

## 1.36 Activation of White Phosphorus (P<sub>4</sub>) by Main Group Elements and Compounds

G Balázs, A Seitz, and M Scheer, Universität Regensburg, Regensburg, Germany

© 2013 Elsevier Ltd. All rights reserved.

<b>1.36.1</b>	<b>Introduction</b>	1106
1.36.1.1	Brief Survey	1106
1.36.1.2	General Trends in the Stability and Reactivity of P <sub>4</sub> Phosphorus	1106
<b>1.36.2</b>	<b>Activation of P<sub>4</sub></b>	1107
1.36.2.1	Activation of P <sub>4</sub> by Alkaline Metals	1107
1.36.2.2	Activation of P <sub>4</sub> by Alkaline Earth Metals and Compounds	1109
1.36.2.3	Activation of P <sub>4</sub> by Group 13 Elements and Compounds	1109
1.36.2.3.1	Boron	1109
1.36.2.3.2	Aluminum	1110
1.36.2.3.3	Gallium	1111
1.36.2.3.4	Indium	1113
1.36.2.3.5	Thallium	1113
1.36.2.4	Activation of P <sub>4</sub> by Group 14 Elements and Compounds	1113
1.36.2.4.1	Carbon	1113
1.36.2.4.2	Silicon	1119
1.36.2.4.3	Germanium, Tin, and Lead	1124
1.36.2.5	Activation of P <sub>4</sub> by Group 15 Elements and Compounds	1124
1.36.2.5.1	Nitrogen	1124
1.36.2.5.2	Phosphorus	1125
1.36.2.5.3	Arsenic, Antimony, and Bismuth	1128
1.36.2.6	Activation of P <sub>4</sub> by Group 16 Elements and Compounds	1128
1.36.2.7	Activation of P <sub>4</sub> by Group 17 Elements and Compounds	1128
<b>1.36.3</b>	<b>Conclusion</b>	1129
<b>References</b>		1129

### Nomenclature

<b>18-crown-6</b>	1,4,7,10,13,16-Hexaoxacyclooctadecane ([−CH <sub>2</sub> CH <sub>2</sub> −O−] <sub>6</sub> )	<b>ICR</b>	Ion cyclotron resonance
<b>BCP</b>	Bond critical point	<b>M</b>	Metal
<b>Bu</b>	<i>n</i> -Butyl (C <sub>4</sub> H <sub>9</sub> )	<b>MAS</b>	Magic angle spinning
<b>Bu<sup>t</sup></b>	<i>tert</i> -Butyl (C <sub>4</sub> H <sub>9</sub> )	<b>Me</b>	Methyl (CH <sub>3</sub> )
<b>CAAC</b>	Cyclic (alkyl)(amino)carbene	<b>Mes</b>	Mesityl (2,4,6-Me <sub>3</sub> C <sub>6</sub> H <sub>2</sub> )
<b>CBS</b>	Complete basis set	<b>MO</b>	Molecular orbital
<b>Cp*</b>	Pentamethylcyclopentadienyl (C <sub>5</sub> Me <sub>5</sub> )	<b>Naph</b>	Naphthalene
<b>DFT</b>	Density functional theory	<b>NHC</b>	N-heterocyclic carbene
<b>diglyme</b>	Diethyleneglycoldimethylether	<b>NICS</b>	Nucleus-independent chemical shift
<b>Dipp</b>	Diisopropylphenyl (2,6-Pr <sup>i</sup> <sub>2</sub> C <sub>6</sub> H <sub>3</sub> )	<b>NMR</b>	Nuclear magnetic resonance
<b>DME</b>	Dimethoxyethane	<b>NR</b>	Neutralization–reionization
<b>DMF</b>	Dimethylformamide	<b>Ph</b>	Phenyl (C <sub>6</sub> H <sub>5</sub> )
<b>en</b>	Ethylenediamine	<b>ppm</b>	Parts per million
<b>EPR</b>	Electron paramagnetic resonance	<b>Pr</b>	<i>n</i> -Propyl (C <sub>3</sub> H <sub>7</sub> )
<b>Et</b>	Ethyl (C <sub>2</sub> H <sub>5</sub> )	<b>Pr<sup>i</sup></b>	<i>iso</i> -Propyl (C <sub>3</sub> H <sub>7</sub> )
<b>Et<sub>2</sub>O</b>	Diethylether	<b>Q</b>	Chalcogen
<b>HOMO</b>	Highest occupied molecular orbital	<b>SCF</b>	Self-consistent field
		<b>THF</b>	Tetrahydrofuran
		<b>XPD</b>	X-ray powder diffraction

### 1.36.1 Introduction

#### 1.36.1.1 Brief Survey

The activation of white phosphorus by main-group elements and compounds is of ongoing research interest in chemistry. The reason for this lies in the availability of white phosphorus as the first industrial product after generation from phosphate minerals and its use as the starting material for subsequent inorganic and organophosphorus products. Almost all subsequent procedures are based on the transformation of P<sub>4</sub> into chlorinated or oxygenated products such as PCl<sub>3</sub>, PCl<sub>5</sub>, POCl<sub>3</sub>, P<sub>4</sub>O<sub>6</sub>, or P<sub>4</sub>O<sub>10</sub>. However, this represents the general problem for its industrial use, since large amounts of HCl or metal halide are produced during the following industrial processes to obtain the desired inorganic or organoderivatives of tri- and pentavalent phosphorus.<sup>1</sup> To avoid these immense amounts of unproductive by-products and change these processes into more sustainable and environmentally friendly procedures, the direct transformation of P<sub>4</sub> phosphorus is necessary to yield the requested subsequent industrial products. These general problems were identified a long time ago and had an initially high impact in academic research of phosphorus in the 1970s and 1980s. However, the discovery that transition metals can coordinate,<sup>2</sup> activate,<sup>3</sup> and transform<sup>4</sup> white phosphorus led to a new focus on P<sub>4</sub> activation by transition metals. In the mid 1980s, the period of intensive research of P<sub>4</sub> activation by transition-metal complexes started and is still being developed.<sup>5</sup> Although the main principles of the gradual activation of P<sub>4</sub> phosphorus are understood<sup>6</sup> and this research area has achieved impressive progress over the years,<sup>7</sup> the key steps of a catalytic functionalization of P<sub>4</sub> phosphorus have not been clarified. The combination of activated transition-metal phosphorus species with organic substrates in a more catalytic way is still the main challenge in this area. Parallel to this research in transition-metal-mediated P<sub>4</sub> activation in the mid 2000s, a renaissance of P<sub>4</sub> activation by main-group compounds occurred.<sup>8</sup> This development was induced by metal-free P<sub>4</sub> degradation by Bertrand et al. using N-heterocyclic carbene (NHC) and cyclic (alkyl)(amino)carbene (CAAC) reagents, which are complementary with earlier reported P<sub>4</sub> activation by carbene analogs of group 13 and heavier group 14 elements. Moreover, cationic carbene-like phosphonium species have been successfully inserted into P—P bonds of white phosphorus (the details are discussed in Sections 1.36.2.3 and 1.36.2.4). According to these decisive developments, in the following sections, a comprehensive overview of the status of P<sub>4</sub> activation and degradation by main-group elements and compounds will be given.

#### 1.36.1.2 General Trends in the Stability and Reactivity of P<sub>4</sub> Phosphorus

P<sub>4</sub> phosphorus reveals a relatively high stability as a platonic body, with high symmetric tetrahedral geometry. For such tetrahedra, a spherical aromaticity was discussed based on the nucleus-independent chemical shift (NICS),<sup>9</sup> which ranges from N<sub>4</sub>(T<sub>d</sub>) ( $\delta = -69.6$ ) over P<sub>4</sub>(T<sub>d</sub>) ( $\delta = -52.9$ ) to finally Bi<sub>4</sub>(T<sub>d</sub>) ( $\delta = -36.6$ ). It is interesting that the NICS value for As<sub>4</sub>(T<sub>d</sub>) ( $\delta = -53.3$ ) is similar to that of P<sub>4</sub>, whereas the value for Sb<sub>4</sub>(T<sub>d</sub>) ( $\delta = -38.8$ ) is close to that of Bi<sub>4</sub>(T<sub>d</sub>), revealing a lower spherical aromatic character. Note that the NICS value in

the center of the T<sub>d</sub> body is slightly lower than those at the center of the E<sub>3</sub> triangles.

Such calculations are based on E<sub>4</sub> tetrahedra with P—P bond lengths of 2.200 Å for P<sub>4</sub>, which is close to that determined for gaseous P<sub>4</sub> at 470 K by electron diffraction, 2.21(2) Å.<sup>10</sup> Analysis of the vibration-rotation Raman spectrum gives a P—P distance of 2.2228(5) Å,<sup>11</sup> whereas in the solid state at 88 K P—P, distances of 2.199–2.212 Å are found for β-P<sub>4</sub><sup>12</sup> by applying a rigid-body libration correction. The long-accepted value of a P—P bond distance in P<sub>4</sub> of 2.21(2) Å as a benchmark for a P—P single bond length disagreed with the value of 2.194 Å determined by quantum chemical calculations.<sup>13</sup> However, recently, the electronic structure of P<sub>4</sub> in the gas phase has been redetermined at 373 K and provides a value of 2.1994(3) Å for the P—P distance.<sup>14</sup> As a consequence, the value of 2.194 Å should be used as a benchmark to reference a P—P single bond distance.

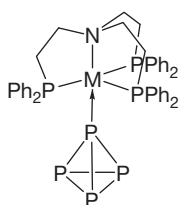
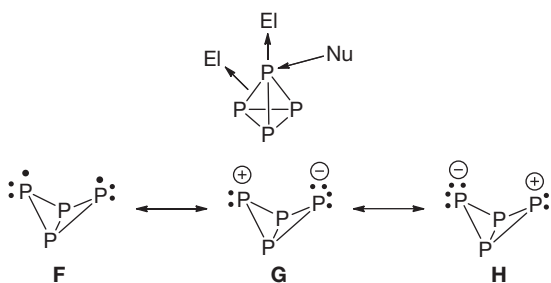
The relatively high reactivity of tetrahedral P<sub>4</sub> is usually attributed to the high bond strain energy.<sup>15</sup> However, newer analyses of the bonding in P<sub>4</sub><sup>16</sup> modify the role of bond strain since, in the singlet ground state of P<sub>4</sub>, the vector linking the P nuclei and the direction of the bond critical point is only about 5°. The excited triplet state of P<sub>4</sub> reveals a butterfly-like structure and is 102.3 kJ mol<sup>-1</sup> higher in energy compared to the neutral singlet state.<sup>16</sup> Using the Bader topological theory,<sup>17</sup> the oxidation of P<sub>4</sub> is a highly energetic process of 1138.1 kJ mol<sup>-1</sup>, leading formally to a P<sub>4</sub><sup>+</sup> species with a favored D<sub>2h</sub> symmetry with four “short” and two “long” bonds. In comparison, the reduction of neutral P<sub>4</sub> to P<sub>4</sub><sup>-</sup> is lower in energy (only 119.7 kJ mol<sup>-1</sup> higher than P<sub>4</sub>), revealing a distorted D<sub>2h</sub> structure as the most favored one.<sup>16</sup> These calculations agree well with the experimental fact that P<sub>4</sub> reacts predominantly under nucleophilic attack. It is interesting that the radical anion P<sub>4</sub><sup>-</sup> was detected and identified by EPR as a spin-adduct with a nitrene during the electrochemical reduction of P<sub>4</sub> in the presence of a spin-trap-like phenyl-*N-tert*-butylnitrene in an electrolysis cell.<sup>18</sup>

From a simple Lewis formula picture, which shows the lone pairs on the vertices of the P atoms, one would expect a good nucleophilicity of P<sub>4</sub>. In the ground-state analysis of P<sub>4</sub>, electron densities are, in fact, found at these positions of electron lone pairs. Nonetheless, the electronic structure reveals that the molecular orbital which would be responsible for such reactivity is only the HOMO-3 orbital. In accordance with this, the nucleophilicity of P<sub>4</sub> is less pronounced and usually observed in main-group chemistry in the reaction with organohalides under drastic thermal conditions (>250 °C). Often, I<sub>2</sub> is added to increase the yield of the products PX<sub>3</sub> and R<sub>4</sub>PX.<sup>19</sup> According to the *ab initio* calculations of Fluck et al., the protonation of P<sub>4</sub> should occur at an apex of the P<sub>4</sub> molecule,<sup>20</sup> followed by an edge protonation, whereas attack at a P<sub>3</sub> face was excluded. Later calculations of Abboud et al.<sup>21</sup> in 1996, using the MP2/6-31G(d,p) method for the gas-phase basicity of P<sub>4</sub>, revealed that an H<sup>+</sup> bridged opened P—P edge structure is, by 45.2 kJ mol<sup>-1</sup>, more stable than an apex-attached moiety.

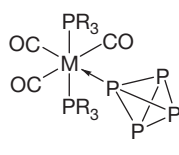
In the main-group chemistry of P<sub>4</sub>, the nucleophilicity is less pronounced, and only in transition-metal chemistry are there a few examples of the Lewis basicity of an apex of the P<sub>4</sub> tetrahedron. Thus, in 1982, the first vertex fixation was found for neutral Lewis-acidic complexes of type A by Di Vaira and Sacconi,<sup>22</sup> followed in 1999 by Gröer and Scheer<sup>23</sup> for

complexes of type B. Using Lewis-acidic cationic complexes, type C complexes containing intact P<sub>4</sub> recently were synthesized by the Stoppioni group.<sup>24</sup> Early examples of Ginsberg exist for an edge fixation of P<sub>4</sub> in D in which, for a long time, the coordinated P—P bond length of 2.462(2) Å was viewed to be a still existing bonding between P atoms.<sup>25</sup> However, in 2002, Krossing et al.<sup>26</sup> could show the side-on fixation of two P<sub>4</sub> moieties on an Ag<sup>+</sup> and, later, on a Cu<sup>+</sup> cation in type E molecules containing weak coordinating counter ions. By NMR investigations and DFT calculations, they could show that, with 2.329(2) Å (Ag derivative), the observed P—P distance is still a bond revealing an intact side-on coordinated P<sub>4</sub> moiety, whereas in the case of the Ginsberg compound D, a P<sub>4</sub><sup>2-</sup> moiety with an open P—P bond is present.

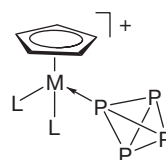
As already mentioned in main-group chemistry, the nucleophilicity of P<sub>4</sub> plays almost no role. Often, the reactions of electrophiles with P<sub>4</sub> are catalyzed by the presence of nucleophiles such as HO<sup>-</sup>, and the combined action of electrophiles and nucleophiles leads to a consecutive cleavage of all P—P bonds to yield P<sub>1</sub> moieties. The experimental details of these few reactions with electrophiles as well as the electrochemical degradation of P<sub>4</sub> are summarized in a review on organophosphorus compounds.<sup>19</sup> In contrast, the P<sub>4</sub> tetrahedron is attacked primarily by a nucleophile as the major reactivity pattern of P<sub>4</sub>. Theoretical as well as experimental findings show that the nucleophiles attack predominantly at an apex P atom. As a result, a P—P bond opening occurs either by a heteroleptic or a homoleptic cleavage accompanied by further degradation of the P<sub>4</sub> tetrahedron. It is interesting that the homoleptic cleavage of a P—P bond, for example, by ultraviolet radiation, is a high-energy process<sup>27</sup> and would lead to a biradical F, which can, alternatively, be described in a zwitterionic structure (G and H).



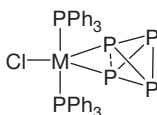
M = Ni, Pd  
A



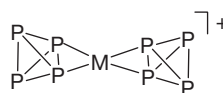
M = Mo, R = Cy  
M = W, R = Cy, Pr<sup>i</sup>  
B



M = Fe, Ru, L = PPh<sub>3</sub>  
LL = dppe  
C



M = Rh, Ir  
D



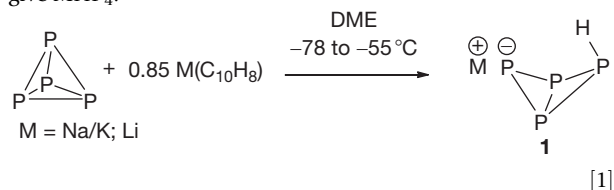
M = Cu, Ag  
E

In light of the lack of detailed mechanistic knowledge of P<sub>4</sub> reactivity, not many general conclusions can be drawn. However, for carbenes and carbene-like species, as a general tendency, it is doubtless that nucleophilic carbenes will attack an apex of the P<sub>4</sub> tetrahedron to result in end-on bound derivatives, whereas more electrophilic carbenes and carbene-like species will formally insert into P—P bonds (details are found in Sections 1.36.2.4 and 1.36.2.5.2).

## 1.36.2 Activation of P<sub>4</sub>

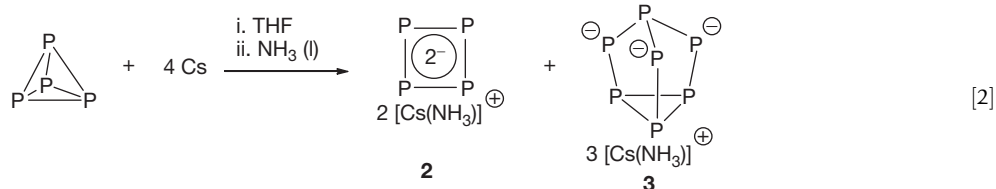
### 1.36.2.1 Activation of P<sub>4</sub> by Alkaline Metals

White phosphorus P<sub>4</sub> reacts readily with alkali metals, leading to, depending on the reaction conditions and stoichiometry, alkali metal phosphides or oligophosphides. Probably, the first step of the reaction is a reductive cleavage of a P—P bond by one or two electron transfers, leading to a radical anion or dianion with a butterfly-like (bicyclo[1.1.0]butane) structure. This phosphide is highly reactive and reacts with P<sub>4</sub>, leading to higher aggregated oligophosphides, which could not be isolated or characterized. However, when the reaction of P<sub>4</sub> with a solution of sodium/potassium naphthalenide or lithium naphthalenide in DME is conducted at -78 to -55 °C, the formation of MHP<sub>4</sub> (1) was observed (eqn [1]).<sup>28</sup> The radical anion P<sub>4</sub><sup>-</sup> or the dianion P<sub>4</sub><sup>2-</sup> is formed as the reaction intermediate, which abstracts hydrogen readily from the solvent to give MHP<sub>4</sub>.



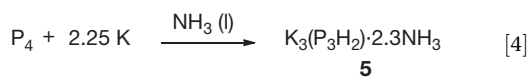
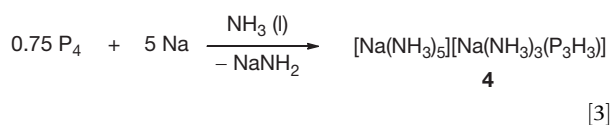
MHP<sub>4</sub> could not be characterized by single-crystal x-ray diffraction, but its structure was definitely determined by NMR spectroscopic methods.

Reacting P<sub>4</sub> with cesium in THF, followed by recrystallization of the reaction product from liquid ammonia, leads to the formation of Cs<sub>2</sub>P<sub>4</sub>·2NH<sub>3</sub> (2), which contains the 6π aromatic cyclotetraphosphide dianion, P<sub>4</sub><sup>2-</sup> (eqn [2]).<sup>29</sup> However, the main reaction product is Cs<sub>3</sub>P<sub>7</sub>·3NH<sub>3</sub> (3), whereas



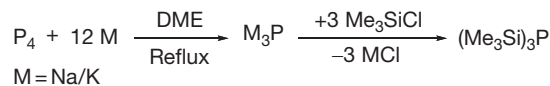
Cs<sub>2</sub>P<sub>4</sub>·2NH<sub>3</sub> is formed only as a side product. A more convenient synthetic route for **2** is the reaction of metallic cesium with the diphosphane P<sub>2</sub>H<sub>4</sub>.<sup>29</sup>

Stronger fragmentation of P<sub>4</sub> to phosphides, containing three phosphorus atoms, was also reported. The reaction of P<sub>4</sub> with excess Na (atomic ratio P:Na = 3:5) in liquid ammonia gives [Na(NH<sub>3</sub>)<sub>5</sub>][Na(NH<sub>3</sub>)<sub>3</sub>P<sub>3</sub>H<sub>3</sub>] (**4**), containing the *catena*-trihydrogen triphosphide P<sub>3</sub>H<sub>3</sub><sup>2-</sup> (eqn [3]).<sup>30</sup> The hydrogen substituents in P<sub>3</sub>H<sub>3</sub><sup>2-</sup> are in all-*trans* configuration, as determined by single-crystal x-ray diffraction studies. The synthesis of the compounds [Rb(18-crown-6)]<sub>2</sub>(P<sub>3</sub>H<sub>3</sub>)·7.5NH<sub>3</sub> and [Cs(18-crown-6)]<sub>2</sub>(P<sub>3</sub>H<sub>3</sub>)·7NH<sub>3</sub>, containing the *catena*-P<sub>3</sub>H<sub>3</sub><sup>2-</sup> anion, was also reported by dissolving P<sub>2</sub>H<sub>4</sub> and a cyclohexaphosphide, P<sub>6</sub><sup>4-</sup>, in liquid ammonia.<sup>31</sup> Interestingly, by reducing P<sub>4</sub> and potassium in liquid ammonia in similar conditions as for the synthesis of **4**, the potassium salt of the *catena*-dihydrogen triphosphide P<sub>3</sub>H<sub>2</sub><sup>3-</sup> was obtained (eqn [4]).<sup>31</sup> The rubidium derivative Rb<sub>3</sub>(P<sub>3</sub>H<sub>2</sub>)·NH<sub>3</sub> can be obtained by dissolving the corresponding hexaphosphide, P<sub>6</sub><sup>4-</sup>, in liquid ammonia, followed by crystallization.<sup>31</sup>

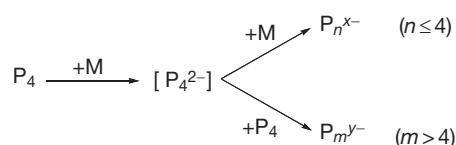


By the reaction of alkali metals with P<sub>4</sub>, not only phosphides, but even neutral compounds can be obtained. If P<sub>4</sub> is reacted with Na in liquid NH<sub>3</sub> in a 2:1 or 1.5:1 atomic ratio, the 1,3-diaminotriphosphane P<sub>3</sub>H<sub>3</sub>(NH<sub>2</sub>)<sub>2</sub> is formed, which is, however, stable only in liquid NH<sub>3</sub>.<sup>32</sup> According to <sup>31</sup>P NMR spectroscopic investigations, from the three possible diastereomers, only the *erythro*, *erythro* isomer with transoid-oriented NH<sub>2</sub> groups is formed. Side products of this reaction are NaPH<sub>2</sub>, Na<sub>2</sub>HP<sub>7</sub>, and higher phosphides.<sup>33</sup>

Fragmentation of P<sub>4</sub> by alkali metals to phosphides containing one or two phosphorus atoms can be achieved by employing a larger excess of alkali metal and higher reaction temperatures. Thus, reacting P<sub>4</sub> with Na in a 1:3 atomic ratio in THF or 1,2-dimethoxyethane under reflux leads to the formation of Na<sub>3</sub>P. This can be subsequently quenched by alkyl halides to give a varying mixture of organophosphanes and organophosphonium salts.<sup>34</sup> Using CH<sub>3</sub>C(CH<sub>2</sub>Br)<sub>3</sub> as the quenching agent, the triphosphanortricyclane derivative CH<sub>3</sub>C(CH<sub>2</sub>P)<sub>3</sub> is obtained in low yield.<sup>35</sup> Similarly, P<sub>4</sub> reacts with Na/K alloy (P:M = 1:3) in boiling THF or DME to give M<sub>3</sub>P, which can be subsequently treated with Me<sub>3</sub>SiCl to give (Me<sub>3</sub>Si)<sub>3</sub>P (**Scheme 1**).<sup>36</sup> Employing a 1:0.6 atomic ratio of P to M in the latter reaction, followed by quenching of the



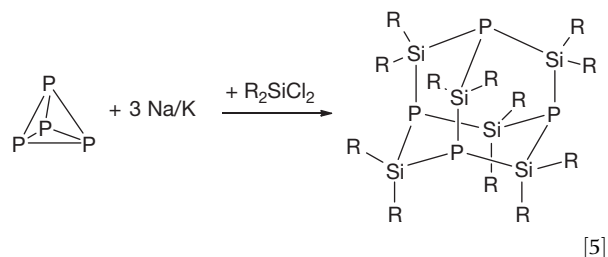
**Scheme 1** Degradation of P<sub>4</sub> by alkali metals to M<sub>3</sub>P, and subsequent reaction with Me<sub>3</sub>SiCl.



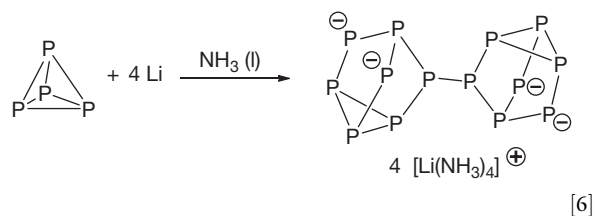
**Scheme 2** General pathway for the conversion of P<sub>4</sub> by alkali metals.

reaction mixture with Me<sub>3</sub>SiCl, leads to the higher phosphanes (Me<sub>3</sub>Si)<sub>3</sub>P<sub>7</sub>, (Me<sub>3</sub>Si)<sub>4</sub>P<sub>14</sub>, and (Me<sub>3</sub>Si)<sub>5</sub>P<sub>13</sub>, in addition to (Me<sub>3</sub>Si)<sub>3</sub>P and (Me<sub>3</sub>Si)<sub>2</sub>P—P(SiMe<sub>3</sub>)<sub>2</sub>.<sup>37</sup> The silylated nortricyclane derivative {(Me<sub>3</sub>Si)<sub>3</sub>Si}<sub>3</sub>P<sub>7</sub> is, likewise, obtained by employing (Me<sub>3</sub>Si)<sub>3</sub>SiCl in the reaction with M<sub>3</sub>P.<sup>38</sup>

When the *in-situ*-generated M<sub>3</sub>P (M = Na/K) is reacted with RR'SiCl<sub>2</sub>, the polycyclic silylphosphanes (Me<sub>2</sub>Si)<sub>3</sub>P<sub>4</sub><sup>39</sup> and (RR'Si)<sub>6</sub>P<sub>4</sub> (R = Me, R' = Et; R = R' = Et, R = Ph, R' = Me; R = vinyl, R' = Me; R = Me, R' = H)<sup>40</sup> are the reaction products. The latter has an adamantane-like structure (eqn [5]).

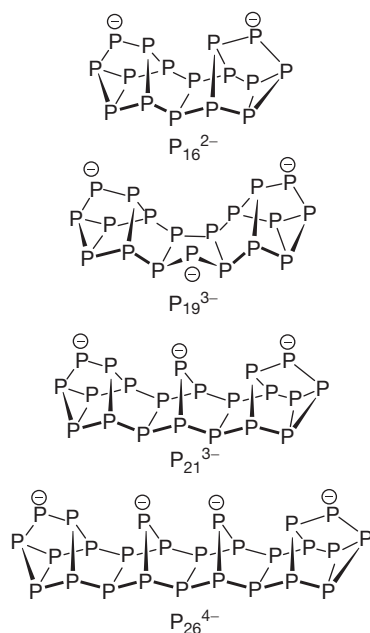


One of the first reactive intermediates formed by the reduction of P<sub>4</sub> with alkali metals, namely, the phosphide P<sub>4</sub><sup>2-</sup>, can undergo two different reaction pathways (**Scheme 2**): (i) it can react with additional alkali metal, leading to the cleavage of further P—P bonds and, hence, to the formation of 'simple' phosphides (phosphides containing less than four phosphorus atoms), or (ii) it can react as a nucleophile with P<sub>4</sub>, which is still present in solution, leading to the aggregation and formation of higher phosphides. Hence, oligophosphides are formed by employing a low M:P ratio in the reaction of alkali metals with P<sub>4</sub>.



The reaction of P<sub>4</sub> with metallic lithium in liquid ammonia in a 1:1 atomic ratio or with sodium naphthalenide in 1,2-dimethoxyethane gives [Li(NH<sub>3</sub>)<sub>4</sub>]<sub>4</sub>P<sub>14</sub>·NH<sub>3</sub><sup>41</sup> (eqn [6]) and Na<sub>4</sub>(DME)<sub>8</sub>P<sub>14</sub><sup>42</sup> respectively. Both compounds contain the tetradecaphosphide P<sub>14</sub><sup>4-</sup>, which is built up from two nortricyclane-like units connected by a P–P bond. A facile way to synthesize Na<sub>4</sub>(DME)<sub>7.5</sub>P<sub>14</sub> is the reaction of PCl<sub>3</sub> with sodium in a 1:3.2 molar ratio.<sup>43</sup> When the reaction of P<sub>4</sub> with Na in THF is performed in the presence of 18-crown-6 in a 3:1 atomic ratio, the phosphorus-rich phosphide Na<sub>2</sub>P<sub>16</sub>·8THF is formed. The structure of the P<sub>16</sub><sup>2-</sup> anion was determined by <sup>31</sup>P NMR spectroscopy. It contains two deltacyclane units joined by a P<sub>2</sub> bridge (Scheme 3),<sup>44</sup> and is isostructural with the analogous (Ph<sub>4</sub>P)<sub>2</sub>P<sub>16</sub>, whose structure was determined by single-crystal x-ray diffraction.<sup>45</sup> An alternative access to P<sub>16</sub><sup>2-</sup> can be achieved by reacting P<sub>4</sub> with LiPH<sub>2</sub><sup>46</sup> or LiP(SiMe<sub>3</sub>)<sub>2</sub><sup>47</sup> even if the latter synthetic route strongly depends on the concentration of the reactants and their molar ratio. As reaction products, polyphosphides (i.e., Li<sub>3</sub>P<sub>7</sub>, Li<sub>2</sub>P<sub>16</sub>), partly silylated polyphosphides such as Li<sub>2</sub>P<sub>7</sub>SiMe<sub>3</sub>, as well as P(SiMe<sub>3</sub>)<sub>3</sub> are formed. Applying an excess of LiPH<sub>2</sub> in the reaction with P<sub>4</sub> leads to the formation of Li<sub>3</sub>P<sub>7</sub> in high yield.<sup>48</sup>

The size of the polyphosphides is not limited to P<sub>16</sub><sup>2-</sup>. Mixtures of higher aggregated phosphides such as M<sub>3</sub>P<sub>19</sub>, M<sub>2</sub>P<sub>16</sub>, M<sub>3</sub>P<sub>21</sub>, M<sub>4</sub>P<sub>26</sub>, M<sub>2</sub>HP<sub>7</sub>, MH<sub>2</sub>P<sub>7</sub>, and M<sub>2</sub>H<sub>2</sub>P<sub>14</sub> (M = Li, Na, K) can be generated by reacting P<sub>4</sub> with Na, K, or LiPH<sub>2</sub> (in a molar ratio varying from 2.5:1 to 1:2) in THF or DME.<sup>49</sup> The individual compounds, such as M<sub>2</sub>P<sub>16</sub>, M<sub>3</sub>P<sub>21</sub>, and M<sub>3</sub>P<sub>19</sub> can only be enriched in solution, but not isolated as pure substances. By reacting P<sub>4</sub> with either LiPH<sub>2</sub> or Na in ratios varying from 1.4:1 to 1:1.5, the polyphosphides M<sub>4</sub>P<sub>26</sub> (M = Li, Na) can be synthesized. The compound Li<sub>4</sub>P<sub>26</sub>·16THF (Scheme 3) could be isolated as crystalline material.<sup>50</sup> More conveniently, Li<sub>4</sub>P<sub>26</sub>·16THF can be obtained and isolated from the decomposition reaction of LiH<sub>2</sub>P<sub>7</sub> in THF. Although alkali metal



**Scheme 3** Structural representation of the oligophosphides P<sub>16</sub><sup>2-</sup>, P<sub>19</sub><sup>3-</sup>, P<sub>21</sub><sup>3-</sup> and P<sub>26</sub><sup>4-</sup>.

phosphides are moisture-sensitive, in some cases, the use of wet solvents can lead to the formation of novel polyphosphides. The reaction of P<sub>4</sub> with K in a mixture of THF and DME, followed by extraction with wet EtOH, leads to K<sub>2</sub>P<sub>16</sub>. The replacement of EtOH with THF as the solvent leads to clean conversion of K<sub>2</sub>P<sub>16</sub> to K<sub>3</sub>P<sub>21</sub> and elemental phosphorus.<sup>51</sup> Even though the reaction of P<sub>4</sub> with alkali metals does not lead selectively to one compound, stoichiometrically pure compounds can be isolated by carefully choosing the reaction conditions. So, by reacting P<sub>4</sub> with Na in a 2:1 ratio, Na<sub>3</sub>P<sub>21</sub>·15THF<sup>52,53</sup> can be isolated from the reaction mixture, whereas the remaining solution contains the aromatic P<sub>5</sub><sup>-</sup> anion.<sup>54</sup> NaP<sub>5</sub> as a pure 18-crown-6 complex is prepared by reacting white phosphorus with NaPH<sub>2</sub> (P/NaPH<sub>2</sub> = 5:1–5.6:1) in boiling THF in the presence of 18-crown-6.<sup>55</sup> If P<sub>4</sub> and Na are reacted in boiling diglyme, the unexpected 1,2,3,4-tetraphospha- and 1,2,3-triphosphacyclopentadienide anions (P<sub>4</sub>CH<sup>-</sup> and P<sub>3</sub>(CH)<sub>2</sub><sup>-</sup>, respectively) are formed, together with NaP<sub>5</sub>.<sup>54a,56</sup>

Summing up, the first step of the reaction of P<sub>4</sub> with alkali metals is a one- or two-electron transfer from alkali metal to P<sub>4</sub>, leading to a radical anion P<sub>4</sub><sup>-</sup> or dianion P<sub>4</sub><sup>2-</sup>. This can react further, either with the alkali metal inducing further fragmentation of the P<sub>4</sub> unit or with P<sub>4</sub> leading to aggregation, and, hence, to more highly aggregated phosphides. Nevertheless, different compounds can be isolated by carefully choosing the reaction conditions (solvent, reaction temperature, and stoichiometry). Generally, high reaction temperatures and excess of alkali metal lead to simple P-pure phosphides, whereas low temperatures and high P:M (M = alkali metal) ratio favor the formation of higher aggregated polyphosphides.

### 1.36.2.2 Activation of P<sub>4</sub> by Alkaline Earth Metals and Compounds

To the best of our knowledge, reactions in which P<sub>4</sub> is reacted only with group 2 metals have not been reported so far. However, some reactions in which white phosphorus is involved as a phosphorus source were described. The addition of P<sub>4</sub> to the dehalogenation reaction of alkyl dihalophosphanes by Mg leads to the formation of phosphorus-rich polyphosphanes. Accordingly, reaction of Bu<sup>t</sup>PCl<sub>2</sub> with Mg in the presence of P<sub>4</sub> gives mixtures of organophosphanes,<sup>57</sup> from which the polycyclic phosphanes P<sub>9</sub>Bu<sup>t</sup><sub>7</sub>, P<sub>10</sub>Bu<sup>t</sup><sub>8</sub>, and P<sub>13</sub>Bu<sup>t</sup><sub>9</sub> were isolated and spectroscopically characterized.<sup>58</sup> The reduction of Pr<sup>i</sup>PCl<sub>2</sub> with magnesium in the presence of P<sub>4</sub> is strongly dependent on the reaction conditions and stoichiometry, giving rise to different cyclic and polycyclic phosphanes. However, when the reduction is followed by thermolysis of the reaction mixture, the polycyclic phosphanes P<sub>11</sub>Pr<sup>i</sup><sub>3</sub>,<sup>59</sup> P<sub>11</sub>Pr<sup>i</sup><sub>5</sub>,<sup>60</sup> P<sub>12</sub>Pr<sup>i</sup><sub>4</sub>,<sup>61,62</sup> P<sub>13</sub>Pr<sup>i</sup><sub>5</sub>,<sup>61</sup> P<sub>14</sub>Pr<sup>i</sup><sub>4</sub>,<sup>63</sup> P<sub>14</sub>Pr<sup>i</sup><sub>6</sub>,<sup>64</sup> P<sub>18</sub>Pr<sup>i</sup><sub>6</sub>,<sup>65</sup> and P<sub>20</sub>Pr<sup>i</sup><sub>6</sub><sup>66</sup> are formed. Similar monocyclic and polycyclic phosphanes<sup>57a</sup> are obtained by the reduction of R<sup>i</sup>PCl<sub>2</sub> (R = Me, Et) with Mg in the presence of P<sub>4</sub>.<sup>67</sup>

### 1.36.2.3 Activation of P<sub>4</sub> by Group 13 Elements and Compounds

#### 1.36.2.3.1 Boron

Reactions of white phosphorus with boron or boron-containing compounds are very scarcely studied. The only example was

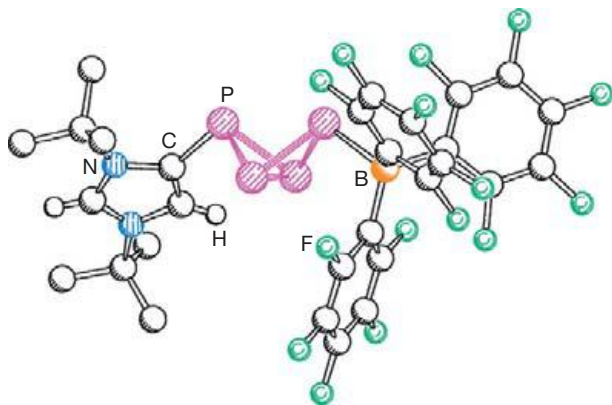


**Figure 1** Molecular structure of **6**. Only the hydrogen atoms attached to the imidazolium ring are depicted. Adapted from Holschumacher, D.; Bannenberg, T.; Ibrom, K.; Daniliuc, C. G.; Jones, P. G.; Tamm, M. *Dalton Trans.* **2010**, *39*, 10590.

reported very recently and describes the interaction of a frustrated Lewis acid/base pair with P<sub>4</sub>.<sup>68</sup> Adding a mixture of 1,3-di-*tert*-butylimidazolin-2-ylene and B(C<sub>6</sub>F<sub>5</sub>)<sub>3</sub> to P<sub>4</sub> in a 5:5:1 molar ratio, the formation of the zwitterionic compound **6** was observed (eqn [7]). The molecular structure of **6** is depicted in Figure 1. For the first step of this reaction, the coordination of P<sub>4</sub> to the Lewis-acidic B(C<sub>6</sub>F<sub>5</sub>)<sub>3</sub> is proposed, which is followed by the nucleophilic attack of the carbene at one phosphorus atom of the opposite P<sub>3</sub> face of the P<sub>4</sub> tetrahedron, leading to the cleavage of a P—P bond and to the formation of a butterfly-like core. Finally, the *normal* carbene adduct rearranges to the *abnormal* adduct, which is thermodynamically more stable by 59.86 kJ mol<sup>-1</sup>, determined by quantum chemical calculations.<sup>68</sup> Although the *cis,trans* isomer of **6** is 8.37 kJ mol<sup>-1</sup> lower in energy compared to the *trans/trans* isomer, experimentally, only the latter was observed. It has to be noted that, in some cases in solution, compounds of this type present identical <sup>31</sup>P NMR data for both the *trans,trans* and *cis,trans* isomers (*vide infra*; Section 1.36.2.3.5). Interestingly, at higher temperatures, **6** decomposes, with the formation of P<sub>4</sub> and the *abnormal* carbene-B(C<sub>6</sub>F<sub>5</sub>)<sub>3</sub> adduct.

### 1.36.2.3.2 Aluminum

Base metals like aluminum and gallium react exothermally with P<sub>4</sub> to give the bulk materials AlP and GaP, respectively. The ΔH<sub>298</sub><sup>0</sup> values have been determined experimentally to be -164 and -102 kJ mol<sup>-1</sup> for AlP and GaP, respectively.<sup>69</sup> In contrast to these high formation enthalpies, there are only a few reactions described in which Al compounds are reacted with P<sub>4</sub>.

The reaction of aluminum(I) compounds with P<sub>4</sub> usually leads to the oxidative addition and fragmentation of the P<sub>4</sub> tetrahedron. When the bulky aluminum(I) species [HC(CMeNDipp)<sub>2</sub>Al] (Dipp = 2,6-Pr<sup>*i*</sup><sub>2</sub>C<sub>6</sub>H<sub>3</sub>) (**7**) is reacted with

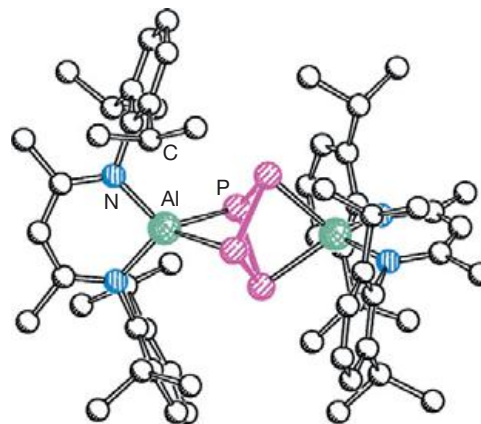
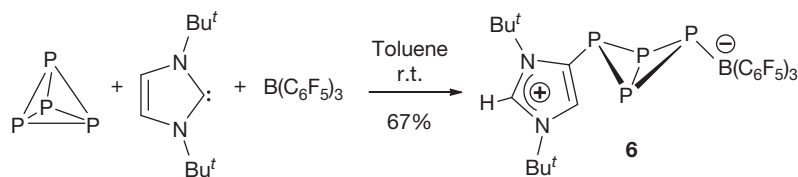


**Figure 2** Molecular structure of **8**. Hydrogen atoms are omitted for clarity. Adapted from Peng, Y.; Fan, H.; Zhu, H.; Roesky, H. W.; Magull, J.; Hughes, C. H. *Angew. Chem. Int. Ed.* **2004**, *43*, 3443.

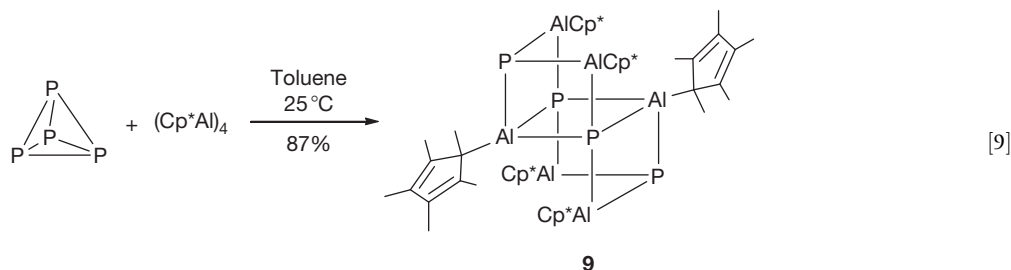
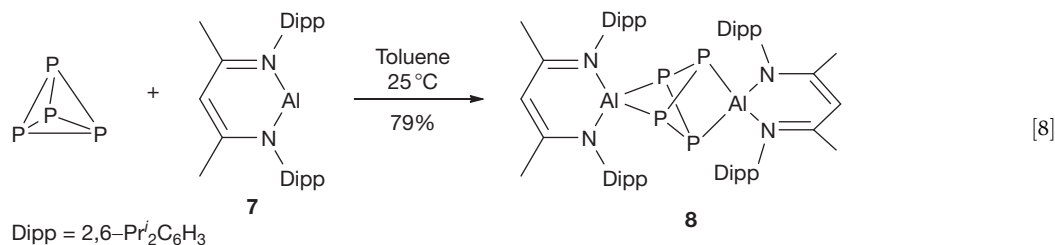
P<sub>4</sub>, the doubly oxidative addition product **8**, in which two RAl units are inserted in two opposite P—P bonds, is obtained (eqn [8], Figure 2).<sup>70</sup> Quantum chemical calculations show that the Al—P bonds in **8** are mainly ionic in nature and that a high bonding energy exists between the asterane-like P<sub>4</sub> unit and the Al atoms. The existence of Al(III) in **8** was also confirmed by <sup>27</sup>Al MAS NMR spectroscopy. A stronger fragmentation of P<sub>4</sub> appears in the reaction with the sterically less crowded (Cp\*Al)<sub>4</sub>, which dissociates in toluene solutions into monomeric Cp\*Al units. The Cp\*Al fragments insert in each P—P bond forming the electron-deficient compound (Cp\*Al)<sub>6</sub>P<sub>4</sub> (**9**) (eqn [9]).<sup>71</sup> Compound **9** is built up from two face-sharing heterocubanes, with two opposite corners being unoccupied. The Cp\* ligands in **9** bind either in η<sup>1</sup> or η<sup>5</sup> fashion, depending on the two- or threefold coordination pattern of the Al center. According to quantum chemical calculations, the higher stability of **9** compared to its adamantane-like isomer is due to the presence of weak Al•••Al interactions.

Al(I) species possess a lone pair of electrons, as well as an empty orbital. Hence, they can act both as nucleophiles and as electrophiles. Nevertheless, the reactions of Al(I) compounds with P<sub>4</sub> seem to proceed via redox processes. This is mainly illustrated with the formation of compound **8** (eqn [8]), in which two [HC(CMeNDipp)<sub>2</sub>Al] (Dipp = 2,6-Pr<sup>*i*</sup><sub>2</sub>C<sub>6</sub>H<sub>3</sub>) units transfer four electrons to P<sub>4</sub>, leading to the reductive cleavage of two P—P bonds and the formation of **8**.

Usually, solutions of Al(I) halides decompose at room temperature through disproportionation to bulk metal and Al(III) halide. Interestingly, the AlR species with R = PR'<sub>2</sub> and NR'<sub>2</sub> substituents decompose to the bulk salts AlP, AlN, and the dimers of the substituents (e.g., R'<sub>2</sub>), which are thermodynamically more favored.<sup>72</sup>



[7]

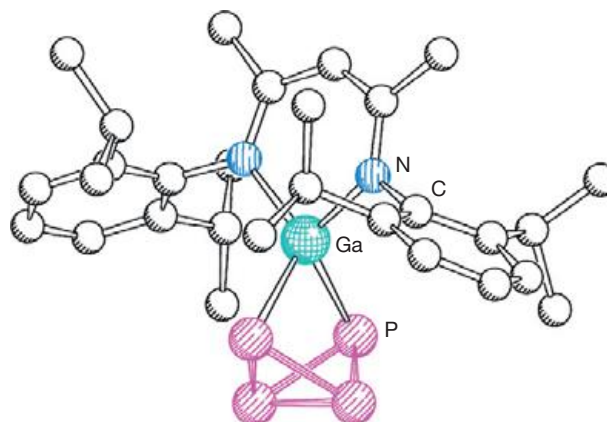


### 1.36.2.3.3 Gallium

Just like aluminum, metallic gallium reacts with P<sub>4</sub> exothermally, with the formation of GaP.<sup>69</sup> But, in contrast to the scarcely studied chemistry of aluminum-containing compounds with P<sub>4</sub>, the reaction of gallium-containing compounds with P<sub>4</sub> was much more broadly investigated.

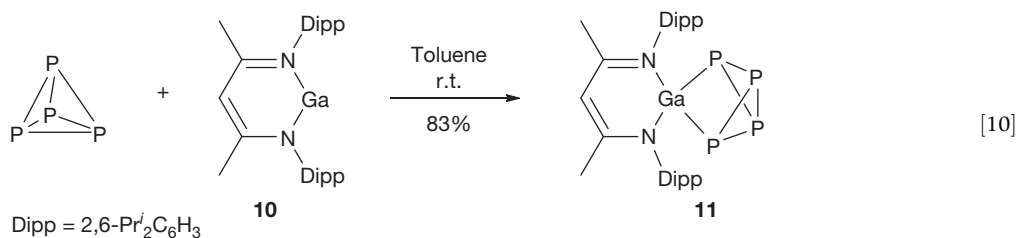
The reaction of the Ga(I) species [HC(CMeNDipp)<sub>2</sub>Ga] (Dipp = 2,6-Pr<sub>2</sub>C<sub>6</sub>H<sub>3</sub>) (10) with P<sub>4</sub> leads to the reductive cleavage of one P—P bond and the formation of [HC(CMeNDipp)<sub>2</sub>GaP<sub>4</sub>] (11) (eqn [10]).<sup>73</sup> It is interesting to note that the corresponding Al derivative [HC(CMeNDipp)<sub>2</sub>Al] (Dipp = 2,6-Pr<sub>2</sub>C<sub>6</sub>H<sub>3</sub>) leads to the cleavage of two P—P bonds in P<sub>4</sub> (*vide infra*). This is probably caused by the lower reduction potential of Ga(I) compared to Al(I). The P<sub>4</sub> core in 11 consists of a bicyclo[1.1.0]butane (butterfly-like) moiety, similar to 1 and 6. The molecular structure of 11 is depicted in Figure 3. Further reaction of 11 with an excess of [Mo(CO)<sub>6</sub>] affords the double Mo(CO)<sub>5</sub>-containing adduct, revealing a heteronuclear [Ga(μ<sub>3</sub>,η<sup>2:1:1</sup>-P<sub>4</sub>)Mo<sub>2</sub>] scaffold, in which the gallium-bound phosphorus atoms coordinate to the molybdenum units.

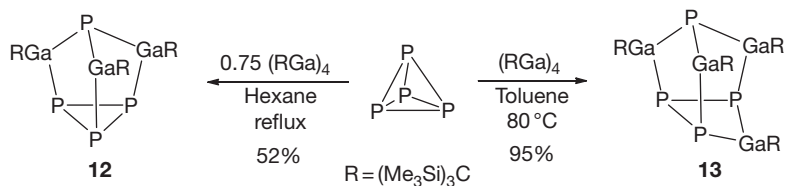
A more extensive fragmentation is achieved when P<sub>4</sub> is treated with the more reactive tetragallane Ga<sub>4</sub>[C(SiMe<sub>3</sub>)<sub>3</sub>]<sub>4</sub>, which dissociates into monomeric RGa units in diluted solutions. Thus, the reaction of Ga<sub>4</sub>[C(SiMe<sub>3</sub>)<sub>3</sub>]<sub>4</sub> with P<sub>4</sub> leads to a threefold insertion of RGa units in three P—P bonds and to the formation of (RGa)<sub>3</sub>P<sub>4</sub> (12), containing a nortricyclane-like structure (Scheme 4).<sup>74</sup> Interestingly, for the apical phosphorus atom in 12, a very unusual <sup>31</sup>P NMR chemical shift is observed at δ = -521.9 ppm, whereas for the basal P<sub>3</sub> unit,



**Figure 3** Molecular structure of 11. Hydrogen atoms are omitted for clarity. Adapted from Prabusankar, G.; Doddi, A.; Gemel, C.; Winter, M.; Fischer, R. A. *Inorg. Chem.* **2010**, *49*, 7976.

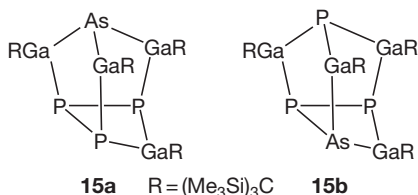
the <sup>31</sup>P NMR resonance appears at δ = -202.8 ppm. In accordance with the redox behavior of the Al(I) compounds (*vide supra*), here, also, an oxidation of the gallium atom from Ga(I) in 10 to Ga(III) in 11 was proposed. If the reaction of Ga<sub>4</sub>[C(SiMe<sub>3</sub>)<sub>3</sub>]<sub>4</sub> with P<sub>4</sub> is performed in a 1:1 ratio in toluene, the quadruple insertion product 13 is obtained (Scheme 4).<sup>75</sup> At room temperature in solution, 13 readily reverts to Ga<sub>4</sub>[C(SiMe<sub>3</sub>)<sub>3</sub>]<sub>4</sub> and unidentified phosphorus-containing products. Although 13 could not be structurally characterized, its constitution was determined by NMR spectroscopy.





**Scheme 4** Reaction of P<sub>4</sub> with (RGa)<sub>4</sub> leading to the insertion of RGa units into P–P bonds.

The very recently reported AsP<sub>3</sub> shows a similar reactivity towards Ga<sub>4</sub>[C(SiMe<sub>3</sub>)<sub>3</sub>]<sub>4</sub> as P<sub>4</sub> (eqn [11]).<sup>75</sup> The major product of the reaction is **14a** (80%), whereas **14b** is formed as a side product in 20% yield. Noteworthy, the insertion isomers **14a** and **14b** are not formed in a statistical ratio, but there is a clear preference for the selective cleavage of the P–As bonds before the P–P bonds are opened. This is in agreement with the expectations, since the As–P bond is considerably weaker than the P–P bond. As observed for **12**, the <sup>31</sup>P NMR resonance for the apical phosphorus atom in **14b** shows a high upfield shift ( $\delta = -495$  ppm). Theoretical calculations on both isomers of the model compound [AsP<sub>3</sub>(GaCH<sub>3</sub>)<sub>3</sub>] reveal quite different molecular properties for **14a** and **14b**. This is also responsible for the facile isolation of **14a** by crystallization and prevents the co-crystallization with **14b**. The molecular structure of **14a** was determined by single-crystal x-ray diffraction, and is depicted in **Figure 4**. Similarly to the case of P<sub>4</sub> (*vide supra*), AsP<sub>3</sub> reacts with 1 equiv. of Ga<sub>4</sub>[C(SiMe<sub>3</sub>)<sub>3</sub>]<sub>4</sub> to give the tetra insertion products **15a** and **15b** in 82% and 18% yields, respectively.<sup>75</sup> A preference for the isomer with the arsenic atom in the apical position is again clearly evident. Selective generation of **15a** is possible by reacting **14a** with 0.25 equiv. of Ga<sub>4</sub>[C(SiMe<sub>3</sub>)<sub>3</sub>]<sub>4</sub>. Just like **13**, the compounds **15a,b** are not stable in solution and decompose to the starting material (RGa)<sub>4</sub> and several unidentified products.



The reaction of P<sub>4</sub> with Ga compounds is not limited to Ga(I) species; even Lewis-acidic Ga(III) compounds react with P<sub>4</sub> under unexpectedly mild conditions. Thus, the reaction of Bu<sup>t</sup><sub>3</sub>Ga with P<sub>4</sub> proceeds already at room temperature via the cleavage of a P–P bond and insertion of a phosphorus atom into a Ga–C bond. Additionally, this phosphorus atom coordinates to the so-formed Bu<sub>2</sub>Ga fragment. The stability of the obtained product is enhanced by further coordination of one phosphorus atom to Bu<sub>3</sub>Ga, leading to **16** (eqn [12]).<sup>76</sup> Although the <sup>31</sup>P NMR data of **16** are similar to those of the

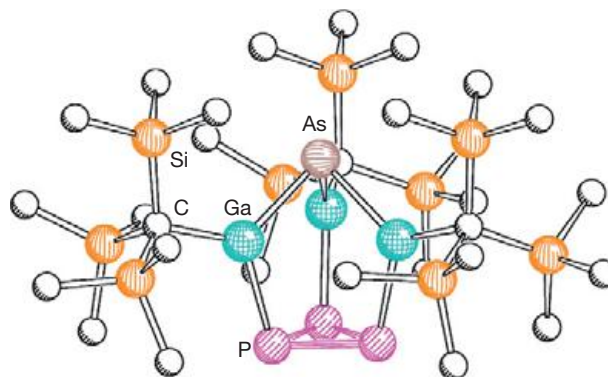
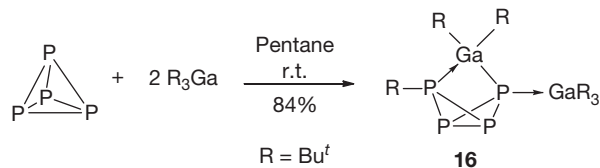


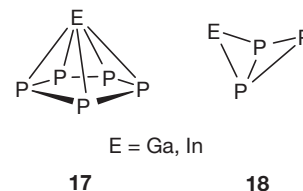
**Figure 4** Molecular structure of [AsP<sub>3</sub>Ga<sub>3</sub>C(SiMe<sub>3</sub>)<sub>3</sub>] (**14a**). Hydrogen atoms are omitted for clarity. Adapted from Cossairt, B. M.; Cummins, C. C. *Chem. Eur. J.* **2010**, *16*, 12603.

structurally related transition-metal-substituted ML<sub>*n*</sub>(η<sup>2</sup>-P<sub>4</sub>) compounds,<sup>77</sup> its electronic structure resembles more that of organophosphorus compounds of the type R<sub>2</sub>P<sub>2</sub>(P<sub>2</sub>).



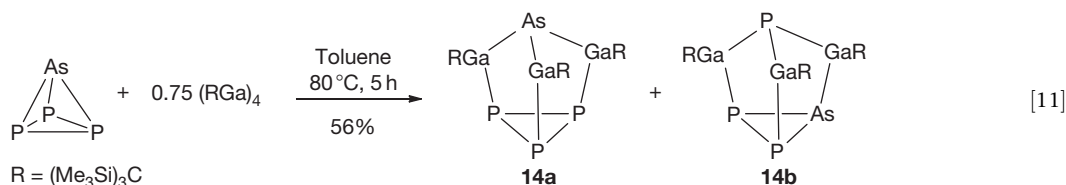
[12]

Highly pure binary phases of GaP and InP can be synthesized starting from red phosphorus and Ga and In, respectively.<sup>78</sup> The existence of the compounds **17** and **18** in the gas phase was proposed on the basis of thermodynamic calculations and their structure and stability were verified by DFT calculations. They play an important role in the transport reactions in the gas phase.



**17**

**18**



[11]

Furthermore, well-crystallized GaP and InP were obtained in aqueous medium by the dismutation of P<sub>4</sub> in alkaline solution in the presence of Ga<sub>2</sub>O<sub>3</sub> and In<sub>2</sub>O<sub>3</sub>, respectively.<sup>79</sup> A key feature of the reaction is the addition of I<sub>2</sub>, which increases the amount of the intermediate PH<sub>3</sub>, and, hence, the yield of GaP nanocrystals.

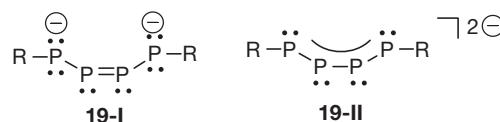
#### 1.36.2.3.4 Indium

The chemistry of indium compounds with white phosphorus is only scarcely studied. However, the preparation of well-crystallized InP, starting from In<sub>2</sub>O<sub>3</sub> and P<sub>4</sub> in alkali solution, similarly to that described for GaP (*vide supra*), was reported.<sup>79</sup> Additionally, nanocrystalline InP can be prepared by the reduction of InCl<sub>3</sub> with KBH<sub>4</sub> in the presence of P<sub>4</sub> in ethylenediamine at 80–160 °C.<sup>80</sup> The addition of HAuCl<sub>4</sub> and performing the reaction at 200 °C leads to the formation of mesoscaled InP hollow spheres.<sup>81</sup> Similarly, InP nanocrystals were obtained by reducing concomitantly PCl<sub>3</sub> and In(OAc)<sub>3</sub> with LiBHET<sub>2</sub>.<sup>82</sup> Moreover, the reaction of P<sub>4</sub> with metal nanoparticles of In, generated by the reduction of InCl<sub>3</sub> with sodium naphthalenide, was reported to form InP nanoparticles.<sup>83</sup> Interestingly, (Cp\*In)<sub>4</sub> reacts with P<sub>4</sub>, but the reaction products could not be identified.<sup>74</sup> This shows the different chemical behavior of (Cp\*In)<sub>4</sub> compared to (Cp\*Al)<sub>4</sub> (*vide supra*).

#### 1.36.2.3.5 Thallium

The reaction of the weakly dimerized 'dithallene' (TlR)<sub>2</sub> (R = 2,6-(2,6-Pr<sup>i</sup><sub>2</sub>C<sub>6</sub>H<sub>3</sub>)<sub>2</sub>C<sub>6</sub>H<sub>3</sub>), protected by very bulky terphenyl substituents with P<sub>4</sub>, results in aryl group transfer from thallium to phosphorus to afford Tl<sub>2</sub>(P<sub>4</sub>R<sub>2</sub>) (19) (Scheme 5).<sup>84</sup> Compound 19 can be viewed as the thallium salt of the diaryltetraphosphabutadienediide. For the description of the bonding in 19, two different models are possible: either the negative charge can be localized on the terminal phosphorus atoms (I) or it can be delocalized over the entire P<sub>4</sub> unit (II). Judged on the basis of Coulomb repulsion between the two negative charges, the localized description I would be more favored. However, the nearly identical P—P distances in 19 (2.136(4) Å and 2.143(6) Å for the peripheral and central P—P bonds, respectively) suggest the presence of a delocalized bonding system of type II. The Tl—P interactions might be responsible for the decreasing interchain electronic repulsion and, hence, stabilization of the electron delocalization. The oxidation of 19 with I<sub>2</sub> leads to the neutral species 20, containing a butterfly-like structure (Scheme 5). Noteworthy, 20 crystallizes as the *trans,trans* or the *cis,trans* isomer, depending on the solvent used. The conformation in the solid state is probably dictated by packing effects. Both isomers were structurally characterized, and, interestingly, show identical <sup>31</sup>P NMR

chemical parameters ( $\delta = -331.8$  (bridgehead P atoms) and  $\delta = -163.0$ ) in solutions.



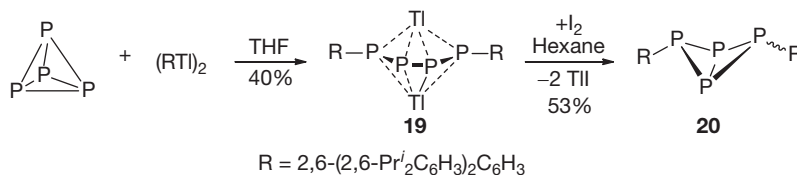
Besides the above discussed reactions, the conversion of P<sub>4</sub> into (C<sub>6</sub>F<sub>5</sub>)<sub>3</sub>P in 70% yield upon treatment with (C<sub>6</sub>F<sub>5</sub>)<sub>2</sub>TlBr under thermal conditions (190 °C, sealed tube) is reported.<sup>85</sup>

#### 1.36.2.4 Activation of P<sub>4</sub> by Group 14 Elements and Compounds

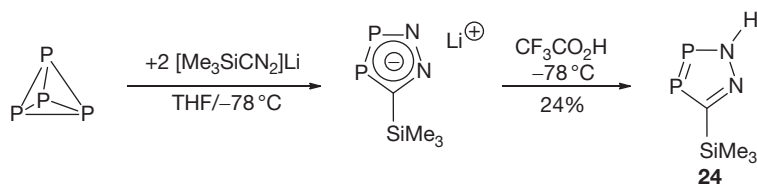
##### 1.36.2.4.1 Carbon

Because of the industrial importance of the organophosphorus reagents, the chemistry of P<sub>4</sub> with a variety of organic molecules was extensively studied in the late 1970s and 1980s. Today, this is, furthermore, supported by the need to use safer and more sustainable methods for the synthesis of organo-phosphorus compounds, omitting the use of hazardous chlorinating agents. Consequently, considerable efforts were made to functionalize P<sub>4</sub> directly, even though a clear breakthrough was not achieved. The achievements of earlier results in this field are summarized in several review articles.<sup>19a,86</sup> Herein, only selected examples and recent developments will be presented.

Strong nucleophiles, such as organolithium and organomagnesium compounds, react with P<sub>4</sub> by nucleophilic attack at one of the phosphorus atoms, leading to a P—P bond cleavage. Depending on the reaction conditions, this initial process can be followed by: (i) further reactions of the so-formed phosphides with P<sub>4</sub> to give more highly aggregated phosphides or oligophosphides;<sup>87</sup> (ii) additional reactions with nucleophiles or electrophiles present in the reaction mixture, leading to additional P—P bond cleavage. In both cases, the formed phosphides can be quenched by different alkylating agents, such as alkyl halides<sup>88</sup> or Me<sub>3</sub>SiCl,<sup>89</sup> to give mixtures of phosphanes. Usually, the reaction cannot be stopped at the first step. But when P<sub>4</sub> is reacted with RLi, which contains the very bulky 2,4,6-Bu<sup>t</sup><sub>3</sub>C<sub>6</sub>H<sub>2</sub> substituent, and the reaction product is quenched with the corresponding organohalide, the diorganotetraphosphane R<sub>2</sub>P<sub>4</sub> (21), containing a bicyclo [1.1.0]tetraphosphabutane core, and the diphosphene derivative 22 are obtained (eqn [13]).<sup>90</sup> Compound 21 could be isolated in rather low yield by fractional crystallization and characterized by single-crystal x-ray diffraction. In contrast to 20, for 21, only the *trans,trans* isomer was reported. A cleaner reaction takes place when donor-free MesLi (Mes = 2,4,6-Me<sub>3</sub>C<sub>6</sub>H<sub>2</sub>) is reacted with P<sub>4</sub>, whereby the *iso*-tetraphosphide (MesPli)<sub>3</sub>P (23) is formed (eqn [14]).<sup>91</sup> Compound 23



Scheme 5 Conversion of P<sub>4</sub> by RTI-TIR.



**Scheme 6** Reaction of P<sub>4</sub> with lithium(trimethylsilyl)-diazomethanide.

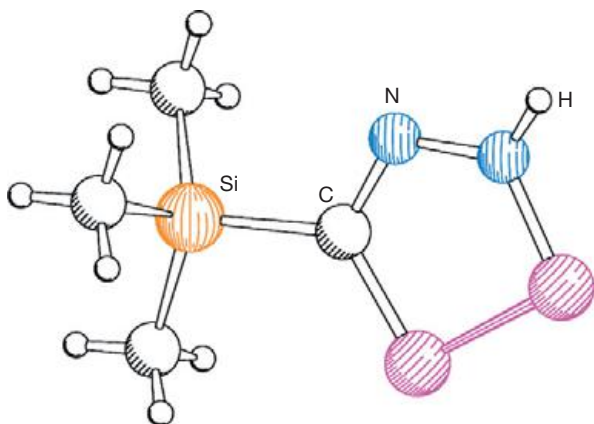
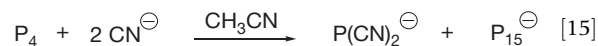


**Figure 5** Molecular structure of **24**. Adapted from Charrier, C.; Maignot, N.; Ricard, L.; Le Floch, P.; Mathey, F. *Angew. Chem. Int. Ed. Engl.* **1996**, *35*, 2133.

crystallizes from THF solutions as a solvated dimer. The LiP core in the solid-state structure of **23** is built up from a trigonal-antiprismatic Li<sub>6</sub> cluster, which is capped by two [P<sub>4</sub>Mes<sub>3</sub>]<sup>3-</sup> anions. Another interesting behavior is observed in the reaction of lithium(trimethylsilyl)-diazomethanide with P<sub>4</sub>. Instead of the expected cyclopentadienide derivative [RCP<sub>4</sub>]<sup>-</sup>, the diazadiphospholide anion [RCN<sub>2</sub>P<sub>2</sub>]<sup>-</sup> (R = Me<sub>3</sub>Si) is formed (**Scheme 6**), which is, formally, a [3+2] cycloaddition product between [P≡P] and the diazomethanide anion.<sup>92</sup> This can easily be protonated by trifluoroacetic acid to give the stable 2-*H*-1,2,3,4-diazadiphosphole **24**. According to x-ray diffraction studies, in the solid state, the hydrogen atom is attached to the nitrogen atom adjacent to the P=P unit. The double bonds in **24** are fairly well localized (P=P 2.0706(6) Å and C=N 1.320(2) Å). The molecular structure is depicted in **Figure 5**.

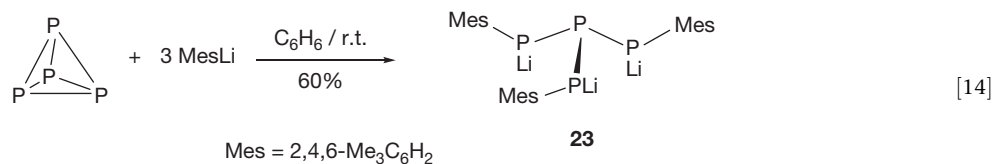
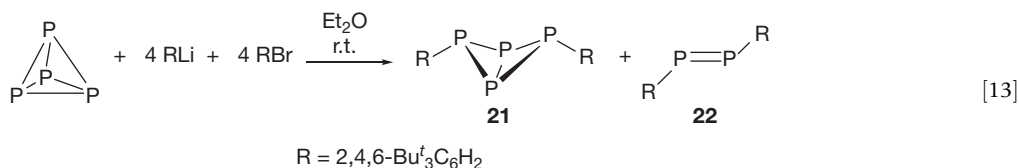
In contrast to the bulky nucleophiles, the sterically less demanding cyanide CN<sup>-</sup> anion leads to a clean reaction with

P<sub>4</sub> with the formation of dicyanophosphanide P(CN)<sub>2</sub><sup>-</sup> and the polyphosphide P<sub>15</sub><sup>-</sup> (eqn [15]).<sup>93</sup> The formation of these products can be rationalized by taking into consideration a possible disproportionation of phosphorus. Thus, the oxidized four-electron P<sup>+</sup> species is stabilized by the addition of two ligand molecules CN<sup>-</sup> to give the closed-shell moiety P(CN)<sub>2</sub><sup>-</sup>. The reduced P<sup>3-</sup> species distributes the high charge by transfer to other phosphorus atoms, leading to the formation of polyphosphanides. Similar to the cyanides, alkali-metal acetylides react with P<sub>4</sub> under complete fragmentation of the P<sub>4</sub> unit. In the presence of alkyl halides as electrophiles, acetylenic phosphanes could be obtained.<sup>88a,e,f</sup> Also, the small carbon anions C<sub>n</sub><sup>-</sup> (n = 3–9) react with gaseous P<sub>4</sub> under the conditions of Fourier transform ICR mass spectrometry to carbon phosphide anions, such as C<sub>n</sub>P<sup>-</sup>, C<sub>n</sub>P<sub>2</sub><sup>-</sup>, C<sub>n</sub>P<sub>5</sub><sup>-</sup> (n = 3–9), and C<sub>4</sub>P<sub>4</sub><sup>-</sup>.<sup>94</sup> Their structure and stability were investigated by theoretical methods. Furthermore, strong nucleophiles, such as carbon-centered nucleophiles, can be generated by electrochemical methods, which, in the presence of electrophilic reagents, react with P<sub>4</sub>, leading to the degradation of P<sub>4</sub> and the formation of various organophosphorus compounds, such as esters of phosphoric, phosphorous, and phosphonic acids, tertiary phosphanes, and other organophosphorus compounds.<sup>95</sup>



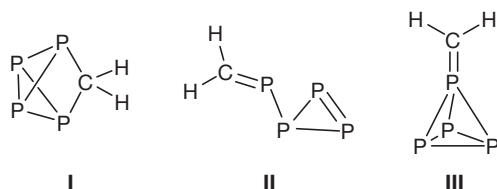
White phosphorus either does not react or reacts only very slowly with weak nucleophiles. The rate of the reaction is strongly increased if electrophiles are present. This leads to a complete degradation of the P<sub>4</sub> unit to monophosphorus species. Usually, CCl<sub>4</sub> is used both as a solvent and as an electrophile.<sup>86c,e</sup> An alternating sequence of nucleophilic attacks with P–P bond cleavage and electrophilic substitutions was proposed as the reaction mechanism, although no definite experimental proof could be established.

A renaissance of the activation of white phosphorus by organic molecules was initiated by the synthesis of stable



singlet carbenes. This opened up an extremely dynamic research area, in which very interesting derivatives of carbene and carbene analogs have been obtained.

The interaction of the parent carbene H<sub>2</sub>C with P<sub>4</sub> was investigated by quantum chemical calculations using different methods.<sup>96</sup> The results show that the triplet carbene does not react with P<sub>4</sub>, probably due to the lack of either electrophilic or nucleophilic character. In contrast, the singlet methylene should react with P<sub>4</sub>. On the potential energy surface, three energy-minimum structures I–III were located. They derive from the electrophilic behavior of H<sub>2</sub>C rather than a nucleophilic one. The most stable structure is I, which contains a CH<sub>2</sub> group inserted in a P–P bond. Structure II is higher in energy than I by ~134 kJ mol<sup>-1</sup>, and is formally obtained by the cleavage of two P–P bonds. The energetically highest-lying structure III is higher in energy by ~172 kJ mol<sup>-1</sup> (MP2/6-311++G(3df,3p) level of theory) than I and represents the first product of a direct attack of an electrophilic carbene at the apex of the P<sub>4</sub> tetrahedron.

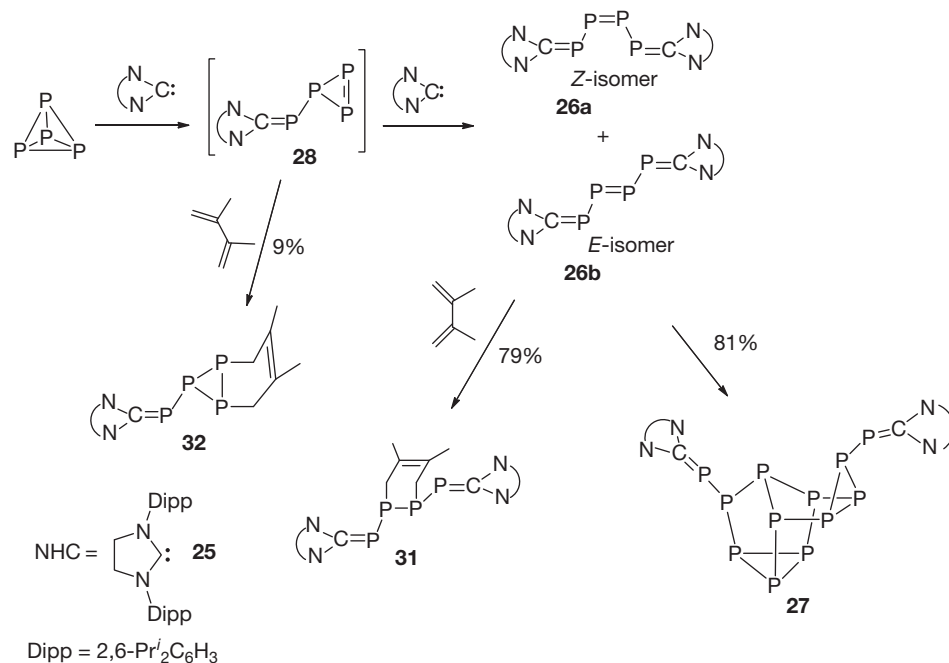


Bertrand and coworkers reported the reaction of the sterically demanding N-heterocyclic carbene **25** with P<sub>4</sub>, leading to the formation of tetraphosphahexatriene derivative **26** (Scheme 7).<sup>97</sup> Both *Z* and *E* isomers of **26** are formed, the *E* isomer (**26b**) being the major product. However, **26** is not stable at room temperature and reacts further to give the P<sub>12</sub> derivative **27** (Scheme 7). For this process, a complex reaction pathway, including reactions with intermediates of type II, carbene

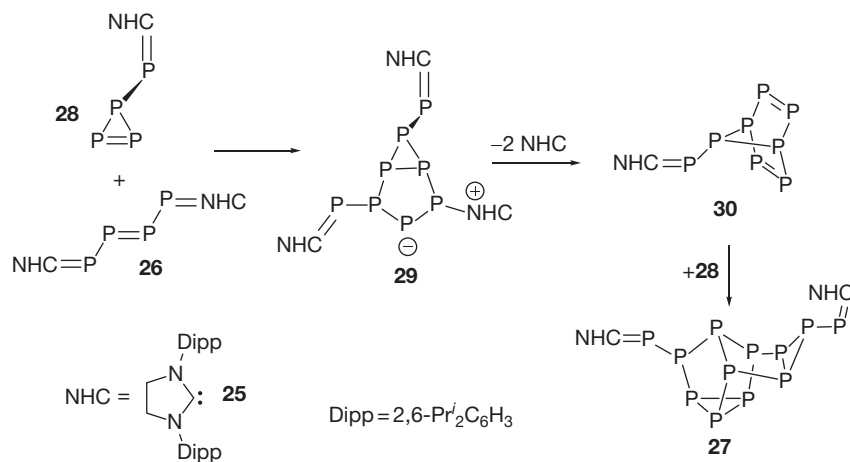
dissociation, and cycloaddition reactions were postulated based on DFT calculations (Scheme 8). Thus, the transient compound of type II, **28** reacts via an exothermic ( $\Delta E = 55.7$  kJ mol<sup>-1</sup>) [3+2]-cycloaddition with **26** to give the bicyclic intermediate **29**. This rearranges easily with the elimination of two carbenes to give the neutral heptaphosphanorbomadiene derivative **30**, which reacts without an activation barrier, through a [ $\pi^2+\pi^2+\pi^2$ ] reaction with **28**, leading to **27**. The structure of **27** was determined by x-ray diffraction and is depicted in Figure 6. In order to identify experimentally the possible reaction intermediates, trapping reactions were performed in the presence of 2,3-dimethylbutadiene. In consequence, the compounds **31** and **32** were isolated, which are the [4+2]-cycloaddition products of 2,3-dimethylbutadiene with the P=P double bond in **26a** and in intermediate **28**, respectively (Scheme 7).

Reaction of the more nucleophilic and simultaneously more electrophilic cyclic (alkyl)-(amino)carbene **32** (CAAC) with P<sub>4</sub> leads to the cleavage of a P–P bond and formation of the intermediate **33**, which reacts subsequently with a second equivalent of **32** to form both isomers of **34** (Scheme 9).<sup>98</sup> Since CAACs are stronger electrophiles than NHCs and, hence, bind more strongly to phosphorus, no elimination reactions can take place (cf. Scheme 8), which inhibits the formation of more highly aggregated products, such as **27**. The identification of the intermediate **33** was achieved by performing the reaction in the presence of a large excess of 2,3-dimethylbutadiene when the [4+2] cycloaddition product **35** was isolated. Similarly to **26b**, the isomer **34b** reacts with 2,3-dimethylbutadiene to give the cycloaddition product **36**. The compounds **34b**, **35**, and **36** were characterized by single-crystal x-ray diffraction and their structures are depicted in Figures 7, 8, and 9, respectively.

The nature of the products obtained by the degradation of P<sub>4</sub> with carbenes depends strongly on the degree of the electrophilic nature and bulkiness of the carbenes. Strong electrophilic carbenes favor the fragmentation of P<sub>4</sub>, leading to



**Scheme 7** Degradation of P<sub>4</sub> induced by the NHC **25** and trapping reactions of **26** and **28** with 2,3-dimethylbutadiene.



**Scheme 8** Proposed reaction pathway for the formation of **27**.

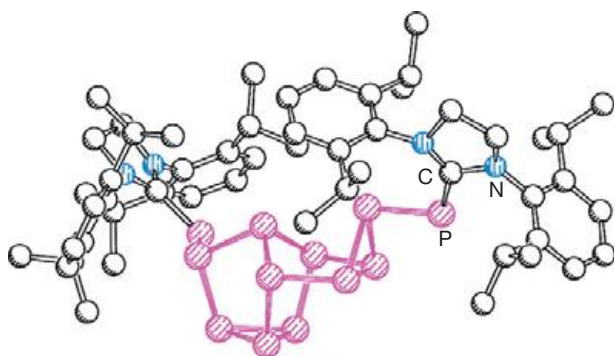


**Figure 6** Molecular structure of **27**. Hydrogen atoms are omitted for clarity. Adapted from Masuda, J. D.; Schoeller, W. W.; Donnadieu, B.; Bertrand, G. *J. Am. Chem. Soc.* **2007**, *129*, 14180.

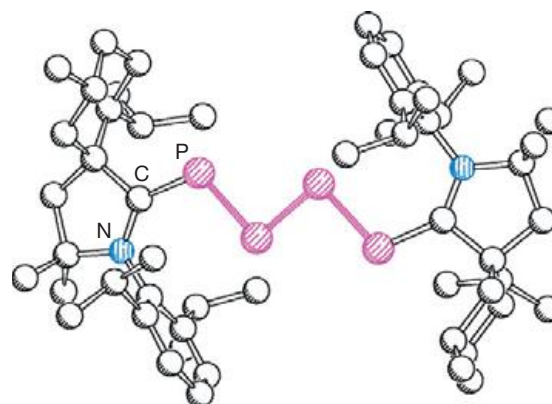
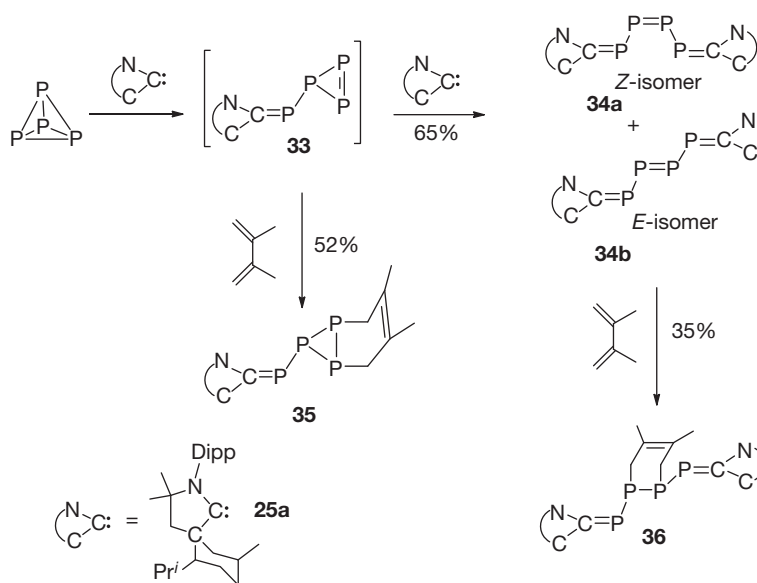


**Figure 7** Molecular structure of **34b**. Hydrogen atoms are omitted for clarity. Adapted from Masuda, J. D.; Schoeller, W. W.; Donnadieu, B.; Bertrand, G. *Angew. Chem. Int. Ed.* **2007**, *46*, 7052.



**Scheme 9** Degradation of P<sub>4</sub> induced by the CAAC **25a** and trapping reactions of **33** and **34** with 2,3-dimethylbutadiene.

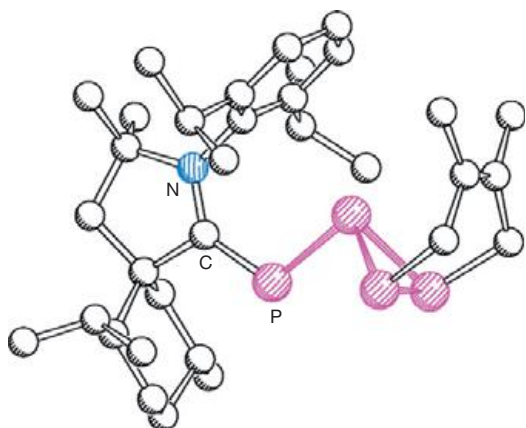


**Figure 8** Molecular structure of **35**. Hydrogen atoms are omitted for clarity. Adapted from Masuda, J. D.; Schoeller, W. W.; Donnadiu, B.; Bertrand, G. *Angew. Chem. Int. Ed.* **2007**, *46*, 7052.

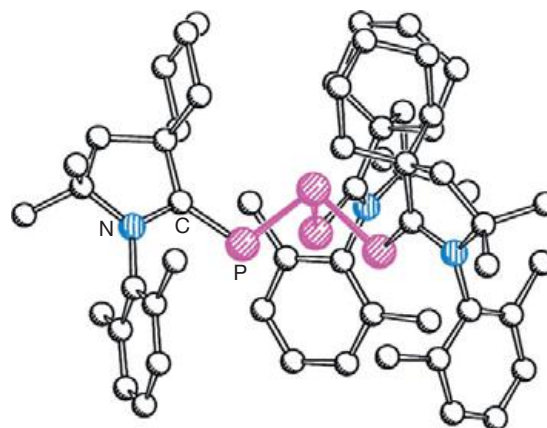


**Figure 10** Molecular structure of **40**. Hydrogen atoms and CH<sub>3</sub> groups of the 2,6-Pr<sub>2</sub>C<sub>6</sub>H<sub>3</sub> substituents are omitted for clarity. Adapted from Back, O.; Kuchenbeiser, G.; Donnadiu, B.; Bertrand, G. *Angew. Chem. Int. Ed.* **2009**, *48*, 5530.

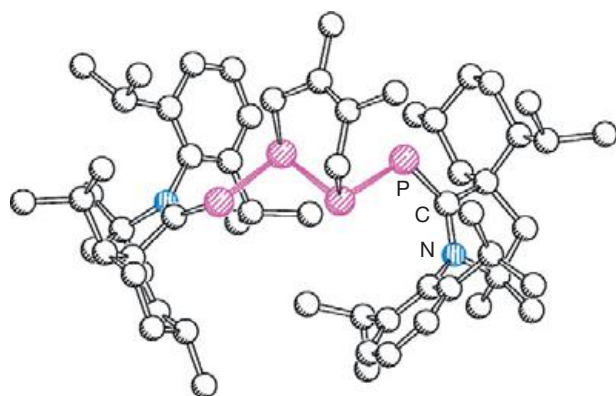


**Figure 9** Molecular structure of **36**. Hydrogen atoms are omitted for clarity. Adapted from Masuda, J. D.; Schoeller, W. W.; Donnadiu, B.; Bertrand, G. *Angew. Chem. Int. Ed.* **2007**, *46*, 7052.

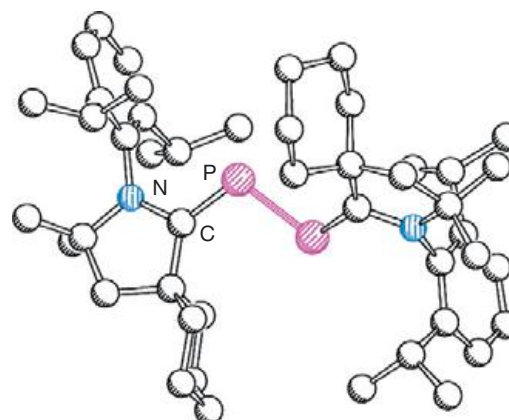
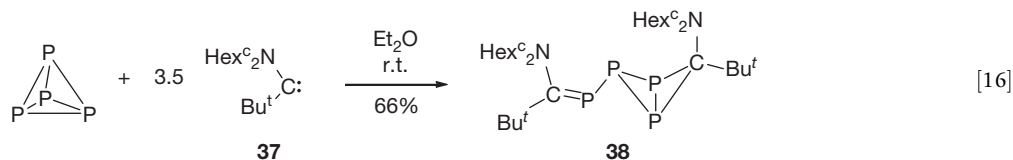


**Figure 11** Molecular structure of **41**. Hydrogen atoms are omitted for clarity. Adapted from Back, O.; Kuchenbeiser, G.; Donnadiu, B.; Bertrand, G. *Angew. Chem. Int. Ed.* **2009**, *48*, 5530.

compounds containing smaller phosphorus fragments, whereas the high steric bulk of the carbenes prevents the formation of small phosphorus fragments, such as P<sub>1</sub> units. Accordingly, the small and electrophilic acyclic (alkyl) (amino)carbene **37** reacts with P<sub>4</sub> to give the bis(carbene)-adduct **38** (eqn [16]).<sup>99</sup> The origin of **38** can be explained by the formation of an intermediate analogous to **28** or **33** (cf. Schemes 7 and 9), which rapidly undergoes a cycloaddition reaction with **37** to give **38**. When the less electrophilic CAAC **39** is reacted with P<sub>4</sub>, the fragmentation products **40** and **41** are obtained (eqn [17]).<sup>99</sup> Interestingly, the formation of **40** implies that the transient analog of **28** reacts with 2 equiv. of **39**, which is rather unexpected due to the steric repulsion of two molecules of **39**. Both **40** and **41** were structurally characterized. The molecular structures of **40** and **41** are depicted in Figures 10 and 11, respectively.

When sterically crowded and strongly electrophilic carbenes are reacted with white phosphorus, the fragmentation of the P<sub>4</sub> tetrahedron is observed, but fragments smaller than P<sub>2</sub> units could not be stabilized. However, when the sterically least demanding stable carbene known to date, namely, the bis (diisopropylamino)cyclopropylidene (**42**), was reacted with P<sub>4</sub> in the presence of chloroform, the stabilization of the cationic P<sub>1</sub> species **43** could be accomplished (eqn [18]; Figure 12).<sup>99</sup> In the reaction mixture, the formation of the P<sub>3</sub><sup>-</sup> anion was observed by <sup>31</sup>P NMR spectroscopy, which, however, decomposed during work-up and could not be isolated.

Very recently, an intriguing and rather unexpected way to incorporate phosphorus directly from P<sub>4</sub> into organic molecules was reported.<sup>100</sup> The irradiation of a mixture of P<sub>4</sub> and a slight excess of 2,3-dimethyl-1,3-butadiene with a mercury



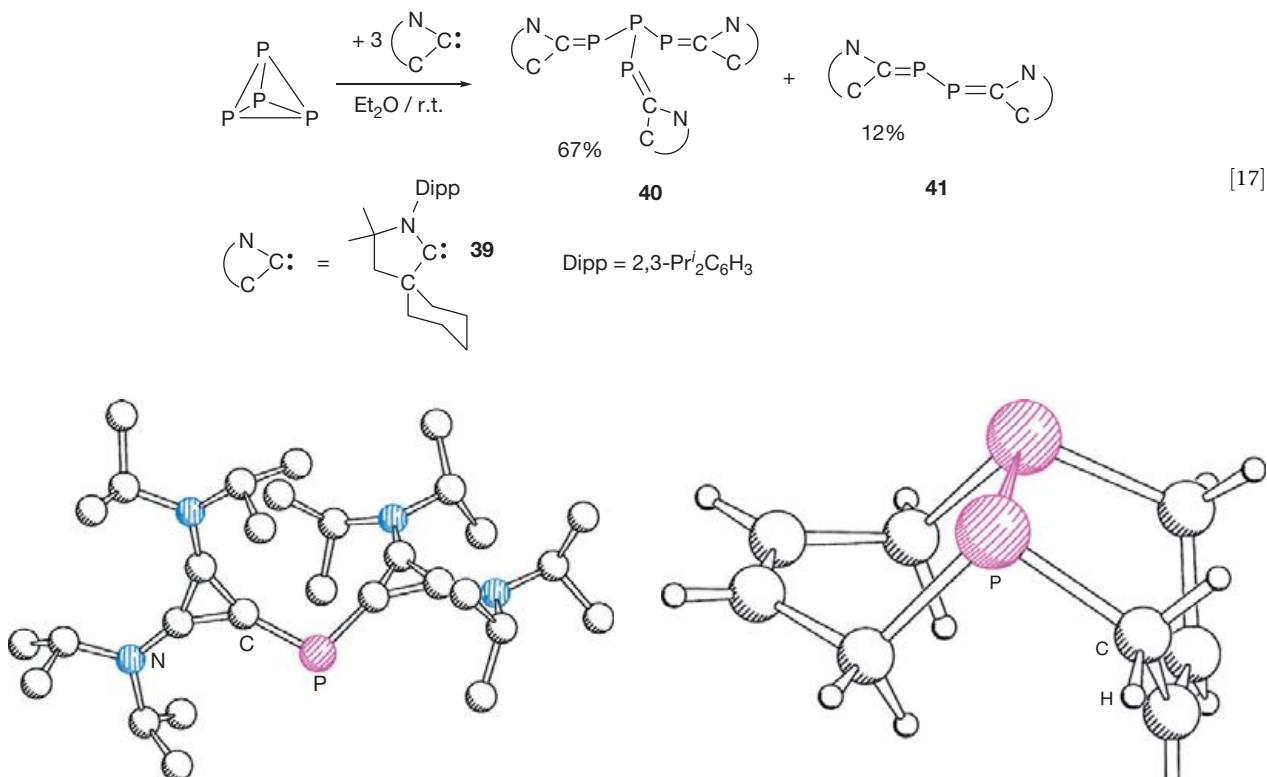
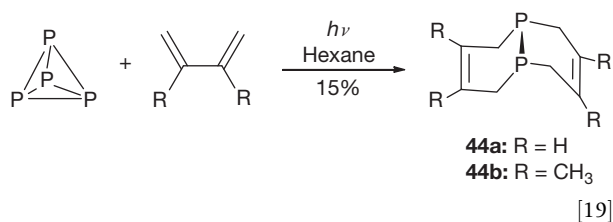


**Figure 12** Molecular structure of the anion  $[(\text{Pr}'_2\text{N})_2\text{C}_3]_2\text{P}^-$  (**43**). Hydrogen atoms are omitted for clarity. Adapted from Back, O.; Kuchenbeiser, G.; Donnadieu, B.; Bertrand, G. *Angew. Chem. Int. Ed.* **2009**, *48*, 5530.

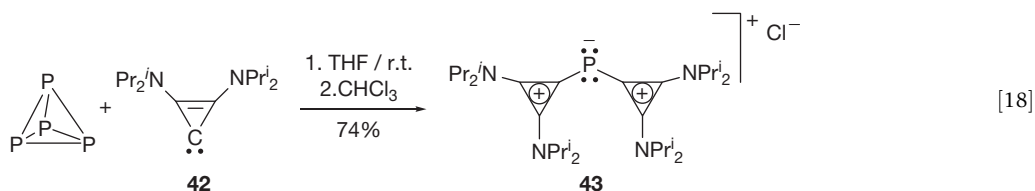
**Figure 13** Molecular structure of **44a**. Adapted from Tofan, D.; Cummins, C. C. *Angew. Chem. Int. Ed.* **2010**, *49*, 7516.

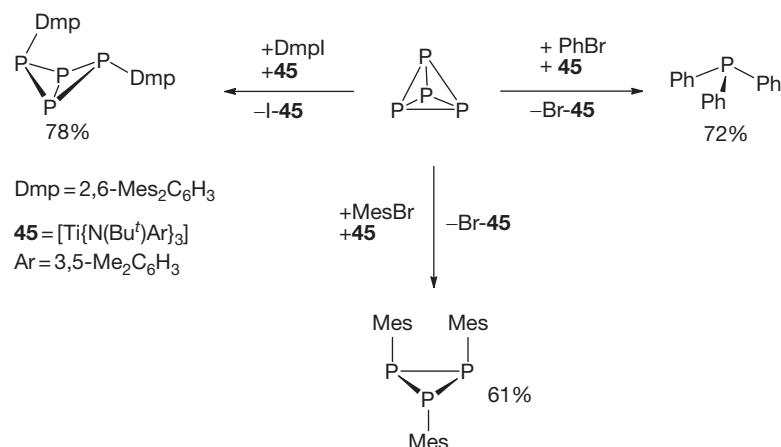
lamp ( $\lambda_{\text{max}}$  mainly 254 nm) leads, among other unidentified products, to **44b** (eqn [19]). The formation of **44b** can be rationalized as the double Diels–Alder product of the diene with a  $\text{P}=\text{P}$  molecule. Under similar conditions, 2,3-butadiene reacts with  $\text{P}_4$  to give **44a** in very low yields ( $\sim 1\%$ ). Both molecules **44a** and **44b** were structurally characterized by single-crystal x-ray diffraction. In the solid state, they adopt a  $\text{C}_s$  symmetric conformation, but fluctuate rapidly on the NMR timescale at room temperature in solution. The molecular structure of **44a** is depicted in **Figure 13**.



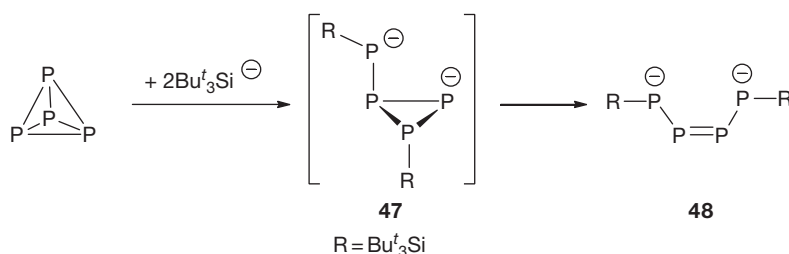
White phosphorus acts as a radical trap for carbon-centered radicals in solution to give the phosphonic acid  $\text{RP}(\text{O})(\text{OH})_2$

upon oxidative work-up.<sup>86f,101</sup> A source of organic radicals, *O*-acyl derivatives of *N*-hydroxy-2-thiopyridone were used under photolytic conditions. However, the generation of organic radicals is not limited to photolytic conditions. When the three-coordinated Ti(III) complex  $[\text{Ti}\{\text{N}(\text{Bu}^t)\text{Ar}\}_3]$  ( $\text{Ar} = 3,5\text{-Me}_2\text{C}_6\text{H}_3$ ; **45**), which is a powerful halogen abstraction reagent in aprotic media at room temperature or below, is reacted with organic halides  $\text{RX}$ , the extraction of  $\text{X}$  and the formation of carbon-centered radicals  $\text{R}$ , which react readily with  $\text{P}_4$ , is observed.<sup>102</sup> Depending on the stoichiometry of  $\text{P}_4$  and  $\text{RX}$ , besides  $[\text{XTi}\{\text{N}(\text{Bu}^t)\text{Ar}\}_3]$  ( $\text{X} = 45$ ), different products can be obtained. The reaction of  $\text{P}_4$  with 5 equiv. of  $\text{PhBr}$  and  $[\text{Ti}\{\text{N}(\text{Bu}^t)\text{Ar}\}_3]$  leads to the formation of  $\text{Ph}_3\text{P}$  (95% conversion) in 72% yield (**Scheme 10**). When, however, only 3 equiv. of  $\text{PhBr}$  and  $[\text{Ti}\{\text{N}(\text{Bu}^t)\text{Ar}\}_3]$  are reacted with  $\text{P}_4$ , the diphosphane  $\text{P}_2\text{Ph}_4$  (29%) is obtained in addition to  $\text{Ph}_3\text{P}$  (71%). Since the degradation of  $\text{P}_4$  occurs in a stepwise manner, it is possible to isolate intermediate structures by tuning the steric protection of the  $\text{RX}$  substrate. Thus, the reaction of 1.5 equiv. of  $\text{MesBr}$  ( $\text{Mes} = 2,4,6\text{-Me}_3\text{C}_6\text{H}_2$ ) and 1.5 equiv. of  $[\text{Ti}\{\text{N}(\text{Bu}^t)$





**Scheme 10** Degradation of P<sub>4</sub> by organic radicals generated from RX and the Ti complex 45.



**Scheme 11** Reaction pathway of the activation of P<sub>4</sub> by the silanide Bu<sup>t</sup><sub>3</sub>Si<sup>-</sup>.

Ar<sub>3</sub>] with 0.25 equiv. of P<sub>4</sub> gave the *cyclo*-triphosphirane P<sub>3</sub>Me<sub>3</sub> as the main reaction product (61%). The diphosphane P<sub>2</sub>Me<sub>4</sub> is also formed in small quantities. Under similar conditions DmpI (Dmp = 2,6-Mes<sub>2</sub>C<sub>6</sub>H<sub>3</sub>) and [Ti{N(Bu<sup>t</sup>)Ar}<sub>3</sub>] react with P<sub>4</sub>, leading to the formation of P<sub>4</sub>(Dmp)<sub>2</sub>, containing a butterfly-like P<sub>4</sub> core. The synthesis of organophosphorus compounds via this method is generally limited to organobromine or organoiodine substrates, since the Cl extraction from RCl induced by 45 is rather slow. However, this method can be extended to the synthesis of P(SiMe<sub>3</sub>)<sub>3</sub> and P(SnPh<sub>3</sub>)<sub>3</sub> (*vide infra*), which can be obtained in 86% and 75% yields, respectively, by reacting the corresponding R<sub>3</sub>ECl (E = Si and Sn) derivatives with P<sub>4</sub> and 45.

An interesting host–guest-type chemistry was observed when a solution of C<sub>60</sub> is treated with P<sub>4</sub>, whereupon a black–blue, highly crystalline solid with the composition {(P<sub>4</sub>)<sub>2</sub>C<sub>60</sub>} precipitates.<sup>103</sup> Its structure was determined by XPD measurements and solved by Rietveld refinement, suggesting an AAA stacking of closely packed C<sub>60</sub> layers with tetrahedral P<sub>4</sub> units between them. Solid-state <sup>31</sup>P MAS NMR spectroscopic investigations revealed a single resonance at δ = −490 ppm, suggesting that no charge transfer between C<sub>60</sub> and P<sub>4</sub> has occurred.

### 1.36.2.4.2 Silicon

Since silanides R<sub>3</sub>Si<sup>-</sup> are strong nucleophiles, they react readily with P<sub>4</sub>, leading to the reductive cleavage of a P–P bond and formation of the [R<sub>3</sub>SiP<sub>4</sub>]<sup>-</sup> anion, which has a butterfly-like core similar to that of 1 (*vide supra*). Although this anion was not isolated, it is proposed to be a reactive intermediate and,

formally, is the first product of the reaction of silanides with P<sub>4</sub>. Further reactions of [R<sub>3</sub>SiP<sub>4</sub>]<sup>-</sup> with additional silanides leads to the degradation and formation of partly silylated phosphides containing smaller polyphosphorus units. Alternatively, aggregation reactions leading to polyphosphorus cage compounds were also observed.

The nature of the reaction products and the degree of degradation of the P<sub>4</sub> tetrahedron is strongly dependent on the stoichiometry and the solvent used, when silicon-centered bulky nucleophiles such as Bu<sup>t</sup><sub>3</sub>Si<sup>-</sup>, Bu<sup>t</sup><sub>2</sub>PhSi<sup>-</sup>, or (Me<sub>3</sub>Si)<sub>3</sub>Si<sup>-</sup> are reacted with P<sub>4</sub>. Generally, an excess of silanide R<sub>3</sub>Si<sup>-</sup> and polar solvents favor a stronger degradation, whereas a deficit of silanide and less polar solvents degrade P<sub>4</sub> to a lower extent.

The reaction of P<sub>4</sub> with [(Me<sub>3</sub>Si)<sub>3</sub>SiK(18-crown-6)] leads to the formation of the octaphosphide 46. Obviously, in this reaction, the intermediate [RP<sub>4</sub>]<sup>-</sup> (R = Si(Me<sub>3</sub>Si)<sub>3</sub>) is formed, which dimerizes and rearranges through intramolecular nucleophilic attacks to give 46.<sup>104</sup> In contrast, reacting the only slightly smaller silanide Bu<sup>t</sup><sub>3</sub>SiM (M = Na, K) with P<sub>4</sub> in a 2:1 stoichiometry leads to the formation of the intermediate 47 (M = K), instead of more highly aggregated phosphides as observed for the reaction of (Me<sub>3</sub>Si)<sub>3</sub>SiK with P<sub>4</sub>. Compound 47 is not stable and rearranges intramolecularly to the tetraphosphenediide 48 (**Scheme 11**). A series of derivatives of 48 with different substituents (R = Bu<sup>t</sup><sub>3</sub>Si, Bu<sup>t</sup><sub>2</sub>PhSi) and alkaline as well as alkaline earth metals (M = Li, Na, K, Rb, Cs, and Ba) were synthesized.<sup>105</sup> Characteristic for the central phosphorus atoms (P=P) in 48 is their <sup>31</sup>P NMR chemical shift at low fields (δ = 408.3 ppm for K<sub>2</sub>-48), whereas the peripheral

phosphorus atoms are found at considerably higher fields ( $\delta = -5.1$  ppm).<sup>105c</sup> Although, a stable compound of type 47 could not be isolated, the core structure can be found in the compounds 35 and 38, which are formed by the fragmentation of P<sub>4</sub> caused by the carbenes 32 and 37 (*vide supra*), respectively, as well as in different organophosphanes of the type P<sub>3</sub>R<sub>2</sub>(PR<sub>2</sub>).<sup>106</sup> In THF solutions, the P<sub>4</sub> chain in Na<sub>2</sub>[(Bu<sup>t</sup>Si)<sub>2</sub>P<sub>4</sub>] (Na<sub>2</sub>-48) adopts a *cis* configuration, as determined by <sup>31</sup>P NMR spectroscopy, whereas the ion-separated compound [Na(18-crown-6)(THF)<sub>2</sub>]<sub>2</sub>[(Bu<sup>t</sup>Si)<sub>2</sub>P<sub>4</sub>] adopts a *trans* configuration in the solid state. The structure of the anion in [Na(18-crown-6)(THF)<sub>2</sub>]<sub>2</sub>[(Bu<sup>t</sup>Si)<sub>2</sub>P<sub>4</sub>] is depicted in Figure 14.<sup>105d</sup> According to the very similar P—P distances (P—P 2.126(9) Å and 2.133(6) Å), the negative charges in the anionic part of [Na(18-crown-6)(THF)<sub>2</sub>]<sub>2</sub>[(Bu<sup>t</sup>Si)<sub>2</sub>P<sub>4</sub>] might be delocalized over the entire P<sub>4</sub> unit, as observed for 19. The sodium salt Na<sub>2</sub>-48 is stable in THF, but it dimerizes in weakly polar solvents to the octaphosphide Na<sub>4</sub>-49. In less polar solvents, Na<sub>4</sub>-49 can be converted via a reversible [2+2] retrocycloaddition to Na<sub>2</sub>-48 (eqn [21]). The reversibility of this equilibrium is ascribed to the cluster-like structure of Na<sub>4</sub>-49.<sup>105a</sup> The structure of [Na(DME)]<sub>4</sub>[(Bu<sup>t</sup>Si)<sub>4</sub>P<sub>8</sub>] (DME = 1,2-dimethoxyethane) is depicted in Figure 15.

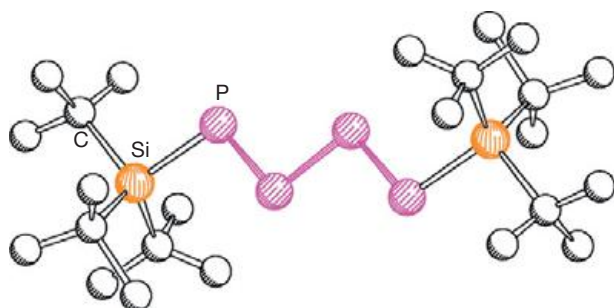


**Figure 14** Molecular structure of the anion in [Na(18-crown-6)(THF)<sub>2</sub>]<sub>2</sub>[(Bu<sup>t</sup>Si)<sub>2</sub>P<sub>4</sub>]. Hydrogen atoms are omitted for clarity. Adapted from Lorbach, A.; Nadj, A.; Tüllmann, S.; Dornhaus, F.; Schödel, F.; Sängler, I.; Margraf, G.; Bats, J. W.; Bolte, M.; Holthausen, M. C.; Wagner, M.; Lerner, H.-W. *Inorg. Chem.* **2009**, *48*, 1005.

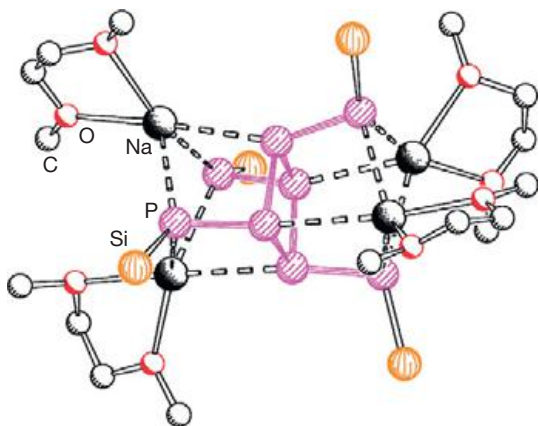
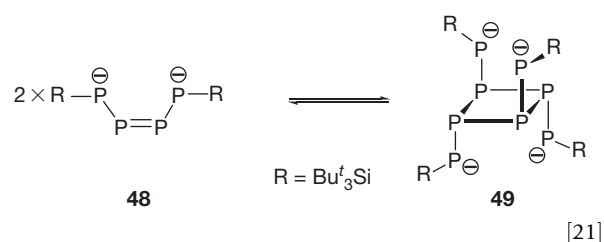
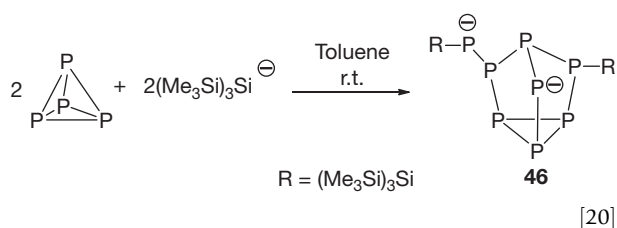
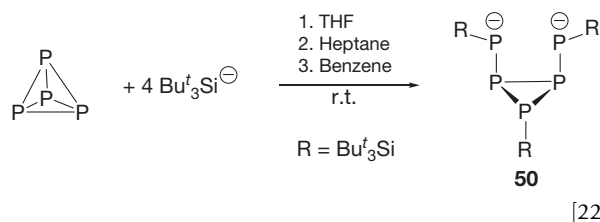


**Figure 15** Molecular structure of [Na(DME)]<sub>4</sub>[(Bu<sup>t</sup>Si)<sub>4</sub>P<sub>8</sub>]. Hydrogen atoms and Bu<sup>t</sup> groups are omitted for clarity. Adapted from Wiberg, N.; Wörner, A.; Karaghiosoff, K.; Fenske, D. *Chem. Ber.* **1997**, *130*, 135.

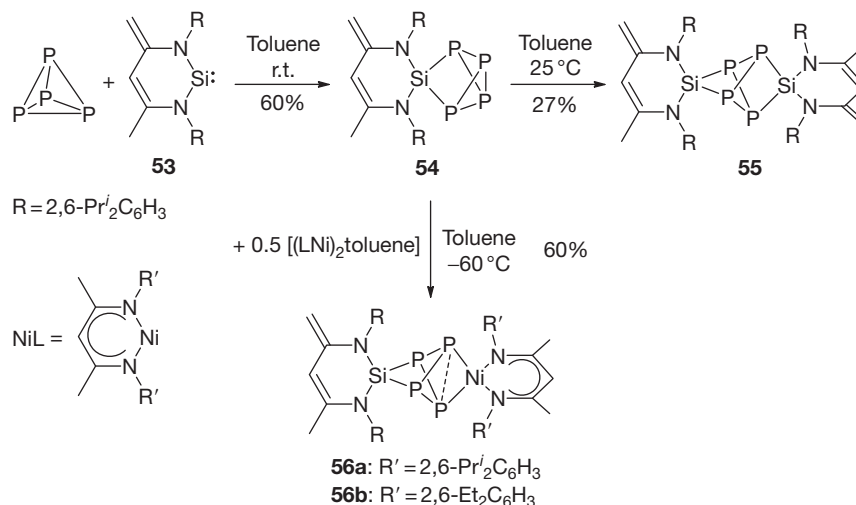


When the Bu<sup>t</sup>SiNa:P<sub>4</sub> molar ratio is increased to 4:1 and the reaction is performed in benzene, the pentaphosphide [(Bu<sup>t</sup>Si)<sub>3</sub>P<sub>5</sub>]Na<sub>2</sub> (Na<sub>2</sub>-50) is formed (eqn [22]).<sup>105b,107</sup> Different derivatives of M<sub>2</sub>-50 (M = Na, K and Ag), as well as different approaches for the synthesis of Na<sub>2</sub>-50, such as protolysis of the tetraphosphide [(Bu<sup>t</sup>Si)<sub>2</sub>P<sub>4</sub>][Na<sub>2</sub>(THF)<sub>n</sub>] with CF<sub>3</sub>CO<sub>2</sub>H in THF or by dissolving crystals of [(Bu<sup>t</sup>Si)<sub>2</sub>P<sub>4</sub>][Na<sub>2</sub>(THF)<sub>n</sub>] in toluene, were reported.<sup>105b,c,108</sup> The degradation of Na<sub>4</sub>-49 with silanides also leads to the formation of Na<sub>2</sub>-50, which is monomeric in THF but has a dimeric structure in the solid state. The silver salt [(Bu<sup>t</sup>Si)<sub>3</sub>P<sub>5</sub>]Ag<sub>2</sub> (Ag<sub>2</sub>-50) is also dimeric in the solid state.



The reaction of Bu<sup>t</sup>SiM (M = Li, Na) with P<sub>4</sub> in a 3:1 molar ratio produces the *iso*-tetraphosphide derivative M<sub>3</sub>-51 (Scheme 12).<sup>109</sup> The Bu<sup>t</sup>PhSi derivative of Na<sub>3</sub>-51, [(Bu<sup>t</sup>PhSi)<sub>3</sub>P<sub>4</sub>]Na<sub>3</sub>, can be synthesized in a similar manner. The phosphides 51 were investigated in solutions by <sup>31</sup>P NMR spectroscopy, and, as expected, the chemical shifts are strongly dependent on the solvent used. In THF solution, the salts M<sub>3</sub>-51 (M = Li, Na) are not stable and decompose slowly at room temperature to give M-52 (M = Li, Na) and Bu<sup>t</sup>SiPM<sub>2</sub> (Scheme 12).<sup>109</sup> A remarkable feature of the triphosphide derivative [(Bu<sup>t</sup>Si)<sub>2</sub>P<sub>3</sub>][Na(thf)<sub>4</sub>] is the unusual <sup>31</sup>P NMR chemical shift of the central phosphorus atom in C<sub>6</sub>D<sub>6</sub> solution, which appears at  $\delta = 732.5$  ppm. The resonance of the peripheral phosphorus atoms appears at  $\delta = 212.5$  ppm and shows a large coupling (<sup>1</sup>J(P,P) = 553 Hz) to the central phosphorus atom. This can be explained by the multiple-bond character of the P<sub>3</sub> core.<sup>110</sup> Interestingly, the Bu<sup>t</sup>PhSi derivatives of Na<sub>3</sub>-51 decompose to the corresponding pentaphosphides Na<sub>2</sub>-50, rather than to the corresponding triphosphides Na-52.<sup>109</sup> The reaction of Bu<sup>t</sup>SiK with P<sub>4</sub> in a 3:1 stoichiometry in THF leads, in the first step, to the formation of the tetraphosphide K<sub>2</sub>-48 and the octaphosphide K<sub>4</sub>-49.





**Scheme 14** Reaction pathway of the activation of P<sub>4</sub> by the electrophilic silylene **53** and subsequent reactions.

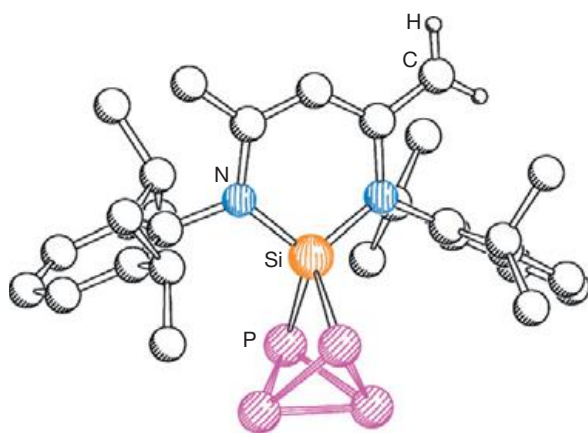


**Figure 16** Molecular structure of **54**. Some hydrogen atoms are omitted for clarity. Adapted from Xiong, Y.; Yao, S.; Brym, M.; Driess, M. *Angew. Chem. Int. Ed.* **2007**, *46*, 4511.

between the bridgehead phosphorus atoms is attributed to a partial  $\pi$ -bond character, which should facilitate the subsequent reaction with an electrophilic silylene (*vide supra*). Indeed, **54** reacts slowly with 1 equiv. of **53**, leading to the insertion of **53** into the bridgehead P—P bond and the formation of **55**, containing an asterane-like P<sub>4</sub> core (**Scheme 14**).<sup>115</sup> The coordination of the bridgehead phosphorus atoms in **54** to the  $\beta$ -diketiminonickel(I) complex [(LNi)<sub>2</sub>·toluene] (L = CH{CMeN(2,6-R<sub>2</sub>C<sub>6</sub>H<sub>3</sub>)<sub>2</sub>})<sub>2</sub>; R = Pr<sup>i</sup>, Et) was also reported (**Scheme 14**).<sup>116</sup> Thereby, the coordination causes the considerable elongation of the coordinated P—P bond, which, nevertheless, remains in the range of a bonding interaction. The P—P distances in **56a** and **56b** are 2.335(4) Å and 2.351(3)/2.354(2) Å (two independent molecules), respectively. The presence of Ni(I) centers in **56** was confirmed by EPR measurements. Thus, these derivatives represent rare examples of heterodinuclear tetraphosphorus complexes with different stages of P—P bond activation.

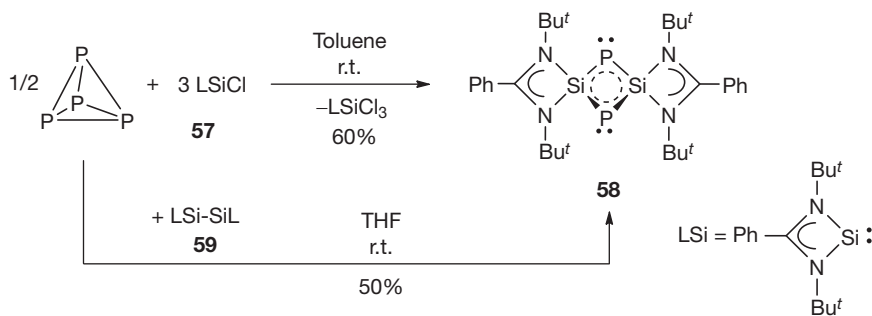
It is interesting to compare the reactivity of **53** with its aluminum and gallium derivatives **7** and **10**, respectively. While the aluminum derivative **7** inserts into two P—P bonds,

the gallium derivative **10** inserts into only one P—P bond of the P<sub>4</sub> tetrahedron. The silylene **53** is able to insert into two P—P bonds, although the second insertion is rather slow.

A most vivid reaction is observed when the chlorosilylene LSiCl (L = PhC(NBu<sup>t</sup>)<sub>2</sub>) **57** is reacted with P<sub>4</sub>. In this reaction, all P—P bonds are cleaved and the zwitterionic compound **58** containing a planar Si—P—Si—P unit stabilized by two amidinato ligands PhC(NBu<sup>t</sup>)<sub>2</sub> (**Scheme 15**) is formed.<sup>117</sup>

According to heteronuclear NMR spectroscopic investigations, **58** contains two naked phosphorus atoms and the silicon centers are not protonated. This was also confirmed by cross-polarization built-up curves. (An NMR method which makes use of the transfer of magnetization from abundant spins such as <sup>1</sup>H or <sup>31</sup>P to dilute spins, in this case, <sup>29</sup>Si by means of cross-polarization.) The structure of **58** was determined by single-crystal x-ray diffraction and is depicted in **Figure 17**. The solid-state <sup>31</sup>P NMR spectrum of **58** shows a signal with almost the same chemical shift ( $\delta = -166.4$  ppm) as the <sup>31</sup>P NMR spectrum of **58** in solutions ( $\delta = -166$  ppm). The Si—P bond lengths (2.1737(6) Å and 2.1742(6) Å) are intermediate between a typical Si—P single bond (2.25 Å) and a Si=P double bond (2.09 Å), indicating the presence of a bis-ylide structure. The bonding in **58** was investigated by quantum chemical calculations. The NICS values show that the ring has no antiaromatic character. This is in agreement with the electron localizability index, which indicates the presence of two lone pairs of electrons at each phosphorus atom. The results of an NBO analysis show an electron delocalization over the whole Si<sub>2</sub>P<sub>2</sub> skeleton. The natural charges obtained from the NBO analysis show that there is a strong charge separation (+1.12 for silicon atoms and -0.69 for phosphorus atoms). Thus, the stability of the Si<sub>2</sub>P<sub>2</sub> four-membered ring in **58** is based on its zwitterionic character.<sup>117</sup> A much cleaner synthesis of **58** can be achieved by the reaction of the bis-silylene **59** with P<sub>4</sub>. According to <sup>31</sup>P and <sup>29</sup>Si NMR spectroscopic investigations, the reaction proceeds without the formation of by-products. However, crystalline **58** was only isolated in 50% yield.<sup>117</sup>

The activation of P<sub>4</sub> is not limited to the silanides or silylenes. The Si=Si double bond in disilenes also reacts with white phosphorus by fragmentation of the P<sub>4</sub> tetrahedron



**Scheme 15** Degradation of P<sub>4</sub> by the chlorosilylene **57** and the bis-silylene **59**.

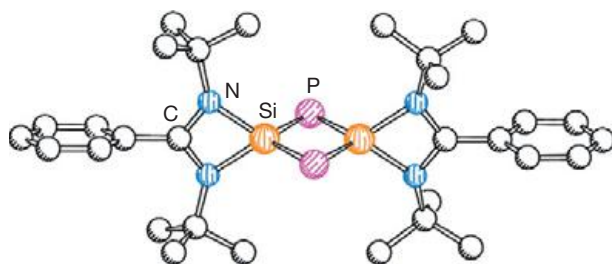
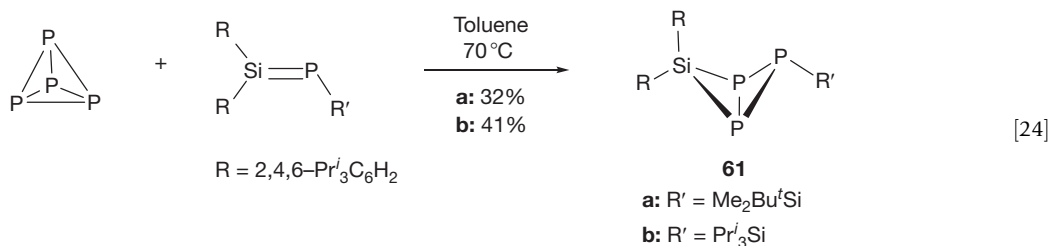
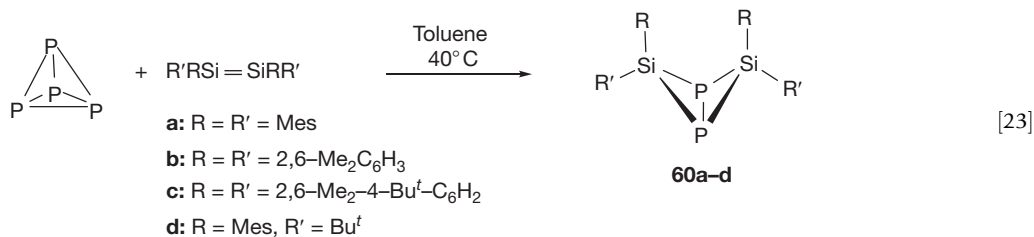


**Figure 17** Molecular structure of **58**. Hydrogen atoms are omitted for clarity. Adapted from Sen, S. S.; Khan, S.; Roesky, H. W.; Kratzert, D.; Meindl, K.; Henn, J.; Stalke, D.; Demers, J.-P.; Lange, A. *Angew. Chem. Int. Ed.* **2011**, *50*, 2322.

and formation of 1,3-diphospha-2,4-disilabicyclo[1.1.0]butanes **60** (eqn [23]).<sup>118</sup> The constitution of **60** was confirmed by multinuclear NMR spectroscopy. In the <sup>31</sup>P NMR spectrum, the bridgehead phosphorus atoms exhibit a sharp resonance at high fields (e.g.,  $\delta = -324.0$  for **60a**), with a relatively large <sup>1</sup>J(Si,P) coupling constant (77 Hz for **60a**).<sup>118a</sup> The crystal structure of **60d** was determined, although the synthesis was achieved via a P<sub>4</sub>-free approach. The reaction mechanism of the formation of **60** is not known; however,

for the Mes/Bu<sup>t</sup> derivative of the disilene, a stable intermediate with the composition Mes<sub>4</sub>(Bu<sup>t</sup>)<sub>4</sub>Si<sub>4</sub>P<sub>4</sub> was isolated and characterized by spectroscopic methods. Based on the <sup>31</sup>P NMR data, two possible isomeric structures were proposed.<sup>118b</sup> Furthermore, **60d** is formed as a mixture of *exo-exo* and *endo-exo* isomers. The latter reorganizes at elevated temperatures to the *exo-exo* form. It was also shown that the phosphorus lone pairs in **60a** can coordinate successively to one or two W(CO)<sub>5</sub> fragments, leading to the corresponding mono and bis-adducts, respectively. The *side-on* coordination of the P—P bond toward Pt(PPh<sub>3</sub>)<sub>2</sub> fragments was observed when **60a** is reacted with [Pt(PPh<sub>3</sub>)<sub>2</sub>(C<sub>2</sub>H<sub>4</sub>)]. The crystal structures of the bis-W(CO)<sub>5</sub> adducts of **60a** and **60d** were reported.<sup>118a,b</sup>

Similarly to the disilenes, phosphasilenes containing an Si=P double bond are also able to react with P<sub>4</sub>, leading to 1,2,3-triphospha-4-sila-bicyclo[1.1.0]butanes **61** (eqn [24]).<sup>119</sup> The compounds **61a,b** were isolated as the *exo* diastereomers and characterized spectroscopically. As usual for the phosphabicyclo[1.1.0]butanes, the bridgehead phosphorus atoms resonate at high fields (**61a**:  $\delta = -331.5$ , **61b**:  $\delta = -328.3$ ), whereas the resonance signal for the wing-tip phosphorus atom appears at lower fields (**61a**:  $\delta = -257.5$ , **61b**:  $\delta = -247.2$ ) in the <sup>31</sup>P NMR spectrum.



### 1.36.2.4.3 Germanium, Tin, and Lead

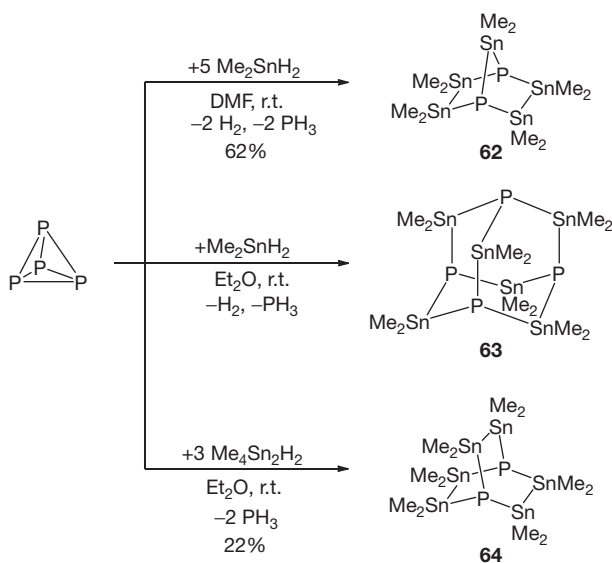
Very little is reported in the literature about the reactivity of P<sub>4</sub> towards germanium-, tin-, or lead-containing compounds. However, in line with the investigations of the reactivity of the silylene 53 with P<sub>4</sub>, it was reported that the germanium analog of 53 does not react with P<sub>4</sub>, even in boiling toluene.<sup>115</sup> This was attributed to the lower reduction potential of Ge(II) compared to the Si(II) species.

Interestingly, it was found that P<sub>4</sub> reacts with dimethyltin dihydride with the formation of Sn—P bonds and elimination of H<sub>2</sub> as well as PH<sub>3</sub>. The nature of the products depends strongly on the solvent used. When Me<sub>2</sub>SnH<sub>2</sub> is reacted with P<sub>4</sub> in DMF, which also acts as a base, the formation of (Me<sub>2</sub>Sn)<sub>5</sub>P<sub>2</sub> (62) containing a norbornane-like core was observed (Scheme 16).<sup>120</sup> However, performing the reaction in the absence of an organic base and in Et<sub>2</sub>O results in the formation of the adamantane derivative (Me<sub>2</sub>Sn)<sub>6</sub>P<sub>4</sub> (63). A more tin-rich product, the bicyclo[2.2.2]octane derivative 64, is formed if Me<sub>4</sub>Sn<sub>2</sub>H<sub>2</sub> is used in the reaction with P<sub>4</sub> (Scheme 16).<sup>121</sup> Under the influence of light, 64 decomposes to 62 and dimethylstannylene. The structures of 62 and 64 were confirmed by single-crystal x-ray diffraction. Furthermore, tetraphenyltin reacts with P<sub>4</sub> in a sealed tube above 220 °C to form Ph<sub>3</sub>P and alloy-like tin phosphides.<sup>122</sup> Ph<sub>3</sub>Sn radicals, generated from Ph<sub>3</sub>SnCl and the titanium complex 45, react with P<sub>4</sub>, leading to the formation of P(SnPh<sub>3</sub>)<sub>3</sub> in 75% yield (cf. Scheme 10).<sup>102</sup>

### 1.36.2.5 Activation of P<sub>4</sub> by Group 15 Elements and Compounds

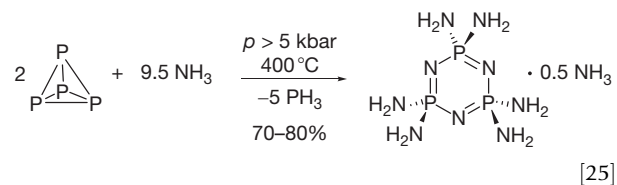
#### 1.36.2.5.1 Nitrogen

Since amines are relatively weak nucleophiles, they react only slowly with P<sub>4</sub>, leading to insoluble precipitates, which are proposed to be another modification of phosphorus.<sup>123</sup> However, the reaction of N-hydroxymethylalkylamines with P<sub>4</sub> produces tertiary phosphane oxides as the main reaction products, together with phosphonic and phosphinic acids.<sup>124</sup> When primary or secondary amines are used, the reaction with P<sub>4</sub> is faster and proceeds with gas evolution. For this process, a



Scheme 16 Conversion of P<sub>4</sub> by organotin hydrides.

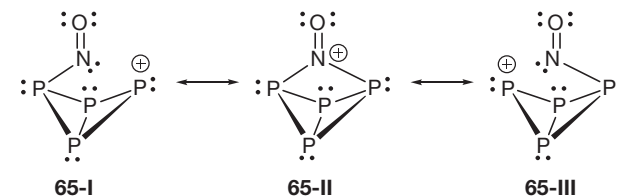
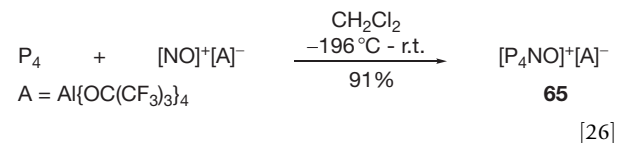
reaction mechanism with the formation of intermediates containing a butterfly-like P<sub>4</sub> core similar to 1 was proposed. Nevertheless, the reaction of P<sub>4</sub> with NH<sub>3</sub> at pressures higher than 5 kbar and temperatures above 250 °C produces the hexaaminocyclotriphosphazene P<sub>3</sub>N<sub>3</sub>(NH<sub>2</sub>)<sub>6</sub>·0.5NH<sub>3</sub> and red phosphorus (eqn [25]).<sup>125</sup>



If the reaction of amines with P<sub>4</sub> is performed in the presence of CCl<sub>4</sub> as the electrophile, followed by hydrolysis, trisamides of phosphoric acid are the main reaction products. The additional use of the HF donor Et<sub>3</sub>NHF leads to the formation of HPF<sub>5</sub><sup>-</sup>, R<sub>2</sub>NHPF<sub>5</sub>, and (R<sub>2</sub>NH)<sub>2</sub>P(O)F.<sup>126</sup> The generation of phosphorus esters containing P—N bonds by the reaction of P<sub>4</sub> with electrochemically generated nucleophiles was also reported.<sup>95</sup>

Since amides are strong nucleophiles, a rapid reaction with P<sub>4</sub> is expected. Interestingly, when P<sub>4</sub> is reacted with (2-pyridylmethyl)(trialkylsilyl)amide, an oxidative C—C coupling reaction is observed, leading to P<sub>7</sub><sup>3-</sup> as the phosphorus-containing product and 1,2-dipyridyl-1,2-bis(tert-butyl)dimethylsilylamido)ethane.<sup>127</sup>

An interesting reaction of the carbene-analogous NO<sup>+</sup> with P<sub>4</sub> was recently reported. Thus, [NO]<sup>+</sup>[A]<sup>-</sup> (A = Al{OC(CF<sub>3</sub>)<sub>3</sub>}<sub>4</sub>) reacts with P<sub>4</sub> via insertion into a P—P bond to yield 65 as a yellow compound (eqn [26]).<sup>128</sup> Based on the experimentally observed red-colored solution at low temperature and on quantum chemical calculations, the C<sub>s</sub> symmetric adduct [P<sub>4</sub>→NO]<sup>+</sup> was proposed to be an intermediate of this reaction. This adduct is 27 kJ mol<sup>-1</sup> higher in energy than the [P<sub>4</sub>NO]<sup>+</sup> cation. Although 65 could not be characterized by single-crystal x-ray diffraction, its structure was elucidated by spectroscopic methods and mass spectrometry. Interestingly, the resonance signal of the phosphorus atoms bonded to the nitrogen appears in the <sup>31</sup>P NMR spectrum at rather low fields (δ = 360), suggesting that the positive charge is mostly localized on these atoms. This was also confirmed by theoretical calculations. The resonance signal of the bridgehead phosphorus atoms appears at δ = -232 in the <sup>31</sup>P NMR spectrum. The bonding situation in 65 can be best described by the Lewis resonance structures 65-I to 65-III, of which the structures 65-I and 65-III contribute mostly to the bonding.



### 1.36.2.5.2 Phosphorus

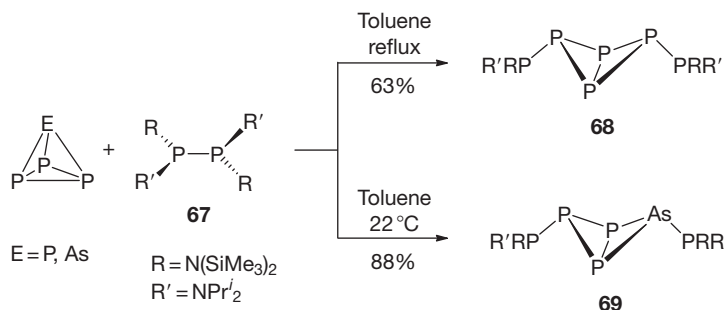
Phosphides of the type R<sub>2</sub>P<sup>−</sup> are strong nucleophiles and react readily with white phosphorus. The reaction proceeds in the first step via a nucleophilic attack of the phosphide on P<sub>4</sub>, leading to the cleavage of a P—P bond, together with concomitant formation of a new P—P bond. This step can then be followed by rearrangements or by further degradation processes. A widely used phosphide which was reacted with P<sub>4</sub> is the parent H<sub>2</sub>P<sup>−</sup>, for which alkali metals are frequently introduced. In these reactions, P<sub>4</sub> serves as the phosphorus source, while, usually, oligophosphides are the reaction products. The reactions of P<sub>4</sub>, H<sub>2</sub>P<sup>−</sup>, and alkali metals were described in Section 1.36.2.1 (*vide supra*).

The nature of the products obtained from the reaction of MPH<sub>2</sub> with P<sub>4</sub> depends strongly on the molar ratio, solvent, and reaction conditions. Thus, oligophosphides containing up to 26 phosphorus atoms can be synthesized by using THF or DME as the solvent and implying a LiPH<sub>2</sub>:P<sub>4</sub> ratio varying from 2.5:1 to 1:2.<sup>46,49,50</sup> Larger amounts of LiPH<sub>2</sub> lead to the formation of Li<sub>3</sub>P<sub>7</sub> in high yield.<sup>48</sup> If NaPH<sub>2</sub> is reacted with P<sub>4</sub> (P:NaPH<sub>2</sub> = 5:1 to 5.6:1) in the presence of 18-crown-6 in boiling THF, the complex [P<sub>5</sub>Na(18-crown-6)], containing an aromatic P<sub>5</sub><sup>−</sup> anion can be prepared.<sup>55b,c</sup> The reaction of KPH<sub>2</sub> with P<sub>4</sub> in DME leads to the formation of the pentaphosphide, KP<sub>5</sub>H<sub>2</sub>, with a bicyclo[1.1.0]tetraphosphabutane core, similar to that of 1.<sup>129</sup> However, it was only characterized by <sup>31</sup>P NMR spectroscopy and molecular weight determinations. The phosphide Ph<sub>2</sub>P<sup>−</sup> reacts with P<sub>4</sub> to give the triphosphide (Ph<sub>2</sub>P)<sub>2</sub>P<sup>−</sup>, the diphosphane (Ph<sub>2</sub>P)<sub>2</sub>, and polyphosphides (eqn [27]; X = Ph<sub>2</sub>P). When however, the linear phosphides of the type (PhP)<sub>n</sub><sup>2−</sup> (n = 1, 2 and 3) are reacted with P<sub>4</sub>, the extension of their chain length up to n = 4 was observed. The cyclopentaphosphide Ph<sub>4</sub>P<sub>5</sub><sup>−</sup> is formed by reacting *catena*-(PhP)<sub>4</sub><sup>2−</sup>

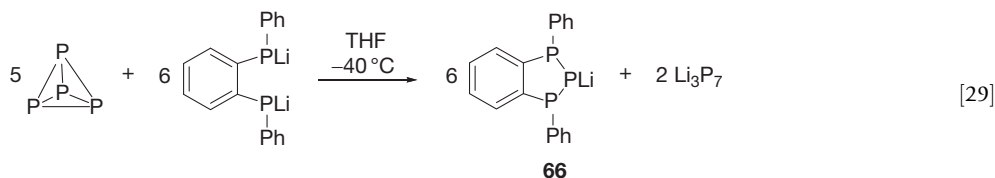
with P<sub>4</sub>.<sup>130</sup> Using a deficit of R<sub>2</sub>POM (M = Li, Na; R = Et, Ph) as nucleophiles in the reaction with P<sub>4</sub> results in the formation of M[OP(R<sub>2</sub>)P(R<sub>2</sub>)PO], together with polyphosphanides such as P<sub>7</sub><sup>3−</sup> and P<sub>16</sub><sup>2−</sup> (eqn [27]; X = R<sub>2</sub>PO). An excess of nucleophile leads to the formation of M<sub>2</sub>[OP(R<sub>2</sub>)PP(R<sub>2</sub>)PO] and polyphosphides (eqn [28]; X = R<sub>2</sub>PO).<sup>131</sup> This behavior was explained by the disproportionation of phosphorus into a P<sup>+</sup> as well as a P<sup>3−</sup> species, as described for the reaction of cyanides with P<sub>4</sub> (*vide supra*). Likewise, *o*-phenylene-bis(lithium phenylphosphanide) reacts with P<sub>4</sub>, with the formation of a benzotriphosphole derivative 66 in addition to Li<sub>3</sub>P<sub>7</sub> (eqn [29]).<sup>131,132b</sup> According to <sup>31</sup>P NMR spectroscopic investigations, the reaction proceeds quantitatively. The structure of 66•3THF was confirmed by single-crystal x-ray diffraction. Furthermore, 66 can be easily alkylated with RX (R = H, Me, Me<sub>3</sub>Si, Ph<sub>2</sub>P). The phosphorus-rich phosphides Cs<sub>3</sub>P<sub>11</sub>(en)<sub>3</sub> (en = ethylenediamine) and M<sub>4</sub>P<sub>14</sub>(en)<sub>x</sub> (M = Na, Cs) can be obtained by the reaction of P<sub>4</sub> in en with Cs<sub>4</sub>P<sub>6</sub> and Na<sub>3</sub>P<sub>7</sub>, respectively.<sup>133</sup>

Recently, it was reported that the ionic complex [Li]<sup>+</sup>[(MoCp)<sub>2</sub>(μ-PCy<sub>2</sub>)(μ-CO)<sub>2</sub>]<sup>−</sup>, containing a Mo≡Mo triple bond, reacts at room temperature with P<sub>4</sub> by a formal addition of a P<sub>2</sub> unit to the Mo≡Mo triple bond to give the complex [Li]<sup>+</sup>[(MoCp)<sub>2</sub>(μ-PCy<sub>2</sub>)(CO)<sub>2</sub>(μ-κ<sup>2</sup>:κ<sup>2</sup>-P<sub>2</sub>)]<sup>−</sup>.<sup>134</sup> The latter reacts with electrophiles such as MeI or Ph<sub>3</sub>SnCl, leading to the neutral complexes [(MoCp)<sub>2</sub>(μ-PCy<sub>2</sub>)(CO)<sub>2</sub>(μ-κ<sup>2</sup>:κ<sup>2</sup>-P<sub>2</sub>R)] (R = Me, SnPh<sub>3</sub>), which were structurally characterized.

Phosphorus-centered radicals are able to react with P<sub>4</sub>, leading to P—P bond cleavage. Thus, the sterically encumbered diphosphane [P{N(SiMe<sub>3</sub>)<sub>2</sub>}(NPr'<sub>2</sub>)<sub>2</sub>] (67), which, in hot toluene solution, dissociates reversibly to the corresponding RR'P radical, reacts with P<sub>4</sub> to form 68 (Scheme 17).<sup>135</sup> The diphosphanyl-bicyclotetraphosphane 68 was obtained as a mixture of



**Scheme 17** Reaction pathway of the activation of P<sub>4</sub> and AsP<sub>3</sub> by P-centered radicals formed in solutions of sterically strained diphosphanes.



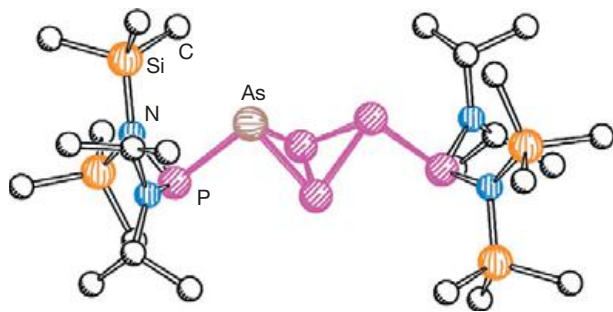
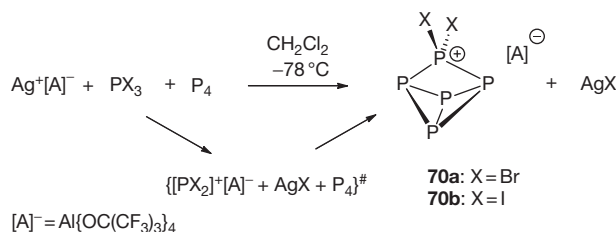


**Figure 18** Molecular structure of **69**. Hydrogen atoms are omitted for clarity. Adapted from Cossairt, B. M.; Cummins, C. C. *J. Am. Chem. Soc.* **2009**, *131*, 15501.

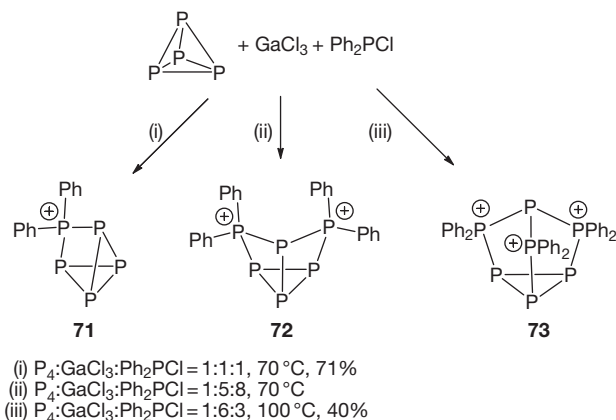


**Scheme 18** Reaction pathway of the activation of P<sub>4</sub> by in-situ generated phosphonium cation PX<sub>2</sub><sup>+</sup>.

*meso*- and *rac*-diastereomers. Correspondingly, AsP<sub>3</sub> reacts with **67** by the selective cleavage of an As—P bond and the formation of **69**. It is interesting to note the lower reaction temperature at which the reaction takes place (**Scheme 17**).<sup>136</sup> Both **68** and **69** were structurally characterized by single-crystal x-ray diffraction studies. The molecular structure of **69** is depicted in **Figure 18**.

Just like the isoelectronic NO<sup>+</sup> (*vide supra*, cf. **Section 1.36.2.5.1**), P<sub>4</sub> reacts with PX<sub>2</sub><sup>+</sup> (X = Br, I), generated by halogen extraction from the corresponding PX<sub>3</sub> by Ag[Al{OC(CF<sub>3</sub>)<sub>3</sub>}<sub>4</sub>], via the insertion of a PX<sub>2</sub> unit into a P—P bond and formation of the ionic compound [P<sub>5</sub>X<sub>2</sub>]<sup>+</sup>[A]<sup>-</sup> (**70a**, X = Br; **70b** X = I) (A = Al{OC(CF<sub>3</sub>)<sub>3</sub>}<sub>4</sub>) (**Scheme 18**).<sup>137</sup> According to <sup>31</sup>P NMR spectroscopic investigations, the reactions proceed almost quantitatively, and **70a** was isolated as a crystalline solid in 85% yield. The structure of **70a** was determined by x-ray crystallography. The structure of the [P<sub>5</sub>Br<sub>2</sub>]<sup>+</sup> cation is depicted in **Figure 19**. In the solid state, the P<sub>5</sub>Br<sub>2</sub><sup>+</sup> represents a C<sub>2v</sub> symmetric cage, which is also preserved in solutions, as determined by spectroscopic methods. An alternative synthetic route to **70b** is the reaction of [Ag(P<sub>4</sub>)<sub>2</sub>][Al{OC(CF<sub>3</sub>)<sub>3</sub>}<sub>4</sub>] with I<sub>2</sub>.<sup>137a</sup>

The disadvantage of the dichlorophosphonium cation [X<sub>2</sub>P]<sup>+</sup>/P<sub>4</sub> system is that it is limited to low temperatures and, consequently, insertion into only one P—P bond can be achieved. In contrast, the diphenylphosphonium cation [Ph<sub>2</sub>P]<sup>+</sup> is considerably more stable and can be used for multiple insertions into P—P bonds of P<sub>4</sub>. As a source of [Ph<sub>2</sub>P]<sup>+</sup>, a melt of Ph<sub>2</sub>PCL and GaCl<sub>3</sub> was used.<sup>138</sup> Consequently, the treatment of P<sub>4</sub> with GaCl<sub>3</sub> and Ph<sub>2</sub>PCL in a 1:1:1 molar ratio results in a relatively clean reaction in which a Ph<sub>2</sub>P<sup>+</sup> cation inserts into one P—P bond of the P<sub>4</sub> tetrahedron to form **71** (**Scheme 19**).<sup>139</sup> The reaction depends strongly on stoichiometry and the reaction temperature. When a 1:5:8 molar ratio of the reactants (P:GaCl<sub>3</sub>:



**Scheme 19** Reaction pathway of the activation of P<sub>4</sub> by the in-situ generated phosphonium cation Ph<sub>2</sub>P<sup>+</sup>.

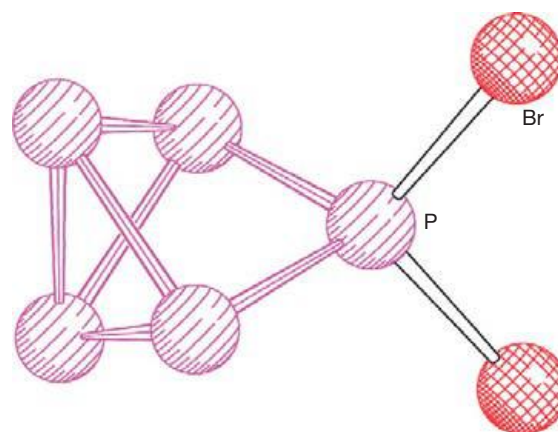


**Figure 19** Molecular structure of the cation [P<sub>5</sub>Br<sub>2</sub>]<sup>+</sup> in **70a**. Adapted from Gonsior, M.; Krossing, I.; Müller, L.; Raabe, I.; Jansen, M.; van Wüllen, L. *Chem. Eur. J.* **2002**, *8*, 4475.

Ph<sub>2</sub>PCL) is used, the formation of a mixture containing the mono-insertion product **71** as well as the double insertion product **72** is formed. Compound **72** is stable only in solutions and could not be isolated. It was characterized by spectroscopic methods. Interestingly, the formation of the other possible isomer of **72**, in which the Ph<sub>2</sub>P<sup>+</sup> cations are inserted into two opposite P—P bonds in P<sub>4</sub>, was not observed. Increasing the ratio of GaCl<sub>3</sub>, hence, generating a Lewis-acidic medium by using a P:GaCl<sub>3</sub>:Ph<sub>2</sub>PCL stoichiometry of 1:6:3, leads to the formation of the triple insertion product **73** in moderate yield. The structures of **71**[GaCl<sub>4</sub>] and **73**[Ga<sub>2</sub>Cl<sub>7</sub>] were determined by single-crystal x-ray diffraction. The molecular structure of **71** is depicted in **Figure 20**.

By comparing the reactions of the silylene **53** and of the isolobal phosphonium cations R<sub>2</sub>P<sup>+</sup> (R = Br, I, Ph) with P<sub>4</sub>, interesting parallels become apparent. In both cases, an insertion into a P—P bond occurs first, but the double insertion product differs. While Ph<sub>2</sub>P<sup>+</sup> inserts into two neighboring P—P bonds, leading to **72**, the silylene **53** inserts into two opposite P—P bonds, leading to **55**. Until now, it has not been clear if this is an electronic or a steric effect, but since **53** is sterically more bulky than Ph<sub>2</sub>P<sup>+</sup>, this difference might be attributed to steric rather than electronic effects.

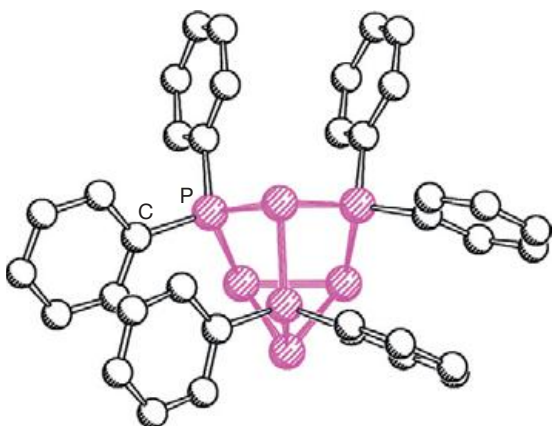


**Figure 20** Molecular structure of the cation **71**. Adapted from Weigand, J. J.; Holthausen, M.; Fröhlich, R. *Angew. Chem. Int. Ed.* **2009**, *48*, 295.

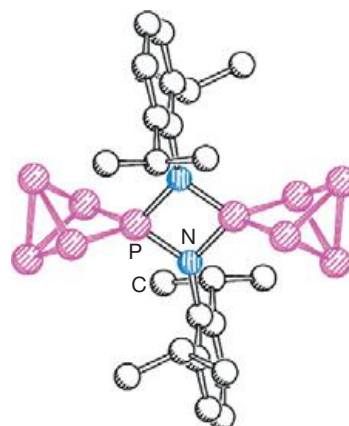
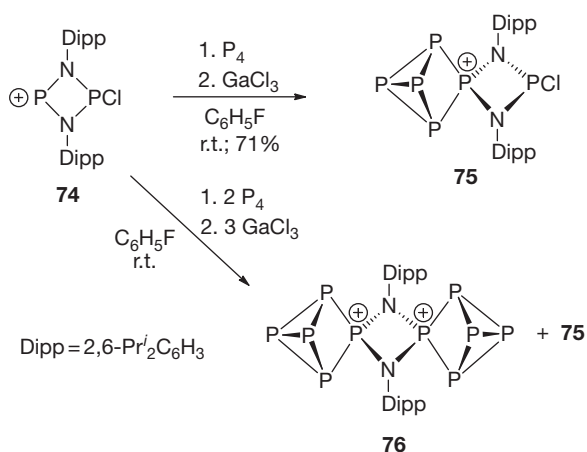


**Figure 21** Molecular structure of the cation **76**. Adapted from Holthausen, M. H.; Weigand, J. J. *J. Am. Chem. Soc.* **2009**, *131*, 14210.



**Scheme 20** Reaction pathway of the activation of P<sub>4</sub> by the in-situ generated cyclic phosphonium cation **74**.

The generation of phosphonium cations is not limited to X<sub>2</sub>P<sup>+</sup> and Ph<sub>2</sub>P<sup>+</sup>. Reacting the *cyclo*-1,3-diphospha-2,4-diazane [DippN<sup>+</sup>PCl]<sub>2</sub> (Dipp = 2,6-Pr<sub>2</sub>C<sub>6</sub>H<sub>3</sub>) with GaCl<sub>3</sub> leads to the generation of the corresponding cyclic phosphonium cation **74**. With P<sub>4</sub>, it reacts similarly to X<sub>2</sub>P<sup>+</sup> and Ph<sub>2</sub>P<sup>+</sup> by insertion into one P—P bond to form **75** (**Scheme 20**).<sup>140</sup> The cation **75** can be isolated as a very air- and moisture-sensitive solid as [75][GaCl<sub>4</sub>] $\cdot$ C<sub>6</sub>H<sub>5</sub>F. If **74** is reacted with 2 equiv. of P<sub>4</sub> in the presence of an excess of GaCl<sub>3</sub>, the formation of the phosphorus-rich dication **76** as well as **75** was observed (**Scheme 20**). According to <sup>31</sup>P NMR spectroscopic studies, **76** is formed in 60% yield, and consists of two C<sub>2v</sub> symmetric P<sub>5</sub> cages bridged by two imido groups. The dimer **76** is not stable in solution and decomposes to unidentified products; however, [76][Ga<sub>2</sub>Cl<sub>7</sub>] could be crystallized as a conglomerate with [75][GaCl<sub>4</sub>]. The molecular structure of **76** is depicted in **Figure 21**. The reactions of phosphonium cations with P<sub>4</sub> can be extended further. The four-membered phosphorus–nitrogen–silicon heterocycle **77** acts as a phosphonium cation source if an excess of the Lewis acid GaCl<sub>3</sub> is added, leading to the expected insertion into a P—P bond and formation of **78** in good yield (eqn [30]).<sup>141</sup> The aluminum derivative **79**, reacts with P<sub>4</sub> similarly to **77**, forming the zwitterionic

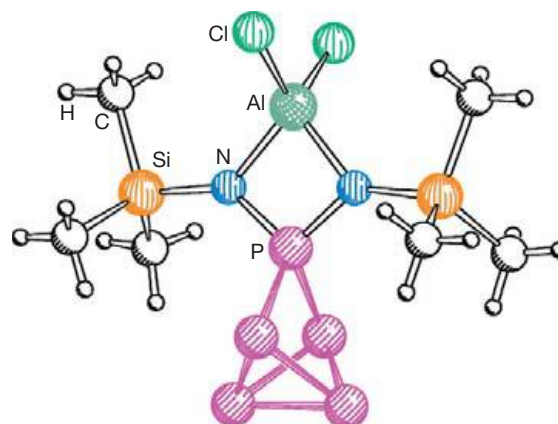
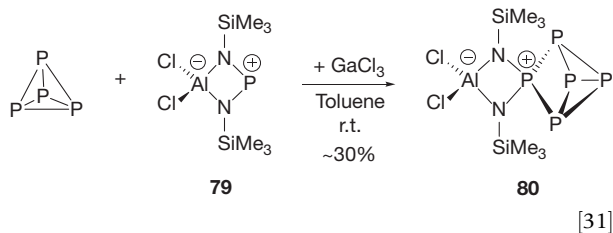
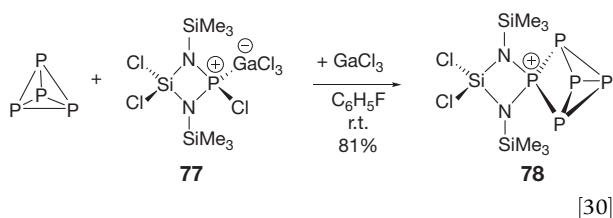


**Figure 22** Molecular structure of **80**. Adapted from Holthausen, M. H.; Richter, C.; Hepp, A.; Weigand, J. J. *Chem. Commun.* **2010**, 46, 6921.

compound **80** (eqn [31]).<sup>141</sup> Both **78** and **80** were isolated as crystalline solids as their [GaCl<sub>4</sub>]<sup>−</sup> salts, and were characterized crystallographically. The structure of **80** is depicted in **Figure 22**. Furthermore, in solution, **78** and **80** were characterized by <sup>31</sup>P NMR spectroscopy.



### 1.36.2.5.3 Arsenic, Antimony, and Bismuth

In the gas phase under mass spectrometric conditions, P<sub>4</sub> reacts with As<sub>4</sub> at 300–350 °C to produce predominantly the three mixed molecules As<sub>3</sub>P, As<sub>2</sub>P<sub>2</sub>, and AsP<sub>3</sub>. At higher temperatures (above ~800 °C), the tetraatomic molecules are unstable with respect to dissociation into the corresponding diatomic species.<sup>142</sup> To the best of our knowledge, no further reaction was reported in which P<sub>4</sub> is reacted with compounds containing heavier group 15 elements.

### 1.36.2.6 Activation of P<sub>4</sub> by Group 16 Elements and Compounds

White phosphorus reacts readily with oxygen, leading to the oxides P<sub>4</sub>O<sub>6</sub> and P<sub>4</sub>O<sub>10</sub>.<sup>1</sup> The suboxides P<sub>2</sub>O, as well as PO and PO<sub>2</sub>, were generated by the oxidation of gaseous P<sub>4</sub> and detected by IR laser spectroscopy.<sup>143,144</sup> Attempts were made to employ the oxidation of P<sub>4</sub> with moist air in order to decompose toxic organic compounds. Hereby, the species PO and PO<sub>2</sub> and, finally, phosphoric acid as well as O<sub>3</sub> were detected.<sup>145</sup> Furthermore, the oxidation of P<sub>4</sub> with oxygen in the presence of organic compounds like olefins,<sup>146</sup> phenols,<sup>147,148</sup> or alcohols<sup>149</sup> were reported to lead to triorganophosphates as the phosphorus-containing product. A series of phosphorus oxides (PO, PO<sub>2</sub>, P<sub>2</sub>O, P<sub>2</sub>O<sub>2</sub>, P<sub>2</sub>O<sub>3</sub>, P<sub>2</sub>O<sub>4</sub>, P<sub>2</sub>O<sub>5</sub>, and P<sub>4</sub>O) were generated by reacting ozone with P<sub>2</sub> molecules in a matrix, which is generated from P<sub>4</sub>.<sup>150</sup> The monoxide P<sub>4</sub>O could be directly generated by the ozonolysis of P<sub>4</sub>.<sup>151</sup> Furthermore, it has been shown that oxygen–phosphorus systems reveal chemiluminescence properties.<sup>152</sup>

Hydroxide or alkoxide anions are strong nucleophiles and, hence, react with P<sub>4</sub>, leading to dark-red solutions, which probably contain a mixture of uncharacterized phosphanides. These solutions decompose slowly to H<sub>2</sub>, PH<sub>3</sub>, and Na<sub>3</sub>PO<sub>2</sub>.<sup>153</sup> Quenching the dark-red solutions with MeI followed by oxidation with HNO<sub>3</sub> leads to mixtures of MePH<sub>2</sub>, MePO<sub>3</sub>H<sub>2</sub>, Me<sub>2</sub>PO<sub>2</sub>H, and Me<sub>3</sub>PO. Some other alkylating agents, such as acrylonitrile, acrylamide, ethyl acrylate, and vinylphosphonate, were also used, leading mainly to the formation of the corresponding phosphane oxides.<sup>154</sup> Phosphane oxides are obtained also by the reaction of allyl halides with P<sub>4</sub> in superbases media.<sup>155,156</sup> When the reaction of P<sub>4</sub> with NaOR is performed in CCl<sub>4</sub>, which is also a source of electrophiles, the corresponding trialkylphosphite is obtained (RO)<sub>3</sub>P.<sup>157</sup> P<sub>4</sub> reacts with MeOH or EtOH only upon heating, giving a mixture of the corresponding alkylphosphanes and phosphonium salts.<sup>158</sup> Using H<sub>3</sub>PO<sub>4</sub> as the solvent, P<sub>4</sub> reacts with benzaldehyde under KI catalysis to give the isophosphindoline derivative, 1-phenyl-1,3-dihydro-2λ<sup>5</sup>-benzophosphonic acid.<sup>159</sup> In the first step, the conversion of P<sub>4</sub> into H<sub>3</sub>PO<sub>2</sub> was proposed, which reacts further with benzaldehyde to give the benzophosphonic acid.

Hydrogen peroxide or different organic peroxides react with P<sub>4</sub> in both aqueous and alcoholic solutions under aerobic conditions, leading to, depending on the reaction conditions, derivatives of hypophosphorous acid, phosphorous acid, mono- and diorgano hydrogen phosphonates, and phosphoric acid or triorganophosphates.<sup>160</sup> Trialkylphosphates (RO)<sub>3</sub>P(O) and dialkylphosphites (RO)<sub>2</sub>P(O)H can be obtained by catalytic

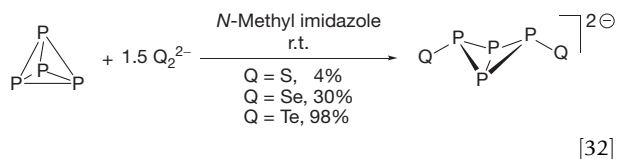
oxidative alkoxylation of P<sub>4</sub> with oxygen using Pd(II) and Ru(II) catalyst and co-oxidants, such as CuCl<sub>2</sub>, NaNO<sub>2</sub>, or FeCl<sub>3</sub>.<sup>161</sup>

White phosphorus is self-igniting when exposed to air. However, when it is encapsulated in a self-assembled tetrahedral capsule by means of host–guest type chemistry, it becomes air-stable and, additionally, water-soluble.<sup>162</sup> P<sub>4</sub> can be released if a stronger guest such as benzene is added. Exposure to air leads to the complete conversion of P<sub>4</sub> to phosphoric acid.

Sulfur or selenium react with P<sub>4</sub> in a melt to give the phosphorus sulfides P<sub>4</sub>S<sub>n</sub> (n = 2–10) or the corresponding selenides.<sup>1,163</sup> At temperatures below 100 °C, evidence for the existence of an S<sub>8</sub> diradical as intermediate in the reaction between P<sub>4</sub> and S<sub>8</sub> was reported.<sup>164</sup> The reaction of thiolates, for example, NaSR, with P<sub>4</sub> in the presence of CCl<sub>4</sub> leads to the formation of (RS)<sub>3</sub>P, which can be converted to (RS)<sub>3</sub>PO under oxidizing conditions.<sup>165</sup> Different thiophosphates are the products of the reaction of P<sub>4</sub> with S<sub>8</sub> in the presence of H<sub>2</sub>S<sup>166</sup> or by the reaction of P<sub>4</sub> with polysulfides.<sup>167</sup> Furthermore, on the basis of NMR evidence, the formation of phosphorus-rich cages with P<sub>5</sub>S<sub>2</sub> and P<sub>6</sub>S skeletons was proposed in the reaction of P<sub>4</sub> with S<sub>8</sub> and I<sub>2</sub> in CS<sub>2</sub> solutions.<sup>168</sup>

The reaction of P<sub>4</sub> with RSSR proceeds at rather high temperatures via a radical mechanism to yield (RS)<sub>3</sub>P.<sup>169</sup> The addition of catalytic amounts of hydroxide ions induces an ionic reaction mechanism and increases the reaction rate.

Interestingly, the reaction of P<sub>4</sub> with Na<sub>2</sub>Q<sub>2</sub> (Q = S, Se and Te) in *N*-methyl imidazole at ambient temperature leads to the dianion P<sub>4</sub>Q<sub>2</sub><sup>2-</sup> (eqn [32]).<sup>170</sup> In the case of the tellurium derivative, the reaction proceeds cleanly (only small amounts of NaP<sub>5</sub> are additionally formed), whereas in the case of the selenium derivative, more by-products are formed. When P<sub>4</sub> is reacted with Na<sub>2</sub>S<sub>2</sub>, the expected P<sub>4</sub>S<sub>2</sub><sup>2-</sup> anion is formed only in traces. This was attributed to the stability of the P<sub>4</sub>Q<sub>2</sub><sup>2-</sup> anions, which decreases from tellurium to sulfur. The stoichiometry and solvent are essential for the formation of P<sub>4</sub>Q<sub>2</sub><sup>2-</sup>. According to heteronuclear NMR studies, the P<sub>4</sub>Q<sub>2</sub><sup>2-</sup> anions have a tetraphosphabicyclo[1.1.0]butane butterfly-like structure with the chalcogen atoms in the sterically more favorable *exo* positions.



[32]

### 1.36.2.7 Activation of P<sub>4</sub> by Group 17 Elements and Compounds

White phosphorus reacts exothermically with halogens, leading to PX<sub>3</sub> or PX<sub>5</sub> derivatives. Using mixtures of halogens leads to the formation of mixed phosphorus halides.<sup>171</sup> Attempts to oxidize P<sub>4</sub> by reacting it with Li<sup>+</sup>[Al{OC(CF<sub>3</sub>)<sub>3</sub>}<sub>4</sub>]<sup>-</sup> and I<sub>2</sub> produces an amorphous solid, probably red phosphorus. The reaction of the silver salt Ag<sup>+</sup>[Al{OC(CF<sub>3</sub>)<sub>3</sub>}<sub>4</sub>]<sup>-</sup> with P<sub>4</sub> and I<sub>2</sub> or Br<sub>2</sub> generates the P<sub>5</sub><sup>+</sup> cation as a reactive intermediate, which decomposes with the formation of [Cl<sub>2</sub>P(CDCl<sub>2</sub>)<sub>2</sub>]<sup>+</sup>[A]<sup>-</sup> (**81**) and [P<sub>3</sub>I<sub>6</sub>]<sup>+</sup>[A]<sup>-</sup> (**82**) (A = {(CF<sub>3</sub>)<sub>3</sub>CO}<sub>3</sub>Al–F–Al{OC(CF<sub>3</sub>)<sub>3</sub>}<sub>3</sub>).<sup>172</sup> The generation of the P<sub>5</sub><sup>+</sup> cation is supported

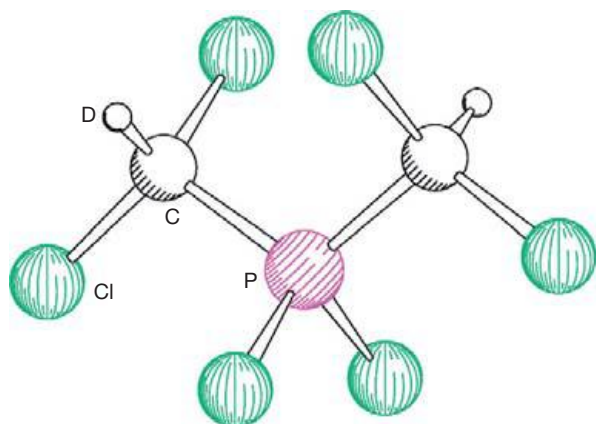


**Figure 23** Molecular structure of the cation  $[\text{Cl}_2\text{P}(\text{CDCl}_2)_2]^+$  in **81**. Adapted from Krossing, I. *J. Chem. Soc. Dalton Trans.* **2002**, 500.

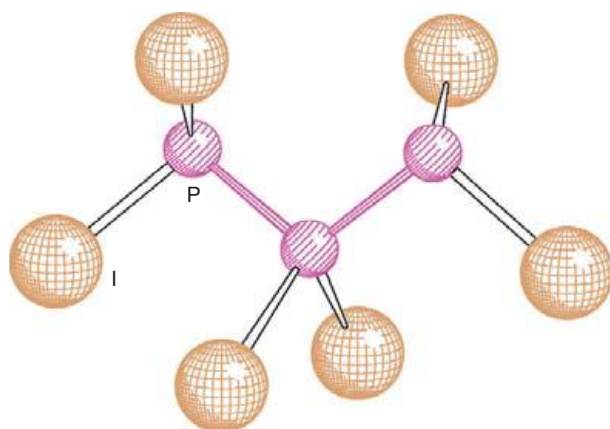


**Figure 24** Molecular structure of the cation  $[\text{P}_3\text{I}_6]^+$  in **82**. Adapted from Krossing, I. *J. Chem. Soc. Dalton Trans.* **2002**, 500.

by thermochemical calculations of Born–Haber cycles of different formation and decomposition processes. Both **81** and **82** were characterized by single-crystal x-ray diffraction analysis (Figures 23 and 24).

### 1.36.3 Conclusion

The activation of white P<sub>4</sub> phosphorus is a significant part of the general interest in the field of activation of small molecules like, for example, N<sub>2</sub>, CH<sub>4</sub>, CO<sub>2</sub>, and H<sub>2</sub> for a direct and energy-efficient transfer into useful derivatives and products. Thereby, not only potential applications are in the main focus of research, but, also, the understanding of the elementary steps of their activation. Since the organophosphorus compounds are widely used, the activation and functionalization of P<sub>4</sub> attract much attention. Earlier results showed the possible direct functionalization of P<sub>4</sub>, leading to organophosphorus compounds, although none of the reactions is yet clean enough and, thus, suitable for industrial applications. More recently, the degradation of P<sub>4</sub> by N-heterocyclic carbenes reignited the search for the direct functionalization of P<sub>4</sub> by main-group-element compounds, and considerable efforts are

expected towards the understanding of the reaction mechanism and especially the initial steps of the P<sub>4</sub> activation. As seen by the photochemical activation of P<sub>4</sub> in the presence of butadienes, a rational approach to P<sub>2</sub> containing organic derivatives comes within reach. All these developments in carbon chemistry stimulated likewise the use of neighbor-group elements and, thus, lead to a growing interest for the activation of P<sub>4</sub> by other main-group elements and compounds. Accordingly, reactions of P<sub>4</sub> with derivatives of almost every main-group element have been reported. These results were summarized in this chapter, with the main focus on recent developments as well as on the mechanistic considerations of P<sub>4</sub> activation. The presented state of knowledge in this field will stimulate more activities for the activation of white phosphorus and, thus, contribute to the further rapid growth of our knowledge in this fascinating field of chemistry. For a related chapter in this Comprehensive, we refer to **Chapter 1.04**.

### References

- Corbridge, D. E. C. *Phosphorus 2000; Chemistry, Biochemistry and Technology*. Elsevier: Amsterdam, 2000.
- (a) Dapporto, S.; Midollini, S.; Sacconi, L. *Angew. Chem. Int. Ed. Engl.* **1979**, *18*, 469; (b) Di Vaira, M.; Ghilardi, C. A.; Midollini, S.; Sacconi, L. *J. Am. Chem. Soc.* **1978**, *100*, 2550.
- Ginsberg, A. P.; Lindsell, W. E. *J. Am. Chem. Soc.* **1979**, *93*, 2082.
- (a) Scherer, O. J.; Sitzmann, H.; Wolmershäuser, G. *Angew. Chem. Int. Ed. Engl.* **1985**, *24*, 351; (b) Scherer, O. J.; Brück, T. *Angew. Chem. Int. Ed.* **1987**, *26*, 59.
- (a) Scheer, M.; Hermann, E. Z. *Chem.* **1990**, *30*, 41; (b) Scherer, O. J. *Angew. Chem. Int. Ed. Engl.* **1990**, *29*, 1104; (c) Scherer, O. J. *Acc. Chem. Res.* **1999**, *32*, 751; (d) Scherer, O. J. *Chem. unserer Zeit* **2000**, *34*, 374; (e) Ehses, M.; Romero, A.; Peruzzini, M. *Top. Curr. Chem.* **2005**, *220*, 107; (f) Peruzzini, M.; Gonsalvi, L.; Romero, D. *Chem. Soc. Rev.* **2005**, *34*, 1038.
- For details cf. (a) Scheer, M.; Troitzsch, C.; Hilfert, L.; Dargatz, M.; Kleinpeter, E.; Jones, P. G.; Sieler, J. *Chem. Ber.* **1995**, *128*, 251; (b) Scheer, M.; Becker, U.; Chisholm, M. H.; Huffman, J. C.; Lemoigno, F.; Eisenstein, O. *Inorg. Chem.* **1995**, *34*, 3117; (c) Scheer, M.; Schuster, K.; Becker, U. *Phosphorus, Sulfur Silicon Relat. Elem.* **1996**, *109–110*, 141; (d) Scheer, M.; Becker, U. *Chem. Ber.* **1996**, *129*, 1307; (e) Scheer, M.; Becker, U. *J. Organomet. Chem.* **1997**, *545–546*, 451; (f) Scheer, M.; Becker, U.; Magull, J. *Polyhedron* **1998**, *17*, 1983.
- (a) Crossairt, B. M.; Piro, N. A.; Cummins, C. C. *Chem. Rev.* **2010**, *110*, 4161; (b) Caporali, M.; Gonsalvi, L.; Rossin, A.; Peruzzini, M. *Chem. Rev.* **2010**, *110*, 4178.
- (a) Scheer, M.; Balázs, G.; Seitz, A. *Chem. Rev.* **2010**, *110*, 4236; (b) Giffin, N. A.; Masuda, J. D. *Coord. Chem. Rev.* **2011**, *255*, 1342.
- Hirsch, A.; Chen, Z.; Jiao, H. *Angew. Chem. Int. Ed.* **2001**, *40*, 2834.
- Maxwell, L. R.; Hendrichs, S. B.; Mosley, V. J. *Chem. Phys.* **1935**, *3*, 699.
- Brassington, N. J.; Edwards, H. G. M.; Long, D. A. *J. Raman Spectrosc.* **1981**, *11*, 346; cf. also: Östermark, H.; Wallin, S.; More, N.; Launila, O. *J. Chem. Phys.* **2003**, *119*, 5918.
- (a) Simon, A.; Bormann, H.; Horakh, J. *Chem. Ber./Recl.* **1997**, *130*, 1235; (b) Simon, A.; Bormann, H.; Craubner, H. *Phosphorus, Sulfur Silicon Relat. Elem.* **1987**, *30*, 507; (c) Okudera, H.; Dinnebie, R. E.; Simon, A. Z. *Kristallogr.* **2005**, *220*, 259.
- Häser, M.; Treutler, O. *J. Chem. Phys.* **1995**, *102*, 3703.
- Crossairt, B. M.; Cummins, C. C.; Head, A. R.; Lichtenberger, D. L.; Berger, R. J. F.; Hayes, S. A.; Mitzel, N. W.; Wu, G. *J. Am. Chem. Soc.* **2010**, *132*, 8459.
- (a) Jones, R. D.; Holl, D. J. *J. Chem. Phys.* **1990**, *92*, 6710; (b) Schoeller, W. W.; Staemmler, V.; Rademacher, P.; Niecke, E. *Inorg. Chem.* **1986**, *25*, 4382.
- Tsirelson, V. G.; Tarasova, M. F.; Smetannikov, Yu. V. *Heteroat. Chem.* **2006**, *17*, 572.
- (a) Bader, R. F. W. *Atoms in Molecules. A Quantum Theory*. Clarendon Press: Oxford, UK, 1990; (b) Tsirelson, V. G.; Ozerov, R. P. *Electron Density and Bonding in Crystals*. Institute of Physics Publishing: Bristol, UK, 1996; (c) Tsirelson, V. G. *Chemical Bond and Thermal Agitation of Atoms in the Crystals*. VINITI: Moscow, 1993.
- Kadirov, M. K.; Budnikova, Yu. G.; Kholin, K. V.; Valitov, M. I.; Krasnov, S. A.; Gryaznova, T. V.; Sinyashin, O. G. *Russ. Chem. Bull.* **2010**, *59*, 466.

19. (a) Milyukov, V. A.; Budnikova, Yu.H.; Sinyashin, O. G. *Russ. Chem. Rev.* **2005**, *74*, 781; (b) Petrov, K. A.; Smirnov, V. V.; Emel'yanov, V. I. *Zh. Obshch. Khim.* **1968**, *38*, 122.
20. Fluck, E.; Pavlidou, C. M. E.; Janoschek, R. *Phosphorus, Sulfur Silicon Relat. Elem.* **1979**, *6*, 469.
21. Abboud, J.-L. M.; Herreros, M.; Notario, R.; Essefar, M.; M<sup>o</sup>, O.; Y<sup>a</sup>ñez, M. *J. Am. Chem. Soc.* **1996**, *118*, 1126; For P<sub>4</sub>Li<sup>+</sup>, cf.: Abboud, J.-L.; Alkorta, M. I.; Davalos, J. Z.; Gal, J.-F.; Herreros, M.; Maria, P.-C.; M<sup>o</sup>, O.; Molina, M. T.; Notario, R.; Y<sup>a</sup>ñez, M. *J. Am. Chem. Soc.* **2000**, *122*, 4451.
22. Di Vaira, M.; Sacconi, L. *Angew. Chem. Int. Ed. Engl.* **1982**, *21*, 330.
23. Gr<sup>o</sup>er, T.; Scheer, M. *Organometallics* **2000**, *19*, 3683.
24. (a) Peruzzini, M.; Marvelli, M.; Romerosa, A.; Rossi, R.; Vizza, F.; Zanobini, F. *Eur. J. Inorg. Chem.* **1999**, 931; (b) Di Vaira, M.; Frediani, P.; Seniori Costantini, S.; Peruzzini, M.; Stoppioni, P. *Acta Crystallogr.* **2005**, *A61*, C298; (c) Barbaro, P.; Di Vaira, M.; Peruzzini, M.; Seniori Costantini, S.; Stoppioni, P. *Chem. Eur. J.* **2007**, *13*, 6682; (d) Caporali, M.; Di Vaira, M.; Peruzzini, M.; Seniori Costantini, S.; Stoppioni, P.; Zanobini, F. *Eur. J. Inorg. Chem.* **2010**, 152.
25. Ginsberg, A. P.; Lindsell, W. E.; McCullough, K. J.; Sprinkle, C. R.; Welch, A. J. *J. Am. Chem. Soc.* **1986**, *108*, 403.
26. (a) Krossing, I.; van W<sup>u</sup>llen, L. *Chem. Eur. J.* **2002**, *8*, 700; (b) Santiso-Quinones, G.; Reisinger, A.; Slattery, J.; Krossing, I. *Chem. Commun.* **2007**, 5046.
27. Cf. comment in quotation [52] in: Schoeller, W. W. *Phys. Chem. Chem. Phys.* **2009**, *11*, 5273.
28. Baudler, M.; Adamek, C.; Opiela, S.; Budzikiewicz, H.; Ouzounis, D. *Angew. Chem. Int. Ed. Engl.* **1988**, *27*, 1059.
29. Kraus, F.; Aschenbrenner, J. C.; Korber, N. *Angew. Chem.* **2003**, *115*, 4162; *Angew. Chem. Int. Ed.* **2003**, *42*, 4030.
30. Korber, N.; Aschenbrenner, J. C. *J. Chem. Soc. Dalton Trans.* **2001**, 1165.
31. Kraus, F.; Aschenbrenner, J. C.; Klamroth, T.; Korber, N. *Inorg. Chem.* **2009**, *48*, 1911.
32. Baudler, M.; Duester, D. *Z. Naturforsch.* **1987**, *B42*, 330.
33. Baudler, M. *Angew. Chem.* **1987**, *99*, 429–451; *Angew. Chem. Int. Ed. Engl.* **1987**, *26*, 419.
34. (a) Peterson, D. J.; Logan, T. J. *J. Inorg. Nucl. Chem.* **1966**, *28*, 53; (b) Cahours, A. *Ann. Chem.* **1862**, *122*, 329.
35. Ellermann, J.; Demuth, A. A. M. *Monatsh. Chem.* **1987**, *118*, 183.
36. (a) Becker, G.; H<sup>o</sup>lderich, W. *Chem. Ber.* **1975**, *108*, 2484; (b) Karsch, H. H.; Bienlein, F.; Rupprich, T.; Uhlrig, F.; Herrmann, E.; Scheer, M. *Synth. Methods Organomet. Inorg. Chem.* **1996**, *3*, 58.
37. Fritz, G.; H<sup>o</sup>lderich, W. *Naturwissenschaften* **1975**, *62*, 573.
38. Siegl, H.; Krumlacher, W.; Hassler, K. *Monatsh. Chem.* **1999**, *130*, 139.
39. Fritz, G.; Uhlmann, M. R. *Z. Anorg. Allg. Chem.* **1978**, *440*, 168.
40. Fritz, G.; Reuter, J. *Z. Anorg. Allg. Chem.* **1989**, *578*, 27.
41. Hanauer, T.; Aschenbrenner, J. C.; Korber, N. *Inorg. Chem.* **2006**, *45*, 6723.
42. Lerner, H.-W.; Bolte, M. *Acta Cryst.* **2007**, *E63*, m1013.
43. Milyukov, V.; Kataev, A.; Sinyashin, O.; L<sup>o</sup>nnecke, P.; Hey-Hawkins, E. Z. *Anorg. Allg. Chem.* **2006**, *632*, 1728.
44. Baudler, M.; Duester, D. *Z. Naturforsch.* **1987**, *B42*, 335.
45. von Schnering, H. G.; Manriquez, V.; H<sup>o</sup>hle, W. *Angew. Chem. Int. Ed. Engl.* **1981**, *20*, 594.
46. Baudler, M.; Exner, O. *Chem. Ber.* **1983**, *116*, 1268.
47. Fritz, G.; H<sup>o</sup>rer, J.; Stoll, K.; Vaahs, T. *Phosphorus, Sulfur Silicon Relat. Elem.* **1983**, *18*, 65.
48. Baudler, M.; Faber, W. *Chem. Ber.* **1980**, *113*, 3394.
49. Baudler, M.; D<sup>u</sup>ster, D.; Germeshausen, J. Z. *Anorg. Allg. Chem.* **1986**, *534*, 19.
50. Baudler, M.; Heum<sup>u</sup>ller, R.; D<sup>u</sup>ster, D.; Germeshausen, J.; Hahn, J. Z. *Anorg. Allg. Chem.* **1984**, *518*, 7.
51. Guerin, F.; Richeson, D. *Inorg. Chem.* **1995**, *34*, 2793.
52. Baudler, M.; Glinka, K. *Inorg. Synth.* **1990**, *27*, 227.
53. Baudler, M.; D<sup>u</sup>ster, D.; Langerbeins, K.; Germeshausen, J. *Angew. Chem. Int. Ed. Engl.* **1984**, *23*, 317.
54. (a) Baudler, M.; D<sup>u</sup>ster, D.; Ouzounis, D. Z. *Anorg. Allg. Chem.* **1987**, *544*, 87; (b) Baudler, M.; Akpogolou, S.; Ouzounis, D.; Wasgestian, F.; Meinigke, G.; Budzikiewicz, H.; M<sup>u</sup>nster, H. *Angew. Chem. Int. Ed.* **1988**, *27*, 280.
55. (a) Baudler, M.; Etzbach, T. *Chem. Ber.* **1991**, *124*, 1159; (b) Milyukov, V. A.; Kataev, A. V.; Sinyashin, O. G.; Hey-Hawkins, E.-M. *Russ. Chem., Bull. Int. Ed.* **2006**, *55*, 1297; (c) Baudler, M.; Ouzounis, D. Z. *Naturforsch. B* **1989**, *44*, 381.
56. Baudler, M.; Hahn, J. Z. *Naturforsch.* **1990**, *45*, 1139.
57. (a) Baudler, M. *Angew. Chem. Int. Ed. Engl.* **1982**, *21*, 492; (b) Baudler, M.; Glinka, K. *Chem. Rev.* **2002**, *93*, 1623.
58. (a) Baudler, M.; Schnalke, M.; Wiaterk, Ch. Z. *Anorg. Allg. Chem.* **1990**, *585*, 7; (b) Baudler, M.; Schnalke, M. Z. *Anorg. Allg. Chem.* **1990**, *585*, 18.
59. Baudler, M.; Jachow, H.; Germeshausen, J. Z. *Anorg. Allg. Chem.* **1987**, *553*, 15.
60. Baudler, M.; Jachow, H.; Floruss, A.; Hasenbach, J. *Chem. Ber.* **1991**, *124*, 1153.
61. Baudler, M.; Aktalay, Y.; Arndt, V.; Tebbe, K.-F.; Feh<sup>e</sup>r, M. *Angew. Chem. Int. Ed. Engl.* **1983**, *22*, 1002.
62. Baudler, M.; Jachow, H.; Tebbe, K. F. Z. *Anorg. Allg. Chem.* **1991**, *593*, 9.
63. (a) Baudler, M.; Jachow, H.; Lieser, B.; Tebbe, K.-F.; Feh<sup>e</sup>r, M. *Angew. Chem. Int. Ed. Engl.* **1989**, *28*, 1231; (b) Baudler, M.; Jachow, H. Z. *Anorg. Allg. Chem.* **1990**, *580*, 27.
64. Baudler, M.; Hasenbach, J.; Jachow, H. Z. *Anorg. Allg. Chem.* **1994**, *620*, 2021.
65. Baudler, M.; Oehlert, W.; Kmiecick, A.; Floruss, A. Z. *Anorg. Allg. Chem.* **1992**, *611*, 43.
66. Baudler, M.; Jachow, H.; Oehlert, W.; Kmiecick, A.; Floruss, A. Z. *Anorg. Allg. Chem.* **1992**, *616*, 19.
67. (a) Baudler, M.; Arndt, V. Z. *Naturforsch.* **1984**, *B39*, 275; (b) Baudler, M.; Schlitte, S.; Hasenbach, J. Z. *Anorg. Allg. Chem.* **1988**, *560*, 7; (c) Baudler, M.; Hahn, J.; Arndt, V.; Koll, B.; Kazmierczak, K.; Daerr, E. Z. *Anorg. Allg. Chem.* **1986**, *538*, 7.
68. Holschumacher, D.; Bannenberg, T.; Ibrorn, K.; Daniliuc, C. G.; Jones, P. G.; Tamm, M. *Dalton Trans.* **2010**, *39*, 10590.
69. Binnewies, M.; Milke, E. *Thermochemical Data of Elements and Compounds*. Wiley-VCH: Weinheim, 2002.
70. Peng, Y.; Fan, H.; Zhu, H.; Roesky, H. W.; Magull, J.; Hughes, C. H. *Angew. Chem. Int. Ed.* **2004**, *43*, 3443.
71. Dohmeier, C.; Schn<sup>o</sup>ckel, H.; Robl, C.; Schneider, U.; Ahlrichs, R. *Angew. Chem. Int. Ed. Engl.* **1994**, *33*, 199.
72. Henke, P.; Schn<sup>o</sup>ckel, H. *Chem. Eur. J.* **2009**, *15*, 13391.
73. Prabusankar, G.; Doddi, A.; Gemel, C.; Winter, M.; Fischer, R. A. *Inorg. Chem.* **2010**, *49*, 7976.
74. Uhl, W.; Beuter, M. *Chem. Commun.* **1999**, 771.
75. Cossairt, B. M.; Cummins, C. C. *Chem. Eur. J.* **2010**, *16*, 12603.
76. Power, M. B.; Barron, A. R. *Angew. Chem. Int. Ed. Engl.* **1991**, *30*, 1353.
77. (a) Scherer, O. J.; Swarowsky, M.; Wolmersh<sup>u</sup>ser, G. *Angew. Chem. Int. Ed. Engl.* **1988**, *27*, 694; (b) Scherer, O. J.; Swarowsky, M.; Wolmersh<sup>u</sup>ser, G. *Organometallics* **1989**, *8*, 841; (c) Yakhvarov, D.; Barbaro, P.; Gonsalvi, L.; Carpio, S. M.; Midollini, S.; Orlandini, A.; Peruzzini, M.; Sinyashin, O.; Zanobini, F. *Angew. Chem. Int. Ed.* **2006**, *45*, 4182; (d) Scheer, M.; Troitzsch, C.; Jones, P. G. *Angew. Chem. Int. Ed. Engl.* **1992**, *31*, 1377; (e) Scheer, M.; Becker, U.; Huffman, J. C.; Chisholm, M. H. J. *Organomet. Chem.* **1993**, *461*, C1.
78. K<sup>o</sup>ppe, R.; Steiner, J.; Schn<sup>o</sup>ckel, H. Z. *Anorg. Allg. Chem.* **2003**, *629*, 2168.
79. Gao, S.; Lun, J.; Chen, N.; Zhano, Y.; Xie, Y. *Chem. Commun.* **2002**, 3064.
80. Yan, P.; Xie, Y.; Wang, W.; Liu, F.; Qian, Y. *J. Mat. Chem.* **1999**, *9*, 1831.
81. Zheng, X.; Liu, C.; Xie, Y. *Eur. J. Inorg. Chem.* **2006**, 2364.
82. Liu, Z.; Kumbhar, A.; Xu, D.; Zhang, J.; Sun, Z.; Fang, J. *Angew. Chem. Int. Ed.* **2008**, *47*, 3540.
83. Carenon, S.; Demange, M.; Shi, J.; Boissiere, C.; Sanchez, C.; Le Floch, P.; M<sup>e</sup>zailles, N. *Chem. Commun.* **2010**, *46*, 5578.
84. Fox, A. R.; Wright, R. J.; Rivard, E.; Power, P. P. *Angew. Chem. Int. Ed.* **2005**, *44*, 7729.
85. Deacon, G. B.; Parrott, J. C. J. *Organomet. Chem.* **1970**, *22*, 287.
86. (a) Maier, L. *Fortschr. Chem. Forsch.* **1971**, *19*, 1; (b) Riesel, L. Z. *Chem.* **1979**, *19*, 161; (c) Lehmann, H. A.; Grossmann, G. *Pure Appl. Chem.* **1980**, *52*, 905; (d) Schmidpeter, A. *Nova Acta Leopoldina* **1985**, *59*, 69; (e) Riesel, L. *Mitteilungsblatt Chem.* **1987**, *34*, 74; (f) Trofimov, B. A.; Gusarova, N. K. *Mendeleev Commun.* **2009**, *19*, 295.
87. Rauhut, M. M.; Semsel, A. M. J. *Org. Chem.* **1963**, *28*, 471.
88. (a) Rauhut, M. M.; Semsel, A. M. J. *Org. Chem.* **1963**, *28*, 473; (b) Cowley, A. H.; Pinnel, R. P. *Inorg. Chem.* **1966**, *5*, 1463; (c) Rauhut, M. M.; Semsel, A. M. J. *Org. Chem.* **1962**, *28*, 473; (d) Trofimov, B.; Brandsma, L.; Arbutzova, S.; Gusarova, N. *Russ. Chem. Bull.* **1997**, *46*, 849; (e) Trofimov, B. A.; Brandsma, L.; Arbutzova, S. N.; Gusarova, N. K. *Russ. J. Gen. Chem.* **1997**, *67*, 322; (f) Arbutzova, S. N.; Brandsma, L.; Gusarova, N. K.; Nikitin, M. V.; Trofimov, B. A. *Mendeleev Commun.* **2000**, *10*, 66.
89. Fritz, G.; H<sup>o</sup>rer, J. Z. *Anorg. Allg. Chem.* **1983**, *504*, 23.
90. Riedel, R.; Hausen, H.-D.; Fluck, E. *Angew. Chem. Int. Ed. Engl.* **1985**, *24*, 1056.
91. H<sup>u</sup>bner, A.; Bernert, T.; S<sup>o</sup>nger, I.; Allig, E.; Bolte, M.; Fink, L.; Wagner, M.; Lerner, H.-W. *Dalton Trans.* **2010**, *39*, 7528.
92. Charrier, C.; Maigrot, N.; Ricard, L.; Le Floch, P.; Mathey, F. *Angew. Chem. Int. Ed. Engl.* **1996**, *35*, 2133.
93. (a) Schmidpeter, A.; Burget, G.; Zwaschka, F.; Sheldrick, W. S. Z. *Anorg. Allg. Chem.* **1985**, *527*, 17; (b) Schmidpeter, A.; Burget, G. *Inorg. Synth.* **1989**, *25*, 126.
94. (a) Fisher, K.; Dance, I.; Willet, G. *Eur. Mass Spectrom.* **1997**, *3*, 331; (b) Fisher, K. J.; Dance, I. G.; Willet, G. D. *Eur. Mass Spectrom.* **1996**, *2*, 369.

95. (a) Budnikova, Y. H.; Yakhvarov, D. G.; Sinyashin, O. G. *J. Organomet. Chem.* **2005**, *690*, 2416 and references cited therein; (b) Kargin, Y. M.; Budnikova, Y. H.; Martynov, B. I.; Turygin, V. V.; Tomilov, A. P. *J. Electroanalytical Chem.* **2001**, *507*, 157; (c) Budnikova, Y.; Tazeev, D.; Gryaznova, T.; Sinyashin, O. *Russ. J. Electrochem.* **2006**, *42*, 1127; (d) Budnikova, Y. H.; Krasnov, S. A.; Graznova, T. V.; Tomilov, A. P.; Turygin, V. V.; Magdeev, I. M.; Sinyashin, O. G. *Phosphorus, Sulfur Silicon Relat. Elem.* **2008**, *183*, 513; (e) Budnikova, Y. H.; Katiyatullina, A. G.; Sinyashin, O. G.; Abdreimova, R. R. *Russ. Chem. Bull.* **2003**, *52*, 929; (f) Budnikova, Y. H.; Kargin, Y. M.; Sinyashin, O. G. *Phosphorus, Sulfur Silicon Relat. Elem.* **1999**, *144–146*, 565; (g) Turygin, V. V.; Igumnov, M. S.; Tomilov, A. P. *Russ. J. Electrochem.* **1999**, *35*, 303; (h) Turygin, V. V.; Khudenko, A. V.; Tomilov, A. P. *Russ. J. Electrochem.* **1999**, *35*, 306; (i) Romakhin, A. S.; Nikitin, E. V. *Russ. J. General Chem.* **1998**, *68*, 1023; (j) Fritz, H. P.; Huber, O. S. *Z. Naturforsch.* **1980**, *B35*, 530.
96. Damrauer, R.; Pusede, S. E.; Staton, G. M. *Organometallics* **2008**, *27*, 3399.
97. Masuda, J. D.; Schoeller, W. W.; Donnadieu, B.; Bertrand, G. *J. Am. Chem. Soc.* **2007**, *129*, 14180.
98. Masuda, J. D.; Schoeller, W. W.; Donnadieu, B.; Bertrand, G. *Angew. Chem. Int. Ed.* **2007**, *46*, 7052.
99. Back, O.; Kuchenbeiser, G.; Donnadieu, B.; Bertrand, G. *Angew. Chem. Int. Ed.* **2009**, *48*, 5530.
100. Tofan, D.; Cummins, C. C. *Angew. Chem. Int. Ed.* **2010**, *49*, 7516.
101. (a) Barton, D. H. R.; Zhu, J. *J. Am. Chem. Soc.* **1993**, *115*, 2071; (b) Barton, D. H. R.; Embse, R. A. V. *Tetrahedron* **1998**, *54*, 12475.
102. Cossairt, B. M.; Cummins, C. C. *New J. Chem.* **2010**, *34*, 1533.
103. Douthwaite, R. E.; Green, M. L. H.; Heyes, S. J.; Rosseinsky, M. J.; Turner, J. F. C. *J. Chem. Soc., Chem. Commun.* **1994**, 1367.
104. Chan, W. T. K.; Garcia, F.; Hopkins, A. D.; Martin, L. C.; McPartlin, M.; Wright, D. S. *Angew. Chem. Int. Ed.* **2007**, *46*, 3084.
105. (a) Wiberg, N.; Wörner, A.; Karaghiosoff, K.; Fenske, D. *Chem. Ber.* **1997**, *130*, 135; (b) Lerner, H.-W.; Margraf, G.; Kaufmann, L.; Bats, J. W.; Bolte, M.; Wagner, M. *Eur. J. Inorg. Chem.* **2005**, 1932; (c) Lerner, H.-W.; Bolte, M.; Karaghiosoff, K.; Wagner, M. *Organometallics* **2004**, *23*, 6073; (d) Lorbach, A.; Nadj, A.; Tüllmann, S.; Dornhaus, F.; Schödel, F.; Sängler, I.; Margraf, G.; Bats, J. W.; Bolte, M.; Holthausen, M. C.; Wagner, M.; Lerner, H.-W. *Inorg. Chem.* **2009**, *48*, 1005.
106. (a) Piro, N. A.; Cummins, C. C. *J. Am. Chem. Soc.* **2009**, *131*, 8764; (b) Baudler, M.; de Riese-Meyer, L. Z. *Naturforsch. B* **1996**, *51*, 101; (c) Fritz, G.; Vaahs, T.; Jarmer, M. Z. *Anorg. Allg. Chem.* **1990**, *589*, 12; (d) Fritz, G.; Stoll, K. Z. *Anorg. Allg. Chem.* **1986**, *538*, 113; (e) Fritz, G.; Haerer, J. Z. *Anorg. Allg. Chem.* **1983**, *500*, 14.
107. Wiberg, N.; Wörner, A.; Lerner, H.-W.; Karaghiosoff, K.; Nöth, H. Z. *Naturforsch. B* **1998**, *53*, 1004.
108. Lerner, H.-W. *Coord. Chem. Rev.* **2005**, *249*, 781.
109. Lerner, H.-W.; Wagner, M.; Bolte, M. *Chem. Commun.* **2003**, 990.
110. Wiberg, N.; Wörner, A.; Lerner, H.-W.; Karaghiosoff, K.; Fenske, D.; Baum, G.; Dransfeld, A.; von Rague Dransfeld, P. *Eur. J. Inorg. Chem.* **1998**, 833.
111. Damrauer, R.; Pusede, S. E. *Organometallics* **2009**, *28*, 1289.
112. Schoeller, W. W. *Theor. Chem. Acc.* **2010**, *127*, 223.
113. Nyíri, K.; Szilvási, T.; Veszprémi, T. *Dalton Trans.* **2010**, *39*, 9347.
114. Haaf, M.; Schmiedl, T.; Schmedake, T. A.; Powell, D. R.; Millevoite, A. J.; Denk, M.; West, R. *J. Am. Chem. Soc.* **1998**, *120*, 12714.
115. Xiong, Y.; Yao, S.; Brym, M.; Driess, M. *Angew. Chem. Int. Ed.* **2007**, *46*, 4511.
116. Xiong, Y.; Yao, S.; Bill, E.; Driess, M. *Inorg. Chem.* **2009**, *48*, 7522.
117. Sen, S. S.; Khan, S.; Roesty, H. W.; Kratzert, D.; Meindl, K.; Henn, J.; Stalke, D.; Demers, J.-P.; Lange, A. *Angew. Chem. Int. Ed.* **2011**, *50*, 2322.
118. (a) Driess, M.; Fanta, A. D.; Powell, D.; West, R. *Angew. Chem. Int. Ed. Engl.* **1989**, *28*, 1038; (b) Fanta, A. D.; Tan, R. P.; Comerlato, N. M.; Driess, M.; Powell, D. R.; West, R. *Inorg. Chim. Acta* **1992**, *198–200*, 733; (c) Driess, M.; Pritzkow, H.; Reisgys, M. *Chem. Ber.* **1993**, *124*, 124.
119. Driess, M. *Angew. Chem. Int. Ed. Engl.* **1991**, *30*, 1022.
120. Mathiasch, B.; Dräger, M. *Angew. Chem. Int. Ed. Engl.* **1978**, *17*, 767.
121. Dräger, M.; Mathiasch, B. *Angew. Chem. Int. Ed. Engl.* **1981**, *20*, 1029.
122. (a) Schuhmann, H. *Angew. Chem. Int. Ed. Engl.* **1969**, *8*, 937; (b) Schuhmann, H.; Köpf, H.; Schmidt, M. Z. *Anorg. Allg. Chem.* **1964**, *331*, 200; (c) Schuhmann, H.; Köpf, H.; Schmidt, M. *Chem. Ber.* **1964**, *97*, 1458.
123. (a) Krebs, H. Z. *Anorg. Allg. Chem.* **1951**, *266*, 175; (b) Street, E. H., Jr.; Gardner, D. M.; Evers, E. C. *J. Am. Chem. Soc.* **1958**, *80*, 1819.
124. (a) Maier, L. *Angew. Chem. Int. Ed. Engl.* **1965**, *4*, 527; (b) Maier, L. *Helv. Chim. Acta* **1967**, *50*, 1723; (c) Maier, L. *Helv. Chim. Acta* **1968**, *51*, 1608; (d) Badeeva, E. K.; Krokhina, S. S.; Ivanov, B. E. *Russ. J. General Chem.* **2003**, *73*, 1376.
125. (a) Jacobs, H.; Kirchgässner, R. Z. *Anorg. Allg. Chem.* **1990**, *581*, 125; (b) Golinski, F.; Jacobs, H. Z. *Anorg. Allg. Chem.* **1994**, *620*, 965.
126. Riesel, L.; Kant, M. Z. *Anorg. Allg. Chem.* **1985**, *531*, 73.
127. Westerhausen, M.; Kneifel, A. N.; Mayer, P. Z. *Anorg. Allg. Chem.* **2006**, *632*, 634.
128. Köchner, T.; Riedel, S.; Lehner, A. J.; Scherer, H.; Raabe, I.; Engesser, T. A.; Scholz, F. W.; Gellrich, U.; Eiden, P.; Paz Schmidt, R. A.; Plattner, D. A.; Krossing, I. *Angew. Chem. Int. Ed.* **2010**, *49*, 8139.
129. Knoll, F.; Bergerhoff, G. *Monatsh. Chem.* **1966**, *97*, 808.
130. Schmidpeter, A.; Burget, G. *Phosphorus, Sulfur Rel. Elem.* **1985**, *22*, 323.
131. (a) Schmidpeter, A.; Burget, G.; von Schnering, H.-G.; Weber, D. *Angew. Chem. Int. Ed. Engl.* **1984**, *23*, 816; (b) Schmidpeter, A.; Lochschmidt, S.; Burget, G.; Sheldrick, W. S. *Phosphorus, Sulfur Silicon Relat. Elem.* **1983**, *18*, 23.
132. Schmidpeter, A.; Burget, G.; Sheldrick, W. S. *Chem. Ber.* **1985**, *118*, 3849.
133. (a) Hönle, W.; von Schnering, G. H. *Phosphorus, Sulfur Silicon Relat. Elem.* **1987**, *30*, 775; (b) von Schnering, H. G.; Hönle, W. *Chem. Rev.* **1988**, *88*, 243.
134. Alvarez, M. A.; García, M. E.; García-Vivó, D.; Ramos, A.; Ruiz, M. A. *Inorg. Chem.* **2011**, *50*, 2064.
135. Bezombes, J.-P.; Hitchcock, P. B.; Lappert, M. F.; Nycz, J. E. *Dalton Trans.* **2004**, 499.
136. Cossairt, B. M.; Cummins, C. C. *J. Am. Chem. Soc.* **2009**, *131*, 15501.
137. (a) Krossing, I.; Raabe, I. *Angew. Chem. Int. Ed.* **2001**, *40*, 4406; (b) Gonsior, M.; Krossing, I.; Müller, L.; Raabe, I.; Jansen, M.; van Wüllen, L. *Chem. Eur. J.* **2002**, *8*, 4475.
138. Dyker, C. A.; Burford, N. *Chem. Asian J.* **2008**, *3*, 28 and references therein.
139. Weigand, J. J.; Holthausen, M.; Fröhlich, R. *Angew. Chem. Int. Ed.* **2009**, *48*, 295.
140. Holthausen, M. H.; Weigand, J. J. *J. Am. Chem. Soc.* **2009**, *131*, 14210.
141. Holthausen, M. H.; Richter, C.; Hepp, A.; Weigand, J. J. *Chem. Commun.* **2010**, *46*, 6921.
142. Wood, E. E. C.; Johnson, F. G. *J. Appl. Phys.* **1995**, *78*, 4444.
143. Bell, I. S.; Qian, H.-B.; Hamilton, P. A.; Davies, P. B. *J. Chem. Phys.* **1997**, *107*, 8311.
144. Ahmad, I. K.; Hamilton, P. A. *J. Am. Chem. Soc.* **1996**, *118*, 1126.
145. Chang, S.-G.; Hu, K.; Wang, Y. *J. Environ. Sci.* **1994**, *6*, 1.
146. Grossmann, G.; Ryong, C. M. Z. *Chem.* **1984**, *24*, 135.
147. Hu, K.; Wang, Y.; Chang, S.-G. *Huanjing Kexue Xuebao* **1995**, *15*, 199.
148. Miao, X.; Chu, S.; Xu, X.; Hu, K. *Zhongguo Huanjing Kexue* **1996**, *16*, 373.
149. (a) Dorfman, Ya. A.; Aleshkova, M. M.; Polimbetova, G. S.; Levina, L. V.; Petrova, T. V.; Abdreimova, R. R.; Doroshkevich, D. M. *Russ. Chem. Rev.* **1993**, *62*, 877; (b) Dorfman, Ya. A.; Abdreimova, R. R.; Polimbetova, G. S.; Aibasova, S. M.; Akbaeva, D. N. *Kinetics and Catalysis* **1996**, *37*, 183; (c) Abdreimova, R. R.; Tamuleniene, J.; Peruzzini, M.; Balevicius, M. L. *Inorg. Chim. Acta* **2000**, *307*, 71.
150. Andrews, L.; Mc Cluskey, M.; Mielke, Z.; Whitnall, R. J. *Mol. Struct.* **1990**, *222*, 95.
151. Andrews, L.; Whitnall, R. J. *J. Am. Chem. Soc.* **1988**, *110*, 5605.
152. Hamilton, P. A.; Murrells, T. P. *J. Phys. Chem.* **1986**, *90*, 182.
153. (a) Auger, V. *Compt. Rend.* **1904**, *139*, 639; (b) Michaelis, A.; Pitch, M. *Chem. Ber.* **1899**, *32*, 337; (c) Michaelis, A.; Pitch, M. *Liebigs Ann.* **1900**, *310*, 45; (d) Michaelis, A.; Chapman, D. L.; Lindbury, A. F. *J. Chem. Soc.* **1899**, *75*, 973; (e) Michaelis, A.; von Arend, K. *Liebigs Ann.* **1901**, *314*, 259; (f) Michaelis, A.; Burgess, C. H.; Chapman, D. L. *J. Chem. Soc.* **1901**, *79*, 1235.
154. Rauhut, M. M.; Bernheimer, R.; Semsel, A. M. *J. Org. Chem.* **1963**, *28*, 478.
155. (a) Malysheva, S.; Sukhov, B.; Gusarova, N.; Shaikhudinova, S.; Kazantseva, T. I.; Belogorlova, N. I.; Kuimov, V.; Trofimov, B. *Phosphorus, Sulfur Silicon Relat. Elem.* **2003**, *178*, 425; (b) Gusarova, N. K.; Arbuszova, S. N.; Shaikhudinova, S. I.; Kazantseva, T. I.; Reutskaya, A. M.; Ivanova, N. I.; Papernaya, L.; Trofimov, B. A. *Phosphorus, Sulfur Silicon Relat. Elem.* **2001**, *175*, 163.
156. (a) Trofimov, B.; Gusarova, N.; Malysheva, S.; Kuimov, V.; Sukhov, B.; Shaikhudinova, S.; Tarasova, N.; Smetannikov, Y.; Sinyashin, O.; Budnikova, Y.; Kazantseva, T.; Smirnov, V. *Russ. J. Gen. Chem.* **2005**, *75*, 1367; (b) Gusarova, N. K.; Shaikhudinova, S. I.; Kazantseva, T. I.; Sukhov, B. G.; Dmitriev, V. I.; Sinegovskaya, L. M.; Smetannikov, Y. V.; Tarasova, N. P.; Trofimov, B. A. *Chem. Heterocycl. Compd.* **2001**, *37*, 576; (c) Gusarova, N. K.; Sukhov, B. G.; Malysheva, S. F.; Kazantseva, T. I.; Smetannikov, Y. V.; Tarasova, N. P.; Trofimov, B. A. *Russ. J. Gen. Chem.* **2001**, *71*, 721.
157. (a) Brown, C.; Hudson, R. F.; Wartew, G. A.; Coates, H. *Phosphorus, Sulfur Silicon Relat. Elem.* **1979**, *6*, 481; (b) Brown, C.; Hudson, R. F.; Wartew, G. A.; Coates, H. *J. Chem. Soc., Chem. Commun.* **1978**, *7*; (c) Brandsma, L.; van Doom, J. A.; de Lang, R.-J.; Gusarova, N. K.; Trofimov, B. A. *Mendeleev Commun.* **1995**, *5*, 14; (d) Riesel, L. Z. *Chem.* **1979**, *19*, 161 and references cited therein.
158. Berthaud, J. *Compt. Rend.* **1906**, *143*, 1166.
159. Fluck, E.; Riedel, R.; Fischer, P. *Phosphorus, Sulfur Silicon Relat. Elem.* **1987**, *33*, 115.
160. (a) Akbayeva, D. N.; Faisova, F. K.; Abdreimova, R. R.; Peruzzini, M. *J. Mol. Catal. A: Chem.* **2007**, *267*, 181; (b) Trofimov, B.; Timokhin, B.; Gusarova, N.;

- Kazantseva, M.; Golubin, A. *Phosphorus, Sulfur Silicon Relat. Elem.* **2002**, *177*, 2385.
161. Abdreimova, R. R.; Akbayeva, D. N.; Polimbetova, G. S.; Caminade, A.-M.; Majorals, J.-P. *Phosphorus, Sulfur Silicon Relat. Elem.* **2000**, *156*, 239.
162. Mal, P.; Breiner, B.; Rissanen, K.; Nitschke, J. R. *Science* **2009**, *324*, 1697.
163. For a newer publication: Jason, M. E.; Ngo, T.; Rahman, S. *Phos. Res. Bull.* **1996**, *6*, 127.
164. Jason, M. E.; Ngo, T.; Rahman, S. *Inorg. Chem.* **1997**, *36*, 2633.
165. (a) Badeeva, E. K.; Batyeva, E. S.; Gubaidullin, A. T.; Litvinov, I. A.; Sinyashin, O. G. *Russ. J. General Chem.* **2005**, *75*, 835; (b) Brown, C.; Hudson, R. F.; Wartew, G. A. *Phosphorus, Sulfur Silicon Relat. Elem.* **1978**, *5*, 67; (c) Brown, C.; Hudson, R. F.; Wartew, G. A. *Phosphorus, Sulfur Silicon Relat. Elem.* **1978**, *5*, 121; (d) Brown, C.; Hudson, R. F.; Wartew, G. A. *J. Chem. Soc., Perkin Trans. 1* **1979**, 1799; (e) Brown, C.; Hudson, R. F.; Wartew, G. A. *Inorg. Synth.* **1983**, *22*, 131.
166. (a) Falius, H.; Krause, W.; Sheldrick, W. S. *Angew. Chem. Int. Ed. Engl.* **1981**, *20*, 103; (b) Falius, H.; Schliephake, A. *Inorg. Synth.* **1989**, *25*, 5.
167. (a) Krause, W.; Falius, H. Z. *Anorg. Allg. Chem.* **1983**, *496*, 80; (b) Falius, H.; Schliephake, A.; Schomburg, D. Z. *Anorg. Allg. Chem.* **1992**, *611*, 141; (c) Gruber, H.; Müller, U. Z. *Anorg. Allg. Chem.* **1997**, *623*, 957.
168. Tattershall, B. W.; Kendall, N. L. *Polyhedron* **1994**, *13*, 2629.
169. (a) Wu, C. *J. Am. Chem. Soc.* **1965**, *87*, 2522; (b) Milyukov, V. A.; Zverev, A. V.; Podlesnov, S. M.; Krivolapov, D. B.; Litvinov, I. A.; Gubaidullin, A. T.; Kataeva, O. N.; Ginzburg, A. G.; Sinyashin, O. G. *Eur. J. Inorg. Chem.* **2000**, 225.
170. Rotter, C.; Schuster, M.; Karaghiosoff, K. *Inorg. Chem.* **2009**, *48*, 7531.
171. Tattershall, B. W.; Kendall, N. L. *Polyhedron* **1994**, *13*, 1517.
172. Crossing, I. J. *J. Chem. Soc. Dalton Trans.* **2002**, 500.

## 1.37 Alkaline Earth Chemistry: Synthesis and Structures

TP Hanusa, EJ Bierschenk, LK Engerer, KA Martin, and NR Rightmire, Vanderbilt University, Nashville, TN, USA

© 2013 Elsevier Ltd. All rights reserved.

<b>1.37.1</b>	<b>Introduction</b>	1134
1.37.1.1	Occurrence and General Properties	1134
1.37.1.2	Oxidation States and Metal–Metal Bonding	1134
<b>1.37.2</b>	<b>Synthesis</b>	1135
1.37.2.1	Redox Reactions	1136
1.37.2.1.1	Direct metallation	1136
1.37.2.1.2	Transmetallation	1136
1.37.2.2	Metathetical Methods	1136
1.37.2.2.1	Salt metathesis	1136
1.37.2.2.2	Transamination reactions	1137
1.37.2.2.3	Elimination reactions	1137
1.37.2.2.4	Alkoxide transfer	1137
<b>1.37.3</b>	<b>Structural Features</b>	1137
1.37.3.1	General Considerations	1137
1.37.3.2	Specialized Features	1138
1.37.3.2.1	Group 2 metals and their electropositive neighbors	1138
1.37.3.2.2	'Bent' molecules; use of d orbitals in bonding	1138
1.37.3.2.3	Cation– $\pi$ interactions	1139
<b>1.37.4</b>	<b>Ligand Types</b>	1139
1.37.4.1	Macrocyclic Compounds	1139
1.37.4.1.1	Porphyrins and phthalocyanines	1139
1.37.4.1.2	Crown Ethers	1141
1.37.4.2	Nonmacrocyclic Compounds	1143
1.37.4.2.1	Hydrides and hydroborates	1143
1.37.4.2.2	Group 14 ligands	1145
1.37.4.2.3	Group 15 ligands	1157
1.37.4.2.4	Group 16 ligands	1165
1.37.4.2.5	Group 17 ligands	1176
<b>1.37.5</b>	<b>Conclusion</b>	1180
<b>References</b>		1180

### Abbreviations

<b>acac</b>	2,4-Pentanedionate	<b>dmsO</b>	Dimethylsulfoxide
<b>Ae</b>	Alkaline-earth (group 2) metal	<b>hmpa</b>	Hexamethylphosphoramide
<b>ALD</b>	Atomic layer deposition	<b>hppH</b>	1,3,4,6,7,8-Hexahydro-2H-pyrimido[1,2-a]pyrimidine
<b>BHT</b>	2,6-Di- <i>t</i> -Bu-4-methylphenolate	<b><i>i</i>-Pr-carbene</b>	Isopropyl-4,5-dimethylimidazol-2-ylidene
<b>Bu</b>	Butyl	<b>mes</b>	2,4,6-Trimethylphenyl
<b>Bz</b>	Benzyl	<b>mes*</b>	2,4,6-Tri- <i>t</i> -butylphenyl
<b>COT</b>	Cyclooctatetrene	<b>MOF</b>	Metal–organic framework
<b>Cp</b>	Cyclopentadienyl	<b>nacnac</b>	$\beta$ -Diketiminato, particularly [CH{ArNCR} <sub>2</sub> ] <sup>−</sup> (Ar = aryl; R = CH <sub>3</sub> or bulkier group)
<b>Cp'</b>	1,2,3,4-Tetraphenylcyclopentadienyl		
<b>Cp<sup>3Si</sup></b>	1,2,4-Tris(trimethylsilyl)cyclopentadienyl	<b>nta</b>	Nitrilotriacetic acid
<b>CVD</b>	Chemical vapor deposition	<b>OAc</b>	Acetate
<b>Cy</b>	Cyclohexyl	<b>Odbp</b>	2,6-Dibenzylphenolate
<b>DFT</b>	Density functional theory	<b>Odipp</b>	2,6-Diisopropylphenolate
<b>diglyme</b>	2,5,8-Trioxanonane	<b>Odpp</b>	2,6-Diphenylphenolate
<b>dipp</b>	2,6-Diisopropylphenyl	<b>pmdeta</b>	<i>N,N,N',N',N''</i> -pentamethyldiethylenetriamine
<b>DIPP-nacnac</b>	[CH{2,6-( <i>i</i> -Pr) <sub>2</sub> C <sub>6</sub> H <sub>3</sub> N}(CMe) <sub>2</sub> ] <sup>−</sup>	<b>pta</b>	5,5-Dimethyl-1,1,1-trifluorohexane-2,4-dionate
<b>dmap</b>	4-Dimethylaminopyridine	<b>py</b>	Pyridyl
<b>dme</b>	Dimethoxyethane		
<b>dmf</b>	Dimethylformamide		
<b>dmit</b>	2-Thioxo-1,3-dithiole-4,5-dithiolate		

pz	Pyrazol-1-yl	tmhd	2,2,6,6-Tetramethylheptane-3,5-dionate
tetraglyme	2,5,8,11,14-Pentaoxapentadecane	tmp	2,2,6,6-Tetramethylpiperidine
TFA	Trifluoroacetate	tmpH	2,2,6,6-Tetramethylpiperidine
thd	2,2,6,6-Tetramethylheptane-3,5-dionate	Tp	Tris(pyrazolyl)borate
THF	Tetrahydrofuran	triglyme	2,5,8,11-Tetraoxododecane
thp	Tetrahydropyran	trip	2,4,6-Triisopropylphenyl
tmeda	<i>N,N,N',N'</i> -tetramethylethylenediamine	Tsi	Tris(trimethylsilyl)methyl

## 1.37.1 Introduction

### 1.37.1.1 Occurrence and General Properties

The elements that comprise group 2 in the periodic table (the alkaline-earth metals, Be to Ra) constitute about 7.5% by mass of the earth's crust, and two of them (Ca and Mg) are among the six most common elements on earth. Even beryllium, the rarest nonradioactive group 2 element (~2 parts per million [ppm]), is about as common as tin and arsenic.<sup>1</sup> Compounds of the alkaline-earth metals have played extraordinarily important roles in human history and science, from the limestone and mortar building materials (containing CaCO<sub>3</sub>, CaO, and MgO) used since the civilizations of ancient Mesopotamia to the radium sources that were essential to establishing the structure of the atom in the early 20th century.

The importance of the group 2 elements to biology cannot be underestimated. Both calcium and magnesium are indispensable to a broad range of cellular functions. Magnesium is critical for photosynthesis in plants (photosystems I and II)<sup>2,3</sup> and for the activity of adenosine triphosphate. Calcium is broadly employed in biological systems as a signal transducer, enzyme cofactor, and structural element (e.g., cell membranes, bones, and teeth). Although strontium is not an essential element for higher life forms (where it behaves much like calcium), marine protozoa belonging to the class *Acantharea* construct their skeletons out of strontium sulfate.<sup>4</sup> Barium sulfate is used as a gravity sensor in the ciliate *Loxodes*.<sup>5</sup> Apart from their direct use by living systems, group 2 compounds find various applications in medicine (e.g., BaSO<sub>4</sub> is employed as a radiopaque agent in x-ray imaging, and one of the first uses for radium salts was as a source of radiation to treat cancer).

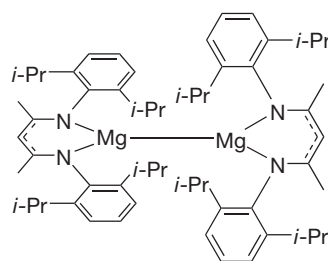
The group 2 elements are all lustrous, silvery metals that, with the exception of beryllium, are relatively soft (Mohs hardness 1.5–2.5; that for Be is 5.5, about the same as molybdenum). The free elements are not found in nature because the metals react in air and all rapidly form an oxide coating on their surface or, in the case of radium, a nitride layer. The oxide layer of beryllium passivates the metal and inhibits further reaction with oxygen or water. One of the few commercial applications for elemental barium takes advantage of its reactivity to air; thin films of the metal are used as getters in vacuum and cathode ray tubes and chemically remove traces of oxygen that otherwise could cause tube failure. Various physical and chemical properties of the metals are listed in Table 1.<sup>6,7</sup>

### 1.37.1.2 Oxidation States and Metal–Metal Bonding

The group 2 metals are divalent elements, and their isolated compounds almost always exhibit the +2 oxidation state. Under

gas phase or low-temperature conditions, low-oxidation-state group 2 species can be generated. Organoalkaline-earth gas-phase radicals MR containing the monovalent metals (M = Mg–Sr; R = Me, CCH, η-Cp, η-pyrrolyl, C≡CCH<sub>3</sub>)<sup>8</sup> have been studied with both experimental and theoretical methods.<sup>9–12</sup> The gas-phase [RaC<sub>2</sub>]<sup>−</sup> ion, formally a radium(I) acetylide, has been produced with a Cs sputter ion source.<sup>13</sup> An IR study of the reaction of laser-ablated beryllium and magnesium atoms with acetylene in argon at 10 K indicates that BeCCH and MgCCH are products<sup>14</sup>; under similar conditions in a methane/argon matrix, BeCH<sub>3</sub> has been identified.<sup>15</sup> Cluster Grignard reagents PhMg<sub>4</sub>X (X = F, Cl, Br) have been prepared by metal-vapor synthesis.<sup>16</sup> The magnesium subhalide MgCl is formed when HCl is passed over hot MgB<sub>2</sub> (700 °C); it transforms into the linear metal–metal-bonded Mg<sub>2</sub>Cl<sub>2</sub> when condensed in a helium matrix at 12 K.<sup>17</sup> Such compounds will not be covered further here; a review of the chemistry of the gas-phase radical species is available,<sup>18</sup> as is a general review of low-oxidation-state group 2 species.<sup>19</sup>

A new era in low-oxidation-state main-group metal<sup>20</sup> chemistry emerged with the synthesis of (C<sub>5</sub>Me<sub>5</sub>)Zn–Zn(C<sub>5</sub>Me<sub>5</sub>), a thermally stable compound (mp = 110 °C) with zinc in the +1 oxidation state.<sup>21</sup> A variety of related compounds soon appeared, featuring either cyclopentadienyl<sup>22</sup> or aryl<sup>23</sup> supporting ligands, and the chemistry was extended to cadmium (I).<sup>23</sup> The LM–ML structural motif was also found to be applicable to magnesium, but with substituted guanidinate and nacnac nitrogen-donor ligands.<sup>24</sup> The Mg–Mg bond length in the LMg–MgL complex with L = [(Ar)NC(N(*i*-Pr)<sub>2</sub>)N(Ar)]<sup>−</sup> and Ar = 2,6-(*i*-Pr)<sub>2</sub>C<sub>6</sub>H<sub>3</sub> **1** (Figure 1) is 2.851(1) Å, and is 2.846(1) Å in the nacnac derivative with L = [(Ar)NC(Me)<sub>2</sub>CH]<sup>−</sup> **2**. These distances are substantially less than the metal–metal separation in elemental magnesium (3.20 Å),<sup>7</sup> and the bonds resist disruption on the addition of base donors such as tetrahydrofuran (THF) or pyridines.<sup>25</sup> Related complexes have been made, such as [K(thf)<sub>2</sub>][LMg–MgL] (L = [2,6-(*i*-Pr)<sub>2</sub>C<sub>6</sub>H<sub>3</sub>]NC(Me)<sub>2</sub>)<sup>2−</sup> with Mg–Mg = 2.9370(18) Å,<sup>26</sup> but this structural motif has not yet been extended to the other group 2 metals.<sup>27</sup> Calculations suggest that CpM–MCp (M = Be, Mg, Ca) complexes might be isolable.<sup>28</sup>

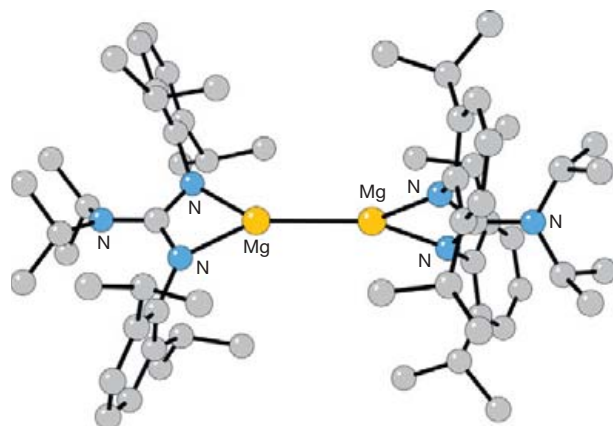
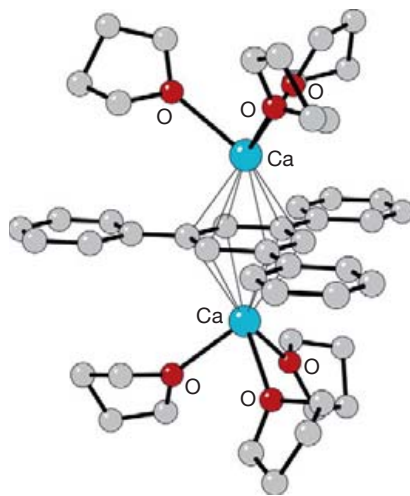


**2**

**Table 1** Atomic and physical properties of the group 2 metals

	<i>Be</i>	<i>Mg</i>	<i>Ca</i>	<i>Sr</i>	<i>Ba</i>	<i>Ra</i>
Atomic number	4	12	20	38	56	88
No. of naturally occurring isotopes	1	3	6	4	7	4 (all radioactive)
Atomic mass	9.01	24.31	40.08	87.62	137.33	226.03 <sup>a</sup>
Electronic configuration	[He]2 s <sup>2</sup>	[Ne]3 s <sup>2</sup>	[Ar]4 s <sup>2</sup>	[Kr]5 s <sup>2</sup>	[Xe]6 s <sup>2</sup>	[Rn]7 s <sup>2</sup>
Ionization energy (kJ mol <sup>-1</sup> )	899.4 (1st); 1757 (2nd)	737.7 (1st); 1451 (2nd)	589.8 (1st); 1145.4 (2nd)	549.2 (1st); 1064 (2nd)	502.7 (1st); 965 (2nd)	509.3 (1st); 979.0 (2nd)
Metal radius (Å) 2.22 Å	1.12	1.60	1.97	2.15	2.24	~2.3
Ionic radius (six-coordinate)(Å)	0.45	0.72	1.00	1.18	1.35	1.48
E° for M <sup>2+</sup> (aq) + 2e <sup>-</sup> → M(s) (V)	-1.97	-2.36	-2.84	-2.89	-2.91	-2.92
Melting point (°C)	1287	650	842	777	727	700
Boiling point (°C)	2469	1090	1484	1382	1870	1737
Density (20 °C)	1.85	1.74	1.55	2.63	3.51	5.5
Δ <i>H</i> <sub>fus</sub> (kJ mol <sup>-1</sup> )	15	8.9	8.6	8.2	7.8	8.5
Δ <i>H</i> <sub>vap</sub> (kJ mol <sup>-1</sup> )	309	127	155	137	136	113
Electrical resistivity (20 °C) μ ohm <sup>-1</sup> cm <sup>-1</sup>	3.7	4.5	3.4	13.5	34	100

<sup>a</sup>Isotope with the longest half-life (<sup>226</sup>Ra, 1600 years).

**Figure 1** Structure of the Mg–Mg-bonded complex **1**.**Figure 2** Structure of the Ca(I) complex (thf)<sub>3</sub>Ca<sup>+</sup>[1,3,5-Ph<sub>3</sub>C<sub>3</sub>H<sub>3</sub>]<sup>2-</sup>Ca<sup>+</sup>(thf)<sub>3</sub> **3**.

The exact nature of the metal–metal bond in the diamagnetic magnesium–magnesium-bonded complexes (like their zinc and cadmium analogs) has been a subject of some dispute, although the metal centers are generally considered to be monovalent.<sup>19</sup> Calculations have suggested that the charges on the magnesium in **2** are low ( $q < +1.2$ ) and that the compound contains covalently bonded Mg in an [Mg<sub>2</sub>]<sup>2+</sup> unit ionically coordinated to the anionic ligands.<sup>29</sup> On formal grounds, however, the metal centers have been described as divalent, given that both valence electrons of the metal centers are involved in bonding.<sup>30</sup>

An indisputably monovalent group 2 complex **3** that is stable above room temperature (dec. >71 °C) was isolated from the reduction of 1,3,5-triphenylbenzene with calcium metal and isolated as a THF adduct (**Figure 2**). Although several different distributions of bonding electrons could be proposed for the black, neutral complex, the results of structural, magnetic ( $S = 1$  [triplet]; ESR resonance at  $g = 2.0023$ ), and computational investigations indicate that the complex should be formulated as (thf)<sub>3</sub>Ca<sup>+</sup>[1,3,5-Ph<sub>3</sub>C<sub>3</sub>H<sub>3</sub>]<sup>2-</sup>Ca<sup>+</sup>(thf)<sub>3</sub>; that is, that the calcium centers have 4s<sup>1</sup> electron configurations. The L<sub>n</sub>M(μ, η<sup>6</sup>-arene) ML<sub>n</sub> framework has not yet been replicated with other alkaline-earth metals. The burgeoning area of low-oxidation-state group 2 chemistry, from both an experimental and a computational viewpoint, has been critically reviewed.<sup>19,31</sup>

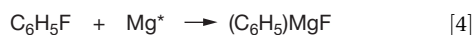
### 1.37.2 Synthesis

A general overview of strategies that have been developed for the synthesis of alkaline-earth coordination and organometallic compounds is given below. These categories are meant to be suggestive, and some preparative routes could fall under more than one grouping. Specialized approaches will be detailed in the context of specific compounds. Reviews of synthetic approaches to group 2 compounds have been published previously.<sup>32,33</sup>

### 1.37.2.1 Redox Reactions

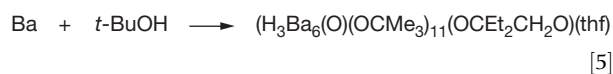
#### 1.37.2.1.1 Direct metallation

The alkaline-earth metals themselves serve as the starting point for many compounds, although the success of the method depends on the acidity of the ligand (e.g., eqns [1]–[3]). The metals have been used in the form of ingots,<sup>34</sup> powders<sup>35–37</sup> (including ball-milled<sup>38,39</sup>), vapor,<sup>40–45</sup> or as activated by amalgamation,<sup>46</sup> treatment with iodine, ammonia,<sup>47–51</sup> or the application of ultrasound.<sup>52–54</sup> These approaches represent attempts to overcome the often low reactivity of the bulk metals in nonaqueous media, a consequence of their readily passivated metal surfaces. The “Rieke metal” approach, which produces the finely divided metal (M\*) by reduction of a group 2 halide with an alkyl lithium or the alkali metals themselves,<sup>35,36,55</sup> extends the range of substrates that are accessible to group 2 species. For example, aryl fluorides, which are unreactive with bulk magnesium, can be used to produce the corresponding Grignard reagents (e.g., eqn [4]).<sup>55</sup>



In other cases, finely divided metals greatly enhance the speed of reactions. For example, the formation of calcium hexa- and trifluoroacetylacetonate from bulk calcium and the respective acetylacetonates requires 5 days or more,<sup>56</sup> whereas with activated Ca powder, the corresponding reactions require only 1 h,<sup>35</sup> a 100-fold enhancement in rate. Sonoelectrochemistry has been used to produce nanometer-sized particles of magnesium, although these have not yet been used in synthesis.<sup>57</sup>

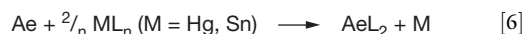
Despite whether the metal is activated, the direct metallation route has limitations, apart from the necessary acidity of the ligand. The toxicity of mercury must be considered in the use of metals activated by amalgamation, although the possible formation of mercury-containing by-products rarely seems to be a problem in practice. Potentially more serious is attack on the solvent media itself by the metals, which, in the case of ethers, may lead to the formation of oxido ligands. When *t*-butanol reacts with barium metal, for example, a diolato ligand is found coordinated to the metal in the product (eqn [5]). Because the diolate is not formed in toluene, the THF solvent is its most likely source.<sup>58</sup>



In some cases, it is possible to dispense with the solvent entirely. Heating alkaline-earth metals in sealed glass vessels under a vacuum in the presence of a desired ligand alone or with a low-melting flux agent (e.g., 1,3,5-(*t*-Bu)<sub>3</sub>C<sub>6</sub>H<sub>3</sub>, 1,2,4,5-Me<sub>4</sub>C<sub>6</sub>H<sub>2</sub>) can generate base-free complexes. The method has been used to prepare pyrazolate complexes (e.g., [Sr{(t-Bu)<sub>2</sub>pz}<sub>2</sub>]<sub>4</sub>)<sup>59</sup> and a variety of aryloxide complexes (e.g., KBa(Odpp)<sub>3</sub>, Ae(Odbp)<sub>2</sub> (Ae = Sr, Ba)<sup>61</sup>) that are not readily obtained by other methods. Reaction times at 225–250 °C range from several days to a week.<sup>60</sup>

#### 1.37.2.1.2 Transmetalation

Both mercury and tin compounds have been used to generate alkaline-earth species by metal exchange (eqn [6]). Organomercury reagents HgR<sub>2</sub> (R = N(SiMe<sub>3</sub>)<sub>2</sub>,<sup>62</sup> Ph,<sup>63</sup> C<sub>6</sub>F<sub>5</sub>)<sup>64</sup> have been the most commonly employed; although, in theory, tin reagents are equivalently suitable, they have been used less frequently (e.g., eqn [7]).<sup>65</sup> Related reactions between calcium metal and phenyl copper yield the solvent-separated cuprate [(thf)<sub>3</sub>Ca(μ-Ph)<sub>3</sub>Ca(thf)<sub>3</sub>]<sup>+</sup>[Ph-Cu-Ph]<sup>-66</sup>; diphenylmanganese and calcium react to form the heterobimetallic ion pair [(thf)<sub>3</sub>Ca(μ-Ph)<sub>3</sub>Ca(thf)<sub>3</sub>]<sup>+</sup>[(thf)<sub>2</sub>PhCa(μ-Ph)<sub>3</sub>MnPh]<sup>-67</sup>

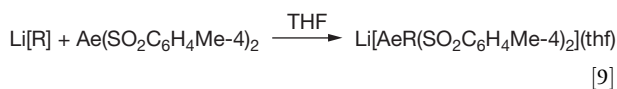
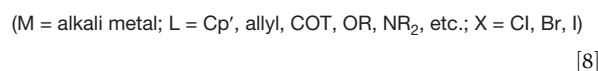
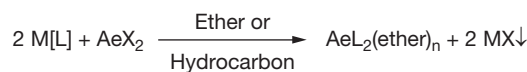


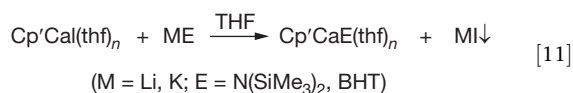
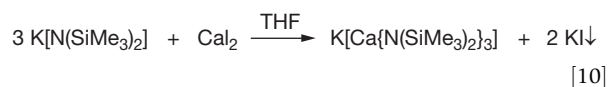
In principle, transmetalation is one of the more versatile synthetic methods and is tolerant of a range of solvent polarities. In practice, it is limited by the availability of the appropriate metal reagents and by the neurotoxicity of mercury and tin compounds.

### 1.37.2.2 Metathetical Methods

#### 1.37.2.2.1 Salt metathesis

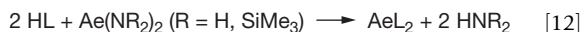
The reaction of an alkali metal salt of a hydrocarbon, alcohol, or amine provides a convenient way to prepare a range of both coordination and organometallic complexes (eqn [8]). It is, perhaps, the most broadly applicable of the general methods, usable with the group 2 metals from beryllium to barium. The most common pairing of reagents has been with potassium salts and alkaline-earth dihalides, particularly the iodides, because removal of the by-product (insoluble alkali metal salts) is the most straightforward with this combination. The use of BeBr<sub>2</sub>(SMe<sub>2</sub>)<sub>2</sub> provides a soluble form of beryllium bromide when ethers must be avoided because it is soluble in Me<sub>2</sub>S and CH<sub>2</sub>Cl<sub>2</sub>.<sup>68</sup> Complications can occur with lithium-based reagents, which seem especially prone to the formation of anionic “ate” complexes (e.g., eqn [9]).<sup>69,70</sup> Such reactions also can occur with potassium salts (e.g., eqn [10]) and can be insidious because the presence of the potassium may not be easy to detect.<sup>71</sup> For example, some types of calcate complexes, e.g., K<sub>x</sub>Ca<sub>y</sub>[N(SiMe<sub>3</sub>)<sub>2</sub>]<sub>x+2y</sub>, can form with substoichiometric amounts of K[N(SiMe<sub>3</sub>)<sub>2</sub>], and calcates of the type (L)<sub>n</sub>K<sub>2</sub>Ca [N(Ph)R]<sub>4</sub> (L = neutral coligands) form during the metathesis reaction of K[N(Ph)R] with CaI<sub>2</sub> if any excess of the potassium amide is present, even if not in exact stoichiometric ratio.<sup>72</sup> Halide metathesis can also be used to derivatize existing group 2 compounds, as in eqn [11].<sup>73</sup>





### 1.37.2.2.2 Transamination reactions

This reaction involves the use of an alkaline-earth amide, most commonly a bis(trimethylsilylamide), in an acid–base reaction (eqn [12]).<sup>74</sup> The bis(trimethylsilyl)amides have been especially popular reagents because of their superior solubility (even in hydrocarbons) and the high p*K*<sub>a</sub> of HN(SiMe<sub>3</sub>)<sub>2</sub> (~26 in THF).<sup>75</sup> The use of the bulky bis(trimethylsilyl)amides can be helpful when solvent-free products are desired; the bulky hexamethyldisilazane by-product usually does not bind to the metal centers.<sup>76</sup> In contrast, THF and even Et<sub>2</sub>O used as solvents may form tenacious adducts, and extraction procedures such as the “toluene reflux” method may be required<sup>77</sup>; however, the latter is not always successful.<sup>78</sup> Transamination has been used to synthesize a variety of organometallic and inorganic compounds, including metallocenes,<sup>76,79</sup> heterobimetallic alkoxides,<sup>80</sup> tetraphenylborates,<sup>81</sup> aminotroponate and aminotroponimate calcium amides,<sup>82</sup> heterobimetallic amides,<sup>83</sup> and *N*-heterocyclic carbene adducts.<sup>84,85</sup> They also have been used in hydroamination reactions.<sup>86,87</sup> There are limitations to transamination chemistry; for example, certain substrates (e.g., thiols,<sup>88</sup> fluorinated alcohols<sup>89</sup>) may react with bis(trimethylsilyl)amides and initiate N–Si cleavage reactions.



### 1.37.2.2.3 Elimination reactions

Transfer of a ligand group from an organoalkaline-earth metal complex to form another, typically by protonolysis (eqn [13]), historically has been confined to compounds of magnesium because of the ready availability of dialkyl species (e.g., the commercially available “MgBu<sub>2</sub>,” which is a statistical mixture of (*n*-Bu)<sub>2</sub>Mg and (*s*-Bu)<sub>2</sub>Mg). Magnesocenes,<sup>47</sup> alkoxides,<sup>90,91</sup> aryloxides,<sup>92</sup> thiolates,<sup>93–95</sup> amides,<sup>96–103</sup> pyrazolates,<sup>64</sup> siloxides,<sup>104</sup> molecular hydrides,<sup>105</sup> soluble hydroxides,<sup>106</sup> and inverse crown complexes,<sup>107–110</sup> among many other species, have been formed with this route. The heavier alkaline-earth dibenzyl complexes, Ae(CH<sub>2</sub>Ar)<sub>2</sub>, which eliminate toluene upon reaction, have found specialized applications. The reaction of dibenzyl calcium<sup>71</sup> or substituted derivatives (*p*-Me<sub>3</sub>SiBz, *p*-(*t*-Bu)Bz)<sup>111</sup> and HN(SiMe<sub>3</sub>)<sub>2</sub> provides a halide-free route to Ca[N(SiMe<sub>3</sub>)<sub>2</sub>]<sub>2</sub>.<sup>71</sup> Some application has been made of the heavier Sr(CH<sub>2</sub>Ph)<sub>2</sub> and Ba(CH<sub>2</sub>Ph)<sub>2</sub>,<sup>112–114</sup> but the limited thermal stability of these compounds in solution has prevented their extensive use.



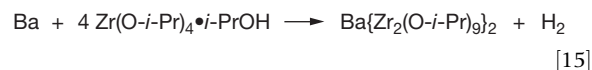
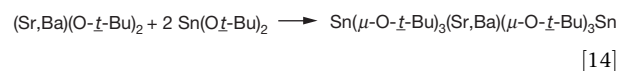
Mixed-metal magnesium/alkali metal reagents can display substantial, yet selective, basicity. For example, bis(benzene)chromium can be deprotonated with a mixture of BuNa or BnK with MgBu<sub>2</sub>, TMPH, and tmeda (1:1:3:1 equiv.).<sup>115</sup> Monometallation occurs on one ring only, yielding MMg[Cr(C<sub>6</sub>H<sub>5</sub>)

(C<sub>6</sub>H<sub>6</sub>)]TMP<sub>2</sub>·tmeda (M=Na, K); in contrast, lithiation reactions metallate both of the benzene rings. Related mixed-metal systems can deprotonate toluene regioselectively at the meta position.<sup>116</sup> The presence of MgBu<sub>2</sub> can affect the toluene metallation ability of NaBu, through the formation of magnesiate anions (e.g., NaMgBu<sub>3</sub> and Na<sub>2</sub>MgBu<sub>4</sub>).<sup>117</sup>

A process based on triphenylbismuth has been used to prepare complexes containing calcium, strontium, and barium.<sup>118,119</sup> Effectively, the BiPh<sub>3</sub> is used to generate a diphenyl metal complex in situ; the latter then reacts with a sufficiently acidic ligand to form the desired product (Scheme 1). The method has been used with alcohols, amines,<sup>118</sup> and cyclopentadienes.<sup>118</sup> To avoid unduly long reaction times with some substrates (up to 4 weeks with HN(SiMe<sub>3</sub>)(dipp)), the alkaline-earth metal should be used in the form of filings and the reaction mixture ultrasonicated; under these conditions, reaction times can be reduced by three-quarters.

### 1.37.2.2.4 Alkoxide transfer

Related to the elimination reactions in Section 1.37.2.2.3 are those involving the transfer of an alkoxide ligand group from a preformed alkoxide. This may be used to generate heterometallic species (e.g., eqn [14]).<sup>120,121</sup> The latter are sometimes available by direct reaction with the metal (e.g., eqn [15]).<sup>122</sup>

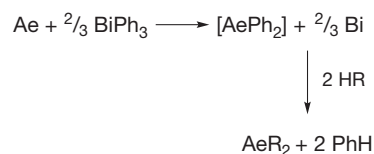


## 1.37.3 Structural Features

### 1.37.3.1 General Considerations

The conventional approach to understanding bonding in group 2 compounds emphasizes the highly electropositive nature of the metals, and, consequently, the strongly polar nature of their bonds to other elements. To the extent that the metal–ligand interactions are essentially electrostatic, ligands will be arranged around the ions in a largely nondirectional manner, so that cation/anion contacts are maximized and intramolecular steric interactions are minimized. Structural evidence for such bonding in the group 2 elements is found in the ability of the sum of cation and anion radii (as far as ‘radii’ can be meaningfully assigned to irregularly shaped ligands) to reproduce the observed metal–ligand distances (i.e.,  $R = r_+ + r_-$ ).

Despite the simplicity of the electrostatic analysis, it provides for an enormous variety of structural motifs. A major reason for this is the large range found in the metal radii and coordination numbers in group 2 complexes. The change from four-coordinate Be<sup>2+</sup> (0.27 Å) to twelve-coordinate Ba<sup>2+</sup>



Scheme 1 Formation of group 2 complexes with BiPh<sub>2</sub>.

(1.61 Å)<sup>123</sup> represents nearly a sixfold difference in size, for example, and it is generally the case that, with small, monodentate ligands, the coordination number of a complex rises steadily with the size of the metal ion. For example, the analysis of water-coordinated ions indicates that the most common coordination number for Be<sup>2+</sup>,<sup>124</sup> Mg<sup>2+</sup>,<sup>125</sup> and Ca<sup>2+</sup> are 4, 6, and 6–8, respectively.<sup>126</sup> When more complex aggregates or those containing sterically bulky or macrocyclic ligands are considered, however, the relationship between ion size and coordination number is weakened. Sterically bulky groups support lower formal coordination numbers in metal complexes than their counterparts with smaller ligands, sometimes as small as 3 for barium.<sup>127</sup> In such cases, secondary intramolecular contacts between the ligand and metal can occur. These can be subtle, as in the agostic interactions between the SiMe<sub>3</sub> groups on amido ligands and metal centers (e.g., in [(Me<sub>3</sub>Si)<sub>2</sub>N]<sub>3</sub>LiMg<sup>128</sup>), or more obvious, as in the cation–π interactions discussed in Section 1.37.3.2.3. The existence of the latter also contravenes the standard prediction that, for the group 2 metal ions, ligands with hard (type a) donor atoms (e.g., O, N, halogens) will routinely be preferred over softer (type b) donors. It has been suggested that the toxicity of certain barium compounds may be related to the Ba<sup>2+</sup> ion's ability to coordinate to 'soft' disulfide linkages, even in the presence of harder oxygen-based residues.<sup>129</sup>

### 1.37.3.2 Specialized Features

#### 1.37.3.2.1 Group 2 metals and their electropositive neighbors

To a first approximation, and with a change in cation charge, an electrostatic analysis of bonding applies not only to group 2 compounds, but also to the alkali metals, lanthanides, and actinides. The correspondences are considerable; for example, like the alkali metals, the alkaline-earth elements have only *ns*<sup>x</sup> valence electron configurations, and, apart from rare exceptions, such as the alkali anions<sup>130–138</sup> and the monovalent compounds mentioned in Section 1.37.1.2, are found only with *ns*<sup>0</sup> electron configurations in compounds. The alkaline-earth metals are highly electropositive ( $\chi = 1.47$  (Be)–0.97 (Ra)), a feature they share with their neighbors (e.g.,  $\chi = 0.97$  (Li)–0.86 (Cs);  $\chi = 1.08$  (La)–1.06 (Yb)). There are also pairings in sizes across the metal families: the radii of six-coordinate Na<sup>+</sup>, Ca<sup>2+</sup>, and Yb<sup>2+</sup> are near matches (1.02, 1.00, and 1.02 Å, respectively), for example, as are those of Sr<sup>2+</sup> and Sm<sup>2+</sup>/Eu<sup>2+</sup> (1.18 and 1.17 Å, respectively) and K<sup>+</sup> and Ba<sup>2+</sup> (1.38 and 1.35 Å, respectively).<sup>123</sup> Such similarities in size and polar bonding lead to parallels in structural features,<sup>85</sup> although not necessarily in reactivity.<sup>139</sup>

#### 1.37.3.2.2 'Bent' molecules; use of d orbitals in bonding

Despite being members of the s-block metals, experimental and computational evidence has been accumulating for several decades that the heavy members of the group 2 elements (Ca, Sr, Ba) represent a type of bridge between the main group and the d-block transition metals; for some purposes, they could be regarded as the earliest members of the d-block series.<sup>140</sup> Beginning in the 1960s, it was established through molecular-beam experiments that the gaseous group 2 dihalides (MF<sub>2</sub> (M = Ca, Sr, Ba); MCl<sub>2</sub> (M = Sr, Ba); BaI<sub>2</sub>) are nonlinear,<sup>141–143</sup>

contrary to the expectations of purely electrostatic bonding. The nonparallel cyclopentadienyl rings in group 2 (and divalent lanthanide) metallocenes<sup>85,144–147</sup> and bulky dialkyls<sup>148,149</sup> are considered to be manifestations of the same phenomenon, although experimental difficulties (e.g., intermolecular interactions in the solid state, thermal averaging effects in the gas phase) make quantifying the amount of bending problematic.

One approach to rationalizing the bending in these compounds proposes a 'reverse polarization' of the metal-core electrons by the ligands; this analysis makes correct predictions about the ordering of the bending for the dihalides (i.e., Ca < Sr < Ba; F > Cl > Br > I).<sup>142,143,150</sup> A polarization argument moves away from a hard-sphere model of the group 2 ions, however, as an ion is 'polarizable' to the extent that it has energetically accessible orbitals that can be influenced by ligands.<sup>150</sup> Support for this interpretation is provided by calculations that indicate a wide range of small molecules, AeX<sub>2</sub> (X = H, BH<sub>2</sub>, CH<sub>3</sub>, NH<sub>2</sub>, OH; Ae = Ca, Sr, Ba), should be bent, at least partially, as an effect of metal d orbital occupancy.<sup>151–156</sup> The energies involved in bending are low, but not negligible (e.g., the energy required to linearize Ba(NH<sub>2</sub>)<sub>2</sub> is calculated to be ~7 kcal mol<sup>-1</sup>).<sup>153</sup> In analogy to the bent AeL<sub>2</sub> compounds, complexes of Ba<sup>2+</sup> with three NH<sub>3</sub>, H<sub>2</sub>O, or HF ligands have been computed to prefer pyramidal over trigonal-planar arrangements, although the pyramidalization energy is less than 1 kcal mol<sup>-1</sup>. Spectroscopic confirmation of the bending angles in most of these small molecules is not yet available.

Other systems provide evidence that d-orbital participation may be important with the heavy alkaline-earth metals. For example, mass spectroscopic studies have demonstrated that up to 32 Ca, Sr, or Ba atoms can bind to the faces of the C<sub>60</sub> fullerene.<sup>157</sup> Furthermore, calculations indicate that the calcium-coated fullerene could adsorb considerable amounts of hydrogen (6–8 wt%), owing to a charge-transfer mechanism involving the calcium d orbitals.<sup>158,159</sup> Systems such as these are of interest in the search for practical hydrogen-storage materials. Barium vapor and NH<sub>3</sub> form BaNH, rather than the amide, as occurs with the lighter group 2 metals. Computations indicate that the short Ba–N distance (2.08 Å) reflects a π-type interaction, with donation from filled N 2p orbitals into the empty Ba 5d orbitals. The amount of d orbital character in the imido linkage is substantial (22%).<sup>160</sup>

The general rationalization for the use of d orbitals in the group 2 elements is that the filled 'semicore' (*n*–1)p and the valence (*n*–1)d orbitals of the heavier alkaline-earth metals have similar radial maxima, and their wave functions will mix during the process of core polarization. Thus, polarization and d orbital participation are not physically separable phenomena.<sup>150</sup> In the case of barium, the energy level of the 5d orbitals has been calculated to lie below the Fermi level in the metal,<sup>161,162</sup> and the extensive involvement of such orbitals in bonding has been used to warrant the claim that barium should be titled an 'honorary d element'.<sup>163</sup> Whether such language is justified or not, the interdependence of the 'core polarization' phenomenon on the accessibility of the (*n*–1)p and, to a lesser extent, the (*n*–1)d orbitals in the group 2 metals seems well established, and their involvement must be explicitly allowed if calculations are to reproduce experimental geometries (Figure 3).<sup>164</sup> This interpretation has been examined in detail with calculations on RaF<sub>2</sub>.<sup>165</sup>

### 1.37.3.2.3 Cation- $\pi$ interactions

A type of noncovalent influence that has gained increasing recognition in the past quarter of a century is the cation- $\pi$  interaction, which describes the involvement of cations with a ligand's  $\pi$ -electrons (usually, but not necessarily, those in an aromatic ring).<sup>166</sup> The interaction can be quite robust; that for benzene with the 'hard'  $K^+$  ion has been measured at  $17.7 \text{ kcal mol}^{-1}$ ,<sup>167</sup> which is almost the same as that to water in the gas phase.<sup>166</sup> Several factors are thought to contribute to the cation- $\pi$  phenomenon, including induced dipole in aromatic rings, donor-acceptor and charge-transfer effects, and that  $sp^2$ -hybridized carbon is more electronegative than hydrogen.

The cation- $\pi$  interaction is operative in many biological systems, such as  $K^+$ -selective channel pores,<sup>168</sup>  $Na^+$ -dependent allosteric regulation in serine proteases,<sup>169</sup> and  $Ca^{2+}$  blockage of voltage-gated sodium channels.<sup>170</sup> There are also coordination complexes of the group 2 elements that display pronounced  $Ae^{n+}$ - $\pi$  interactions to coordinated ligands. Although the strength of the interaction is expected to decrease with the increasing size of the cation,<sup>166</sup> most of the structurally authenticated examples involve the heaviest members, especially barium. This is partially a result of the greater 'softness' of the larger cations, but also reflects the fact that the coordination spheres are greater in the heavier metals, where there is more room to accommodate additional ligands. Thus, there are no experimentally verified examples of cation- $\pi$  interactions in beryllium complexes, and cases with magnesium are rare: the unsolvated allyl complex  $[Mg\{C_3(SiMe_3)_2H_3\}_2]_2$  **4** (Figure 4) is an example in which bridging allyl ligands exhibits cation- $\pi$  interactions with the metal centers ( $Mg \cdots C = 2.44 - 2.51 \text{ \AA}$ ).<sup>171</sup> With

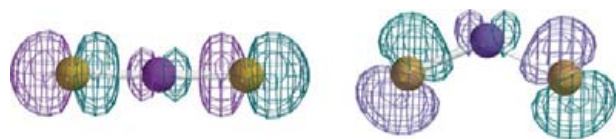


**Figure 3** The HOMO of linear  $CaF_2$  (left) is largely an antibonding combination of F 2p and 'semicore' Ca 3p orbitals. On bending with the assistance of the 3d orbitals, the antibonding interaction is reduced, stabilizing the molecule. A similar analysis applies to the heavier group 2 dihalides.

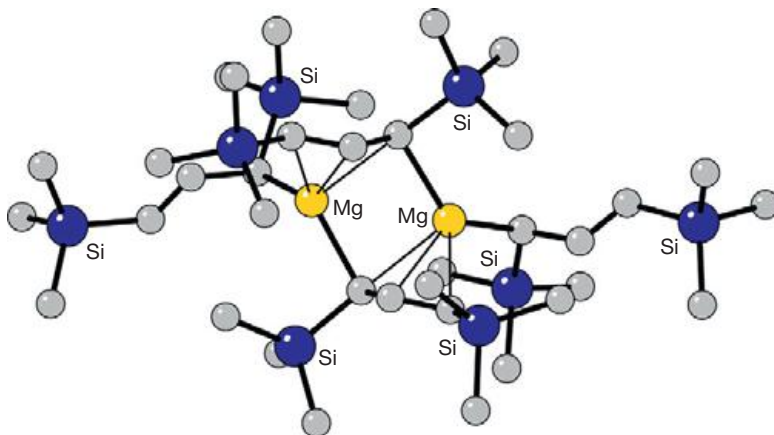


**Figure 4** Structure of  $[Mg\{C_3(SiMe_3)_2H_3\}_2]_2$  **4**.

barium, many examples exist, some with extensive interactions, such as in the structure of  $Ba_2(Odpp)_4$  **5** (Figure 5), with multiple  $Ba \cdots C(\text{arene})$  contacts  $< 3.5 \text{ \AA}$ .<sup>46</sup>

Considering the prevalence of cation- $\pi$  interactions, it is not surprising that, in some cases, group 2 ions may play an important role in modifying the structure and bonding of metal complexes. One of the clearest manifestations of this effect is the formation of 2D and 3D coordination polymers, in which the structure adopted is critically dependent on the identity of the metal ion. The dichromium complexes  $\{Ca(H_2O)_3\}[Cr_2(\mu-OH)_2(NTA)_2] \cdot 3H_2O$ ,  $\{Sr(H_2O)_3\}[Cr_2(\mu-OH)_2(NTA)_2] \cdot 3H_2O$ , and  $\{Ba(H_2O)_3dmsO\}[Cr_2(\mu-OH)_2(NTA)_2] \cdot 2H_2O$  **6** illustrate this property, as the Ca and Sr complexes form 3D frameworks, whereas **6** forms 2D sheets (Figure 6). The corresponding Mg complex does not form a coordination polymer at all, but, rather, exists as separated ions,  $\{Mg(H_2O)_6\}[Cr_2(\mu-OH)_2(NTA)_2] \cdot 4H_2O$ .<sup>172</sup>

## 1.37.4 Ligand Types

### 1.37.4.1 Macrocyclic Compounds

#### 1.37.4.1.1 Porphyrins and phthalocyanines

Historically, alkaline-earth metal porphyrin systems have been synthesized mainly as analogs to study naturally occurring magnesium and iron porphyrin systems.<sup>173</sup> There is increasing use of porphyrins with substituents that can confer unusual electronic properties on their complexes. For example, [5,10,15,20-tetraphenyl-2,3,7,8,12,13,17,18-octakis(phenylethynyl)porphyrinato]magnesium **7** can be synthesized from a solution of the substituted porphyrin in methylene chloride charged with  $MgI_2$  and diisopropylethylamine, and can be isolated as a metallic green crystalline solid.<sup>174</sup> The 24-atom core is nearly planar (to within  $0.039 \text{ \AA}$ ), yet it (and an analogous Zn counterpart) exhibits a substantial red-shift of the Soret band, contrary to theories that link porphyrin distortion and band shifts.<sup>175,176</sup> A study of bis(pyridine)(5,10,15,20-tetraphenylporphyrinato)magnesium **8** revealed octahedral coordination to the four nitrogen atoms from the porphyrin ring and two nitrogen atoms from the axial pyridine ligands in addition to the largest  $^{25}Mg$  quadrupole coupling constant ( $C_Q$ ) ( $15.32 \pm 0.02 \text{ MHz}$ ) so far observed for  $^{25}Mg$  nuclei.<sup>177</sup> A 'weak-link' approach method

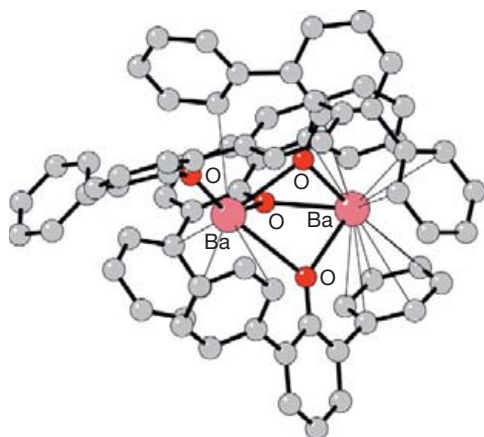
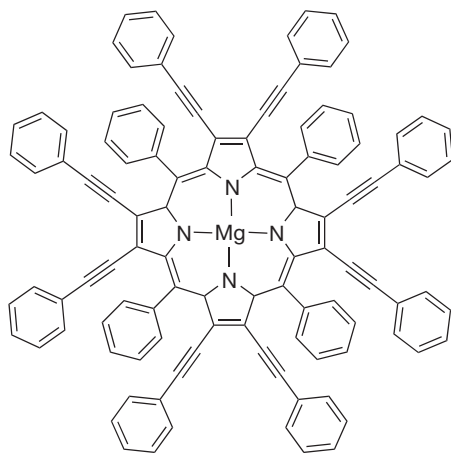
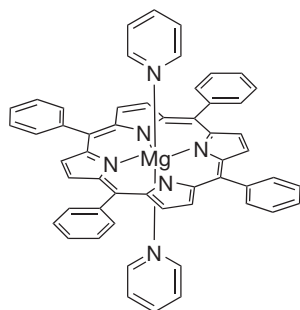


**Figure 5** Structure of  $\text{Ba}_2(\text{Odpp})_4$  **5**.

for preparing dissymmetric cofacial porphyrin superstructures has been developed that allows for selective modulation of the porphyrin–porphyrin distance and orientation, as well as the production of multimetallic species.<sup>178</sup>



**7**



**8**

The biological focus of most porphyrin studies with Mg has dictated the use of protic solvents and prevented the isolation of the more hydrolytically sensitive Ca, Sr, and Ba porphyrin complexes. Use of the nonprotic solvent THF enables the isolation of crystalline calcium porphyrins. In particular, the

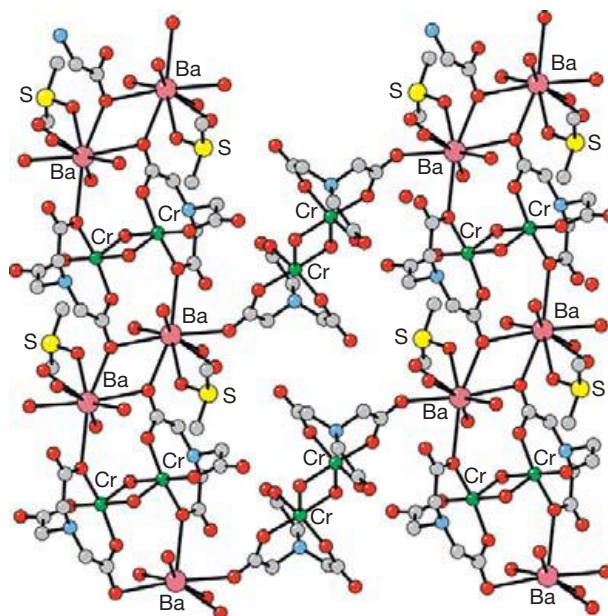


**Figure 6** Structure of  $(\{\text{Ba}(\text{H}_2\text{O})_3\text{dmsO}\}[\text{Cr}_2(\mu\text{-OH})_2(\text{nta})_2] \cdot 2 \text{H}_2\text{O})_\infty$  **6**.

treatment of 5,10,15,20-tetrakis(4-*tert*-butylphenyl)porphyrin  $\text{H}_2(t\text{-BuPP})$  with activated calcium yields a neutral calcium complex that can be crystallized as a pyridine adduct. Alternatively, the complex can be treated with  $\text{CaI}_2(\text{thf})_4$  in MeCN to yield the trimetallic complex  $(\text{MeCN})_2\text{ICa}(t\text{-BuPP})\text{Ca}(t\text{-BuPP})\text{Ca}(\text{MeCN})_2$  **9** (Figure 7).<sup>179</sup>

The metallation of *meso*-octaalkylporphyrinogens with Ca, Sr, and Ba gives  $\text{Ae}_2\text{N}_4\text{R}_8$  ( $\text{R}=\text{Et}$ ;  $\text{Ae}=\text{Ca}$ , Sr, or Ba;  $\text{R}=\textit{n}$ -Bu,  $\text{M}=\text{Ba}$ ) complexes. In the coordination sphere of each metal are two thf molecules; with the barium complex, they are replaceable by several different aromatics to give  $\text{Ba}_2\text{N}_4(\textit{n}\text{-Bu})_8(\eta^6\text{-arene})_2$  (arene = benzene, toluene, durene, or naphthalene) complexes.<sup>180</sup> NMR evidence indicates that the structures are retained in solution.

Metal phthalocyanine (Pc) complexes are structurally related to porphyrin species, but possess distinctive optoelectronic properties and are the basis of many dyes and pigments. As with porphyrins, the majority of studies involve magnesium derivatives. Magnesium phthalocyanine (MgPc) **10** is a semiconductor with a thin film optical band gap of 2.6 eV.<sup>181</sup> Crystallographic studies<sup>182</sup> have found that the blue-violet **10** is not planar, as is typical for  $\text{M}^{\text{II}}\text{Pc}$  complexes, but that the Mg is displaced from the  $\text{N}_4$ -isoindole plane by 0.43 Å at 260 K; the deviation of the magnesium cation from the plane increases at lower temperatures.<sup>183</sup> **10** forms dimers in the solid state that are stabilized by 4 + 1 coordination of the Mg ions (Figure 8). Under ambient,  $\text{O}_2$ , and  $\text{N}_2$  atmospheres, **10** forms  $(\text{MgPc})_2\text{X}_2$  ( $\text{X}=\text{O}$ , N) complexes in a reversible, temperature-dependent process.<sup>183</sup>

A complex of dipyridinated **10** has been synthesized by heating the complex in pyridine at 160 °C. The magnesium-atom coordination is approximately tetragonal-bipyramidal, though the bonds between the Mg atom and the axial base ligands are slightly longer than expected.<sup>184</sup> When **10** is dissolved in wet benzonitrile, triclinic crystals of  $\text{10}\cdot\text{H}_2\text{O}$  are produced after slow recrystallization at 80 °C, again displaying

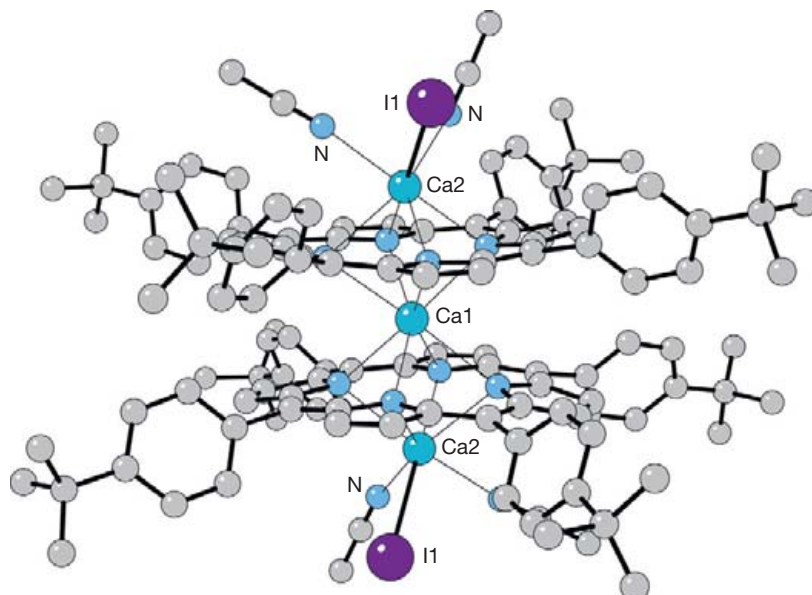


**Figure 7** Structure of  $(\text{MeCN})_2\text{I}_2\text{Ca}(t\text{-BuPP})\text{Ca}(t\text{-BuPP})\text{CaI}_2(\text{MeCN})_2$  **9**.

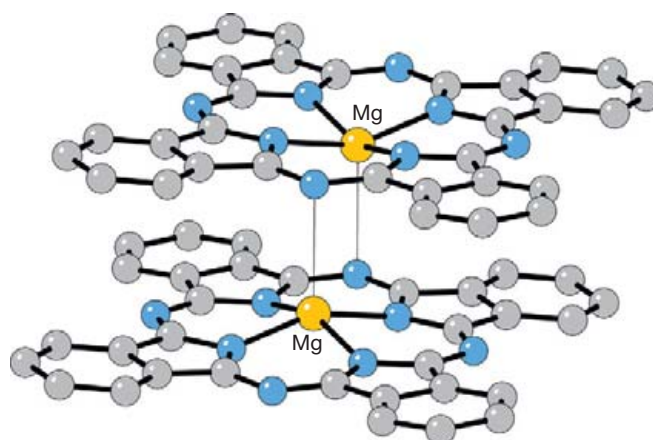
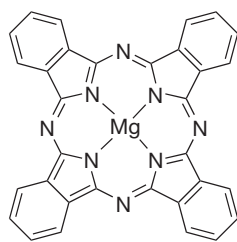


**Figure 8** Structure of magnesium phthalocyanine ( $\text{MgPc}$ ) **10**.

4 + 1 coordination of the central magnesium and dimer formation with strong  $\pi$ - $\pi$  interactions between the distorted Pc macro rings.<sup>185</sup> The redox properties of a phthalocyanine-like tetrakis(thiadiazole)porphyrazine,  $[\text{TDPzMg}]$  **11**, have been examined with cyclic voltammetry and density functional theory (DFT) calculations; its  $E_{1/2}$  value is less negative than the corresponding reduction potential for its phthalocyanine counterpart.<sup>186</sup>



**11**

The reaction of beryllium metal with 1,2-dicyanobenzene at 270 °C produces beryllium phthalocyanine ( $\text{BePc}$ ), which is planar with no intermolecular interactions between molecules in stacks.<sup>187</sup> The complex is unstable in air and is converted to (2-ethoxyethanol)-aqua-beryllium phthalocyanine, indicating the joint action of aerobic water and carbon dioxide molecules in the ambient-air degradation process.<sup>187</sup> Studies of  $\text{BePc}$  and **10** with 4-picoline demonstrated that the central metal ion of  $\text{BePc}$  is mono-axially ligated by the ring nitrogen atom, whereas  $\text{MgPc}$  exhibits biaxial ligation. The ligand-releasing temperature is higher for Mg than Be.<sup>188</sup>

#### 1.37.4.1.2 Crown Ethers

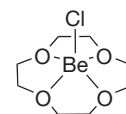
Crown ethers are common ligands in group 2 chemistry,<sup>189</sup> and the range of metal radii and available ring sizes leads to a variety of structural arrangements. This is evident when the metal is held constant and the ring size is steadily increased. A study using DFT and ab initio calculations showed that

solvated  $[\text{Be}(12\text{-crown-4})]^{2+}$  is fivefold coordinated in water or ammonia as  $[\text{Be}(\text{H}_2\text{O})(12\text{-crown-4})]^{2+}$  or  $[\text{Be}(\text{NH}_3)(12\text{-crown-4})]^{2+}$ , respectively. These complexes undergo water and ammonia exchange according to an associative interchange mechanism, much as do  $[\text{Be}(\text{H}_2\text{O})_4]^{2+}$  and  $[\text{Be}(\text{NH}_3)_4]^{2+}$ .<sup>190</sup> The reaction of  $\text{BeCl}_2$  with 1 equiv. of the larger 15-crown-5 in  $\text{CH}_2\text{Cl}_2$  gives  $[\text{BeCl}_2(15\text{-crown-5})]$ , in which distorted tetrahedral coordination of a  $\text{BeO}_2\text{C}_2$  five-membered heterocycle with terminal chlorine atoms is observed.<sup>191</sup> The centrosymmetric complex  $[(\text{BeCl}_2)_2(18\text{-crown-6})]$  was synthesized in  $\text{CH}_2\text{Cl}_2$  suspension from  $\text{BeCl}_2$  and 18-crown-6. Upon exposure to moist atmosphere,  $[\{\text{Be}_3(\mu\text{-OH})_3(\text{H}_2\text{O})_6\}(18\text{-crown-6})]\text{Cl}_3 \cdot 3\text{H}_2\text{O}$  **12** (Figure 9) is formed; there is no direct interaction between the Be atoms and the crown ether.<sup>192</sup>

Although the small size of 12-crown-4 and the large diameters of the heavy alkaline-earth metals Ca, Sr, and Ba would seem to offer a poor fit for each other, the consequences of the mismatch have been examined carefully.<sup>193</sup> Owing to the small diameter of 12-crown-4, the metal ions either stay above the plane of the ligand and fill the remaining coordination sites with other anions, or they form sandwich complexes, residing between two crown ligands. The large size of  $\text{Ba}^{2+}$  allows it to adopt the sandwich orientation, but the rest of the group 2 anions are too small and must adopt the 'one-faced' orientation with 12-crown-4. Variations in anion coordination strength and the presence of hydrogen-bond donor anions can affect these outcomes.<sup>193</sup> Studies with 18-crown-6 and 15-crown-5 found that the metal ions (from perchlorates or halides) are normally encapsulated in the crown under aqueous conditions, yielding  $[\text{M}(18\text{-crown-6})(\text{H}_2\text{O})_3]_2$  and  $[\text{M}(15\text{-crown-5})(\text{H}_2\text{O})_3]_2$  cations, respectively, except for the combination of barium and 15-crown-5, for which a variety of structures is possible.<sup>194</sup>

A rare cationic beryllium complex with direct Be–crown bonding was synthesized in two different ways; the reaction of  $\text{BeCl}_2$  with 1 equiv. of 12-crown-4 with  $\text{SbCl}_5$  in dichloromethane gave  $[\text{BeCl}(12\text{-crown-4})][\text{SbCl}_4]$  **13**, whereas when 2 equiv. of 12-crown-4 and  $\text{SbCl}_5$  were used, the product was a mixture of **13** and  $\text{SbCl}_3(12\text{-crown-4})$ . In the beryllium

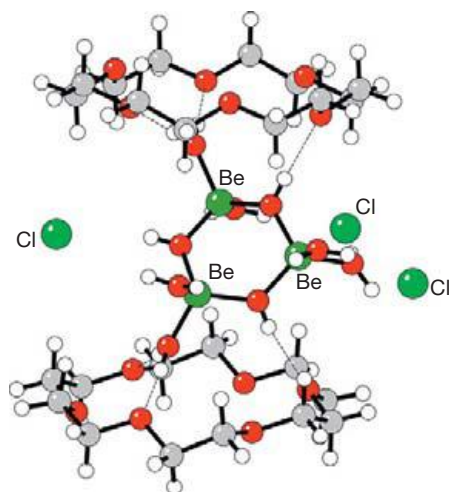
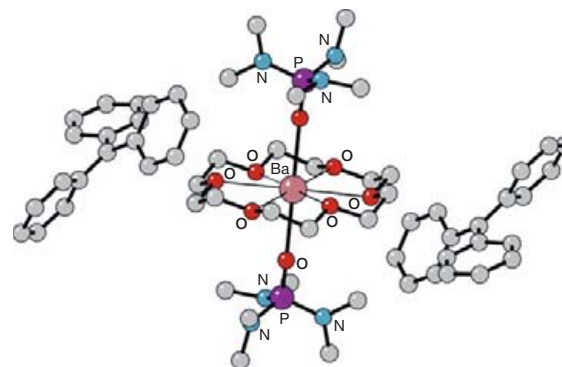
complex, the anions form zigzag chains in the crystal to accommodate the stereochemical effect of the antimony lone pair.<sup>195</sup>

**13**

The crystal structure of  $(i\text{-Bu})\text{MgOAr}(18\text{-crown-6})$  was reported in a study in which the conjugate bases of cyclopentadiene, indene, and fluorene or a hindered phenol were used as counterions to the  $[\text{RMg}(\text{macrocycle})]^+$  ion.<sup>196</sup> Exchange studies revealed that 15-crown-5 showed more effective coordination to  $\text{RMg}^+$  than 18-crown-6. Reactions of  $\text{RMgOAr}$  with 15-crown-5 lead to  $[\text{RMg}(\text{macrocycle})]^+[\text{RMg}(\text{OAr})_2]^-$  instead of to the expected  $[\text{RMg}(\text{macrocycle})]^+[\text{OAr}]^-$ , and when 18-crown-6 is used, the principal product is  $\text{RMgOAr}(18\text{-crown-6})$ .

The combination of calcium–crown ether supramolecular dications and monovalent  $[\text{Ni}(\text{dmit})_2]^-$  anions produces salts with unusual arrangements of anions in the crystal. The presence of  $\pi\text{-}\pi$  dimers of  $[\text{Ni}(\text{dmit})_2]^-$  and sandwich  $[\text{Ca}(\text{crown ether})_2]^{2+}$  complexes coexist with monomeric  $[\text{Ni}(\text{dmit})_2]^-$  anions in the structures of  $\text{Ca}^{2+}(12\text{-crown-4})_2[\text{Ni}(\text{dmit})_2]_2$  and  $\text{Ca}^{2+}(15\text{-crown-5})_2[\text{Ni}(\text{dmit})_2]_2(\text{CH}_3\text{CN})_{0.7}$ .<sup>197</sup> With the larger (1-aza-18-crown-6) and (1,10-diaza-18-crown-6) rings, the calcium ions are included inside the cavities, and are additionally coordinated with two axial  $\text{CH}_3\text{CN}$  molecules. The  $\text{Ca}^{2+}(1\text{-aza-18-crown-6})[\text{Ni}(\text{dmit})_2]_2(\text{CH}_3\text{CN})_2$  and  $\text{Ca}^{2+}(1,10\text{-diaza-18-crown-6})[\text{Ni}(\text{dmit})_2]_2(\text{CH}_3\text{CN})_2$  structures are accompanied by uniform zigzag chains of  $[\text{Ni}(\text{dmit})_2]^-$  anions, whose magnetic properties are consistent with 1D Heisenberg antiferromagnets.

Charge-separated barium triphenylmethanide  $[\text{Ba}(18\text{-crown-6})(\text{HMPA})_2](\text{CPh}_3)_2$  **14** (Figure 10) was synthesized from  $\text{Ba}(\text{CH}_2\text{Ph})_2$  with 2 equiv. of  $\text{HCPh}_3$ , 18-crown-6, and HMPA in THF. Dark-red crystals of both the barium compound and its strontium analog were synthesized.<sup>112,113</sup> Examples of Ca, Sr, or Ba azide complexes with crown ethers are known; these include  $\text{Ba}(18\text{-crown-6})(\text{N}_3)_2(\text{MeOH})$ ,  $\text{Sr}(15\text{-crown-5})(\text{N}_3)_2(\text{H}_2\text{O})$ ,  $\text{Ca}(15\text{-crown-5})(\text{N}_3)_2(\text{H}_2\text{O})$ , and  $\text{Sr}(15\text{-crown-5})(\text{N}_3)(\text{NO}_3)$ . The azide moiety is not always bonded in the same fashion, however; coordination modes include  $\kappa^1$ -,  $\mu$ -1,3-, and linkages via H-bonded  $\text{H}_2\text{O}$  molecules.

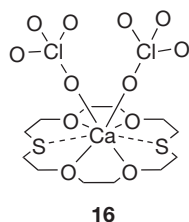
**Figure 9** Structure of  $[(\text{Be}_3(\mu\text{-OH})_3(\text{H}_2\text{O})_6)(18\text{-crown-6})]\text{Cl}_3 \cdot 3\text{H}_2\text{O}$  **12**.**Figure 10** Structure of barium triphenylmethanide  $[\text{Ba}(18\text{-crown-6})(\text{HMPA})_2](\text{CPh}_3)_2$  **14**.

The triazido complex  $[\text{Ba}(18\text{-crown-6})(\text{N}_3)_2(\text{MeOH})]\cdot 1/3\text{MeOH}$  **15** (Figure 11) is the first main-group compound to exhibit dinuclear cations with three  $\mu$ -1,3-NNN bridges ( $\text{Ba-N} = 2.804(4)\text{-}2.856(4)\text{ \AA}$ ).<sup>198</sup>

Crown ethers have been featured in several pyridine-containing barium complexes.  $[\text{Ba}(\text{C}_9\text{H}_7)(18\text{-crown-6})(\text{py})]^+ [\text{C}_9\text{H}_7]^- \cdot \text{py}$ ,  $[\text{Ba}\{\text{C}_9\text{H}_6(\text{CH}_2\text{CH}_2\text{O})_5\text{C}_6\text{H}_4\text{O}\}_2\cdot 4\text{py}]$ ,  $[\text{Ba}(\text{C}_9\text{H}_7)(\text{dibenzo-18-crown-6})(\text{py})]^+ [\text{C}_9\text{H}_7]^- \cdot 0.5(\text{dibenzo-18-crown-6})\cdot 0.65\text{py}$ , and  $[\text{Ba}(\text{benzo-crown-5})_2]^{2+} [\text{Ba}(\text{C}_9\text{H}_7)_3(\text{py})]_2^-$  were synthesized from bis(indenyl)barium and a crown ether in pyridine as the solvent.<sup>199</sup>  $[\text{Ba}(\text{C}_{13}\text{H}_9)(18\text{-crown-6})(\text{py})]^+ [\text{C}_{13}\text{H}_9]^- \cdot \text{py}$  and  $[\text{Ba}(\text{C}_{13}\text{H}_9)(\text{dibenzo-18-crown-6})(\text{pyridine})]^+ [\text{C}_{13}\text{H}_9]^- \cdot 2\text{py}$  were synthesized from bis(flourenyl)barium and a crown ether in pyridine.<sup>200</sup> Air-sensitive, colorless crystals of monomeric  $\text{Ba}(\text{C}_5\text{H}_5)_2(18\text{-crown-6})$  were synthesized from  $\text{Ba}(\text{C}_5\text{H}_5)_2$  and 18-crown-6. The geometry around the barium is hexagonal-bipyramidal, with the Cp rings at the top and bottom of the bipyramid.<sup>201</sup>

The heterometallic species  $[\text{Ba}(18\text{-crown-6})(\text{HMPA})_2][\text{SnPh}_3]_2$ ,  $[\text{Ca}(18\text{-crown-6})(\text{HMPA})_2][\text{Sn}(\text{SnPh}_3)_3]_2$ , and  $[\text{Sr}(18\text{-crown-6})(\text{HMPA})_2][\text{Sn}(\text{SnPh}_3)_3]_2$  have been synthesized by the insertion of the metals into the Sn—Sn bond of hexaphenyldistannane in liquid ammonia.<sup>202</sup>  $[\text{Ca}(18\text{-crown-6})(\text{HMPA})_2][\text{SeMes}^*]_2$  was prepared by the reaction of elemental Ca dissolved in anhydrous liquid  $\text{NH}_3$  with either  $\text{HSMes}^*$  or  $\text{Mes}^*\text{SeSeMes}^*$ .<sup>203</sup>

Colorless crystals of  $\text{Ca}(1,10\text{-dithia-18-crown-6})(\text{ClO}_4)_2$  **16** were isolated from an equimolar mixture of 1,10-dithia-18-crown-6 and  $\text{Ca}(\text{ClO}_4)_2\cdot 4\text{H}_2\text{O}$  in benzonitrile at room temperature by slow evaporation. The six-coordinate calcium center is only coordinated to four crown oxygens and the two monodentate perchlorato ligands, giving it a distorted trigonal prismatic geometry; the contacts to sulfur are at  $3.0\text{ \AA}$ .<sup>204</sup>



The reaction of metallic barium with 1 equiv. of 18-crown-6 and 2 equiv. of Hpta gave the white solid  $\text{Ba}(\text{pta})_2(18\text{-crown-6})$ .<sup>205</sup> The two pta ligands are situated trans to the planar 18-crown-6 ring. Related to this are the complexes  $[\text{Ba}(\text{pta})_2(18\text{-dibenzocrown-6})]$  and  $[\text{Ba}(\text{pta})_2(18\text{-dibenzocrown-6})]$

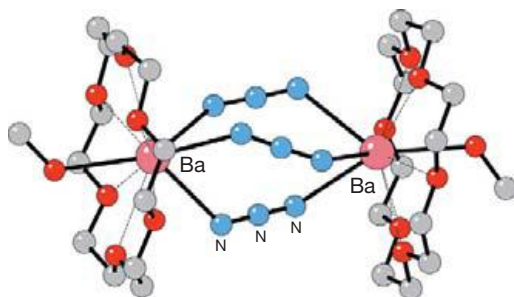


Figure 11 Structure of  $\text{Ba}(18\text{-crown-6})(\text{N}_3)_2(\text{MeOH})$  **15**.

( $\text{C}_6\text{H}_5\text{CH}_3$ ). The 18-dibenzocrown-6 ligand is curved, with the pta ligands on the same side.

Distantly related to crown ethers are calixarenes, the cyclic oligomers formed from condensation reactions between para-substituted phenols and formaldehyde; they are inexpensive compounds that are stable to both basic and acidic media.<sup>206,207</sup> Their ability to complex both neutral and ionic species has driven their employment as complexing agents and extractants,<sup>208-212</sup> in chemical sensing (detection) devices,<sup>213-215</sup> and as catalysts;<sup>216,217</sup> their chemistry has been reviewed elsewhere<sup>218</sup> (see Chapter 1.38).

Calixarenes excel in the complexation of large ions, and this has been exploited in the development of ligands for metals as large as radium.<sup>219</sup> Thus, it is not surprising that beryllium was the last of the group 2 metals to be incorporated into a structurally characterized calixarene complex.<sup>220</sup> The compound  $p$ -(*t*-Bu)-calix[4](OMe)<sub>2</sub>(OBeCl)<sub>2</sub> **17** (Figure 12) possesses the doubly-flattened partial-cone conformation that has been observed for Al, Ga, and Zn species. In **17**, the two Be atoms generate a  $\text{Be}_2\text{O}_2$  motif in the center of the flattened calixarenes.

### 1.37.4.2 Nonmacrocylic Compounds

#### 1.37.4.2.1 Hydrides and hydroborates

The binary hydrides of the group 2 elements differ in their solid-state structures ( $\text{BeH}_2$  is a coordination polymer, whereas  $\text{MgH}_2$  adopts a tetragonal  $\text{TiO}_2$  (rutile) lattice, and  $\text{CaH}_2$ ,  $\text{SrH}_2$ , and  $\text{BaH}_2$  have orthorhombic  $\text{PbCl}_2$  structures), but all are nonmolecular species, insoluble in media with which they do not react. Increasing interest in generating soluble molecular hydride complexes that could have potential applications in catalysis<sup>221</sup> and hydrogen storage<sup>222</sup> has stimulated the development of compounds such as the Mg hydride **18**. Treatment of **18** with DMAP yields **19**, the first structurally authenticated magnesium complex with a terminal hydride ( $\text{Mg-H} = 1.75(7)\text{ \AA}$ ) (Scheme 2).<sup>27</sup> The hydrocarbon-soluble calcium hydride complex  $[(\text{DIPP-nacnac})\text{CaH}(\text{thf})]_2$  **20**, produced from the reaction of  $(\text{DIPP-nacnac})\text{Ca}[\text{N}(\text{SiMe}_3)_2](\text{thf})$  with  $\text{PhSiH}_3$ ,<sup>223</sup> is stable under reflux conditions and displays

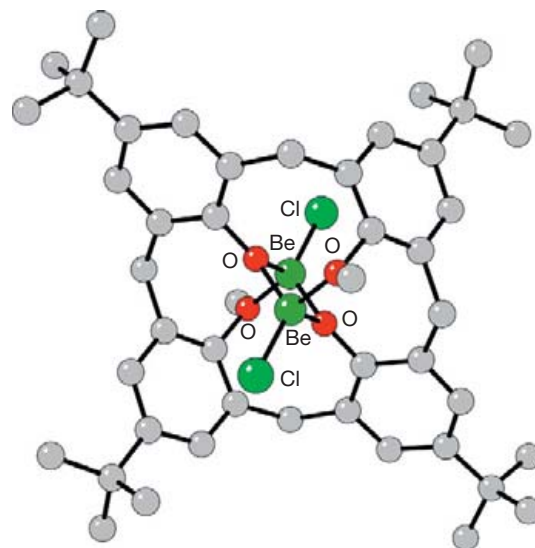
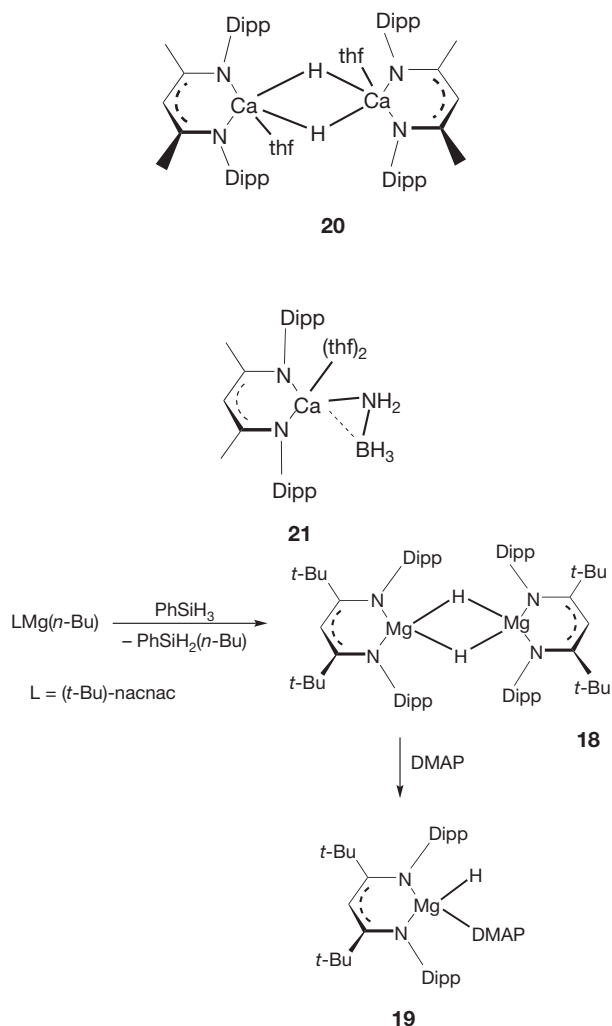


Figure 12 Structure of  $p$ -(*t*-Bu)-calix[4](OMe)<sub>2</sub>(OBeCl)<sub>2</sub> **17**.

Ca–H distances of 2.09(4)–2.21(3) Å. The reaction of **20** with benzophenone and various epoxides readily generates alkoxide complexes.<sup>224</sup>

The reaction of **20** with various aminoboranes generates a variety of derivatives. The bulky DIPP-nacnac bulky ligand prevents the formation of coordination polymers with bridging B–N ligands and allows crystallization of the products (DIPP-nacnac)CaNH(R)BH<sub>3</sub>(thf)<sub>x</sub> (x = 1, 2; R = H, Me, *i*-Pr, DIPP) as monomers. (DIPP-nacnac)CaNH<sub>2</sub>BH<sub>3</sub>(thf)<sub>2</sub> **21** contains the NH<sub>2</sub>BH<sub>3</sub> anion coordinated side-on with an eclipsed conformation and the THF ligands are easily lost. As the steric bulk of the substituent R on nitrogen increases, the result is slight elongation of the N–Ca bond distance (from 2.399(2) to 2.460(2) Å), shortening of the BH<sub>3</sub>···Ca contact (from 2.867(4) to 2.570(3) Å), and linearization of the R–N–Ca angle. Magnesium analogs of the type (DIPP-nacnac)MgNH(R)BH<sub>3</sub> (R = H, Me, *i*-Pr, DIPP) are also known; the magnesium amidoboranes decompose at a higher temperature than the calcium amidoboranes. The complexes with smaller R substituents give a mixture of decomposition products, while the one with the larger R group DIPP decomposes into a borylamide complex (DIPP-nacnac)MgN(DIPP)BH<sub>2</sub>.<sup>225–227</sup>



**Scheme 2** Formation of a soluble magnesium complex with a terminal hydride ligand.

The long-known Mg(BH<sub>4</sub>)<sub>2</sub> **22**, of interest in studies of hydrogen storage, has a problematic synthetic history, and classical metathetical preparations (e.g., from MgCl<sub>2</sub> and LiBH<sub>4</sub> or NaBH<sub>4</sub>) produce low yields or mixtures of salts.<sup>228,229</sup> Additional syntheses of **22** have been developed that may be more reliable. The first is a metathetical reaction between Mg(C<sub>4</sub>H<sub>9</sub>)<sub>2</sub> and Al(BH<sub>4</sub>)<sub>3</sub>, yielding **22** and Al(C<sub>4</sub>H<sub>9</sub>)<sub>3</sub>. The second is an insertion reaction of a BH<sub>3</sub> species (released from BH<sub>3</sub>·S(CH<sub>3</sub>)<sub>2</sub>) into the Mg–C bonds of Mg(C<sub>4</sub>H<sub>9</sub>)<sub>2</sub>;<sup>230</sup> this is a modification of a previously reported route.<sup>231</sup> Both methods afford analytically pure polycrystalline material and use commercially available reagents. The structural characteristics of **22** are uniquely complex, given the simpler structures of its beryllium and calcium analogs. Each Mg<sup>2+</sup> ion is surrounded by four [BH<sub>4</sub>]<sup>−</sup> tetrahedra arranged in a deformed tetrahedron, and the orientation of the [BH<sub>4</sub>]<sup>−</sup> tetrahedra is such that each Mg<sup>2+</sup> ion is coordinated by tetrahedral edges only (**Figure 13**). This results in hexagonal symmetry in which five symmetry-independent Mg<sup>2+</sup> ions and ten symmetry-independent [BH<sub>4</sub>]<sup>−</sup> ions are connected into an eightfold, relatively irregular hydrogen coordination environment.<sup>229</sup>

The synthesis of calcium alanate can be accomplished from the reaction of CaCl<sub>2</sub> and NaAlH<sub>4</sub>, with or without the assistance of ball-milled reagents. The product, crystallized as Ca(AlH<sub>4</sub>)<sub>2</sub>(thf)<sub>2</sub>, contains octahedrally coordinated calcium and *trans* η<sup>1</sup>-bonded AlH<sub>4</sub> ligands (Ca–μ-H = 1.92 Å; Al–μ-H = 1.65 Å).<sup>232</sup> The structure is similar to that of Mg(AlH<sub>4</sub>)<sub>2</sub>(thf)<sub>2</sub>.<sup>233,234</sup>

Colorless crystals of the first magnesium borohydride complex containing only two donor atoms (N) coordinated to the Mg atom, Mg(BH<sub>4</sub>)<sub>2</sub>·tmeda **23**, were prepared from TMEDA addition to a solution of **22** in diethyl ether. The Mg atom has distorted pseudotetrahedral geometry and the BH<sub>4</sub> groups are tridentate. Mg(BH<sub>4</sub>)<sub>2</sub>·6NH<sub>3</sub> was prepared by bubbling gaseous NH<sub>3</sub> through **22** dissolved in ether; the decomposition of the

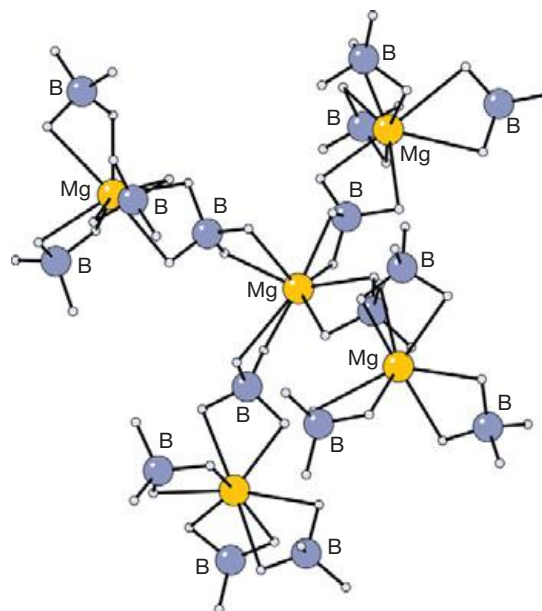
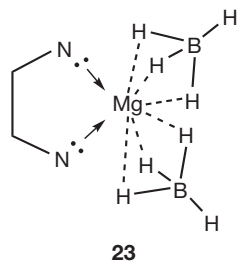


**Figure 13** Portion of the lattice of Mg(BD<sub>4</sub>)<sub>2</sub>. The protio version (**22**) is isostructural.

resulting white solid in a vacuum at 125 °C yields Mg(BH<sub>4</sub>)<sub>2</sub>·2NH<sub>3</sub> as a viscous colorless liquid that crystallizes into a white solid.<sup>235,236</sup>



The aminoborane complex Mg(NH<sub>2</sub>BH<sub>3</sub>)<sub>2</sub>·NH<sub>3</sub>, in which the coordinated NH<sub>3</sub> and BH<sub>3</sub> of [NH<sub>2</sub>BH<sub>3</sub>]<sup>−</sup> exhibit dihydrogen bonds, was formed from a reaction between MgNH and NH<sub>3</sub>BH<sub>3</sub>.<sup>237</sup> The borane complex Mg(B<sub>3</sub>H<sub>8</sub>)<sub>2</sub> was synthesized as a white solid from the sublimation of the solid-state reaction mixture of MgBr<sub>2</sub> and NaB<sub>3</sub>H<sub>8</sub>. The dimethyl and diethyl ethers 24 of this complex were crystallographically characterized and the Mg exhibits distorted cis-octahedral geometry with two Et<sub>2</sub>O ligands and the two bidentate B<sub>3</sub>H<sub>8</sub> ligands (Figure 14).<sup>238</sup>

Work has progressed in the area of β-diketimate-stabilized borohydride complexes of group 2 elements. When treated with 4 or 2 equiv. of Me<sub>2</sub>NHBH<sub>3</sub>, the complex (DIPP-nacnac)Mg(*n*-Bu) and its calcium counterpart produces products containing the [H<sub>3</sub>BNMe<sub>2</sub>BH<sub>2</sub>Me<sub>2</sub>N]<sup>−</sup> ion. Subsequent thermolysis at 60 °C gives (H<sub>2</sub>BNMe<sub>2</sub>)<sub>2</sub> and magnesium or calcium hydride species through δ-hydride elimination. The calcium compound is less reactive, and this is attributed to the dependence of the δ-hydride elimination step on the charge density and polarizing capability of the group 2 metal involved.<sup>239</sup> A β-diketimate-stabilized calcium borohydride was synthesized from calcium diphenylamide and 9-borabicyclo[3.3.1]nonane (9-BBN). An amidoborane coproduct was observed and explained as the result of σ-bond metathesis.<sup>240</sup> Another β-diketimate-stabilized calcium borohydride (DIPP-nacnac)CaB(*s*-Bu)<sub>3</sub>H<sub>3</sub>·thf was produced from the reaction of KB(*s*-Bu)<sub>3</sub>H with [LCa(μ-1)<sub>3</sub>thf]<sub>2</sub>; a similar reaction with strontium iodide produced the equivalent strontium tri(*s*-Bu)borohydride. Both monomeric products exhibit hydride ligation between the metal and boron centers.<sup>241</sup>

A series of monomeric amide or aryloxide complexes of the form LCaX, where L=a bulky tris-pyrazolylborate (i.e.,

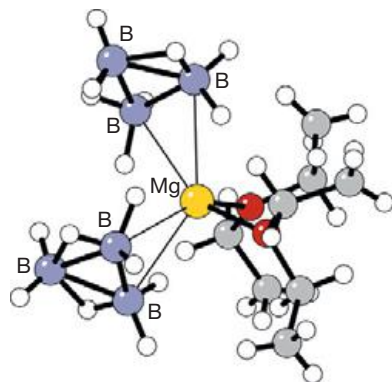


Figure 14 Structure of Mg(B<sub>3</sub>H<sub>8</sub>)<sub>2</sub>·Et<sub>2</sub>O 24.

tris[3-(2-methoxy-1,1-dimethylethyl)pyrazolyl]hydroborate, tris[3-isopropylpyrazole]hydroborate, or tris[3-*tert*-butylpyrazole]hydroborate) and X = N(SiMe<sub>3</sub>)<sub>2</sub> or β-diiminate ligands (DIPP-nacnac and CH[CM<sub>2</sub>NC<sub>6</sub>H<sub>4</sub>-2-OMe]<sub>2</sub>) have been made as part of studies to access their ability to serve as catalyst precursors for the ring-opening polymerizations of lactide. The hard N<sub>3</sub>-O<sub>3</sub>-κ<sup>6</sup> binding of the tris-pyrazolylborate results in tight binding to Mg<sup>2+</sup> and Ca<sup>2+</sup> ions, and larger alkaline-earth metals like Sr<sup>2+</sup> and Ba<sup>2+</sup> achieve 7- and 8-coordination. This stabilizes the discrete monomeric calcium complex and prevents the formation of Schlenk equilibrium products L<sub>2</sub>Ca and Ca[N(SiMe<sub>2</sub>)<sub>2</sub>]<sub>2</sub>. Interestingly, [HB(3-*t*-Bupz)<sub>3</sub>]Ca(O-2,6-*i*-Pr<sub>2</sub>C<sub>6</sub>H<sub>3</sub>)·(PO) is found to bind one molecule of propylene oxide (PO), but the resulting complex, [HB(3-*t*-Bupz)<sub>3</sub>]Ca(O-2,6-*i*-Pr<sub>2</sub>C<sub>6</sub>H<sub>3</sub>)·(PO)<sub>2</sub> 25 (Figure 15; Ca-O(PO)=2.454(2) Å), is inert<sup>242-246</sup> (see Chapter 1.38).

The tris(pyrazolyl)borates of the heavier group 2 metals are of interest in chemical vapor deposition (CVD) and atomic layer deposition (ALD) processes, and can be made by halide metathetical routes. Strontium tris(pyrazolyl)borate, SrTp<sub>2</sub>, is a monomer in the solid state, whereas the barium counterpart exists as a dimer containing two bridging Tp ligands.<sup>247</sup> The room-temperature reaction of AeI<sub>2</sub> (Ae=Ca, Sr, Ba) with 2 equiv. of potassium tris(3,5-diethylpyrazolyl)borate or potassium tris(3,5-di-*n*-propylpyrazolyl)borate in hexane yields monomeric tris(3,5-diethylpyrazolyl)borate or tris(3,5-di-*n*-propylpyrazolyl)borate complexes. Of all these compounds, only the dimeric (BaTp<sub>2</sub>)<sub>2</sub> displays low volatility, perhaps because of its dimeric structure. A related reaction of AeI<sub>2</sub> with thallium bis(3,5-di-*tert*-butylpyrazolyl)borate in THF yields monomeric bis(3,5-di-*tert*-butylpyrazolyl)borate compounds in greater than 60% yields. The κ<sup>3</sup>-*N,N,H*-bis(3,5-di-*tert*-butylpyrazolyl)borate ligands are highly distorted, with Ae-N-N-B torsion angles ranging from 20.0° to 60.9°, evidently to avoid intra- and interligand *tert*-butyl group steric repulsions.<sup>248</sup>

#### 1.37.4.2.2 Group 14 ligands

##### 1.37.4.2.2.1 Organometallic compounds

For well over 100 years, use of the synthetically important Grignard reagents (RMgX) has dominated organoalkaline-earth chemistry. Attempts were made starting in the first decade of the twentieth century to extend the chemistry of the RMgX reagents to calcium,<sup>249</sup> and, for the next 50 years, the target compounds were almost always dialkyl complexes or alkyl metal halides, which remained intractably difficult to

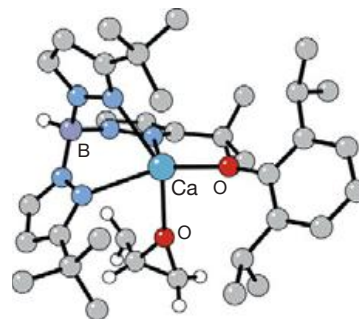


Figure 15 Structure of [HB(3-*t*-Bupz)<sub>3</sub>]Ca(O-2,6-*i*-Pr<sub>2</sub>C<sub>6</sub>H<sub>3</sub>)·(PO) 25.

manipulate.<sup>250–252</sup> Even the bis(cyclopentadienyl) compounds of calcium, strontium, and barium, although thermally stable, displayed low solubility and were isolated in low to trace yields (0.2% in the case of barium).<sup>253,254</sup>

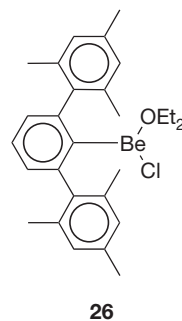
Substantial progress with the organic chemistry of the heavy metals began in the mid-1980s, largely through the recognition that the size of calcium, strontium, and barium places them in a different category from the smaller beryllium and magnesium.<sup>255</sup> The parallels noted above (Section 1.37.3.2.1) between the sizes of the alkaline-earth metals and several divalent lanthanide ions extends to their organometallic compounds as well, and the use of ligands more appropriately sized to the larger metals had a transformative effect on the field. The revival of interest has expanded from the original emphasis on metallocenes<sup>256,257</sup> to include many varieties of noncyclopentadienyl derivatives.<sup>258</sup> More recent advances have demonstrated that direct analogs of Grignard compounds can be isolated if special conditions are enforced (e.g., low temperatures, minimal use of ethereal solvents).<sup>259</sup> Applications in material science (e.g., CVD reagents<sup>260,261</sup> and catalysis<sup>257</sup>) have helped fuel research in this area (see Chapter 1.38).

The organic ligand in an organometallic complex may be a pendant substituent<sup>46,262–264</sup> or it may be supplied by the solvent. For the purposes of this section, complexes in which the only M–C contacts are from coordinated solvent will not generally be included. Similarly, metal cyanides (i.e.,  $M(\text{CN})_2$ ) and salt-like carbides containing the methanide ( $\text{C}^{4-}$ ), acetylide ( $\text{C}_2^{2-}$ ), or allylenide ( $\text{C}_3^{4-}$ ) ions (e.g.,  $\text{Be}_2\text{C}$ ,  $\text{CaC}_2$ ,  $\text{Mg}_2\text{C}_3$ ) or more complex metal species such as  $\text{MgB}_{12}\text{C}_{12}$ <sup>265</sup> or the graphite analog  $\text{BeB}_2\text{C}_2$ <sup>266</sup> are not detailed here; the formation, structures, and spectroscopy of carbides have been reviewed elsewhere.<sup>17</sup>

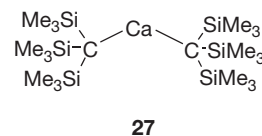
The sterically bulky groups that have been used with the heavy group 2 metals have also been employed with beryllium and magnesium, for which coordination numbers as low as 2 are now known in several classes of complexes. The chemistry of beryllium has always been hindered over concerns about toxicity,<sup>267</sup> and the monumental work of Coates in the 1960s and 1970s on alkyl and aryl complexes still stands as a benchmark in this area.<sup>268</sup> A survey of solution  $^9\text{Be}$  NMR has been published,<sup>269</sup> and organoberyllium species occupy both extremes of the known chemical shift range ( $-27.7$  ppm for  $\text{CpBeSiMe}_3$ ;  $+20.8$  ppm for  $\text{Me}_2\text{BeOEt}_2$ ). Advances in heavy group 2 organometallic chemistry have been repeatedly reviewed.<sup>256,258,270,271</sup>

**1.37.4.2.2.1.1 Compounds with  $\sigma$ -bonded ligands** A variety of structurally authenticated low-coordinate complexes of beryllium is known; the reaction in toluene of base-free  $\text{Ph}_2\text{Be}$  with *i*-Pr-carbene gives the adduct  $\text{Ph}_2\text{Be}(i\text{-Pr-carbene})$  ( $\text{BeC}(\text{carbene}) = 1.807(4) \text{ \AA}$ ;  $\text{Be-C}(\text{Ph}) = 1.751(6) \text{ \AA}$  (av)); in addition, the three-coordinate complex  $\text{Ph}_2\text{Be}(n\text{-Bu}_2\text{O})$  is also known.<sup>272</sup> The bulky terphenyl substituent  $-\text{C}_6\text{H}_3-2,6\text{-}(\text{mesityl})_2$  ( $\text{Ar}^*$ ) has been used to generate aryl beryllium complexes with coordination numbers less than 4. For example, the reaction of 1 equiv. of  $\text{Li}[\text{Ar}^*]$  with  $\text{BeCl}_2(\text{OEt}_2)_2$  or  $\text{BeBr}_2(\text{OEt}_2)_2$  gives the monomeric complexes  $\text{Ar}^*\text{BeX}(\text{OEt})_2$  ( $\text{X} = \text{Cl}$  **26** or  $\text{Br}$ ), which possess three-coordinate beryllium atoms.<sup>273</sup> The reaction of **26** with  $\text{LiNHP}$  affords the thermally unstable dimer  $(\text{Ar}^*\text{BeNHP})_2$ , which decomposes at room temperature to yield  $\text{HAr}^*$  and the imide  $(\text{MeNHP})_x$ .<sup>273</sup> The treatment of **26** with 1 equiv. of  $\text{Li}[\text{SMes}^*]$  produces the colorless three-coordinate thiolate derivative,  $\text{Ar}^*\text{BeSMes}^*$

$(\text{OEt}_2)$ , which has been crystallographically characterized.<sup>273</sup> When **26** reacts with  $\text{LiNHSiPh}_3$  or  $\text{LiN}(\text{SiMe}_3)_2$ , the crystallographically characterized monomers  $\text{Ar}^*\text{BeNHSiPh}_3(\text{OEt}_2)$  and  $\text{Ar}^*\text{BeN}(\text{SiMe}_3)_2$  can be isolated. The latter is a rare example of a compound with a two-coordinate Be center in the solid state ( $\text{Be-C} = 1.519(4)$ ;  $\text{Be-N} = 1.519(4) \text{ \AA}$ ). Organometallic *m*-terphenyl derivatives of beryllium have been reviewed.<sup>274</sup>



Sterically bulky ligands have been increasingly used to enforce low coordination numbers (as low as 2) in  $\sigma$ -bonded compounds of magnesium and the heavier alkaline-earth metals. The dialkyl  $\text{Mg}(\text{Tsi})_2$  has a linear structure, with  $\text{Mg-C} = 2.116(2) \text{ \AA}$ .<sup>275</sup> The calcium analog  $\text{Ca}(\text{Tsi})_2$  **27** is made from the reaction of  $\text{K}[\text{C}(\text{SiMe}_3)_3]$  and  $\text{CaI}_2$  in benzene.<sup>148</sup> In the solid state, **27** is bent, with  $\text{Ca-C} = 2.459(9) \text{ \AA}$  and  $\text{C-Ca-C} = 149.7(7)^\circ$ , and displays several close intramolecular contacts that could influence the bending angle (e.g.,  $\text{Ca} \cdots \text{C}(\text{Me})$  distances of  $\sim 3.0 \text{ \AA}$  with  $\text{Ca} \cdots \text{H}$  distances of  $2.5 \text{ \AA}$ ). Dialkyls of the type  $\text{Ae}[\text{CH}(\text{SiMe}_3)_2]_2(\text{thf})_n$  ( $\text{Ae} = \text{Ca}$ ,  $n = 2$ ;  $\text{Ae} = \text{Sr}$ ,  $\text{Ba}$ ,  $n = 3$ ) react with a diimine ligand precursor to form either the heteroleptic  $\beta$ -diketiminato alkyl when  $\text{Ae} = \text{Ca}$ , or C–H activation products involving ligand methyl group deprotonation when  $\text{Ae} = \text{Sr}$  or  $\text{Ba}$ .<sup>276</sup> A review of the chemistry of compounds containing the Tsi ligand and related bulky groups is available.<sup>277</sup>

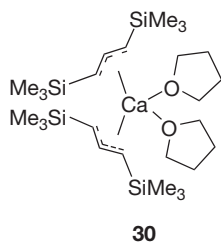


Di(allyl)beryllium and several adducts were reported by Wiegand and Thiele,<sup>278</sup> who prepared the parent compound from the reaction of diethylberyllium and tri(allyl)boron. It is presumably polymeric, although its structure has not been determined. With the use of the bulky allyl ligand  $[\text{1,3-(SiMe}_3)_2\text{C}_3\text{H}_3]^-$  ( $\text{A}'$ ), the colorless complex  $\text{BeA}'_2(\text{Et}_2\text{O})$  **28** can be synthesized via the salt metathesis reaction of  $\text{BeCl}_2$  and  $\text{KA}'$  in  $\text{Et}_2\text{O}$ .<sup>78</sup> Each Be center is surrounded by two  $\sigma$ -coordinated allyl moieties and the oxygen of a diethyl ether molecule in a trigonal-planar environment (Figure 16). **28** is fluxional in solution, and  $^9\text{Be}$  NMR spectroscopy was used to identify the operation of Schlenk-type equilibria between it and  $\text{BeCl}_2$ .

In an unusual transformation, the crystallographically characterized cyclic hexanuclear species  $[\text{HC}\{\text{C}(t\text{-Bu})\text{N}(\text{dipp})\}]_2\text{Mg}(\text{C}_3\text{H}_5)_6$  **29** is formed on thermal treatment under vacuum of the  $\beta$ -diketiminate  $\text{HC}\{\text{C}(t\text{-Bu})\text{N}(\text{dipp})\}_2\text{Mg}(\text{C}_3\text{H}_5)(\text{thf})$  (Scheme 3). The allyl groups in **29** (Figure 17) exhibit  $\mu\text{-}\eta^1\text{:}\eta^1$  bonding, an uncommon arrangement for an organoalkaline-earth

species;<sup>279</sup> it is also observed in a polymeric calcium complex,  $[\text{Ca}(\mu^2\text{-}\eta^1\text{:}\eta^1\text{-C}_3\text{H}_5)(18\text{-crown-6})][\text{Zn}(\eta^1\text{-C}_3\text{H}_5)_4]$ .<sup>280</sup>

Despite the compact size of its ligands, the parent bis(allyl) calcium,  $(\text{C}_3\text{H}_5)_2\text{Ca}$ , is readily soluble in THF and has been recrystallized as a triglyme adduct; the allyl ligands are  $\pi$ -bonded (2.671(1)–2.846(1) Å). Treatment with iodine initiates C–C coupling to produce 1,5-hexadiene;<sup>281</sup> dissolution in pyridine results in dearomatization of the ring and the formation of a calcium 4-allyl-1,4-dihydropyridyl complex.<sup>282</sup> The colorless bis(allyl) complex  $[1,3\text{-}(\text{SiMe}_3)_2\text{C}_3\text{H}_3]_2\text{Ca}(\text{thf})_2$  **30**<sup>283</sup> and its strontium counterpart are isostructural.<sup>284</sup> Attempts to form a barium derivative through halide metathesis led to the heterometallic coordination polymer  $[\text{K}(\text{thf})\text{Ba}_2\{1,3\text{-}(\text{SiMe}_3)_2\text{C}_3\text{H}_3\}]_\infty$ . The ligands in all three compounds react with iodine and undergo C–C coupling reactions.<sup>284</sup>



The reaction of  $(\text{C}_3\text{H}_5)_2\text{Ca}$  with 18-crown-6 at  $-30^\circ\text{C}$  leads to a highly fluxional complex that contains one  $\pi$ - and one  $\sigma$ -bonded allyl ligand in the solid state,  $\text{Ca}(\eta^1\text{-C}_3\text{H}_5)(\eta^3\text{-C}_3\text{H}_5)$  (18-crown-6) **31**.<sup>285</sup> DFT calculations indicate that this is the lowest energy conformation for two allyl ligands and a crown ether around the metal center. This is another manifestation of the  $\eta^3 \rightarrow \eta^1$  transformation of the allyl ligand that can occur on the complexation of donor molecules to a group 2 metal, first observed in the magnesium complex **4**.<sup>171</sup> Warming **31** to room temperature results in rapid cleavage of the crown ether ( $t_{1/2} = 2.5$  h) and the formation of vinyl-terminated alcoholates of different chain lengths. Use of the more soluble starting material **30** did not lead to the isolation of a crown ether adduct, but, in principle, displays the same decomposition reaction. The

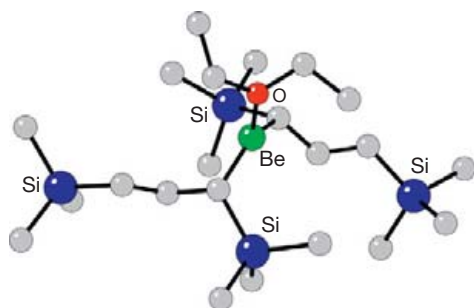
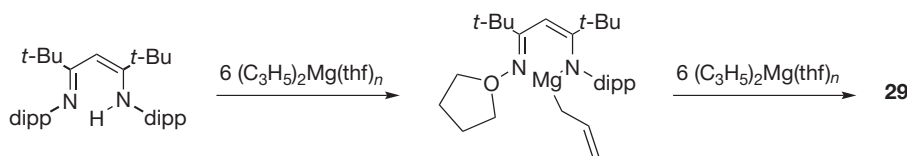
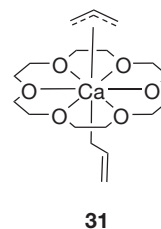


**Figure 16** Structure of the Be allyl complex **28**.



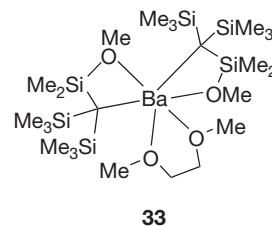
**Scheme 3** Formation of the hexanuclear allyl-bridged complex **29**.

chemistry of s-block complexes of the related azaallyl ligand has been previously reviewed.<sup>286</sup>



The x-ray crystal structure of  $\text{Mes}^*_2\text{Mg}$  reveals an almost linear two-coordinate diaryl. The average Mg–C distances and C–Mg–C angle are 2.116(3) Å and  $158.2(1)^\circ$ , respectively. There are also close ( $\sim 2.2\text{--}2.3$  Å) contacts involving the metal and hydrogens from the *o*-(*t*-Bu) groups.<sup>287</sup> The reaction of diphenylmethane with dibenzylbarium in THF or barium *t*-butoxide with  $\text{Ph}_2\text{CH}(\text{SiMe}_3)$  in the presence of *n*-BuLi forms barium diphenylmethanide by hydrocarbon elimination and desilylation mechanisms, respectively.<sup>114</sup> Crystallized in the form of its 18-crown-6 ether derivative **32** (Figure 18), the complex displays direct Ba–C bonds of 3.065(3) and 3.097(3) Å, and a longer contact at 3.39 Å.

Metathesis between either  $\text{SrI}_2$  or  $\text{BaI}_2$  and 2 equiv. of  $\text{K}[(\text{Me}_3\text{Si})_2(\text{MeOMe}_2\text{Si})\text{C}]$  in THF yields the dialkyls  $[(\text{Me}_3\text{Si})_2(\text{MeOMe}_2\text{Si})\text{C}]_2\text{Ae}(\text{L})$  ( $\text{Ae}(\text{L}) = \text{Sr}(\text{thf}), \text{Ba}(\text{dme})$ ) **33**.<sup>288</sup> The metals are bonded to the ligand C and O atoms in four-membered chelate rings, with Sr–C = 2.786(3) and 2.849(3) Å, and Ba–C = 3.049(2) and 3.036(2) Å. The geometry around barium in **33** is a distorted trigonal antiprism.



A variety of benzyl complexes containing calcium, strontium, or barium is now known. The bis(benzyl) complexes of calcium and strontium are synthesized by transmetalation of the appropriate potassium salts with  $\text{CaI}_2$ <sup>111,289–292</sup> or  $\text{SrI}_2$ ,<sup>293</sup> respectively; a barium derivative forms from  $\text{LiCH}_2\text{Ph-tmeda}$  with  $\text{Ba}[\text{N}(\text{SiMe}_3)_2]_2(\text{thf})_2$  or  $\text{Ba}[\text{O}(\text{Mes}^*)]_2$ .<sup>294</sup> As expected, the complexes are quite basic: dibenzylcalcium will deprotonate triphenylmethane ( $\text{p}K_a = 31.5$ ), leading to the solvent-separated ion pairing  $[\text{Ca}(\text{thf})_6][\text{Ph}_3\text{C}]_2$ ,<sup>111</sup> and dibenzylbarium reacts with diphenylmethane ( $\text{p}K_a = 33.5$ ) in THF to yield bis(diphenylmethyl)barium in 90% yield, and with 1,1-diphenylethene in THF to form bis(1,1,3-triphenylpropyl)barium in near-quantitative yield.<sup>294</sup>

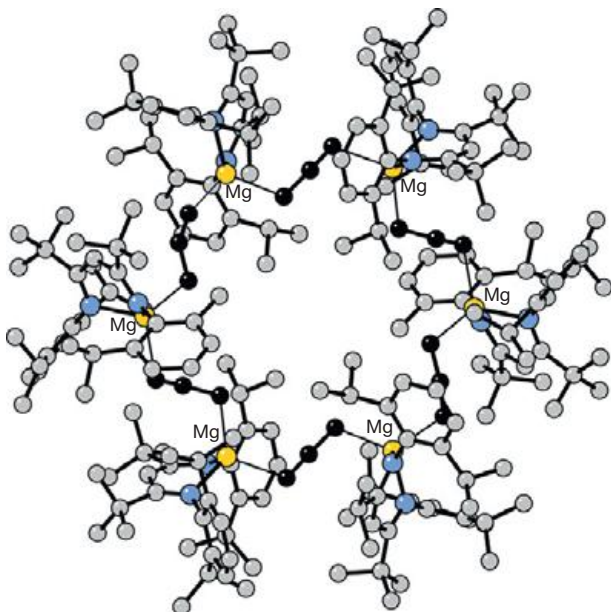


**Figure 17** Structure of  $[\text{HC}(\text{C}(t\text{-Bu})\text{N}(\text{dipp}))_2 \text{Mg}(\text{C}_3\text{H}_5)]_6$  **29**. The atoms of the bridging allyl ligands are in black.

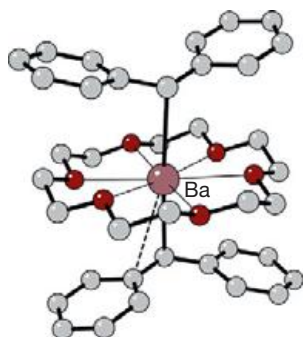


**Figure 18** Structure of  $\text{Ba}(\text{CHPh})_2(18\text{-crown-6})$  **32**.

The latter is soluble in hydrocarbon solvents, while dibenzylbarium and bis(diphenylmethyl)barium are soluble only in THF. As expected for complexes with a high degree of ionic bonding, the calculated energy differences between *cis*- and *trans*-geometries of  $(p\text{-}t\text{-Bu})\text{Bz}_2\text{Ca}(\text{thf})_4$ ,  $(p\text{-Me}_3\text{SiBz})_2\text{Ca}(\text{thf})_4$ , and  $(\text{Bz})_2\text{Ca}(\text{thf})_4$  are very small ( $<2 \text{ kcal mol}^{-1}$ ), and crystal-packing effects likely affect the geometries observed in the solid state.<sup>111</sup> Several benzyl complexes of the heavy group 2 metals are polymerization initiators, and their activity is often sensitive to the identity of the metal and the presence of additional coordinated bases<sup>292</sup> (see **Chapter 1.38**).

In a comparison of the crystal structures, NMR and IR spectra of various  $\text{Yb}^{\text{II}}$  and calcium complexes demonstrated that they are strikingly similar, a reflection of the nearly identical radii of  $\text{Yb}^{2+}$  and  $\text{Ca}^{2+}$ .<sup>139</sup> Nevertheless, the dibenzylterbium(II) analog of **34** produces polystyrene of high syndiotacticity ( $r = 94.9\%$ ,  $rr = 90.0\%$ ), whereas **34** itself yields only atactic or slightly syndiotactic polymer. A difference in  $\text{Yb-L}$  and  $\text{Ca-L}$  bond strengths, despite their similar lengths, has been proposed as the source of the difference.<sup>139</sup> It should

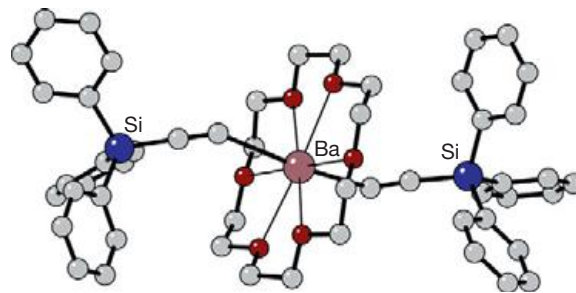
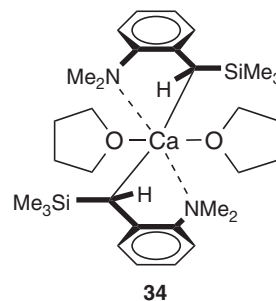


**Figure 19** Structure of  $\text{Ba}(\text{C}\equiv\text{CSiPh}_3)_2(18\text{-crown-6})$  **35**.

be noted that the structural similarities between calcium and ytterbium(II) complexes is not always close; the  $\text{M-allyl}$  distances in  $[1,3\text{-}(\text{SiMe}_3)_3\text{C}_5\text{H}_5]_2 \text{M}(\text{thf})_2$  complexes differ by an average of  $0.09 \text{ \AA}$ , and the calcium compound **30** is far more active as a polymerization imitator than the lanthanide analog<sup>295</sup> (see **Chapter 1.38**).

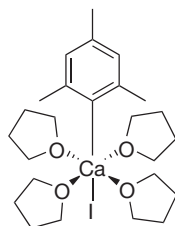
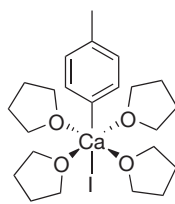
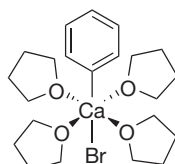
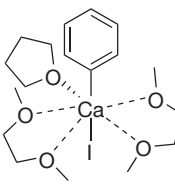


The reaction of the amido complexes  $\text{M}[\text{N}(\text{SiMe}_3)_2]_2$  ( $\text{M} = \text{Ca}, \text{Sr}, \text{Ba}$ ) with triphenylsilylthyne in the presence of 18-crown-6 leads to the formation of the bis(acetylide) compounds  $\text{Ae}(\text{C}\equiv\text{CSiPh}_3)_2(18\text{-crown-6})$ .<sup>296</sup> The compounds are monomers, with terminal acetylides ( $\text{Ca-C} = 2.523(7), 2.558(7) \text{ \AA}$ ;  $\text{Sr-C} = 2.692(4), 2.723(4) \text{ \AA}$ ;  $\text{Ba-C} = 2.852(3), 2.853(2) \text{ \AA}$ ). All three compounds display bent  $\text{C-M-C}$  and  $\text{M-C}\equiv\text{C}$  angles, with the latter strongly affected by the identity of the metal: from nearly  $160^\circ$  for  $\text{M} = \text{Ca}$  and  $\text{Sr}$  to  $126.6(3)^\circ$  and  $141.3(3)^\circ$  in the barium compound **35** (**Figure 19**). Further study of these systems, accompanied with computational modeling, has indicated that intramolecular interactions between the acetylides and the crown ethers play a significant role in the bending.<sup>297</sup>

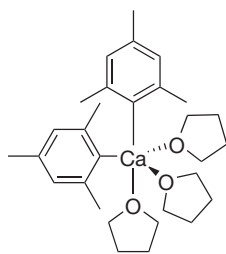
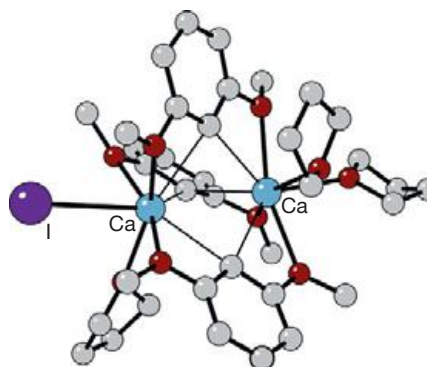
For many decades after their first report in 1905,<sup>249</sup> the literature on the synthesis and reactions of the aryl halides and diaryls of  $\text{Ca}$ ,  $\text{Sr}$ , and  $\text{Ba}$  was contradictory (see 'Calcium, Strontium, and Barium' in *Comprehensive Organometallic Chemistry-I*). Extensive reinvestigations of the chemistry of these compounds in recent years have clarified the status of these species, and reviews on the area are available.<sup>298,299</sup>

Activated calcium reacts with aryl halides to give compounds of the type  $\text{RCaX}$ , which can be isolated in the form of adducts (i.e.,  $\text{MesCaI}(\text{thf})_4$  **36**,  $(p\text{-tolyl})\text{CaI}(\text{thf})_4$  **37**,  $\text{PhCaX}(\text{thf})_4$  ( $\text{X} = \text{Br}$  **38**, **I**), and  $\text{PhCaI}(\text{thf})(\text{dme})_2$  **39**) in reasonable yields. The synthesis and isolation must be conducted at low temperatures ( $< -30^\circ \text{C}$ ) to avoid ether cleavage reactions.<sup>300,301</sup> The calcium centers in the  $\text{ArCaX}(\text{thf})_4$  complexes are in octahedral environments and the organic and halide groups are *trans* to each other; the  $\text{Ae-C}$  distances range between  $2.556(5) \text{ \AA}$  for **37** and  $2.583$

(3) Å for **38**. The more saturated coordination environment in **39** (accompanied by a longer Ca–C bond of 2.621(5) Å) is apparently the reason for its improved stability (it can be handled at 0 °C).<sup>300</sup>

**36****37****38****39**

The diaryl calcium compound  $\text{CaMes}_2(\text{thf})_3$  **40** has been isolated by fractional crystallization of  $\text{MesCaI}(\text{thf})_4$  **36** at temperatures ranging from  $-30$  to  $-90$  °C. Complex **40** is extremely soluble in THF, even at  $-90$  °C, and is more reactive than **36**, cleaving ethers at temperatures above  $-55$  °C.<sup>302</sup> The formation of the highly reactive **40** by Schlenk redistribution from **36** is probably a general phenomenon, and may be the source of the reactivity of  $\text{ArCaI}$  compounds.

**40****Figure 20** Structure of  $(\text{thf})_2\text{Ca}[\mu\text{-C}_6\text{H}_3\text{-2,6-(OMe)}_2]_3\text{Ca}(\text{thf})\text{I}$  **41**.

Interestingly, the Schlenk equilibrium of  $\text{Ca}(\text{Ar})\text{I}$  ( $\text{Ar} = \text{Ph}$ , naphthyl) can be shifted quantitatively in favor of the soluble  $\text{CaAr}_2$  by the addition of stoichiometric amounts of  $\text{K}(\text{O}-t\text{-Bu})$ , exploiting the insolubility of  $\text{KI}$  in organic media.<sup>67</sup> Recrystallization of  $\text{CaPh}_2(\text{thf})_4$  from TMEDA yields the thf-free dinuclear complex,  $[(\text{tmEDA})\text{Ca}(\text{Ph})(\mu\text{-Ph})]_2$ .<sup>67</sup> Alternatively, modification of the ortho substituents on an arene ring can be used to influence the position of Schlenk equilibrium, as in the formation of the dinuclear, aryl-rich  $(\text{thf})_2\text{Ca}[\mu\text{-C}_6\text{H}_3\text{-2,6-(OMe)}_2]_3\text{Ca}(\text{thf})\text{I}$  **41** (Figure 20), either from the direct reaction of calcium with 1-iodo-2,6-dimethoxybenzene or from the reaction of phenylcalcium iodide and 1,3-dimethoxybenzene.<sup>302</sup> As with **40**, **41** displays high solubility in THF at low temperature.

Calcium atoms react with methyl-substituted benzene derivatives under cocondensation conditions to yield arylcalcium hydrides.<sup>44</sup> With  $\text{C}_6\text{H}_5\text{CH}_3$ ,  $\text{C}_6\text{H}_5(t\text{-Bu})$ , and  $\text{C}_6\text{H}_5\text{Si}(\text{CH}_3)_3$ , the reaction displays no selectivity for C–H activation, giving the ortho, meta, and para isomers of each arylcalcium hydride. With  $m\text{-C}_6\text{H}_4(\text{CH}_3)_2$ , the reaction selectively activates the bond meta to the  $\text{CH}_3$  groups. The reaction between  $\text{HCaC}_6\text{H}_5(t\text{-Bu})$  and  $(t\text{-Bu})$ -substituted phenols ( $2,6\text{-}(t\text{-Bu})_2\text{C}_6\text{H}_3\text{OH}$ ,  $4\text{-Me-2,6-(}t\text{-Bu)}_2\text{C}_6\text{H}_2\text{OH}$ ,  $2,4,6\text{-}(t\text{-Bu})_3\text{C}_6\text{H}_2\text{OH}$ ) produces the corresponding aryloxides in high yields.

A DFT study was performed in order to determine the structures of phenyl calcium hydride and its magnesium analog in donor solvents.<sup>303</sup> A dimeric phenyl calcium hydride was found to be the most stable species in solution, but monomers or tetramers cannot be excluded at very low or very high concentrations. The structure and bonding of  $\text{CpBeH}$ ,  $\text{CpMgH}$ , and  $\text{CpCaH}$  have also been the subject of DFT calculations.<sup>304</sup>

The decomposition products of organocalcium aryls in ethers have received considerable attention, and usually take the form of oxygen-centered calcium cages such as  $[\text{Ca}(\text{C}_6\text{H}_3\text{-2,6-(OMe)}_2)_2]_3\text{-CaO}$ ,<sup>305</sup>  $[(\text{thf})_2\text{Ca}(\text{Ph})\text{I}]_3\text{-(thf)CaO}$ ,<sup>306</sup>  $[(\text{Et}_2\text{O})\text{CaPh}_2]_4\text{-(Et}_2\text{O)CaO}$ ,<sup>307</sup>  $[(\text{thf})\text{Ca}(\text{O-CH=CH}_2)_2]_4\text{-CaO-Ca}_2$  **42** (Figure 21), and  $(\text{CaO})_4\text{-4(thf)}_3\text{Ca}_2$  **43** (Figure 22),<sup>308</sup> stemming from  $\alpha$ -deprotonation of THF. The aggregate **43**, for example, forms when  $\text{PhCaI}$  is heated under reflux in THF; the phenyl groups are converted into benzene. The vinylalcoholate **42** is believed to be an intermediate in the formation of **43**; it is isolated at lower temperatures ( $< -10$  °C) from the reaction of  $\text{PhCaI}$  and  $\text{ZnEt}_2$ , which accelerates the decomposition of the organocalcium halide. These results underscore the unreliability of earlier investigations of organocalcium aryls that were conducted at room temperature or above.

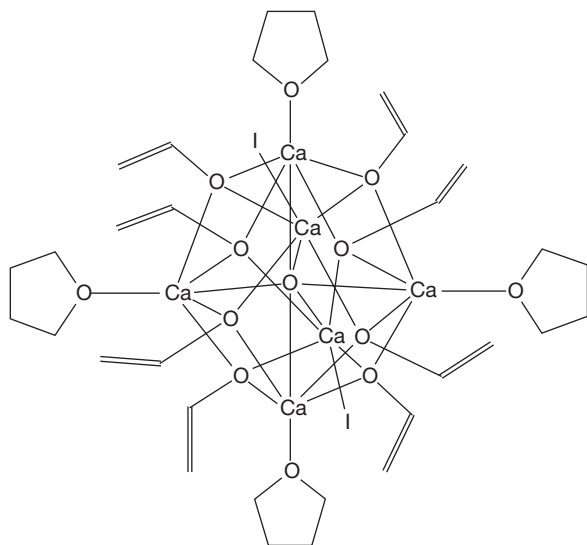


**Figure 21** Structure of  $((\text{thf})\text{Ca}(\text{O}-\text{CH}\equiv\text{CH}_2)_4) \cdot \text{CaO} \cdot \text{Ca}_2$  **42**.

When the dimeric salt **44** is treated with  $\text{CaI}_2$  in THF, cleavage of the methoxy methyl group occurs, and the tetramer **45** containing a  $\text{Ca}_4\text{O}_4$  cuboidal core is isolated in low yield (**Figure 23**).<sup>309</sup> The molecule has crystallographic  $S_4$  symmetry, and each calcium center is coordinated by the oxygen and phosphanyl phosphorus atoms on one ligand, the oxygen and anionic carbon of a second ligand ( $\text{Ca}-\text{C}=2.591(5)\text{Å}$ ), and the oxygen atom of a third ligand.  $\text{Ca}-\text{O}$  distances in the cube range from 2.346(4) to 2.430(3) Å.

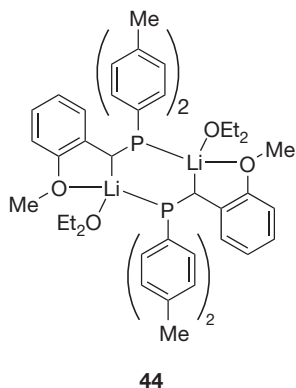


**Figure 22** Structure of  $(\text{CaO})_4 \cdot 4(\text{thf})_3\text{Ca}_2$  **43**.

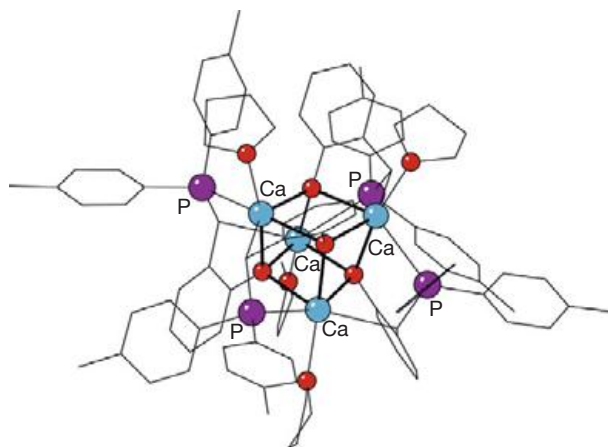


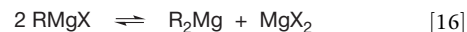
**Figure 23** Structure of  $[\text{Ca}(\text{thf})\{\text{CH}[\text{P}(\text{C}_6\text{H}_4\text{Me}-4)_2]\text{C}_6\text{H}_4\text{O}-2\}]_4$  **45**.

#### 1.37.4.2.2.1.2 Grignard reagents and related complexes

Grignard reagents are normally represented by the simple formula  $\text{RMgX}$  ( $\text{R}$ =organic group,  $\text{X}$ =halogen), although solvation, dimerization, aggregation, and deviations from this stoichiometry are common. Despite extensive work in the area, as documented in previous reviews,<sup>310–313</sup> the mechanisms of Grignard reagent formation are still under study. The many variables involved, including the identity of the substrates, the nature of the solvents used, and the physical form of the magnesium, greatly complicate the research. Both radical and anionic pathways have been implicated in Grignard formation.<sup>314</sup> Grignard formation is found to be dramatically affected by the presence of magnesium halides<sup>315</sup> and iron(II) chloride.<sup>316</sup> Several books and reviews on Grignard reagents, stressing applications in organic

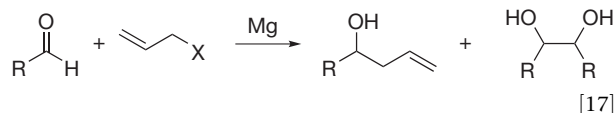
synthesis,<sup>317–319</sup> and the chemistry of highly functionalized organomagnesium reagents<sup>320</sup> have been published.

Schlenk equilibrium<sup>321</sup> (eqn [16]) occurs normally with many Grignard reagents, especially in ethereal solvents, but deliberate manipulation of the equilibrium can affect the progress of reactions and the product distribution. Di- or polyfunctionalized Grignard reagents remain comparatively rare, although they can offer enhanced reactivity relative to their monofunctional counterparts  $\text{RMgX}$ ; their chemistry has been reviewed elsewhere.<sup>322</sup>



For over a century after the initial reports of Grignard chemistry, it was uncritically assumed that the high reactivity of the magnesium–carbon bond mandated the use of anhydrous experimental conditions. This assumption was disproved in the case of Barbier–Grignard allylation of aldehydes (eqn [17]).<sup>323</sup> In dry THF, the reaction between benzaldehyde, allyl bromide, and  $\text{Mg}$  proceeds quantitatively,

but when the water content in THF reaches 7%, the reaction stops. When neat water is the solvent, however, the allyl halide is apparently confined to the magnesium surface because of hydrophobic interactions, shielding the metal from the water. The allylation reaction then proceeds, but with low conversion. The reaction of allyl bromide or iodide with benzaldehyde and Mg in 0.1 N aqueous HCl or NH<sub>4</sub>Cl again produces quantitative conversion of the aldehyde to allylation and pinacol coupling products. Such aqueous systems have received additional investigation,<sup>324,325</sup> as aqueous Grignard chemistry is attractive for its use of an environmentally benign solvent; it has been the subject of several reviews.<sup>326–330</sup>



Grignard reagents that are chiral at the metal should give strong asymmetric induction, and if the chirality were controlled, they could have great potential in stereoselective syntheses. There are also possibilities for studying single-electron transfer (SET) in the reaction of Grignard reagents, in which the metal-bearing carbon is the only stereogenic center. Reactions in which SET is involved include amination,<sup>331</sup> allylation,<sup>332,333</sup> oxidation,<sup>334</sup> and transmetalation.<sup>335</sup> This chemistry has been reviewed elsewhere.<sup>336</sup>

The majority of Grignard reagents are four-coordinate, but the *cis* isomers of octahedral complexes would be useful in the study of stereoselective synthesis. A variety of such systems are known<sup>337,338</sup>; as an example, the absolute asymmetric synthesis of the *D* and *L* enantiomers for both *cis*-[MgBr(4-MeC<sub>6</sub>H<sub>4</sub>)(dme)<sub>2</sub>] and *cis*-[MgMe(dme)<sub>2</sub>(thf)]I has been accomplished. Subsequent reaction with RCHO (R = (*i*-Pr) or Ph) yields the corresponding alcohol in up to 22% enantiomeric excess.<sup>339</sup>

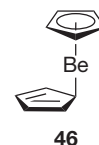
Determination of the structures of Grignard reagents continues to be of interest, and reviews on this subject have been published.<sup>340,341</sup> Most of the structure authentications are done on crystalline materials, although solution studies performed with extended x-ray absorption fine structure (EXAFS) spectroscopy are also available. Halide-bridged structures are common<sup>342,343</sup>; for example, the Grignard compounds MeMgBr and EtMgBr were found to be dimers in (*n*-Bu)<sub>2</sub>O at both room temperature and –85 °C.<sup>344</sup>

The traditional uses of Grignard reagents in organic synthesis are documented in many references outside this chapter.<sup>317–319</sup> There are numerous cases in which a Grignard reagent is used as a source of magnesium or as a ligand transfer reagent. In many reactions, the products are not organometallic species (e.g., phosphoranes,<sup>345</sup> alkoxides<sup>346</sup>) and are not detailed here.

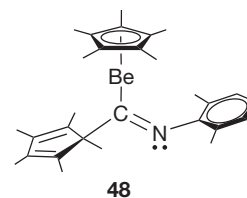
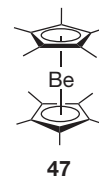
**1.37.4.2.2.1.3 Metallocenes and other cyclopentadienyl derivatives** As is true with other metals of the periodic table, the cyclopentadienyl ring and its derivatives are common in group 2 chemistry. The first organometallic compounds of Ca,<sup>347</sup> Sr,<sup>41</sup> and Ba<sup>348</sup> to be crystallographically characterized were cyclopentadienyl complexes. Cyclopentadienyl derivatives of beryllium are described in reviews that include main-group<sup>349,350</sup> and, specifically group 2, metallocenes.<sup>257,351</sup> A review focused specifically on beryllocenes has also been published.<sup>352</sup> Summaries of quantum chemical calculations

on main-group metallocenes that include group 2 species are available.<sup>146,147</sup>

For many years after the synthesis of the hydrocarbon-soluble dicyclopentadienylberyllium 46 by Fischer and Hofmann in 1959,<sup>353</sup> it remained the only crystallographically characterized beryllocene. The difficulty in establishing and understanding the nonclassical structure of 46 has made it one of the most intensively studied main-group metallocenes.<sup>351</sup> There is now general agreement that 46 adopts an η<sup>5</sup>/η<sup>1</sup> slip-sandwich structure in solution and the solid state,<sup>354</sup> and it is fluxional in both phases.<sup>354,355</sup> Calculations<sup>356–358</sup> support the slip-sandwich structure as the global minimum on the potential energy surface, which is thought to reflect a balance between Be–C bond strength, favored by σ-bonding, and Cp delocalization energy, which is favored by π-bonding.<sup>359</sup>

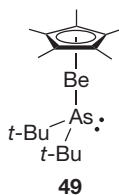


The failure of attempts<sup>77,360</sup> to prepare the permethylated derivative of 46, (C<sub>5</sub>Me<sub>5</sub>)<sub>2</sub>Be 47, was, at one time, ascribed to a possible steric oversaturation of the metal center.<sup>256</sup> Nevertheless, 47 and related beryllocenes (C<sub>5</sub>Me<sub>4</sub>H)<sub>2</sub>Be and (C<sub>5</sub>Me<sub>5</sub>)Be (C<sub>5</sub>Me<sub>4</sub>H) can be prepared from BeCl<sub>2</sub> and the appropriate KCp' reagent in Et<sub>2</sub>O or toluene/Et<sub>2</sub>O mixtures. The generation of 47 requires prolonged reaction times (3–4 days) and high temperatures (115 °C reflux). Like the parent 46, the beryllocene 47 is a sublimable, air- and oxygen-sensitive solid that is fluxional in solution. It reacts with CNC<sub>6</sub>H<sub>3</sub>Me<sub>2</sub>-2,6 to give a half-sandwich iminoacyl product, (C<sub>5</sub>Me<sub>5</sub>)BeC(=NXyl) (C<sub>5</sub>Me<sub>5</sub>) 48, via insertion into the Be–C σ bond.<sup>361</sup>

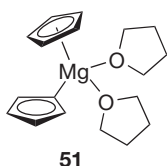


Low-temperature x-ray crystallography demonstrated that 47 exhibits a ferrocene-like η<sup>5</sup>/η<sup>5</sup> parallel-sandwich structure. The Be–C<sub>5</sub>Me<sub>5</sub> centroid distance (1.655(1) Å) and the Be–C distance (av 2.049 Å) are noticeably longer than in 46 (by 0.12 Å). Interestingly, calculations at various levels of theory place an η<sup>5</sup>/η<sup>1</sup> C<sub>s</sub> symmetric conformation for 47 at 1–3 kcal mol<sup>–1</sup> lower in energy than a ferrocene-like η<sup>5</sup>/η<sup>5</sup> D<sub>5d</sub> form.<sup>362</sup> Although the energy difference is small, it is possible that the η<sup>5</sup>-rings of 47 observed in the solid state are an artifact of crystal-packing.

The monocyclopentadienyl complexes  $(C_5Me_5)BeX$  ( $X=Cl, Br$ ) are versatile starting materials for other half-sandwich complexes.<sup>363</sup> Reaction with alkyllithium reagents  $LiR$  in  $Et_2O$  ( $R=Me, CMe_3, CH_2CMe_3, CH_2Ph$ ) produces the monomeric  $(\eta^5-C_5Me_5)BeR$  derivatives. Both the halide and alkyl derivatives are volatile; the alkyl derivatives are stable toward ligand rearrangement. The diorganoarsenide derivative  $\eta^5-(C_5Me_5)BeAs(t-Bu)_2$  **49** was prepared from the reaction of  $(C_5Me_5)BeCl$ <sup>77</sup> with  $LiAs(t-Bu)_2$  in  $Et_2O$  at  $0^\circ C$ .<sup>364</sup> The  $^9Be$  NMR shift of  $+14.16$  ppm is highly unusual for  $Cp-Be-X$  complexes, which are usually in the  $-27$  to  $-16$  ppm range; lower-ring hapticity in solution (either a static  $\eta^3$  or an average between  $\eta^1$  and  $\eta^5$ ) would explain the observed downfield NMR shift.<sup>269</sup>



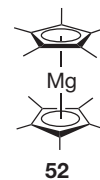
Magnesocene,  $Cp_2Mg$  **50**, was the first of the group 2 metallocenes to be synthesized,<sup>365</sup> and its ferrocene-like structure ( $Mg-C=2.304(8)$  Å (solid state)<sup>366</sup>;  $2.339(4)$  Å (gas phase)<sup>367</sup>) and usefulness as a cyclopentadienyl transfer reagent for transition-metal complexes have long been known.<sup>368-371</sup> The lability of the rings of **50** is displayed in other ways. The reaction of **50** with DMSO affords the ionic compound  $[Mg(dmsO)_6]^{2+}[C_5H_5]_2^-$  with uncoordinated cyclopentadienyl rings.<sup>372</sup> The reaction of **50** with the less strongly donating THF leads to the neutral complex  $Cp_2Mg(thf)_2$  **51** with differently ligated cyclopentadienyl rings: one with  $\eta^1$  coordination ( $Mg-C=2.282(3)$  Å) and the other with  $\eta^5$  ( $Mg-C=2.417-2.479(3)$  Å). Steric crowding presumably leads to the change in bonding arrangement.<sup>372</sup>



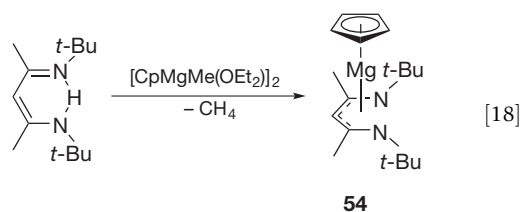
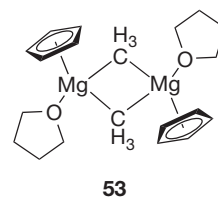
The lability of the  $Cp$  rings of **50** has also made it a useful source of the  $Mg^{2+}$  ion. **50** has been used to deposit  $MgO$  by atomic layer epitaxy,<sup>373</sup> and is commonly employed as a p-type dopant for semiconductors, particularly  $GaAs$ ,<sup>374</sup>  $GaN$ ,<sup>375,376</sup> and  $AlGaN$ .<sup>377</sup> In  $GaN$ ,  $Mg$  doping induces a blue 2.8-eV photoluminescence band arising from donor-acceptor (D-A) pair recombination.<sup>378-380</sup> The reaction of **50** with alkylamines has been examined in the context of  $Cp_2Mg-MR_3-NH_3$  ( $M=$  group 13 metal) mixtures as CVD precursors. The addition of primary

and secondary amines to **50** at ambient temperature in toluene affords stable amine adducts in good yield.<sup>381,382</sup>

Although it was the earliest known group 2 decamethylmetallocene,<sup>383</sup>  $(C_5Me_5)_2Mg$  **52** was the last of the group 2 decamethylmetallocenes to be structurally authenticated with x-ray or electron diffraction. Unlike its counterparts with the heavier group 2 metals, **52** is linear, with  $Mg-C=2.302$  Å.<sup>231</sup> Both **52** and other magnesocenes react with *i*-Pr-carbene to form adducts.<sup>47</sup>



$[CpMgMe(Et_2O)]_2$  **53**, a versatile reagent for (monocyclopentadienyl)magnesium chemistry, is prepared by dissolving **50** and  $Me_2Mg$  in  $Et_2O$ .<sup>384</sup> It reacts readily with a variety of amines and 2,5-bis(dimethylaminomethyl)pyrrole to form substitution products.<sup>384</sup> Monocyclopentadienyl complexes containing the  $\beta$ -diketiminato ligand can display either  $\eta^2$ - or  $\pi$ -coordination to a magnesium center. The reaction of **53** with the diketimine  $N-(t-Bu)-4-(t-Bu-imino)-2-penten-2-amine$  in  $Et_2O$  (eqn [18]) produces  $CpMg(HC(C(Me)N(t-Bu))_2)$  **54**.<sup>385</sup> In the solid state, **54** contains a  $\pi$ -coordinated  $\beta$ -diketiminato ligand ( $Mg-N=2.006(4), 2.021(3)$  Å; the  $Mg-C_z$  distances of  $2.689(3)$  and  $2.729(3)$  Å represent weak bonding interactions).



The structure of unsolvated  $Cp_2Ca$  was described in 1974,<sup>347</sup> but attempts to crystallize the strontium and barium analogs for characterization with x-ray crystallography were unsuccessful, owing to their insolubility in common solvents. The parent metallocene  $Cp_2Ca$  undergoes H/D exchange when heated in  $DMSO-d_6$  to yield  $Cp_2Ca\{d_{10}\}$  (97% D) in 95% yield. For the ring-substituted bis(1-cyclopentenyl)calcocene, H/D exchange occurs at the cyclopentadienyl rings and the 2,5-positions of the 1-cyclopentenyl substituents.<sup>386</sup>

The reaction of  $C_5H_6$  with  $Ba[N(SiMe_3)_2]_2(thf)_2$  gives  $Cp_2Ba$ , which can be recrystallized from DMSO to give  $Cp_2Ba-dmsO$  **55**. The latter forms an extended structure with four  $Cp^-$  groups surrounding the central  $Ba^{2+}$  ion ( $Ba-C=3.138(6)-3.164(5)$

Å) (Figure 24). The reaction of  $\text{Cp}_2\text{Ba}$  with 18-crown-6 affords monomeric  $\text{Cp}_2\text{Ba}(18\text{-crown-6})$  with two axial  $\text{Cp}^-$  rings ( $\text{Ba}-\text{C}=3.180(6)\text{-}3.257(7)\text{Å}$ ).<sup>201</sup>

Metallocenes with methylated rings were among the first heavy alkaline-earth cyclopentadienyl complexes to be structurally characterized, but many other substituents (e.g., *t*-Bu,<sup>387</sup> 4-(*n*-Bu)- $\text{C}_6\text{H}_4$ <sup>388</sup>) have been incorporated into bis(cyclopentadienyl) complexes. Under this classification are included compounds with indenyl ligands,<sup>389</sup> which, in heavy group 2 compounds, function as benzo-Cp groups, without the slippage that is observed in many transition-metal complexes.<sup>390</sup> Various organometallic complexes containing heterocyclic group 15 rings are known. These are often formed in complex reactions.<sup>391,392</sup> Some of them resemble metallocenes, such as  $(\eta^5\text{-}2,5\text{-Ph}_2\text{C}_4\text{As})_2\text{Ca}(\text{thf})_2$ .<sup>393</sup>

Fulvenes or their analogs have been used as precursors to bis(cyclopentadienyl) complexes, both without bridges and *ansa*-bridged; some of latter are chiral. Substituents on fulvenes affect whether calocenes with or without bridges are formed preferentially.<sup>394</sup> Hydrogen atom or proton transfer between dialkylfulvenes and their radical anions is responsible for the formation of bridged calocenes.<sup>395</sup> The reductive coupling of guaiazulene, a fulvene analog, with activated calcium in THF affords a 60:40 mixture of two isomers,

8,8'- (56, Figure 25) and 8,6'-(diguaiiazulene)bis(tetrahydrofuran)calcium, respectively.<sup>396</sup>

Phosphonium-bridged species (i.e., the diylides  $[\text{R}_2\text{PCp}'_2]^-$ )<sup>397</sup> are attractive ligands for group 2 elements, as they provide a metallocene-like framework, but only a uninegative charge. By treatment of the phosphonium salt  $[\text{Me}(t\text{-Bu})\text{P}(\text{C}_5\text{Me}_4\text{H})_2]\text{I}$  with 1 equiv. of KH followed by  $\text{Ca}[\text{N}(\text{SiMe}_3)_2]_2$ , the calcium complex  $[\text{Me}(t\text{-Bu})\text{P}(\text{C}_5\text{Me}_4)_2]\text{CaN}(\text{SiMe}_3)_2$  57 (Figure 26) is produced, which is structurally analogous to  $\text{Cp}'_2\text{LnX}$  organolanthanides. DFT studies of the  $\text{H}_3\text{E}$  ( $\text{E}=\text{C}, \text{Si}, \text{P}$ )-substituted cyclopentadienyl ring indicate that the energy required for out-of-plane bending of the substituent decreases in the order  $\text{H}_3\text{C} > \text{H}_3\text{Si} > \text{H}_3\text{P}$ . Related examples of phosphonium-bridged organometallic compounds are known.<sup>398</sup>

Most metallocenes of calcium, strontium, or barium are bent, even when unsolvated. The exceptions to this are complexes with extremely bulky ligands (e.g., the sterically crowded  $(\text{C}_5(i\text{-Pr})_5)_2\text{Ba}$ ,<sup>399</sup>  $(\text{Ph}_5\text{C}_5)_2\text{Ae}$  ( $\text{Ae}=\text{Ca}, \text{Ba}$ ),<sup>63</sup> or  $(\text{Cp-BIG})_2\text{Ae}$  ( $\text{Cp-BIG}=(4\text{-}(n\text{-Bu})\text{-C}_6\text{H}_4)_5\text{Cp}$ ;  $\text{Ae}=\text{Ca}, \text{Sr}, \text{Ba}$  58) (Figure 27).<sup>388</sup> All three  $(\text{C}_5(i\text{-Pr})_5\text{H})_2\text{M}$  ( $\text{M}=\text{Ca}, \text{Sr}, \text{Ba}$ ) species display exceptional levels of air stability (on the order of weeks for the calcium and strontium derivatives), undoubtedly a result of the complete enclosure of the metal centers. All of these metallocenes possess high symmetry; the  $\text{S}_{10}$

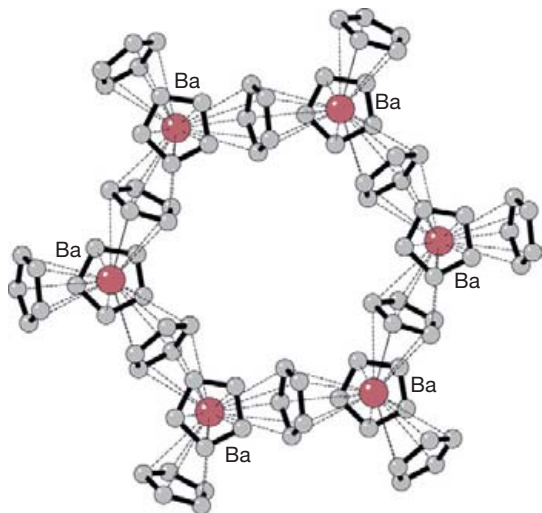


Figure 24 Structure of  $[\text{Cp}_2\text{Ba} \cdot \text{dmsol}]_n$  55.

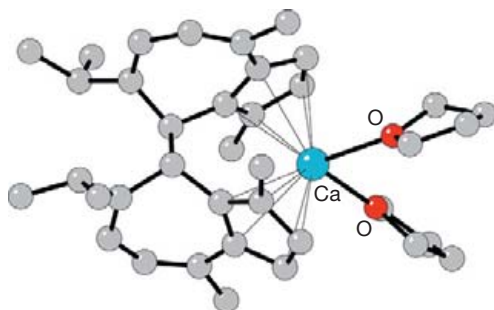


Figure 25 Structure of 8,8'-(diguaiiazulene)bis(tetrahydrofuran)calcium 56.

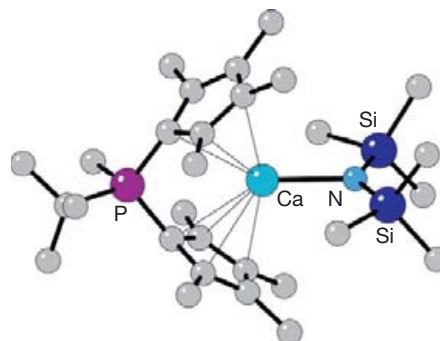


Figure 26 Structure of  $[\text{Me}(t\text{-Bu})\text{P}(\text{C}_5\text{Me}_4)_2]\text{CaN}(\text{SiMe}_3)_2$  57.

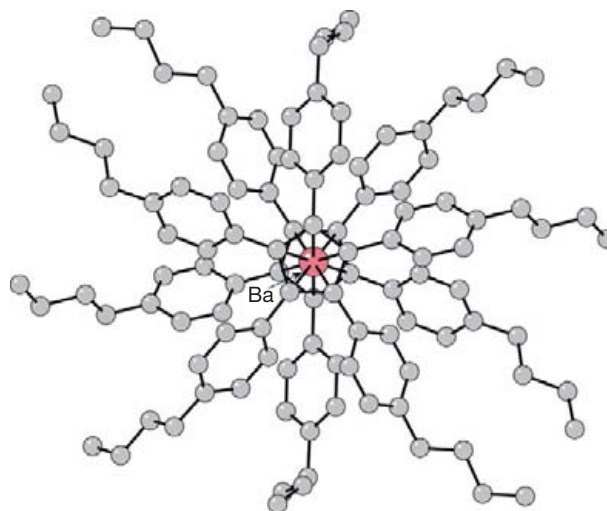


Figure 27 Structure of  $(\text{Cp-BIG})_2\text{Ba}$  58.

geometries of the  $(\text{Cp-BIG})_2\text{Ae}$  complexes have been analyzed with DFT calculations on simplified  $(\text{C}_5\text{Ph}_5)_2\text{Ae}$  models, and arene–arene interactions are believed to play a substantial role in supporting their structures.<sup>400</sup>

The reaction of  $[(\text{C}_5(i\text{-Pr})_5)\text{Ba}(\text{thf})_2]_2$  with  $\text{Na}_2\text{COT}$  in THF/hexane produces the triple-decker sandwich complex  $(\text{C}_5(i\text{-Pr})_5)\text{Ba}(\text{COT})\text{Ba}(\text{C}_5(i\text{-Pr})_5)$  **59** (Figure 28). It crystallizes as a slightly bent stack (Cp' centroid–Ba–COT centroid angle =  $169.5^\circ$ ).<sup>401</sup> Related complexes have been made with terminal  $(\text{C}_5(i\text{-Pr})_4\text{H})$  ligands for Ca, Sr, and Ba.<sup>402</sup>

The reaction of CO with  $(\text{C}_5\text{Me}_5)_2\text{Ae}$  (Ae = Mg–Ba) has been studied in toluene or methylcyclohexane solution in a high-pressure IR cell.<sup>403,404</sup> Only with the calcium and strontium complexes are carbonyl stretches observed that could be interpreted as the formation of monocarbonyl complexes  $(\text{C}_5\text{Me}_5)_2\text{AeCO}$  (for  $(\text{C}_5\text{Me}_5)_2\text{CaCO}$ ,  $2158\text{ cm}^{-1}$ ;  $(\text{C}_5\text{Me}_5)_2\text{SrCO}$ ,  $2159\text{ cm}^{-1}$ ). These are greater than that of free CO in toluene or methylcyclohexane ( $2134\text{ cm}^{-1}$ ). Equilibrium-constant measurements indicate that the M–CO binding is weak; the CO appears to function as a pure  $\sigma$ -donor to the metals.

Compounds of the general form  $\text{Cp}'\text{AeX}(\text{L})_n$  (Ae = Ca, Sr, Ba; X = a monoanionic ligand; L = optional neutral Lewis base (s)) can be derivatized by exchanging X, and the addition or removal of ligands L (ethers, amines) allows adjustment of the coordination environment. Nevertheless, a persistent challenge with studying mono(cyclopentadienyl) and other heteroleptic alkaline-earth compounds is the operation of Schlenk-type equilibria (cf. eqn [16]). The mono[(tetraisopropyl)cyclopentadienyl]strontium halide  $[(\text{C}_5(i\text{-Pr})_4\text{H})\text{Sr}(\text{thf})_2]_2$ , for example, has been obtained from both  $\text{SrI}_2$  and  $\text{Na}[(\text{C}_5(i\text{-Pr})_4\text{H})]$  or by ligand redistribution between octaisopropylstrontocene and  $\text{SrI}_2$ .<sup>405</sup> The mono(ring) complexes  $[(\text{C}_5((t\text{-Bu})_{3-1,2,4})\text{H}_2)\text{Ba}(\text{thf})_2]_\infty$  and  $[(\text{C}_5(i\text{-Pr})_4\text{H})\text{Ba}(\text{thf})_2]_2$  have been synthesized from  $\text{BaI}_2$  and the corresponding sodium cyclopentadienides.<sup>406</sup> The heavier metal compounds are more susceptible to loss of donor solvent and ring redistribution than their calcium counterparts.<sup>73</sup>

The chlorido-bridged calcium complex  $[(\text{C}_5((t\text{-Bu})_{3-1,2,4})\text{H}_2)\text{CaCl}(\text{dme})]_2$  is available from  $\text{CaCl}_2$  and  $\text{Na}[(\text{C}_5((t\text{-Bu})_{3-1,2,4})\text{H}_2)]$ .<sup>405</sup> The related mono(ring) complexes  $[(\text{C}_5((\text{SiMe}_3)_{3-1,2,4})\text{H}_2)\text{Ae}(\text{thf})_n]$  can be prepared as crystalline solids by halide displacement reactions between  $\text{K}[(\text{C}_5((\text{SiMe}_3)_{3-1,2,4})\text{H}_2)]$  and the metal diiodides;<sup>406</sup> the calcium and strontium iodide complexes are dimers with bridging iodide ligands, whereas the barium complex crystallizes from THF/toluene as a coordination polymer. The polymeric structure of the mono(ring) complex  $[(\text{C}_5((t\text{-Bu})_{3-1,2,4})\text{H}_2)\text{Ba}(\text{thf})_2]$  is similar.<sup>405</sup>

Derivatization of some mono(cyclopentadienyl) complexes to yield new monosubstituted species can often be accomplished by metathetical exchange (eqn [19]) or protonation

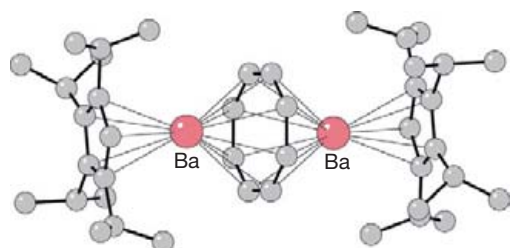
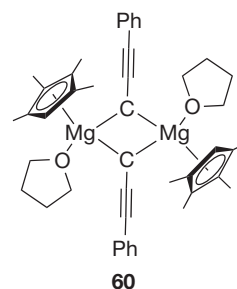
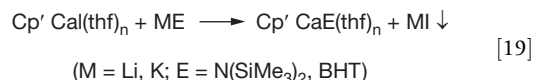
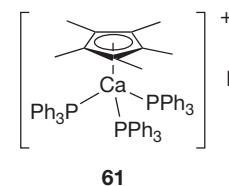


Figure 28 Structure of  $(\text{C}_5(i\text{-Pr})_5)\text{Ba}(\text{COT})\text{Ba}(\text{C}_5(i\text{-Pr})_5)$  **59**.

reactions.<sup>73</sup> Protonolysis of  $(\text{C}_5(i\text{-Pr})_4\text{H})\text{Ca}[\text{N}(\text{SiMe}_3)_2](\text{thf})$  with several terminal alkynes  $\text{HC}\equiv\text{CR}$  in either toluene or hexanes produces the corresponding calcium acetylide complexes  $[(\text{C}_5(i\text{-Pr})_4\text{H})\text{CaC}\equiv\text{CR}(\text{thf})_2]$  (R = Ph, ferrocenyl,  $\text{SiMe}_3$ ,  $\text{Si}(i\text{-Pr})_3$ ,  $\text{SiPh}_3$ ) in good yield.<sup>407</sup> The related  $[(\text{C}_5\text{HMe}_4)\text{MgC}\equiv\text{CPh}(\text{thf})_2]$  **60** has been synthesized from the reaction of  $[(\text{C}_5\text{HMe}_4)\text{Mg}(n\text{-Bu})]$  and  $\text{HC}\equiv\text{CPh}$ ,<sup>50</sup> as has  $[(\text{C}_5\text{HMe}_4)\text{CaC}\equiv\text{CPh}(\text{thf})_2]$  from metallic Ca,  $\text{C}_5\text{H}_2\text{Me}_4$  and  $\text{HC}\equiv\text{CPh}$ .<sup>50</sup> All of these are acetylide-bridged dimers, with Mg–C(acetylide) distances in **60** ranging from 2.218(2) to 2.399(2) Å.



The cationic complex  $[(\text{C}_5\text{Me}_5)\text{Ca}(\text{OPPh}_3)_3]^+\text{I}^-$  **61** is obtained by the displacement of an iodide from  $(\text{C}_5\text{Me}_5)\text{Ca}(\text{thf})_2$  with triphenylphosphane oxide.<sup>408</sup> The latter's ability to substitute for  $\text{I}^-$  and THF but not  $[(\text{C}_5\text{Me}_5)]^-$  on calcium follows the approximate  $\text{pK}_b$  of the bases (i.e.,  $-12$  ( $[(\text{C}_5\text{Me}_5)]^-$ )  $< \sim 8$  ( $\text{OPPh}_3$ )  $< \sim 12$  (THF)  $< \sim 24$  ( $\text{I}^-$ )). The piano-stool geometry of **61** is coupled with a longer than average Ca–C distance of 2.684(4) Å,<sup>408</sup> evidently reflecting the strong electron-donor properties of the  $\text{OPPh}_3$  ligands.



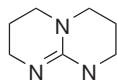
61

#### 1.37.4.2.2.1.4 Other organometallics (including heterobimetallics)

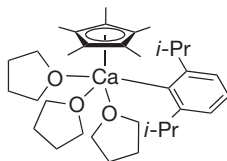
The weak interactions that may exist between group 2 cations and anionic hydrocarbyl ligands are demonstrated in the 'metal-in-a-box' compounds such as  $[\text{Ae}(\text{thf})_6][\text{Me}_3\text{Si}(\text{fluorenyl})_2]$  (Ae = Ca or Mg),<sup>409</sup> which are formed by the addition of THF to solutions of the bis(fluorenyl) complexes in nonpolar solvents. A similar situation exists with compounds containing the  $[(\text{C}_5\text{Ph}_5)]^-$  ion, giving rise to complexes such as  $[\text{Ca}(\text{thf})_6][\text{C}_5\text{Ph}_5]_2$  **62** (Figure 29).<sup>63</sup> The disruption of the metal–carbon bonds is thought to reflect a combination of robust Ae–thf interactions, the stability of the free carbanions, and the formation of numerous C–H $\cdots\pi$  interactions between THF and the anions.

Alkylmagnesium complexes stabilized by a bulky  $\beta$ -diketiminato ligand have been known for some time.<sup>410,411</sup> Structurally characterized examples of these include  $[\text{Mg}(\text{L})\text{Me}(\text{OEt})_2]$ ,  $[\text{Mg}(\text{L})(\mu\text{-Me})_2]$ , and  $[\text{Mg}(\text{L})(t\text{-Bu})]$  (L = DIPP–nacnac).<sup>410</sup> Related compounds with aminotroponimate<sup>411</sup>

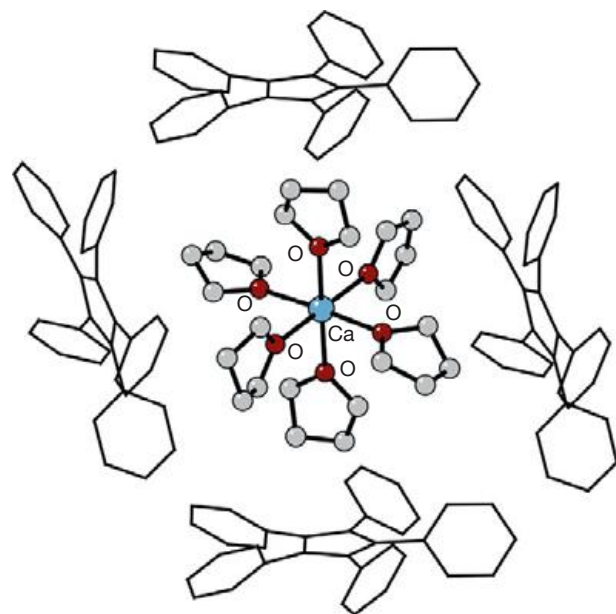
and guanidinate<sup>412,413</sup> ligands are known. In particular, the reaction between hppH **63** and MeMgBr results in the tetranuclear species [MgBr(hpp)]<sub>4</sub>, in which each magnesium is coordinated by four nitrogen atoms and one Br atom in a distorted square pyramid. The Mg···Mg' contacts are as short as 2.943(3) Å, which is only 0.1 Å longer than in the monovalent **1** and **2**.

**63**

The use of Grignard reagents to synthesize aryloxide complexes, which are not formally organometallic species, has been mentioned earlier (Section 1.37.4.2.2.1.2). Combined cyclopentadienyl/aryloxide complexes can be formed from the reaction of ICa(Odipp)(thf)<sub>4</sub> with K[C<sub>5</sub>Me<sub>5</sub>], (Cp<sup>3Si</sup>)<sub>2</sub>Ca with K[Odipp], and IBa(BHT)(thf)<sub>3</sub> with K[C<sub>5</sub>Me<sub>5</sub>] in THF.<sup>414</sup> The products, (C<sub>5</sub>Me<sub>5</sub>)Ca(Odipp)(thf)<sub>3</sub> **64**, (Cp<sup>3Si</sup>)Ca(Odipp)(thf)<sub>2</sub>, and (C<sub>5</sub>Me<sub>5</sub>)Ba(BHT)(thf), respectively, are stable against Schlenk rearrangement in THF and aromatic solvents.

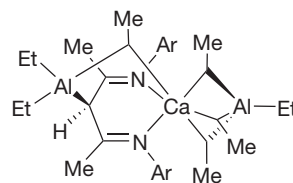
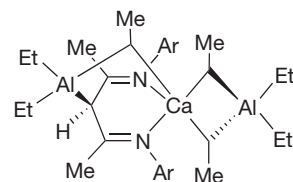
**64**

A review of magnesium organodiamides and mixed magnesium–aluminum-bridged oligomers, with a focus on heterocumulene reactivity, is available in the literature.<sup>415</sup> Reaction of the β-diketiminato calcium complex (DIPP-nacnac)Ca[N(SiMe<sub>3</sub>)<sub>2</sub>](OEt)<sub>2</sub> with Et<sub>3</sub>Al produces a calcium aluminate complex κ<sup>3</sup>-(DIPP-nacnac)Ca[Et<sub>4</sub>Al], in which the calcium is

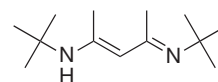
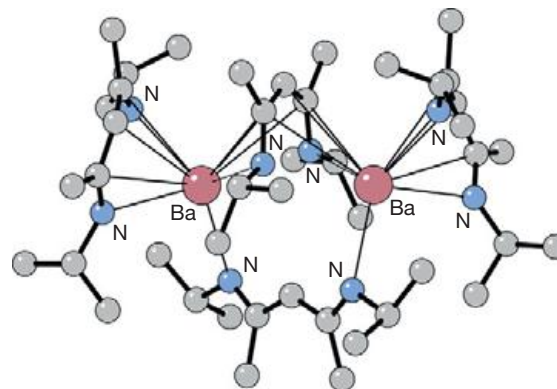


**Figure 29** Partial packing diagram of the 'metal-in-a-box' compound [Ca(thf)<sub>6</sub>][C<sub>5</sub>Ph<sub>5</sub>]<sub>2</sub> **62**.

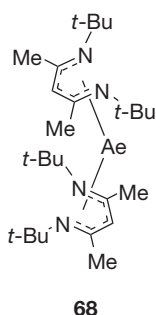
coordinated by bridging ethyl groups from the aluminate anion (disordered over μ<sub>3</sub>-**65** and μ<sub>2</sub>-**66** coordination modes). The coordination sphere is completed by a tripodal κ<sup>3</sup>-N,N,C-coordinated ligand derived from the reaction of the β-diketiminato ligand with Et<sub>3</sub>Al.<sup>416</sup>

**65****66**

Treatment of the amine **67** (L(*t*-Bu)H) in a 2:1 ratio with Ae[N(SiMe<sub>3</sub>)<sub>2</sub>]<sub>2</sub>(thf)<sub>2</sub> (Ae = Ca, Sr, Ba) in toluene at ambient temperatures affords (η<sup>5</sup>-L(*t*-Bu))<sub>2</sub>M **68** in ≥ 93% yields.<sup>417</sup> All three compounds possess bent sandwich structures with η<sup>5</sup>-coordinated β-diketiminato ligands. The reaction of Ba[N(SiMe<sub>3</sub>)<sub>2</sub>]<sub>2</sub>(thf)<sub>2</sub> with the *i*-Pr analog of **67** yields the C<sub>2</sub>-symmetric dinuclear complex **69** (Figure 30). The latter exhibits three different bonding modes for the β-diketiminato ligands: η<sup>5</sup> (Ba–N = 2.685, 2.722 Å), μ-η<sup>1</sup>:η<sup>1</sup> (Ba–N = 2.790 Å), and μ-η<sup>5</sup>:η<sup>5</sup> (Ba–N = 2.814, 2.927 Å). NMR evidence indicates that its dinuclear structure remains intact in solution.<sup>417</sup> Various other β-diketiminato ligand systems have been investigated for their stability against Schlenk redistribution and ability to resist protonation from aromatic amines.<sup>418</sup>

**67**

**Figure 30** Structure of the dinuclear β-diketiminato complex **69**.



#### 1.37.4.2.2.2 Silicon, germanium, and tin ligands

Although silicon-containing ligands (e.g., those with  $-\text{SiR}_3$  ( $\text{R}=\text{alkyl, aryl}$ ) substituents) are frequently incorporated into compounds of the group 2 metals, direct Ae–Si bonds are uncommon. Compounds containing Ae–SiMe<sub>3</sub> bonds are rare,<sup>419</sup> but closely related ligands containing different R groups have been used in group 2 compounds. ‘Supersilanides’ replace the methyl groups with *tert*-butyl groups,<sup>420</sup> and the supersilanides  $(t\text{-Bu})_3\text{SiAeX}$  and  $(t\text{-Bu})_3\text{Si-Ae-Si}(t\text{-Bu})_3$  ( $\text{Ae}=\text{Be, Mg; X}=\text{Cl, Br}$ ) have been synthesized from the appropriate Ae halides and  $\text{NaSi}(t\text{-Bu})_3$ , structurally characterized, and tested for reactivity. The analogous Grignard compound  $(t\text{-Bu})_3\text{SiMgBr}$  undergoes coordination interactions with THF solvent to form the dimer  $[(t\text{-Bu})_3\text{SiMg}(\text{thf})(\mu\text{-Br})_2]$ .<sup>420</sup>

The first  $\alpha,\omega$ -dianionic unsaturated oligosilane was synthesized as a magnesium salt from the reaction of the lithium disilene **70** with  $(\text{trip})\text{SiCl}_3$ , followed by reduction with activated Mg (**71**, Figure 31).<sup>421</sup> The structure was confirmed with <sup>29</sup>Si NMR and x-ray crystallography. The UV–vis spectrum of **71** displays a maximum absorption at 415 nm, corresponding closely with that of **70** at 417 nm; this suggests that the charge remains localized on the silicon atoms of the two compounds.<sup>421</sup>

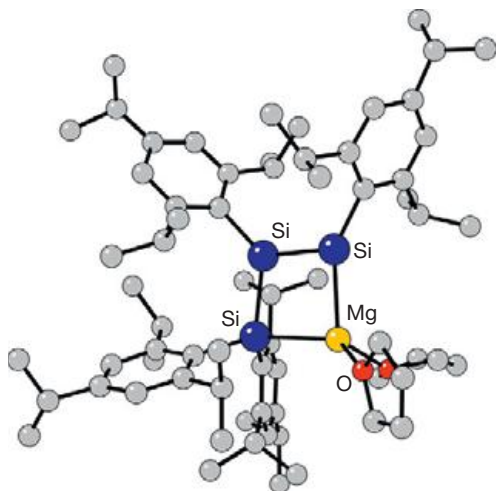
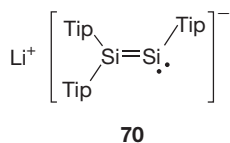


**Figure 31** Structure of the magnesium trisilene-1,3-diide **71**.

The so-called ‘hypersilanide’ anion  $([\text{Si}(\text{SiMe}_3)_3]^-)$  has been incorporated into the monomeric magnesium compounds  $\text{Mg}[\text{Si}(\text{SiMe}_3)_3]_2(\text{thf})_2$  and  $\text{MgBr}[\text{Si}(\text{SiMe}_3)_3](\text{thf})_2$ .<sup>422</sup> Both compounds were synthesized from  $\text{MgBr}_2$  and the appropriate stoichiometric equivalent of lithium or potassium hypersilanide in diethyl ether and THF,<sup>422</sup> and have been characterized with NMR and x-ray crystallographic studies.

Hypersilanides of the heavier group 2 elements have been synthesized through halide metathesis reactions and characterized to determine the effects of coordinating solvents on Ae–Si bonding in the solid state.<sup>423,424</sup> The barium hypersilanides are represented by  $\text{Ba}(\text{thf})_4[\text{Si}(\text{SiMe}_3)_3]_2$  and  $[\text{Ba}(\text{hmpa})_6][\text{Si}(\text{SiMe}_3)_3]_2$ . The former exhibits direct Ba–Si bonding with a heavily distorted octahedral geometry and a bent *trans* Si–Ba–Si bond ( $140.62(3)^\circ$ ; Ba–Si =  $2.74(1)\text{Å}$  (av)).<sup>423,424</sup> The latter compound consists of separated ionic species owing to the hmpa ligand that quantitatively produces the separated ions in the solid state.<sup>423,424</sup> Hypersilanides of Ca and Sr have also been synthesized in a similar manner with coordinated thf and TMEDA in appropriate ratios to fill each element’s coordination sphere (i.e.,  $\text{Ae}(\text{thf})_3[\text{Si}(\text{SiMe}_3)_3]_2$  ( $\text{Ae}=\text{Ca, Sr}$ )).<sup>424</sup> The center silicon atoms in the hypersilanide anions display distortions toward pyramidal geometry, indicative of considerable charge transfer from the metal to the anion. All of the heavy alkaline-earth hypersilanides undergo rapid decomposition with the formation of  $\text{Si}(\text{SiMe}_3)_4$  in THF solution, and separation into ions in  $\text{C}_6\text{D}_6$  solution. Such solution instability may place limits on their effectiveness as potential catalyst initiators (see Chapter 1.38).

The 1,1′-oligoferrocene derivative **72** containing a magnesium bridging between silicon atoms was prepared through the reaction of 1,1′-bis[bis(trimethylsilyl)potassiosilyl]ferrocene with the electrophilic species  $\text{MgBr}_2\cdot\text{Et}_2\text{O}$ . The Cp rings of ferrocene remain parallel, and the tetrahedral coordination environment is constructed from the silicon ligands and two thf molecules (Figure 32).<sup>425</sup>

Heavy alkaline-earth metal germanides for calcium, strontium, and barium  $\text{Ae}(\text{thf})_n(\text{Ge}(\text{SiMe}_3)_3)_2$  ( $\text{Ae}=\text{Ca, } n=3$ ;  $\text{Sr, } n=3$ ; and  $\text{Ba, } n=4$ ) have been prepared with halide metathesis

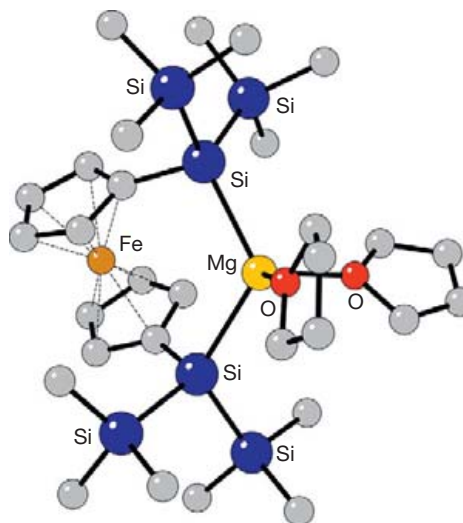


**Figure 32** Structure of the magnesium 1,1′-oligoferrocene derivative **72**.

methods analogous to those used for the silanides.<sup>426</sup> Nearly identical Ae–Si and Ae–Ge bond lengths are observed in corresponding compounds, with slightly shorter bond distances for the germanium analogs (e.g., for  $\text{Ca}(\text{thf})_3(\text{M}(\text{SiMe}_3)_3)_2$ , Ca–Si = 3.06 Å (av), Ca–Ge = 3.04 Å (av)), which is probably a consequence of slightly higher bond polarity in the heavier derivatives.<sup>426</sup>

Unique ‘nonclassical’ dianionic species of  $^3\Delta$ -1,2,3,4-disiladigermetene were synthesized through the reduction of the digermetene by magnesium or calcium in THF, or through halide metathesis (Ca, Sr 73 (Figure 33), and Ba) with the dipotassium salt of the digermetide dianion.<sup>427</sup> The highly air- and moisture-sensitive products contain a bicyclo[1.1.0]butane 2,4-dianion skeleton not present in the starting material.

Compounds containing direct bonds between the group 2 elements and tin-containing ligands are rare. Structurally authenticated compounds containing Ca–Sn (i.e.,  $\text{Ca}(\text{SnMe}_3)_2(\text{thf})_4$ ),<sup>428</sup> Sr–Sn, or Ba–Sn bonds were first reported only in 1994.<sup>429</sup> More recently, various cluster-type compounds (e.g.,  $[\text{Sn}_3\text{Mg}(\text{thf})(\mu_3\text{-N}(t\text{-Bu})_4)]$  74 (Figure 34))<sup>430</sup>

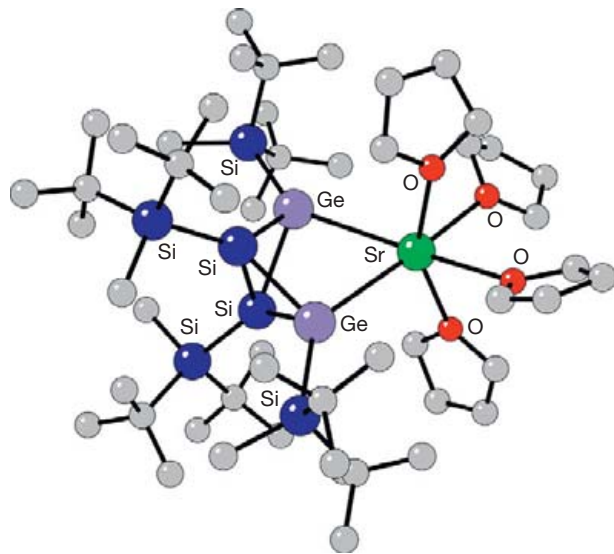


Figure 33 Structure of the strontium  $^3\Delta$ -1,2,3,4-disiladigermetene 73.

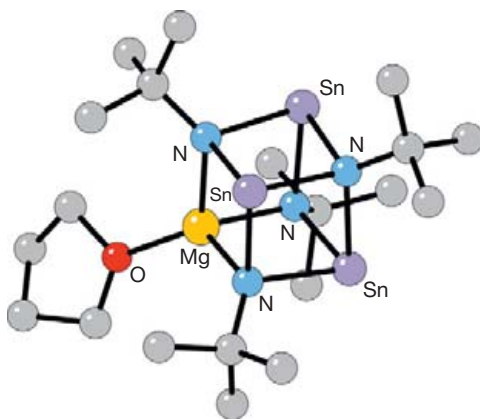


Figure 34 Structure of the heterobimetallic cubane complex  $\text{Sn}_3\text{Mg}(\text{thf})(\mu_3\text{-N}(t\text{-Bu})_4)$  74.

and ion-separated compounds containing alkaline-earth metals and tin (e.g.,  $[\text{Ba}(18\text{-crown-6})(\text{hmpa})_2][\text{SnPh}_3)_2]$  have been synthesized.<sup>402</sup> None of the latter complexes incorporate direct bonding between group 2 elements and Sn.

### 1.37.4.2.3 Group 15 ligands

#### 1.37.4.2.3.1 Nitrogen-donor ligands

**1.37.4.2.3.1.1 Amides, especially bis(trimethylsilyl) amides** The heavier group 2 elements (Ca–Ba) dissolve in liquid ammonia to form ammoniates,  $\text{Ae}(\text{NH}_3)_x$ , which, on standing, will convert to the parent amides ( $\text{Ae}(\text{NH}_2)_2$ ); they possess ionic lattices.<sup>7</sup> Pure magnesium dissolves in liquid  $\text{NH}_3$  to generate a blue color, although an ammoniate cannot be isolated. In contrast, an Mg/Hg alloy will react in liquid  $\text{NH}_3$  to generate the  $\text{Mg}(\text{NH}_3)_6\text{Hg}_{22}$  aggregate, which possesses an octahedrally coordinated magnesium center.<sup>48</sup> Replacement of the hydrogen atoms of amides with groups of increasing size leads to molecular complexes. Alkaline-earth amido complexes are used both in organic synthesis<sup>431</sup> and to prepare a wide variety of derivatives of other main-group and transition-metal complexes.

A widely used class of s-block amido complexes is that containing the bis(trimethylsilyl) group,  $-\text{N}(\text{SiMe}_2)_2$ . Early examples of these compounds were synthesized by Wannagat in the 1960s,<sup>432</sup> and all the group 2 metals (except for Ra) are now represented. The chemistry of the heavy alkaline-earth derivatives has been extensively developed by Westerhausen,<sup>433</sup> this chemistry has already been reviewed in the literature.<sup>74</sup>

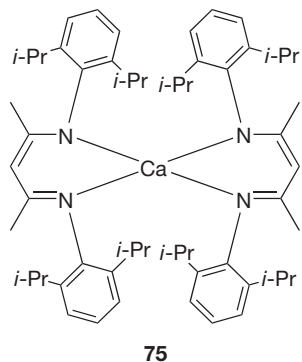
Synthesis of the s-block metal bis(trimethylsilyl)amides is varied, and representative routes were described in Section 1.37.2. Synthesis of the compounds is sensitive to the reaction conditions and identity of the metals, and the exact products to be expected can be difficult to predict; for example, the addition of  $\text{LiN}(\text{SiMe}_3)_2$  to  $\text{Ca}[\text{N}(\text{SiMe}_3)_2]_2$  in THF produces the heterometallic species  $\text{Ca}[\text{N}(\text{SiMe}_3)_2][\mu\text{-N}(\text{SiMe}_3)_2]_2\text{Li}(\text{thf})$ ; if the barium amido complex is used instead,  $\text{Ba}[\text{N}(\text{SiMe}_3)_2]_2(\text{thf})_3\text{Li}_2[\mu\text{-N}(\text{SiMe}_3)_2]_2(\text{thf})_2$  can be isolated.<sup>434</sup>

The beryllium bis(trimethylsilyl)amido complex is monomeric,<sup>435,436</sup> probably for steric reasons, but the Mg–Ba compounds are dimers.<sup>127</sup> Although the M–Si distances change as expected with the increasing size of the cation, the difference between terminal and bridging N–Si distances decreases with the larger metals. Partial multiple bonding between Si and N, in which the lone-pair electrons on nitrogen are delocalized onto silicon, has been suggested as an explanation for the Si–N distance/Si–N–Si’ angle relationships, but steric interactions may also play a critical role in determining the geometries. Bis(trimethylsilyl)amido complexes containing short Si–N bonds must necessarily possess relatively large Si–N–Si’ angles to avoid violating a minimum  $\text{SiMe}_3 \cdots \text{SiMe}_3'$  separation.

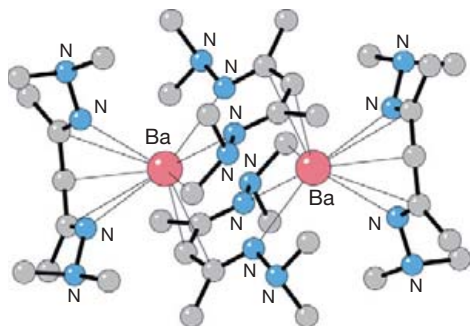
The trimethylsilyl groups are primarily responsible for the hydrocarbon solubility of the base-free and ether adducts, supported by the strong ion-pairing interaction between the  $\text{Ae}^{2+}$  and the  $[\text{N}(\text{SiMe}_3)_2]^-$  ions.<sup>437</sup> Extensive NMR data ( $^1\text{H}$ ,  $^{13}\text{C}$ ,  $^{15}\text{N}$ ,  $^{29}\text{Si}$ ) exist for these species<sup>74</sup>; the  $\delta(\text{N})$  and  $\delta(\text{SiMe}_3)$  shifts are sensitive to the identity of the metal center. In the case of the barium compounds, differences in the chemical shifts and coupling constants for the bridging and terminal  $-\text{N}(\text{SiMe}_3)_2$  groups disappear, an indication that they are in fast exchange.

**1.37.4.2.3.1.2  $\beta$ -Diketiminates and guanidinates** The  $\beta$ -diketiminato ligand has become one of the more widely used supporting groups in alkaline-earth metal chemistry.

Besides the homoleptic complexes that are known, such as  $(\text{NIPP-nacnac})_2\text{Ca}$  **75**<sup>243</sup> and several others,<sup>244,417,438</sup>  $\beta$ -diketiminate ligands have been used to support a wide variety of ligand types, including halides (F, Cl),<sup>439</sup> amides,<sup>440,441</sup> cyanides,<sup>442</sup> acetylides,<sup>443,444</sup> hydroxides,<sup>445</sup> oxides,<sup>446</sup> alkoxides and enolates,<sup>447</sup> aryls,<sup>448</sup> and alkyls.<sup>279,410,449</sup> The bonding modes of the  $\beta$ -diketiminate ligand range from  $\eta^2$  to  $\eta^5$ , which depend upon the identity of the metal and the molecularity of the complex.<sup>450</sup>

**75**

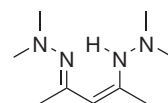
Treatment of  $\text{Ae}[\text{N}(\text{SiMe}_3)_2]_2(\text{thf})_2$  with the ((2,2-dimethylhydrazinyl)pent-3-en-2-ylidene)-1,1-dimethylhydrazine **76** produces a series of homoleptic  $\beta$ -diketiminate complexes of Ca (monomeric), Sr, and Ba **77** (Figure 35; both dinuclear).<sup>451</sup> They display improved volatility, perhaps as a result of the lattice energy-lowering effects of the dimethylamino groups' lone pairs



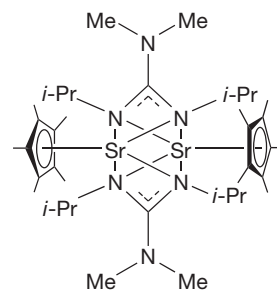
**Figure 35** Structure of the  $[\text{Ba}(\eta^5\text{-LNMe}_2)(\mu\text{-}\eta^2\text{:}\eta^3\text{-LNMe}_2)]_2$  dimer, with  $\text{L} = ((2,2\text{-dimethylhydrazinyl)pent-3-en-2-ylidene)-1,1\text{-dimethylhydrazine}$  **77**.



of electrons. Reviews covering the chemistry of  $\beta$ -diketiminato complexes have been published in the literature.<sup>452,453</sup>

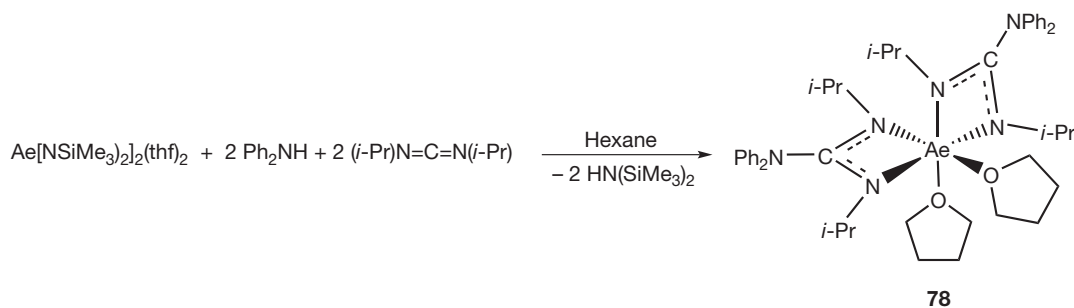
**76**

As monoanionic chelating N-donor ligands, guanidates (and amidinates,  $[\text{RC}(\text{NR}')(\text{NR}'')]^-$ <sup>275,454-465</sup>) share similarities with  $\beta$ -diketimينات. Insertion reactions of carbodiimides into M–N and M–P bonds (Scheme 4) can generate guanidinate-type complexes of calcium and strontium **78**.<sup>460</sup> Similarly,  $(\text{thf})_4\text{Ca}(\text{PPh}_2)_2$  reacts with di-*iso*-propyl- and dicyclohexylcarbodiimides to yield the phospho(III)guanidates  $(\text{thf})_2\text{Ca}[\text{RNC}(\text{PPh}_2)\text{NR}]_2$ .<sup>461</sup> The reaction of alkaline-earth halides, bis(trimethylsilyl)methylamides, and decamethylmetallocenes with various guanidine or guanidinate ligands generates a range of both homoleptic and mixed-ligand guanidinate complexes.<sup>412</sup> For example, the treatment of  $[\text{Sr}\{\text{N}(\text{SiMe}_3)_2\}_2]_2$  with 4.0 equiv of  $(i\text{-Pr})\text{N}=\text{C}(\text{NMe}_2)\text{N}(\text{H})(i\text{-Pr})$  (LH) yields the dimeric complex  $(\eta^2\text{-L})\text{Sr}(\mu^2, \eta^2\text{:}\eta^2\text{-L})(\mu^2, \eta^1\text{:}\eta^1\text{-L})\text{Sr}(\eta^2\text{-L})$  **79** (Figure 36); the same guanidine with  $(\text{C}_5\text{Me}_5)_2\text{Sr}$  produces the complex  $(\text{C}_5\text{Me}_5)\text{Sr}(\mu^2, \eta^2\text{:}\eta^2\text{-L})_2\text{Sr}(\text{C}_5\text{Me}_5)$  **80** with liberation of  $\text{C}_5\text{Me}_5\text{H}$ .

**80**

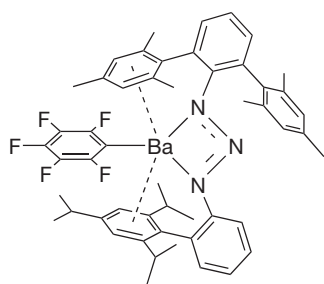
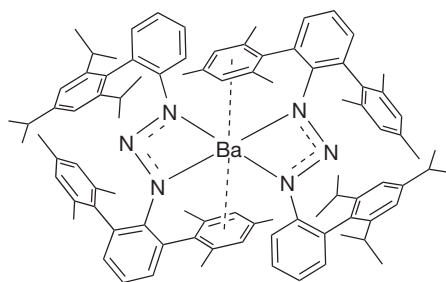
Guanidinate-ligated complexes have been of interest for their ability to initiate polymerization reactions (e.g., with *l*- and *rac*-lactide<sup>462</sup> and styrene<sup>463</sup>) (see Chapter 1.38). The ability of bulky guanidinate complexes to stabilize low-oxidation-state metallacycles has been reviewed previously.<sup>464</sup>

Triazenido ligands,  $[\text{N}(\text{NR}')(\text{NR}'')]^-$ , extend the chelating N-donor motif of  $\beta$ -diketimينات, guanidates, and amidinates, but are less commonly encountered. As a class,

**78**

**Scheme 4** Insertion reactions of carbodiimides into Ae–N bonds.

triazenides are weaker donors than amidinates, and often undergo undesired ligand redistribution. Strategies for stabilizing the compounds, which are not always successful, include the use of sterically bulky R groups, such as 2,6-diisopropylphenyl,<sup>465,466</sup> or pendant R groups that provide secondary coordination to the metal, as in the heteroleptic pentafluorophenyl triazenides [Ae(C<sub>6</sub>F<sub>5</sub>)(N<sub>3</sub>ArAr')] (Ae = Sr, Ba **81**) or the solvated Ca(C<sub>6</sub>F<sub>5</sub>)(N<sub>3</sub>ArAr')(thf).<sup>467</sup> Treating **81** or its strontium analog with PhSiH<sub>3</sub> initiates a  $\sigma$ -bond metathesis reaction, yielding the yellow homoleptic triazenides Ae [N<sub>3</sub>Dmp(Tph)]<sub>2</sub> (Dmp = 2,6-Mes<sub>2</sub>C<sub>6</sub>H<sub>3</sub>; Tph = 2-TripC<sub>6</sub>H<sub>4</sub> with Trip = 2,4,6-(*i*-Pr)<sub>3</sub>C<sub>6</sub>H<sub>2</sub>).<sup>468</sup> In the barium complex **82**, the Ba–N distances average 2.926 Å, which is substantially longer than in **81** (2.726 Å), even though there is only a difference of 1 in the formal coordination numbers, and the Ba···C( $\pi$ -arene) contact distances are similar (3.31–3.42 Å in **82**; 3.29–3.43 Å in **81**).

**81****82**

**1.37.4.2.3.1.3 Pyrazolates** Isoelectronic with the cyclopentadienyl anion, the pyrazolate anion, [C<sub>3</sub>H<sub>3</sub>N<sub>2</sub>]<sup>−</sup>, has been

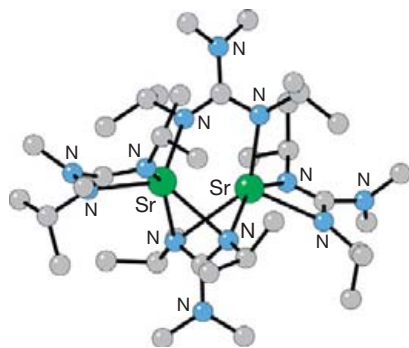


**Figure 36** Structure of the guanidinate complex ( $\eta^2$ -L)Sr( $\mu^2, \eta^1: \eta^1$ -L)( $\mu^2, \eta^1: \eta^1$ -L)Sr( $\eta^2$ -L) **79**.

incorporated into various group 2 metal complexes. Reaction of the disubstituted pyrazoles 3,5-R<sub>2</sub>pzH (R = *t*-Bu, Ph, Me) with KH yields the corresponding potassium salts, which are common reagents for forming pyrazolato complexes by halide metathesis;<sup>469,470</sup> other substituted pyrazoles have also been used in the synthesis of pyrazolato complexes,<sup>59,247,471,472</sup> as have thallium salts.<sup>248</sup>

The reaction of magnesium bromide with potassium 3,5-di-*tert*-butylpyrazolate, K[*t*-Bu<sub>2</sub>pz], in toluene affords Mg<sub>2</sub>(*t*-Bu<sub>2</sub>pz)<sub>4</sub>; in THF, the product is Mg<sub>2</sub>(*t*-Bu<sub>2</sub>pz)<sub>4</sub>(thf)<sub>2</sub>.<sup>473</sup> Both of these are dinuclear complexes with two bridging pyrazolato and two chelating  $\eta^2$ -pyrazolato ligands. TMEDA binds to the unsolvated compound or displaces THF from the solvate to give Mg(*t*-Bu<sub>2</sub>pz)<sub>2</sub>(TMEDA), which is a mononuclear species with two  $\eta^2$ -pyrazolates and chelating TMEDA.

The reaction of CaBr<sub>2</sub> with 2 equiv. of K[*t*-Bu<sub>2</sub>pz] in THF yields Ca(*t*-Bu<sub>2</sub>pz)<sub>2</sub>(thf)<sub>2</sub>, which, on treatment with various donors L (L = pyridine, TMEDA, PMDETA, triglyme, and tetraglyme), generates the corresponding adducts Ca(*t*-Bu<sub>2</sub>pz)<sub>2</sub>(L)<sub>*n*</sub> (*n* = 3 for py; *n* = 1 for the others). A related series of THF, PMDETA, triglyme, and tetraglyme adducts of the 3,5-dimethylpyrazolate anion can also be prepared.<sup>469</sup> The *t*-Bu pyrazolato complexes are mononuclear, with  $\eta^2$ -bound ligands. The compounds have been investigated for their potential use in CVD, but only Ca(Bu<sub>2</sub>pz)<sub>2</sub>(triglyme) displays appreciable volatility, and the rate of triglyme dissociation is comparable to that of sublimation. In other complexes, unfavorable steric interactions between the pyrazolato ligands and the neutral donors lead to the latter's loss on heating before sublimation occurs.

In an unanticipated result, the reaction of barium metal and 3,5-dimethylpyrazole cleaves the cyclic dimethylsiloxane oligomer in silicone grease, forming the complex (thf)<sub>6</sub>Ba<sub>6</sub>(3,5-dimethylpyrazolato)<sub>8</sub>[(OSiMe<sub>2</sub>)<sub>2</sub>O]<sub>2</sub> **83**. Two [O(SiMe<sub>2</sub>O)<sub>2</sub>]<sup>2−</sup> bidentate-chelating siloxane anions are coordinated above and below a nearly hexagonal Ba<sub>6</sub><sup>12+</sup> layer that has been compared to the (110) plane in cubic body-centered metallic barium (**Figure 37**). Eight  $\sigma/\pi$ -coordinated pyrazolate anions flank the barium layer, and six coordinated THF molecules are located at the periphery of the Ba<sub>6</sub> plane.<sup>474</sup>

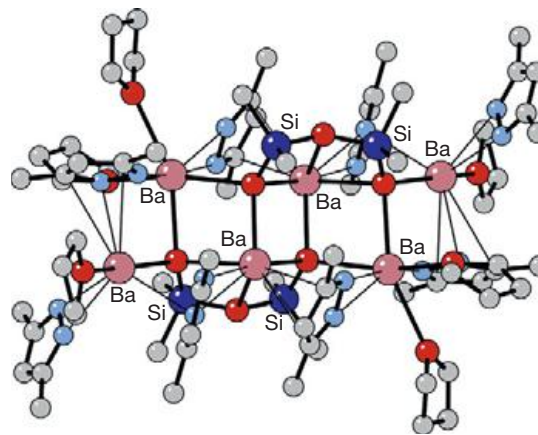


**Figure 37** Structure of (thf)<sub>6</sub>Ba<sub>6</sub>(3,5-dimethylpyrazolato)<sub>8</sub>[(OSiMe<sub>2</sub>O)<sub>2</sub>]<sub>2</sub> **83**.

**1.37.4.2.3.1.4 Inverse crowns** A particularly interesting development in heterometallic amido complexes are the so-called 'inverse-crown ether' complexes. Often, these are 8-membered (M–N–Mg–N)<sub>2</sub> rings (M=Li, Na, K)<sup>128,475,476</sup> that act as polymeric hosts to anionic species (e.g., O<sup>2-</sup>,<sup>109</sup> O<sub>2</sub><sup>2-</sup>, H<sup>-</sup><sup>(477)</sup>). Larger 12-membered (NaMgNNaN)<sub>2</sub><sup>2+</sup> or 24-membered (KNMgN)<sub>6</sub><sup>2+</sup> variants, which function as single or multiple traps for arene-based anions, are also known.<sup>478</sup> In a typical preparation of an inverse crown, the reaction of (*n*-Bu)Li with MgBu<sub>2</sub> and oxygenated 2,2,6,6-tetramethylpiperidine (LH) affords the complex [L<sub>4</sub>Li<sub>2</sub>Mg<sub>2</sub>O]. The same reaction with (*n*-Bu)Na in place of (*n*-Bu)Li and HN(SiMe<sub>3</sub>)<sub>2</sub> in place of tetramethylpiperidine yields [(Me<sub>3</sub>Si)<sub>2</sub>N]<sub>4</sub>Na<sub>2</sub>Mg<sub>2</sub>(O<sub>2</sub>)<sub>x</sub>(O)<sub>1-x</sub>.<sup>475</sup>

The inverse crown [NaMg(N(*i*-Pr)<sub>2</sub>)<sub>3</sub>]<sub>n</sub> reacts with ferrocene in a regioselective fourfold deprotonation at the 1,1',3,3' positions. The product, Na<sub>4</sub>Mg<sub>4</sub>(N(*i*-Pr)<sub>2</sub>)<sub>8</sub>Fe(C<sub>5</sub>H<sub>3</sub>)<sub>2</sub> **84** (Figure 38), contains a 16-membered, centrosymmetric Na<sub>4</sub>Mg<sub>4</sub>N<sub>8</sub> ring. As is

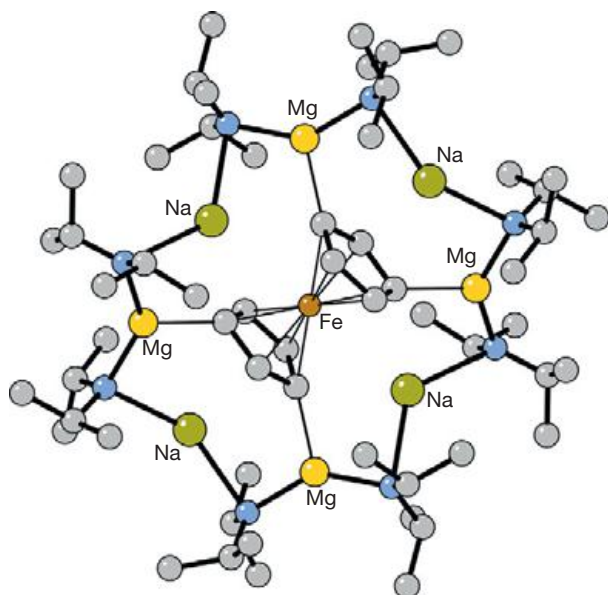


**Figure 38** Structure of the inverse-crown derivative, Na<sub>4</sub>Mg<sub>4</sub>(N(*i*-Pr)<sub>2</sub>)<sub>8</sub>Fe(C<sub>5</sub>H<sub>3</sub>)<sub>2</sub> **84**.

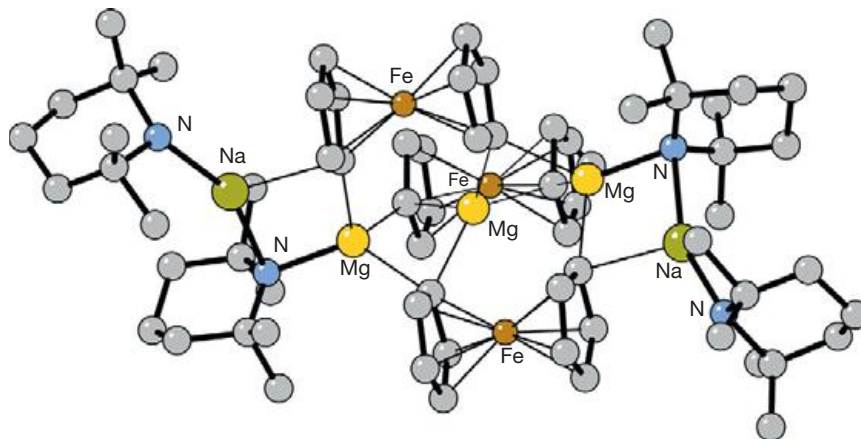


**Figure 39** Structure of an inverse crown with multiple deprotonated ferrocenes [Fe(C<sub>5</sub>H<sub>4</sub>)<sub>2</sub>]<sub>3</sub>[Na<sub>2</sub>Mg<sub>3</sub>(tmp)<sub>2</sub>·(tmpH)<sub>2</sub>] **85**.

common with inverse crowns, the deprotonation positions are dictated by the positions of magnesium in the ring. The ring is severely flexed in order to anchor the dideprotonated edge of each Cp ring.<sup>479</sup> Analogous compounds have been made from ruthenocenes and osmocene.<sup>480</sup> A series of inverse crowns with multiple deprotonated ferrocenes and the general formula [Fe(C<sub>5</sub>H<sub>4</sub>)<sub>2</sub>]<sub>3</sub>[M<sub>2</sub>Mg<sub>3</sub>(tmp)<sub>2</sub>L<sub>2</sub>] (M=Li, L=tmpH or py; M=Na, L=tmpH) **85** (Figure 39) have also been prepared.<sup>107</sup> The mixed  $\pi$ -metallocene- $\pi$ -arene complex K( $\eta^5$ -Cp<sub>2</sub>Fe)<sub>2</sub>( $\eta^3$ -C<sub>6</sub>H<sub>5</sub>CH<sub>3</sub>)<sub>2</sub> Mg[N(SiMe<sub>3</sub>)<sub>2</sub>]<sub>3</sub> is similarly known.<sup>481</sup> The metallocene complexes are special cases of the selective deprotonation of arenes at thermodynamically unfavorable ring sites that produce anions bound within the central cavities of inverse crowns.<sup>110</sup>

The reaction of the phosphinimine Me<sub>3</sub>SiNPPH<sub>2</sub>CH<sub>3</sub> with (CH<sub>3</sub>)<sub>2</sub>CHMgCl produces Mg<sub>4</sub>(Me<sub>3</sub>SiNPPH<sub>2</sub>CH<sub>2</sub>)<sub>4</sub>( $\mu_4$ -O)( $\mu_2$ -Cl)<sub>2</sub> **86**, which is a type of inverse crown ether (Figure 40).<sup>482</sup> Each magnesium is coordinated to a central O<sup>2-</sup> and one of the two outer Cl<sup>-</sup>. Four six-membered MgNPCMgO rings are joined through the central O atom.

The heterotrimetallic inverse crown Li<sub>2</sub>K<sub>2</sub>Mg<sub>4</sub>(*t*-Bu)(Me<sub>3</sub>Si)N]<sub>4</sub>(*t*-Bu){Me<sub>2</sub>(H<sub>2</sub>C)Si}N]<sub>4</sub>(hexane)<sub>x</sub> **87** (Figure 41) is prepared from the reaction of Mg[N(SiMe<sub>3</sub>)(*t*-Bu)]<sub>2</sub> with Me<sub>3</sub>Si(*t*-Bu)NH, followed by sequential treatment with BuLi and KCH<sub>2</sub>Ph. The molecule consists of a 16-membered (KNMgNLiNMgN)<sub>2</sub> primary ring with four six-membered (MgCSiNLiN) appendant secondary rings; the usual anionic core in inverse crowns is part of the ring structure in **87**.<sup>483</sup>

Alkoxide-based inverse-crown complexes of general formula [MMg(N(*i*-Pr)<sub>2</sub>)<sub>2</sub>OR]<sub>2</sub> (M=Li, R=*n*-Oct; M=Na, R=*n*-Bu or *n*-Oct) are also known. They contain octagonal (NaNMgN)<sub>2</sub> cationic rings with both faces capped by a  $\mu_3$ -alkoxide ion that only interacts with the sodium center that is in a *syn* relationship to itself (e.g., [NaMg{N(*i*-Pr)<sub>2</sub>}<sub>2</sub>O(*n*-Bu)]<sub>2</sub> **88**; Figure 42).<sup>108</sup> Reviews of metal inverse-crown chemistry are available in the literature.<sup>484,485</sup>

**1.37.4.2.3.1.5 Other N-bound ligands** The thiocyanate (SCN<sup>-</sup>) ion is among the classic ambidentate ligands, but, apart from ionic salts, is found in comparatively few structurally authenticated coordination complexes of the group 2 metals. The conventional expectation is that they should display N-coordination to the 'class a' metals,<sup>486,487</sup> but when bis(tetra-phenylphosphonium) hexachlorodiberyllate, (Ph<sub>4</sub>P)<sub>2</sub>[Be<sub>2</sub>Cl<sub>6</sub>],

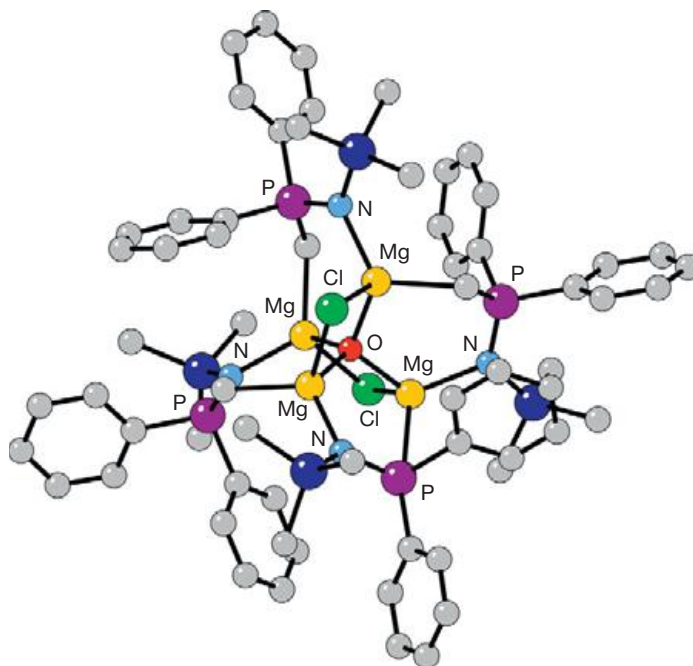


**Figure 40** Structure of the tetrametallic inverse crown  $\text{Mg}_4(\text{Me}_3\text{SiNPPh}_2\text{CH}_2)_4(\mu_4\text{-O})(\mu_2\text{-Cl})_2$  **86**.

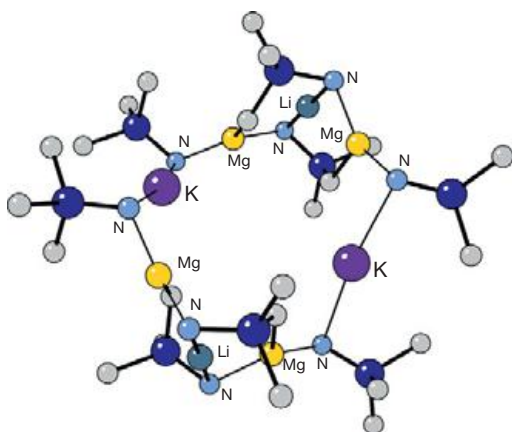


**Figure 41** Structure of the heterotrimetallic inverse crown  $\text{Li}_2\text{K}_2\text{Mg}_4[(t\text{-Bu})(\text{Me}_3\text{Si})\text{N}]_4[(t\text{-Bu})(\text{Me}_2(\text{H}_2\text{C})\text{Si})\text{N}]_4(\text{hexane})_x$  **87**. For clarity, the *t*-Bu groups in the nitrogen atoms have been removed.

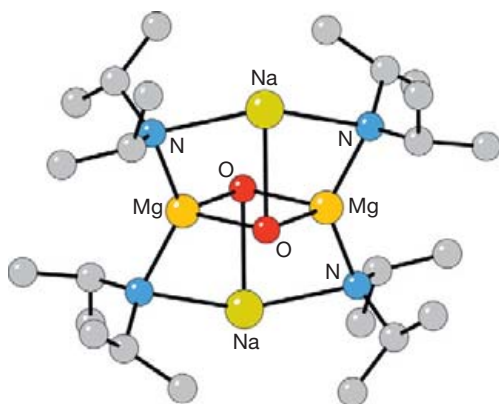
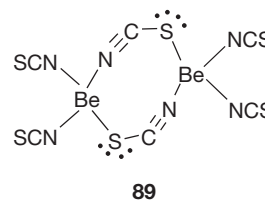


**Figure 42** Structure of  $[\text{NaMg}[\text{N}(i\text{-Pr})_2]_2\text{O}(n\text{-Bu})]_2$  **88**.

is allowed to react with excess (trimethylsilyl)isothiocyanate, a mixture of products is obtained.<sup>488</sup> One of these,  $(\text{Ph}_4\text{P})_2[\text{Be}_2(\text{NCS})_4(\mu\text{-NCS})_2]$  **89**, is constructed from a centrosymmetric eight-membered  $\text{Be}_2(\text{NCS})_2$  ring, with Be–N and Be–S distances of 1.68(1) and 2.352(9) Å, respectively.



The 1,4-di-*tert*-butyl-1,4-diazabutadiene ligand ((*t*-Bu)<sub>2</sub>DAB) is able to stabilize triplet biradicals with magnesium, calcium, and strontium.<sup>489</sup> Activated magnesium will react with (*t*-Bu)<sub>2</sub>DAB in THF to form the deep-red  $\text{Mg}[(t\text{-Bu})_2\text{DAB}]_2$ . EPR measurements ( $g_{\text{av}} = 2.0036$ <sup>490</sup>) and an x-ray single-crystal structural study has been used to characterize the product. The magnesium center is tetrahedrally coordinated, but the molecule possesses nearly *2mm* symmetry, and both ligands display features consistent with radical anions (Mg–N = 2.070(7), 2.067(7) Å; Mg–N = 82.1(3)°, 82.4(3)°). It is also possible to prepare beryllium, calcium, and barium complexes of the diazabutadiene ligand that contain doubly-reduced ligands.<sup>491,492</sup>

#### 1.37.4.2.3.2 Phosphorus-donor ligands

The interaction of group 2 metals and phosphorus-based ligands takes many forms, from neutral phosphanes and anionic diphosphides ( $[\text{PR}]^{2-}$ ), to mixed (P,N) and (P,S) donors. The area has witnessed considerable growth in the past several decades; prior to 1990, only a single compound containing a group 2 element bonded to phosphorus had been structurally authenticated<sup>493</sup>; by the end of 2010, the total was

over 100. Extensive reviews of the area have appeared in the literature,<sup>74,494–497</sup> including complexes with phosphorus-stabilized carbanions<sup>498</sup> and of molecular clusters of magnesium dimetallated primary phosphanes.<sup>499</sup>

**1.37.4.2.3.2.1 Neutral donor ligands** As expected from the mismatch between the type a group 2 metals and the type b character of neutral phosphanes, adducts of the metals with coordinated  $\text{PR}_3$  groups are rare, and are known only with polydentate ligands (e.g.,  $(\text{trimpsi})\text{Mg}[\text{SeSi}(\text{SiMe}_3)_3]_2$ ;  $\text{trimpsi} = \text{tris}((\text{dimethylphosphino})\text{methyl})-(\text{tert-butyl})\text{silane}$ ).<sup>500</sup> Pendant phosphanes that form part of a chelating ligand can be isolated, however, such as in the  $\text{Ca}_4\text{O}_4$  heterocubane complex  $[\text{Ca}(\text{thf})(\text{OC}_6\text{H}_4\text{CH}(\text{P}(\text{tolyl-}i>p)_2))]_4$  **90**.<sup>309</sup> Isolated in low yield from the reaction of the lithium salt of the multidentate O-substituted phosphane  $2\text{-MeOC}_6\text{H}_4\text{CH}(\text{P}(\text{tolyl-}i>p)_2)$  with  $\text{CaI}_2$  in THF, **90** contains a formally six-coordinate  $\text{Ca}^{2+}$  center, bound by the oxygen and phosphanyl phosphorus atoms on one ligand, the oxygen and anionic carbon of a second ligand ( $\text{Ca}-\text{C} = 2.591(5) \text{ \AA}$ ), and the oxygen atom of a third ligand. It displays  $\text{Ca} \cdots \text{P}$  contacts at  $2.986(3) \text{ \AA}$  (Figure 43).

**1.37.4.2.3.2.2 Monosubstituted phosphido complexes**

Group 2 compounds containing the dinegative  $\text{PR}^{2-}$  unit are not common, but complex structures can be formed from them. Magnesium forms several types with  $\text{Mg}_{2n}\text{P}_{2m}$  cores. The magnesianation of  $\text{PSi}(t\text{-Bu})_3$  with  $\text{Mg}(n\text{-Bu})_2$  in THF yields tetrameric  $[(\text{thf})\text{MgPSi}(t\text{-Bu})_3]_4$  **91**.<sup>501</sup> In the central  $\text{Mg}_4\text{P}_4$  cube, the  $\text{Mg}-\text{P}$  distances range from 2.55 to 2.59 Å. When the reaction is conducted in toluene, the larger aggregate  $\text{Mg}_6[\text{P}(\text{H})\text{Si}(t\text{-Bu})_3]_4\text{P}[\text{Si}(t\text{-Bu})_3]_2$  is generated. An  $\text{Mg}_4\text{P}_2$  octahedron is at the center, with the phosphorus atoms in a trans position. The  $\text{Mg} \cdots \text{Mg}$  edges are bridged by the  $\text{P}(\text{H})\text{Si}(t\text{-Bu})_3$  substituents.

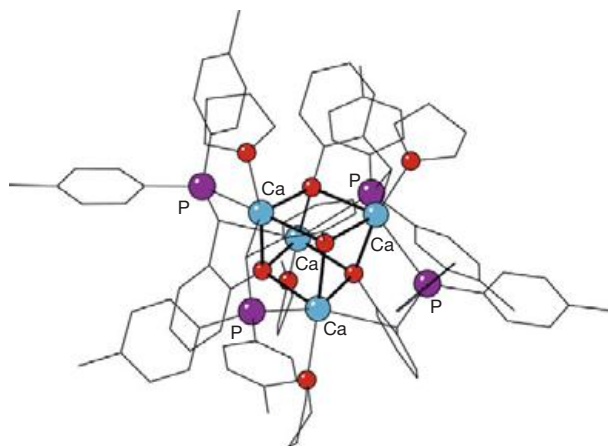
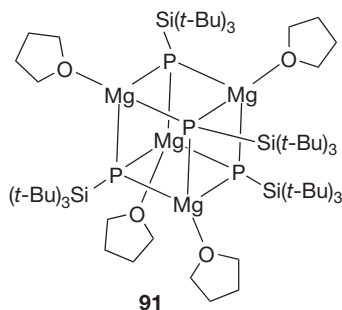


Figure 43 Structure of the cuboidal  $[\text{Ca}(\text{thf})(\text{OC}_6\text{H}_4\text{CH}(\text{P}(\text{tolyl-}i>p)_2))]_4$  **90**.

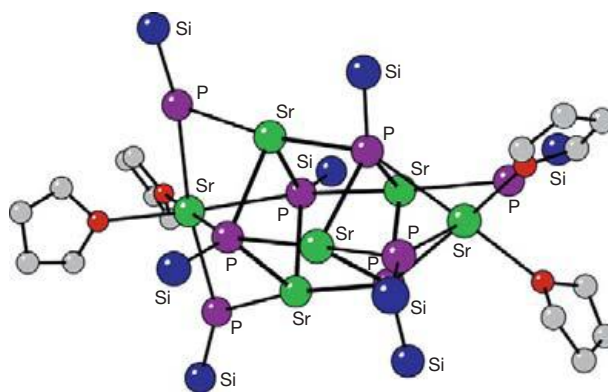


Figure 44  $\text{Sr}(\text{thf})_2(\mu\text{-PHSi}(i\text{-Pr})_3)_2[\text{Sr}_2(\mu_4\text{-PSi}(i\text{-Pr})_3)_2]_2\text{Sr}(\mu\text{-PHSi}(i\text{-Pr})_3)_2(\text{thf})_2$  **92**. For clarity, the isopropyl groups on the silicon atoms have been removed.

The triisopropylsilylphosphido ligand has been used to generate a variety of polymetallic species. For example, the metallation of  $\text{H}_2\text{PSi}(i\text{-Pr})_3$  with  $\text{Ca}(\text{thf})_2[\text{N}(\text{SiMe}_3)_2]$  in tetrahydropyran in a molar ratio of 3:2 yields  $(\text{Me}_3\text{Si})_2\text{Nca}[\mu\text{-P}(\text{H})\text{Si}(i\text{-Pr})_3]_3\text{Ca}(\text{thf})_3$ ; the complex contains a trigonal-bipyramidal  $\text{Ca}_2\text{P}_3$  core, with the metal atoms on the apices.<sup>502</sup> An  $\text{Sr}_4\text{P}_4$  cube serves as the core of  $\text{Sr}(\text{thf})_2(\mu\text{-PHSi}(i\text{-Pr})_3)_2[\text{Sr}_2(\mu_4\text{-PSi}(i\text{-Pr})_3)_2]_2\text{Sr}(\mu\text{-PHSi}(i\text{-Pr})_3)_2(\text{thf})_2$  **92** (Figure 44), which is formed by the elimination of  $\text{PH}_2\text{Si}(i\text{-Pr})_3$  from  $\text{Sr}(\text{thf})_4(\text{PH}(i\text{-Pr})_3)_2$  in toluene.<sup>433</sup>

Depending on the metal involved, the use of the 1,1,3,3-tetraisopropyl-1,3-diphosphinodisiloxane ligand **93** leads to monomeric, dimeric, and trimeric structures.<sup>503</sup> The reaction of  $\text{MgBu}_2$  with the diphosphinodisiloxane forms a polycyclic trimer  $[\text{Mg}\{\text{P}(\text{H})\text{Si}(i\text{-Pr})_2\text{O}\}(\text{thf})]_3$  **94**, in which one end of the bidentate ligand bridges two magnesium cations to form a six-membered  $(\text{Mg}_3\text{P}_3)$  ring ( $\text{Mg}-\text{P} = 2.58 \text{ \AA}$  (av)); the

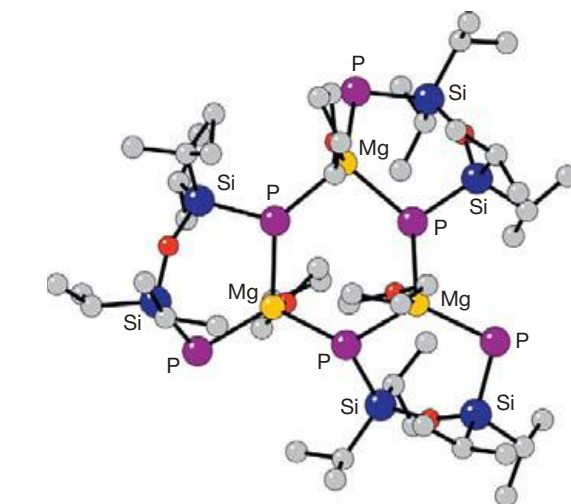
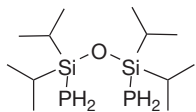


Figure 45 Structure of  $[\text{Mg}\{\text{P}(\text{H})\text{Si}(i\text{-Pr})_2\text{O}\}(\text{thf})]_3$  **94**.

$[\text{Ba}\{\text{P}(\text{H})\text{Si}(i\text{-Pr})_2\text{O}\}(\text{dme})_2]_2$  **95** has four bridging phosphorus atoms of two diphosphinosiloxane ligands, forming an octahedron (Figure 46); the Ba–P distances range from 3.302(1) to 3.334(1) Å.



93

#### 1.37.4.2.3.2.3 Disubstituted phosphido complexes

Disubstituted phosphido ligands  $[\text{PRR}']^-$  have been incorporated into various group 2 complexes. Many examples are covered in detail in previously cited reviews; only representative systems are presented here. A particularly well-studied class of these complexes are those with trialkylsilyl groups as substituents, especially the bis(trimethyl)silyl moiety.<sup>74</sup> Synthetic methods for these compounds vary, from direct metallation (e.g., the reaction of  $(n\text{-Bu})_2\text{Mg}$  and  $\text{HPN}(\text{SiMe}_3)_2$  generates  $\text{Mg}[\text{P}(\text{SiMe}_3)_2]$  to metathesis (e.g.,  $\text{Ae}[\text{N}(\text{SiMe}_3)_2]_2$  ( $\text{Ae} = \text{Mg}, \text{Ca}, \text{Sr}, \text{Ba}$ ) react with  $\text{HP}(\text{SiR}_3)$  to produce the corresponding phosphides). In donor solvents (ether, THF), the complexes are monomeric; in hydrocarbons, monomer/dimer equilibria can be observed in NMR spectra.

Diphenylphosphanide can form either monomers or polymers with the group 2 metals. Octahedral calcium and strontium monomers of the formula  $\text{Ae}(\text{PPh}_2)_2(\text{thf})_4$  are formed by allowing diphenylphosphane and  $\text{Ae}[\text{N}(\text{SiMe}_3)_2]_2(\text{thf})_2$  ( $\text{Ae} = \text{Ca}$  or  $\text{Sr}$ ) to react. In the solid state, the two diphenylphosphide substituents are in a trans arrangement ( $\text{Ca}-\text{P} = 2.9882(4)$  Å;  $\text{Sr}-\text{P} = 3.1427(7)$  Å).<sup>504</sup> In contrast, the analogous barium counterpart  $[\text{Ba}_3(\text{PPh}_2)_6(\text{thf})_4]_n$  **96** forms a polymer with two diphenylphosphanides, bridging the barium cations (Figure 47). The addition of 18-crown-6 prevents polymer formation, generating the monomeric (18-crown-6) $\text{Ba}(\text{PPh}_2)_2$ .

Not surprisingly, a change in the number of aryl groups on a phosphane strongly influences the nature of the derivative phosphide complexes. For example, the metallation reaction of  $\text{MgEt}_2$  with diphenylphosphane generates the polymeric  $[(\text{thf})\text{Mg}(\text{Et})\text{PPh}_2]_\infty$ , which possess bridging  $\text{PPh}_2$  ligands.<sup>505</sup> The related reactions of  $\text{MgEt}_2$  with  $\text{HPPH}_2$  and  $\text{H}_2\text{PPh}$  with a 1:2 stoichiometry yields  $(\text{thf})_4\text{Mg}(\text{PPh}_2)_2$  and  $(\text{thf})_6\text{Mg}_4(\text{P}(\text{H})\text{Ph})_8$

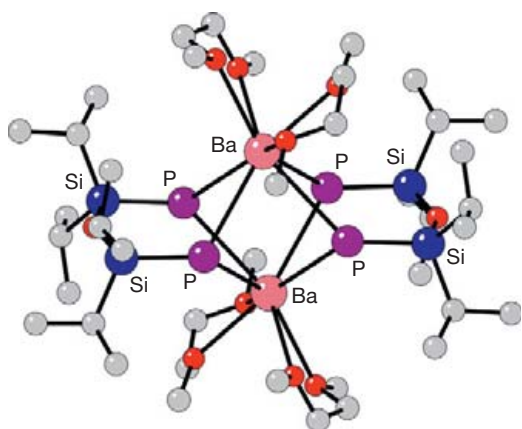


Figure 46 Structure of  $[\text{Ba}\{\text{P}(\text{H})\text{Si}(i\text{-Pr})_2\text{O}\}(\text{dme})_2]_2$  **95**.

**97** (Figure 48), respectively. The two magnesium atoms of **97** possess different environments. Hexacoordinate  $\text{Mg1}$  binds to four bridging phosphanide ligands and to two thf molecules in a cis arrangement. The tetracoordinate atom  $\text{Mg2}$  is in a distorted tetrahedral environment with two bridging phosphanide groups, a terminally bound phosphanide, and one thf. The three chemically distinct phosphanides display separate P–H stretching frequencies in the IR region, at 2261, 2286, and  $2310\text{ cm}^{-1}$ . Depending on the reactant stoichiometry, when  $\text{Et}_2\text{O}$  is added to a mixture of  $\text{KPh}_2$  and  $\text{Mg}(\text{PPh}_2)_2$  in THF, either of the potassium diphenylphosphinomagnesiates  $(\text{Et}_2\text{O})\text{K}[(\text{thf})\text{Mg}(\text{PPh}_2)_3]$  or  $(\text{Et}_2\text{O})_x(\text{thf})_y\text{K}_2[\text{Mg}(\text{PPh}_2)_4]$  will crystallize. They have extended structures in the solid state.<sup>505</sup>

The structural consequences of using the  $[\text{P}(\text{H})\text{Ph}]^-$  anion with the heavier alkaline-earth metals were examined with the metathetical reactions of  $\text{K}[\text{P}(\text{H})\text{Ph}]$  and  $\text{AeI}_2$ . The reaction with  $\text{CaI}_2$  yields the dinuclear  $(\text{thf})_3\text{Ca}[\mu\text{-P}(\text{H})\text{Ph}]_3\text{Ca}(\text{thf})_2\text{P}(\text{H})\text{Ph}$ , whereas the corresponding reactions with  $\text{SrI}_2$  and  $\text{BaI}_2$  gives polymeric  $[(\text{thf})_2\text{Sr}\{\text{P}(\text{H})\text{Ph}\}_2]_\infty$  and  $[(\text{thf})\text{Ba}\{\text{P}(\text{H})\text{Ph}\}_2]_\infty$ , respectively. Despite the different numbers of coordinated thf molecules on the metals, the strontium and barium

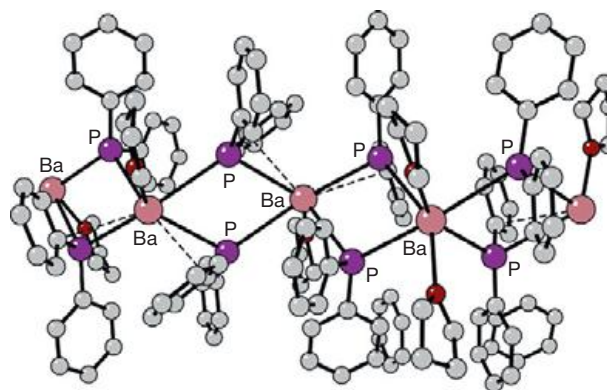


Figure 47 Structure of  $[\text{Ba}_3(\text{PPh}_2)_6(\text{thf})_4]_n$  **96**.

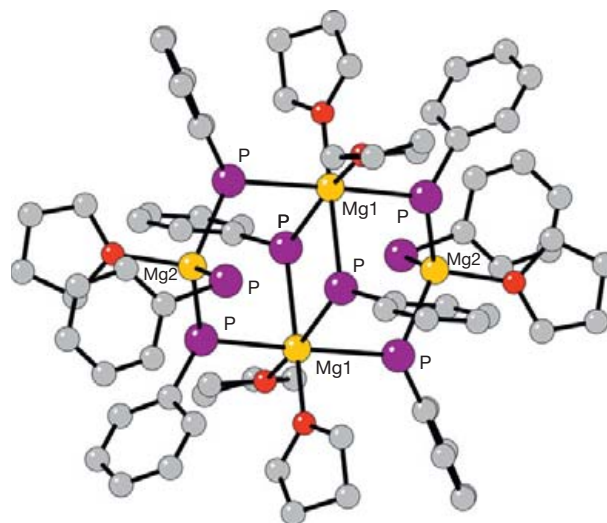
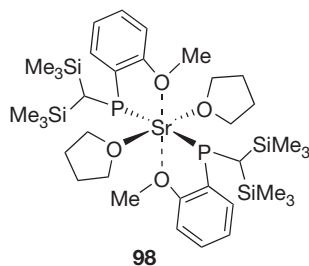


Figure 48 Structure of  $(\text{thf})_6\text{Mg}_4(\text{P}(\text{H})\text{Ph})_8$  **97**.

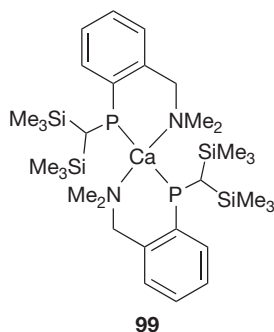
compounds have almost identical P–H stretching frequencies (2286 and 2284  $\text{cm}^{-1}$ ).<sup>505</sup>

Similarities between calcium and ytterbium(II) species were the inspiration to explore the halide metathesis between  $\text{CaI}_2$  and  $\text{K}[\text{P}\{(\text{SiMe}_3)_2\text{CH}\}(\text{C}_6\text{H}_4\text{-2-O-Me})]$ , which forms the tetrameric alkoxy-phosphide cluster  $[\text{Ca}\{\text{P}\{(\text{SiMe}_3)_2\text{CH}\}(\text{C}_6\text{H}_4\text{-2-O})\}(\text{thf})]_4 \cdot 4\text{thf}$  through a ligand cleavage reaction, presumably involving a bisphosphanide intermediate  $\text{Ca}(\text{thf})_n[\{(\text{SiMe}_3)_2\text{CH}\}(\text{C}_6\text{H}_4\text{-2-O-Me})\text{P}]_2$ ,<sup>506</sup> and leaving the tertiary phosphane  $[(\text{Me}_3\text{Si})_2\text{CH}\}(\text{C}_6\text{H}_4\text{-2-O-Me})\text{P}(\text{Me})]$  as a side-product.<sup>507</sup> The calcium cluster contains a  $\text{Ca}_4\text{O}_4$  cuboidal core and  $\mu_2$ -phosphide groups, and is isostructural with its ytterbium counterpart.<sup>508</sup> In contrast, the metathesis reaction of  $\text{SrI}_2$  or  $\text{BaI}_2$  with  $\text{K}[\text{P}\{(\text{SiMe}_3)_2\text{CH}\}(\text{C}_6\text{H}_4\text{-2-O-Me})]$  forms the corresponding monomeric complexes  $[\{(\text{SiMe}_3)_2\text{CH}\}(\text{C}_6\text{H}_4\text{-2-O-Me})\text{P}]_2\text{Ae}(\text{thf})_n$  ( $\text{Ae} = \text{Sr}, n = 2; \text{Ba}, n = 3$ ).<sup>506</sup>

The salt of a slightly more bulky phosphanide,  $\text{K}[\{(\text{SiMe}_3)_2\text{CH}\}(\text{C}_6\text{H}_3\text{-2-O-Me-3-Me})\text{P}]$ , reacts with  $\text{AeI}_2$  ( $\text{Ae} = \text{Ca-Ba}$ ) to yield the monomeric isostructural  $[\{(\text{SiMe}_3)_2\text{CH}\}(\text{C}_6\text{H}_3\text{-2-O-Me-3-Me})\text{P}]_2\text{Ae}(\text{thf})_2$  complexes; the calcium complex proves to be thermally sensitive, and it must be kept below 0 °C during preparation and handling in order to avoid extensive decomposition. The strontium **98** and barium complexes are isostructural with the calcium complex.<sup>506,509</sup>

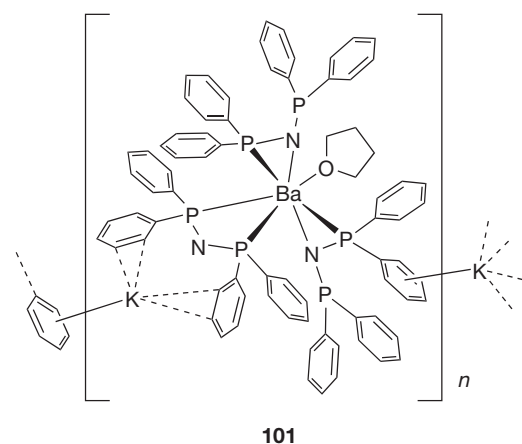
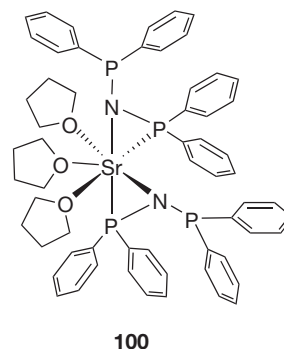


A phosphanide similar to that above, with nitrogen replacing oxygen, forms complexes with the metals Mg–Ba. Specifically, the phosphane  $\text{R}(\text{Me}_2\text{NCH}_2\text{-2-C}_6\text{H}_4)\text{PH}$  ( $\text{R} = (\text{Me}_3\text{Si})_2\text{CH}$ ) reacts with  $\text{MgBu}_2$  to form  $\text{Mg}[\text{PR}(\text{C}_6\text{H}_4\text{-2-CH}_2\text{NMe}_2)]_2$ , and the phosphanide  $\text{K}[\text{PR}(\text{C}_6\text{H}_4\text{-2-CH}_2\text{NMe}_2)]$  reacts with  $\text{CaI}_2$ ,  $\text{SrI}_2$ , or  $\text{BaI}_2$  to generate the corresponding  $(\text{thf})_n\text{Ae}[\text{PR}(\text{C}_6\text{H}_4\text{-2-CH}_2\text{NMe}_2)]_2$  compounds by salt metathesis. The Ca **99**, Sr, and Ba species are fluxional on the NMR timescale, displaying monomer–dimer equilibria.<sup>510</sup>



A bis(diphosphanyl-amido) complex of strontium,  $[(\text{Ph}_2\text{P})_2\text{N}]_2\text{Sr}(\text{thf})_3$  **100**, can be formed from the reaction of  $[\text{K}(\text{thf})_n][\text{N}(\text{PPh}_2)_2]$  and  $\text{SrI}_2$ . The single-crystal x-ray structure of **100** indicates  $\eta^2$  coordination of the ligand via the nitrogen

and one phosphorus atom. In solution, rapid exchange of the two different phosphorus atoms occurs. With  $\text{BaI}_2$ , the same reaction yields a coordination polymer  $\{[(\text{Ph}_2\text{P})_2\text{N}]_2\text{Ba}(\text{THF})\}[\text{K}(\text{thf})_n]_n$  **101**, in which two of the three  $[(\text{Ph}_2\text{P})_2\text{N}]^-$  ligands bind to the metal in an  $\eta^2$  (N,P) mode, while the third is in a heteroallylic (P,P) coordination mode. In the solid state, cation– $\pi$  interactions between the potassium atoms and the phenyl rings generate the infinite chains.<sup>511,512</sup>



#### 1.37.4.2.3 Arsenic donor ligands

Early reports describing the preparation of group 2 arsenides such as  $\text{Ca}(\text{AsH}_2)_2$  and  $\text{Ca}(\text{AsHMe})_2$  provided few details on their properties.<sup>513</sup> That situation has changed with the use of silyl-substituted arsenic ligands, and compounds containing them display considerable structural diversity. This area has been reviewed in the literature.<sup>514</sup>

Many arsenic derivatives have been synthesized from bis(trimethylsilyl)amido complexes. The 2:1 reaction of  $\text{AsH}_2\text{Si}(i\text{-Pr})_3$  with  $\text{Ba}[\text{N}(\text{SiMe}_3)_2]_2 \cdot 2(\text{thf})$  in THF affords the bis(arsenide) complex  $\text{Ba}(\text{thf})_3[\mu\text{-As}(\text{H})\text{Si}(i\text{-Pr})_3]_2\text{BaAs}(\text{H})\text{Si}(i\text{-Pr})_3(\text{thf})_2$ .<sup>502</sup> The metallation of  $\text{As}[\text{SiMe}_2(t\text{-Bu})]_2\text{H}$  with  $\text{Ba}[\text{N}(\text{SiMe}_3)_2]_2 \cdot 4(\text{thf})$  generates  $\text{Ba}[\text{As}(\text{SiMe}_2(t\text{-Bu}))_2]_2 \cdot 4(\text{thf})$  **102** (Figure 49), which, in the solid state, exists as a distorted pentagonal bipyramid with apical arsenic atoms and a vacant equatorial site shielded by the trialkylsilyl groups. The As–Ba–As' angle is 140.8°. The magnesiumation of  $\text{AsH}_2\text{Si}(i\text{-Pr})_3$  in THF yields  $[\text{Mg}(\text{thf})\text{AsSi}(i\text{-Pr})_3]_4$  **103** (Figure 50), constructed around an  $\text{Mg}_4\text{As}_4$  cube.<sup>515</sup> The transmetallation of  $\text{Zn}(\text{SiMe}_3)_2$  with calcium in THF produces **104**, which, on further metallation with triisopropylsilylarsine, yields the calcium dizinc(diansacyclobutane-2,4-diide) **105**

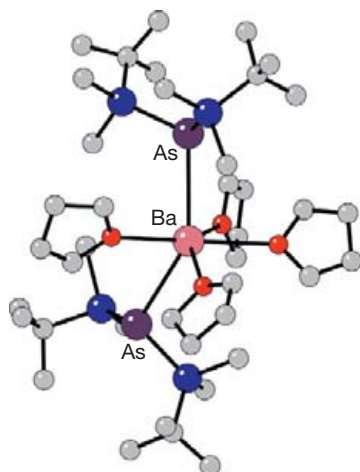


Figure 49 Structure of  $\text{Ba}[\text{As}(\text{SiMe}_2(\text{t-Bu}))_2]_2 \cdot 4(\text{thf})$  **102**.

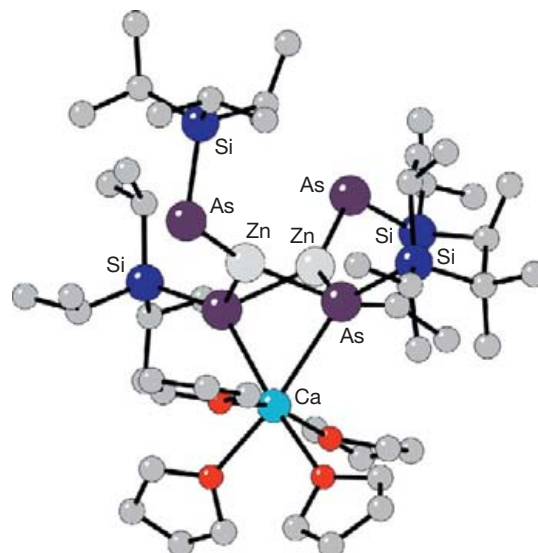


Figure 51 Structure of the calcium dizinca(diasacyclobutane-2,4-diide) **105**.

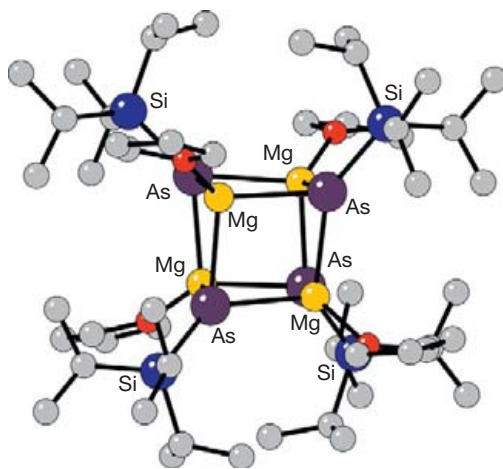
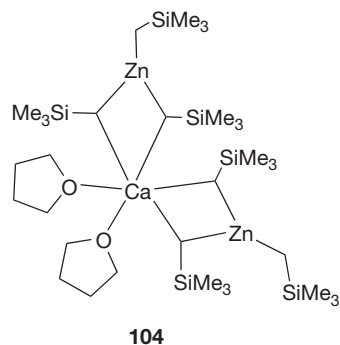


Figure 50 Structure of  $[\text{Mg}(\text{thf})\text{AsSi}(\text{i-Pr})_3]_4$  **103**.

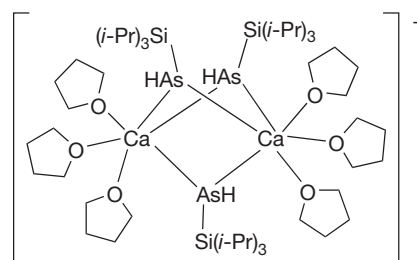
(Figure 51), which is constructed around a distorted trigonal  $\text{As}_2\text{CaZn}_2$  bipyramid with the As atoms in apical positions. The Ca–As bond lengths had an average of 2.914 Å.<sup>516</sup>



**104**

The reaction of  $\text{AsH}_2(\text{Si}(\text{i-Pr})_3)$  with  $\text{Ae}[\text{N}(\text{SiMe}_3)_2]_2 \cdot 2(\text{thf})$  ( $\text{Ae} = \text{Ca}$  or  $\text{Sr}$ ) produces  $\text{Ae}[\text{As}(\text{H})\text{Si}(\text{i-Pr})_3]_2(\text{thf})_4$ , which is in equilibrium with the dimers  $\text{Ae}[\text{As}(\text{H})\text{Si}(\text{i-Pr})_3][\mu\text{-As}(\text{H})\text{Si}(\text{i-Pr})_3]_3\text{M}(\text{thf})_3$  by the elimination of THF. The reaction of the equilibrium mixtures with diphenylbutadiyne gives the metal bis(thf)bis(2,5-diphenylarsolide) species. A mechanism based

on intermolecular  $\text{H}/\text{Si}(\text{i-Pr})_3$  exchange has been proposed that explains the formation of both the  $[\text{As}(\text{Si}(\text{i-Pr})_3)_2]^-$  and 2,5-diphenyl-3,4-bis(phenylethynyl)arsolide anions; the latter was isolated as a solvent-separated ion pair with the dinuclear  $[(\text{thf})_3\text{Ca}\{\mu\text{-As}(\text{H})\text{Si}(\text{i-Pr})_3\}_3\text{Ca}(\text{thf})_3]^+$  cation **106**.<sup>393</sup>



**106**

A dimeric magnesium arsenide compound was serendipitously synthesized from  $\text{MgBu}_2$  and NASH (NASH =  $\text{NHC}_6\text{H}_4\text{AsMe}_2$ ). Isolation of the product,  $[\text{Mg}_2(\mu^2:\eta^1\text{-NHC}_6\text{H}_4\text{AsMe}_2)_2(\mu^3:\eta^3\text{-OSiMe}_2\text{NC}_6\text{H}_4\text{AsMe}_2)(\text{thf})]_2$  **107** (Figure 52), was the result of dimethylsilane insertion into the Mg–N bond, stemming from exposure to dimethylsilane grease.<sup>517</sup>

The planar pentagonal  $\text{As}_5^-$  anion and square  $\text{As}_4^{2-}$  dianion have been examined computationally for the extent of their aromaticity.<sup>518,519</sup> DFT calculations on the  $[\text{As}_5]^-$  anion indicated that the  $C_{5v}$  pyramidal structures for the corresponding  $[\text{AeAs}_5]^+$  ( $\text{Ae} = \text{Be-Ba}$ ) complexes contained three delocalized  $\pi$  molecular orbitals.<sup>518</sup> Calculations of the square dianion confirmed the presence of six aromatic  $\pi$ -electrons and the generation of square-pyramidal  $\text{AeAs}_4$  clusters.<sup>519</sup>

### 1.37.4.2.4 Group 16 ligands

#### 1.37.4.2.4.1 Oxygen-donor ligands

Alkaline-earth complexes containing oxygen-donor ligands represent a large and diverse group of compounds. The interest

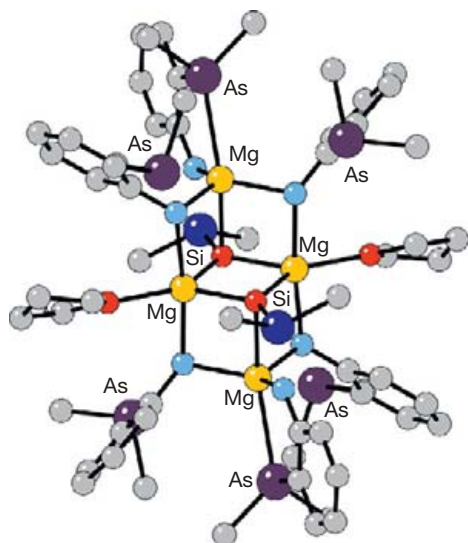


**Figure 52** Structure of  $[\text{Mg}_2(\mu^2\text{-}\eta^1\text{-NHC}_6\text{H}_4\text{AsMe}_2)_2(\mu^3\text{-}\eta^3\text{-OSiMe}_2\text{NC}_6\text{H}_4\text{AsMe}_2)(\text{thf})_2]$  **107**.

in their properties encompasses inorganic synthesis (many s-block complexes are used as transfer reagents for p-, d-, and f-block complexes), materials chemistry (e.g., precursors to metal oxides), and the biological realm (water- and oxygen-containing organic functional groups play a critical role in defining the structure and reactions of many proteins and enzymes). Their chemistry has been repeatedly and extensively reviewed.<sup>520–523</sup>

**1.3.7.4.2.4.1.1 Carboxylates** Compared to other group 2 metal complexes with anionic oxygen donors, the metal carboxylates are particularly robust; although often hygroscopic, they will not decompose upon absorption of water, and are, as a class, thermally stable. Their handling is, thus, simpler than alkoxides and aryloxides. The bonding arrangements of calcium carboxylates were reviewed in the early 1980s,<sup>524</sup> and the chemistry of group 2 carboxylates and their applications as precursors in CVD have been extensively examined.<sup>261,525</sup>

Carboxylates can form structurally complex units that generate 3D networks. For example, in the crystal structure of  $[\text{Mg}\{\text{C}_2\text{H}_4(\text{CO}_2\text{Et})_2\}_3][\text{MgCl}_4]$ , the cations are linked by other diethyl succinate ligands to form a linear polymer. In the cation, each magnesium atom is octahedrally coordinated by six carbonyl oxygen atoms of ethyl succinate molecules.<sup>526</sup> A more complex infinite 3D structure exists in barium diethyl 1,3-dithiepane-2-ylidenemalonate **108** via intermetallic coordination of the dicarboxylic groups. The metal center adopts a nine-coordinate geometry with three different carboxylate bonding arrangements (chelated monodentate, bidentate  $\eta^2$ , monodentate) and two water molecules. Each ligand is associated with five barium atoms, in the form of a layer structure (Figure 53).<sup>527</sup>

Comparatively few examples of beryllium carboxylates have been structurally characterized, and among the most well known are the molecular oxide-carboxylates  $\text{OBe}_4(\text{RCO}_2)_6$  ( $\text{R} = \text{H, Me, Et, Pr, Ph}$ ). The structure of 'basic beryllium acetate' ( $\text{R} = \text{Me}$ ) is constructed from a central O atom surrounded by four Be; the edges of the tetrahedron are bridged by the acetate groups. The

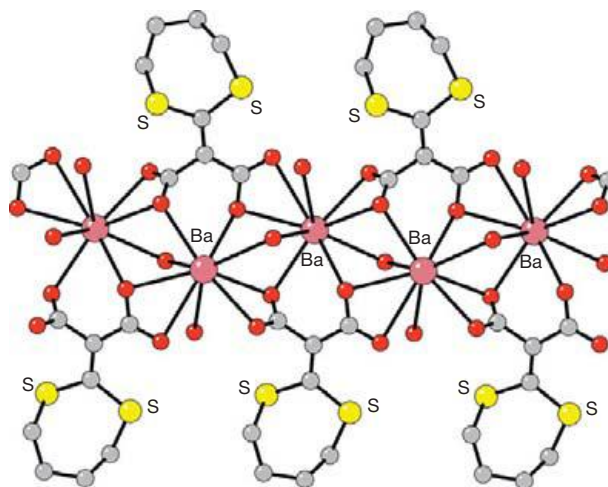


**Figure 53** Portion of the lattice of barium diethyl 1,3-dithiepane-2-ylidenemalonate **108**, illustrating the various carboxylate-binding modes present.

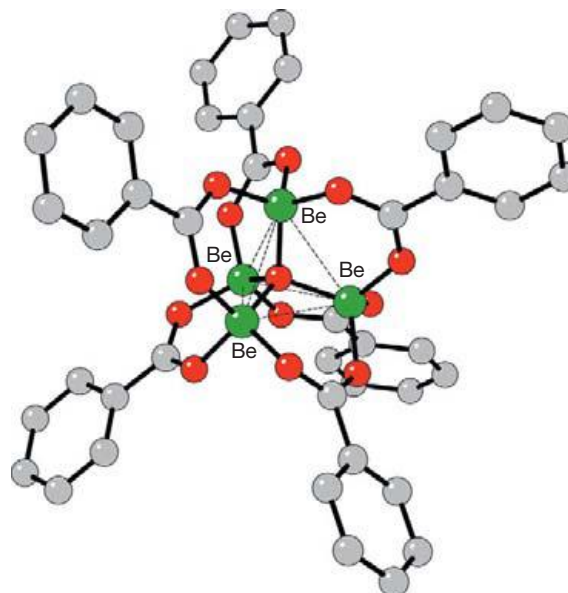


**Figure 54** Structure of tetraberylliumoxohexabenzozoate **109**.

same structure is observed in tetraberylliumoxohexabenzozoate **109**, prepared from beryllium hydroxide and benzoic acid.<sup>528</sup> The terminal atoms of the carboxylates lie at the vertices of an octahedron enclosing the  $\text{Be}_4\text{O}$  cluster (Figure 54).

A truly vast number of carboxylic acids have been used to form carboxylate derivatives of Mg, Ca, Sr, and Ba, and structural characterization has confirmed that the majority form coordination polymers in the solid state. Reviews focusing on their structural chemistry are available in the literature.<sup>529,530</sup> Carboxylate ligands can be formed from the direct reaction of a Grignard reagent with  $\text{CO}_2$ ,<sup>531</sup> but insertion into Mg–N bonds can occur as well. The reaction of  $\text{CO}_2$  gas with  $\text{Ph}_2\text{NMgBr}$  in THF yields the salt  $[\text{Mg}_3(\text{O}_2\text{CNPh}_2)_4(\text{thf})_5\text{Br}][(\text{thf})\text{MgBr}_3]$  **110** (Figure 55) and the neutral dimer  $[\text{Mg}(\text{O}_2\text{CN}(\text{Me})\text{Ph})(\text{thf})_2\text{Br}]_2$  **111**.<sup>532</sup> The former features a trinuclear magnesium

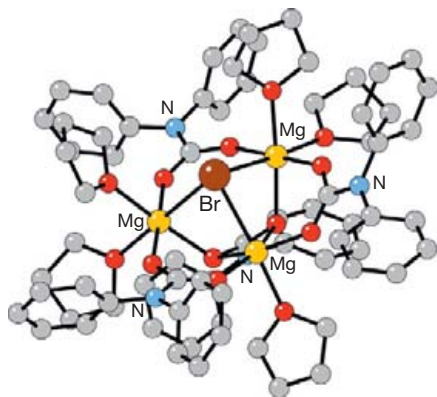
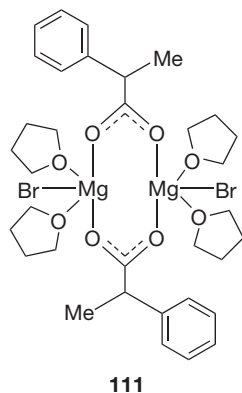


**Figure 55** Structure of  $[\text{Mg}_3(\text{O}_2\text{CNPh}_2)_4(\text{thf})_5\text{Br}]^+[(\text{thf})\text{MgBr}_3]^-$  **110**.

core that is supported by a pyramidal  $\mu_3$ -bromide ion and four carbamato anions. In contrast, **111** contains two bridging *N*-phenyl-*N*-methylcarbamato ligands, and each magnesium center exhibits a five-coordinate trigonal-bipyramidal geometry. The formation of the two related but distinct compounds, which do not interconvert in solution, underscores how substituents on the carbamato ligands can interfere with predictions of structures in these systems.



**111**

Bubbling gaseous  $\text{CO}_2$  through a mixed THF/HMPA solution of  $\text{Mg}_2(\text{NCy}_2)_4$  yields the colorless dinuclear  $\text{Mg}_2(\text{O}_2\text{CN-Cy}_2)_4(\text{hmpa})$  **112** (Figure 56). The dinuclear structure contains four carbamato ligands that are bonded to magnesium in three different modes – two  $\mu_2, \eta^2$ , one  $\mu_2, \eta^3$ , and one  $\eta^2$ .<sup>533</sup>

Magnesium acetate crystallizes upon reaction with imidazole in dimethylformamide to form  $[\text{Mg}_2(\text{C}_2\text{H}_3\text{O}_2)_2\text{O}(\text{C}_3\text{H}_4\text{N}_2)_4(\text{C}_2\text{H}_4\text{O}_2)_2]$  **113**.<sup>534</sup> It contains two octahedral magnesium centers, each of which is coordinated by two imidazole ligands, two bridging acetate ligands, and a terminal acetic acid ligand. A bridging oxygen atom links the two centers together along the symmetry axis. A related structure is formed from the reaction of aqueous  $\text{MgCl}_2$  with the sodium salt of 4-nitrobenzoic acid and *N*-methylimidazole.<sup>535</sup> In the dinuclear complex  $[\text{Mg}(\text{H}_2\text{O})(\text{N-Melm})_2(4\text{-nba})_2]_2$  **114**, each Mg center is hexacoordinated to an aqua ligand, two monodentate methylimidazole ligands, and a monodentate benzoate ligand; they are connected through two nitrobenzoate ligands. The dimers are linked through intra- and intermolecular hydrogen bonding into 1D chains.

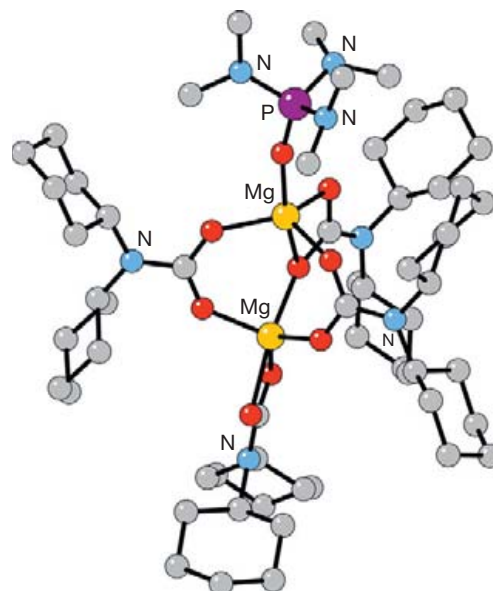
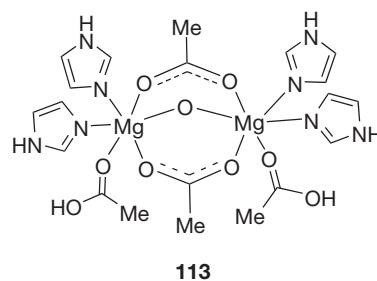
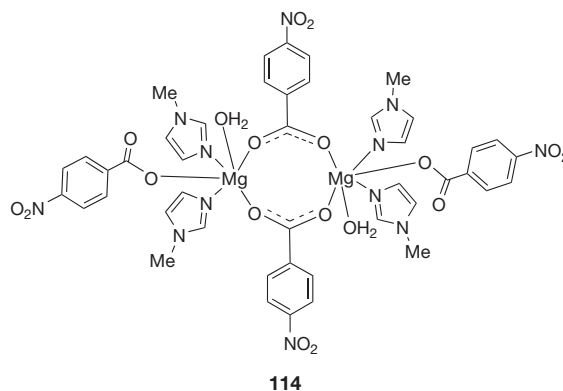


**Figure 56** Structure of  $\text{Mg}_2(\text{O}_2\text{CNCy}_2)_4(\text{hmpa})$  **112**.



**113**



**114**

Magnesium oxide reacts with dimethylammonium dimethylcarbamate,  $[\text{Me}_2\text{NH}_2][\text{O}_2\text{CNMe}_2]$ , in toluene to give the carbonato-carbamato complex  $[\text{Me}_2\text{NH}_2]_3[\text{Mg}_8(\text{CO}_3)_2(\text{O}_2\text{CNMe}_2)_{15}]$  **115** (Figure 57).<sup>536</sup> It is an octanuclear aggregate that contains hexacoordinate magnesium in an octahedral geometry. The magnesium cations are bonded to the oxygens of the carbamato and carbonato groups.

Recent work has taken advantage of the tendency of carboxylate ligands to bridge metal centers and has employed them as functional groups as organic linkers in metal-organic

frameworks (MOFs).<sup>537</sup> By adding additional carboxylate functional groups to the organic linker, the dimensionality of the coordination can be increased.<sup>538</sup> The reaction of  $\text{Mg}(\text{NO}_2)_2 \cdot 6\text{H}_2\text{O}$  with 2,4-dioxidoterephthalate generates the porous MOF Mg-MOF-74, which displays the ability to capture  $\text{CO}_2$  at capacities of up to 8.9 wt%.<sup>539</sup> Heating

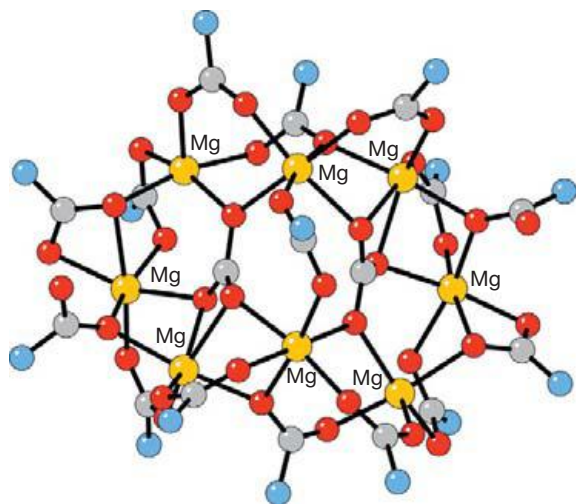


**Figure 57** Structure of  $[\text{Me}_2\text{NH}_2]_3[\text{Mg}_8(\text{CO}_3)_2(\text{O}_2\text{CNMe}_2)_{15}]$  **115**. For clarity, the methyl groups on the nitrogen atoms have been removed.

$\text{Mg}(\text{NO}_2)_2 \cdot 6\text{H}_2\text{O}$  and  $\text{H}_4\text{TCPBDA}$  ( $\text{TCPBDA}^{2-} = N,N,N',N'$ -tetrakis(4-carboxyphenyl)-biphenyl-4,4'-diamine) in DMF-EtOH- $\text{H}_2\text{O}$  yields the doubly-interpenetrated magnesium-based MOF,  $[\text{Mg}(\text{TCPBDA})(\text{H}_2\text{O})_2] \cdot 6\text{DMF} \cdot 6\text{H}_2\text{O}$  **116**. In **116**, the magnesium ions possess an octahedral coordination geometry from the binding of four  $\text{TCPBDA}^{2-}$  ligands at the equatorial positions and two water molecules at the axial positions (Figure 58). The desolvated solid of **116**,  $\text{Mg}(\text{TCPBDA})$ , exhibits selective gas-sorption properties for  $\text{H}_2$  and  $\text{O}_2$  gases over  $\text{N}_2$  at 77 K, and for  $\text{CO}_2$  gas over  $\text{CH}_4$  at temperatures ranging from 195 to 298 K.<sup>540</sup>

A magnesium MOF ( $\text{Mg}_3(\text{BPT})_2(\text{H}_2\text{O})_4$  **117**), derived from the asymmetrical ligand biphenyl-3,4',5-tricarboxylate ( $\text{H}_3\text{BPT}$ ), consists of 1D hexagonal nanotube-like channels (Figure 59). At 77 K, **117** displays hydrogen-sorption hysteresis up to 1.3 wt% at atmospheric pressure.<sup>541</sup> Interestingly, the excitation of solid **117** at 328 nm produces an intense violet-blue luminescence peak at 372 nm, which may stem from a ligand-based  $\pi-\pi^*$  transition. This suggests that the MOF might find use as a fluorescent porous material.

Most calcium carboxylate complexes form coordination polymers in the solid state; however, it is possible, through the use of bulky ligands, to limit their oligomerization. In an effort to model the active sites of calcium-binding proteins, the mononuclear calcium complex  $(\text{NEt}_4)_2[\text{Ca}\{\text{O}_2\text{C}-2,6-(t\text{-BuCONH})_2\text{C}_6\text{H}_3\}_4]$  **118** was generated from the reaction of an aqueous solution of  $\text{Ca}(\text{OAc})_2 \cdot \text{H}_2\text{O}$  and  $(\text{NEt}_4)(\text{OAc}) \cdot 4\text{H}_2\text{O}$  with an ethanol solution of 2,6-(*t*-BuCONH) $_2\text{C}_6\text{H}_4\text{CO}_2\text{H}$ .<sup>542</sup> The tetrakis(carboxylato)

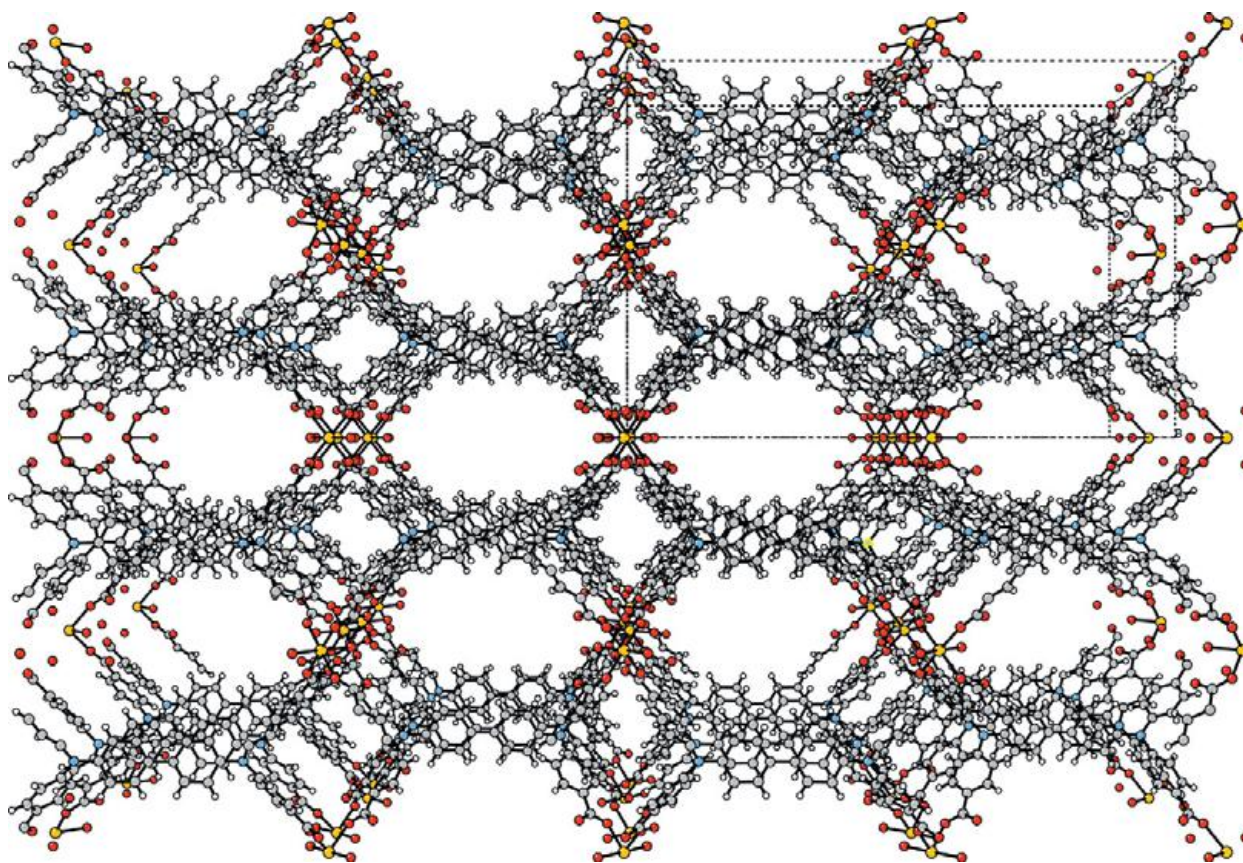


**Figure 58** Portion of the lattice of  $[\text{Mg}(\text{TCPBDA})(\text{H}_2\text{O})_2] \cdot 6\text{DMF} \cdot 6\text{H}_2\text{O}$  **116**. A unit cell is outlined in black.

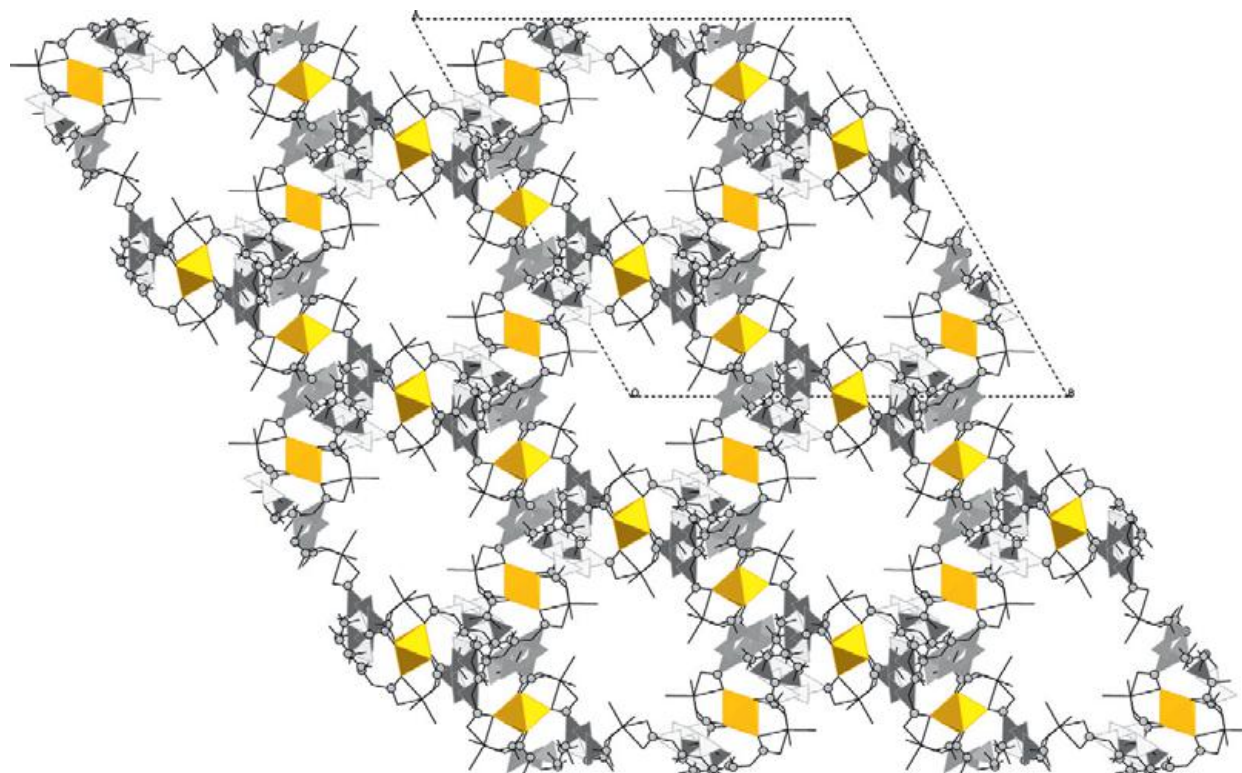
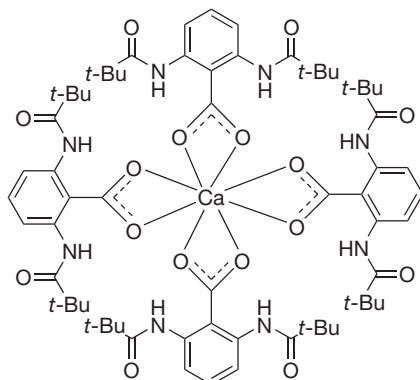


**Figure 59** Structure of  $\text{Mg}_3(\text{BPT})_2(\text{H}_2\text{O})_4$  **117**.

calcium complex contains four bidentate-bridging carboxylate ligands and the calcium center is eight-coordinate.



**118**

A heterometallic precursor for the deposition of barium-copper oxide thin films was produced from the reaction of barium *N,N*-dimethylaminopropanolate (dmap) and copper(II) acetate in THF.<sup>543</sup> The eight-coordinate barium ion in  $\text{Ba}(\text{dmap})_4\text{Cu}_4(\text{OAc})_6 \cdot \text{thf}$  **119** displays a distorted square-pyramidal geometry (Figure 60). It is sandwiched between two dicopper  $\text{Cu}_2(\mu\text{-dmap})_2(\mu\text{-OAc})_2$  units. A similar structure is observed when trifluoroacetate is used in place of the acetate ligand.

**1.37.4.2.4.1.2 Diketonates and enolates** Group 2 metal diketonates, the salts of  $\beta$ -diketones and  $\beta$ -ketoimines, are of principal interest for their usefulness as potential precursors for CVD,<sup>544</sup> and the  $\beta$ -diketonates used for this purpose have been

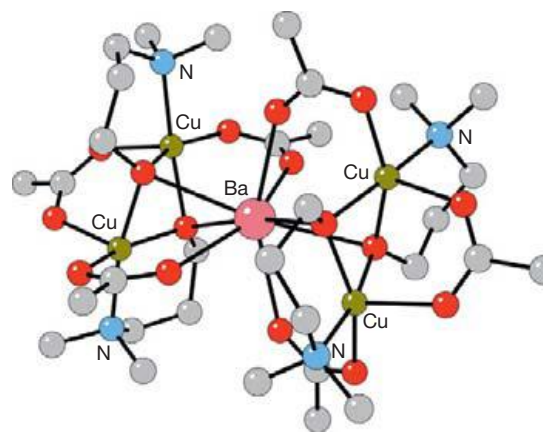


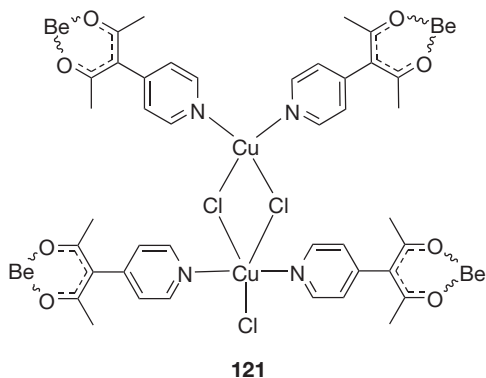
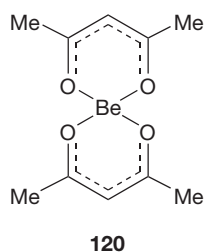
**Figure 60** Structure of  $\text{Ba}(\text{dmap})_4\text{Cu}_4(\text{OAc})_6 \cdot \text{thf}$  **119**.

extensively reviewed.<sup>260,261,525,545,546</sup> Considerable interest has been expressed in fluorinated derivatives, which can display substantially increased volatility relative to the hydrocarbon compounds.<sup>547</sup>

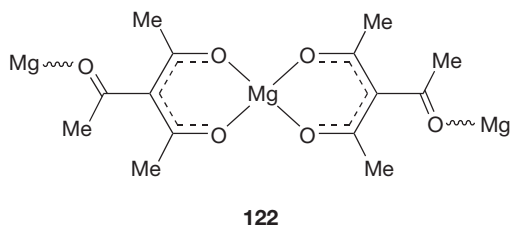
The deprotonation of  $\beta$ -diketones and  $\beta$ -ketoimines can be accomplished by a variety of methods, including reaction with aqueous solutions of metal chlorides,<sup>548</sup> hydroxides, carbonates,<sup>549</sup> or ethoxides.<sup>550,551</sup> Metalla- $\beta$ -diketonates of the group 2 metals are sensitive compounds, and differences in handling procedures (e.g., the inclusion of bases such as  $\text{NH}_3$ , THF, pyridine, and thd) have led to conflicting reports on reactivity and volatility. As with the  $\beta$ -diketonates, metal enolates of the s-block metals encompass a variety of forms, from monomers to large clusters, depending on the nature of

the R group and the presence of auxiliary bases coordinated to the metal.

Structurally characterized  $\beta$ -diketonates of beryllium have been known for over 50 years, starting with the monomeric  $\text{Be}(\text{acac})_2$  **120**.<sup>552</sup> Functionalized acac ligands have been features in more recent work with beryllium. For example, the addition of 3-(4-pyridyl)-2,4-pentanedione to an aqueous solution of  $\text{BeSO}_4$  and pyridine yields the complex  $\text{Be}(3\text{-(4-pyridyl)-2,4-pentanedione})_2$  ( $\text{BeL}_2$ ), which is isostructural with **120**.<sup>553</sup> Mixing  $\text{BeL}_2$  with cobalt or copper dihalides generates multinuclear species such as  $\text{Co}[\text{BeL}_2]_2\text{Cl}_2\cdot\text{H}_2\text{O}$ ,  $\text{Co}[\text{BeL}_2](\text{CH}_3\text{OH})_2\cdot\text{SO}_4\cdot\text{H}_2\text{O}\cdot\text{CH}_3\text{OH}$ , the mixed-valence complex  $\text{Cu}_2\text{X}_3[\text{BeL}_2]_2$  ( $\text{X}=\text{Cl}$  **121**, Br), and the univalent complex  $\text{Cu}_2\text{Br}_2[\text{BeL}_2]_2\cdot 5.33\text{CHCl}_3$ . In **121**, the beryllium coordination environment is the same as  $\text{BeL}_2$ ; the copper atoms are attached to two pyridyl functional groups from separate  $\text{BeL}_2$  fragments and either two or three halide ions for Cu(I) and Cu(II), respectively.



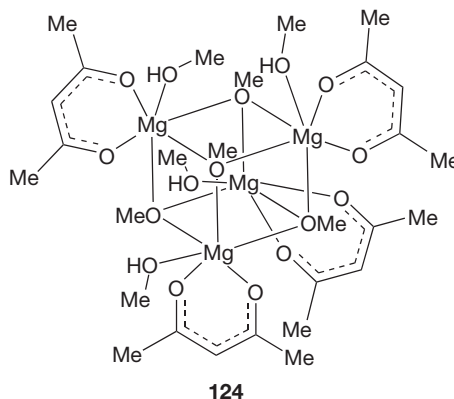
A magnesium compound containing a functionalized acac ligand, bis(3-acetyl-2,4-pentanedionato-O2,O3) magnesium,  $\text{Mg}[\text{C}_7\text{H}_9\text{O}_3]_2$  **122**, was made in the search for linear complexes of potential use in the construction of MOFs.<sup>554</sup> The complex is formed from the addition of  $(n\text{-Bu})_2\text{Mg}$  in *n*-heptane to a solution of triacetyl methane in toluene. In the solid state, **122** crystallizes in a layered structure constructed around magnesium centers that are bound octahedrally to two bidentate acac ligands, and two oxygen atoms from two backside acetyl groups.



The tetrahemispheraplex **123** is formed from the reaction between diethyl ketipinate (diethyl 3,4-dihydroxyhexa-2,

4-dienedioate) and magnesium chloride in THF.<sup>555</sup> The tetranuclear structure of **123** contains four magnesium cations linked through three doubly-bidentate diethyl 2,3-dioxobutane-1,4-dicarboxylato(2<sup>-</sup>) bridges (Figure 61). Ethylammonium counterions balance the charge. Similar structures are also found with ammonium and methylammonium counterions.<sup>556</sup>

$\text{Mg}_4(\text{acac})_4(\mu_3\text{-OMe})_4(\text{MeOH})_4$  **124** is obtained as the only isolable product of the reaction of  $\text{Mg}(\text{OMe})_2(\text{MeOH})_{3,5}$  and  $\text{CH}(\text{CH}_3)\text{CH}_2\text{NMe}_2\text{OH}$  in toluene with  $\text{Cu}(\text{acac})_2$ .<sup>557</sup> It crystallizes as colorless needles containing an  $\text{M}_4\text{O}_4$  cubane-like core. The center of **124** formed from four Mg atoms located at the vertex of the cubane, bonded to three triply-bridging oxygens from  $\mu_3\text{-OMe}$  and a solvating oxygen from MeOH. The coordination is completed by a bidentate acac group.



Bis(1-adamantyl acetoacetato)magnesium **125** is formed by the reaction of 1-adamantanol, magnesium chloride, and triethylamine in DMF.<sup>558</sup> It displays a trinuclear structure in the solid state, with the terminal magnesium atoms bound in a distorted octahedral arrangement to three bidentate 1-adamantyl acetoacetato ligands (Figure 62). The central magnesium is also octahedrally coordinated to six oxygen atoms from six separate 1-adamantyl acetoacetato ligands. Related derivatives have been made with hexyl-, dodecyl-,

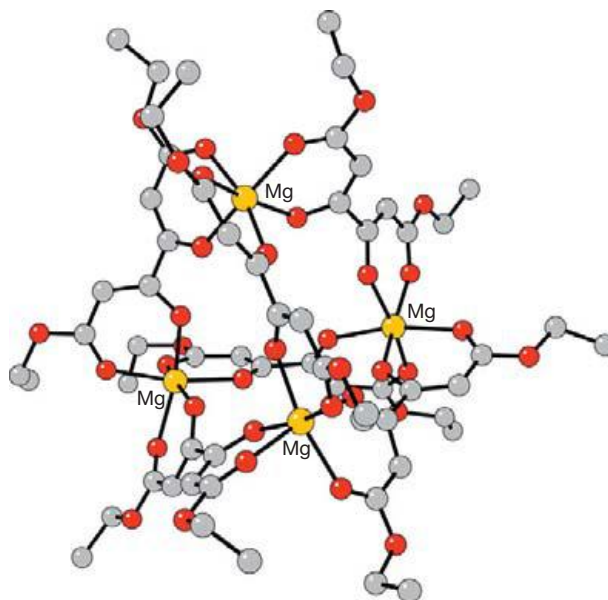


**Figure 61** Structure of the magnesium tetrahemispheraplex **123**.

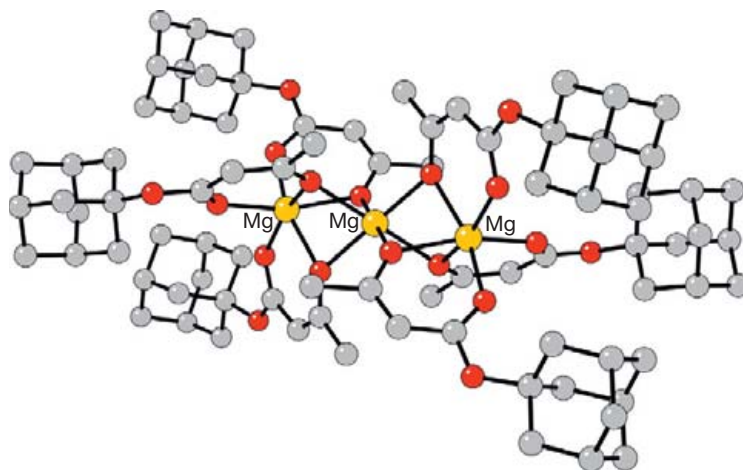


**Figure 62** Structure of bis(1-adamantyl acetoacetato)magnesium **125**.

*tert*-butyl-, cyclohexyl-, and bornyl-groups in place of the 1-adamantyl acetoacetate, and are believed to retain their oligomeric structures in solution.

The reaction products between  $\text{Mg}[\text{N}(\text{SiMe}_3)_2]_2$  and 2,4,6-trimethylacetophenone in hexane solution have been determined with  $^1\text{H}$  NMR spectroscopic analysis of the solids precipitated from solution.<sup>559</sup> Only enolate and unenolized ketone are present in the solids, and the absence of any amide suggests the formation of a magnesium bis(enolate). The structure of the isolated bis(enolate),  $\text{Mg}_4[\text{OC}(2,4,6\text{-trimethylphenyl})=\text{CH}_2]_8[\text{O}=\text{C}(2,4,6\text{-trimethylphenyl})\text{Me}]_2$  **126**, reveals four metals in a linear arrangement with six bridging and two terminal enolates, and two terminal ketones; the result is the formation of three orthogonal  $(\text{Mg}-\text{O})_2$  rings (Figure 63).

The equimolar reaction of  $\text{Ca}[\text{N}(\text{SiMe}_3)_2]_2$  with Hthd in THF yields mononuclear tris- $\text{Ca}(\text{tmhd})\{\text{N}(\text{SiMe}_3)_2\}(\text{thf})_3$ , which melts below room temperature (at  $4^\circ\text{C}$ ).<sup>560</sup> The calcium center in the complex is hexacoordinated in a distorted octahedral geometry. It is bound to the nitrogen atom of one bis(trimethylsilyl) amide ligand, two oxygen atoms from a bidentate diketone ligand, and three furan oxygens in a meridional arrangement. If a 3:2 calcium to dione ratio is used, the dinuclear complex  $[(\text{thf})\text{Ca}]_2(\text{tmhd})_2(\mu\text{-tmhd})\{\mu\text{-N}(\text{SiMe}_3)_2\}$  **127** is isolated instead. The calcium centers are each bound to a bridging  $\text{N}(\text{SiMe}_3)_2$  ligand, a terminal bidentate  $\beta$ -diketonate ligand, a doubly-bridging bidentate diketonate ligand, and a molecule of THF solvent. These compounds are catalytically active for the ring-opening polymerization of cyclic esters such as lactones and lactides (see Chapter 1.38).

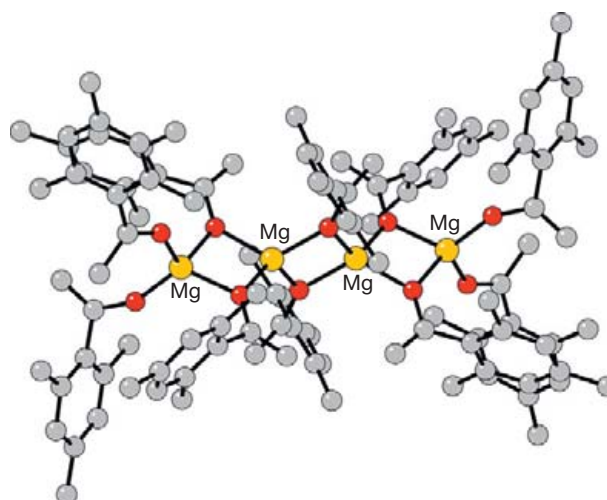
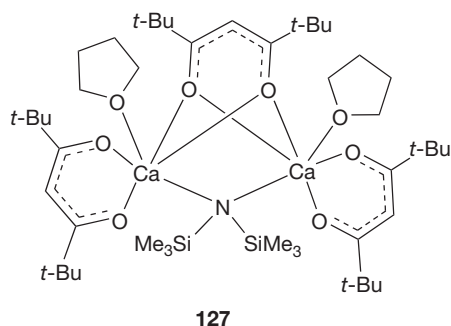
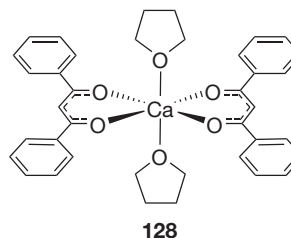
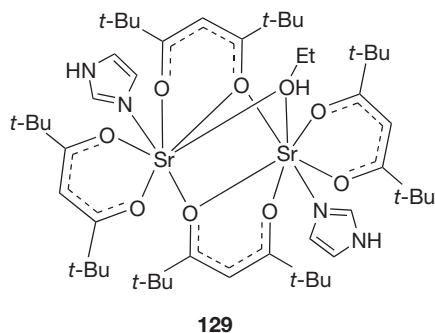


**Figure 63** Structure of  $\text{Mg}_4[\text{OC}(2,4,6\text{-trimethylphenyl})=\text{CH}_2]_8[\text{O}=\text{C}(2,4,6\text{-trimethylphenyl})\text{Me}]_2$  **126**.

The reactions of (Hthd), 1,1,1,5,5,5-hexafluoro-2,4-pentanedione (Hhfa), or 1,3-diphenyl-1,3-propanedione (Hdpp) with calcium methoxide in hexane or toluene leads to the oligomeric  $\beta$ -diketonates  $\text{Ca}_3(\text{thd})_6$ ,  $[\text{Ca}(\text{hfa})_2]_n$ , and  $[\text{Ca}(\text{dpp})_2]_n$ , respectively.<sup>561</sup> They can be deoligomerized by reaction with THF, triglyme, or 18-crown-6. The complex with dpp and thf ligands,  $\text{Ca}(\text{dpp})_2(\text{thf})_2$  **128**, contains octahedrally coordinated calcium with *trans* thf ligands and nearly symmetrically bound  $\beta$ -ketoenolate O atoms (Ca–O distances of 2.260 (2) and 2.292(2) Å).

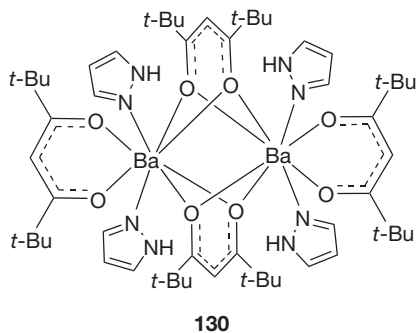


An exploratory search for volatile CVD precursors containing strontium led to the preparation of substituted  $\beta$ -diketonates using 1,1,1-trifluoro-2,4-pentanedione (Htfac), 1,1,1-trifluoro-4-phenyl-2,4-butanedione (Htfbz), Hhfa, and imidazole cations.<sup>562</sup> In particular, the addition of metallic strontium to an ethanol solution of imidazole (imH) and Htfbz in a 1:1:3 ratio of metal:imidazole: $\beta$ -diketonate gives the dinuclear complex (imH<sub>2</sub>)<sub>2</sub>[Sr<sub>2</sub>(tbz)<sub>6</sub>] **129**. It contains two octahedrally coordinated Sr centers that are bound to four oxygens from two terminal bidentate tbz ligands and four oxygens from doubly-bridging bidentate tbz ligands. Two imidazolium cations balance the charge of the compound. If a ratio of 1:2:4 of metal:methylimidazole: $\beta$ -diketonate is used, the mononuclear complex (MimH<sub>2</sub>)<sub>2</sub>[Sr(tbz)<sub>4</sub>] is formed instead. The strontium atom is eight-coordinate, surrounded by four tbz diketonate ligands.



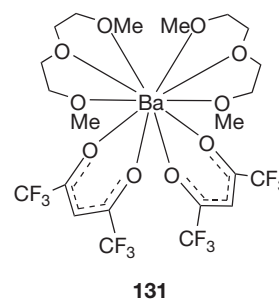
The 1:1:2 ratio of metal:imidazole: $\beta$ -diketonate reaction of Sr metal with imidazole and thd in ethanol gives the compound Sr<sub>2</sub>(thd)<sub>4</sub>(imH)<sub>2</sub>(EtOH). It features two strontium atoms coordinated to the nitrogen from a terminal imH, two oxygens from a terminal bidentate thd ligand, two oxygens from an  $\eta^1, \eta^2$ -O<sub>2</sub>-thd ligand, one oxygen from another  $\eta^1, \eta^2$ -O<sub>2</sub>-thd ligand, and the oxygen from a bridging ethanol molecule. If the reactants are added in a 3:2:6 ratio, **129** is formed, along with the mononuclear Sr(thd)<sub>2</sub>(H<sub>2</sub>O)<sub>2</sub>(EtOH).<sup>562</sup>

In a reaction similar to that used for the strontium analogs, Hthd, barium metal, and pyrazole (Hpz) react in toluene to produce the dinuclear complex [Ba(thd)<sub>2</sub>(Hpz)<sub>2</sub>]<sub>2</sub> **130**.<sup>563</sup> The barium centers are eight-coordinate from the two oxygens of three thd groups and two pyrazole nitrogen atoms. Two of the thd groups are tetradentate and doubly-bridging, while the other thd groups are bidentate. The same reaction with dimethyl pyrazole in place of pyrazole yields an isostructural compound.



The Ca, Sr, and Ba complexes of hfa and diglyme have been made by the addition of the appropriate metal carbonate to a

solution of Hhfa and diglyme in hexanes, and were examined for their potential to serve as CVD precursors.<sup>564</sup> The calcium and strontium compounds Ca(hfa)<sub>2</sub>(diglyme)(H<sub>2</sub>O) and Sr(hfa)<sub>2</sub>(diglyme)(H<sub>2</sub>O) are isostructural, with distorted anti-prismatic geometries. The metals are bonded to four oxygens from two [hfa]<sup>-</sup> anions, three oxygen atoms from diglyme, and an oxygen from a water molecule. The barium structure Ba(hfa)<sub>2</sub>(diglyme)<sub>2</sub> **131** is constructed around a ten-coordinate center. The barium atom is bonded to two tridentate diglyme molecules and two chelating [hfa]<sup>-</sup> anions (average Ba–O<sub>hfa</sub> = 2.74 Å; Ba–O<sub>diglyme</sub> = 2.93 Å). After the coordinated water is removed, only the calcium complex Ca(hfa)<sub>2</sub>(diglyme)<sub>n</sub> exhibits appreciable thermal stability; it can evaporate intact in the range of 298–330 K.



**1.37.4.2.4.1.3 Alkoxides and aryloxides** Alkaline-earth derivatives of phenol and the lower alcohols (methoxides, ethoxides) have been known for more than a century, and, traditionally, have found use as polymerization catalysts and surfactant stabilizers (see [Chapter 1.38](#)). Based on their solubility and volatility (both of which are generally low), group 2 alkoxides were presumed to be oligomeric or polymeric substances, although, until the last third of the previous century, comparatively little was known of their structural chemistry.<sup>565</sup>

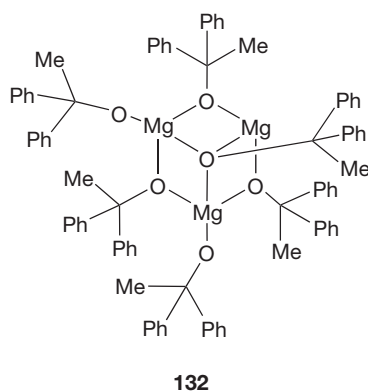
The biological interest in ion transport across membranes in the 1970s<sup>566,567</sup> and early 1980s and the discovery of superconducting oxides in the mid-1980s<sup>568</sup> initiated intensive study of alkoxides, especially in their role as precursors to metal oxides and halides. The area has expanded considerably in the last 30 years, and extensive reviews of various subjects in alkoxide and aryloxide chemistry, especially the alkaline-earth derivatives, are now available.<sup>92,261,569,570</sup>

The number of structurally characterized homo- and heterometallic alkoxides and aryloxides of the group 2 elements now numbers in the hundreds, and the previously cited review articles should be consulted for extensive listings. A large amount of structural diversity exists in the compounds, and monomers to discrete multimetallic aggregates (species with 12 or more group 2 metals are known<sup>571</sup>) and many polymeric species are represented. The ability of the larger metals to accommodate more ligands in their coordination spheres and, thus, form more extensive aggregates is counterbalanced by their lower Lewis acidity; it is not axiomatic, for example, that barium compounds will have higher coordination numbers than their calcium analogs.<sup>572</sup> This inherent electronic effect can be reinforced by the presence of sterically demanding ligands, and their packing around the metal may control coordination geometries.<sup>573</sup> The variety of Ae–O bonding modes available (e.g., terminal,  $\mu_2$ ,  $\mu_3$ ) and the potential

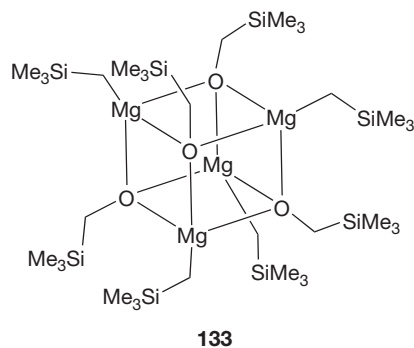
contribution from Ae–O  $\pi$ -bonding have made quantitative and even qualitative predictions of structures problematic,<sup>574</sup> although progress is still being made in this area.<sup>575,576</sup>

There is continuing interest in the group 2 alkoxide and aryloxide complexes in organic synthesis,<sup>577–579</sup> polymerization initiators<sup>346,244,580–587</sup> (see **Chapter 1.38**), sol-gel processes,<sup>588</sup> and CVD precursors,<sup>589</sup> and detailed coverage of this chemistry is outside the scope of this chapter.

The sensitivity of the nuclearity of complexes to the presence of auxiliary ligands is illustrated by the products of  $\text{MgBu}_2$  with various bulky alkoxides and siloxides. The reaction of  $\text{MgBu}_2$  with 1,1-diphenylethanol in toluene yields the trinuclear product  $\text{Mg}(\mu_3\text{-OCPh}_2\text{CH}_3)(\mu\text{-OCPh}_2\text{CH}_3)_3(\text{OCPh}_2\text{CH}_3)_2$  **132**.<sup>104</sup> If the reaction is conducted in the presence of THF, the dinuclear product  $[\text{Mg}(\text{OCPh}_2\text{CH}_3)_2(\text{thf})_2]$  is isolated instead. A related transformation is observed when the oligomeric  $[\text{Mg}(\text{OC}_6\text{H}_3(2,6\text{-Me})_2)_2]_n$  is split into the monomeric  $\text{Mg}(\text{OC}_6\text{H}_3(2,6\text{-Me})_2)(\text{py})_3$  complex in the presence of pyridine.<sup>91</sup>



Owing to the sensitivity of alkaline-earth alkoxides and their derivatives to air and moisture, unanticipated products can be generated in the course of their synthesis. Early reports on the thermal behavior of the widely used barium oxide precursor 'Ba(thd)<sub>2</sub>' for example, indicated that ~25–40% of the material remained unsublimed under oxide-forming conditions.<sup>590,591</sup> Further investigation indicated that the use of partially hydrolyzed and/or adducted material was responsible for the large amount of residue.<sup>550</sup> Similarly, when a solution of  $\text{ClMgCH}_2\text{SiMe}_3$  in light petroleum/diethyl ether is allowed to stand for over a week, crystals of the tetrametallic complex  $[\text{Mg}(\text{CH}_2\text{SiMe}_3)(\mu_3\text{-OCH}_2\text{SiMe}_3)]_4$  **133** can be isolated. Evidently, the  $\text{ClMgCH}_2\text{SiMe}_3$  undergoes Schlenk redistribution to form  $\text{MgCl}_2$  and  $\text{Mg}(\text{CH}_2\text{SiMe}_3)_2$ . The latter then reacts with traces of  $\text{O}_2$  to generate **133** by direct insertion into the Mg–C bond.<sup>592</sup>



The variety of structures that can be assumed by group 2 coordination spheres is particularly evident with heterometallic alkoxide clusters. The reaction of the mixed-metal alkoxides  $\text{BaTi}(\text{O}(i\text{-Pr})\text{OMe})_6$  or  $\text{BaZr}(\text{O}(i\text{-Pr})\text{OMe})_6$  with methacrylic acid produce methacrylate-modified barium oxoclusters.<sup>593</sup> The product from the barium–titanium alkoxide,  $\text{Ba}_2\text{Ti}_{10}(\mu_3\text{-O})_8(\mu_2\text{-OH})_5(\mu_2\text{-OMc})_{20}(\text{O}(i\text{-Pr})\text{OMe})_2$  ( $\text{Mc}$  = methacrylate) **134** (**Figure 64**), is constructed of two  $\text{BaO}_{10}$  cores surrounded by ten  $\text{TiO}_6$  octahedra. This framework is surrounded by a shell of ten methacrylate groups that serve as bridging ligands between titanium atoms. The product from the barium–zirconium alkoxide is the homometallic  $[\text{Ba}(\text{OMc})_2(\text{McOH})_3]_n$ , based on zigzag chains of edge-sharing  $\{\text{BaO}_9\}$  polyhedra linked through bridging bidentate methacrylate anions.

An example of a coordination motif found in homometallic species that persists in a heterometallic counterpart is provided by the product of the reaction of elemental barium and europium in boiling 2-propanol. It crystallizes from THF as  $\text{H}_2[\text{Eu}_2\text{Ba}_6\text{O}_2(\text{O}(i\text{-Pr}))_{16}(\text{thf})_4]$  **135** (**Figure 65**).<sup>34</sup> Rather than

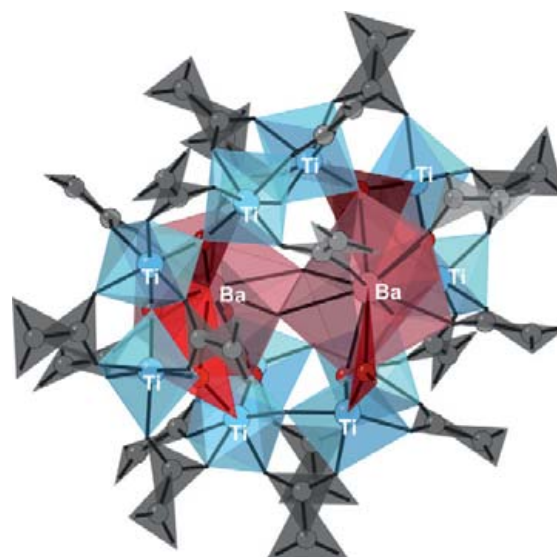


**Figure 64** Structure of  $\text{Ba}_2\text{Ti}_{10}(\mu_3\text{-O})_8(\mu_2\text{-OH})_5(\mu_2\text{-OMc})_{20}(\text{O}(i\text{-Pr})\text{OMe})_2$  ( $\text{Mc}$  = methacrylate) **134**. The coordination sphere of barium is in red; that of titanium is in blue.

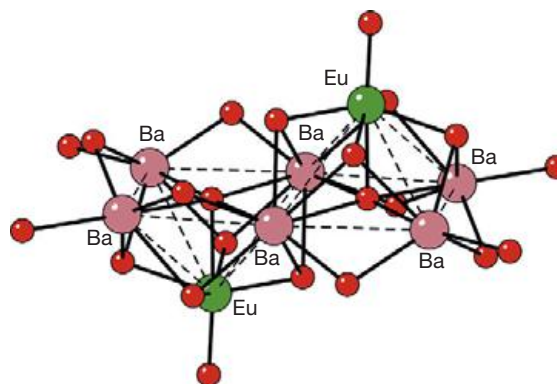


**Figure 65** Structure of  $\text{H}_2[\text{Eu}_2\text{Ba}_6\text{O}_2(\text{O}(i\text{-Pr}))_{16}(\text{thf})_4]$  **135**. The carbon atoms have been removed for clarity.

assume a geometry based on eight-coordinate metal centers, which would be typical for these metals, the structure comprises two square-based pyramids with coplanar bases (Ba) that share a basal edge and have apices (Eu) on opposite sides, a motif found previously in barium and strontium aryloxides.<sup>594</sup> In 135, the metal atoms of each square pyramid are bound by one  $\mu_5$ -oxygen, four  $\mu_3$ -O(*i*-Pr) ligands bridging the triangular faces, and three  $\mu$ -O(*i*-Pr) ligands bridging the unshared basal edges of the square pyramid. The europium atoms also display a terminal O(*i*-Pr) ligand, and a thf ligand is coordinated to the unshared basal corners of the square pyramids.

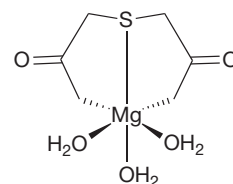
The solution chemistry of group 2 alkoxides is often complex, with various redistribution and solvation equilibria in play. This is illustrated by the behavior of magnesium aryloxides containing the bulky OAr (Ar = C<sub>6</sub>H<sub>3</sub>(*t*-Bu)<sub>2</sub>, 2,6) ligand. Several dimeric and mononuclear species can be synthesized containing OAr (e.g., [Mg(*s*-Bu)( $\mu$ -OAr)]<sub>2</sub>, [Mg( $\mu$ -N(*i*-Pr)<sub>2</sub>OAr)]<sub>2</sub>, Mg(OAr)<sub>2</sub>(thf)<sub>2</sub> 136, and Mg(OAr)<sub>2</sub>(tmeda)), and partial rearrangement of the heteroleptic species occurs in THF solution to yield their homoleptic counterparts.<sup>595</sup> Interestingly, when the unsolvated complex [Mg(OAr)<sub>2</sub>]<sub>2</sub> is dissolved in thf-d<sub>8</sub>, some of the compound forms the magnesiate [Mg(OAr)]<sub>2</sub>[Mg(OAr)<sub>3</sub>] 137, whereas part of it is converted into 136. Evidently, unsymmetrical cleavage of the dimer [Mg(OAr)<sub>2</sub>]<sub>2</sub> is responsible for this behavior (Scheme 5). If 136 alone is dissolved in thf-d<sub>8</sub>, 137 is not observed.

#### 1.37.4.2.4.2 Sulfur-donor ligands

Given the relatively high Lewis acidity of the group 2 ions, it is, perhaps, not surprising that their chemistry with sulfur-donor ligands has developed more slowly than that to oxygen donors. Nevertheless, there has been steady growth in the field, and reviews of the area are available in the literature.<sup>596–598</sup>

Several different routes are available for sulfur-bound group 2 compounds. The reaction of MgCl<sub>2</sub> with thiocarboxylic acids produces the corresponding derivatives; for example, an aqueous solution of MgCl<sub>2</sub> with a mixture of Na<sub>2</sub>CO<sub>3</sub> and thiodiacetic acid (S(CH<sub>2</sub>COOH)<sub>2</sub>) produces the colorless complex Mg(S(CH<sub>2</sub>COO)<sub>2</sub>)(H<sub>2</sub>O)<sub>3</sub> 138 (Mg–S = 2.7294(5) Å).<sup>599</sup> Similarly, the reaction of AeCl<sub>2</sub>·*n*H<sub>2</sub>O (Ae = Ca, Sr, or Ba) with 2-mercaptobenzoic acid in an EtOH/H<sub>2</sub>O/NH<sub>3</sub> mixture produces [{Ae(O<sub>2</sub>CC<sub>6</sub>H<sub>4</sub>SSC<sub>6</sub>H<sub>4</sub>CO<sub>2</sub>)(H<sub>2</sub>O)<sub>2</sub>}·0.5EtOH]<sub>*n*</sub>

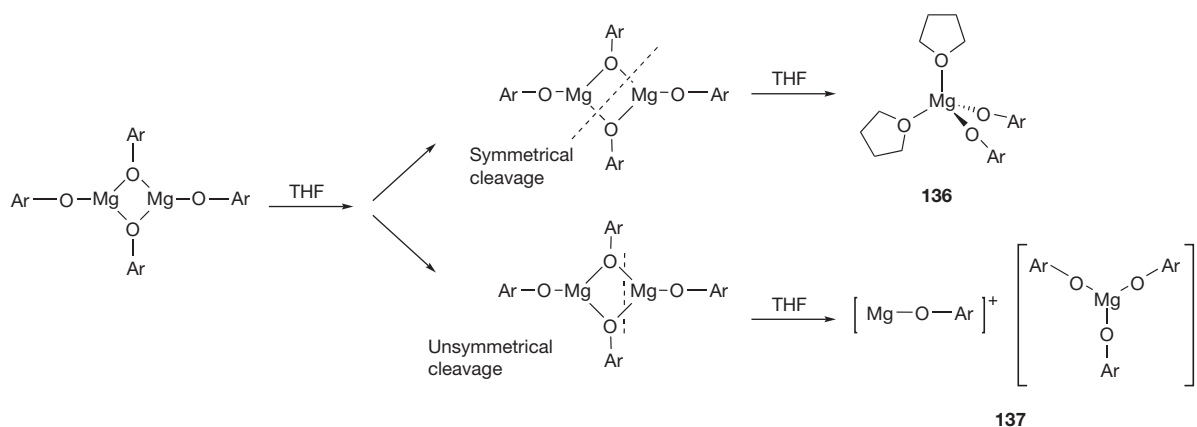
(Ae = Ca or Sr) and [{Ba<sub>2</sub>(O<sub>2</sub>CC<sub>6</sub>H<sub>4</sub>SSC<sub>6</sub>H<sub>4</sub>CO<sub>2</sub>)(H<sub>2</sub>O)<sub>2</sub>}·0.5EtOH]<sub>*n*</sub> 139; the acid has been oxidized to 2,2'-dithiobis (benzoic acid). The metals are coordinated only through the carboxylate groups in the calcium and strontium compounds; in contrast, reflecting the lowering acidity of barium, in 139, the metal is linked to both carboxylate and disulfide moieties (Figure 66; Ba'–O = 2.68(1) Å; Ba'–S = 3.610(6) Å).<sup>129</sup>



138

Elimination reactions (Section 1.37.2.2.3) involving (*n*-Bu)<sub>2</sub>Mg are useful for forming a range of compounds with sulfur derivatives. Bis(diphenylthiophosphinoyl)methane, CH<sub>2</sub>(PPh<sub>2</sub>=S)<sub>2</sub>, reacts with (*n*-Bu)<sub>2</sub>Mg to produce [MgC(PPh<sub>2</sub>=S)<sub>2</sub>(thf)<sub>2</sub>] 140 (Figure 67; Mg–S(av) = 2.46(3) Å).<sup>600</sup> Cyclohexylphosphane (CyPH<sub>2</sub>) reacts with 1 equiv. of (*n*-Bu)<sub>2</sub>Mg and 3/8 equiv. of S<sub>8</sub> in THF to yield the magnesium salt of the [CyPS<sub>3</sub>]<sup>2-</sup> dianion, [MgS<sub>3</sub>PCy(thf)<sub>2</sub>]<sub>2</sub> 141.<sup>601</sup> The magnesium atoms are bonded to the sulfur atoms in a  $\mu_2$ - $\eta^2$ ,  $\eta^2$  manner, with Mg–S = 2.558(2)–2.700(2) Å. The Mg–O bonds from the *cis* THF ligands are at a distance of 2.080(3) and 2.094(3) Å, completing the distorted octahedral geometry around the metal (Figure 68). The [P<sub>2</sub>S<sub>6</sub>]<sup>4-</sup> core in 141 is similar to that in the Li(tmeda) analog.

Various mercaptopyridines react with (*n*-Bu)<sub>2</sub>Mg in THF and form the magnesium pyridine-2-thiolates, Mg(R-pyS)<sub>2</sub>(thf)<sub>2</sub> (R = H 142, 3-CF<sub>3</sub>, 5-CF<sub>3</sub>, 3-SiMe<sub>3</sub>).<sup>95</sup> The S–C bonds of all the compounds fall in a narrow range (averaging 1.732–1.753 Å), indicating that they are normal single bonds (as in a thiol) and not the shortened bonds that would be associated with S=C character in an  $\alpha$ -thiopyridone. The compounds are instructive model systems for the magnesium centers in Photosystem I, in which the metal, bound in the porphyrin ring of chlorophyll, also interacts with a neighboring methionine residue.



Scheme 5 Divergent reaction pathways resulting from alkoxide bond cleavage.

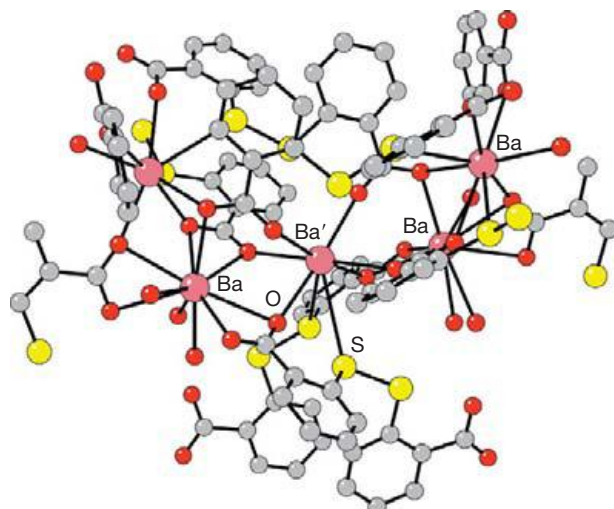


**Figure 66** Portion of the lattice of  $[(\text{Ba}_2(\text{O}_2\text{CC}_6\text{H}_4\text{SSC}_6\text{H}_4\text{CO}_2)_2(\text{H}_2\text{O})_2) \cdot 0.5\text{EtOH}]_n$ , **139**. The labeled atom is referred to in the text.

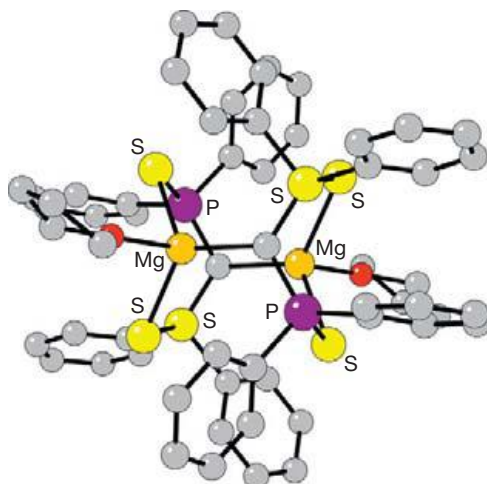


**Figure 67** Structure of  $[\text{MgC}(\text{PPh}_2=\text{S})_2(\text{thf})_2]$  **140**.

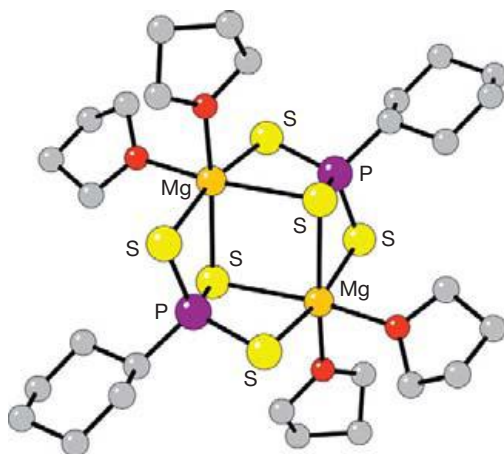
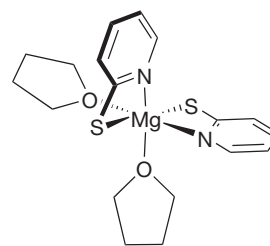
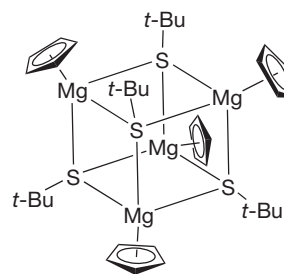


**Figure 68** Structure of  $[\text{MgS}_3\text{PCy}(\text{thf})_2]$  **141**.



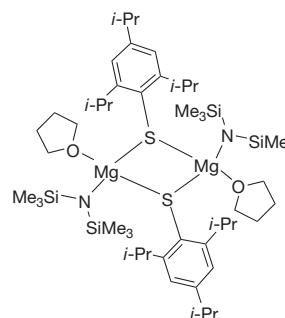
**142**

Elimination reactions can also be conducted with cyclopentadienyl ligands, as with the reaction of  $\text{Cp}_2\text{Mg}$  with thiols HSR ( $\text{R} = i\text{-Pr}$ ,  $t\text{-Bu}$ ,  $\text{Cy}$ ) to form the cubane complexes  $[\text{MgCp}(\mu_3\text{-SR})_4]$  ( $\text{R} = i\text{-Pr}$ ,  $t\text{-Bu}$ , or  $\text{Cy}$ ).<sup>602</sup> When the  $t\text{-Bu}$  compound **143** is treated with THF or *tert*-butylpyridine, the dimeric complexes  $[\text{MgCp}(\mu_2\text{-}(t\text{-Bu}))(\text{L})_2]$  are the result. **143** is centrosymmetric and displays a planar central  $\text{Mg}_2\text{S}_2$  ring; in the thf-ligated compound, the  $\text{Mg}_2\text{S}_2$  ring is puckered.<sup>602</sup>



**143**

The nuclearity of the products of the reaction of  $[\text{Mg}(\text{N}(\text{SiMe}_3)_2)_2]$  with magnesium thiolates varies with solvent systems used and the steric bulk of thiolate.<sup>603</sup> For example, the more compact thiolates  $[\text{Mg}(\text{thf})_2(\text{SR})_2]_n$  ( $\text{R} = \text{Ph}$ ,  $\text{trip}$ ) yield dimeric species,  $[\text{Mg}(\text{thf})(\text{N}(\text{SiMe}_3)_2)(\mu\text{-SR})_2]$ , when hexane alone ( $\text{R} = \text{Ph}$ ) or a hexane/toluene mixture ( $\text{R} = \text{trip}$  **144**) is the solvent. Use of the bulkier  $[\text{Mg}(\text{SMes}^*)_2]$  in hexane/THF produces the four-coordinate, monomeric species  $\text{Mg}(\text{thf})_2(\text{N}(\text{SiMe}_3)_2)(\text{SMes}^*)$ . Slight changes in reaction conditions alter the products, however; the reaction of  $[\text{Mg}(\text{N}(\text{SiMe}_3)_2)_2]$  with  $\text{Mg}(\text{thf})_2(\text{SMes}^*)_2$  in a toluene/hexane mixture produces the symmetrical dimeric, four-coordinate magnesium thiolate  $[\text{Mg}(\text{thf})\{\text{SMes}^*\}\{\mu\text{-SMes}^*\}]_2$ . Such variability complicates the production of potential precursors to important quaternary phases, such as  $\text{Zn}_{2n-x}\text{Mg}_x\text{SSe}$ .<sup>604,605</sup>



**144**

## 1.37.4.2.4.3 Selenium and tellurium donor ligands

The isolation of well-characterized coordination or organometallic compounds of the group 2 elements containing bonds to Se (or Te) generally requires that the donor ligands possess large, sterically demanding substituents that confer kinetic stability on the complexes. Much of the work in this area dates from only the early 1990s, and the area has been reviewed.<sup>598</sup>

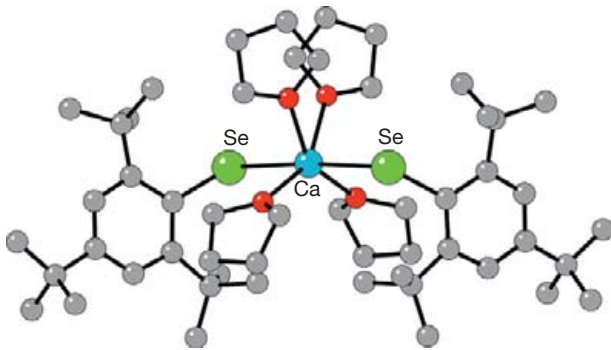


Figure 69 Structure of  $\text{Ca}(\text{thf})_4(\text{SeMes}^*)_2$  **145**.

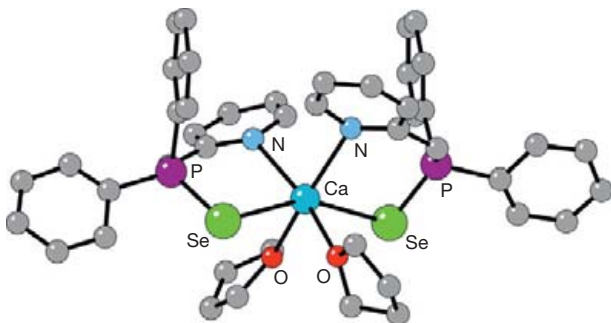


Figure 70 Structure of  $\text{Ca}(\text{thf})_2[(\text{PyCH})(\text{Se})\text{PPh}_2]_2$  **146**.

The calcium selenolate  $\text{Ca}(\text{thf})_4(\text{SeMes}^*)_2$  **145** has been prepared by direct metallation of  $(\text{Mes}^*\text{Se})_2$  with calcium in liquid ammonia.<sup>203</sup> In the solid state, **145** exhibits a Ca–Se contact pair in a monomeric structure with the selenolate ligands in approximate trans positions (Se–Ca–Se = 175.40 (5)°) (Figure 69).<sup>203</sup> The experimentally determined bond length (2.9936(4) Å) is believed to reflect primarily ionic bonding, in agreement with previous ab initio calculations.<sup>606</sup>

After **145**, the synthesis and characterization of  $\text{Ca}(\text{thf})_2[(\text{PyCH})(\text{Se})\text{PPh}_2]_2$  **146** from  $(\text{thf})_2\text{Ca}[\text{N}(\text{SiMe}_3)_2]_2$  and  $\text{Ph}_2\text{P}(\text{CH}_2\text{Py})$  mark only the second reported compound containing a direct Ca–Se bond (2.945(1) Å) (Figure 70).<sup>607</sup> Differential thermal analysis (DTA) of the yellow compound indicated that it might be a possible candidate for the formation of CaSe by CVD. The structurally authenticated compounds  $\text{Ba}[\text{Se}(\text{Mes}^*)]_2(\text{thf})_4$  (monomer, Ba–Se = 3.279(1) Å),  $[\text{Ba}(18\text{-crown-6})(\text{hmpa})_2][[\text{Se}(\text{Mes}^*)]_2]$  (solvent-separated ion triple),  $[\text{Ba}\{\text{Se}(\text{trip})\}_2(\text{py})_3(\text{thf})]_2$  **147** (Figure 71) (dimer,  $\mu\text{-Ba-Se} = 3.2973(3), 3.4189(3)$  Å; terminal Ba–Se = 3.2768 (3) Å), and  $\text{Ba}[\text{Se}(\text{trip})]_2(18\text{-crown-6})$  (monomer, Ba–Se = 3.2326(7)–3.2361(7) Å) have been prepared by the reductive insertion of Ba (dissolved in  $\text{NH}_3$ ) into the Se–Se bond of the corresponding diorganodiselenides.<sup>608</sup>

After a flurry of activity in the early 1990s,<sup>500,609,610</sup> the investigation of molecular group 2 compounds with tellurium donor ligands seems to have entered a quiescent phase; in particular, no crystal structures of compounds displaying Ae–Te bonds have been published since 2000.

## 1.37.4.2.5 Group 17 ligands

Halides of the group 2 metals such as  $\text{MgCl}_2$  and  $\text{CaCl}_2$  are among the most widely known of all compounds, and their uses are legion.<sup>611</sup> The molecular structure and spectra of the group 2 halides have been reviewed in the literature.<sup>612–615</sup> The use of the halides as reagents means that numerous group 2

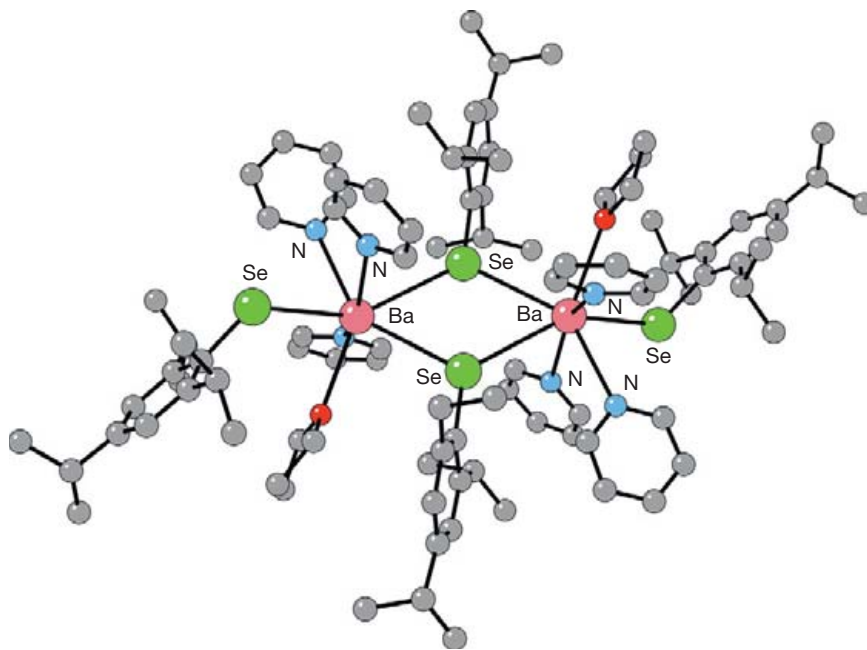
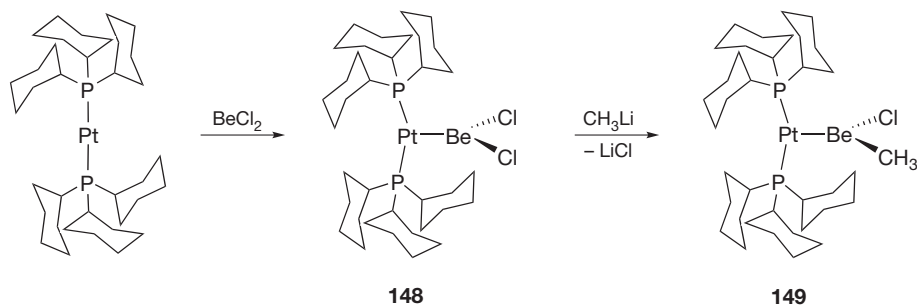


Figure 71 Structure of  $[\text{Ba}\{\text{Se}(\text{trip})\}_2(\text{py})_3(\text{thf})]_2$  **147**.



**Scheme 6** Formation of the platinum-beryllium bonded complexes **148** and **149**.

compounds with halide ligands have been structurally characterized (e.g., adducts with nitrogen and mixed nitrogen-oxygen bases such as MeCN, py, en, dien, tmeda, DMF, phen, bipy, terpy, substituted pyridines, water, and ROH (R=Me, Pr, Bu)).<sup>616–625</sup> A review of the coordination chemistry of beryllium halides is available in the literature.<sup>626</sup>

Although simple haloberyllates of the form  $[\text{BeX}_4]^{2-}$  (X=Cl, Br, I) have not been prepared in either aqueous or organic media, complexed haloberyllates in a variety of forms can be synthesized.<sup>37,627–635</sup> Among these are compounds with phosphorus- or nitrogen-donor ligands containing  $\text{BeCl}_3$  or  $\text{Be}_2\text{Cl}_3$  moieties; these have been characterized with crystallographic studies.<sup>628,630,633</sup> The anion of  $[\text{Be}_2\text{F}_6]^{2-}$  was isolated and identified with an x-ray crystal structure and IR spectroscopy as part of the complex  $(\text{Ph}_4\text{P})_2[\text{Be}_2\text{F}_6] \cdot 2\text{CH}_3\text{CN}$ .<sup>635</sup>

The treatment of  $\text{BeCl}_2$  with  $\text{Pt}(\text{PCy}_3)_2$  in  $\text{C}_6\text{D}_6$  yields the colorless adduct  $(\text{Cy}_3\text{P})_2\text{PtBeCl}_2$  **148**. The Be atom is in a trigonal-planar arrangement (Pt–Cl=1.922 Å (av); Pt–Be=2.168(4) Å).<sup>636</sup> Further treatment with methyl lithium replaces one of the chlorine atoms, generating  $(\text{Cy}_3\text{P})_2\text{PtBeCl}(\text{CH}_3)$  **149** (Scheme 6), with Pt–Cl=1.933(3) Å, Pt–Be=2.195(3) Å. In both **148** and **149**, the platinum-beryllium interactions represent genuine two-center-two-electron bonds.

A series of 1D, 2D, and 3D lithiumberyllofluoro frameworks has been synthesized and characterized (e.g.,  $[\text{Li}_2\text{Be}_2\text{F}_7][\text{CH}_3\text{NH}_3]$  **150**, Figure 72).<sup>637–640</sup> Control over the dimensionality is exercised by varying the organoamine templates used during synthesis, ultimately leading to structures resembling zeolites.<sup>638,639</sup>

As part of a study of anhydrous sol-gel synthesis of metal fluorides,  $\text{Mg}(\text{OCH}_3)_2$  was treated with an alcoholic HF solution ( $3\text{Mg}(\text{OCH}_3)_2 \cdot 1\text{HF}$ ), yielding the magnesium alcoholate fluoride  $[\text{Mg}_6(\mu_4\text{-F})_2(\mu_3\text{-OME})_4(\text{OME})_4(\text{MeOH})_{12}][\text{H}(\text{MeO})_2]_2$  **151**.<sup>641</sup> The hexanuclear, cationic dicubane unit comprises two trinuclear fragments joined by a four-membered  $(\text{MgF})_2$  ring that features  $\mu_4\text{-F}$  atoms (Mg–F=2.138(1) Å) (Figure 73). The cation is hydrogen-bonded to two  $(\text{MeOH} \cdots \text{OME})^-$  anions, producing the triple-ion structure.

A series of magnesium iodides has been synthesized as by-products from an aryl exchange of the Grignard reagent 2,6-Et<sub>2</sub>C<sub>6</sub>H<sub>3</sub>MgI(thf).<sup>642</sup> The  $\text{MgI}_2(\text{thf})_3$  by-product was easily oxidized to  $\text{MgI}(\text{thf})_5\text{I}_3$  and fully characterized. A unique donor-free Grignard-type reagent exists in  $[(\text{C}_5\text{Me}_5)_2\text{Al}][\text{Mg}_6\text{Cl}_8(\text{C}_5\text{Me}_5)_5]$  **152**, which was synthesized from  $(\text{C}_5\text{Me}_5)_2\text{Mg}$  and  $\text{AlCl}_3$  in an ether-toluene mixture.<sup>643</sup> The anion of **152** possesses the inverse magnesocene motif  $\mu\text{-}(\text{C}_5\text{Me}_5)_2\text{Mg}_2$  (Figure 74).<sup>643</sup>

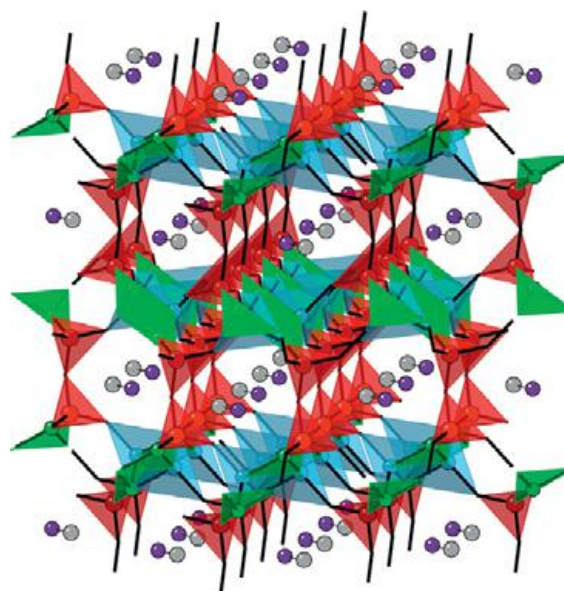


**Figure 72** Partial polyhedral packing diagram of  $[\text{Li}_2\text{Be}_2\text{F}_7][\text{CH}_3\text{NH}_3]$  **150**, illustrating the porous framework surrounding the methylamine templates. Lithium-centered tetrahedra are in blue, beryllium in red, and fluoride in green; nitrogen atoms are purple and carbons are gray.

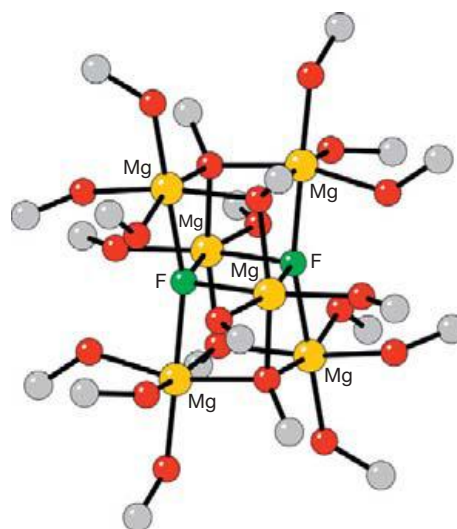


**Figure 73** Structure of the cation of  $[\text{Mg}_6(\mu_4\text{-F})_2(\mu_3\text{-OME})_4(\text{OME})_4(\text{MeOH})_{12}][\text{H}(\text{MeO})_2]_2$  **151**.

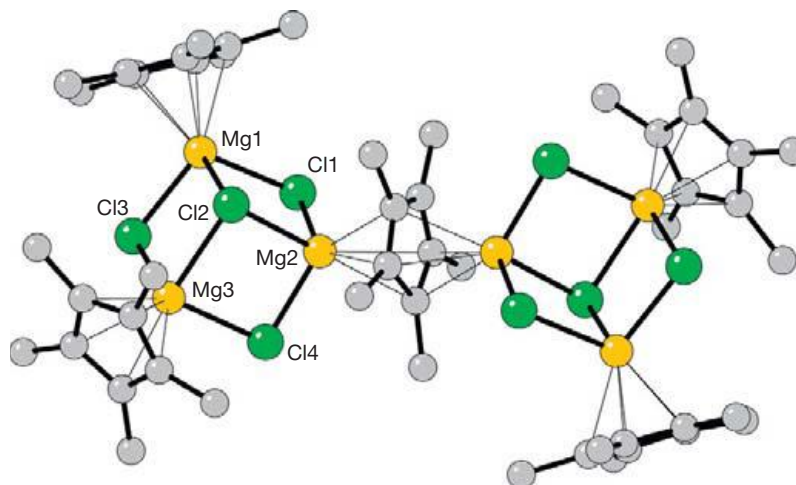


**Figure 74** Structure of the anion of  $[(C_5Me_5)_2Al]^+[Mg_6Cl_8(C_5Me_5)_5]$  **152**.

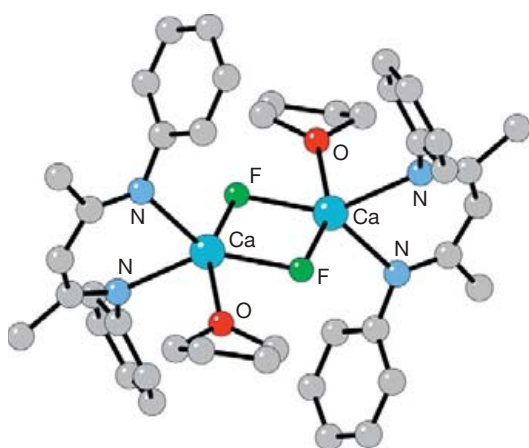
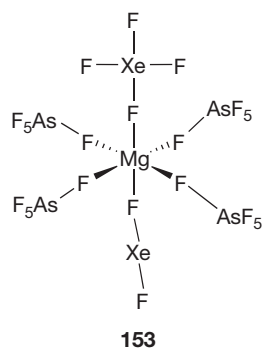


**Figure 75** Structure of  $[(DIPP-nacnac)Ca(\mu-F)(thf)_2]$  **154**.

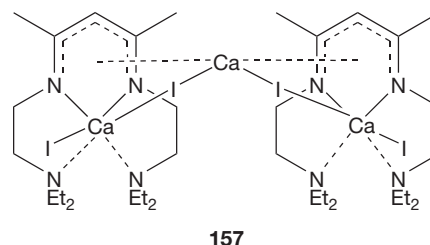
When a mixture of  $XeF_2$  and  $XeF_4$  is allowed to react with Mg ( $AsF_6$ )<sub>2</sub> in anhydrous HF, crystals of  $[Mg(XeF_2)(XeF_4)](AsF_6)_2$  **153** can be obtained.<sup>644</sup> The compound is the only known example in which  $XeF_4$  functions as a ligand, a metal center (Mg–F ( $XeF_3$ ) = 1.956(7) Å), and in which both  $XeF_2$  (Mg–F( $XeF$ ) = 1.935(7) Å) and  $XeF_4$  ligands are concurrently bound to a metal.



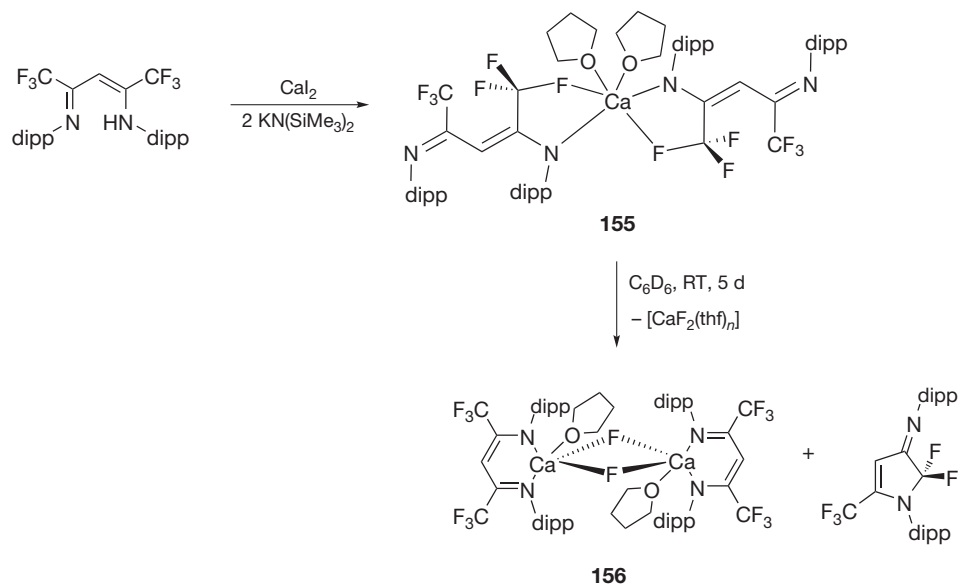
Obtained from the reaction of  $(DIPP-nacnac)Ca[N(SiMe_3)_2](thf)$  with  $Me_3SnF$ , the unusual calcium monofluoride complex

$[(DIPP-nacnac)Ca(\mu-F)(thf)_2]$  **154** possesses high solubility in organic solvents (Figure 75; Ca–F = 2.170(2), 2.189(2) Å).<sup>645</sup> Layers of transparent  $CaF_2$  can be formed from **154** at room temperature with dip-coating. By replacing the DIPP substituent with  $CF_3$  groups, the calcium  $\beta$ -diketiminato complex **155** is generated, which displays an unusual binding mode of a  $CF_3$  group (Ca  $\cdots$  F = 2.489(3) Å; Scheme 7).<sup>646</sup> The C–F bonds of the coordinated fluorine atoms are elongated (by an average of 0.043 Å) compared to uncoordinated fluorine atoms. Compound **155** proves to be unstable, and converts into the symmetrical complex **156** on standing in  $C_6D_6$  for 5 days.

The reaction of the  $\beta$ -diketiminato ligand HL (L =  $Et_2NCH_2CH_2NC(Me)CHC(Me)NCH_2CH_2NEt_2$ ) with KN ( $SiMe_3$ )<sub>2</sub> and  $CaI_2$  in THF leads to the formation of  $LCaI(\mu-ICaI-\mu)ICaL$  **157**, which contains a  $[I-Ca-I-Ca-I-Ca-I]^{2+}$  chain supported by two  $\beta$ -diketiminato ligands.<sup>647</sup> The central I–Ca–I' angle is strongly bent (102.64(7)°), whereas the comparable angle around the terminal calcium atoms is nearly linear (173.61(5)°). The average Ca–I bond length (3.166 Å) in **157** does not differ greatly from that in the dimeric complex  $[Ca(\eta^5-CH(CMe(t-Bu)N)_2)(\mu-I)(thf)_2]$  (3.144 Å).<sup>450</sup>



Hydrocarbon-soluble strontium fluoride and chloride compounds of the form  $(DIPP-nacnac)Sr(thf)(\mu-X)_2Sr(thf)_2(DIPP-nacnac)$  **158** were isolated from the reaction of  $(DIPP-nacnac)SrN(SiMe_3)_2(thf)$  with  $Me_3SnF$  and  $(DIPP-nacnac)AlCl(CH_3)$ , respectively.<sup>439</sup> Both the fluoro and chloro derivatives possess central four-membered  $(SrX)_2$  rings (Sr–F = 2.345(1), 2.397(1) Å; Sr–Cl = 2.898(1), 2.954(1) Å), and the metal centers differ in the number of coordinated THF molecules, generating penta- and hexacoordinate arrangements.



**Scheme 7** Formation of the soluble calcium fluoride complex **156**.

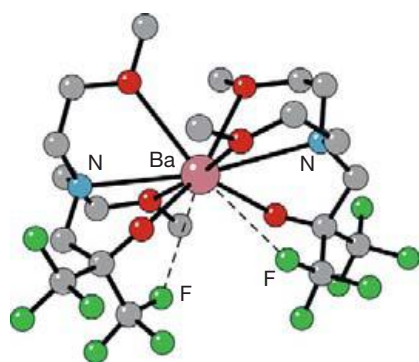
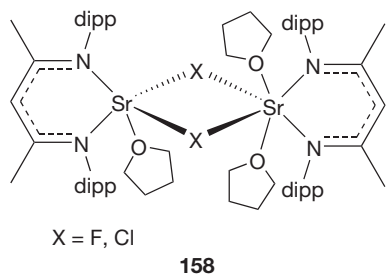


**Figure 76** Structure of  $\text{Ba}(\text{amak})_2$  ( $\text{amak} = [\text{OC}(\text{CF}_3)_2\text{CH}_2\text{N}(\text{CH}_2\text{CH}_2\text{OMe})_2]^-$ ) **159**.



An unusual barium–fluorine interaction is observed in the aminoalkoxide complex  $\text{Ba}(\text{amak})_2$  ( $\text{amak} = [\text{OC}(\text{CF}_3)_2\text{CH}_2\text{N}(\text{CH}_2\text{CH}_2\text{OMe})_2]^-$ ) **159**.<sup>648</sup> The ten-coordinate barium center in **159** bonds to six oxygen and two nitrogen atoms, and displays dative contacts at 3.212(3) and 3.132(2) Å to a fluorine from each amak ligand (Figure 76).

With the use of capillary-wetting techniques,<sup>649</sup>  $\text{Ba}_2$  has been combined with single-walled carbon nanotubes of 1.6 nm in diameter to create a 1D chain of edge-linked coordination polyhedra.<sup>650</sup> The barium centers display five- and

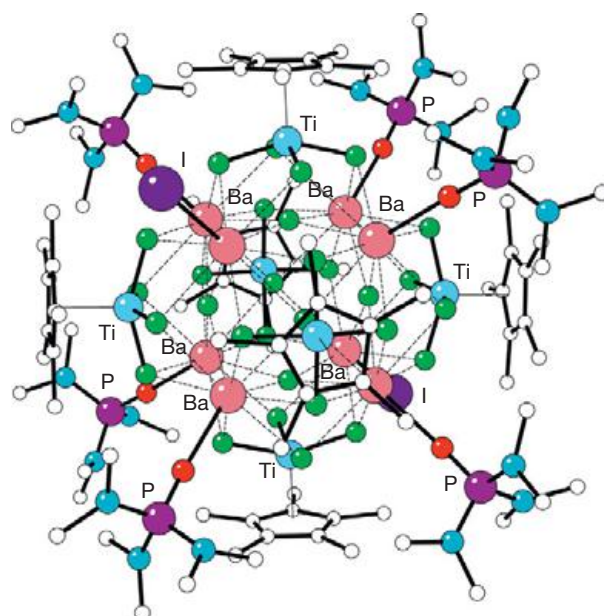
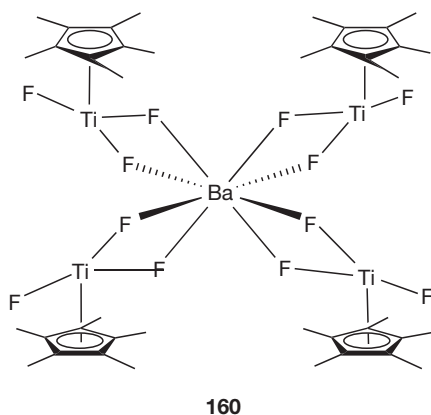


**Figure 77** Structure of  $[\text{Ba}_8\text{Ti}_6\text{F}_{30}\text{I}_2(\text{C}_5\text{Me}_5)_6(\text{hmpa})_6][\text{I}_3]_2$  **161**.

six-coordination along the edges and in the center of the chain, respectively, environments that are unknown in bulk  $\text{BaF}_2$ .

A mixture of  $[\text{Hdmpy}][(\text{C}_5\text{Me}_5)_2\text{Ti}_2\text{F}_7]$  ( $\text{dmpy} = 2,6$ -dimethylpyridine),  $\text{Ba}_2$ , and hmpa will produce the bimetallic barium halide complex  $\text{Ba}[(\text{C}_5\text{Me}_5)_2\text{Ti}_2\text{F}_7]_2(\text{hmpa})$  **160** ( $\text{Ba}-\text{F}_{\text{term}} = 2.664(2) - 2.878(2)$  Å).<sup>651</sup> A solution of **160** cooled to 4 °C deposits crystals of  $[\text{Ba}_8\text{Ti}_6\text{F}_{30}\text{I}_2(\text{C}_5\text{Me}_5)_6(\text{hmpa})_6][\text{I}_3]_2$  **161** after 10 weeks. The latter is constructed around a cube of barium atoms, with each face capped by a  $(\text{C}_5\text{Me}_5)\text{TiF}_4$  fragment; the  $\text{Ba}-\mu\text{-F}$  distances range from 2.764(6) to 2.849(6) Å (Figure 77). Although **160** displays complex equilibria in solution, both it and **161** are resistant to the formation of  $\text{BaF}_2$ .



### 1.37.5 Conclusion

Since the last quarter of the twentieth century, the coordination and organometallic chemistry of the Group 2 elements has gained new-found appreciation in areas as diverse as materials science, catalysis, and biology. Developments have been accelerated by the expanded use of sterically bulky ligands, which are more appropriate to the larger Group 2 cations, and by the recognition that simple electrostatic views of the interaction of these metals with their ligands are no longer adequate.

Accompanying the greater understanding of the fundamental chemistry is an increased range of applications, including uses in molecular absorption, gas storage, and ion exchange. Organoalkaline-earth complexes in particular have expanded from their traditional role in organic synthesis (e.g., the Grignard reagents) to include precursors for chemical vapor deposition and polymerization initiators for polar monomers. The potential for new discoveries and uses with the earth-abundant Group 2 elements appears brighter than ever.

### References

- Emsley, J. *The Elements*, 3rd ed.; Oxford University Press: New York, 1998.
- Voet, D.; Voet, J.G. In *Biochemistry*, Wiley: New York, 2011; pp 901–940.
- Jordan, P.; Fromme, P.; Witt, H. T.; Klukas, O.; Saenger, W.; Krausz, N. *Nature* **2001**, *411*, 909–917.
- De Deckker, P. *Hydrobiologia* **2004**, *517*, 1–13.
- Hemmersbach, R.; Braun, M. *Signal Transduct.* **2006**, *6*, 432–442.
- Greenwood, N. N.; Earnshaw, A. *Chemistry of the Elements*, 2nd ed.; Butterworth-Heinemann: Oxford, 1997.
- Wells, A. F. *Structural Inorganic Chemistry*, 5th ed.; Clarendon Press: Oxford, 1984.
- Corlett, G. K.; Patel, K.; Wheeler, M. D.; Ellis, A. M. *Phys. Chem. Chem. Phys.* **2003**, *5*, 36–40.
- Chan, W.-T.; Hamilton, I. P. *Chem. Phys. Lett.* **1998**, *297*, 217–224.
- Chan, W. T.; Hamilton, I. P. *Chem. Phys. Lett.* **2000**, *316*, 171–175.
- Ketvirtis, A. E.; Simons, J. *J. Am. Chem. Soc.* **2000**, *122*, 369–377.
- Mahadevi, A. S.; Sastry, G. N. *J. Phys. Chem. B* **2010**, *115*, 703–710.
- Zhao, X. L.; Nadeau, M. J.; Garwan, M. A.; Kilius, L. R.; Litherland, A. E. *Nucl. Instrum. Methods Phys. Res., Sect. B* **1994**, *92*, 258–264.
- Thompson, C. A.; Andrews, L. *J. Am. Chem. Soc.* **1996**, *118*, 10242–10249.
- Greene, T. M.; Lanzisera, D. V.; Andrews, L.; Downs, A. J. *J. Am. Chem. Soc.* **1998**, *120*, 6097–6104.
- Tjurina, L. A.; Smirnov, V. V.; Barkovskii, G. B.; Nikolaev, E. N.; Espipov, S. E.; Beletskaya, I. P. *Organometallics* **2001**, *20*, 2449–2450.
- Köppe, R.; Henke, P.; Schnöckel, H. *Angew. Chem., Int. Ed.* **2008**, *47*, 8740–8744.
- Bernath, P. F. *Adv. Photochem.* **1997**, *23*, 1–62.
- Krieck, S.; Yu, L.; Reiher, M.; Westerhausen, M. *Eur. J. Inorg. Chem.* **2010**, *2010*, 197–216.
- Jensen, W. B. *J. Chem. Educ.* **2003**, *80*, 952–961.
- Resa, I.; Carmona, E.; Gutierrez-Puebla, E.; Monge, A. *Science* **2004**, *305*, 1136–1138.
- Griirane, A.; Resa, I.; Rodríguez, A.; Carmona, E.; Alvarez, E.; Gutierrez-Puebla, E.; Monge, A.; Galindo, A.; Del Rio, D.; Andersen, R. A. *J. Am. Chem. Soc.* **2007**, *129*, 693–703.
- Zhu, Z.; Brynda, M.; Wright, R. J.; Fischer, R. C.; Merrill, W. A.; Rivard, E.; Wolf, R.; Fettingner, J. C.; Olmstead, M. M.; Power, P. P. *J. Am. Chem. Soc.* **2007**, *129*, 10847–10857.
- Green, S. P.; Jones, C.; Stasch, A. *Science* **2007**, *318*, 1754–1757.
- Green, S. P.; Jones, C.; Stasch, A. *Angew. Chem., Int. Ed.* **2008**, *47*, 9079–9083.
- Liu, Y.; Li, S.; Yang, X.-J.; Yang, P.; Wu, B. *J. Am. Chem. Soc.* **2009**, *131*, 4210–4211.
- Bonyhady, S. J.; Jones, C.; Nembenna, S.; Stasch, A.; Edwards, A. J.; McIntyre, G. J. *Chem.—Eur. J.* **2010**, *16*, 938–955.
- Velazquez, A.; Fernández, I.; Frenking, G.; Merino, G. *Organometallics* **2007**, *26*, 4731–4736.
- Overgaard, J.; Jones, C.; Stasch, A.; Iversen, B. B. *J. Am. Chem. Soc.* **2009**, *131*, 4208–4209.
- Parkin, G. *Science* **2004**, *305*, 1117–1118.
- Schulz, S. *Chem.—Eur. J.* **2010**, *16*, 6416–6428.
- Buchanan, W. D.; Allis, D. G.; Ruhlandt-Senge, K. *Chem. Commun.* **2010**, *46*, 4449–4465.
- Sarish, S. P.; Nembenna, S.; Nagendran, S.; Roesky, H. W. *Acc. Chem. Res.* **2011**, *44*, 157–170.
- Evans, W. J.; Giarikos, D. G.; Greci, M. A.; Ziller, J. W. *Eur. J. Inorg. Chem.* **2002**, *2002*, 453–456.
- McCormick, M. J.; Moon, K. B.; Jones, S. R.; Hanusa, T. P. *J. Chem. Soc., Chem. Commun.* **1990**, 778–779.
- Wu, T. C.; Xiong, H.; Rieke, R. D. *J. Org. Chem.* **1990**, *55*, 5045–5051.
- Neumüller, B.; Dehnicke, K. Z. *Anorg. Allg. Chem.* **2010**, *636*, 1438–1440.
- Harrowfield, J. M.; Hart, R. J.; Whitaker, C. R. *Aust. J. Chem.* **2001**, *54*, 423–425.
- Liu, Y.; Liu, T.; Xiong, Z.; Hu, J.; Wu, G.; Chen, P.; Wee, A. T. S.; Yang, P.; Murata, K.; Sakata, K. *Eur. J. Inorg. Chem.* **2006**, *2006*, 4368–4373.
- Gowenlock, B. G.; Lindsell, W. E.; Singh, B. J. *Chem. Soc., Dalton Trans.* **1978**, 657–664.
- Engelhardt, L. M.; Junk, P. C.; Raston, C. L.; White, A. H. *J. Chem. Soc., Chem. Commun.* **1988**, 1500–1501.
- Mochida, K.; Takeuchi, H.; Hiraga, Y.; Ogawa, H. *Organometallics* **1987**, *6*, 2293–2297.
- Mochida, K.; Yamanishi, T. *J. Organomet. Chem.* **1987**, *332*, 247–252.
- Dunne, J. P.; Tacke, M.; Selinka, C.; Stalke, D. *Eur. J. Inorg. Chem.* **2003**, 1416–1425.
- Mendoza, O.; Tacke, M. *J. Organomet. Chem.* **2006**, *691*, 1110–1116.
- Deacon, G. B.; Forsyth, C. M.; Junk, P. C. *J. Organomet. Chem.* **2000**, *607*, 112–119.
- Schumann, H.; Gottfriedsen, J.; Glanz, M.; Dechert, S.; Demtschuk, J. *J. Organomet. Chem.* **2001**, *617–618*, 588–600.
- Hwang, I.-C.; Drews, T.; Seppelt, K. *J. Am. Chem. Soc.* **2000**, *122*, 8486–8489.
- Lorenz, V.; Blaurock, S.; Edelman, F. T. *Z. Anorg. Allg. Chem.* **2008**, *634*, 441–444.
- Schumann, H.; Steffens, A.; Hummert, M. *Z. Anorg. Allg. Chem.* **2009**, *635*, 1041–1047.
- O'Brien, A. Y.; Hitzbleck, J.; Torvisco, A.; Deacon, G. B.; Ruhlandt-Senge, K. *Eur. J. Inorg. Chem.* **2008**, *2008*, 172–182.
- Tuulmets, A.; Mikk, M.; Panov, D. *J. Organomet. Chem.* **1996**, *523*, 133–138.
- Tuulmets, A.; Panov, D. *J. Organomet. Chem.* **1999**, *575*, 182–186.
- Tuulmets, A.; Raik, P. *Ultrason. Sonochem.* **1999**, *6*, 85–87.
- Rieke, R. D.; Burns, T. P.; Wehmeyer, R. M.; Kahn, B. E. *ACS Symp. Ser.* **1987**, *333*, 223–245.
- Purdy, A. P.; Berry, A. D.; Holm, R. T.; Fatemi, R. T.; Gaskill, D. K. *Inorg. Chem.* **1989**, *28*, 2799–2803.
- Haas, I.; Gedanken, A. *Chem. Commun.* **2008**, 1795–1797.
- Caulton, K. G.; Chisholm, M. H.; Drake, S. R.; Folting, K. *J. Chem. Soc., Chem. Commun.* **1990**, 1349–1351.
- Hitzbleck, J.; Deacon, G. B.; Ruhlandt-Senge, K. *Angew. Chem., Int. Ed.* **2004**, *43*, 5218–5220.
- Zuniga, M. F.; Deacon, G. B.; Ruhlandt-Senge, K. *Chem.—Eur. J.* **2007**, *13*, 1921–1928.
- Cole, M. L.; Deacon, G. B.; Forsyth, C. M.; Junk, P. C.; Proctor, K. M.; Scott, J. L.; Strauss, C. R. *Polyhedron* **2007**, *26*, 244–249.

62. Bradley, D. C.; Hursthouse, M. B.; Ibrahim, A. A.; Abdul Malik, K. M.; Motevalli, M.; Mösele, R.; Powell, H. *Polyhedron* **1990**, *9*, 2959–2964.
63. Deacon, G. B.; Forsyth, C. M.; Jaroschik, F.; Junk, P. C.; Kay, D. L.; Maschmeyer, T.; Masters, A. F.; Wang, J.; Field, L. D. *Organometallics* **2008**, *27*, 4772–4778.
64. Hitzbleck, J.; Deacon, G. B.; Ruhlandt-Senge, K. *Eur. J. Inorg. Chem.* **2007**, 592–601.
65. Westerhausen, M. *Inorg. Chem.* **1991**, *30*, 96–101.
66. Fischer, R.; Görls, H.; Westerhausen, M. *Organometallics* **2007**, *26*, 3269–3271.
67. Langer, J.; Kriech, S.; Görls, H.; Westerhausen, M. *Angew. Chem., Int. Ed.* **2009**, *48*, 5741–5744.
68. Himmel, D.; Krossing, I. Z. *Anorg. Allg. Chem.* **2006**, *632*, 2021–2023.
69. Sockwell, S. C.; Hanusa, T. P.; Huffman, J. C. *J. Am. Chem. Soc.* **1992**, *114*, 3393–3399.
70. Frankland, A. D.; Lappert, M. F. *J. Chem. Soc., Dalton Trans.* **1996**, 4151–4152.
71. Johns, A. M.; Chmely, S. C.; Hanusa, T. P. *Inorg. Chem.* **2009**, *48*, 1380–1384.
72. Glock, C.; Görls, H.; Westerhausen, M. *Inorg. Chem.* **2009**, *48*, 394–399.
73. Burke, D. J.; Alexander, E. K.; Hanusa, T. P. *Organometallics* **1994**, *13*, 2773–2786.
74. Westerhausen, M. *Coord. Chem. Rev.* **1998**, *176*, 157–210.
75. Fraser, R. R.; Mansour, T. S.; Savard, S. J. *Org. Chem.* **1985**, *50*, 3232–3234.
76. Tanner, P. S.; Burke, D. J.; Hanusa, T. P. *Polyhedron* **1995**, *14*, 331–333.
77. Burns, C. J.; Andersen, R. A. *J. Organomet. Chem.* **1987**, *325*, 31–37.
78. Chmely, S. C.; Hanusa, T. P.; Brennessel, W. W. *Angew. Chem., Int. Ed.* **2010**, *49*, 5870–5874.
79. Brady, E. D.; Chmely, S. C.; Jayaratne, K. C.; Hanusa, T. P.; Young, V. G., Jr. *Organometallics* **2008**, *27*, 1612–1616.
80. Hernandez-Sanchez, B. A.; Boyle, T. J.; Baros, C. M.; Brewer, L. N.; Headley, T. J.; Tallant, D. R.; Rodriguez, M. A.; Tuttle, B. A. *Chem. Mater.* **2007**, *19*, 1459–1471.
81. Verma, A.; Guino-o, M.; Gillett-Kunnath, M.; Teng, W.; Ruhlandt-Senge, K. Z. *Anorg. Allg. Chem.* **2009**, *635*, 903–913.
82. Datta, S.; Roesky, P. W.; Blechert, S. *Organometallics* **2007**, *26*, 4392–4394.
83. Wendell, L. T.; Bender, J.; He, X.; Noll, B. C.; Henderson, K. W. *Organometallics* **2006**, *25*, 4953–4959.
84. Barrett, A. G. M.; Crimmin, M. R.; Hill, M. S.; Kociok-Köhn, G.; MacDougall, D. J.; Mahon, M. F.; Procopiou, P. A. *Organometallics* **2008**, *27*, 3939–3946.
85. Williams, R. A.; Hanusa, T. P.; Huffman, J. C. *Organometallics* **1990**, *9*, 1128–1134.
86. Lachs, J. R.; Barrett, A. G. M.; Crimmin, M. R.; Kociok-Köhn, G.; Hill, M. S.; Mahon, M. F.; Procopiou, P. A. *Eur. J. Inorg. Chem.* **2008**, *26*, 4173–4179.
87. Barrett, A. G. M.; Boorman, T. C.; Crimmin, M. R.; Hill, M. S.; Kociok-Köhn, G.; Procopiou, P. *Chem. Commun.* **2008**, 5206–5208.
88. Chadwick, S.; English, U.; Ruhlandt-Senge, K. *Angew. Chem., Int. Ed.* **1998**, *37*, 3007–3009.
89. Bradley, D. C.; Chudzynska, H.; Hammond, M. E.; Hursthouse, M. B.; Motevalli, M.; Ruowen, W. *Polyhedron* **1992**, *11*, 375–379.
90. Hanawalt, E. M.; Farkas, J., Jr.; Richey, H. G., Jr. *Organometallics* **2004**, *23*, 416–422.
91. Zechmann, C. A.; Boyle, T. J.; Rodriguez, M. A.; Kemp, R. A. *Polyhedron* **2000**, *19*, 2557–2564.
92. Zuniga, M. F.; Kreutzer, J.; Teng, W.; Ruhlandt-Senge, K. *Inorg. Chem.* **2007**, *46*, 10400–10409.
93. Chadwick, S.; English, U.; Senge, M. O.; Noll, B. C.; Ruhlandt-Senge, K. *Organometallics* **1998**, *17*, 3077–3086.
94. Chadwick, S.; English, U.; Ruhlandt-Senge, K. *Inorg. Chem.* **1999**, *38*, 6289–6293.
95. Pedrares, A. S.; Teng, W.; Ruhlandt-Senge, K. *Chem.—Eur. J.* **2003**, *9*, 2019–2024.
96. Wannagat, U.; Autzen, H.; Kuckertz, H.; Wismar, H.-J. *Z. Anorg. Allg. Chem.* **1972**, *394*, 254–262.
97. Clegg, W.; Horsburgh, L.; Mulvey, R. E.; Ross, M. J.; Rowlings, R. B.; Wilson, V. *Polyhedron* **1998**, *17*, 1923–1930.
98. Forbes, G. C.; Kennedy, A. R.; Mulvey, R. E.; Rodger, P. J. A.; Rowlings, R. B. *J. Chem. Soc., Dalton Trans.* **2001**, 1477–1484.
99. Kennedy, A. R.; Mulvey, R. E.; Schulte, J. H. *Acta Crystallogr., Sect. C* **2001**, *57*, 1288–1289.
100. Drummond, A. M.; Gibson, L. T.; Kennedy, A. R.; Mulvey, R. E.; O'Hara, C. T.; Rowlings, R. B.; Weightman, T. *Angew. Chem., Int. Ed.* **2002**, *41*, 2382–2384.
101. Hevia, E.; Kenley, F. R.; Kennedy, A. R.; Mulvey, R. E.; Rowlings, R. B. *Eur. J. Inorg. Chem.* **2003**, 3347–3353.
102. Olmstead, M. M.; Grigsby, W. J.; Chacon, D. R.; Hascall, T.; Power, P. P. *Inorg. Chim. Acta* **1996**, *251*, 273–284.
103. Lian, B.; Thomas, C. M.; Casagrande, O. L., Jr.; Roisnel, T.; Carpentier, J.-F. *Polyhedron* **2007**, *26*, 3817–3824.
104. Zechmann, C. A.; Boyle, T. J.; Rodriguez, M. A.; Kemp, R. A. *Inorg. Chim. Acta* **2001**, *319*, 137–146.
105. Andrikopoulos, P. C.; Armstrong, D. R.; Kennedy, A. R.; Mulvey, R. E.; O'Hara, C. T.; Rowlings, R. B. *Eur. J. Inorg. Chem.* **2003**, 3354–3362.
106. Sanchez-Barba, L. F.; Hughes, D. L.; Humphrey, S. M.; Boehmann, M. *Organometallics* **2006**, *25*, 1012–1020.
107. Henderson, K. W.; Kennedy, A. R.; Mulvey, R. E.; O'Hara, C. T.; Rowlings, R. B. *Chem. Commun.* **2001**, 1678–1679.
108. Drewette, K. J.; Henderson, K. W.; Kennedy, A. R.; Mulvey, R. E.; O'Hara, C. T.; Rowlings, R. B. *Chem. Commun.* **2002**, 1176–1177.
109. Kennedy, A. R.; MacLellan, J. G.; Mulvey, R. E. *Acta Crystallogr., Sect. C* **2003**, *59*, m302–m303.
110. Hevia, E.; Gallagher, D. J.; Kennedy, A. R.; Mulvey, R. E.; O'Hara, C. T.; Talmard, C. *Chem. Commun.* **2004**, 2422–2423.
111. Harder, S.; Mueller, S.; Huebner, E. *Organometallics* **2004**, *23*, 178–183.
112. Alexander, J. S.; Ruhlandt-Senge, K. *Angew. Chem., Int. Ed.* **2001**, *40*, 2658–2660.
113. Alexander, J. S.; Ruhlandt-Senge, K.; Hope, H. *Organometallics* **2003**, *22*, 4933–4937.
114. Alexander, J. S.; Ruhlandt-Senge, K. *Chem.—Eur. J.* **2004**, *10*, 1274–1280.
115. Hevia, E.; Honeyman, G. W.; Kennedy, A. R.; Mulvey, R. E.; Sherrington, D. C. *Angew. Chem., Int. Ed.* **2005**, *44*, 68–72.
116. Andrikopoulos, P. C.; Armstrong, D. R.; Graham, D. V.; Hevia, E.; Kennedy, A. R.; Mulvey, R. E.; O'Hara, C. T.; Talmard, C. *Angew. Chem., Int. Ed.* **2005**, *44*, 3459–3462.
117. Andrikopoulos, P. C.; Armstrong, D. R.; Hevia, E.; Kennedy, A. R.; Mulvey, R. E.; O'Hara, C. T. *Chem. Commun.* **2005**, 1131–1133.
118. Gillett-Kunnath, M. M.; MacLellan, J. G.; Forsyth, C. M.; Andrews, P. C.; Deacon, G. B.; Ruhlandt-Senge, K. *Chem. Commun.* **2008**, 4490–4492.
119. Verma, A.; Weismann, D.; Powers, A.R.; Gillett-Kunnath, M.M.; Sitzmann, H.; Ruhlandt-Senge, K. In 239th National Meeting of the American Chemical Society, San Francisco, CA, March 21–25, 2010, American Chemical Society, Washington, DC, 2010 INOR-776.
120. Veith, M.; Kaefer, D.; Huch, V. *Angew. Chem.* **1986**, *98*, 367–368.
121. Bidell, W.; Shklover, V.; Berke, H. *Inorg. Chem.* **1992**, *31*, 5561–5571.
122. Vaartstra, B. A.; Huffman, J. C.; Streib, W. E.; Caulton, K. G. *Inorg. Chem.* **1991**, *30*, 3068–3072.
123. Shannon, R. D. *Acta Crystallogr., Sect. A* **1976**, *32*, 751–767.
124. Bock, C. W.; Glusker, J. P. *Inorg. Chem.* **1993**, *32*, 1242–1250.
125. Bock, C. W.; Kaufman, A.; Glusker, J. P. *Inorg. Chem.* **1994**, *33*, 419–427.
126. Katz, A. K.; Glusker, J. P.; Beebe, S. A.; Bock, C. W. *J. Am. Chem. Soc.* **1996**, *118*, 5752–5763.
127. Vaartstra, B. A.; Huffman, J. C.; Streib, W. E.; Caulton, K. G. *Inorg. Chem.* **1991**, *30*, 121–125.
128. Kennedy, A. R.; Mulvey, R. E.; Rowlings, R. B. *J. Am. Chem. Soc.* **1998**, *120*, 7816–7824.
129. Murugavel, R.; Baheti, K.; Anantharaman, G. *Inorg. Chem.* **2001**, *40*, 6870–6878.
130. Huang, R. H.; Huang, S. Z.; Dye, J. L. *J. Coord. Chem.* **1998**, *46*, 13–31.
131. Dye, J. L. *J. Phys. Chem.* **1984**, *88*, 3842–3846.
132. DeBacker, M. G.; Mkadmi, E. B.; Sauvage, F. X.; Lelieur, J.-P.; Wagner, M. J.; Concepcion, R.; Kim, J.; McMills, L. E. H.; Dye, J. L. *J. Am. Chem. Soc.* **1996**, *118*, 1997–2003.
133. Kim, J.; Ichimura, A. S.; Huang, R. H.; Redko, M.; Phillips, R. C.; Jackson, J. E.; Dye, J. L. *J. Am. Chem. Soc.* **1999**, *121*, 10666–10667.
134. Redko, M. Y.; Vlassa, M.; Jackson, J. E.; Misiolek, A. W.; Huang, R. H.; Dye, J. L. *J. Am. Chem. Soc.* **2002**, *124*, 5928–5929.
135. Wagner, M. J.; Dye, J. L. *Compr. Supramol. Chem.* **1996**, *1*, 477–510.
136. Dye, J. L. *Macromol. Symp.* **1998**, *134*, 29–39.
137. Dye, J. L. *Inorg. Chem.* **1997**, *36*, 3816–3826.
138. Redko, M. Y.; Huang, R. H.; Jackson, J. E.; Harrison, J. F.; Dye, J. L. *J. Am. Chem. Soc.* **2003**, *125*, 2259–2263.
139. Harder, S. *Angew. Chem., Int. Ed.* **2004**, *43*, 2714–2718.
140. Kaupp, M. *Angew. Chem., Int. Ed.* **2001**, *40*, 3535–3565.
141. Wharton, L.; Berg, R. A.; Klemperer, W. J. *J. Chem. Phys.* **1963**, *39*, 2023–2031.
142. Kasparov, V. V.; Ezhov, Y. S.; Rambidi, N. G. *J. Struct. Chem.* **1979**, *20*, 260–266.
143. Guido, M.; Gigli, G. *J. Chem. Phys.* **1976**, *65*, 1397–1402.
144. Evans, W. J.; Hughes, L. A.; Hanusa, T. P.; Doedens, R. J. *Organometallics* **1986**, *5*, 1285–1291.
145. Andersen, R. A.; Blom, R.; Burns, C. J.; Volden, H. V. *J. Chem. Soc., Chem. Commun.* **1987**, 768–769.

146. Kwon, O.; McKee, M. L. In *Computational Organometallic Chemistry*; Cundari, T. R., Ed.; Marcel Dekker: New York, 2001.
147. Rayón, V. M.; Frenking, G. *Chem.—Eur. J.* **2002**, *8*, 4693–4707.
148. Eaborn, C.; Hawkes, S. A.; Hitchcock, P. B.; Smith, J. D. *Chem. Commun.* **1997**, 1961–1962.
149. Eaborn, C.; Hitchcock, P. B.; Izod, K.; Smith, J. D. *J. Am. Chem. Soc.* **1994**, *116*, 12071–12072.
150. von Szentpály, L.; Schwerdtfeger, P. *Chem. Phys. Lett.* **1990**, *170*, 555–560.
151. Kaupp, M.; Schleyer, P. V. R.; Stoll, H.; Preuss, H. *J. Am. Chem. Soc.* **1991**, *113*, 6012–6020.
152. Kaupp, M.; Schleyer, P. V. R.; Stoll, H.; Preuss, H. *J. Chem. Phys.* **1991**, *94*, 1360–1366.
153. Kaupp, M.; Schleyer, P. V. R. *J. Am. Chem. Soc.* **1992**, *114*, 491–497.
154. Kaupp, M.; Schleyer, P. V. R. *J. Phys. Chem.* **1992**, *96*, 7316–7323.
155. Seijo, L.; Barandiarán, Z.; Huzinaga, S. *J. Chem. Phys.* **1991**, *113*, 3762–3773.
156. Hassett, D. M.; Marsden, C. J. *Chem. Commun.* **1990**, 667–669.
157. Zimmermann, U.; Malinowski, N.; Näher, U.; Frank, S.; Martin, T. P. *Phys. Rev. Lett.* **1994**, *72*, 3542–3545.
158. Yoon, M.; Yang, S.; Hicke, C.; Wang, E.; Geohegan, D.; Zhang, Z. *Phys. Rev. Lett.* **2008**, *100*, 206806.
159. Wang, Q.; Sun, Q.; Jena, P.; Kawazoe, Y. *J. Chem. Theory Comput.* **2009**, *5*, 374–379.
160. Janczyk, A.; Lichtenberger, D. L.; Ziurys, L. M. *J. Am. Chem. Soc.* **2006**, *128*, 1109–1118.
161. Moriarty, J. A. *Phys. Rev. B* **1986**, *34*, 6738–6745.
162. Zeng, W. S.; Heine, V.; Jepsen, O. *J. Phys. Condens. Matter* **1997**, *9*, 3489.
163. Gagliardi, L.; Pyykkö, P. *Theor. Chem. Acc.* **2003**, *110*, 205–210.
164. Pyykkö, P. *J. Chem. Soc., Faraday Trans. 2* **1979**, *75*, 1256–1276.
165. Lee, E. P. F.; Soldan, P.; Wright, T. G. *Inorg. Chem.* **2001**, *40*, 5979–5984.
166. Ma, J. C.; Dougherty, D. A. *Chem. Rev.* **1997**, *97*, 1303–1324.
167. Feller, D.; Dixon, D. A.; Nicholas, J. B. *J. Phys. Chem. A* **2000**, *104*, 11414–11419.
168. Nakamura, R. L.; Anderson, J. A.; Gaber, R. F. *J. Biol. Chem.* **1997**, *272*, 1011–1018.
169. Dang, Q. D.; Guinto, E. R.; Di Cera, E. *Nat. Biotechnol.* **1997**, *15*, 146–149.
170. Santarelli, V. P.; Eastwood, A. L.; Dougherty, D. A.; Ahern, C. A.; Horn, R. *Biophys. J.* **2007**, *93*, 2341–2349.
171. Chmely, S. C.; Carlson, C. N.; Hanusa, T. P.; Rheingold, A. L. *J. Am. Chem. Soc.* **2009**, *131*, 6344–6345.
172. Novitschi, G.; Costes, J.-P.; Ciornea, V.; Shova, S.; Filippova, I.; Simonov, Y. A.; Gulea, A. *Eur. J. Inorg. Chem.* **2005**, 2005, 929–937.
173. Biesaga, M.; Pyrzyńska, K.; Trojanowicz, M. *Talanta* **2000**, *51*, 209–224.
174. Chandra, T.; Kraft, B. J.; Huffman, J. C.; Zaleski, J. M. *Inorg. Chem.* **2003**, *42*, 5158–5172.
175. Miura, M.; Majumder, S. A.; Hobbs, J. D.; Renner, M. W.; Furenli, L. R.; Shelnut, J. A. *Inorg. Chem.* **1994**, *33*, 6078–6085.
176. Parusel, A. B. J.; Wondimagegn, T.; Ghosh, A. *J. Am. Chem. Soc.* **2000**, *122*, 6371–6374.
177. Wu, G.; Wong, A.; Wang, S. *Can. J. Chem.* **2003**, *81*, 275–283.
178. Oliveri, C. G.; Heo, J.; Nguyen, S. T.; Mirkin, C. A.; Wawrzak, Z. *Inorg. Chem.* **2007**, *46*, 7716–7718.
179. Bonomo, L.; Lehaire, M.-L.; Solari, E.; Scopelliti, R.; Floriani, C. *Angew. Chem., Int. Ed.* **2001**, *40*, 771–774.
180. Bonomo, L.; Solari, E.; Scopelliti, R.; Floriani, C. *Chem.—Eur. J.* **2001**, *7*, 1322–1332.
181. Rajesh, K. R.; Menon, C. S. *J. Non-Cryst. Solids* **2005**, *351*, 2414–2420.
182. Mizuguchi, J. *J. Phys. Chem. A* **2001**, *105*, 1121–1124.
183. Janczak, J.; Kubiak, R. *Polyhedron* **2001**, *20*, 2901–2909.
184. Janczak, J.; Kubiak, R. *Polyhedron* **2002**, *21*, 265–274.
185. Janczak, J.; Marina, I. Y. *Polyhedron* **2003**, *22*, 1167–1181.
186. Donzello, M. P.; Ercolani, C.; Kadish, K. M.; Ricciardi, G.; Rosa, A.; Stuzhin, P. A. *Inorg. Chem.* **2007**, *46*, 4145–4157.
187. Kubiak, R.; Waskowska, A.; Sledz, M.; Jezierski, A. *Inorg. Chim. Acta* **2006**, *359*, 1344–1350.
188. Kubiak, R.; Janczak, J.; Sledz, M.; Bukowska, E. *Polyhedron* **2007**, *26*, 4179–4186.
189. Lehn, J.-M.; Ball, P. In *The New Chemistry*; Hall, N., Ed.; Cambridge University Press, 2000; pp 300–351.
190. Puchta, R.; Van, E. R. Z. *Anorg. Allg. Chem.* **2008**, *634*, 735–739.
191. Neumueller, B.; Dehnicke, K.; Puchta, R. Z. *Anorg. Allg. Chem.* **2008**, *634*, 1473–1476.
192. Putcha, R.; Kolbig, R.; Weller, F.; Neumuller, B.; Massa, W.; Dehnicke, K. Z. *Anorg. Allg. Chem.* **2010**, *636*, 2364–2371.
193. Junk, P. C.; Louis, L. M.; Smith, M. K. Z. *Anorg. Allg. Chem.* **2002**, *628*, 1196–1209.
194. Junk, P. C.; Steed, J. W. *J. Coord. Chem.* **2007**, *60*, 1017–1028.
195. Neumueller, B.; Dehnicke, K. Z. *Anorg. Allg. Chem.* **2006**, *632*, 1681–1686.
196. Pajerski, A. D.; Squiller, E. P.; Parvez, M.; Whittle, R. R.; Richey, H. G., Jr. *Organometallics* **2005**, *24*, 809–814.
197. Akutagawa, T.; Takamatsu, N.; Shitagami, K.; Hasegawa, T.; Nakamura, T.; Inabe, T.; Fujita, W.; Awaga, K. *J. Mater. Chem.* **2001**, *11*, 2118–2124.
198. Brown, M. D.; Davis, M. F.; Dyke, J. M.; Ferrante, F.; Levason, W.; Ogden, J. S.; Webster, M. *Chem.—Eur. J.* **2008**, *14*, 2615–2624.
199. Fichtel, K.; Behrens, U. Z. *Anorg. Allg. Chem.* **2005**, *631*, 2508–2516.
200. Fichtel, K.; Höxter, S.; Behrens, U. Z. *Anorg. Allg. Chem.* **2006**, *632*, 2003–2009.
201. Fichtel, K.; Hofmann, K.; Behrens, U. *Organometallics* **2004**, *23*, 4166–4168.
202. Englisch, U.; Ruhlandt-Senge, K.; Uhlrig, F. *J. Organomet. Chem.* **2000**, *613*, 139–147.
203. Englisch, U.; Ruhlandt-Senge, K. Z. *Anorg. Allg. Chem.* **2001**, *627*, 851–856.
204. Park, I.-H.; Park, K.-M.; Lee, S. S. *Dalton Trans.* **2010**, *39*, 9696–9704.
205. Pochekutova, T. S.; Khamylov, V. K.; Kurskii, Y. A.; Fukin, G. K.; Petrov, B. I. *Polyhedron* **2010**, *29*, 1381–1386.
206. Pochini, A.; Ungaro, R. *Compr. Supramol. Chem.* **1996**, *2*, 103–142.
207. Gutsche, C. D. In *Calixarenes 2001*; Asfari, M.-Z., Böhmer, V., Harrowfield, J., Vicens, J., Eds.; Kluwer: Dordrecht, 2001; pp 1–25.
208. Gutsche, C. D. *ACS Symp. Ser.* **2000**, *757*, 2–9.
209. Milbradt, R.; Böhmer, V. In *Calixarenes 2001*; Asfari, M.-Z., Böhmer, V., Harrowfield, J., Vicens, J., Eds.; Kluwer: Dordrecht, 2001; pp 663–676.
210. Ludwig, R. *Fresenius J. Anal. Chem.* **2000**, *367*, 103–128.
211. Kolarik, Z. *Miner. Process Extract Metall. Rev.* **2000**, *21*, 89–141.
212. Wipff, G. In *Calixarenes 2001*; Asfari, M.-Z., Böhmer, V., Harrowfield, J., Vicens, J., Eds.; Kluwer: Dordrecht, 2001; pp 312–333.
213. Hayashita, T.; Teramae, N.; Kuboyama, T.; Nakamura, S.; Yamamoto, H.; Nakamura, H. *J. Inclusion Phenom. Mol. Recognit. Chem.* **1998**, *32*, 251–265.
214. Diamond, D.; Nolan, K. *Anal. Chem.* **2001**, *73*, 22A–29A.
215. Dakanale, E.; Levi, S.; Rosler, S.; Auge, J.; Hartmann, J.; Henning, B. *GIT Lab. J.* **1998**, *2*, 118–121.
216. Cacciopaglia, R.; Mandolini, L. In *Calixarenes in Action*; Mandolini, L., Ungaro, R., Eds.; Imperial College Press: London, 2000; pp 241–264.
217. Steyer, S.; Jeunesse, C.; Armspach, D.; Matt, D.; Harrowfield, J. In *Calixarenes 2001*; Asfari, M.-Z., Böhmer, V., Harrowfield, J., Vicens, J., Eds.; Kluwer: Dordrecht, 2001; pp 513–535.
218. Guillemot, G.; Solari, E.; Rizzoli, C.; Floriani, C. *Chem.—Eur. J.* **2002**, *8*, 2072–2080.
219. Chen, X.; Ji, M.; Fisher, D. R.; Wai, C. M. *Inorg. Chem.* **1999**, *38*, 5449–5452.
220. Gottfriedsen, J.; Blaurock, S. Z. *Anorg. Allg. Chem.* **2005**, *631*, 3037–3039.
221. Spielmann, J.; Buch, F.; Harder, S. *Angew. Chem., Int. Ed.* **2008**, *47*, 9434–9438.
222. Eigen, N.; Keller, C.; Dornheim, M.; Klassen, T.; Bormann, R. *Scr. Mater.* **2007**, *56*, 847–851.
223. Harder, S.; Brettar, J. *Angew. Chem., Int. Ed.* **2006**, *45*, 3474–3478.
224. Spielmann, J.; Harder, S. *Chem.—Eur. J.* **2007**, *13*, 8928–8938.
225. Spielmann, J.; Jansen, G.; Bandmann, H.; Harder, S. *Angew. Chem., Int. Ed.* **2008**, *47*, 6290–6295.
226. Spielmann, J.; Harder, S. *J. Am. Chem. Soc.* **2009**, *131*, 5064–5065.
227. Spielmann, J.; Piesik, D. F. J.; Harder, S. *Chem.—Eur. J.* **2010**, *16*, 8307–8318.
228. Konoplev, V. N.; Bakulina, V. M. *Izv. Akad. SSSR, Ser. Khim.* **1971**, 159–161.
229. Černý, R.; Filinchuk, Y.; Hagemann, H.; Yvon, K. *Angew. Chem., Int. Ed.* **2007**, *46*, 5765–5767.
230. Zanella, P.; Crociani, L.; Masciocchi, N.; Giunchi, G. *Inorg. Chem.* **2007**, *46*, 9039–9041.
231. Bremer, M.; Nöth, H.; Warchhold, M. *Eur. J. Inorg. Chem.* **2003**, *2003*, 111–119.
232. Fichtner, M.; Frommen, C.; Fuhr, O. *Inorg. Chem.* **2005**, *44*, 3479–3484.
233. Nöth, H.; Schmidt, M.; Treit, A. *Chem. Ber.* **1995**, *128*, 999–1006.
234. Fichtner, M.; Fuhr, O. *J. Alloys Compd.* **2002**, *345*, 286–296.
235. Soloveichik, G. L.; Andrus, M.; Lobkovsky, E. B. *Inorg. Chem.* **2007**, *46*, 3790–3791.
236. Soloveichik, G.; Her, J.-H.; Stephens, P. W.; Gao, Y.; Rijssenbeek, J.; Andrus, M.; Zhao, J. C. *Inorg. Chem.* **2008**, *47*, 4290–4298.
237. Chua, Y. S.; Wu, G.; Xiong, Z.; Karkamkar, A.; Guo, J.; Jian, M.; Wong, M. W.; Autrey, T.; Chen, P. *Chem. Commun.* **2010**, *46*, 5752–5754.
238. Kim, D. Y.; Yang, Y.; Abelson, J. R.; Girolami, G. S. *Inorg. Chem.* **2007**, *46*, 9060–9066.
239. Liptrot, D. J.; Hill, M. S.; Mahon, M. F.; MacDougall, D. J. *Chem.—Eur. J.* **2010**, *16*, 8508–8515.
240. Barrett, A. G. M.; Crimmin, M. R.; Hill, M. S.; Hitchcock, P. B.; Procopiou, P. A. *Organometallics* **2007**, *26*, 4076–4079.

241. Pillai, S. S.; Jana, A.; Roesky, H. W.; Schulz, T.; John, M.; Stalke, D. *Inorg. Chem.* **2010**, *49*, 3816–3820.
242. Chisholm, M. H.; Ellerts, N. W.; Huffman, J. C.; Iyer, S. S.; Pacold, M.; Phomphrai, K. *J. Am. Chem. Soc.* **2000**, *122*, 11845–11854.
243. Chisholm, M. H.; Gallucci, J.; Phomphrai, K. *Chem. Commun.* **2003**, 48–49.
244. Chisholm, M. H.; Gallucci, J. C.; Phomphrai, K. *Inorg. Chem.* **2004**, *43*, 6717–6725.
245. Chisholm, M. H.; Gallucci, J. C.; Yaman, G. *Dalton Trans.* **2009**, 368–374.
246. Chisholm, M. H.; Gallucci, J. C.; Yaman, G.; Young, T. *Chem. Commun.* **2009**, 1828–1830.
247. Saly, M. J.; Heeg, M. J.; Winter, C. H. *Inorg. Chem.* **2009**, *48*, 5303–5312.
248. Saly, M. J.; Winter, C. H. *Organometallics* **2010**, *29*, 5472–5480.
249. Beckmann, E. *Ber. Dtsch. Chem. Ges.* **1905**, *38*, 904–906.
250. Gilman, H.; Schulze, F. *J. Am. Chem. Soc.* **1926**, *48*, 2463–2467.
251. Gilman, H.; Haubein, A. H.; O'Donnell, G.; Woods, L. *J. Am. Chem. Soc.* **1943**, *65*, 268–270.
252. Gilman, H.; Woods, L. *J. Am. Chem. Soc.* **1945**, *67*, 520–522.
253. Ziegler, K.; Froitzheim-Kühlhorn, H.; Häfner, H. *Chem. Ber.* **1956**, *89*, 434–443.
254. Fischer, E. O.; Stölzle, G. *Chem. Ber.* **1961**, *94*, 2187–2193.
255. Alexander, J. S.; Ruhlandt-Senge, K. *Eur. J. Inorg. Chem.* **2002**, 2761–2774.
256. Hanusa, T. P. *Chem. Rev.* **1993**, *93*, 1023–1036.
257. Hanusa, T. P. *Organometallics* **2002**, *21*, 2559–2571.
258. Hanusa, T. P. *Coord. Chem. Rev.* **2000**, *210*, 329–367.
259. Westerhausen, M. *Coord. Chem. Rev.* **2008**, *252*, 1516–1531.
260. Matthews, J. S.; Rees, W. S., Jr. *Adv. Inorg. Chem.* **2000**, *50*, 173–192.
261. Wojtczak, W. A.; Fleig, P. F.; Hampden-Smith, M. J. *Adv. Organomet. Chem.* **1996**, *40*, 215–340.
262. Molander, G. A.; Schumann, H.; Demtschuk, J. *Organometallics* **1996**, *15*, 3817–3824.
263. Schumann, H.; Schutte, S.; Kroth, H.-J.; Lentz, D. *Angew. Chem., Int. Ed.* **2004**, *43*, 6208–6211.
264. Wiecko, M.; Eidamshaus, C.; Koppe, R.; Roesky, P. W. *Dalton Trans.* **2008**, 4837–4839.
265. Adasch, V.; Hess, K.-U.; Ludwig, T.; Vojteer, N.; Hillebrecht, H. *Chem.—Eur. J.* **2007**, *13*, 3450–3458.
266. Hofmann, K.; Rocquefelte, X.; Halet, J.-F.; Bähz, C.; Albert, B. *Angew. Chem., Int. Ed.* **2008**, *47*, 2301–2303.
267. Scott, B. L.; McCleskey, T. M.; Chaudhary, A.; Hong-Geller, E.; Gnanakaran, S. *Chem. Commun.* **2008**, 2837–2847.
268. Coates, G. E.; Morgan, G. L. In: Stone, F. G. A., West, R., Eds.; *Advances in Organometallic Chemistry* Academic Press: New York, 1970; vol. 9, pp 195–257.
269. Plieger, P. G.; John, K. D.; Keizer, T. S.; McCleskey, T. M.; Burrell, A. K.; Martin, R. L. *J. Am. Chem. Soc.* **2004**, *126*, 14651–14658.
270. Hanusa, T. P. *Polyhedron* **1990**, *9*, 1345–1362.
271. Westerhausen, M. *Z. Anorg. Allg. Chem.* **2009**, *635*, 13–32.
272. Gottfriedsen, J.; Blaurock, S. *Organometallics* **2006**, *25*, 3784–3786.
273. Niemeyer, M.; Power, P. P. *Inorg. Chem.* **1997**, *36*, 4688–4696.
274. Clyburne, J. A. C.; McMullen, N. *Coord. Chem. Rev.* **2000**, *210*, 73–99.
275. Al-Juaid, S. S.; Eaborn, C.; Hitchcock, P. B.; Kundu, K.; McGeary, C. A.; Smith, J. D. *J. Organomet. Chem.* **1994**, *480*, 199–203.
276. Crimmin, M. R.; Barrett, A. G. M.; Hill, M. S.; MacDougall, D. J.; Mahon, M. F.; Procopiou, P. A. *Dalton Trans.* **2009**, 9715–9717.
277. Eaborn, C.; Smith, J. D. *J. Am. Chem. Soc., Dalton Trans.* **2001**, 1541–1552.
278. Wiegand, G.; Thiele, K. H. *Z. Anorg. Allg. Chem.* **1974**, *405*, 101–108.
279. Bailey, P. J.; Liddle, S. T.; Morrison, C. A.; Parsons, S. *Angew. Chem., Int. Ed.* **2001**, *40*, 4463–4466.
280. Lichtenberg, C.; Jochmann, P.; Spaniol, T. P.; Okuda, J. *Angew. Chem., Int. Ed.* **2011**, *50*, 5753–5756.
281. Jochmann, P.; Dols, T. S.; Spaniol, T. P.; Perrin, L.; Maron, L.; Okuda, J. *Angew. Chem., Int. Ed.* **2009**, *48*, 5715–5719.
282. Jochmann, P.; Dols, T. S.; Spaniol, T. P.; Perrin, L.; Maron, L.; Okuda, J. *Angew. Chem., Int. Ed.* **2010**, *49*, 7795–7798.
283. Harvey, M. J.; Hanusa, T. P.; Young, V. G., Jr. *Angew. Chem., Int. Ed.* **1999**, *38*, 217–219.
284. Quisenberry, K. T.; White, R. E.; Hanusa, T. P.; Brennessel, W. W. *New J. Chem.* **2010**, *34*, 1579–1584.
285. Jochmann, P.; Spaniol, T. P.; Chmely, S. C.; Hanusa, T. P.; Okuda, J. *Organometallics* **2011**, *30*, 5291–5296.
286. Caro, C. F.; Lappert, M. F.; Merle, P. G. *Coord. Chem. Rev.* **2001**, *219*–221, 605–663.
287. Waggoner, K. M.; Power, P. P. *Organometallics* **1992**, *11*, 3209–3214.
288. Izod, K.; Liddle, S. T.; Clegg, W. *J. Am. Chem. Soc.* **2003**, *125*, 7534–7535.
289. Feil, F.; Harder, S. *Organometallics* **2000**, *19*, 5010–5015.
290. Harder, S.; Feil, F.; Weeber, A. *Organometallics* **2001**, *20*, 1044–1046.
291. Harder, S.; Feil, F. *Organometallics* **2002**, *21*, 2268–2274.
292. Feil, F.; Muller, C.; Harder, S. *J. Organomet. Chem.* **2003**, *683*, 56–63.
293. Feil, F.; Harder, S. *Organometallics* **2001**, *20*, 4616–4622.
294. Weeber, A.; Harder, S.; Brintzinger, H. H.; Knoll, K. *Organometallics* **2000**, *19*, 1325–1332.
295. Simpson, C. K.; White, R. E.; Carlson, C. N.; Wroblewski, D. A.; Kuehl, C. J.; Croce, T. A.; Steele, I. M.; Scott, B. L.; Hanusa, T. P.; Sattelberger, A. P.; John, K. D. *Organometallics* **2005**, *24*, 3685–3691.
296. Green, D. C.; Englich, U.; Ruhlandt-Senge, K. *Angew. Chem., Int. Ed.* **1999**, *38*, 354–357.
297. Guino-o, M. A.; Alexander, J. S.; McKee, M. L.; Hope, H.; Englich, U. B.; Ruhlandt-Senge, K. *Chem.—Eur. J.* **2009**, *15*, 11842–11852.
298. Westerhausen, M.; Gärtner, M.; Fischer, R.; Langer, J. *Angew. Chem., Int. Ed.* **2007**, *46*, 1950–1956.
299. Westerhausen, M.; Gaertner, M.; Fischer, R.; Langer, J.; Yu, L.; Reiher, M. *Chem.—Eur. J.* **2007**, *13*, 6292–6306.
300. Fischer, R.; Gaertner, M.; Goerls, H.; Westerhausen, M. *Organometallics* **2006**, *25*, 3496–3500.
301. Fischer, R.; Gaertner, M.; Görls, H.; Westerhausen, M. *Angew. Chem., Int. Ed.* **2006**, *45*, 609–612.
302. Fischer, R.; Gaertner, M.; Görls, H.; Yu, L.; Reiher, M.; Westerhausen, M. *Angew. Chem., Int. Ed.* **2007**, *46*, 1618–1623.
303. Dunne, J. P.; Fox, S.; Tacke, M. *J. Mol. Struct. (Theochem)* **2001**, *543*, 157–166.
304. Hurtado, M.; Lamsabhi, A.-M.; Mo, O.; Yanez, M.; Guillemin, J.-C. *Dalton Trans.* **2010**, *39*, 4593–4601.
305. Ruscic, C.; Harder, S. *Organometallics* **2005**, *24*, 5506–5508.
306. Fischer, R.; Görls, H.; Westerhausen, M. *Inorg. Chem. Commun.* **2005**, *8*, 1159–1161.
307. Gärtner, M.; Görls, H.; Westerhausen, M. *Organometallics* **2007**, *26*, 1077–1083.
308. Kriek, S.; Görls, H.; Westerhausen, M. *J. Organomet. Chem.* **2009**, *694*, 2204–2209.
309. Knapp, V.; Müller, G. *Angew. Chem., Int. Ed.* **2001**, *40*, 183–186.
310. Lawrence, L. M.; Whitesides, G. M. *J. Am. Chem. Soc.* **1980**, *102*, 2493–2494.
311. Walborsky, H. M. *Acc. Chem. Res.* **1990**, *23*, 286–293.
312. Walling, C. *Acc. Chem. Res.* **1991**, *24*, 255–256.
313. Walborsky, H. M.; Zimmermann, C. *J. Am. Chem. Soc.* **1992**, *114*, 4996–5000.
314. Garst, J. F.; Ronald Boone, J.; Webb, L.; Easton Lawrence, K.; Baxter, J. T.; Ungvary, F. *Inorg. Chim. Acta* **1999**, *296*, 52–66.
315. Garst, J. F.; Lawrence, K. E.; Batlaw, R.; Boone, J. R.; Ungvary, F. *Inorg. Chim. Acta* **1994**, *222*, 365–375.
316. Bogdanovic, B.; Schwickardi, M. *Angew. Chem., Int. Ed.* **2000**, *39*, 4610–4612.
317. Wakefield, B. J. In *Organomagnesium Methods in Organic Synthesis, Best Synthetic Methods Ser.*; Katritzky, A. R., Meth-Cohn, O., Rees, C. W., Eds.; Academic Press: San Diego, CA, 1995.
318. Silverman, G. S.; Rakita, P. E. *Handbook of Grignard Reagents*. Marcel Dekker: Monticello, NY, 1996.
319. Richey, H. G., Jr. *Grignard Reagents: New Developments*. Wiley: Chichester, 2000.
320. Knochel, P.; Dohle, W.; Gommermann, N.; Kneisel, F. F.; Kopp, F.; Korn, T.; Sapountzis, I.; Vu, V. A. *Angew. Chem., Int. Ed.* **2003**, *42*, 4302–4320.
321. Tidwell, T. T. *Angew. Chem., Int. Ed.* **2001**, *40*, 331–337.
322. Bickelhaupt, F. *Chem. Soc. Rev.* **1999**, *28*, 17–23.
323. Li, C.-J.; Zhang, W.-C. *J. Am. Chem. Soc.* **1998**, *120*, 9102–9103.
324. Zhang, W.-C.; Li, C.-J. *J. Org. Chem.* **1999**, *64*, 3230–3236.
325. Deng, W.; Tan, X.-H.; Liu, L.; Guo, Q.-X. *Chin. J. Chem.* **2004**, *22*, 747–750.
326. Zhang, W.-C.; Hua, X.-G.; Meng, Y.; Venkatraman, S.; Keh, C. C. K.; Li, C.-J. In *Recent Research Developments in Organic Chemistry 4*, 2000 pp 397–411.
327. Li, C.-J. *Green Chem.* **2002**, *4*, 1–4.
328. Lindstroem, U. M. *Chem. Rev.* **2002**, *102*, 2751–2771.
329. Li, C.-J.; Haberman, J. X.; Keh, C. C. K.; Yi, X.-H.; Meng, Y.; Hua, X.-G.; Venkatraman, S.; Zhang, W.-C.; Nguyen, T.; Wang, D.; Huang, T.; Zhang, J. *ACS Symp. Ser.* **2002**, *819*, 178–190.
330. Li, C.-J.; Wang, D. *Chemtracts* **2003**, *16*, 59–78.
331. Hoffmann, R. W.; Hoelzer, B.; Knopff, O. *Org. Lett.* **2001**, *3*, 1945–1948.
332. Hoffmann, R. W.; Holzer, B. *Chem. Commun.* **2001**, 491–492.
333. Hoelzer, B.; Hoffmann, R. W. *Chem. Commun.* **2003**, 732–733.
334. Hoffmann, R. W.; Holzer, B.; Knopff, O.; Harms, K. *Angew. Chem., Int. Ed.* **2000**, *39*, 3072–3074.
335. Hoffmann, R. W.; Hoelzer, B. *J. Am. Chem. Soc.* **2002**, *124*, 4204–4205.
336. Hoffmann, R. W. *Chem. Soc. Rev.* **2003**, *32*, 225–230.
337. Vestergren, M.; Gustafsson, B.; Davidsson, O.; Hakansson, M. *Angew. Chem., Int. Ed.* **2000**, *39*, 3435–3437.

338. Vestergren, M.; Eriksson, J.; Hakansson, M. *J. Organomet. Chem.* **2003**, *681*, 215–224.
339. Vestergren, M.; Eriksson, J.; Hakansson, M. *Chem.—Eur. J.* **2003**, *9*, 4678–4686.
340. Holloway, C. E.; Melnik, M. *Coord. Chem. Rev.* **1994**, *135–136*, 287–301.
341. Bickelhaupt, F. J. *Organomet. Chem.* **1994**, *475*, 1–14.
342. Al-Juaid, S. S.; Avent, A. G.; Eaborn, C.; El-Hamruni, S. M.; Hawkes, S. A.; Hill, M. S.; Hopman, M.; Hitchcock, P. B.; Smith, J. D. *J. Organomet. Chem.* **2001**, *631*, 76–86.
343. Al-Juaid, S. S.; Eaborn, C.; Hitchcock, P. B.; Hill, M. S.; Smith, J. D. *Organometallics* **2000**, *19*, 3224–3231.
344. Abraham, I.; Hoerner, W.; Ertel, T. S.; Bertagnolli, H. *Polyhedron* **1996**, *15*, 3993–4001.
345. Batsanov, A. S.; Bolton, P. D.; Copley, R. C. B.; Davidson, M. G.; Howard, J. A. K.; Lustig, C.; Price, R. D. *J. Organomet. Chem.* **1998**, *550*, 445–448.
346. Chisholm, M. H.; Huffman, J. C.; Phomphrai, K. *J. Chem. Soc., Dalton Trans.* **2001**, 222–224.
347. Zenger, R.; Stucky, G. *J. Organomet. Chem.* **1974**, *80*, 7–17.
348. Williams, R. A.; Hanusa, T. P.; Huffman, J. C. *J. Chem. Soc., Chem. Commun.* **1988**, 1045–1046.
349. Jutzi, P.; Burford, N. *Chem. Rev.* **1999**, *99*, 969–990.
350. Jutzi, P. *Chem. Unserer Zeit* **1999**, *33*, 343–353.
351. Burkey, D. J.; Hanusa, T. P. *Comments Inorg. Chem.* **1995**, *17*, 41–77.
352. Fernández, R.; Carmona, E. *Eur. J. Inorg. Chem.* **2005**, *2005*, 3197–3206.
353. Fischer, E. O.; Hofmann, H. P. *Chem. Ber.* **1959**, *92*, 482–486.
354. Hung, I.; Macdonald, C. L. B.; Schurko, R. W. *Chem.—Eur. J.* **2004**, *10*, 5923–5935.
355. Nugent, K. W.; Beattie, J. K.; Field, L. D. *J. Phys. Chem.* **1989**, *93*, 5371–5377.
356. Margl, P.; Schwarz, K.; Blochl, P. E. *J. Chem. Phys.* **1995**, *103*, 683–690.
357. Margl, P.; Schwarz, K.; Blochl, P. E. *J. Am. Chem. Soc.* **1994**, *116*, 11177–11178.
358. Mire, L. W.; Wheeler, S. D.; Wagenseller, E.; Marynick, D. S. *Inorg. Chem.* **1998**, *37*, 3099–3106.
359. Beattie, J. K.; Nugent, K. W. *Inorg. Chim. Acta* **1992**, *198–200*, 309–318.
360. Pratten, S. J.; Cooper, M. K.; Aroney, M. J. *J. Organomet. Chem.* **1990**, *381*, 147–153.
361. del Mar Conejo, M.; Fernandez, R.; Carmona, E.; Gutierrez-Puebla, E.; Monge, A. *Organometallics* **2001**, *20*, 2434–2436.
362. del Mar Conejo, M.; Fernandez, R.; del Rio, D.; Carmona, E.; Monge, A.; Ruiz, C.; Marquez, A. M.; Sanz, F. J. *Chem.—Eur. J.* **2003**, *9*, 4452–4461.
363. del Mar Conejo, M.; Fernandez, R.; Carmona, E.; Andersen, R. A.; Gutierrez-Puebla, E.; Monge, M. A. *Chem.—Eur. J.* **2003**, *9*, 4462–4471.
364. Battle, S. L.; Cowley, A. H.; Decken, A.; Jones, R. A.; Koschmieder, S. U. *J. Organomet. Chem.* **1999**, *582*, 66–69.
365. Weiss, E.; Fischer, E. O. *Z. Anorg. Allg. Chem.* **1955**, *278*, 219–224.
366. Bünder, W.; Weiss, E. *J. Organomet. Chem.* **1975**, *92*, 1–6.
367. Haaland, A.; Luszyk, J.; Brunvoll, J.; Starowieyski, K. B. *J. Organomet. Chem.* **1975**, *85*, 279–285.
368. Abis, L.; Calderazzo, F.; Maichle-Mossmer, C.; Pampaloni, G.; Strahle, J.; Tripepi, G. *J. Chem. Soc., Dalton Trans.* **1998**, 841–845.
369. Dohmeier, C.; Robl, C.; Tacke, M.; Schnoekel, H. *Angew. Chem.* **1991**, *103*, 594–595.
370. Bond, A. D.; Layfield, R. A.; MacAllister, J. A.; McPartlin, M.; Rawson, J. M.; Wright, D. S. *Chem. Commun.* **2001**, 1956–1957.
371. Smith, M. E.; Andersen, R. A. *J. Am. Chem. Soc.* **1996**, *118*, 11119–11128.
372. Jaenschke, A.; Paap, J.; Behrens, U. *Organometallics* **2003**, *22*, 1167–1169.
373. Putkonen, M.; Sajavaara, T.; Niinisto, L. *J. Mater. Chem.* **2000**, *10*, 1857–1861.
374. Kuech, T. F.; Wang, P. J.; Tischler, M. A.; Potemski, R.; Scilla, G. J.; Cardone, F. *J. Cryst. Growth* **1988**, *93*, 624–630.
375. Leem, J.-Y.; Lee, C.-R.; Lee, J.-I.; Noh, S. K.; Kwon, Y.-S.; Ryu, Y.-H.; Son, S.-J. *J. Cryst. Growth* **1998**, *193*, 491–495.
376. Hacke, P.; Nakayama, H.; Detchprohm, T.; Hiramatsu, K.; Sawaki, N. *Appl. Phys. Lett.* **1996**, *68*, 1362–1364.
377. Suzuki, M.; Nishio, J.; Onomura, M.; Hongo, C. *J. Cryst. Growth* **1998**, *189–190*, 511–515.
378. Lim, P. H.; Schineller, B.; Schon, O.; Heime, K.; Heuken, M. *J. Cryst. Growth* **1999**, *205*, 1–10.
379. Kwon, Y.-H.; Shee, S. K.; Gainer, G. H.; Park, G. H.; Hwang, S. J.; Song, J. *J. Appl. Phys. Lett.* **2000**, *76*, 840–842.
380. Kaufmann, U.; Kunzer, M.; Maier, M.; Obloh, H.; Ramakrishnan, A.; Santic, B.; Schlotter, P. *Appl. Phys. Lett.* **1998**, *72*, 1326–1328.
381. Xia, A.; Heeg, M. J.; Winter, C. H. *J. Am. Chem. Soc.* **2002**, *124*, 11264–11265.
382. Xia, A.; Knox, J. E.; Heeg, M. J.; Schlegel, H. B.; Winter, C. H. *Organometallics* **2003**, *22*, 4060–4069.
383. Cauletti, C.; Green, J. C.; Kelly, M. R.; Powell, P.; Van Tilborg, J.; Robbins, J.; Smart, J. *J. Electron Spectrosc. Relat. Phenom.* **1980**, *19*, 327–353.
384. Parris, G. E.; Ashby, E. C. *J. Organomet. Chem.* **1974**, *72*, 1–10.
385. El-Kaderi, H. M.; Xia, A.; Heeg, M. J.; Winter, C. H. *Organometallics* **2004**, *23*, 3488–3495.
386. Perrotin, P.; Sinnema, P.-J.; Shapiro, P. J. *Organometallics* **2006**, *25*, 2104–2107.
387. Hatanpää, T.; Ritala, M.; Leskelä, M. *J. Organomet. Chem.* **2007**, *692*, 5256–5262.
388. Orzechowski, L.; Piesik, D. F. J.; Ruspici, C.; Harder, S. *Dalton Trans.* **2008**, 4742–4746.
389. Jaenschke, A.; Olbrich, F.; Behrens, U. *Z. Anorg. Allg. Chem.* **2009**, *635*, 2550–2557.
390. Overby, J. S.; Hanusa, T. P. *Organometallics* **1996**, *15*, 2205–2212.
391. Westerhausen, M.; Digeser, M. H.; Gückel, C.; Noth, H.; Knizek, J.; Ponikvar, W. *Organometallics* **1999**, *18*, 2491–2496.
392. Westerhausen, M.; Gückel, C.; Piotrowski, H.; Mayer, P.; Warchhold, M.; Nöth, H. *Z. Anorg. Allg. Chem.* **2001**, *627*, 1741–1750.
393. Westerhausen, M.; Birg, C.; Piotrowski, H. *Eur. J. Inorg. Chem.* **2000**, 2173–2178.
394. Sinnema, P. J.; Shapiro, P. J.; Hohn, B.; Bitterwolf, T. E.; Twamley, B. *Organometallics* **2001**, *20*, 2883–2888.
395. Sinnema, P.-J.; Hoehn, B.; Hubbard, R. L.; Shapiro, P. J.; Twamley, B.; Blumenfeld, A.; Vij, A. *Organometallics* **2002**, *21*, 182–191.
396. Sinnema, P.-J.; Shapiro, P. J.; Hohn, B.; Twamley, B. *J. Organomet. Chem.* **2003**, *676*, 73–79.
397. Cristau, H.-J. *Chem. Rev.* **1994**, *94*, 1299–1313.
398. Leyser, N.; Schmidt, K.; Brintzinger, H.-H. *Organometallics* **1998**, *17*, 2155–2161.
399. Sitzmann, H.; Dezember, T.; Ruck, M. *Angew. Chem., Int. Ed.* **1998**, *37*, 3114–3115.
400. Kuchenbecker, D.; Harder, S.; Jansen, G. *Z. Anorg. Allg. Chem.* **2010**, *636*, 2257–2261.
401. Sitzmann, H.; Walter, M. D.; Wolmershauser, G. *Angew. Chem., Int. Ed.* **2002**, *41*, 2315–2316.
402. Walter, M. D.; Wolmershaeuser, G.; Sitzmann, H. *J. Am. Chem. Soc.* **2005**, *127*, 17494–17503.
403. Selg, P.; Brintzinger, H. H.; Andersen, R. A.; Horváth, I. T. *Angew. Chem. Int. Ed. Engl.* **1995**, *34*, 791–793.
404. Selg, P.; Brintzinger, H. H.; Schultz, M.; Andersen, R. A. *Organometallics* **2002**, *21*, 3100–3107.
405. Sitzmann, H.; Weber, F.; Walter, M. D.; Wolmershaeuser, G. *Organometallics* **2003**, *22*, 1931–1936.
406. Harvey, M. J.; Hanusa, T. P. *Organometallics* **2000**, *19*, 1556–1566.
407. Burkey, D. J.; Hanusa, T. P. *Organometallics* **1996**, *15*, 4971–4976.
408. Jayaratne, K. C.; Fitts, L. S.; Hanusa, T. P.; Young, V. G., Jr. *Organometallics* **2001**, *20*, 3638–3640.
409. Harder, S.; Feil, F.; Repo, T. *Chem.—Eur. J.* **2002**, *8*, 1991–1999.
410. Gibson, V. C.; Segal, J. A.; White, A. J. P.; Williams, D. J. *J. Am. Chem. Soc.* **2000**, *122*, 7120–7121.
411. Bailey, P. J.; Dick, C. M. E.; Fabre, S.; Parsons, S. *Dalton* **2000**, 1655–1661.
412. Cameron, T. M.; Xu, C.; Dipasquale, A. G.; Rheingold, A. L. *Organometallics* **2008**, *27*, 1596–1604.
413. Ciobanu, O.; Fuchs, A.; Reinmuth, M.; Lebkücher, A.; Kaifer, E.; Wadepohl, H.; Himmel, H.-J. *Z. Anorg. Allg. Chem.* **2010**, *636*, 543–550.
414. Harvey, M. J.; Burkey, D. J.; Chmely, S. C.; Hanusa, T. P. *J. Alloys Compd.* **2008**, *488*, 528–532.
415. Chang, C. C.; Ameerunisha, M. S. *Coord. Chem. Rev.* **1999**, *189*, 199–278.
416. Crimmin, M. R.; Hill, M. S.; Hitchcock, P. B.; Mahon, M. F. *New J. Chem.* **2010**, *34*, 1572–1578.
417. El-Kaderi, H. M.; Heeg, M. J.; Winter, C. H. *Organometallics* **2004**, *23*, 4995–5002.
418. Avent, A. G.; Crimmin, M. R.; Hill, M. S.; Hitchcock, P. B. *Dalton Trans.* **2005**, *2*, 278–284.
419. Saulys, D. A.; Powell, D. R. *Organometallics* **2003**, *22*, 407–413.
420. Lerner, H.-W.; Scholz, S.; Bolte, M.; Wiberg, N.; Nöth, H.; Krossing, I. *Eur. J. Inorg. Chem.* **2003**, *2003*, 666–670.
421. Abersfelder, K.; Güclü, D.; Scheschke, D. *Angew. Chem., Int. Ed.* **2006**, *45*, 1643–1645.

422. Farwell, J. D.; Lappert, M. F.; Marschner, C.; Strissel, C.; Tilley, T. D. *J. Organomet. Chem.* **2000**, *603*, 185–188.
423. Teng, W.; Englisch, U.; Ruhlandt-Senge, K. *Angew. Chem., Int. Ed.* **2003**, *42*, 3661–3664.
424. Teng, W.; Ruhlandt-Senge, K. *Organometallics* **2004**, *23*, 2694–2700.
425. Wagner, H.; Baumgartner, J.; Marschner, C. *Organometallics* **2007**, *26*, 1762–1770.
426. Teng, W.; Ruhlandt-Senge, K. *Organometallics* **2004**, *23*, 952–956.
427. Lee, V. Y.; Takanashi, K.; Ichinohe, M.; Sekiguchi, A. *Angew. Chem., Int. Ed.* **2004**, *43*, 6703–6705.
428. Westerhausen, M. *Angew. Chem., Int. Ed. Engl.* **1994**, *33*, 1493–1495.
429. Veith, M.; Weidner, S.; Kunze, K.; Käfer, D.; Hans, J.; Huch, V. *Coord. Chem. Rev.* **1994**, *137*, 297–322.
430. Eisler, D. J.; Chivers, T. *Chem.—Eur. J.* **2006**, *12*, 233–243.
431. Evans, D. A. In: Morrison, J. D., Ed.; *Asymmetric Synthesis* Academic Press: New York, 1983; vol. 3, Chapter 1, p 1983.
432. Wannagat, U. *Pure Appl. Chem.* **1969**, *19*, 329–342.
433. Westerhausen, M.; Birg, C.; Krofta, M.; Mayer, P.; Seifert, T.; Nöth, H.; Pfitzner, A.; Nilges, T.; Deiseroth, H.-J. *Z. Anorg. Allg. Chem.* **2000**, *626*, 1073–1080.
434. Davies, R. P. *Inorg. Chem. Commun.* **2000**, *3*, 13–15.
435. Clark, A. H.; Haaland, A. J. *Chem. Soc. D, Chem. Commun.* **1969**, 912–913.
436. Clark, A. H.; Haaland, A. *Acta Chem. Scand.* **1970**, *24*, 3024–3030.
437. Tesh, K. F.; Hanusa, T. P.; Huffman, J. C. *Inorg. Chem.* **1990**, *29*, 1584–1586.
438. Harder, S. *Organometallics* **2002**, *21*, 3782–3787.
439. Sarish, S. P.; Roesky, H. W.; John, M.; Ringe, A.; Magull, J. *Chem. Commun.* **2009**, 2390–2392.
440. Avent, A. G.; Crimmin, M. R.; Hill, M. S.; Hitchcock, P. B. *Dalton Trans.* **2004**, 3166–3168.
441. Crimmin, M. R.; Arrowsmith, M.; Barrett, A. G. M.; Casely, I. J.; Hill, M. S.; Procopiou, P. A. *J. Am. Chem. Soc.* **2009**, *131*, 9670–9685.
442. Ruspic, C.; Harder, S. *Inorg. Chem.* **2007**, *46*, 10426–10433.
443. Avent, A. G.; Crimmin, M. R.; Hill, M. S.; Hitchcock, P. B. *Organometallics* **2005**, *24*, 1184–1188.
444. Barrett, A. G. M.; Crimmin, M. R.; Hill, M. S.; Hitchcock, P. B.; Lomas, S. L.; Mahon, M. F.; Procopiou, P.; Suntharalingam, K. *Organometallics* **2008**, *27*, 6300–6306.
445. Ruspic, C.; Nembenna, S.; Hofmeister, A.; Magull, J.; Harder, S.; Roesky, H. W. *J. Am. Chem. Soc.* **2006**, *128*, 15000–15004.
446. Sarish, S. P.; Nembenna, S.; Roesky, H. W.; Ott, H.; Pal, A.; Stalke, D.; Dutta, S.; Pati, S. K. *Angew. Chem., Int. Ed.* **2009**, *48*, 8740–8742.
447. Dove, A. P.; Gibson, V. C.; Hormnirun, P.; Marshall, E. L.; Segal, J. A.; White, A. J. P.; Williams, D. J. *Dalton Trans.* **2003**, 3088–3097.
448. Reinmuth, M.; Wild, U.; Rudolf, D.; Kaifer, E.; Enders, M.; Wadepohl, H.; Himmel, H.-J. *Eur. J. Inorg. Chem.* **2009**, 4795–4808.
449. Barrett, A. G. M.; Casely, I. J.; Crimmin, M. R.; Hill, M. S.; Lachs, J. R.; Mahon, M. F.; Procopiou, P. A. *Inorg. Chem.* **2009**, *48*, 4445–4453.
450. El-Kaderi, H. M.; Heeg, M. J.; Winter, C. H. *Polyhedron* **2006**, *25*, 224–234.
451. Sedai, B.; Heeg, M. J.; Winter, C. H. *Organometallics* **2009**, *28*, 1032–1038.
452. Bourget-Merle, L.; Lappert, M. F.; Severn, J. R. *Chem. Rev.* **2002**, *102*, 3031–3066.
453. Sarish, S. P.; Jana, A.; Roesky, H. W.; Schulz, T.; John, M.; Stalke, D. *Inorg. Chem.* **2010**, *49*, 3816–3820.
454. Barker, J.; Kilner, M. *Coord. Chem. Rev.* **1994**, *133*, 219–300.
455. Averbuj, C.; Tish, E.; Eisen, M. S. *J. Am. Chem. Soc.* **1998**, *120*, 8640–8646.
456. Walther, D.; Gebhardt, P.; Fischer, R.; Kreher, U.; Görls, H. *Inorg. Chim. Acta* **1998**, *281*, 181–189.
457. Kincaid, K.; Gerlach, C. P.; Giesbrecht, G. R.; Hagadorn, J. R.; Whitener, G. D.; Shafir, A.; Arnold, J. *Organometallics* **1999**, *18*, 5360–5366.
458. Chivers, T.; Fedorchuk, C.; Parvez, M. *Organometallics* **2005**, *24*, 580–586.
459. Chivers, T.; Copey, M. C.; Fedorchuk, C.; Parvez, M.; Stubbs, M. *Organometallics* **2005**, *24*, 1919–1928.
460. Barrett, A. G. M.; Crimmin, M. R.; Hill, M. S.; Hitchcock, P. B.; Lomas, S. L.; Mahon, M. F.; Procopiou, P. A. *Dalton Trans.* **2010**, *39*, 7393–7400.
461. Al-Shboul, T. M. A.; Volland, G.; Görls, H.; Westerhausen, M. *Z. Anorg. Allg. Chem.* **2009**, *635*, 1568–1572.
462. Monegan, J. D.; Bunge, S. D. *Inorg. Chem.* **2009**, *48*, 3248–3256.
463. Feil, F.; Harder, S. *Eur. J. Inorg. Chem.* **2005**, *2005*, 4438–4443.
464. Jones, C. *Coord. Chem. Rev.* **2010**, *254*, 1273–1289.
465. Nimitsiriwat, N.; Gibson, V. C.; Marshall, E. L.; Takolpuckdee, P.; Tomov, A. K.; White, A. J. P.; Williams, D. J.; Elsegood, M. R. J.; Dale, S. H. *Inorg. Chem.* **2007**, *46*, 9988–9997.
466. Barrett, A. G. M.; Crimmin, M. R.; Hill, M. S.; Hitchcock, P. B.; Kociok-Köhn, G.; Procopiou, P. A. *Inorg. Chem.* **2008**, *47*, 7366–7376.
467. Hauber, S.-O.; Lissner, F.; Deacon, G. B.; Niemeyer, M. *Angew. Chem., Int. Ed.* **2005**, *44*, 5871–5875.
468. Lee, H. S.; Niemeyer, M. *Inorg. Chem.* **2009**, *49*, 730–735.
469. Pfeiffer, D.; Heeg, M. J.; Winter, C. H. *Inorg. Chem.* **2000**, *39*, 2377–2384.
470. Hitzbleck, J.; O'Brien, A. Y.; Deacon, G. B.; Ruhlandt-Senge, K. *Inorg. Chem.* **2006**, *45*, 10329–10337.
471. Chisholm, M. H.; Gallucci, J. C.; Yaman, G.; Young, T. *Chem. Commun.* **2009**.
472. Chisholm, M. H.; Gallucci, J. C.; Yaman, G. *Dalton Trans.* **2009**.
473. Pfeiffer, D.; Heeg, M. J.; Winter, C. H. *Angew. Chem., Int. Ed.* **1998**, *37*, 2517–2519.
474. Steiner, A.; Lawson, G. T.; Walford, B.; Leusser, D.; Stalke, D. *J. Chem. Soc., Dalton Trans.* **2001**, 219–221.
475. Kennedy, A. R.; Mulvey, R. E.; Rowlings, R. B. *Angew. Chem., Int. Ed.* **1998**, *37*, 3180–3183.
476. Kennedy, A. R.; Mulvey, R. E.; Roberts, B. A.; Rowlings, R. B.; Raston, C. L. *Chem. Commun.* **1999**, 353–354.
477. Gallagher, D. J.; Henderson, K. W.; Kennedy, A. R.; O'Hara, C. T.; Mulvey, R. E.; Rowlings, R. B. *Chem. Commun.* **2002**, 376–377.
478. Andrews, P. C.; Kennedy, A. R.; Mulvey, R. E.; Raston, C. L.; Roberts, B. A.; Rowlings, R. B. *Angew. Chem., Int. Ed.* **2000**, *39*, 1960–1962.
479. Clegg, W.; Henderson, K. W.; Kennedy, A. R.; Mulvey, R. E.; O'Hara, C. T.; Rowlings, R. B.; Tooke, D. M. *Angew. Chem., Int. Ed.* **2001**, *40*, 3902–3905.
480. Andrikopoulos, P. C.; Armstrong, D. R.; Clegg, W.; Gilfillan, C. J.; Hevia, E.; Kennedy, A. R.; Mulvey, R. E.; O'Hara, C. T.; Parkinson, J. A.; Tooke, D. M. *J. Am. Chem. Soc.* **2004**, *126*, 11612–11620.
481. Honeyman, G. W.; Kennedy, A. R.; Mulvey, R. E.; Sherrington, D. C. *Organometallics* **2004**, *23*, 1197–1199.
482. Cárdenas, C. V.; Hernández, M.Á.M.; Grévy, J.-M. *Dalton Trans.* **2010**, *39*, 6441–6448.
483. Forbes, G. C.; Kenley, F. R.; Kennedy, A. R.; Mulvey, R. E.; O'Hara, C. T.; Parkinson, J. A. *Chem. Commun.* **2003**, 1140–1141.
484. Mulvey, R. E. *Chem. Commun.* **2001**, 1049–1056.
485. Mulvey, R. E. *Organometallics* **2006**, *25*, 1060–1075.
486. Esteban, D.; Platas-Iglesias, C.; Avecilla, F.; de Blas, A.; Rodríguez-Blas, T. *Polyhedron* **2005**, *24*, 289–294.
487. Stroud, T. L.; Coker, N. L.; Krause, J. A. *Acta Crystallogr., Sect. E* **2009**, *65*, m1509–m1510.
488. Neumüller, B.; Dehnicke, K. *Z. Anorg. Allg. Chem.* **2010**, *636*, 1206–1211.
489. Corvaja, C.; Pasimeni, L. *Chem. Phys. Lett.* **1976**, *39*, 261–264.
490. Clopath, P.; Von Zelewsky, A. *Helv. Chim. Acta* **1973**, *56*, 980–983.
491. Thiele, K.-H.; Lorenz, V.; Thiele, G.; Zoenchen, P.; Scholz, J. *Angew. Chem.* **1994**, *106*, 1461–1463.
492. Lorenz, V.; Neumueller, B.; Thiele, K.-H. *Z. Naturforsch., B: Chem. Sci.* **1995**, *50*, 71–75.
493. Hey, E.; Engelhardt, L. M.; Raston, C. L.; White, A. H. *Angew. Chem., Int. Ed. Engl.* **1987**, *26*, 81–82.
494. Mulvey, R. E. *Chem. Soc. Rev.* **1991**, *20*, 167–209.
495. Becker, G.; Eschbach, B.; Kaeshammer, D.; Mundt, O. *Z. Anorg. Allg. Chem.* **1994**, *620*, 29–40.
496. Westerhausen, M. *Trends Organomet. Chem.* **1997**, *2*, 89–105.
497. Karsch, H. H.; Graf, V.; Reisky, M. *Phosphorus, Sulfur Silicon Relat. Elem.* **1999**, *144–146*, 553–556.
498. Izod, K. *Coord. Chem. Rev.* **2002**, *227*, 153–173.
499. Driess, M. *Adv. Inorg. Chem.* **2000**, *50*, 235–284.
500. Gindelberger, D. E.; Arnold, J. *Inorg. Chem.* **1994**, *33*, 6293–6299.
501. Westerhausen, M.; Krofta, M.; Mayer, P.; Warchhold, M.; Nöth, H. *Inorg. Chem.* **2000**, *39*, 4721–4724.
502. Westerhausen, M.; Digeser, M. H.; Krofta, M.; Wiberg, N.; Nöth, H.; Knizek, J.; Ponikwar, W.; Seifert, T. *Eur. J. Inorg. Chem.* **1999**, 743–750.
503. Kopecky, P.; von Hänisch, C.; Weigend, F.; Kracke, A. *Eur. J. Inorg. Chem.* **2010**, *2010*, 258–265.
504. Crimmin, M. R.; Barrett, A. G. M.; Hill, M. S.; Hitchcock, P. B.; Procopiou, P. A. *Inorg. Chem.* **2007**, *46*, 10410–10415.
505. Gärtner, M.; Görls, H.; Westerhausen, M. *Inorg. Chem.* **2008**, *47*, 1397–1405.
506. Blair, S.; Izod, K.; Clegg, W.; Harrington, R. W. *Inorg. Chem.* **2004**, *43*, 8526–8531.
507. Izod, K.; Clegg, W.; Liddle, S. T. *Organometallics* **2000**, *19*, 3640–3643.
508. Clegg, W.; Izod, K.; Liddle, S. T.; O'Shaughnessy, P.; Sheffield, J. M. *Organometallics* **2000**, *19*, 2090–2096.
509. Blair, S.; Izod, K.; Clegg, W.; Harrington, R. W. *Eur. J. Inorg. Chem.* **2003**, *2003*, 3319–3324.
510. Blair, S.; Izod, K.; Clegg, W. *Inorg. Chem.* **2002**, *41*, 3886–3893.

511. Roesky, P. W. *Inorg. Chem.* **2005**, *45*, 798–802.
512. Panda, T. K.; Gamer, M. T.; Roesky, P. W. *Inorg. Chim. Acta* **2006**, *359*, 4765–4768.
513. Stone, F. G. A.; Burg, A. J. *Am. Chem. Soc.* **1954**, *76*, 386.
514. Izod, K. *Adv. Inorg. Chem.* **2000**, *50*, 33–107.
515. Westerhausen, M.; Makropoulos, N.; Piotrowski, H.; Warchhold, M.; Nöth, H. *J. Organomet. Chem.* **2000**, *614–615*, 70–73.
516. Westerhausen, M.; Gueckel, C.; Piotrowski, H.; Vogt, M. Z. *Anorg. Allg. Chem.* **2002**, *628*, 735–740.
517. Cole, M. L.; Jones, C.; Junk, P. C. *New J. Chem.* **2002**, *26*, 89–93.
518. Xu, W. G.; Jin, B. J. *Mol. Struct. (Theochem.)* **2006**, *759*, 101–107.
519. Xu, W. G.; Jin, B. J. *Mol. Struct. (Theochem.)* **2005**, *731*, 61–66.
520. Bradley, D. C. *Chem. Rev.* **1989**, *89*, 1317–1322.
521. Bradley, D.; Mehrotra, R. C.; Rothwell, I.; Singh, A. *Alkoxo and Aryloxo Derivatives of Metals*. Academic Press: New York, 2001.
522. Hubert, S. *Coord. Chem. Rev.* **2001**, *215*, 223–242.
523. Fromm, K. M.; Gueneau, E. D. *Polyhedron* **2004**, *23*, 1479–1504.
524. Einspahr, H.; Bugg, C. E. *Acta Crystallogr. Sect. B* **1981**, *37*, 1044–1052.
525. Rees, W. S., Jr. *CVD of Nonmetals*. VCH: Weinheim, 1996; p 282.
526. Sobota, P.; Szafer, S. *Inorg. Struct. (Theochem.)* **1996**, *35*, 1778–1781.
527. Kim, K. M.; Lee, S. S.; Jung, O.-S.; Sohn, Y. S. *Inorg. Chem.* **1996**, *35*, 3077–3078.
528. Berger, R. J. F.; Schmidt, M. A.; Juselius, J.; Sundholm, D.; Sirsch, P.; Schmidbauer, H. Z. *Naturforsch., B: Chem. Sci.* **2001**, *56*, 979–989.
529. Pomogailo, A. D.; Dzhardimalieva, G. I.; Kestelman, V. N. *Macromolecular Metal Carboxylates and Their Nanocomposites*. Springer: Berlin, 2010.
530. Banerjee, D.; Parise, J. B. *Cryst. Growth Des.* **2011**, *11*, 4704–4720.
531. Yang, K.-C.; Chang, C.-C.; Yeh, C.-S.; Lee, G.-H.; Peng, S.-M. *Organometallics* **2000**, *20*, 126–137.
532. Caudle, M. T.; Brennessel, W. W.; Young, V. G. *Inorg. Chem.* **2005**, *44*, 3233–3240.
533. Tang, Y.; Zakharov, L. N.; Rheingold, A. L.; Kemp, R. A. *Organometallics* **2004**, *23*, 4788–4791.
534. Stadie, N. P.; Sanchez-Smith, R.; Groy, T. L. *Acta Crystallogr. Sect. E* **2007**, *63*, m2153–m2154.
535. Srinivasan, B.; Sawant, J.; Näther, C.; Bensch, W. J. *Chem. Sci.* **2007**, *119*, 243–252.
536. Dell'Amico, D. B.; Calderazzo, F.; Labella, L.; Marchetti, F.; Martini, M.; Mazzoncin, I. *Compt. Rend. Chim.* **2004**, *7*, 877–884.
537. Katharina, M. F. *Coord. Chem. Rev.* **2008**, *252*, 856–885.
538. Almeida Paz, F. A.; Klinowski, J.; Vilela, S. M. F.; Tomé, J. P. C.; Cavaleiro, J. A. S.; Rocha, J. *Chem. Soc. Rev.* **2012**, *41*, 201241.
539. Britt, D.; Furukawa, H.; Wang, B.; Glover, T. G.; Yaghi, O. M. *Proc. Natl. Acad. Sci. U.S.A.* **2009**, *106*, 20637–20640.
540. Cheon, Y. E.; Park, J.; Suh, M. P. *Chem. Commun.* **2009**, 5436–5438.
541. Guo, Z.; Li, G.; Zhou, L.; Su, S.; Lei, Y.; Dang, S.; Zhang, H. *Inorg. Chem.* **2009**, *48*, 8069–8071.
542. Onoda, A.; Yamada, Y.; Nakayama, Y.; Takahashi, K.; Adachi, H. *Inorg. Chem.* **2004**, *43*, 4447–4455.
543. Tahir, A. A.; Mazhar, M.; Hamid, M.; Zeller, M.; Hunter, A. D. *New J. Chem.* **2009**, *33*, 1535–1541.
544. Vaartstra, B. A.; Gardiner, R. A.; Gordon, D. C.; Ostrander, R. L.; Rheingold, A. L. *Mater. Res. Soc. Symp. Proc.* **1994**, *335*, 203–208.
545. Otway, D. J.; Rees, W. S., Jr. *Coord. Chem. Rev.* **2000**, *210*, 279–328.
546. Condorelli, G. G.; Malandrino, G.; Fraga, I. L. *Coord. Chem. Rev.* **2007**, *251*, 1931–1950.
547. Fragalà, M. E.; Toro, R. G.; Rossi, P.; Dapporto, P.; Malandrino, G. *Chem. Mater.* **2009**, *21*, 2062–2069.
548. Belcher, R.; Cranley, C. R.; Majer, J. R.; Stephen, W. I.; Uden, P. C. *Anal. Chim. Acta* **1972**, *60*, 109–116.
549. Arunasalam, V. C.; Baxter, I.; Drake, S. R.; Hursthouse, M. B.; Abdul Malik, K. M.; Miller, S. A. S.; Mingos, D. M. P.; Otway, D. J. *J. Chem. Soc., Dalton Trans.* **1997**, 1331–1336.
550. Drake, S. R.; Otway, D. J.; Hursthouse, M. B.; Abdul Malik, K. M. *J. Chem. Soc., Dalton Trans.* **1993**, 2883–2890.
551. Darr, J. A.; Drake, S. R.; Hursthouse, M. B.; Abdul Malik, K. M.; Miller, S. A. S.; Mingos, D. M. P. *J. Chem. Soc., Dalton Trans.* **1997**, 945–950.
552. Amirthalingam, V.; Padmanabhan, V. M.; Shankar, J. *Acta Crystallogr.* **1960**, *13*, 201–204.
553. Vreshch, V. D.; Chernega, A. N.; Howard, J. A. K.; Sieler, J.; Domasevitch, K. V. *Dalton Trans.* **2003**.
554. Tobbens, D. M.; Hummel, M.; Kaindl, R.; Schottenberger, H.; Kahlenberg, V. *CrystEngComm* **2008**, *10*, 327–334.
555. Saalfrank, R. W.; Demleitner, B.; Glaser, H.; Maid, H.; Bathelt, D.; Hampel, F.; Bauer, W.; Teichert, M. *Chem.—Eur. J.* **2002**, *8*, 2679–2683.
556. Saalfrank, R. W.; Demleitner, B.; Glaser, H.; Maid, H.; Reihls, S.; Bauer, W.; Maluenga, M.; Hampel, F.; Teichert, M.; Krautscheid, H. *Eur. J. Inorg. Chem.* **2003**, *2003*, 822–829.
557. Kessler, V. G.; Gohil, S.; Kritikos, M.; Korsak, O. N.; Knyazeva, E. E.; Moskovskaya, I. F.; Romanovsky, B. V. *Polyhedron* **2001**, *20*, 915–922.
558. Koval, L. I.; Dzyuba, V. I.; Bon, V. V.; Il'nitska, O. L.; Pekhnyo, V. I. *Polyhedron* **2009**, *28*, 2698–2702.
559. Allan, J. F.; Henderson, K. W.; Kennedy, A. R.; Teat, S. J. *Chem. Commun.* **2000**, 1059–1060.
560. Westerhausen, M.; Schneiderbauer, S.; Kneifel, A. N.; Soeltl, Y.; Mayer, P.; Noeth, H.; Zhong, Z.; Dijkstra, P. J.; Feijen, J. *Eur. J. Inorg. Chem.* **2003**, 3432–3439.
561. El Habra, N.; Benetollo, F.; Casarin, M.; Bolzan, M.; Sartori, A.; Rossetto, G. *Dalton Trans.* **2010**, *39*, 8064–8070.
562. Marchetti, F.; Pettinari, C.; Pettinari, R.; Cingolani, A.; Gobetto, R.; Chierotti, M. R.; Drozdov, A.; Troyanov, S. I. *Inorg. Chem.* **2006**, *45*, 3074–3085.
563. Pettinari, C.; Marchetti, F.; Pettinari, R.; Vertlib, V.; Drozdov, A.; Timokhin, I.; Troyanov, S.; Min, Y.-S.; Kim, D. *Inorg. Chim. Acta* **2003**, *355*, 157–167.
564. Kuzmina, N. P.; Tsymbarenko, D. M.; Korsakov, I. E.; Starikova, Z. A.; Lysenko, K. A.; Boytsova, O. V.; Mironov, A. V.; Malkerova, I. P.; Alikhanyan, A. S. *Polyhedron* **2008**, *27*, 2811–2818.
565. Bradley, D. C.; Mehrotra, R. C.; Gaur, D. P. *Metal Alkoxides*. Academic Press: New York, 1978; p 50–51.
566. Johnson, S. M.; Herrin, J.; Liu, S. J.; Paul, I. C. *J. Am. Chem. Soc.* **1970**, *92*, 4428–4435.
567. Smith, G. D.; Duax, W. L. *J. Am. Chem. Soc.* **1976**, *98*, 1578–1580.
568. Bednorz, J. G.; Müller, K. A. Z. *Z. Phys. B.* **1986**, *64*, 189–193.
569. Hubert-Pfalzgraf, L. G. *Polyhedron* **1994**, *13*, 1181–1193.
570. Mehrotra, R. C.; Singh, A.; Sogani, S. J. *Chem. Soc. Rev.* **1994**, 215–225.
571. Parola, S.; Khem, R.; Cornu, D.; Chassagneux, F.; Lecocq, S.; Kighelman, Z.; Setter, N. *Inorg. Chem. Commun.* **2002**, *5*, 316–318.
572. Tesh, K. F.; Hanusa, T. P.; Huffman, J. C.; Huffman, C. J. *Inorg. Chem.* **1992**, *31*, 5572–5579.
573. Tesh, K. F.; Burkey, D. J.; Hanusa, T. P. *J. Am. Chem. Soc.* **1994**, *116*, 2409–2417.
574. Drake, S. R.; Streib, W. E.; Chisholm, M. H.; Caulton, K. G. *Inorg. Chem.* **1990**, *29*, 2707–2708.
575. Nunes, P.; Leal, J. P.; Cachata, V.; Raminhos, H.; Minas da Piedade, M. E. *Chem.—Eur. J.* **2003**, *9*, 2095–2101.
576. Fromm, K. M. *Dalton Trans.* **2006**, 5103–5112.
577. Fedushkin, I. L.; Skatova, A. A.; Cherkasov, V. K.; Chudakova, V. A.; Dechert, S.; Hummert, M.; Schumann, H. *Chem.—Eur. J.* **2003**, *9*, 5778–5783.
578. Kloetzing, R. J.; Krasovskiy, A.; Knochel, P. *Chem.—Eur. J.* **2007**, *13*, 215–227.
579. Roberts, C. C.; Fritsch, J. M. *Polyhedron* **2010**, *29*, 1271–1278.
580. Sobota, P.; Utko, J.; Ejfler, J.; Jerzykiewicz, L. B. *Organometallics* **2000**, *19*, 4929–4931.
581. Dove, A. P.; Gibson, V. C.; Hormnirun, P.; Marshall, E. L.; Segal, J. A.; White, A. J. P.; Williams, D. J. *Dalton Trans.* **2003**.
582. Gromada, J.; Mortreux, A.; Nowogrocki, G.; Leising, F.; Mathivet, T.; Carpentier, J.-F. *Eur. J. Inorg. Chem.* **2004**, *2004*, 3247–3253.
583. Chisholm, M. H.; Gallucci, J. C.; Phomphrai, K. *Inorg. Chem.* **2005**, *44*, 8004–8010.
584. Arnold, P. L.; Casely, I. J.; Turner, Z. R.; Bellabarba, R.; Tooze, R. B. *Dalton Trans.* **2009**.
585. Chen, M.-T.; Chang, P.-J.; Huang, C.-A.; Peng, K.-F.; Chen, C.-T. *Dalton Trans.* **2009**.
586. Hung, W.-C.; Lin, C.-C. *Inorg. Chem.* **2008**, *48*, 728–734.
587. Van Nguyen, H.; Matsubara, R.; Kobayashi, S. *Angew. Chem., Int. Ed.* **2009**, *48*, 5927–5929.
588. Teng, W.; Guino-o, M.; Hitzbleck, J.; Englich, U.; Ruhlandt-Senge, K. *Inorg. Chem.* **2006**, *45*, 9531–9539.
589. Chi, Y.; Ranjan, S.; Chung, P.-W.; Hsieh, H.-Y.; Peng, S.-M.; Lee, G.-H. *Inorg. Chim. Acta* **2002**, *334*, 172–182.
590. Yuhya, S.; Kikuchi, K.; Yoshida, M.; Sugawara, K.; Shiohara, Y. *Mol. Cryst. Liq. Cryst.* **1990**, *184*, 231–235.
591. Kim, S. H.; Cho, C. H.; No, K. S.; Chun, J. S. *J. Mater. Res.* **1991**, *6*, 704–711.
592. Moreno, C. A.; Hughes, D. L.; Bochmann, M. *Polyhedron* **2007**, *26*, 2523–2526.
593. Albinati, A.; Faccini, F.; Gross, S.; Kickelbick, G.; Rizzato, S.; Venzo, A. *Inorg. Chem.* **2007**, *46*, 3459–3466.
594. Caulton, K. G.; Chisholm, M. H.; Drake, S. R.; Folting, K.; Huffman, J. C. *Inorg. Chem.* **1993**, *32*, 816–820.

595. Henderson, K. W.; Honeyman, G. W.; Kennedy, A. R.; Mulvey, R. E.; Parkinson, J. A.; Sherrington, D. C. *Dalton Trans.* **2003**, 1365–1372.
596. Janssen, M. D.; Grove, D. M.; Koten, G. V. *Prog. Inorg. Chem.* **1997**, *46*, 97–149.
597. Ruhlandt-Senge, K. *Comments Inorg. Chem.* **1997**, *19*, 351–385.
598. Englich, U.; Ruhlandt-Senge, K. *Coord. Chem. Rev.* **2000**, *210*, 135–179.
599. Gírrirane, A.; Pastor, A.; Álvarez, E.; Galindo, A. *Inorg. Chem. Commun.* **2005**, *8*, 453–456.
600. Leung, W.-P.; Wan, C.-L.; Mak, T. C. W. *Organometallics* **2010**, *29*, 1622–1628.
601. Bjernemose, J. K.; Davies, R. P.; Jurd, A. P. S.; Martinelli, M. G.; Raitby, P. R.; White, A. J. P. *Dalton Trans.* **2004**, 3169–3170.
602. Xia, A.; Heeg, M. J.; Winter, C. H. *J. Organomet. Chem.* **2003**, *669*, 37–43.
603. Teng, W.; Englich, U.; Ruhlandt-Senge, K. *Inorg. Chem.* **2000**, *39*, 3875–3880.
604. Söllner, J.; Schmoranzler, J.; Hamadeh, H.; Bollig, B.; Kubalek, E.; Heuken, M. *J. Electron. Mater.* **1995**, *24*, 1557–1561.
605. Kozlovsky, V. I.; Krysa, A. B.; Korostelin, Y. V.; Shapkin, P. V.; Kalisch, H.; Luenenbuerger, M.; Heuken, M. *J. Cryst. Growth* **1998**, *184–185*, 124–128.
606. Pappas, J. A. *J. Am. Chem. Soc.* **1978**, *100*, 6023–6027.
607. Kling, C.; Ott, H.; Schwab, G.; Stalke, D. *Organometallics* **2008**, *27*, 5038–5042.
608. Ruhlandt-Senge, K.; Englich, U. *Chem.—Eur. J.* **2000**, *6*, 4063–4070.
609. Becker, G.; Klinkhammer, K. W.; Schwarz, W.; Westerhausen, M.; Hildenbrand, T. *Z. Naturforsch., B: Chem. Sci.* **1992**, *47*, 1225–1232.
610. Gindelberger, D. E.; Arnold, J. J. *Am. Chem. Soc.* **1992**, *114*, 6242–6243.
611. Büchner, W.; Schliebs, W.; Winter, G.; Büchel, K. H. In *Industrial Inorganic Chemistry*, VCH: New York, 1989; pp 149 ff., 218 ff.
612. Hargittai, M. *Coord. Chem. Rev.* **1988**, *91*, 35–88.
613. Beattie, I. R. *Angew. Chem., Int. Ed.* **1999**, *38*, 3294–3306.
614. Hargittai, M. *Chem. Rev.* **2000**, *100*, 2233–2301.
615. Hargittai, M. *Acc. Chem. Res.* **2009**, *42*, 453–462.
616. Waters, A. F.; White, A. H. *Aust. J. Chem.* **1996**, *49*, 27–34.
617. Waters, A. F.; White, A. H. *Aust. J. Chem.* **1996**, *49*, 147–154.
618. Skelton, B. W.; Waters, A. F.; White, A. H. *Aust. J. Chem.* **1996**, *49*, 137–146.
619. Kepert, D. L.; Waters, A. F.; White, A. H. *Aust. J. Chem.* **1996**, *49*, 117–135.
620. Skelton, B. W.; Waters, A. F.; White, A. H. *Aust. J. Chem.* **1996**, *49*, 99–115.
621. Waters, A. F.; White, A. H. *Aust. J. Chem.* **1996**, *49*, 87–98.
622. Waters, A. F.; White, A. H. *Aust. J. Chem.* **1996**, *49*, 73–86.
623. Waters, A. F.; White, A. H. *Aust. J. Chem.* **1996**, *49*, 61–72.
624. Kepert, D. L.; Skelton, B. W.; Waters, A. F.; White, A. H. *Aust. J. Chem.* **1996**, *49*, 47–59.
625. Waters, A. F.; White, A. H. *Aust. J. Chem.* **1996**, *49*, 35–46.
626. Dehnicke, K.; Neumüller, B. *Z. Anorg. Allg. Chem.* **2008**, *634*, 2703–2728.
627. Neumüller, B.; Dehnicke, K. *Z. Anorg. Allg. Chem.* **2010**, *636*, 1516–1521.
628. Neumüller, B.; Dehnicke, K. *Z. Anorg. Allg. Chem.* **2003**, *629*, 2529–2534.
629. Neumüller, B.; Dehnicke, K. *Z. Anorg. Allg. Chem.* **2004**, *630*, 347–349.
630. Neumüller, B.; Dehnicke, K. *Z. Anorg. Allg. Chem.* **2004**, *630*, 1374–1376.
631. Neumüller, B.; Dehnicke, K. *Z. Anorg. Allg. Chem.* **2005**, *631*, 74–80.
632. Neumüller, B.; Dehnicke, K. *Z. Anorg. Allg. Chem.* **2006**, *632*, 1681–1686.
633. Neumüller, B.; Weller, F.; Dehnicke, K. *Z. Anorg. Allg. Chem.* **2003**, *629*, 2195–2199.
634. Puchta, R.; Neumüller, B.; Dehnicke, K. *Z. Anorg. Allg. Chem.* **2009**, *635*, 1196–1199.
635. Tonner, R.; Frenking, G.; Neumüller, B.; Dehnicke, K. *Z. Anorg. Allg. Chem.* **2007**, *633*, 1183–1188.
636. Braunschweig, H.; Gruss, K.; Radacki, K. *Angew. Chem., Int. Ed.* **2009**, *48*, 4239–4241.
637. Gerrard, L. A.; Weller, M. T. *Chem. Commun.* **2003**, 716–717.
638. Gerrard, L. A.; Weller, M. T. *Chem. Mater.* **2004**, *16*, 1650–1659.
639. Gerrard, L. A.; Weller, M. T. *Chem.—Eur. J.* **2003**, *9*, 4936–4942.
640. Gerrard, L. A.; Weller, M. T. *J. Chem. Soc., Dalton Trans.* **2002**, 4402–4406.
641. Dimitrov, A.; Wuttke, S.; Troyanov, S.; Kernitz, E. *Angew. Chem., Int. Ed.* **2008**, *47*, 190–192.
642. Wehmschulte, R. J.; Twamley, B.; Khan, M. A. *Inorg. Chem.* **2001**, *40*, 6004–6008.
643. Vollet, J.; Hartig, J. R.; Baranowska, K.; Schnöckel, H. *Organometallics* **2006**, *25*, 2101–2103.
644. Tavčar, G.; Žemva, B. *Angew. Chem., Int. Ed.* **2009**, *48*, 1432–1434.
645. Nembenna, S.; Roesky, H. W.; Nagendran, S.; Hofmeister, A.; Magull, J.; Wilbrandt, P.-J.; Hahn, M. *Angew. Chem., Int. Ed.* **2007**, *46*, 2512–2514.
646. Barrett, A. G. M.; Crimmin, M. R.; Hill, M. S.; Hitchcock, P. B.; Procopiou, P. A. *Angew. Chem., Int. Ed.* **2007**, *46*, 6339–6342.
647. Sarish, S. P.; Jana, A.; Roesky, H. W.; Schulz, T.; Stalke, D. *Organometallics* **2010**, *29*, 2901–2903.
648. Chi, Y.; Ranjan, S.; Chou, T.-Y.; Liu, C.-S.; Peng, S.-M.; Lee, G.-H. *J. Chem. Soc., Dalton Trans.* **2001**, 2462–2466.
649. Sloan, J.; Wright, D. M.; Bailey, S.; Brown, G.; York, A. P. E.; Coleman, K. S.; Green, M. L. H.; Sloan, J.; Wright, D. M.; Hutchison, J. L.; Woo, H.-G. *Chem. Commun.* **1999**, 699–700.
650. Sloan, J.; Grosvenor, S. J.; Friedrichs, S.; Kirkland, A. I.; Hutchison, J. L.; Green, M. L. H. *Angew. Chem., Int. Ed.* **2002**, *41*, 1156–1159.
651. Pevec, A. *Inorg. Chem.* **2004**, *43*, 1250–1256.

This page intentionally left blank

## 1.38 Alkaline Earth Chemistry: Applications in Catalysis

M Arrowsmith and MS Hill, University of Bath, Bath, UK

© 2013 Elsevier Ltd. All rights reserved.

<b>1.38.1</b>	<b>Introduction</b>	1189
1.38.1.1	Background: The Group 2 Elements in Synthesis	1189
1.38.1.2	Reactivity of Heavier Alkaline Compounds: Comparisons with Trivalent Lanthanide Chemistry	1189
1.38.1.3	Catalysis with Group 2 Complexes	1190
1.38.1.4	The Schlenk Equilibrium and Precatalyst Selection	1191
<b>1.38.2</b>	<b>Polymerization Catalysis</b>	1192
1.38.2.1	Polymerization of Polar Monomers	1192
1.38.2.2	Polymerization of Styrene	1194
1.38.2.3	Oligomerization Reactions	1195
<b>1.38.3</b>	<b>Heterofunctionalization of Unsaturated Bonds</b>	1196
1.38.3.1	Intra- and Intermolecular Hydroamination of Unsaturated Bonds	1196
1.38.3.2	Intermolecular Hydrophosphination of Unsaturated Bonds	1201
1.38.3.3	Intermolecular Hydroacetylenation of Carbodiimides	1204
1.38.3.4	Intermolecular Hydrosilylation of Unsaturated Bonds	1204
1.38.3.5	Hydroboration of N-Heterocycles	1206
1.38.3.6	Hydrogenation of Activated Alkenes	1206
<b>1.38.4</b>	<b>Catalytic Dehydrocoupling of <math>\sigma</math>-Bonds</b>	1207
1.38.4.1	Dehydrocoupling of Silanes and Amines	1207
1.38.4.2	Amine Borane Dehydrocoupling	1208
<b>1.38.5</b>	<b>Lewis Acid-Catalyzed Carbon–Carbon Bond Formation</b>	1211
1.38.5.1	Hydroarylation of Alkenes	1211
1.38.5.2	Enantioselective Aldol Reactions	1211
1.38.5.3	Asymmetric 1,4-Addition and [2+3]-Cycloaddition Reactions	1212
1.38.5.4	Asymmetric Addition of Esters and Imidates to Imines (Mannich-Type Reactions)	1213
<b>1.38.6</b>	<b>Conclusion</b>	1214
<b>References</b>		1214

### 1.38.1 Introduction

#### 1.38.1.1 Background: The Group 2 Elements in Synthesis

Although a century has passed since the Nobel Prize award to Victor Grignard,<sup>1</sup> the organometallic and reaction chemistry of the alkaline earth metals remains dominated by his eponymous organomagnesium compounds.<sup>2–4</sup> The ready synthesis of Grignard reagents, RMgX, and Hauser bases, R<sub>2</sub>NMgX (R=alkyl or aryl, X=halide),<sup>5</sup> and their application in the stoichiometric synthesis of new carbon–carbon, transition element–carbon and main group element–carbon  $\sigma$ -bonds have resulted in their position as workhorse reagents in both organic and organometallic syntheses. While early efforts to obtain analogous heavier alkaline earth (Ae) alkyl or aryl halides, R/ArAeX, indicated similar constitutions and chemical behavior,<sup>6,7</sup> the extremely air and moisture sensitivity and thermal instability of these compounds for a long time impeded the development of a related calcium, strontium, or barium chemistry. Although some progress was made during the 1990s through the synthesis of  $\sigma$ -bonded organometallic and amide derivatives (e.g., the bis(trimethylsilyl)-methyl and -amide compounds **1**<sup>8</sup> and **2**<sup>9</sup>), only very limited reactivity was reported, while the need for specialized techniques such as the metal vapor synthesis employed in the preparation of compound **1** hardly encouraged optimism for the

development of a rich and well-defined reaction chemistry. The prevailing opinion of the synthetic potential of the heavier group 2 elements at the end of the twentieth century can, thus, be gauged from a telling commentary provided by an undergraduate textbook published in 1999:<sup>10</sup>

The organic compounds of these elements are of little synthetic use compared to the magnesium compounds.

Although it was only in 2006 that the first definitive identification of a calcium 'Grignard analog,' the thermally sensitive mesitylcalcium iodide, compound **3**,<sup>11–15</sup> was described, the activities of the first decade of the twenty-first century have done much to overturn this prejudice primarily through the emergence of a rapidly expanding catalytic group 2 chemistry.

#### 1.38.1.2 Reactivity of Heavier Alkaline Compounds: Comparisons with Trivalent Lanthanide Chemistry

An assessment of the reactivity of heavier alkaline earth species requires an initial consideration of the nature of the elements themselves and their ability to form complexes suitable for coherent study. Upon descending the group, the divalent alkaline earth cations display a dramatic 88% increase in ionic radius from magnesium to barium (Mg<sup>2+</sup>, 0.72 Å; Ca<sup>2+</sup>,

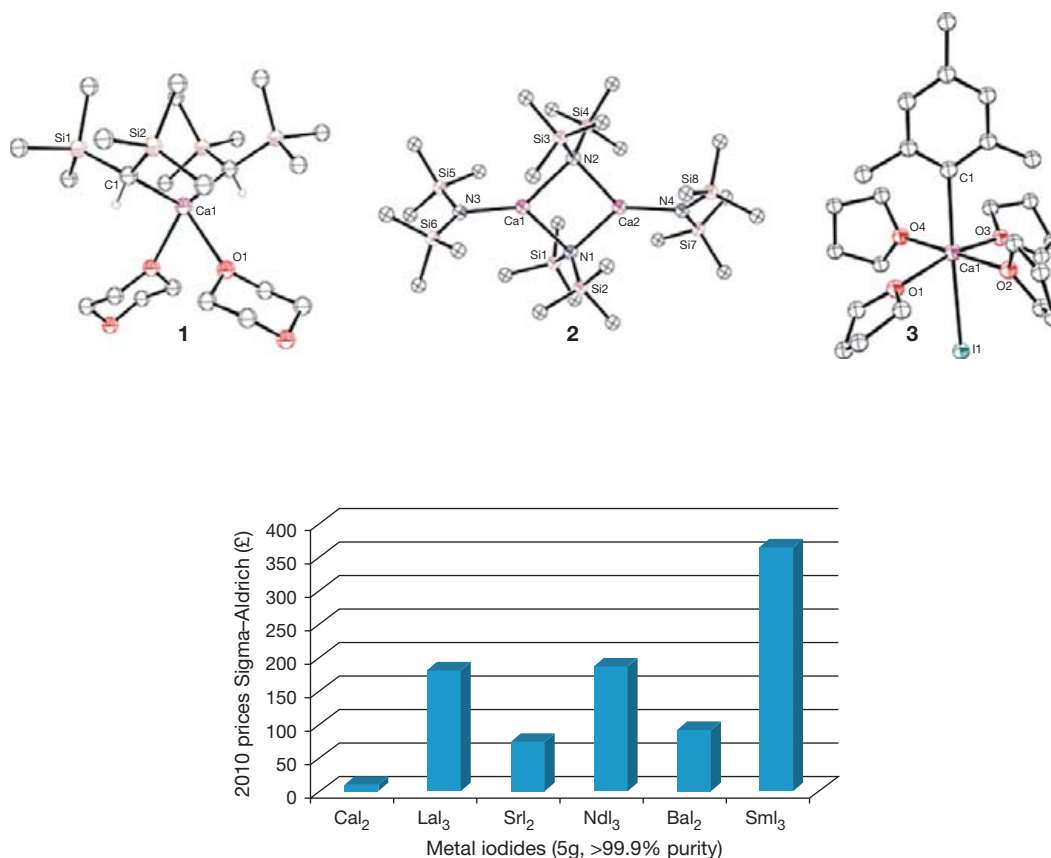


**Figure 1** Comparison between the cost of alkaline earth and rare earth starting materials.<sup>24</sup>

1.00 Å; Sr<sup>2+</sup>, 1.18 Å; Ba<sup>2+</sup>, 1.35 Å)<sup>16</sup> accompanied by a marked decrease in electronegativity.<sup>17</sup> As a result, metal–ligand bonding becomes increasingly ionic and nondirectional. Furthermore, with the exception of a handful of outstanding examples of subvalent Mg(I) and Ca(I) compounds displaying metal–metal bonds and stabilized by either bulky ligands or extended  $\pi$ -systems,<sup>18–20</sup> the vast majority of complexes of the alkaline earth elements are redox inactive and may be viewed as achieving a d<sup>0</sup> electronic configuration upon forming their common 2+ oxidation state. Consequent comparisons have often been made with the properties of similarly d<sup>0</sup> lanthanide cations which are generally found in their principal 3+ oxidation state.<sup>21</sup> Lanthanide complexes are also characterized by their redox inactivity and ionic metal–ligand bonding resulting from a high electropositivity and limited polarizability.<sup>22,23</sup> Moreover, the 4f-orbitals, which remain shielded by the 5s<sup>2</sup>5p<sup>6</sup> outer shell electrons, do not intervene in complex formation. Although parallels have also been drawn between the size of the Ca<sup>2+</sup> dication and the ionic radii of the largest lanthanide cations (La<sup>3+</sup>, 1.03 Å; Nd<sup>3+</sup>, 0.98 Å; Sm<sup>3+</sup>, 0.96 Å), the 88% increase in size down the group from Mg<sup>2+</sup> to Ba<sup>2+</sup> contrasts markedly with the 16% range provided by the lanthanide contraction from La<sup>3+</sup> to Yb<sup>3+</sup>.<sup>16</sup> Similarly, Pauling electronegativity decreases by 35% from magnesium to barium, whereas only a 15% increase is observed from lanthanum to ytterbium.<sup>17</sup> While the larger Ae<sup>2+</sup> dications display higher polarizability, their increasingly diffuse charge induces weaker polarizing power, and it may, thus, be surmised that a wider

variation of reactivity might be expected from complexes of the heavier alkaline earth metals. From an economic and sustainability point of view, the availability of calcium as the fifth most abundant element in the earth's crust (4.15 wt.%) and the relative abundance of the other alkaline earth metals compared with the rare earth metals make research into this nascent area of chemistry even more desirable, as shown by the cost comparison of alkaline earth versus lanthanide starting materials as illustrated in **Figure 1**.

Although, due to a lacuna of appropriate reagents, the entry point into this chemistry remains relatively narrow, the recent development of a variety of stable heavier alkaline earth alkyl,<sup>25</sup> benzyl,<sup>26</sup> hydrido,<sup>27</sup> and amido<sup>9,28</sup> reagents has facilitated the growth of a defined reaction chemistry and the emergence of chemical behavior which is dictated by the fundamental characteristics of the individual elements.

### 1.38.1.3 Catalysis with Group 2 Complexes

Whereas heterogeneous alkaline earth oxide and alkoxide catalysts have been studied for several decades and have found various industrial applications, often in combination with other metals (Li, Al, etc.),<sup>29</sup> homogeneous catalysis with group 2 complexes is still in its infancy.<sup>30</sup> A notable body of work arose during the 1980s centered on the use of lanthanide complexes of the form L<sub>2</sub>LnX (L=monoanionic spectator ligands, e.g., cyclopentadienyl; X=monoanionic substituents, e.g., alkyl, amide, phosphide, and hydride) in a variety of

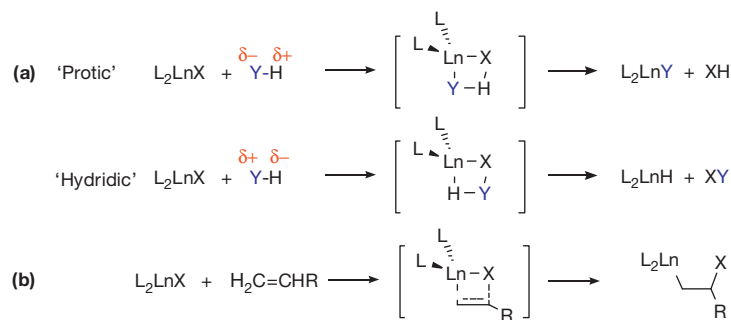


**Figure 2** Stoichiometric reactivity of lanthanide complexes: (a)  $\sigma$ -bond metathesis and (b) insertion.

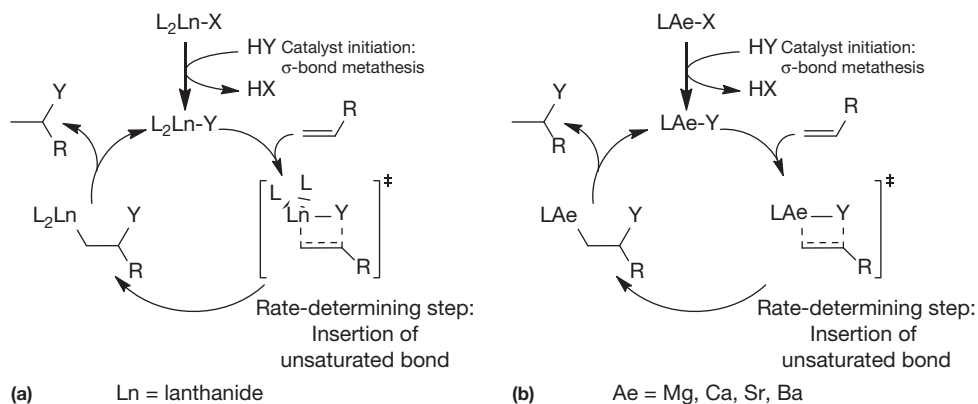


**Figure 3** General catalytic cycle for (a) lanthanide-mediated (b) alkaline earth-mediated heterofunctionalization of carbon-carbon double bonds.

catalytic transformations.<sup>31</sup> In the absence of any notable redox behavior, this is necessarily based on two simple mechanistic pathways: (a) the  $\sigma$ -bond metathesis or protonolysis of a monoanionic substituent X, the chemoselectivity of which is dependent upon the substrate bond polarity and (b) the polarized insertion of unsaturated bonds into the Ln-X  $\sigma$ -bond (Figure 2).

Incorporated into catalytic cycles, these two reactions have enabled a vast number of synthetic reactions ranging from the inter- and intramolecular heterofunctionalization of carbon-carbon multiple bonds (hydroamination, hydrophosphination, hydroalkoxylation, hydrosilylation, hydroboration, etc.) to the polymerization of alkenes.<sup>31</sup> A general catalytic cycle for these lanthanide-catalyzed reactions is presented in Figure 3(a). Activation of the precatalyst occurs through either reversible or irreversible  $\sigma$ -bond metathesis, followed by the rate-determining insertion of the unsaturated bond proceeding via a four-membered cyclic transition state. The resulting highly reactive lanthanide alkyl species is then engaged in a further  $\sigma$ -bond metathesis (or protonolysis) reaction to liberate the functionalized product and regenerate the active catalyst. Sterically encumbered ligands are of importance for the kinetic stabilization of the active species in order to avoid ligand redistribution toward unreactive homoleptic complexes or dimerization leading to a decrease in reactivity. While highly substituted and ansa-bridged cyclopentadienyls have proved the spectator ligands of choice for many of these transformations,<sup>32</sup> recent years have seen a change of focus toward a wide variety of sterically demanding chiral noncyclopentadienyl ligands for stereoselective catalysis.<sup>33</sup>

Figure 3(b) presents an analogous heterofunctionalization pathway based upon a reactive alkaline earth complex, LAeX, where L is a monoanionic supporting ligand and X is a reactive  $\sigma$ -bonded substituent (X = NR<sub>2</sub>, OR, R, and H). Whether based on homoleptic precatalysts of the form AeX<sub>2</sub> (X = NR<sub>2</sub>, OR, and R) or heteroleptic compounds of the form LAeX where L is a bulky monoanionic spectator ligand, the challenge of constructing a cycle such as that illustrated is not simply dependent upon the viability of the individual metathesis and insertion steps. Compounds of the group 2 elements do not benefit from ligand field effects. Any influence over solution behavior, therefore, is largely dependent upon kinetic control of the alkaline earth coordination sphere.

#### 1.38.1.4 The Schlenk Equilibrium and Precatalyst Selection

As homoleptic alkaline earth compounds of the form AeX<sub>2</sub> may often be polymeric or insoluble in hydrocarbon solvents, research has focused on the design of sterically demanding, lipophilic monoanionic ligands, L, to stabilize and solubilize group 2 amide, alkoxide, alkyl, or hydride functionalities in heteroleptic complexes of the form LAeX. Due to a weakening of the metal-ligand bonds down the group, however, the larger alkaline earth metal centers present an increasing problem of ligand exchange and the establishment of Schlenk-type equilibria analogous to the dynamic behavior of Grignard reagents, RMgX, and their propensity toward redistributing to the homoleptic MgR<sub>2</sub> and MgX<sub>2</sub> species.<sup>34</sup> In the case of heteroleptic LAeX complexes, these tend to irreversibly redistribute toward the kinetically stabilized homoleptic AeL<sub>2</sub> and AeX<sub>2</sub> species

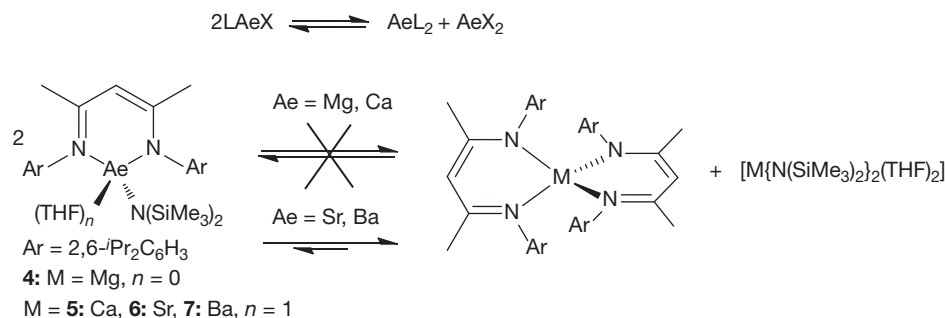


**Figure 4** Schlenk-type ligand redistribution for the  $\beta$ -diketiminato amide complexes of Mg, Ca, Sr, and Ba.

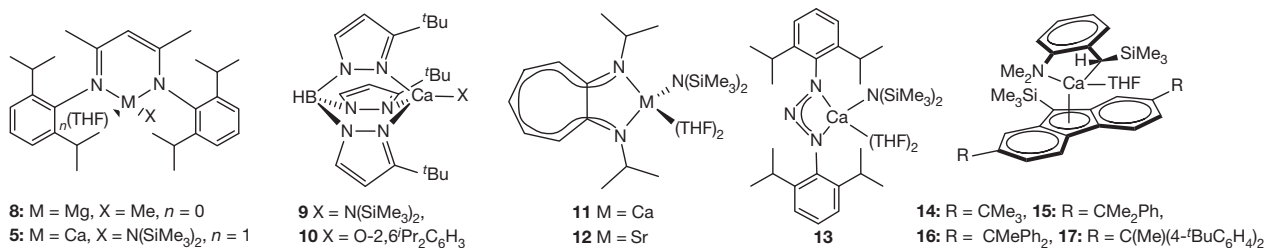


**Figure 5** Examples of heteroleptic alkaline earth pre-catalysts.

(Figure 4), the former being catalytically inactive while the latter, although still active, might be insoluble or cause a dramatic change in catalytic activity and selectivity, especially when dealing with chiral LAeX complexes for potentially enantioselective catalysis. For the case of the  $\beta$ -diketiminato alkaline earth bis(trimethylsilyl)amides (compounds 4–7), for example, shown in Figure 4, the heteroleptic magnesium and calcium analogs can be readily isolated in good purity and show no or little ligand lability in solution even at high temperatures. The related strontium and barium complexes, however, are found to be in solution equilibrium with the homoleptic species, even at room temperature.<sup>35</sup> Another common problem is that of the dimerization of heteroleptic species bearing small monoanionic co-ligands, which may impede catalytic reactions by blocking vacant coordination sites.

While early research focused on sterically demanding cyclopentadienyl ligands to overcome this problem, the resulting half-sandwich calcium amide, acetylide, halide, or borohydride complexes, although heteroleptic in the solid state, often remained prone to Schlenk-type ligand redistribution in solution and thus of limited potential as pre-catalysts.<sup>36</sup> Also, as the synthesis of heteroleptic strontium or barium metallocenes proved to be rather elusive, attention shifted toward monoanionic noncyclopentadienyl ligands bearing bulky substituents which could be easily tuned for steric, electronic, and potentially chiral effects. A landmark in this area was the isolation by Chisholm and coworkers of heteroleptic calcium  $\beta$ -diketiminato and tris(pyrazolyl)borate complexes 5, 9, and 10 and their application to the ring-opening polymerization of lactides in 2004 (Figure 5 and Section 1.38.2.1).<sup>37</sup> Since then the  $\beta$ -diketiminato ligand has been successfully employed to stabilize a wide variety of heteroleptic magnesium, calcium, and strontium complexes bearing small functionalities (F, OH,  $\text{NH}_2$ , CN, H, etc.) obtained via  $\sigma$ -bond metathesis.<sup>38</sup> It is therefore unsurprising that heteroleptic amide and hydride

complexes based on this particular ligand have so far been used in the majority of alkaline earth-catalyzed reactions, together with heteroleptic tris(pyrazolyl)borate (9, 10),<sup>37</sup> amino-troponimate (11, 12),<sup>39</sup> triazene (13),<sup>40</sup> and bis- and tris(imidazolin-2-ylidene-1-yl)borate<sup>42</sup> group 2 amide complexes and dearomatized bis(imino)acenaphthene,<sup>43</sup> and fluorenyl-supported organometallic species (14–17) (Figure 5).<sup>44</sup>

## 1.38.2 Polymerization Catalysis

### 1.38.2.1 Polymerization of Polar Monomers

The catalytic synthesis of polymers with either mechanical or pharmaceutical and medicinal applications, such as poly(methyl methacrylate) (PMMA) or poly(lactide) (PLA),<sup>45</sup> requires the catalyst to be either entirely removable from the finished product or, if this is not the case, at least noncolored or biocompatible. As biocompatible metals, magnesium and calcium have, therefore, been identified as highly desirable for these catalytic transformations. The earliest polymerization studies with homogeneous alkaline earth catalysts date back as far as the early 1970s. In 1974, Lindsell and coworkers reported the highly syndiotactic polymerization of MMA with bis(cyclopentadienyl) calcium pre-catalysts, albeit in very poor yield (8%).<sup>46</sup> Attempts by M. S. Chisholm's group to reproduce the tacticity of these results failed but introduced the use of more soluble  $[(\text{Cp}^*)_2\text{Ca}(\text{THF})_2]$  (THF, tetrahydrofuran) to achieve high yields of essentially atactic PMMA.<sup>47</sup> Later studies by Schumann with similar homoleptic and heteroleptic Mg, Ca, Sr, and Ba pre-catalysts allowed fast and near quantitative polymerization of functionalized methacrylate monomers and the formation of block-copolymers.<sup>48</sup> The use of heteroleptic  $\beta$ -diketiminato magnesium enolate dimer 18 by Dove et al. as shown in Figure 6 provided fast, living, and highly syndioselective polymerization of PMMA ( $\text{tr} = 96\%$ ).<sup>49</sup>

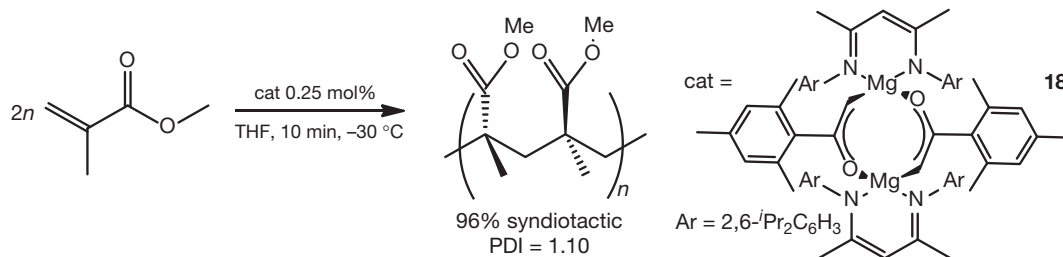


**Figure 6** Syndioselective polymerization of MMA.

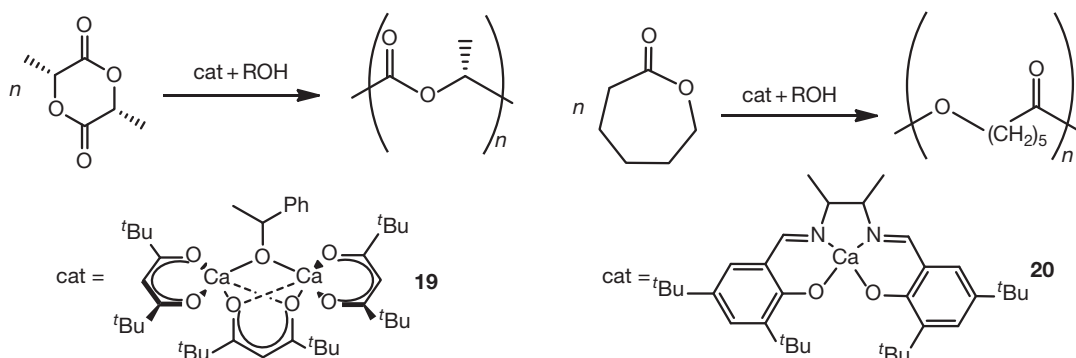


**Figure 7** Polymerization of L-lactide and  $\epsilon$ -caprolactone with examples of group 2 catalysts.

Until recently, the most efficient catalysts for the polymerization of cyclic esters such as lactide (LA),  $\epsilon$ -caprolactone ( $\epsilon$ -CL), and trimethylene carbonate (TMC) were based upon zinc as well as other transition and main group metals. Over the last decade, however, research has turned increasingly toward biocompatible alkaline earth-based catalysts for these polymerization reactions. As early as 1996,  $\text{CaH}_2$  was reported to promote the copolymerization of L-LA and poly(ethylene glycol).<sup>50</sup> Calcium and magnesium acetylacetonate complexes, such as 19, as well as dibutylmagnesium have also been used to catalyze the ring-opening polymerization of both L-LA and  $\epsilon$ -CL with glycolide (Figure 7). The resulting polymers were found to be entirely compatible with brain tissue.<sup>51</sup> In 2001, Feijin and Westerhausen investigated the potential of commercially available  $[\text{Ca}(\text{OMe})_2]$  as well as *in situ*-generated alkoxide species from more soluble  $[\text{Ca}\{\text{N}(\text{SiMe}_3)_2\}_2(\text{THF})_2]$  showing the latter to be efficient precatalysts for the living polymerization of both  $\epsilon$ -CL and L-LA without racemization. The resulting polymers were found to have narrow polydispersities, enabling the formation of block-copolymers.<sup>52</sup> Since then a growing number of heteroleptic monomeric, dimeric, and even trimeric calcium amide, alkoxide and magnesium alkyl species, as well as several complexes bearing bis(phenolate) ligands have been tested for the polymerization and copolymerization of L-LA and  $\epsilon$ -CL.<sup>53</sup> Although there are only very few examples of strontium and barium catalysts for the ring-opening polymerization of L-LA and  $\epsilon$ -CL,<sup>54</sup> a family of cationic heavier alkaline earth complexes ( $\text{Ae} = \text{Mg}, \text{Ca}, \text{Sr}, \text{and Ba}$ ) stabilized by azacrown ether-substituted phenoxide or hexafluoropropoxide ligands has been reported to catalyze the immortal ring-opening polymerization of L-LA when activated with an excess (5–50 equiv.) of external protic nucleophilic agents ( $\text{BnOH}, ^i\text{PrOH}$ ). In this case, an order of reactivity

$\text{Mg} < \text{Ca} < \text{Sr} \approx \text{Ba}$  was established while complexes supported by the aryloxy ligands were more active than those supported by the fluorinated alkoxide ancillary, an observation that was ascribed to the possible additional stabilization through the formation of persistent  $\text{Ae} \cdots \text{F}$  contacts (estimated as 12–40  $\text{kcal mol}^{-1}$  by density functional theory (DFT) calculations).<sup>55</sup> For the polymerization of TMC and its copolymerization with L-LA, Darendsbourg has studied the use of tridentate and tetradentate Schiff base derivatives of calcium and magnesium such as 20.<sup>56</sup>

Stereocontrolled polymerization of *rac*-lactide was first achieved by Chisholm and coworkers using tris(pyrazolyl)borate calcium amide and phenoxide complexes 9 and 10.<sup>37</sup> Thus, with 0.5 mol.% of 10 conversions >90% and heterotacticity of 90% were obtained in <1 min (Figure 8) in THF at room temperature. Similarly, high heteroselectivity has also been obtained with a  $\beta$ -diketiminato magnesium methoxide catalyst,<sup>57</sup> while the first cationic main group tetrahydroborate complex  $[\text{Ca}(\text{BH}_4)(\text{THF})_5][\text{BPh}_4]$  and the charge neutral tris(pyrazolyl)hydroborate complex  $\{\{\text{Tp}^i(\text{BuMe})\}\text{Ca}(\text{BH}_4)(\text{THF})\}$  have been employed as initiators for the living ring-opening polymerization of *rac*-lactide with the latter species providing high levels of heterotactic enrichment (80–90%).<sup>58</sup>

The Union Carbide catalyst  $[(\text{NH}_2)_2\text{Ca}(\text{O}^i\text{Pr})]$  has been shown to promote the ring-opening polymerization of propylene oxide while 3-(S)-isopropylmorpholine-2,5-dione could be polymerized with  $\text{CaH}_2$  in the presence of poly(ethylene oxide).<sup>59</sup> Although several attempts have been made to design bimetallic calcium and magnesium catalysts for the copolymerization of cyclohexene oxide and  $\text{CO}_2$ , the only successful approach has been reported by Xiao et al. whose bimetallic magnesium complex 21 proved to be efficient even at 1 bar  $\text{CO}_2$  pressure (Figure 9).<sup>60</sup>

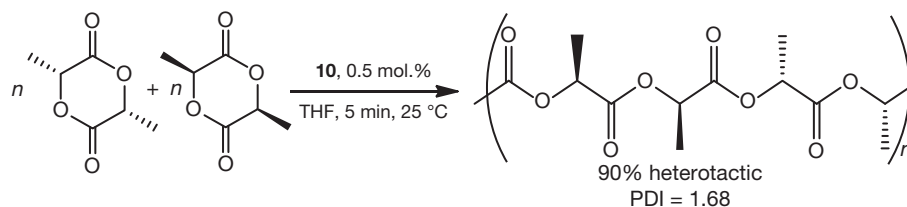


**Figure 8** Stereoselective polymerization of *rac*-lactide with calcium tris(pyrazolyl)borate complex **10**.

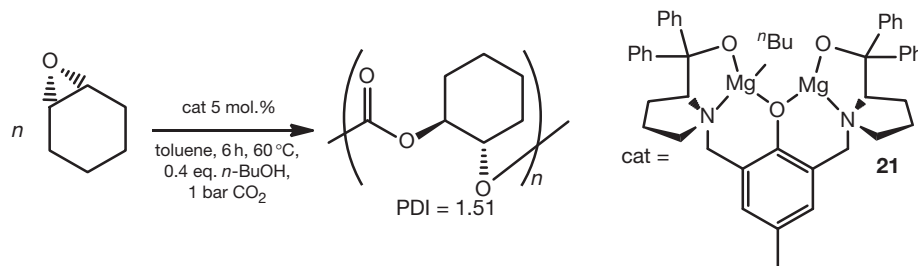


**Figure 9** Copolymerization of cyclohexene oxide and  $\text{CO}_2$  with a bimetallic magnesium catalyst.

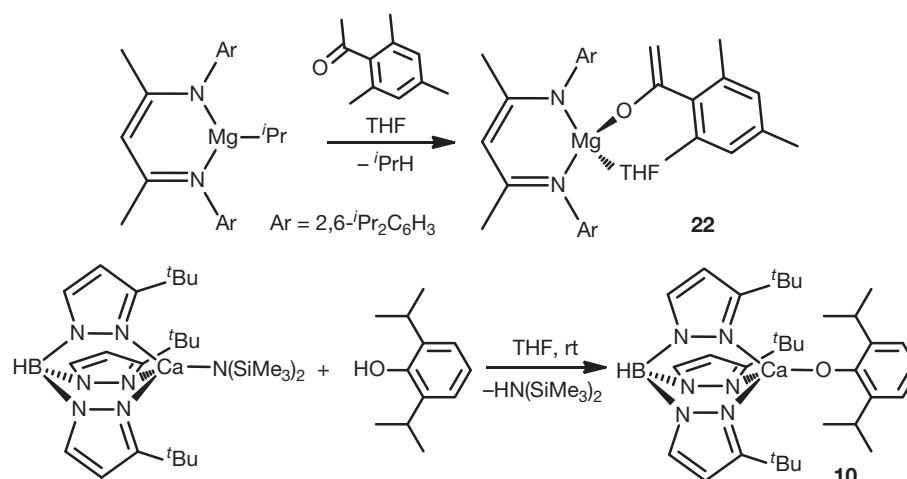


**Figure 10** Examples of catalyst activation through  $\sigma$ -bond metathesis of a magnesium alkyl and a calcium amide precursor with an enolizable ketone and a phenol respectively.<sup>28,39</sup>

In all the above-mentioned studies, catalyst activities were shown to be dependent on the metal center, with turnover frequencies in the order of  $\text{Ca} > \text{Mg} > \text{Zn}$  when analogs of all three metals were compared. In general, reactions are living, first order in monomer and take place without any induction period. Catalyst activation is usually achieved by  $\sigma$ -bond metathesis (protonolysis) of a group 2 amide or alkyl precursor with an alcohol, phenol, or enolizable ketone as shown in **Figure 10**, a step which is well documented in the literature.<sup>49,61,62</sup>

Subsequent polymer propagation proceeds via multiple insertion steps of the carbonyl functionality of the substrate into the metal–alkoxide bond of the active catalyst. The only examples of stoichiometric insertion of this type have been reported by Mingos and coworkers, with the insertion of carbonyl sulfide and carbon dioxide into the M–O bonds of

alkaline earth bis(alkoxide) species,<sup>63</sup> and by Harder and Roesky whose attempt to insert carbon dioxide into the Ca–O bond of heteroleptic calcium hydroxide dimer **23** resulted in the irreversible protonation of the  $\beta$ -diketiminato ligand accompanied by slow precipitation of calcium carbonate according to the reaction pathway proposed in **Figure 11**.<sup>62</sup>

### 1.38.2.2 Polymerization of Styrene

The polymerization of alkenes with group 2 metal centers appears to require conjugation of the alkene monomer. In 2000, Weeber et al. reported the first dibenzylbarium catalyst for the polymerization of styrene.<sup>64</sup> The reaction, however, was neither living nor stereoselective and presented a slow initiation as well as high ligand lability of the catalyst due to the highly diffuse charge density of the large barium center. Efforts

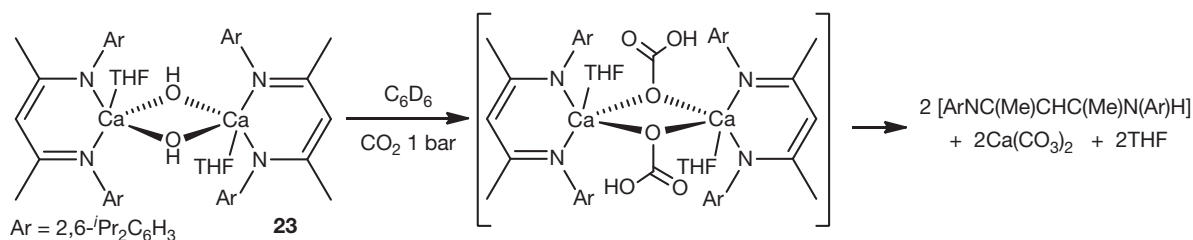


**Figure 11** Insertion of  $\text{CO}_2$  into a Ca–O bond, followed by decomposition into  $[\text{Ca}(\text{CO}_3)_2]$ .

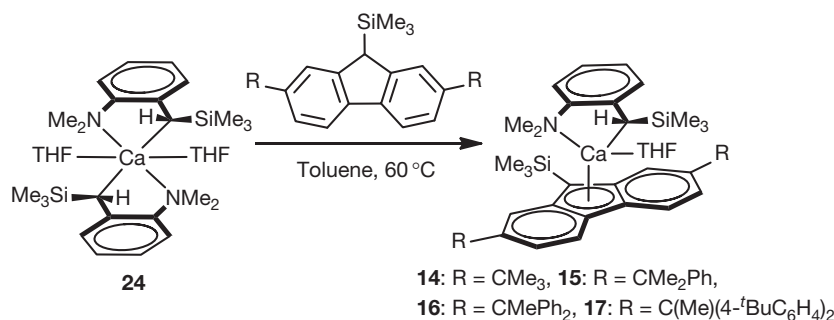


**Figure 12** Synthesis of heteroleptic benzylcalcium initiators by  $\sigma$ -bond metathesis for stereoselective styrene polymerization.

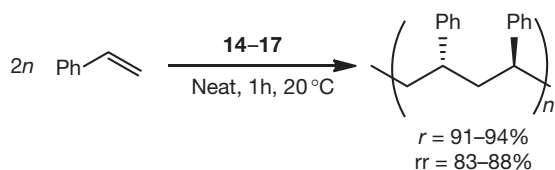


**Figure 13** Syndiospecific polymerization of styrene.

by Harder and coworkers thereafter focused on more readily manipulated calcium initiators based on the chiral bidentate (2- $\text{NMe}_2$ - $\alpha$ - $\text{Me}_3\text{Si}$ -benzyl) ligand, compound 24.<sup>26,65</sup>

Although highly active for the living anionic polymerization reaction, the homoleptic diastereomeric catalyst 24 produced largely atactic polystyrene due to racemization in solution. The heteroleptic versions, however, obtained by  $\sigma$ -bond metathesis between a number of heavily substituted fluorenes (Figure 12), allowed the production of a polymer of up to 94% syndiotacticity in diads from neat styrene at 20 °C (Figure 13).<sup>44,66</sup> Stereoselectivity was found to increase with the steric bulk of the fluorenyl substituents.

In all cases, broad-molecular-weight distributions, due to slow catalyst initiation, prevented the synthesis of block-copolymers. The reaction mechanism was reasoned to involve precoordination of the alkene as the presence of coordinated THF deactivates the precatalyst, with propagation proceeding via multiple insertion of styrene into the metal–alkyl bond. In support of this hypothesis, Harder and coworkers have shown that the reaction of  $[\text{Ba}(\text{CH}_2\text{Ph})_2(\text{THF})_2]$  with 1,1-diphenylethene yields quantitative insertion of the alkene into the Ba–C bonds to form  $[\text{Ba}\{\text{C}(\text{Ph})_2\text{CH}_2\text{CH}_2\text{Ph}\}_2(\text{THF})_2]$ , 25, which was characterized by  $^1\text{H}$  NMR spectroscopy (Figure 14).<sup>64</sup>

### 1.38.2.3 Oligomerization Reactions

A small number of oligomerization reactions mediated by heavier group 2 metals have been reported. In 2007, Crimmin et al. showed that the dimerization of a variety of aldehydes to form the analogous ester, also known as Tischenko reaction, could be catalyzed by the simple homoleptic bis(bis(trimethylsilylamide)) complexes,  $[\text{M}\{\text{N}(\text{SiMe}_3)_2\}_2]_2$  ( $\text{M}$  = group 2 element) with catalyst activity in the order of  $\text{Ca} > \text{Sr} > \text{Ba}$  (Figure 15).<sup>67</sup> Given that the reaction involves the formal reduction of one aldehyde molecule while the other one is oxidized and that group 2 metals are redox inactive, the catalytic process necessarily involves a hydride transfer between aldehydes. Quenching of the catalytic reaction with benzaldehyde in the early stages showed that catalyst initiation generates a calcium alkoxide intermediate with liberation of a benzamide through a Meerwein–Ponndorf–Verley-type reduction of the aldehyde. This is followed by insertion of the second aldehyde equivalent into the metal–alkoxide bond and hydride transfer to another equivalent of aldehyde to regenerate the catalyst and liberate the ester. A similar protocol has also been reported utilizing well-defined magnesium guanidinate complexes.<sup>68</sup>

Harder and coworkers demonstrated that the catalytic trimerization of phenyl and cyclohexyl isocyanate can be achieved with calcium methanediide complex 26 at room temperature (Figure 16).<sup>69</sup> Thanks to the very slow reaction rate of the cyclohexyl substrate, the double-insertion intermediate 27, which also proved active as a catalyst, could be isolated and crystallographically characterized.

In reactivity somewhat reminiscent of organolanthanide and  $d^0$  transition metal alkynyl reactivity, Hill and coworkers reported the unexpected catalytic dimerization of 3-methoxypropyne to form the 2,3,4-hexatriene

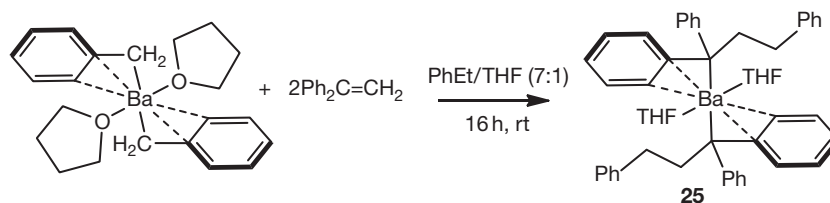


**Figure 14** Insertion of 1,1-diphenylethene into a barium–benzyl bond.

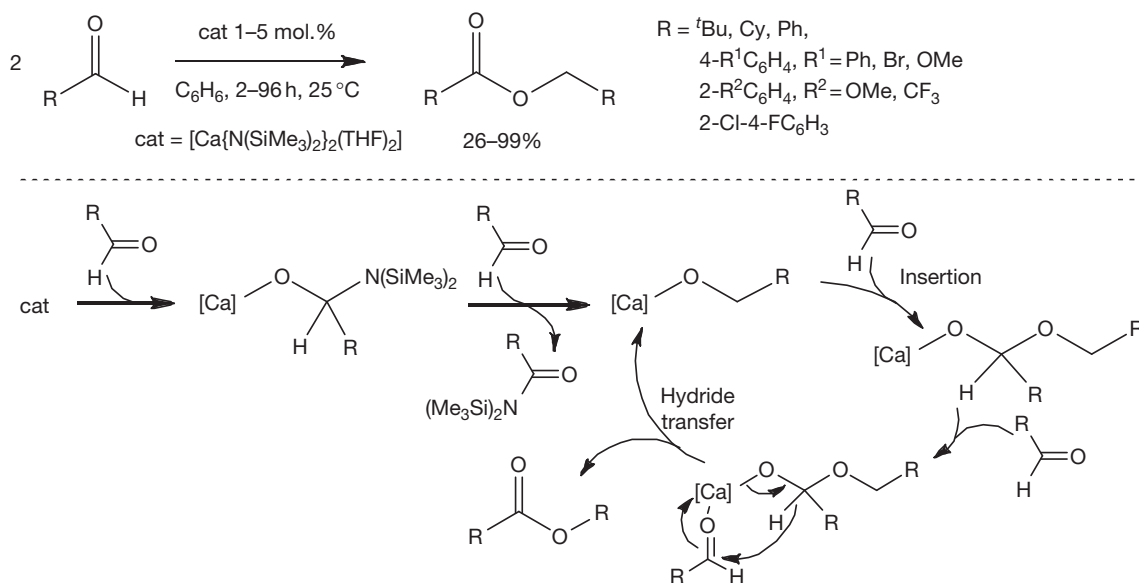


**Figure 15** Tischenko reaction with homoleptic group 2 amides and proposed mechanism.

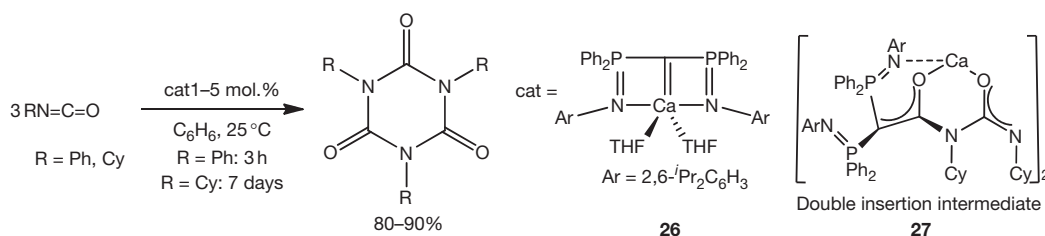


**Figure 16** Calcium-catalyzed trimerization of isocyanates.

[MeOCH<sub>2</sub>CH=C=C=CHCH<sub>2</sub>OMe] in the presence of heteroleptic calcium β-diketiminato and triazenide complexes **5** and **13** (Figure 17).<sup>70</sup> Since the dimerization of terminal alkynes with transition metal and lanthanide catalysts most often results in formation of the more stable enyne products, the exclusive production of the substituted hexatriene was, in this case, quite remarkable.

Catalyst initiation via σ-bond metathesis between the terminal alkyne and the alkaline earth amide precursor has been well documented in numerous stoichiometric reactions to form both homoleptic and heteroleptic group 2 acetylides (Figure 18).<sup>71,72</sup> The coupling reaction is then thought to proceed via a dimeric μ-(Z)-butatriene diyl bridging unit as has been shown to exist with group 3 or the 4f elements,<sup>73</sup> with the carbon–carbon bond formation driven by the asymmetric bridging mode and coordination of the ether moiety to the highly electropositive calcium centers.

### 1.38.3 Heterofunctionalization of Unsaturated Bonds

#### 1.38.3.1 Intra- and Intermolecular Hydroamination of Unsaturated Bonds

Pioneering studies in the early 1990s by Marks et al. demonstrated that achiral and chiral lanthanide compounds are among the most efficient catalysts for the intramolecular hydroamination/cyclization of aminoalkenes, -alkynes, -dienes, and -allenes.<sup>74</sup> In 2005, Crimmin et al. provided the first report of calcium-mediated intramolecular hydroamination of a number of aminoalkenes based on Chisholm's β-diketiminato calcium amide complex **5**, with catalytic activity comparable to the best of the group 3 and lanthanide systems (Figure 19).<sup>75</sup> Reactions proceeded at high rates and under mild conditions (25–60 °C) with moderate catalyst loadings to produce substituted pyrrolidines and piperidines in high yields without apparent ligand redistribution to the homoleptic and

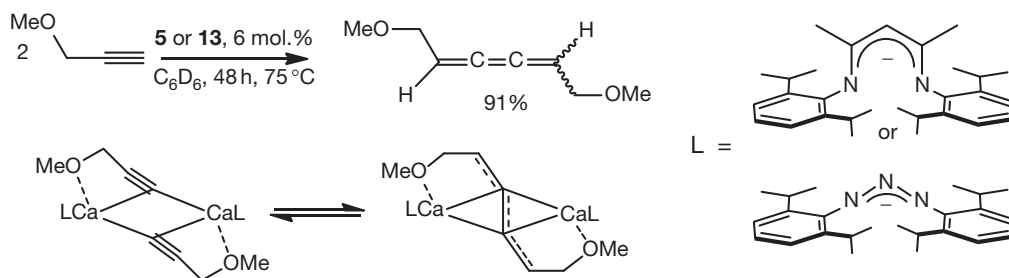


**Figure 17** Calcium-catalyzed dimerization of 3-methoxypropyne and proposed acetylide-butatriene diyl equilibrium.

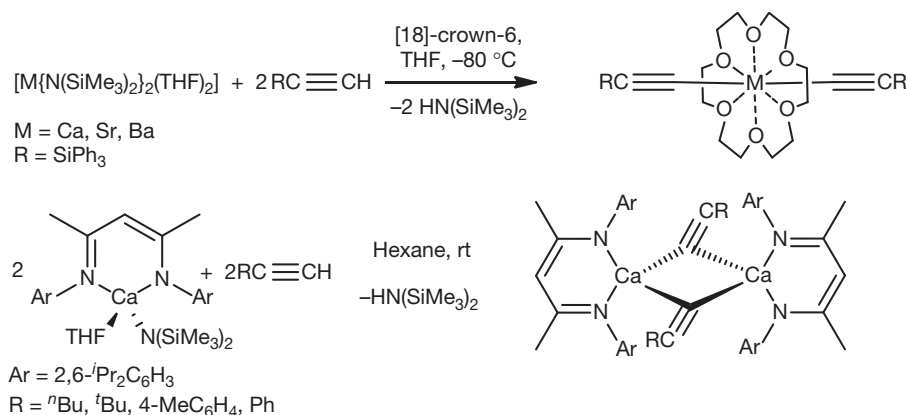


**Figure 18** Synthesis of homoleptic and heteroleptic group 2 acetylides by  $\sigma$ -bond metathesis.

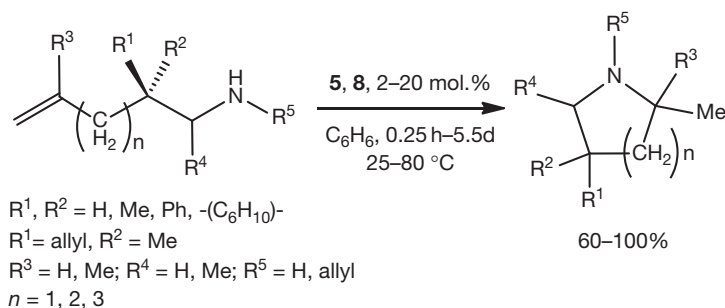


**Figure 19** Intramolecular hydroamination of aminoalkenes with heteroleptic Mg and Ca catalysts.

catalytically inactive calcium species. A subsequent study of an extensive range of aminoalkene substrates showed that the ease of cyclization, following Baldwin's guidelines for ring closure, decreased with ring size. While five-membered heterocyclic pyrrolidines could be obtained at room temperature and with low catalyst loadings (2–10 mol.%) in near quantitative yields within a few minutes, the formation of six- and seven-membered piperidines and hexahydroazepines required longer periods of time (up to 5.5 days), higher catalyst loadings (10–20 mol.%), and sometimes prolonged heating at 80 °C. Bulky substituents in the  $\beta$ -position of the amine facilitated cyclization by favoring reactive conformations of the transition states (Thorpe–Ingold effect), while internal substitution of the alkene moiety significantly hindered the reaction. None of the  $\beta$ -diketiminato precatalysts could achieve the hydroamination of substrates with internal alkenes under the reported reaction

conditions. Whereas prochirality in the  $\beta$ -position of the amine did not lead to diastereoselectivity, the  $\alpha$ -substituted aminoalkenes 1-amino-1-methylpent-4-ene and 1-amino-1-phenylpent-4-ene underwent diastereoselective hydroamination favoring the *trans*-geometry of the pyrrolidine in enantiomeric excess >78%, with the smaller magnesium metal center of precatalyst **8** affording significantly higher selectivity. Similar preference for the *trans*-conformation of the product had already been observed in the case of lanthanide-catalyzed hydroamination, with smaller metal centers providing increased diastereoselectivity induced by a tighter conformation of the rate-determining C=C insertion transition state. Although significantly more active as a catalyst than its magnesium counterpart **8**, the use of calcium complex **5** was limited by its propensity to deleterious Schlenk-like ligand redistribution at high temperatures, alkene isomerization side-reactions of 1-amino-5-hexene substrates, as

well as its inability to cyclize 1-amino-2,2-diphenyl-6-heptene into the resulting hexahydroazepines. In contrast, this latter reaction could be achieved, albeit very slowly and at high temperature (5.5 days, 80 °C, 88% yield) with the magnesium precatalyst.<sup>76</sup> Subsequent extension of this catalytic reactivity to homoleptic silylamides  $[M\{N(SiMe_3)_2\}_2]_2$  and  $[M\{N(SiMe_3)_2\}_2(THF)_2]$  ( $M = Mg, Ca, Sr,$  and  $Ba$ ) and the alkyl species  $[M\{CH(SiMe_3)_2\}_2(THF)_2]$  ( $M = Mg, Ca, Sr,$  and  $Ba$ ) provided similar observations. In general, the calcium precatalysts proved to be more reactive than their strontium analogs, which, in turn, proved to be far more reactive than the magnesium or barium species.<sup>77</sup>

The individual steps of the originally proposed catalytic cycle have been investigated with a series of stoichiometric reactions (Figure 20). Whereas  $\sigma$ -bond metathesis between magnesium alkyl complex 8 and a number of primary and secondary amines was shown to be fast and irreversible, yielding new isolable amide species, a stoichiometric reaction between calcium amide precatalyst 5 and benzylamine resulted in a quantifiable equilibrium with a  $\Delta G^\circ$  (298 K) of  $-11.4 \text{ kJ mol}^{-1}$ , indicating fast but reversible catalyst initiation.<sup>78</sup> Other less acidic amines such as *tert*-butylamine and cyclohexylamine were found to displace the THF of 5 to form an amine adduct, providing proof for precoordination of the amine and potential substrate inhibition during catalysis. Similar observations were provided through the reaction of the analogous strontium species  $[\{ArNC(Me)CHC(Me)NAr\}Sr\{N(SiMe_3)_2\}(THF)]$  ( $Ar = 2,6\text{-di-}i\text{-propylphenyl}$ ) 28 with 2-methoxyethylamine, which resulted in equilibration between the starting silylamide, an isolable amine adduct 29, and the product of amine/silylamide transamination 30.<sup>77</sup>

Use of silylamide precatalysts was, thus, reasoned to provide potentially reversible entry into the catalytic manifold.

Kinetic experiments with variable substrate concentrations at constant catalyst concentration and the resulting rate law both reflected a first-order dependence upon [catalyst] and revealed the importance of substrate and product inhibition, as had previously been demonstrated in analogous lanthanide-based reactions.<sup>74,76</sup> The presence of THF was also found to significantly retard reaction rates, and the catalytic hydroamination of deuterated substrates pointed toward a short-lived alkyl intermediate resulting from intramolecular insertion of the terminal alkene into the metal–amide bond. All these findings led Crimmin et al. to propose two distinct catalytic cycles depending on the nature of the precatalyst, as depicted in Figure 21.<sup>76</sup>

A further kinetic study of the cyclization of (1-allylcyclohexyl) methanamine with each of the homoleptic calcium and strontium silylamide precatalysts  $[M\{N(SiMe_3)_2\}_2]_2$  provided an apparent second-order dependence in [catalyst], while determination of the activation barriers and Eyring analyses provided quantitative evidence that the group 2 catalysts provide activities at least commensurate with previously reported lanthanide-based catalyses.<sup>77</sup> In the particular cases of systems based upon calcium and strontium, an enhanced catalytic performance was proposed to arise from a tangible entropic advantage resulting from the reduced charge density of the larger divalent alkaline earth cations and consequentially less constrained rate-determining alkene insertion transition states. The rate of cyclization was also found to decrease with increasing substrate concentration. This latter finding, along with the observation of large kinetic isotope effects ( $k_H/k_D = 3.4\text{--}4.5$ ) employing N-deuterated aminoalkenes, 29

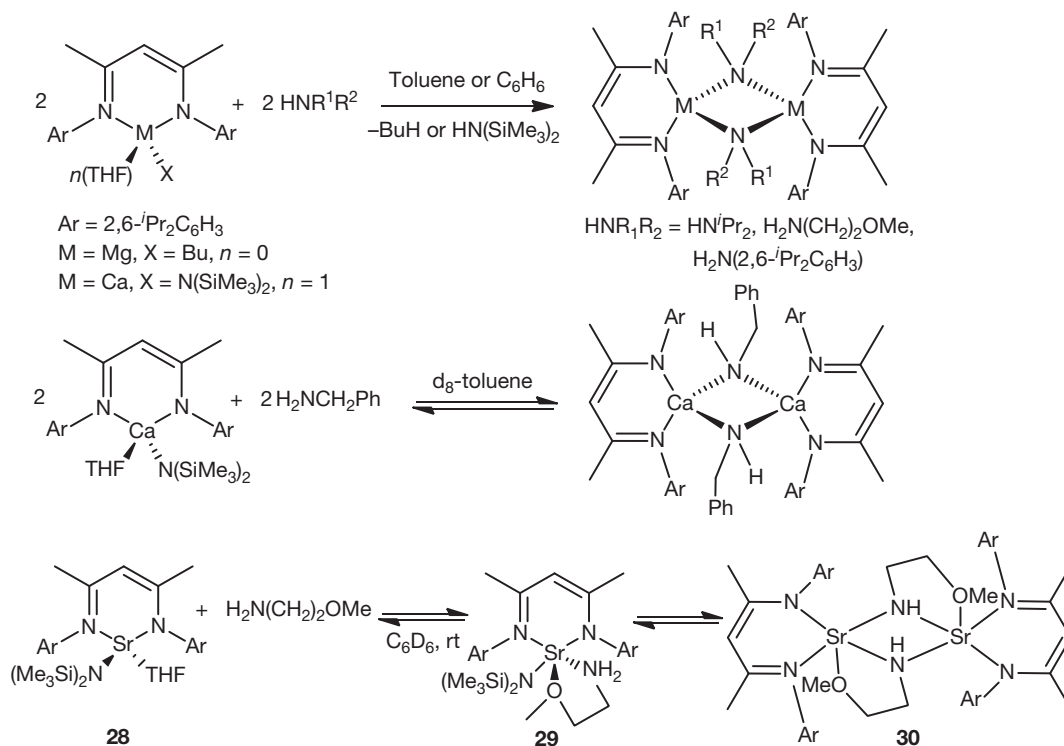
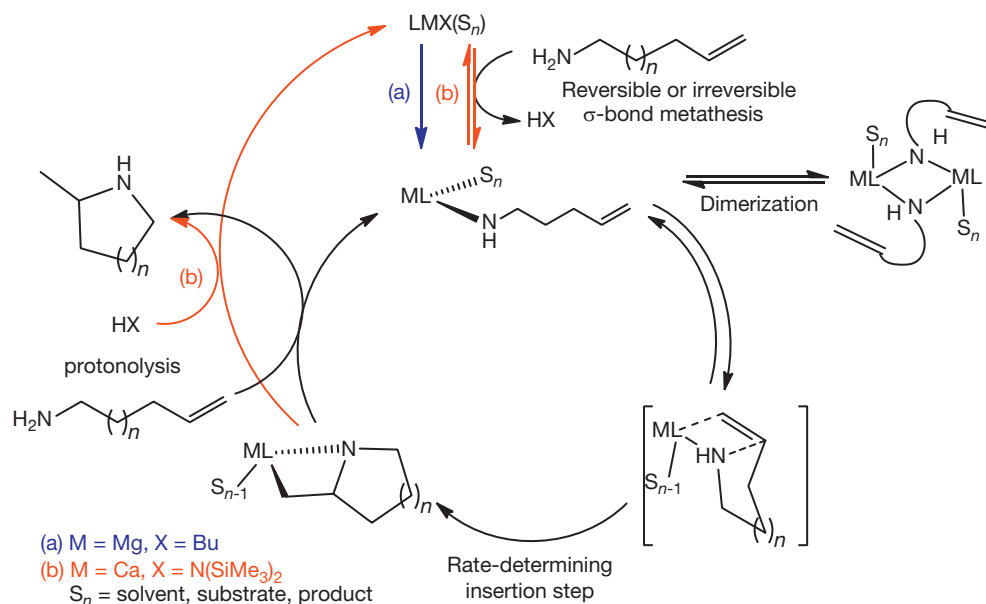


Figure 20 Transamination reactions with group 2 amides.

which were proposed to be a result of a beneficial and concerted proton-transfer step associated with rate-determining alkene insertion, was reasoned to be consistent with Michaelis-Menten-type kinetics.<sup>77</sup> The model presented suggested an augmented polarization of the alkene moiety as a result of both the polarizing effect of the M–N bond and the simultaneous formation of an intramolecular N–H( $\delta^+$ )...C( $\delta^-$ )=C interaction (Figure 22). This hypothesis was supported by the stoichiometric observations of Sadow and coworkers who reported that an isolated magnesium tris(oxazolonyl)borate amidoalkene complex would not undergo cyclization unless a second equivalent of aminoalkene was added to the solution (Figure 23).<sup>79</sup> This result was interpreted as a reflection of the direct involvement of additional amine within the coordination sphere of the group 2 element during the

rate-determining insertion step. In both cases, a similar rationale was presented in which a two-substrate, six-center transition state involving concerted C–N bond formation and N–H bond cleavage was proposed as the turnover-limiting step of the catalytic cycle. In this scenario, both substrate access to the metal center and substrate polarization, affected by the intrinsic properties (i.e., electropositivity and ionic radius) of the individual alkaline earth cation, are key elements in the rate-determining process.

In related work, Hultzsich and coworkers studied the catalytic intramolecular hydroamination activity of a series of magnesium phenoxyamine complexes, in which the cyclization rate of 1-amino-2,2-diphenyl-4-pentene was found to display either a zero-order or a second-order decline in [substrate].<sup>80</sup> Although no explanation was given for these latter



**Figure 21** Proposed catalytic cycle for the intramolecular hydroamination of aminoalkenes with reversible or irreversible catalyst initiation.

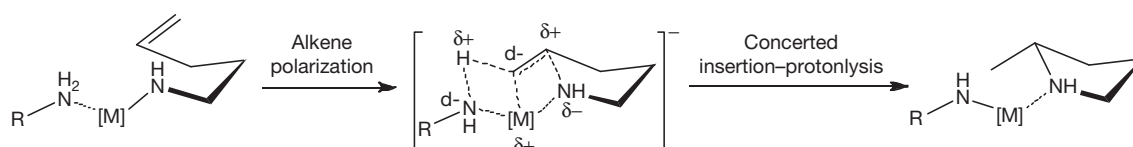


**Figure 22** Possible concerted insertion-protonolysis process accounting for the high kinetic isotope effects observed in group 2-based hydroamination catalysis.

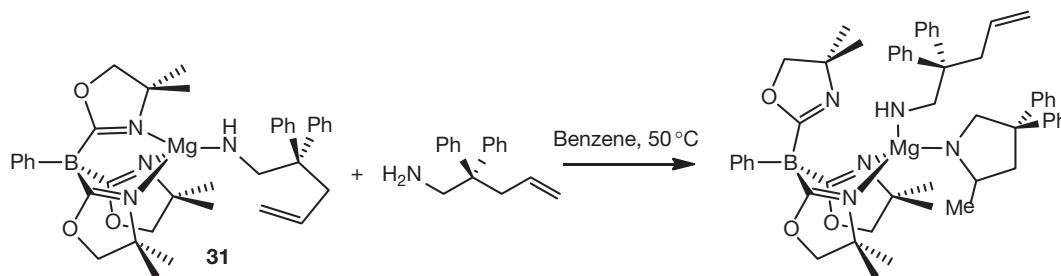


**Figure 23** Cyclization of an isolable magnesium amidoalkene.

observations, the results highlight the complexity of group 2-catalyzed intramolecular hydroamination reactions and the limitations of the mechanism illustrated in **Figure 21** and warn against over-generalization.

A number of further heteroleptic magnesium, calcium, strontium amide complexes bearing triazenide,<sup>40</sup> bis-<sup>41</sup> and tris(imidazolin-2-ylidene-1-yl)borate<sup>42</sup> (**9** and **10**), and aminotroponimate<sup>39</sup> ligands (**11** and **12**) have also been used in the hydroamination of aminoalkenes with similar results. It is, however, notable that the aminotroponimate-stabilized calcium and strontium species **11** and **12** reported by Roesky allowed the facile cyclization of 1-amino-2,2-dimethyl-5-phenyl-4-pentene and 1-amino-7-phenyl-6-hexyne at room temperature, the first examples of group 2 catalyzed hydroamination in which the alkene is terminally substituted. While the calcium precatalysts were shown to produce higher turnover frequencies than their strontium counterparts, the tendency for ligand redistribution toward the homoleptic species, especially with the larger strontium center, did not allow more quantitative comparison of the effect of ionic radii on the rate of catalysis. Reaction of a bis(imino)acenaphthene (BIAN) with heavier alkaline earth dialkyls  $[M\{CH(SiMe_3)_2\}_2(THF)_2]$  ( $M = Mg, Ca, \text{ and } Sr$ ) has been found to result in dearomatization of the aromatic ligand and the isolation of heteroleptic alkyl species, compounds **32–34** which showed unprecedented stability toward Schlenk-type redistribution (**Figure 24**). In this case, the calcium species was also observed to provide substantially faster catalysis at lower temperature and catalyst loading than reported in previous studies, an observation which was ascribed to the irreversibility of the alkyl-based catalyst initiation step, and provided the first cyclization of a terminal-substituted unactivated aminoalkene.<sup>43</sup>

A number of reports have appeared in which this hydroamination catalysis is extended to an enantioselective process. Initial attempts by Buch et al. to achieve stereocontrolled intramolecular hydroamination by using a chiral (*S*)-Ph-pybox-supported calcium amide precatalyst only yielded extremely low enantioselectivities ( $ee < 10\%$ ), mainly due to Schlenk-type ligand redistribution leading to the catalytically inactive homoleptic calcium complex and achiral but catalytically

active  $[Ca\{N(SiMe_3)_2\}_2(THF)_2]$ .<sup>81</sup> While similar issues were encountered during subsequent reports of the use of magnesium and calcium complexes of tris(oxazolonyl)borato ( $ee < 36\%$ )<sup>82</sup> and chiral 1,2-diamine ( $ee < 26\%$ )<sup>83</sup> ligands, application of a more rigid phenoxyamine magnesium complex **35** has enabled the intramolecular hydroamination reaction to be performed with enantioselectivities as high as 93% ee (**Figure 25**).<sup>8</sup>

This latter study also described the use of the chiral magnesium system for the catalytic intermolecular *anti*-Markovnikov addition of pyrrolidine and benzylamine. Similar reactivity had been reported earlier by Barrett et al. who provided the first examples of the intermolecular hydroamination of activated alkenes with heavier alkaline earth metals under mild conditions (5 mol.% catalyst loading, 60 °C) (**Figure 26**).<sup>85</sup> In this case, the homoleptic strontium precatalyst displayed notably higher catalytic activities than its calcium counterpart.

Kinetic analyses revealed that a higher activation energy for the strontium system was counterbalanced by a significantly less negative entropy of activation for strontium, mirroring a much looser four-membered insertion transition state and providing the larger metal center with a significant entropic advantage under the reported reaction conditions. A computational study employing DFT of a model ethane–ammonia system catalyzed by a simplified alkaline earth  $\beta$ -diketiminato amide complex was consistent with these experimental findings and indicated that calcium provided significantly lower activation barriers than magnesium for both the alkene insertion and final protonolysis steps (**Figure 27**).<sup>85</sup>

In 2008, group 2-mediated hydroamination catalysis was extended to the catalytic synthesis of guanidines and ureas from carbodiimides and isocyanates respectively, using heteroleptic calcium complex **5** and the homoleptic  $[M\{N(SiMe_3)_2\}_2(THF)_n]$  series ( $M = Ca, Sr, \text{ and } Ba; n = 0, 2$ ) as precatalysts (**Figure 28**).<sup>86</sup> In both cases, strontium was found to yield significantly higher turnover frequencies than calcium, although this was not quantitatively investigated. Catalysis with barium was much slower and usually accompanied by precipitation of insoluble products which, although not

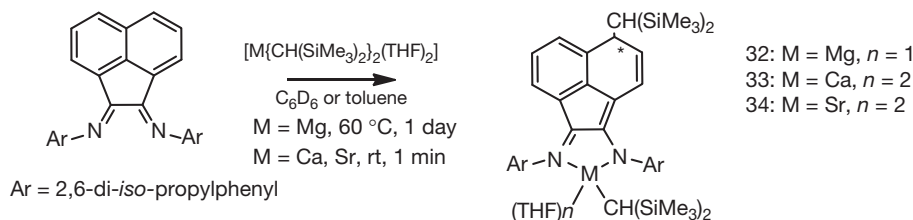


**Figure 24** Group 2 alkyl-induced dearomatization of a BIAN derivative.

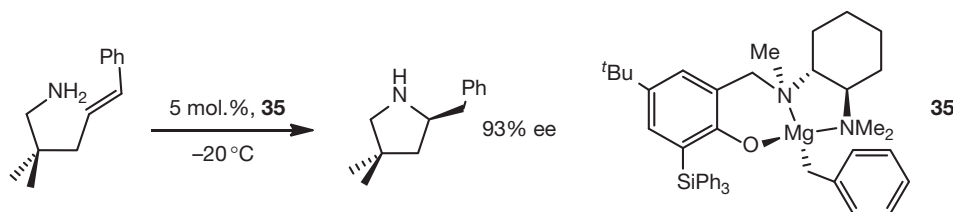


**Figure 25** Enantioselective intramolecular hydroamination of a terminally substituted aminoalkene.

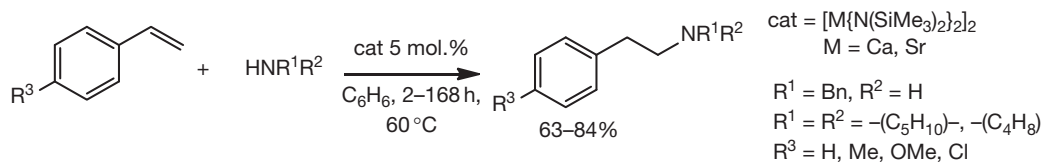


**Figure 26** Intermolecular hydroamination of activated alkenes.

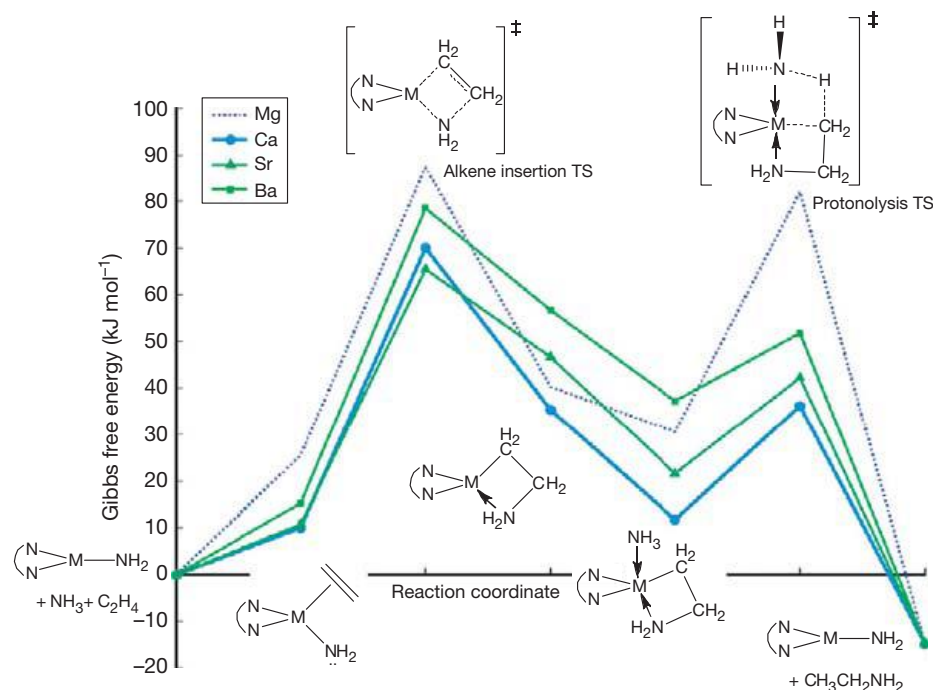


**Figure 27** Computational (DFT) study of the intermolecular hydroamination of ethene with ammonia by group 2 metal centers.

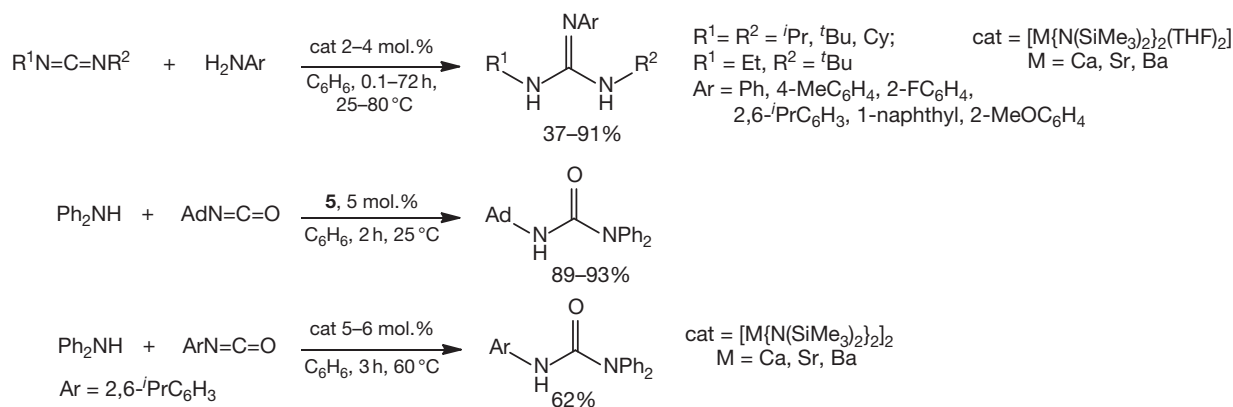


**Figure 28** Catalytic hydroamination of carbodiimides and isocyanates.

characterized, were thought to be polymeric and catalytically inactive species.

Stoichiometric reactions allowed the isolation of both heteroleptic and homoleptic guanidinate insertion products and a heteroleptic calcium urea complex as catalytically active intermediates,<sup>87</sup> demonstrating that catalysis occurs via an amide-carbodiimide or amide-isocyanate coordination-insertion mechanism (Figure 29).

### 1.38.3.2 Intermolecular Hydrophosphination of Unsaturated Bonds

Although lanthanocenes have been applied to the intramolecular hydrophosphination/cyclization of phosphinoalkenes,<sup>88</sup> attempts to achieve the intermolecular organolanthanide-catalyzed version of this reaction remain limited.<sup>89</sup> Based upon the success of the intramolecular hydroamination of

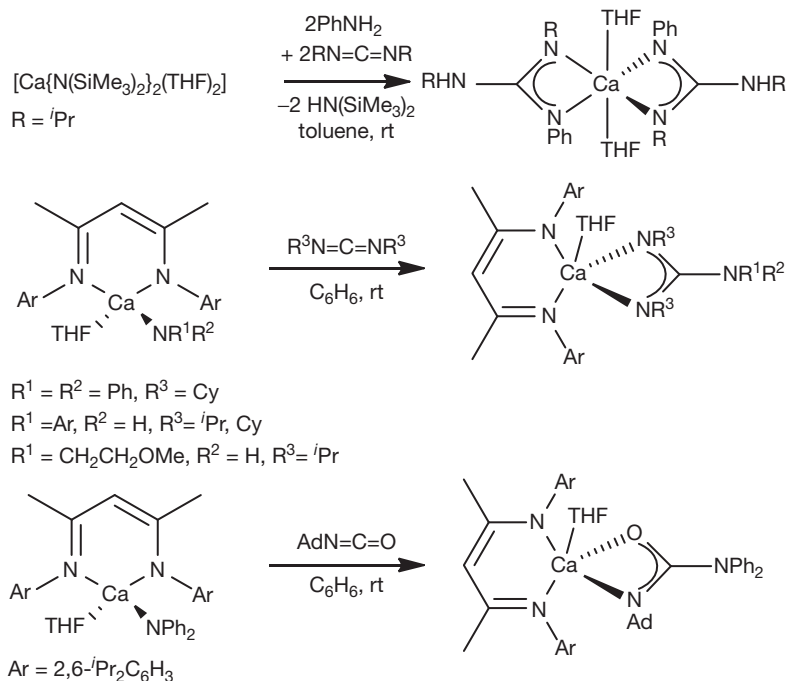


**Figure 29** Insertion of carbodiimides and isocyanates into alkaline earth–amide bonds.

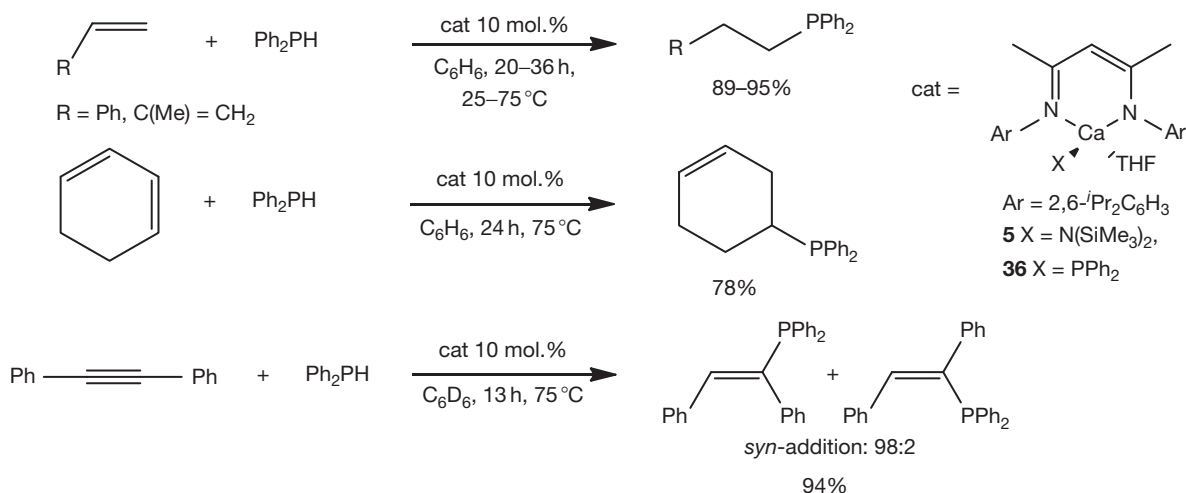


**Figure 30** Intermolecular hydrophosphination of activated alkenes and alkynes.

aminoalkenes with group 2 precatalysts, Crimmin et al. reported in 2007 the use of heteroleptic calcium complex **5** for the intermolecular hydrophosphination of unhindered activated alkenes and alkynes with diphenylphosphane, with activities comparable to those reported for late transition-metal catalysts.<sup>90</sup> Addition of the phosphane across the carbon–carbon double bond was both regioselective, with a marked preference for the *anti*-Markovnikov product, and stereoselective, with nearly exclusive *syn*-addition as shown in the (*Z*) geometry of the product resulting from the hydrophosphination of 1,2-diphenylethyne (**Figure 30**).

Initiation of the precatalyst occurs via  $\sigma$ -bond metathesis to generate heteroleptic calcium diphenylphosphide

complex **36**, which is itself catalytically active. The chemistry of stoichiometric  $\sigma$ -bond metathesis between phosphanes and group 2 amides has been well established by Westerhausen and coworkers since the 1990s and led to the isolation of numerous homoleptic alkaline earth phosphides (**Figure 31**).<sup>91</sup>

The active catalyst then undergoes concerted insertion of the alkene or alkyne into the calcium–phosphorus bond, which leads to the observed *syn*-stereoselectivity. In accordance with this mechanism, Westerhausen and coworkers had earlier described the stoichiometric insertion of one equivalent of diphenylbutadiyne into one of the Mg–P bonds of  $[Mg\{P(SiMe_3)_2\}_2(THF)_4]$  to yield the heteroleptic insertion product as displayed in **Figure 32**.<sup>92</sup>

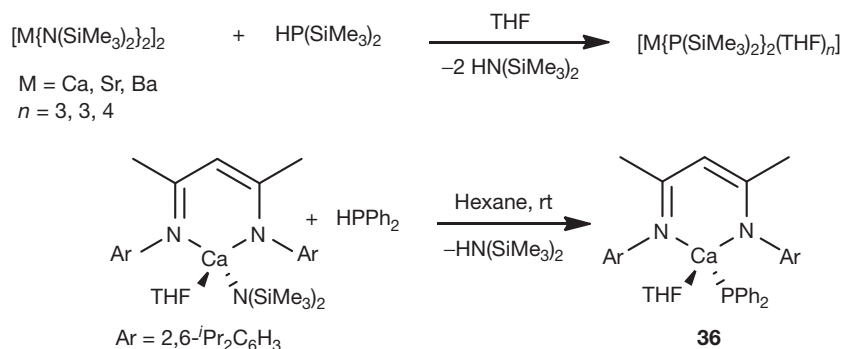


**Figure 31** Synthesis of homoleptic and heteroleptic alkaline earth phosphides by protonolysis.

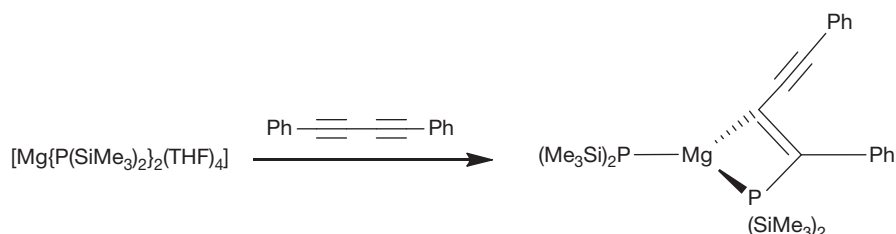


**Figure 32** Insertion of diphenylbutadiyne into an Mg–P bond.

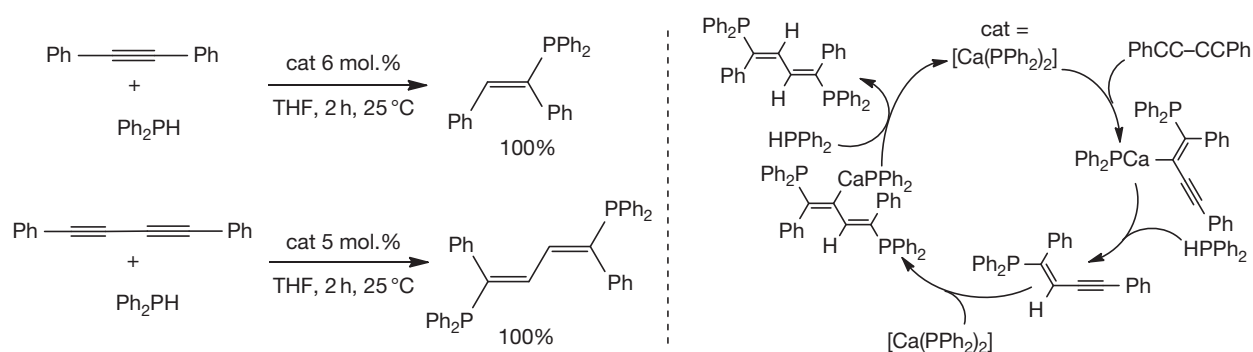


**Figure 33** Hydrophosphination of alkynes using  $[\text{Ca}(\text{PPh}_2)_2]$ .

Attempts by Hill and coworkers to use homoleptic  $[\text{Ca}\{\text{N}(\text{SiMe}_3)_2\}_2(\text{THF})_2]$  under these reaction conditions met with limited success due to formation of homoleptic calcium diphosphide species which are highly insoluble in benzene. Later, however, Westerhausen reported that homoleptic  $[\text{Ca}(\text{PPh}_2)_2]$  efficiently catalyzes the *syn*-addition of diphenylphosphane to both diphenylethyne and diphenylbutadiyne in THF, in which the catalyst is soluble (Figure 33).<sup>93</sup>

As for hydroamination, this reactivity could be extended to other unsaturated substrates such as carbodiimides.<sup>94</sup> Although heteroleptic calcium complex 5 was found to catalyze the reaction, the less hindered homoleptic heavier group 2 bis(amides)  $[\text{M}\{\text{N}(\text{SiMe}_3)_2\}_2(\text{THF})_2]$  ( $\text{M} = \text{Ca, Sr, and Ba}$ ) and the unsolvated  $[\text{Ca}\{\text{N}(\text{SiMe}_3)_2\}_2]$  proved to be more active precatalysts. Although no kinetic studies were undertaken due to extremely fast reaction rates, it appeared that the larger strontium and barium metal centers were more efficient than their calcium counterpart. Hydrophosphination of both symmetric and unsymmetric carbodiimides with diarylphosphanes proceeded

at room temperature with low catalyst loadings to give the analogous phosphaguanidine in high yield (Figure 34). Hydrophosphination of 1,3-di-*tert*-butyl-carbodiimide could not be achieved, presumably because of the steric demands of the carbodiimide substituents. Furthermore, dicyclohexylphosphane did not react with any of the carbodiimide substrates under the reported reaction conditions. In this latter case, the decreased acidity of the dialkylphosphane compared to the diarylphosphanes was shown to prevent catalyst initiation.

As for the hydroamination of carbodiimides, the reaction proceeded via insertion of the carbodiimide into the metal-phosphide bond. Interestingly, addition of one equivalent of phosphane to the isolated calcium phosphaguanidinate insertion product did not result in  $\sigma$ -bond metathesis and liberation of the phosphaguanidine product. Addition of a further equivalent of carbodiimide, however, resulted in liberation of the free phosphaguanidine. The authors explained this by invoking the Curtin–Hammett principle, arguing that the calcium phosphaguanidinate intermediate and diphenylphosphane are in

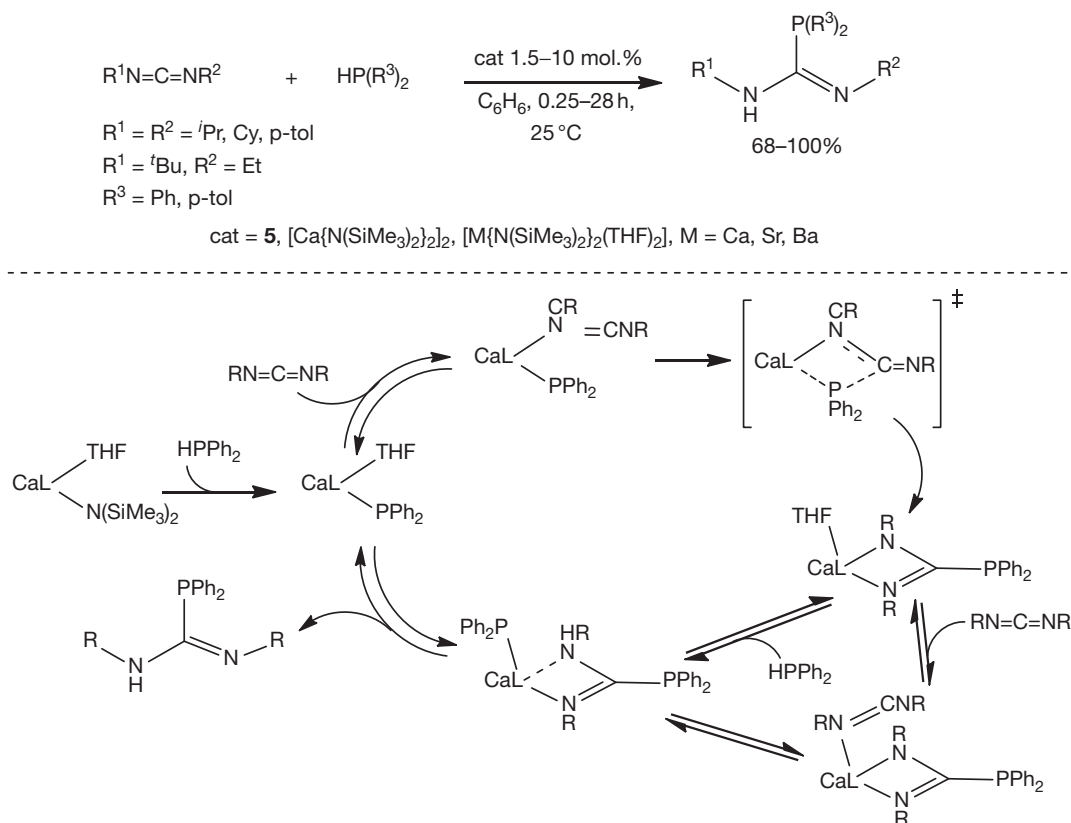


**Figure 34** Hydrophosphination of carbodiimides.

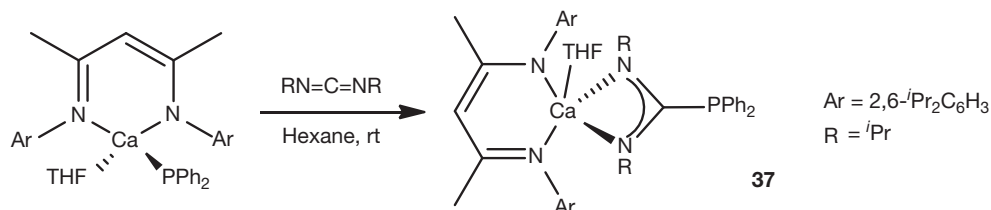


**Figure 35** Stoichiometric synthesis of the insertion phosphaguanidinate intermediate **37**.

equilibrium with a small amount the phosphaguanidine and calcium phosphide complex, which in turn reacts readily with the carbodiimide to achieve catalytic turnover. As a result, Hill and coworkers proposed a catalytic cycle based on mostly reversible processes as shown in **Figure 34** via the intermediacy of isolable group 2 phosphaguanidinate species **37** (**Figure 35**).<sup>94</sup> Following this, Westerhausen also reported that the homoleptic calcium phosphide complex  $[\text{Ca}(\text{PPh}_2)_2(\text{THF})_4]$  undergoes insertion with carbodiimides to form the homoleptic calcium bis(phosphaguanidinate) species, which in turn only display very limited catalytic activity.<sup>95</sup>

### 1.38.3.3 Intermolecular Hydroacetylenation of Carbodiimides

In 2009, Hill and coworkers reported the stoichiometric insertion of carbodiimides into the calcium carbon bond of heteroleptic calcium acetylides (**Figure 36**).<sup>72</sup>

Based upon the precedent of lanthanide-mediated hydroacetylenation, the authors showed in a preliminary experiment that 5 mol.% of calcium complex **5** catalyzes hydroacetylenation of 1,3-diisopropylcarbodiimide with phenylacetylene at 80 °C over a period of 14 h. Nuclear magnetic resonance (NMR) experiments, however, showed that the  $\beta$ -diketiminate ligand is protonated by the acetylene under the reaction conditions, indicating that it is unlikely that either the heteroleptic amide, acetylide, or insertion products shown above are catalytically active species (**Figure 37**).

### 1.38.3.4 Intermolecular Hydrosilylation of Unsaturated Bonds

In 2006, Buch and Harder described the regioselective hydrosilylation of activated alkenes with homoleptic calcium and strontium benzyl precatalysts **38** and **39** under mild reaction conditions (0.5–10 mol.% catalyst loading, 25–50 °C,

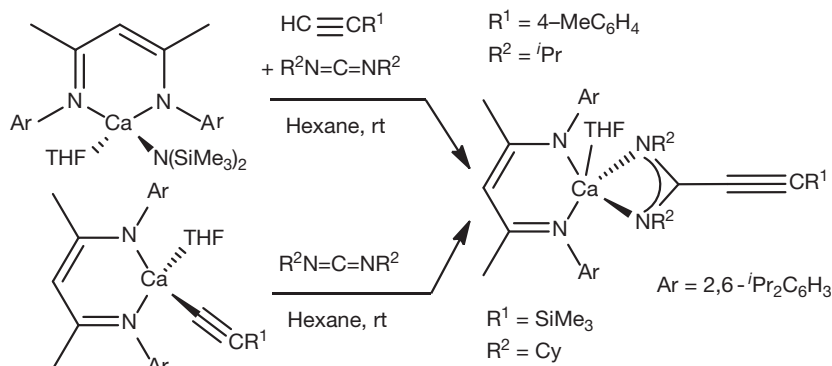


**Figure 36** Stoichiometric insertion of carbodiimides into a heteroleptic calcium acetylide complex.

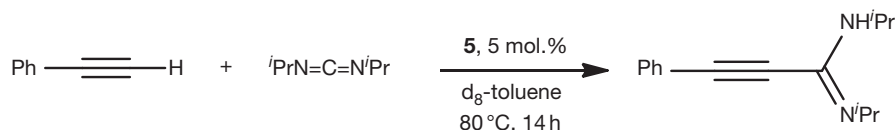


**Figure 37** Catalytic calcium-mediated hydroacetylation of a carbodiimide.

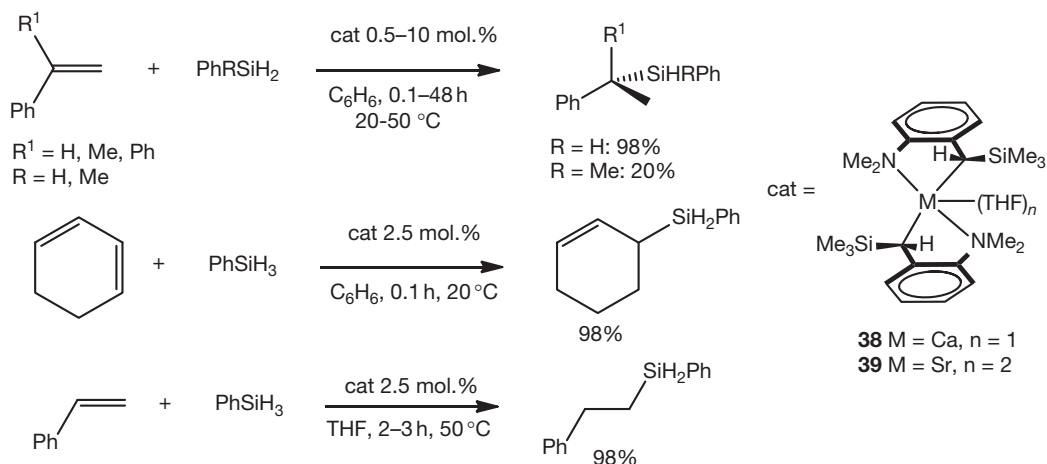


**Figure 38** Regioselective hydrosilylation of activated alkenes.

0.1–48 h), with the larger strontium metal center providing higher turnover frequencies.<sup>96</sup> Although these dibenzyl species are also active as anionic styrene polymerization initiators, clean conversion to the silylated alkene was observed in each case. Regioselectivity could be effectively influenced by choice of the solvent: in apolar benzene exclusive formation of the Markovnikov product was observed, whereas in polar THF only the *anti*-Markovnikov product was obtained (Figure 38). Reactions in diethyl ether yielded a mixture of isomers in the presence of the calcium precatalyst, whereas only the terminal silylated product was obtained with strontium.

In both polar and apolar solvents, catalyst initiation was reported to occur through  $\sigma$ -bond metathesis of the dibenzyl precatalyst with the silane to form a transient, highly reactive heteroleptic group 2 hydride intermediate which, although it could not be isolated, was proposed to form hydride-rich clusters in solution. The successful isolation of heteroleptic calcium hydride complex 40<sup>97</sup> and its magnesium analog<sup>98</sup>

obtained from the reaction of  $\beta$ -diketiminato calcium and magnesium complexes 8 and 5, as well as the synthesis of a hydride-rich  $\text{Mg}_4\text{H}_6$  cluster 41<sup>99</sup> from the reaction of a carbene-supported magnesium bis(amide) with phenylsilane strongly support this mechanism (Figure 39). Commercially available  $\text{CaH}_2$ , however, even if freshly produced and finely ground, did not catalyze the hydrosilylation of alkenes.

In apolar solvents, the reaction was proposed to proceed through conventional insertion of the alkene into the metal–hydride bond to form the most stable alkyl intermediate which then undergoes  $\sigma$ -bond metathesis with another equivalent of silane to reform the metal hydride and the silylated Markovnikov product (Figure 40, (a)). For the reactions performed in the polar solvent THF, the authors presented a catalytic cycle proceeding via a charge-separated ion pair of the form  $[\text{LM}]^+[\text{PhSiH}_4]^-$  which is subsequently converted into a group 2 silanide complex (Figure 40, (b)). Due to steric factors, alkene insertion into the metal–silicon bond would

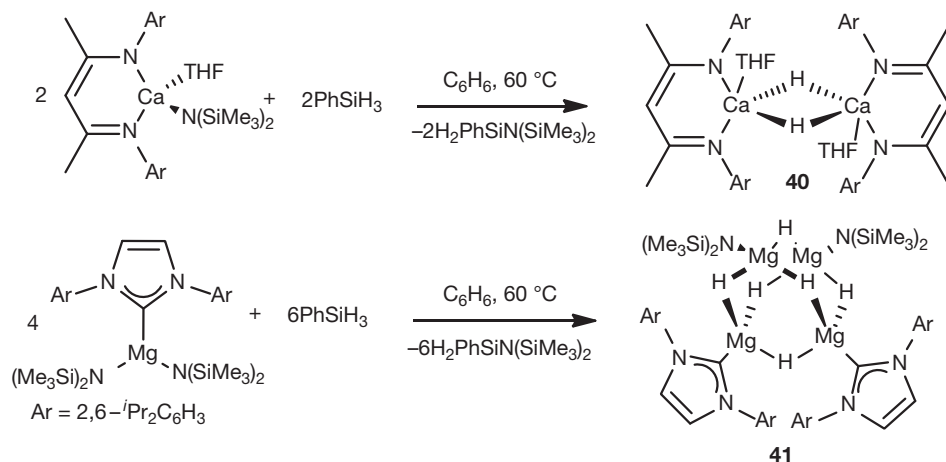


**Figure 39** Synthesis of magnesium and calcium hydride complexes by  $\sigma$ -bond metathesis with  $\text{PhSiH}_3$ .

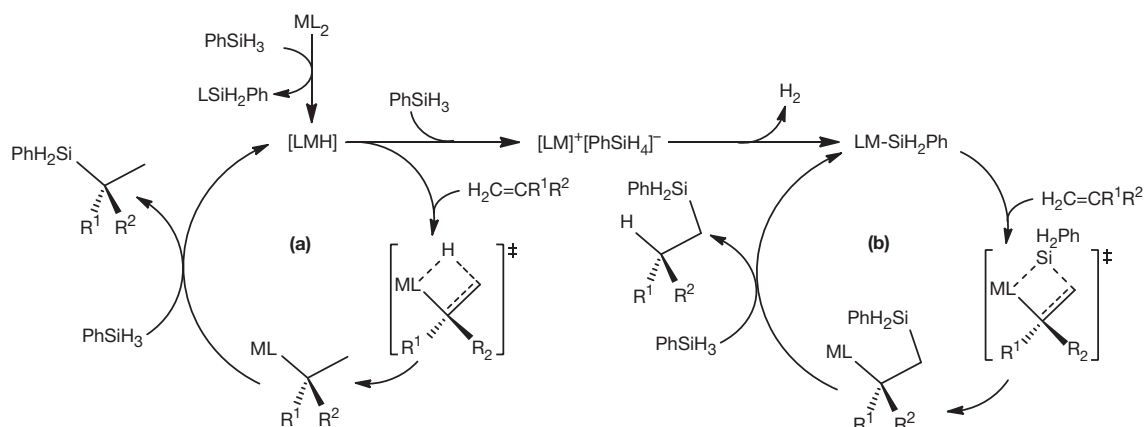


**Figure 40** Proposed catalytic cycles for the hydrosilylation of alkenes in apolar (a) and polar (b) solvents.

yield the *anti*-Markovnikov product, accounting for the observed regioisomer. Although this second catalytic cycle provides a justification for the influence of the solvent on regioselectivity, evidence for the charge-separated ion pair or silanide intermediate in THF, as well as for  $\text{H}_2$  release has yet to be found and the possibility of a polarity-influenced transition state for the  $\sigma$ -bond metathesis between the group 2 alkyl intermediate and the silane in the first catalytic cycle cannot be discounted.

Homoleptic dibenzyl calcium complex **38** and molecular calcium hydride complex **40** were also reported to promote the catalytic hydrosilylation of ketones (Figure 41).<sup>100</sup> Reactions proceeded under mild conditions (1–5 mol.% catalyst loading, 20–50 °C) and yielded almost exclusively the dialkoxysilane, independent of the initial ratio between silane and ketone. Although stoichiometric insertion of ketones into the metal-hydride bond to form calcium alkoxide species (Figure 42) was always accompanied by a substantial amount of enolization, enolization products were virtually absent under catalytic conditions.

The isolated calcium alkoxide species did not react in turn with phenylsilane. Spielman and Harder argued that catalysis does thus not proceed via a calcium alkoxide intermediate. Rather, and although reactions were carried out in apolar benzene, they proposed a catalytic cycle based entirely upon

charge-separated ion pairs, with reactions occurring exclusively at the hypervalent anionic silicon centers.

### 1.38.3.5 Hydroboration of N-Heterocycles

In related, but apparently mechanistically distinct reactivity, Hill and coworkers have described a magnesium-catalyzed protocol for the tandem dearomatization/hydroboration of N-heterocycles.<sup>102</sup> Although attempted extension of stoichiometric phenylsilane/magnesium hydride-promoted dearomatization reactivity to a catalytic regime was unsuccessful,<sup>101</sup> use of the readily available reagent pinacolborane allowed for the hydroboration of a wide range of substituted and fused-ring pyridine derivatives. This reactivity was proposed to occur through a sequence of Mg–H migratory insertion and Mg–N/H–B metathesis steps reminiscent of earlier calcium amide reactivity with the dialkylborane 9-BBN (Figure 43).<sup>103</sup>

### 1.38.3.6 Hydrogenation of Activated Alkenes

Following their successful hydrosilylation catalysis, Spielman and Harder described the catalytic hydrogenation of alkenes with molecular calcium hydride **40** and dibenzylcalcium and -strontium complexes **38–39**.<sup>104</sup> Reactions proceeded under relatively mild conditions (2.5–5 mol.%

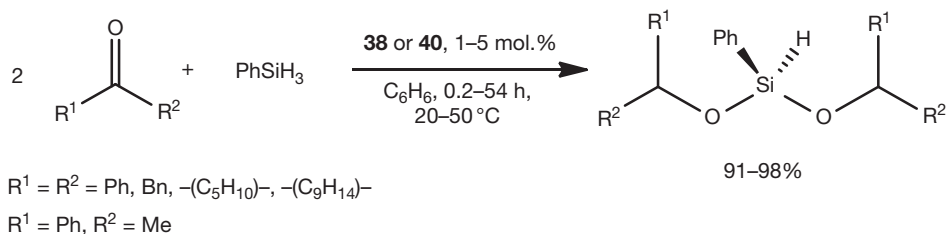


**Figure 41** Catalytic hydrosilylation of ketones.

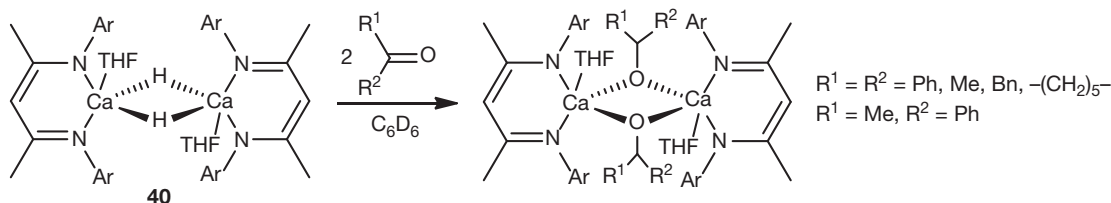


**Figure 42** Stoichiometric insertion of ketones into heteroleptic calcium hydride complex **40**.

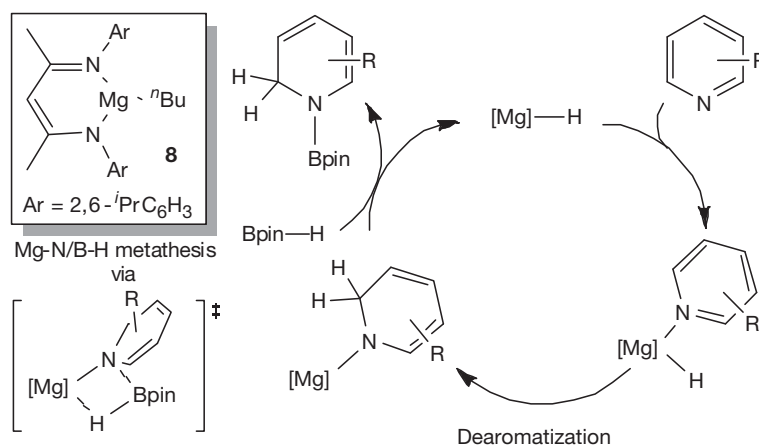


**Figure 43** Magnesium-catalyzed hydroboration and dearomatization of pyridines.

catalyst loading, 20–60 °C, 20 bar H<sub>2</sub>) and provided the mono-hydrogenated products in moderate to high yields (Figure 44). As for the hydrophosphination and hydrosilylation reactions, reactivity was limited to activated alkenes such as 1,1-diphenylethene, styrene,  $\alpha$ -methylstyrene, and cyclohexadiene.

Side-reactions producing dimers or oligomers resulting from single or multiple insertion of the alkene substrate into the calcium alkyl intermediate were limited and reactivity could again be tuned by choice of the solvent: in polar THF or hexamethylphosphoramide (HMPA) the reaction with styrene resulted exclusively in polymerization, whereas in apolar benzene the hydrogenation product was obtained in 81–85% yield. In line with the organolanthanide-catalyzed hydrogenation of alkenes, the authors proposed the catalytic cycle outlined in Figure 45.

Stoichiometric reactions between **40** and 1,1-diphenylethene, 1,3-cyclohexadiene, and myrcene resulted in clean insertion of the terminal, less substituted alkene into the calcium–hydride bond to form the intermediate calcium alkyl (Figure 46).<sup>104,105</sup> Hydrogenation of the latter species under 20 bar of H<sub>2</sub> regenerated the calcium hydride catalyst with liberation of the mono-

hydrogenated alkene. Further evidence of the  $\sigma$ -bond metathesis process was obtained by saturation of a solution of the deuterated version of **40** with H<sub>2</sub> leading to fast H/D exchange.

### 1.38.4 Catalytic Dehydrocoupling of $\sigma$ -Bonds

#### 1.38.4.1 Dehydrocoupling of Silanes and Amines

The catalytic dehydrogenative coupling of  $\sigma$ -bonds remains a challenging type of reaction and, to date, only limited examples have been reported in alkaline earth chemistry. In 2007, Buch and Harder described the dehydrocoupling of terminal alkynes and amines with silanes by the azametallacyclopropane complex [(Ph<sub>2</sub>C–NPh)Ca(HMPA)<sub>3</sub>] **42** at room temperature. Within the limited substrate scope examined, the calcium precatalyst displayed catalytic activity and selectivity similar to its Yb(II) analog (Figure 47).<sup>106</sup>

In contrast to the previously discussed polymerization and heterofunctionalization catalyses, the catalytic cycles illustrated in Figure 47 do not involve any unsaturated insertion steps. Initiation occurs via  $\sigma$ -bond metathesis between the alkyl moiety of the ligand and the substrate to form either the

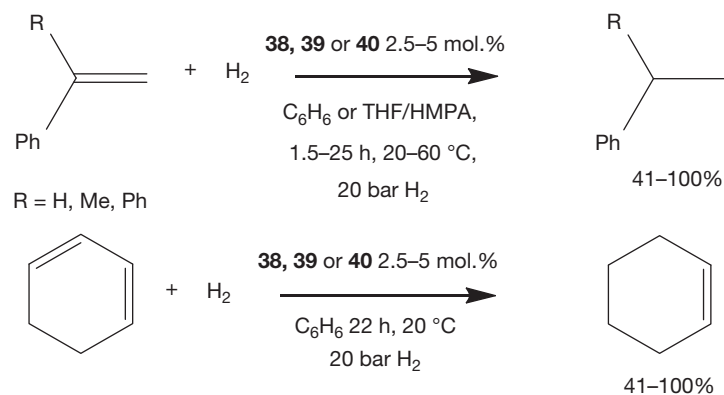


**Figure 44** Catalytic hydrogenation of conjugated alkenes.

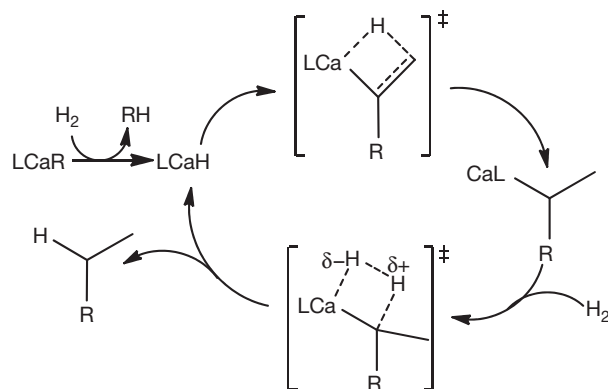


**Figure 45** Catalytic cycle for the calcium-mediated hydrogenation of activated alkenes.

calcium amide or acetylide catalyst which in turn reacts with the silane to form an ill-defined calcium hydride intermediate and liberate the coupled silylated product. Further  $\sigma$ -bond metathesis with another equivalent of amine or acetylene regenerates the active species with quantitative release of  $\text{H}_2$  (Figure 48).

This Si-H/H-N cross-coupling reactivity was subsequently extended by Sadow and coworkers to other amines and the more challenging substrates ammonia and hydrazine employing a tris(oxazolonyl)borato magnesium complex. While kinetic studies of the dehydrocoupling catalysis supported a similar mechanistic cycle to that depicted in Figure 48, a kinetic isotope effect ( $k_{\text{SiH}}/k_{\text{SiD}}$ ) of 1.0 led the authors to deduce that the turnover limiting step of the reaction involved nucleophilic attack of a magnesium amide on silicon rather than a concerted four-membered Mg-centered transition state.<sup>107a</sup> Related phosphorus-centered reactions of triphenylphosphane oxide and diphenylphosphane oxide with calcium alkyls and amides in the presence of  $\text{PhSiH}_3$  have been observed to occur to give apparent P-C bond cleavage in the former case and P(V) to P(III) reduction and P-P coupling in the latter case.<sup>107b</sup>

#### 1.38.4.2 Amine Borane Dehydrocoupling

Although hydrogen release has been reported to be promoted by solid-state ball milling with  $\text{MgH}_2$  and conversion of

$\text{H}_3\text{N}\cdot\text{BH}_3$  to the crystallographically characterized calcium amidotrihydaborates  $[\text{Ca}(\text{NH}_2\text{BH}_3)_2(\text{THF})_n]$  ( $n=0, 1, 2$ ) has been reported to result in significant hydrogen release, these solid-state reactions are, necessarily, mechanistically uncertain.<sup>108</sup> The homogeneous group 2-catalyzed dehydrocoupling of amines and boranes was prefaced by several reports of stoichiometric B-H/H-N dehydrocoupling reactivity. In 2007, Hill and coworkers reported that  $\sigma$ -bond metathesis reactions of the calcium amido compound 5 with the secondary organoborane 9-BBN result in the formation of B-N-bonded species and a calcium diorganoborohydride as the reaction products,<sup>103</sup> while in 2008 Spielmann et al. reported that sequential  $\text{H}_2$ -elimination can be induced from  $\beta$ -diketiminato calcium amidoborane derivatives of both  $\text{H}_3\text{N}\cdot\text{BH}_3$  itself and  $\text{BH}_3$  adducts of primary amines and anilines.<sup>109,110</sup> In these cases further thermally induced B-N formation apparently occurred via the intermediacy of dimeric calcium complexes of the complex dianions  $[\text{RN-BH-NR-BH}_3]^{2-}$  ( $\text{R}=\text{H, Me, and } ^i\text{Pr}$ ). In cases where dimerization was not possible, unimolecular  $\text{H}_2$  elimination provided species containing coordinated imidoborane anions. In 2009, Harder and coworkers described the formation of the bis(amino)borane  $[\text{HB}\{\text{NH}(2,6\text{-}^i\text{Pr}_2\text{C}_6\text{H}_3)\}_2]$  catalyzed by magnesium  $\beta$ -diketiminato complex 43 in the presence of  $[\text{H}_3\text{B}\cdot\text{H}_2\text{N}(2,6\text{-}^i\text{Pr}_2\text{C}_6\text{H}_3)]$  (Figure 46).<sup>110</sup> A heteroleptic magnesium borohydride complex was identified as a catalytically active intermediate and the  $\text{BH}_3$  byproduct observed in the  $^1\text{H}$  NMR spectrum in the form of  $\text{B}_2\text{H}_6$ . The active catalyst, a  $\beta$ -diketiminato-supported magnesium amidoborane, was readily isolated from the  $\sigma$ -bond metathesis of the related magnesium hydride complex with the aniline borane. In view of these observations, the authors proposed the two possible catalytic cycles displayed in Figure 49, both of which are based on an intermediate  $[\text{LMg}(\text{NHAr-BH}_2\text{-NHAr-BH}_3)]$  species which decomposes either through  $\beta$ -hydride elimination to form the bis(amino)borane and a magnesium hydride or through a 1,3-hydride shift to release the product and form a magnesium borohydride intermediate.

Stoichiometric  $\sigma$ -bond metathesis reactions between  $\beta$ -diketiminato-supported calcium and magnesium amides and hydride with  $\text{H}_3\text{B}\cdot\text{NH}_2\text{R}$  ( $\text{R}=\text{H, Me, } ^i\text{Pr, and } 2,6\text{-}^i\text{Pr}_2\text{C}_6\text{H}_3$ ) (Figure 50) by the same authors led to the isolation of a number of heteroleptic amidoborane complexes which thermally decompose either into borylamide complexes ( $\text{M}=\text{Mg, Ca}$ ;



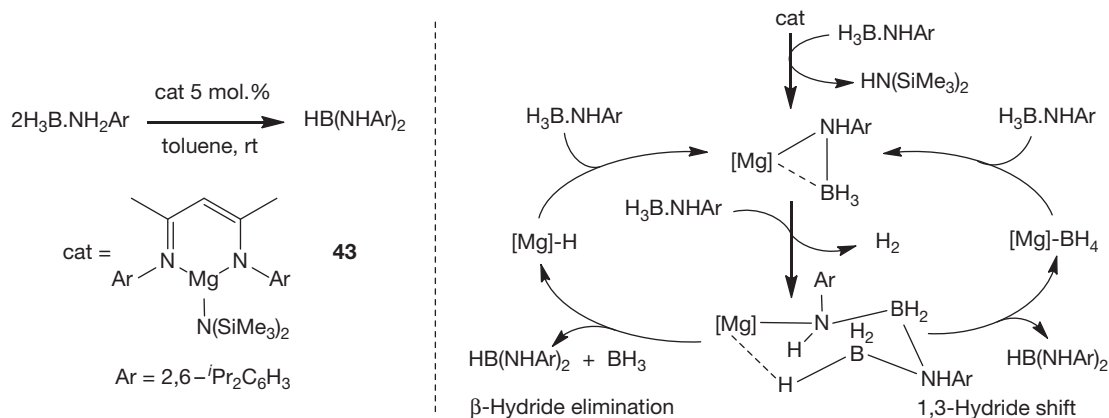


**Figure 49** Possible catalytic cycles for the catalytic dehydrocoupling of  $[\text{H}_3\text{B}\cdot\text{H}_2\text{N}(2,6\text{-}i\text{-Pr}_2\text{C}_6\text{H}_3)]$ .

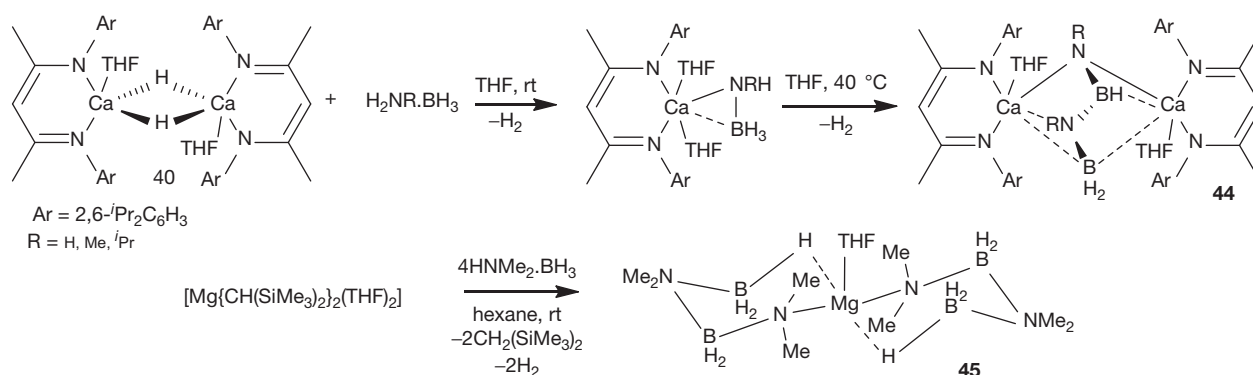


**Figure 50** Stoichiometric  $\sigma$ -bond metathesis reactions of group 2 complexes with amine boranes demonstrating dehydrogenative B–N coupling.

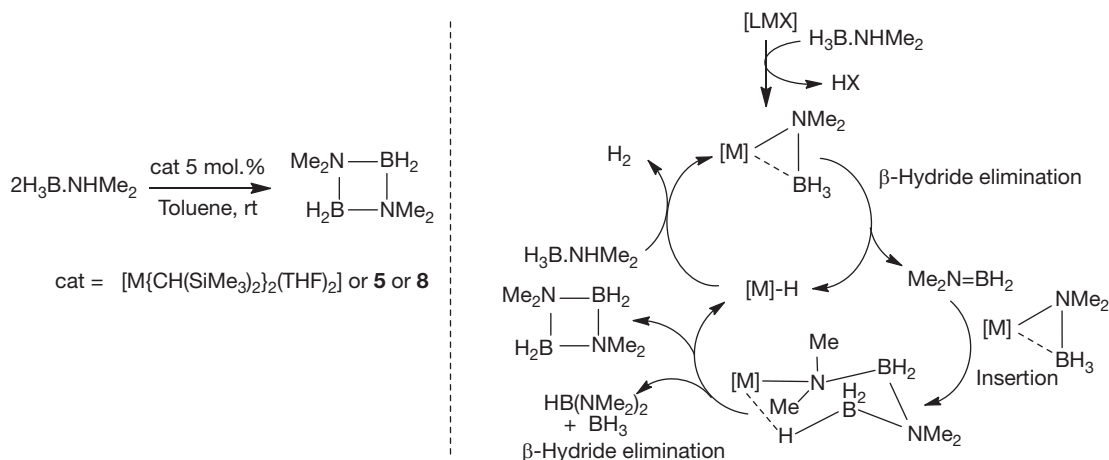


**Figure 51** Proposed catalytic cycle for catalytic dehydrocoupling of  $\text{H}_3\text{B}\cdot\text{NHMe}_2$  into cyclic  $[(\text{H}_2\text{BNMe}_2)_2]$ .

insertion into group 2-amidoborane bonds to form the observed coupled  $[\text{NMe}_2\text{-BH}_2\text{-NMe}_2\text{-BH}_3]^-$  anion. This viewpoint that reactivity is thus dictated by the ability of the catalytic metal center to effect rate-determining hydride elimination was subsequently supported by further stoichiometric and catalytic studies and extensions to potentially more polarizing group 3 systems and a study of the

stoichiometric reactivity of the heteroleptic alkylstrontium amidoborane,  $[\text{Sr}\{\text{CH}(\text{SiMe}_3)_2\}\{\text{NMe}_2\text{BH}_3\}(\text{THF})_2]$ , **46**.<sup>113,114</sup> In this latter case, a sequence of  $\beta$ -H and  $\text{H}_2\text{N}=\text{BH}_2$  insertion steps provides the alkylamidoborane  $[\text{HB}\{\text{CH}(\text{SiMe}_3)_2\}(\text{NMe}_2)]$ , thus providing evidence for the key B–N bond-forming insertion process of the mechanism illustrated in **Figure 51**.

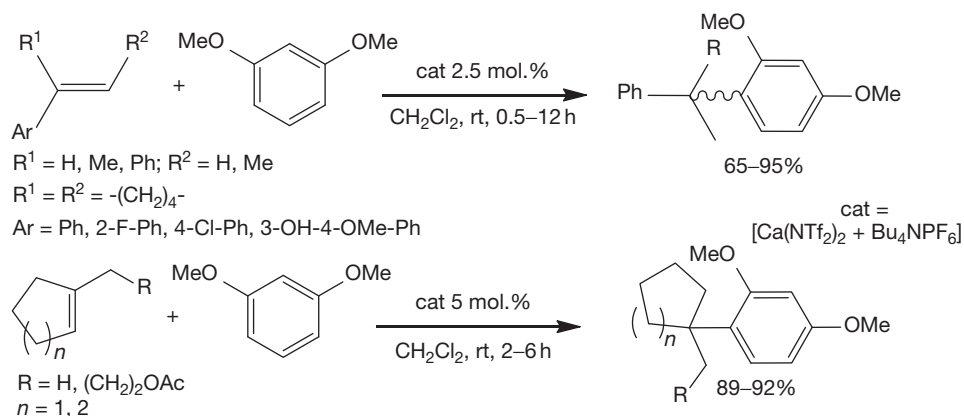


Figure 52 Calcium Lewis acid-catalyzed hydroarylation of alkenes.

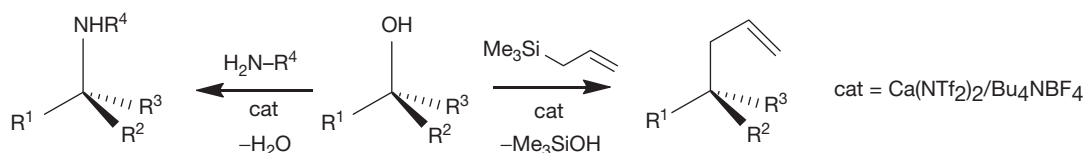


Figure 53 Calcium-catalyzed amination and allylation of alcohols.

### 1.38.5 Lewis Acid-Catalyzed Carbon–Carbon Bond Formation

In recent years, the use of alkaline earth complexes as Lewis acid catalysts in synthetic organic chemistry has increased dramatically. Usually prepared *in situ* over molecular sieves from readily available homoleptic metal alkoxides or amides and a variety of asymmetric ligands, these catalytic systems have attracted much interest owing to their reduced cost compared with more traditional transition metal catalysts, their biocompatibility, and their efficiency at catalyzing a large array of asymmetric nucleophilic addition reactions with excellent yields and high enantio- or diastereoselectivity.

#### 1.38.5.1 Hydroarylation of Alkenes

Niggemann and coworkers have reported the calcium-catalyzed hydroarylation of alkenes employing the Lewis acidic  $[\text{Ca}(\text{NTf}_2)_2 + \text{Bu}_4\text{NPF}_6]$  system.<sup>115</sup> This was found to catalyze the addition of electron-rich aromatic substrates across a variety of activated and even aliphatic alkene bonds at room temperature, under very mild conditions and in excellent yields (2.5–5 mol.% catalyst loading, 0.5–12 h, 65–95% yield) (Figure 52). A variety of functional groups, halides, hydroxides, ethers, furans, and thiophenes, present both on the alkene and on the arene substrates, were tolerated under the mild reaction conditions employed. In contrast to the vast majority of alkaline earth-catalyzed heterofunctionalization reactions mentioned in previous sections, hydroarylation exclusively yielded the Markovnikov products, indicating significant mechanistic differences. Although no mechanism was proposed by the authors, the presence of  $\text{Bu}_4\text{NPF}_6$  proved to be critical for catalytic turnover to occur, suggesting the formation of a more reactive charge-separated  $[\text{Ca}(\text{NTf}_2)]^+\text{PF}_6^-$

species. Moreover, reactions proceeded in dichloromethane without the exclusion of moisture or air, and were even inhibited under strictly anhydrous conditions, which led the authors to propose that a carbinol intermediate might be involved, although this latter species could not be detected.

An identical  $[\text{Ca}(\text{NTf}_2)_2/\text{Bu}_4\text{NPF}_6]$  catalyst system was found to efficiently functionalize electron-rich arenes with secondary and tertiary benzylic, propargylic, and allylic alcohols under very mild Friedel–Crafts alkylation conditions and to catalyze the direct amination of  $\pi$ -activated alcohols with a variety of nitrogen nucleophiles and for C–C coupling between silanes and a similar range of alcohols.<sup>116–118</sup> In these latter cases, efficient conversions were achieved with secondary and tertiary benzylic and allylic alcohols and tertiary propargylic alcohols (Figure 53).

#### 1.38.5.2 Enantioselective Aldol Reactions

The first examples of enantioselective alkaline earth-mediated catalysis date back from the 1990s, when Yamada and Shibasaki reported the asymmetric aldol reaction of a variety of aldehydes with excess acetophenone using a chiral barium catalyst prepared *in situ* from  $[\text{Ba}(\text{O}^i\text{Pr})_2]$  and an excess of an (*R*)-2-hydroxy-2'-methoxy-1,1'-binaphthyl ligand precursor. Enantiomeric excesses remained moderate, ranging from 50 to 70%.<sup>119</sup> Noyori and coworkers reported a more enantioselective system for the same reaction, prepared *in situ* from  $[\text{Ca}\{\text{N}(\text{SiMe}_3)_2\}_2(\text{THF})_2]$ , KSCN, and an excess of (*S,S*)-hydrobenzoin (Figure 54).<sup>120</sup> The calcium catalyst was found to be several times more active than previously described systems, with moderate to good enantioselectivities (66–91%). Cold-spray ionization mass spectrometry (CSI-MS) provided insight into the oligomeric nature of the catalyst, which was otherwise not characterized. The reaction of 3-(benzyloxy)-2,2-

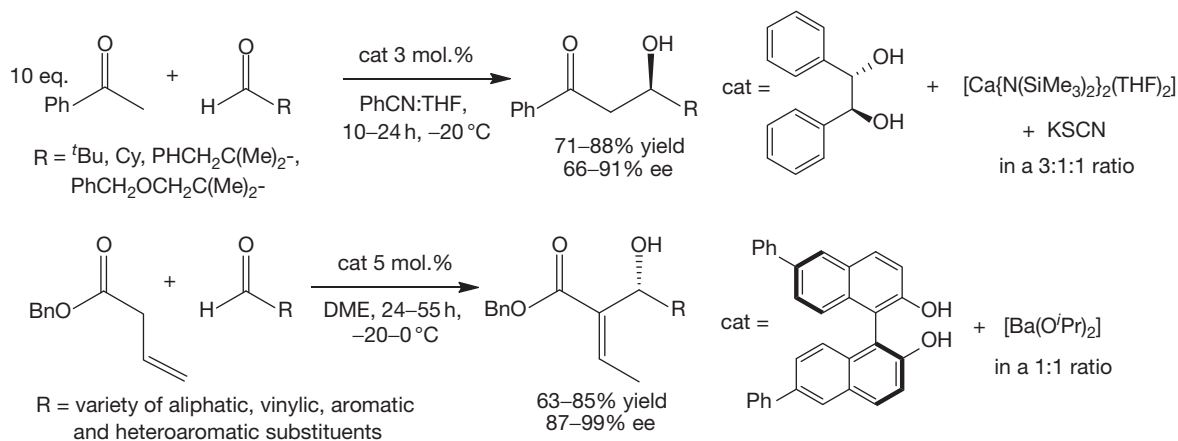


**Figure 54** Asymmetric calcium- and barium-mediated aldol reactions.

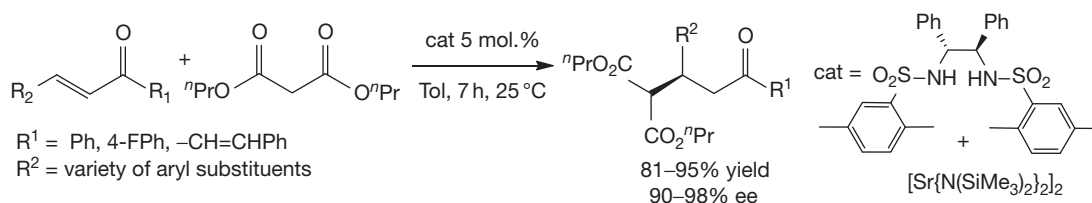


**Figure 55** Asymmetric strontium-catalyzed Michael addition.

dimethylpropanal with acetophenone allowed the synthesis of the aldol (*R*) product, which is an intermediate in the synthesis of epothilone A, a chemotherapeutic drug, in 79% yield and 91% enantiomeric excess, thus paving the way for the application of these chiral alkaline earth catalyst systems in the synthesis of pharmaceutical and natural organic products. More recently, Yamaguchi et al. also described an (*S*)-1-1'-bi-2-naphthol (BINOL)/[Ba(O<sup>*i*</sup>Pr)<sub>2</sub>] system for the asymmetric aldol/retroaldol reaction of β-γ-unsaturated esters with aldehydes leading to high selectivity for the (*E*)-α-adduct and enantiomeric excesses of up to 99%.<sup>121</sup> The analogous lanthanide-based systems did not catalyze the reaction, showing once more that alkaline earth catalysts cannot simply be considered as lanthanide mimetic.

### 1.38.5.3 Asymmetric 1,4-Addition and [2+3]-Cycloaddition Reactions

Asymmetric Michael reactions and other 1,4-addition reactions have also been successfully catalyzed by various homogeneous alkaline earth systems. In 2001, Kumaraswamy et al. described the use of a chiral CaCl<sub>2</sub>/[KO<sup>*t*</sup>Bu]/(*R*)-BINOL system as an inexpensive substitute for [La(O<sup>*i*</sup>Pr)<sub>3</sub>] for the asymmetric Michael addition of dimethylmalonate to linear and cyclic enones, albeit with relatively poor enantiomeric excess of the product.<sup>122</sup> Later, the same authors managed to greatly improve enantioselectivities by using the octahydro-BINOL version of the ligand precursor to generate Michael addition products containing quaternary stereocenters.<sup>123</sup> Kobayashi and coworkers extended this work by using a chiral bis(sulfonamide) ligand precursor with [Sr{N(SiMe<sub>3</sub>)<sub>2</sub>]<sub>2</sub> for the enantioselective Michael addition of di-*iso*-propylmalonate to a series of cyclic and acyclic chalcones.<sup>124</sup> After optimization of

the reaction conditions, high yields (>81%) and excellent selectivity (ee > 90%) were achieved at room temperature within a few hours (Figure 55). The analogous asymmetric 1,4-addition of malonates and β-ketoesters to nitroalkenes was successfully catalyzed by a [Ca{O(4-OMe-C<sub>6</sub>H<sub>4</sub>)<sub>2</sub>]/[*anti*-5,4-diphenyl-PyBox] system (1:2.2 ratio) with good yields (>73%) and moderate to excellent enantioselectivities (65–96%), for the formation of both tertiary and quaternary carbon stereocenters.<sup>125</sup>

Other alkaline earth-catalyzed 1,4-addition reactions include the addition of α-amino acid esters to α,β-unsaturated carbonyl substrates developed by Kobayashi and coworkers using a calcium catalyst prepared *in situ* from a chiral Ph-Box ligand and [Ca(O<sup>*i*</sup>Pr)<sub>2</sub>]. Chiral glutamic acid derivatives were obtained in high yields under mild reaction conditions with enantiomeric excesses above 78% (Figure 56).<sup>126</sup> The analogous magnesium system was catalytically inactive, while strontium and barium afforded much poorer enantioselectivities, likely due to their larger coordination sphere and looser transition states. NMR studies suggested that the catalyst was a monomeric calcium alkoxide complex supported by the chiral anionic ligand.

During the course of these studies, the authors discovered that crotonate derivatives, instead of yielding the expected 1,4-addition product, underwent a [2+3]-cycloaddition process with the α-amino acid to yield highly enantiomerically and diastereomerically pure substituted pyrrolidines containing four stereocenters (Figure 57). A whole range of α-amino acids including glycine, alanine, methionine, leucine, and serine derivatives were successfully used. The reaction between crotonate derivatives and α-substituted α-amino acid esters yielded pyrrolidines containing contiguous, chiral, tertiary,

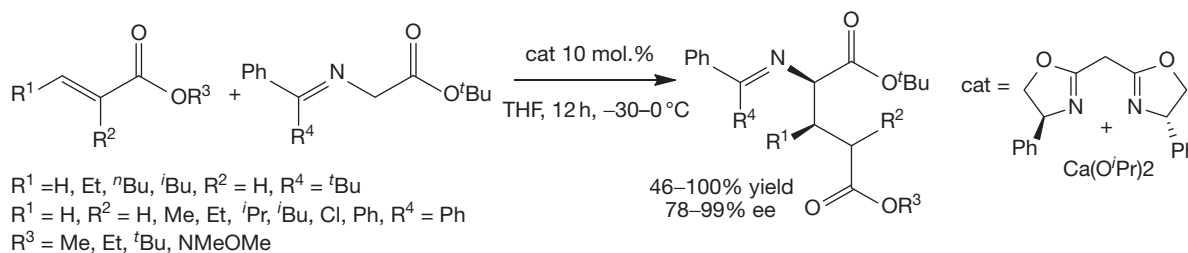


**Figure 56** Highly selective calcium-catalyzed synthesis of chiral glutamic acid derivatives.

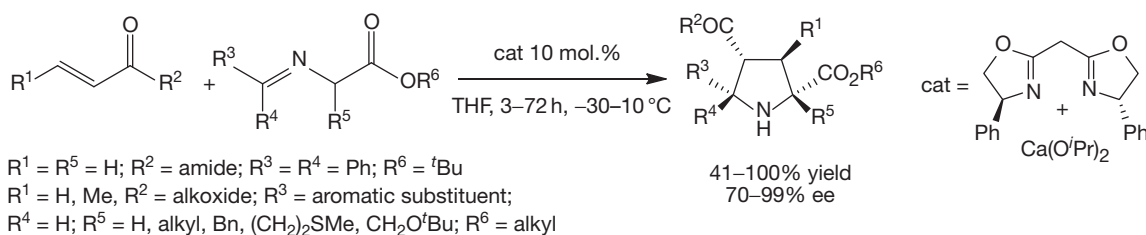


**Figure 57** Highly diastereo- and enantioselective calcium-mediated [2+3]-cycloaddition reactions.

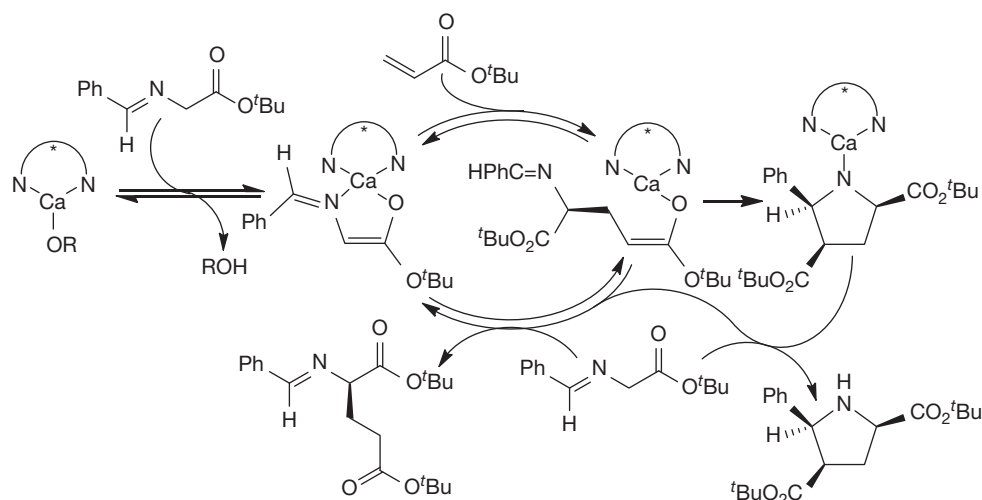


**Figure 58** Proposed catalytic cycles for the 1,4-addition and [2+3]-cycloaddition of  $\alpha,\beta$ -unsaturated carbonyl substrates to  $\alpha$ -amino acid esters.

and quaternary carbon centers in good yields (41–98%) with excellent selectivity ( $ee > 85\%$ ) despite longer reaction times. Such a high stereoselectivity in the direct formation of highly sterically hindered chiral carbon centers is an achievement which places this calcium catalyst system among the very best in asymmetric [2+3]-cycloaddition. Kobayashi and coworkers successfully applied this reactivity to the synthesis of chiral pyrrolidine cores for hepatitis-C virus RNA-dependent polymerase inhibitors in 83% yield and 85–88% enantiomeric excess.

Mechanistic investigation of both the 1,4-addition and [2+3]-cycloaddition processes led the authors to propose the catalytic cycle outlined in **Figure 58**. Catalyst initiation occurs via reversible  $\sigma$ -bond metathesis of the calcium alkoxide pre-catalyst with the  $\alpha$ -amino acid ester, followed by 1,4-addition to the  $\alpha,\beta$ -unsaturated carbonyl substrate. The reaction then proceeds toward either protonolysis and liberation of the

1,4-addition product or intramolecular cyclization and protonolysis to liberate the chiral pyrrolidine.

#### 1.38.5.4 Asymmetric Addition of Esters and Imidates to Imines (Mannich-Type Reactions)

In 2010, Kobayashi and coworkers also reported that the enantioselective Mannich reaction of dibenzylmalonate with aromatic *N*-Boc imines using a  $[\text{Ca}(\text{O}^i\text{Pr})_2]/[\text{PyBox}]$  system (1:1.5 ratio) afforded the resulting amines in excellent yields, with moderate to good selectivity (54–77% ee) within 2 h at  $-20^\circ\text{C}$ .<sup>127</sup> Other Mannich reactions reported by the same group include the highly diastereoselective addition of *N*-Boc amides to *N*-diphenylphosphinoyl imines accompanied by Boc migration in the presence of a  $[\text{Ba}(\text{O}^i\text{Bu})_2]/[2'$ -methoxybiphenyl-2-ol] system.<sup>128</sup> The related reaction of sulfonylimidates with aromatic and aliphatic *N*-Boc imines yielded

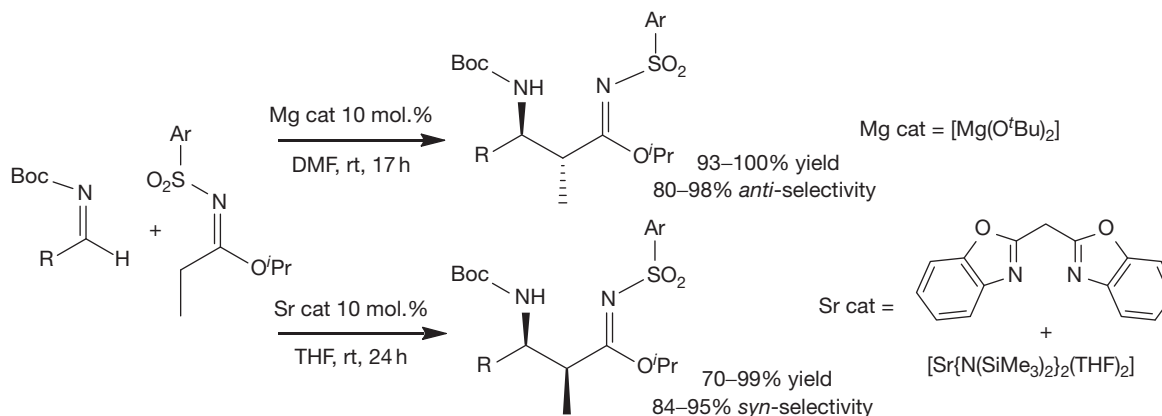


**Figure 59** Diastereoselective reaction of sulfonylimidates with *N*-Boc imines.

interesting results: in the presence of a simple  $[\text{Mg}(\text{O}^t\text{Bu})_2]$  catalyst in dimethylformamide (DMF) without addition of ligand, excellent yields (>80%) and *anti*-diastereoselectivity (>80%) were achieved, whereas with a  $[\text{Sr}\{\text{N}(\text{SiMe}_3)_2\}_2(\text{THF})_2]/[\text{PyBox}]$  system and a less polar solvent like THF, similarly excellent yields and *syn*-selectivity (>84%) were obtained (Figure 59).<sup>129</sup> In 2007, Yamaguchi et al. described a similar Mannich-type reaction between  $\beta,\gamma$ -unsaturated esters and *N*-diphenylphosphinoyl imines, catalyzed by a  $[\text{Ba}\{\text{O}(4\text{-MeO-C}_6\text{H}_4)\}_2]/[(\text{S})\text{-biaryldiol}]$  system with high selectivity for the  $\alpha,\beta$ -unsaturated  $\alpha$ -adduct and good enantioselectivity (77–80%).<sup>130</sup> In all cases, catalyst initiation was thought to proceed through  $\sigma$ -bond metathesis between the metal alkoxide functionality and the carbonyl substrate, followed by insertion of the imine and formation of the carbon–carbon bond.

### 1.38.6 Conclusion

Although catalysis with complexes of the group 2 elements heavier than beryllium has yet to achieve any sort of prominence in organic or inorganic chemistry, much has been achieved in a relatively short period of time. A wide range of bond activation and heterofunctionalization reactivity has been observed and, perhaps more significantly, profound variations in the activity and chemical behavior of the individual alkaline earths effectively belie any opinion that reactivity simply mirrors that of magnesium as group 2 is descended. Although an impressively broad range of catalytic reactivity has now been observed, existing reports are, in many cases, little more than an initial proof-of-concept exercise. Much remains to be done vis-à-vis refinements to selectivity and improvements to absolute activity, which will surely result from future advances in supporting ligand design. Broader applicability in synthesis will require the formulation of more air- and moisture-tolerant precatalytic complexes while mechanistic analyses will continue to inform our understanding of what remains a relatively under-represented but abundant and environmentally benign series of elements. Much remains to be achieved but there is now at least a foundation to build upon.

For related chapters in this Comprehensive, we refer to Chapters 7.01 and 9.30.

### References

- Grignard, M. V. *Comptes Rendus* **1900**, *T. 130*, 1322.
- Silverman, G. S. R.; Phillip, E. *Handbook of Grignard Reagents*. Marcel Dekker, Inc.: New York, 1996.
- Richey, H. G. J. *Grignard Reagents – New Developments*. Wiley: Chichester, 2000.
- Garst, J.; Soriaga, M. *Coord. Chem. Rev.* **2004**, 623.
- See, for example, (a) Krasovskiy, A.; Knochel, P. *Angew. Chem. Int. Ed.* **2004**, *43*, 3333; (b) Krasovskiy, A.; Krasovskaya, V.; Knochel, P. *Angew. Chem. Int. Ed.* **2006**, *45*, 2958; (c) Krasovskiy, A.; Kopp, F.; Knochel, P. *Angew. Chem. Int. Ed.* **2006**, *45*, 497; (d) Metzger, A.; Gavryushin, A.; Knochel, P. *Syn Lett* **2009**, 1433.
- Beckmann, E. *Ber. Dtsch. Chem. Ges.* **1905**, *38*, 904.
- Gilman, H.; Schulze, F. *J. Am. Chem. Soc.* **1926**, *48*, 2463.
- Cloke, F. G. N.; Hitchcock, P. B.; Lappert, M. F.; Lawless, G. A.; Royo, B. J. *Chem. Soc. Chem. Commun.* **1991**, 724.
- Westerhausen, M. *Inorg. Chem.* **1991**, *30*, 96.
- Cotton, F. A.; Wilkinson, G.; Murillo, C. A.; Bochmann, M. *Advanced Inorganic Chemistry*, 6th ed.; John Wiley & Sons: New York, 1999.
- Fischer, R.; Gartner, M.; Gorus, H.; Westerhausen, M. *Angew. Chem. Int. Ed.* **2006**, *45*, 609.
- Fischer, R.; Gartner, M.; Gorus, H.; Westerhausen, M. *Organometallics* **2006**, *25*, 3496.
- Gartner, M.; Gorus, H.; Westerhausen, M. *Synthesis-Stuttgart* **2007**, 725.
- Gartner, M.; Gorus, H.; Westerhausen, M. *Organometallics* **2007**, *26*, 1077.
- Fischer, R.; Gartner, M.; Gorus, H.; Yu, L.; Reiher, M.; Westerhausen, M. *Angew. Chem. Int. Ed.* **2007**, *46*, 1618.
- Shannon, R. *Acta Cryst. Sect. A* **1976**, *32*, 751.
- Allred, A. J. *Inorg. Nucl. Chem.* **1961**, *17*, 215.
- Green, S.; Jones, C.; Stasch, A. *Science* **2007**, *318*, 1754.
- Green, S.; Jones, C.; Stasch, A. *Angew. Chem. Int. Ed.* **2008**, *47*, 9079.
- Kriech, S.; Gorus, H.; Yu, L.; Reiher, M.; Westerhausen, M. *J. Am. Chem. Soc.* **2009**, *131*, 2977.
- Maldivi, P.; Petit, L.; Adamo, C.; Vetere, V. *Comptes Rendus Chimie* **2007**, *10*, 888.
- Zhou, X. G.; Zhu, M. *J. Organomet. Chem.* **2002**, *647*, 28.
- Hunt, P. A. *Dalton Trans.* **2007**, 1743.
- Sigma-Aldrich Catalogue 2010–2011*.
- Crimmin, M. R.; Barrett, A. G. M.; Hill, M. S.; Macdougall, D. J.; Mahon, M. F.; Procopiou, P. A. *Chem. Eur. J.* **2008**, *14*, 11292.
- Feil, F.; Muller, C.; Harder, S. *J. Organomet. Chem.* **2003**, *683*, 56.
- Harder, S.; Brettar, J. *Angew. Chem. Int. Ed.* **2006**, *45*, 3474.

28. Hitchcock, Peter B.; Lappert, M. F.; Lawless, G. A.; Royo, B. *J. Am. Chem. Soc.* **1990**, *30*, 96.
29. (a) Schachte, Y.; Pines, H. *J. Catal.* **1968**, *11*, 147; (b) Zhang, G.; Hattori, H.; Tanabe, K. *Appl. Catal.* **1988**, *36*, 189.
30. For previous reviews, see (a) Barrett, A. G. M.; Crimmin, M. R.; Hill, M. S.; Procopiou, P. A. *Proc. Roy. Soc. A, Math. Phys. Eng. Sci.* **2010**, *466*, 927; (b) Harder, S. *Chem. Rev.* **2010**, *110*, 3852.
31. (a) Molander, G. A.; Romero, J. A. C. *Chem. Rev.* **2002**, *102*, 2161; (b) Molander, G. A. *Chem. Rev.* **1992**, *92*, 29; (c) Hou, Z. M.; Wakatsuki, Y. *Coord. Chem. Rev.* **2002**, *231*, 1.
32. Gottfriedsen, J.; Edelman, F. T. *Coord. Chem. Rev.* **2007**, *251*, 142.
33. (a) Aspinall, H. *Chem. Rev.* **2002**, *102*, 1807; (b) Inanaga, J.; Furuno, H.; Hayano, T. *Chem. Rev.* **2002**, *102*, 2211; (c) Mikami, K.; Terada, M.; Matsuzawa, H. *Angew. Chem. Int. Ed.* **2002**, *41*, 3555; (d) Shibasaki, M.; Yoshikawa, N. *Chem. Rev.* **2002**, *102*, 2187.
34. Schlenk, W.; Schlenk, W., Jr. *Chem. Ber.* **1929**, *62*, 920.
35. Avent, A. G.; Crimmin, M. R.; Hill, M. S.; Hitchcock, P. B. *Dalton Trans.* **2005**, 278.
36. Hanusa, T. P. *Organometallics* **2002**, *21*, 2559.
37. (a) Chisholm, M. H.; Gallucci, J. C.; Phomphrai, K. *Chem. Commun.* **2003**, 48; (b) Chisholm, M. H.; Gallucci, J. C.; Phomphrai, K. *Inorg. Chem.* **2004**, *43*, 6717.
38. (a) Sarish, S.; Roesky, H. W.; John, M.; Ringe, A.; Magull, J. *Chem. Commun.* **2009**, 2390; (b) Nembenna, S.; Roesky, H. W.; Nagendran, S.; Hofmeister, A.; Magull, J.; Wilbrandt, P.; Hahn, M. *Angew. Chem. Int. Ed.* **2007**, *46*, 2512; (c) Ruspice, C.; Harder, S. *Inorg. Chem.* **2007**, *46*, 10426.
39. (a) Datta, S.; Roesky, P. W.; Bleichert, S. *Organometallics* **2007**, *26*, 4392; (b) Datta, S.; Gamer, M. T.; Roesky, P. W. *Organometallics* **2008**, *27*, 1207.
40. Barrett, A.; Crimmin, M.; Hill, M.; Hitchcock, P.; Kociok-Köhn, G.; Procopiou, P. *Inorg. Chem.* **2008**, *47*, 7366.
41. Arrowsmith, M.; Hill, M. S.; Kociok-Köhn, G. *Organometallics* **2009**, *28*, 1730.
42. Arrowsmith, M.; Heath, A.; Hill, M. S.; Hitchcock, P. B.; Kociok-Köhn, G. *Organometallics* **2009**, *28*, 4550.
43. Arrowsmith, M.; Hill, M. S.; Kociok-Köhn, G. *Organometallics* **2011**, *30*, 1291.
44. Harder, S.; Feil, F.; Knoll, K. *Angew. Chem. Int. Ed.* **2001**, *40*, 4261.
45. Dijkstra, P. J.; Du, H.; Feijen, J. *Polym. Chem.* **2011**, *2*, 520.
46. Allen, K. A.; Gowen, B.; Lindsell, W. E. *J. Polym. Sci. A* **1974**, *12*, 1131.
47. Li, Y. F.; Deng, H.; Brittain, W.; Chisholm, M. S. *Polym. Bull.* **1999**, *42*, 635.
48. Steffens, A.; Schumann, H. *Macromol. Symp.* **2006**, *236*, 203.
49. Dove, A. P.; Gibson, V. C.; Marshall, E. L.; White, A. J. P.; Williams, D. J. *Chem. Commun.* **2002**, 1208.
50. (a) Li, S. M.; Rashkov, I.; Espartero, J. L.; Manolova, N.; Vert, M. *Macromolecules* **1996**, *29*, 57 (b); Rashkov, I.; Manolova, N.; Li, S. M.; Espartero, J. L.; Vert, M. *Macromolecules* **1996**, *29*, 50.
51. Dobrzynski, P.; Kasperczyk, J.; Jelonek, K.; Ryba, M.; Walski, M.; Bero, M. *J. Biomed. Mater. Res. A* **2006**, *79A*, 865.
52. (a) Zhong, Z. Y.; Dijkstra, P. J.; Birg, C.; Westerhausen, M.; Feijen, J. *Macromolecules* **2001**, *34*, 3863; (b) Zhong, Z. Y.; Ankone, M. J. K.; Dijkstra, P. J.; Birg, C.; Westerhausen, M.; Feijen, J. *Polym. Bull.* **2001**, *46*, 51; (c) Zhong, Z. Y.; Schneiderbauer, S.; Dijkstra, P. J.; Westerhausen, M.; Feijen, J. *J. Polym. Environ.* **2001**, *9*, 31.
53. (a) Westerhausen, M.; Schneiderbauer, S.; Kneifel, A. N.; Soltl, Y.; Mayer, P.; Noth, H.; Zhong, Z. Y.; Dijkstra, P. J.; Feijen, J. *Eur. J. Inorg. Chem.* **2003**, 3432; (b) Zhong, Z. Y.; Schneiderbauer, S.; Dijkstra, P. J.; Westerhausen, M.; Feijen, J. *Polym. Bull.* **2003**, *51*, 175; (c) Sarazin, Y.; Howard, R. H.; Hughes, D. L.; Humphrey, S. M.; Bochmann, M. *Dalton Trans.* **2006**, 340; (d) Poirier, V.; Roisnel, T.; Carpentier, J.-F.; Sarazin, Y. *Dalton Trans.* **2009**, 9820; (e) Ho, S.-M.; Hsiao, C.-S.; Datta, A.; Hung, C.-H.; Chang, L.-C.; Lee, T.-Y.; Huang, J.-H. *Inorg. Chem.* **2009**, *48*, 8004; (f) Piao, L. H.; Sun, J. R.; Zhong, Z. Y.; Liang, Q. Z.; Chen, X. S.; Kim, J. H.; Jing, X. B. *J. Appl. Polym. Sci.* **2006**, *102*, 2654.
54. Davidson, M. G.; O'Hara, C. T.; Jones, M. D.; Keir, C. G.; Mahon, M. F.; Kociok-Köhn, G. *Inorg. Chem.* **2007**, *46*, 7686.
55. Sarazin, Y.; Liu, B.; Roisnel, T.; Maron, L.; Carpentier, J. F. *J. Am. Chem. Soc.* **2011**, *133*, 9069.
56. (a) Darenbourg, D. J.; Choi, W.; Ganguly, P.; Richers, C. P. *Macromolecules* **2006**, *39*, 4374; (b) Darenbourg, D. J.; Choi, W.; Richers, C. P. *Macromolecules* **2007**, *40*, 3521; (c) Darenbourg, D. J.; Choi, W.; Karroonirun, O.; Bhuvanesh, N. *Macromolecules* **2008**, *41*, 3493.
57. Marshall, E. L.; Gibson, V. C.; Rzepa, H. S. *J. Am. Chem. Soc.* **2005**, *127*, 6048.
58. Cushion, M. G.; Mountford, P. *Chem. Commun.* **2011**, 47, 2276.
59. (a) Chisholm, M. H.; Navarro-Llobet, D.; Simonsick, W. J. *Macromolecules* **2001**, *34*, 8851; (b) Feng, Y.; Klee, D.; Hocker, H. *Macromol. Chem. Phys.* **2001**, *202*, 3120.
60. (a) Piesik, D. F. J.; Range, S.; Harder, S. *Organometallics* **2008**, *27*, 6178; (b) Xiao, Y. L.; Wang, Z.; Ding, K. L. *Macromolecules* **2006**, *39*, 128.
61. (a) Boyle, T.; Hernandez-Sanchez, B.; Baros, C.; Brewer, L.; Rodriguez, M. *Chem. Mater.* **2007**, 2016; (b) He, X. Y.; Morris, J.; Noll, B. C.; Brown, S. N.; Henderson, K. W. *J. Am. Chem. Soc.* **2006**, *128*, 13599; (c) He, X. Y.; Hurley, E.; Noll, B. C.; Henderson, K. W. *Organometallics* **2008**, *27*, 3094; (d) Dove, A.; Gibson, V. C.; Hormnirun, P.; Marshall, E. L.; Segal, J.; White, A. J. P.; Williams, D. W. *Dalton Trans.* **2003**, 3088; (e) Sarish, S.; Nembenna, S.; Nagendran, S.; Roesky, H. W.; Pal, A.; Herbst-Irmer, R.; Ringe, A.; Magull, J. *Inorg. Chem.* **2008**, 5971.
62. Ruspice, C.; Nembenna, S.; Hofmeister, A.; Magull, J.; Harder, S.; Roesky, H. W. *J. Am. Chem. Soc.* **2006**, *128*, 15000.
63. (a) Arunasalam, V.; Mingos, D. M. P.; Plakatouras, J.; Baxter, I.; Hursthouse, M.; Malik, K. *Polyhedron* **1995**, *14*, 1105; (b) Arunasalam, V.; Baxter, I.; Darr, J.; Drake, S.; Hursthouse, M.; Malik, K.; Mingos, D. M. P. *Polyhedron* **1998**, *17*, 641; (c) Bezouglı, I.; Bashall, A.; McPartlin, M.; Mingos, D. M. P. *J. Chem. Soc. Dalton Trans.* **1998**, 2665.
64. Weeber, A.; Harder, S.; Brintzinger, H.; Knoll, K. *Organometallics* **2000**, *19*, 1325.
65. (a) Feil, F.; Harder, S. *Organometallics* **2001**, *20*, 4616; (b) Harder, S.; Feil, F.; Weeber, A. *Organometallics* **2001**, *20*, 1044.
66. (a) Harder, S.; Feil, F. *Organometallics* **2002**, *21*, 2268; (b) Feil, F.; Harder, S. *Eur. J. Inorg. Chem.* **2003**, 3401; (c) Piesik, D. F. J.; Habe, K.; Harder, S. *Eur. J. Inorg. Chem.* **2007**, 5652.
67. Crimmin, M. R.; Barrett, A. G. M.; Hill, M. S.; Procopiou, P. A. *Org. Lett.* **2007**, *9*, 331.
68. Day, B. M.; Mansfield, N. E.; Coles, M. P.; Hitchcock, P. B. *Chem. Commun.* **2011**, 47, 4995.
69. Orzechowski, L.; Harder, S. *Organometallics* **2007**, *26*, 2144.
70. Barrett, A. G. M.; Crimmin, M. R.; Hill, M. S.; Hitchcock, P. B.; Lomas, S. L.; Procopiou, P. A.; Suntharalingam, K. *Chem. Commun.* **2009**, 2299.
71. (a) Burke, D. J.; Hanusa, T. P. *Organometallics* **1996**, *15*, 4971; (b) Guino, M.; Alexander, J.; McKee, M.; Hope, H.; English, U.; Ruhlandt-Senge, K. *Chem. Eur. J.* **2009**, *15*, 11842; (c) Schumann, H.; Steffens, A.; Hummert, M. Z. *Anorg. Allg. Chem. Int. Ed.* **1999**, *38*, 354; (d) Green, D.; English, U.; Ruhlandt-Senge, K. *Angew. Chem. Int. Ed.* **1999**, *38*, 354; (e) Stasch, A.; Sarish, S.; Roesky, H. W.; Meindl, K.; Dall'Antonia, F.; Schulz, T.; Stalke, D. *Chem. Asian J.* **2009**, *4*, 1451; (f) Avent, A. G.; Crimmin, M. R.; Hill, M. S.; Hitchcock, P. B. *Organometallics* **2005**, *24*, 1184.
72. Barrett, A. G. M.; Crimmin, M. R.; Hill, M. S.; Hitchcock, P. B.; Lomas, S. L.; Mahon, M. F.; Procopiou, P. A.; Suntharalingam, K. *Organometallics* **2008**, *27*, 6300.
73. (a) Lee, L.; Berg, D. J.; Bushnell, G. W. *Organometallics* **1995**, *14*, 5021; (b) Heeres, H. J.; Nijhoff, J.; Teuben, J. H.; Rogers, R. D. *Organometallics* **1993**, *12*, 2609.
74. Hong, S.; Marks, T. J. *Acc. Chem. Res.* **2004**, *37*, 673.
75. Crimmin, M. R.; Casely, I. J.; Hill, M. S. *J. Am. Chem. Soc.* **2005**, *127*, 2042.
76. Crimmin, M. R.; Arrowsmith, M.; Barrett, A. G. M.; Casely, I. J.; Hill, M. S.; Procopiou, P. A. *J. Am. Chem. Soc.* **2009**, *131*, 9670.
77. Arrowsmith, M.; Crimmin, M. R.; Barrett, A. G. M.; Hill, M. S.; Kociok-Köhn, G.; Procopiou, P. A. *Organometallics* **2011**, *30*, 1493.
78. (a) Avent, A. G.; Crimmin, M. R.; Hill, M. S.; Hitchcock, P. B. *Dalton Trans.* **2004**, 3166; (b) Barrett, A. G. M.; Crimmin, M. R.; Hill, M. S.; Kociok-Köhn, G.; Lachs, J. R.; Procopiou, P. A. *Dalton Trans.* **2008**, 1292; (c) Barrett, A. G. M.; Casely, I. J.; Crimmin, M. R.; Hill, M. S.; Lachs, J. R.; Mahon, M. F.; Procopiou, P. A. *Inorg. Chem.* **2009**, *48*, 4445.
79. Dunne, J. F.; Fulton, D. B.; Ellern, A.; Sadow, A. D. *J. Am. Chem. Soc.* **2010**, *132*, 17680.
80. Arrowsmith, M.; Crimmin, M. R.; Barrett, A. G. M.; Hill, M. S.; Kociok-Köhn, G.; Procopiou, P. A. *Organometallics* **2011**, *30*, 1493.
81. Buch, F.; Harder, S. Z. *Naturforsch. B* **2008**, *63*, 169.
82. Neal, S. R.; Ellern, A.; Sadow, A. D. *J. Organomet. Chem.* **2011**, *696*, 228.
83. (a) Wixey, J. S.; Ward, B. D. *Chem. Commun.* **2011**, 47, 5449; (b) Wixey, J. S.; Ward, B. D. *Dalton Trans.* **2011**, 40, 7693.
84. Zhang, X.; Enge, T. J.; Hultsch, K. C. *Angew. Chem. Int. Ed.* **2011**, *51*(2), 394–398. <http://dx.doi.org/10.1002/anie.201105079>.
85. Barrett, A. G. M.; Brinkmann, C.; Crimmin, M. R.; Hill, M. S.; Hunt, P.; Procopiou, P. A. *J. Am. Chem. Soc.* **2009**, *131*, 12906.
86. (a) Barrett, A. G. M.; Boorman, T. C.; Crimmin, M. R.; Hill, M. S.; Kociok-Köhn, G.; Procopiou, P. A. *Chem. Commun.* **2008**, 5206–5208; (b) Lachs, J.; Barrett, A. G. M.; Crimmin, M. R.; Kociok-Köhn, G.; Hill, M. S.; Mahon, M. F.; Procopiou, P. A. *Eur. J. Inorg. Chem.* **2008**, 4173.
87. Barrett, A. G. M.; Crimmin, M. R.; Hill, M. S.; Hitchcock, P. B.; Procopiou, P. A. *Dalton Trans.* **2008**, 4474.

88. (a) Kawaoka, A. M.; Douglass, M. R.; Marks, T. J. *Organometallics* **2003**, *22*, 4630; (b) Douglass, M. R.; Stern, C. L.; Marks, T. J. *J. Am. Chem. Soc.* **2001**, *123*, 10221.
89. (a) Takaki, K.; Koshiji, G.; Komeyama, K.; Takeda, M.; Shishido, T.; Kitani, A.; Takehira, K. *J. Org. Chem.* **2003**, *68*, 6554; (b) Takaki, K.; Takeda, M.; Koshiji, G.; Shishido, T.; Takehira, K. *Tetrahedron Lett.* **2001**, *42*, 6357.
90. Crimmin, M. R.; Barrett, A. G. M.; Hill, M. S.; Hitchcock, P. B.; Procopiou, P. A. *Organometallics* **2007**, *26*, 2953.
91. (a) Westerhausen, M.; Low, R.; Schwarz, W. J. *Organomet. Chem.* **1996**, *513*, 213; (b) Westerhausen, M.; Pfitzner, A. J. *Organomet. Chem.* **1995**, *487*, 187; (c) Westerhausen, M.; Schwarz, W. J. *Organomet. Chem.* **1993**, *463*, 51; (d) Westerhausen, M.; Digeser, M.; Krofta, M.; Wiberg, N.; Noth, H.; Krizek, J.; Ponikvar, W.; Seifert, T. *Eur. J. Inorg. Chem.* **1999**, 743; (e) Westerhausen, M.; Birg, C.; Krofta, M.; Mayer, P.; Seifert, T.; Noth, H.; Pfitzner, A.; Nilges, T.; Deiseroth, H. Z. *Anorg. Allg. Chem.* **2000**, *626*, 1073; (f) Westerhausen, M.; Krofta, M.; Mayer, P. Z. *Anorg. Allg. Chem.* **2000**, *626*, 2307.
92. Westerhausen, M.; Digeser, M.; Noth, H.; Ponikvar, W.; Seifert, T.; Polborn, K. *Inorg. Chem.* **1999**, *38*, 3207.
93. Al-Shboul, T. M. A.; Goris, H.; Westerhausen, M. *Inorg. Chem. Commun.* **2008**, *11*, 1419.
94. Crimmin, M. R.; Barrett, A. G. M.; Hill, M. S.; Hitchcock, P. B.; Hitchcock, P. B.; Procopiou, P. A.; Procopiou, P. A. *Organometallics* **2008**, *27*, 497.
95. Al-Shboul, T. M. A.; Volland, G.; Goris, H.; Westerhausen, M. Z. *Anorg. Allg. Chem.* **2009**, *635*, 1568.
96. Buch, F.; Brettar, H.; Harder, S. *Angew. Chem. Int. Ed.* **2006**, *45*, 2741.
97. Harder, S.; Brettar, J. *Angew. Chem. Int. Ed.* **2006**, *45*, 3474.
98. Bonyhady, S.; Jones, C.; Nembenna, S.; Stasch, A.; Edwards, A.; McIntyre, G. *Chem. Eur. J.* **2010**, *15*, 938.
99. Arrowsmith, M.; Hill, M. S.; MacDougall, D. J.; Mahon, M. F. *Angew. Chem. Int. Ed.* **2009**, *48*, 4013.
100. Spielmann, J.; Harder, S. *Eur. J. Inorg. Chem.* **2008**, 1480.
101. (a) Hill, M. S.; MacDougall, D. J.; Mahon, M. F. *Dalton Trans.* **2010**, *39*, 11129; (b) Hill, M. S.; Kociok-Köhn, G.; MacDougall, G.; Mahon, M. F.; Weetman, C. *Dalton Trans.* **2011**, *40*, 12500.
102. Arrowsmith, M.; Hill, M. S.; Hadlington, T.; Kociok-Köhn, G.; Weetman, C. *Organometallics* **2011**, *30*, 5556.
103. Crimmin, M. R.; Barrett, A. G. M.; Hill, M. S.; Hitchcock, P. B.; Procopiou, P. A. *Organometallics* **2007**, *26*, 4076.
104. Spielmann, J.; Buch, F.; Harder, S. *Angew. Chem. Int. Ed.* **2008**, *47*, 9434.
105. Spielmann, J.; Harder, S. *Chem. Eur. J.* **2007**, *12*, 8928.
106. Buch, F.; Harder, S. *Organometallics* **2007**, *26*, 5132.
107. (a) Dunne, J. F.; Neal, S. R.; Engelkemier, J.; Ellern, A.; Sadow, A. D. *J. Am. Chem. Soc.* **2011**, *133*, 16782; (b) Hill, M. S.; Mahon, M. F.; Robinson, T. P. *Chem. Commun.* **2010**, *46*, 2498.
108. (a) Kang, X.; Ma, L.; Fang, Z.; Gao, L.; Luo, J.; Wang, S.; Wang, P. *Phys. Chem. Chem. Phys.* **2009**, *11*, 2507; (b) Diyabalanage, H. V. K.; Shrestha, R. P.; Semelsberger, T. A.; Scott, B. L.; Bowden, M. E.; Davis, B. L.; Burrell, A. K. *Angew. Chem. Int. Ed.* **2007**, *46*, 8995; (c) Wu, H.; Zhou, W.; Yildirim, T. *J. Am. Chem. Soc.* **2008**, *130*, 14834.
109. Spielmann, J.; Jansen, G.; Bandman, H.; Harder, S. *Angew. Chem. Int. Ed.* **2008**, *47*, 6290.
110. (a) Spielmann, J.; Harder, S. *J. Am. Chem. Soc.* **2009**, *131*, 5064; (b) Spielmann, J.; Piesik, D. F. J.; Harder, S. *Chem. Eur. J.* **2010**, *16*, 8307.
111. Spielmann, J.; Bolte, M.; Harder, S. *Chem. Commun.* **2009**, 6934.
112. (a) Liprot, D. J.; Hill, M. S.; Mahon, M. F.; MacDougall, D. J. *Chem. Eur. J.* **2010**, *16*, 8508; (b) Hill, M. S.; Hodgson, M.; Liprot, D. J.; Mahon, M. F. *Dalton Trans.* **2011**, *40*, 7783.
113. Hill, M. S.; Kociok-Köhn, G.; Robinson, T. P. *Chem. Commun.* **2010**, *46*, 7587.
114. Bellham, P.; Hill, M. S.; Liprot, D. J.; MacDougall, D. J.; Mahon, M. F. *Chem. Commun.* **2011**, *47*, 9060.
115. Niggemann, M.; Bisek, N. *Chem. Eur. J.* **2010**, *16*, 11246.
116. Niggemann, M.; Meel, M. J. *Angew. Chem. Int. Ed.* **2009**, *48*, 9117.
117. Haubenreisser, S.; Niggemann, M. *Adv. Synth. Catal.* **2011**, *353*, 469.
118. Meyer, V.; Niggemann, M. *Eur. J. Org. Chem.* **2011**, 3671.
119. Yamada, Y.; Shibasaki, M. *Tetrahedron Lett.* **1998**, *39*, 5561.
120. Suzuki, T.; Yamagiwa, N.; Matsuo, Y.; Sakamoto, S.; Yamaguchi, K.; Shibasaki, M.; Noyori, R. *Tetrahedron Lett.* **2001**, *42*, 4669.
121. Yamaguchi, A.; Matsunaga, S.; Shibasaki, M. *J. Am. Chem. Soc.* **2009**, *131*, 10842.
122. Kumaraswamy, G.; Sastry, M. N. V.; Jena, N. *Tetrahedron Lett.* **2001**, *42*, 8515.
123. Kumaraswamy, G.; Jena, N.; Sastry, M. N. V.; Padmaja, M.; Markondaiah, B. *Adv. Synth. Catal.* **2005**, *347*, 867.
124. (a) Agostinho, M.; Kobayashi, S. *J. Am. Chem. Soc.* **2008**, *130*, 2430; (b) Kobayashi, S.; Yamaguchi, M.; Agostinho, M.; Schneider, U. *Chem. Lett.* **2009**, *38*, 296.
125. Tsubogo, T.; Yamashita, Y.; Kobayashi, S. *Angew. Chem. Int. Ed.* **2009**, *48*, 9117.
126. (a) Kobayashi, S.; Tsubogo, T.; Saito, S.; Yamashita, Y. *Org. Lett.* **2008**, *10*, 807; (b) Tsubogo, T.; Saito, S.; Seki, K.; Yamashita, Y.; Kobayashi, S. *J. Am. Chem. Soc.* **2008**, *130*, 13321; (c) Kobayashi, S.; Yamashita, Y. *Acc. Chem. Res.* **2011**, *44*, 58; (d) Tsubogo, T.; Kano, Y.; Ikemoto, K.; Yamashita, Y.; Kobayashi, S. *Tetrahedron Asym.* **2010**, *21*, 1221.
127. Poisson, T.; Tsubogo, T.; Yamashita, Y.; Kobayashi, S. *J. Org. Chem.* **2010**, *75*, 963.
128. (a) Saito, S.; Tsubogo, T.; Kobayashi, S. *Chem. Commun.* **2007**, 1236; (b) Kobayashi, S.; Matsubara, R. *Chem. Eur. J.* **2009**, *15*, 10694.
129. Van Nguyen, H.; Matsubara, R.; Kobayashi, S. *Angew. Chem. Int. Ed.* **2009**, *48*, 5927.
130. Yamaguchi, A.; Aoyama, N.; Matsunaga, S.; Shibasaki, M. *Org. Lett.* **2007**, *9*, 3387.

## 1.39 Main-Group Catalysts for Lactide Polymerization

B-H Huang, S Dutta, and C-C Lin, National Chung Hsing University, Taichung, Taiwan, ROC

© 2013 Elsevier Ltd. All rights reserved.

<b>1.39.1</b>	<b>Introduction</b>	1217
<b>1.39.2</b>	<b>ROP of LA by Main-Group Metals</b>	1220
1.39.2.1	ROP of LAs by Alkali Metals (Li, Na, and K)	1220
1.39.2.2	ROP of LA by Group 2 Metals (Mg, Ca, Sr, Ba) and Zn	1220
1.39.2.2.1	Tripodal complexes	1222
1.39.2.2.2	BDI complexes	1223
1.39.2.2.3	Tridentate ketiminate complexes	1226
1.39.2.2.4	Bisphenolate complexes	1226
1.39.2.2.5	Schiff base complexes	1228
1.39.2.2.6	Miscellaneous ligands	1228
1.39.2.2.7	Comparison of activity of Mg and Zn complexes	1230
1.39.2.2.8	Calcium complexes	1230
1.39.2.3	Group 13 Metals (Al, Ga, In)	1234
1.39.2.4	Group 14 Metals (Ge, Sn)	1236
1.39.2.5	Group 15 Metals (Bi)	1238
1.39.2.6	ROP of LAs by Mixed-Metal Initiators	1240
<b>1.39.3</b>	<b>Stereocontrolled ROP of LAs</b>	1241
<b>1.39.4</b>	<b>Conclusion</b>	1245
<b>Acknowledgment</b>		1247
<b>References</b>		1247

### Abbreviations

<b>BDI</b>	$\beta$ -Diketiminato	<b>MCIMP</b>	2,2'-Methylenebis(4-chloro-6-isopropyl-3-methylphenol)
<b>BnOH</b>	Benzyl alcohol	<b>MMBP</b>	2,2'-Methylenebis(4-methyl-6- <i>tert</i> -butylphenol)
<b>BSS</b>	Bismuth subsalicylate	$M_w$	Weight average molecular weight of the polymer
<b>DP</b>	Degree of polymerization	$M_w/M_n$	Polydispersity or molecular-weight distribution
<b>EDBP</b>	2,2'-Ethylidenebis(4,6-di- <i>tert</i> -butylphenol)	<b>PDI</b>	Polydispersity index
<b>Hex</b>	Hexanoate	<b>PLA</b>	Poly(lactide)
<b>I</b>	Initiator	<b>ROP</b>	Ring-opening polymerization
$k_{prop}$	Rate of propagation	<b>TBBP</b>	3,3',5,5'-Tetra- <i>tert</i> -butyl-2,2'-biphenol
<b>LA</b>	Lactide	<b>TEG</b>	Tetra(ethylene glycol)
<b>M</b>	Monomer		

### 1.39.1 Introduction

Synthetic polymers are widely used in human life as plastics, fibers, coatings, etc. They were originally developed for their excellent mechanical properties and durability. However, their durability and resistance to all forms of degradation that make synthetic polymers so useful have led to a disposal problem and environmental disaster. Therefore, biodegradable polymers have been attracting considerable attention in the past 20 years due to their potential applications in the environmental protection as well as in the medical field.<sup>1</sup> Among biodegradable polymers, the aliphatic polyesters, such as poly( $\epsilon$ -caprolactone),<sup>2</sup> poly(lactide) (PLA),<sup>3</sup> polycarbonate,<sup>4</sup> and their copolymers, are especially interesting for their applications in the medical field as biodegradable surgical sutures or as a delivery medium for controlled release of drugs.<sup>5,6</sup> Especially, PLA, derived from

annually renewable resources such as starch harvested from corn or sugar beet, is one of the promising synthetic biodegradable polymers (Figure 1).

It has been known that the physical and mechanical properties of PLAs are competitive with those of many conventional petrochemical plastics,<sup>7</sup> yet they degrade to lactic acid and low-molecular-weight oligomers which are metabolized by both soil and marine organisms.<sup>8</sup> A larger-scale application of PLAs as a biodegradable material has only become a reality recently when environmentally friendly packaging materials, food and drinks containers, pillow liners, and many more products have been introduced commercially as schematically represented in Figure 2. In addition, poly(L-lactide) (PLLA) has been investigated as implants for fixation of bones and joints as well as medical screws and pins for surgery.<sup>9</sup> Additionally, PLA copolymers have been utilized for medical applications

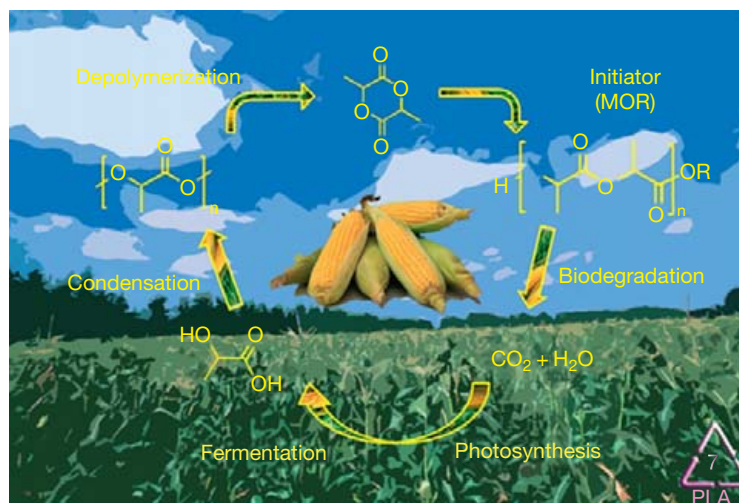


**Figure 1** Synthesis of LA monomer from natural resources, LA polymerization in the presence of a metal catalysts and biodegradation of PLA.

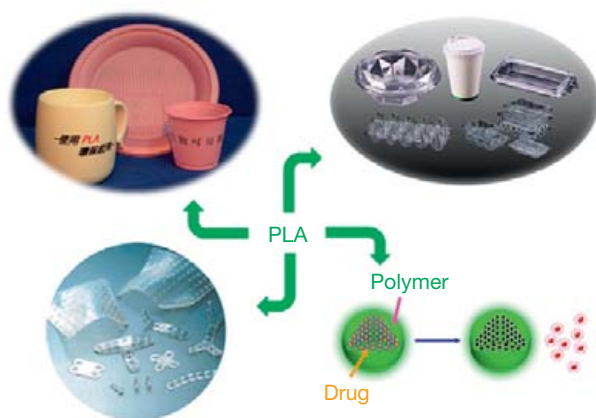
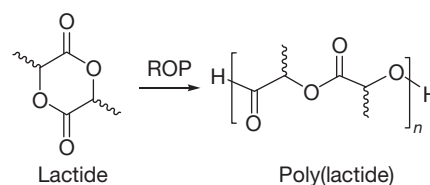


**Figure 2** Applications of PLA.<sup>11</sup>

such as degradable matrix for the controlled drug-delivery matrices.<sup>10</sup>

In the past, PLAs were obtained by condensation of lactic acid-yielding gummy polymeric material with low-molecular weight and poor polydispersities.<sup>12</sup> Synthetically, ring-opening polymerization (ROP) of dilactones, pioneered by Carothers in 1932,<sup>13</sup> was considered as the first initiative for the preparation of PLAs with well-defined molecular weight and polydispersities. During the 1990s, growing interest for sustainable plastics and improvement of the synthetic strategy of lactide (LA) monomer production enabled Carothers' method to be recognized and eventually it has attracted significant interest over the past decades.

Metal-catalyzed ROP of LA is the widely used method in industry and academic laboratories for the preparation of PLA (Scheme 1) with excellent control of polymerization such as high-molecular-weight control with respect to the monomer/initiator ratio, narrow polydispersity, and polymer chain end of polymer, as well as highly selective tacticity. Numerous efforts have been made over the last decade toward the development of efficient metal catalysts that promote the ROP of LA under mild conditions and effectively combine both efficiency and control of

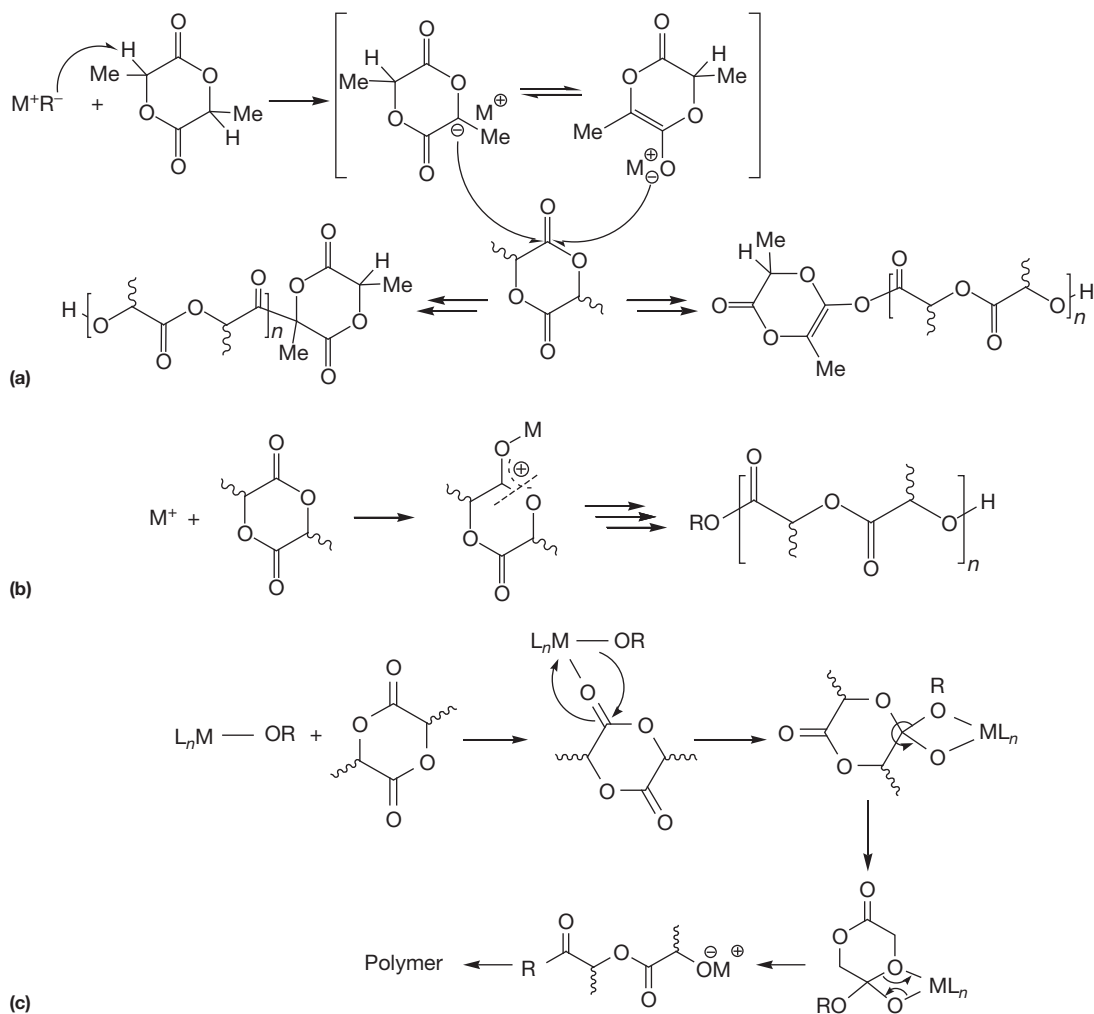


**Scheme 1** Lactide ring-opening polymerization to poly(lactide).

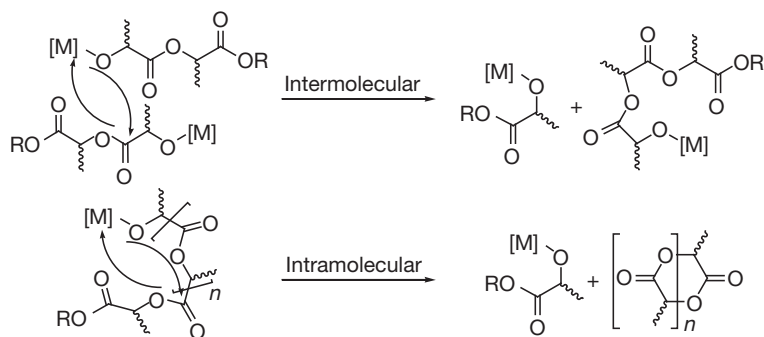
polymerization. It can be reasoned that LAs are among the rare polymerizable six-membered ring compounds with a polymerization enthalpy estimated at approximately  $23 \text{ kJ mol}^{-1}$ <sup>14</sup> which is associated with the relief of their ring strain<sup>15</sup> that stands out as the driving force for the ring-opening step in the polymerization process. In this process, polymerization enthalpy remains modest so that the ROP thermodynamic equilibrium is not highly favorable, especially at high temperature ( $[\text{LA}]_{\text{eq}} = 0.045 \text{ mol l}^{-1}$  at  $20^\circ \text{C}$  and  $0.129 \text{ mol l}^{-1}$  at  $120^\circ \text{C}$ ).<sup>16</sup>

ROP of LAs by metal salts and well-defined complexes has been demonstrated to occur mainly via three routes, namely anionic polymerization (nucleophilic), cationic polymerization, and coordination-insertion polymerization mechanisms. Anionic ROP proceeds through either the deprotonation of the monomer or its ring opening by nucleophilic attack as shown in Scheme 2(a). In acyl cleavage with metal salts such as butyllithium, lithium/potassium *tert*-butoxide, and potassium methoxide, polymerization principally proceeds via attack of the initiating or propagating alkoxide at the ester-carbonyl followed by the ring opening at the acyl C–O bond as shown in Scheme 2(b).<sup>17</sup> The coordination-insertion mechanism, first formulated in 1971 by Dittrich and Schulz, is followed by three steps.<sup>18</sup> This proceeds through coordination of LA by the carbonyl oxygen to the Lewis-acidic metal center which leads to initiation and, subsequently, propagation by a metal alkoxide species, either isolated or generated *in situ* by addition of an alcohol to a suitable metal precursor, to result in the formation of a new chain-extended metal alkoxide complex as shown in Scheme 2(c).<sup>17d</sup>

It is well known that the physical properties of PLA depend dramatically on the molecular weight and polydispersity index



**Scheme 2** Metal-catalyzed ROP of LA (a) anionic, (b) cationic, and (c) coordination insertion.



**Scheme 3** Intramolecular and intermolecular transesterification side reactions.

(PDI) of the polymer. The efficiency of the molecular-weight control depends not only on  $k_{\text{propagation}}/k_{\text{initiation}}$  ( $k_{\text{propagation}}/k_{\text{initiation}}$  = ratio of initiation and propagation rate) but also on the extent of transesterification (intra- and intermolecular backbiting) leading to macrocyclic structures, shorter chains, and polymerization/depolymerization equilibrium in the case of intramolecular transesterification (Scheme 3).<sup>17d</sup> All of these side reactions effectively contribute to the resulting

broad-molecular-weight distributions in product PLA and sometimes in generating irreproducible molecular-weight polymers. In most cases, the extent of the undesirable transesterification reactions has been attributed to the polymerization controllability of the metal initiator.<sup>18</sup>

Recently, several reviews have been published on various aspects of the ROP of LA,<sup>17,19</sup> including stereocontrol of LAs.<sup>20</sup> This chapter delivers an overview of the increasingly expanding

research on ROP of LAs catalyzed by the well-defined main-group metal complexes. Technological aspects such as catalyst efficiency, effects of solvents, and polymerization temperatures on the conversion and polymerization control are discussed. In addition, the effect of the sterics and electronics of the ancillary ligands on the rate of the polymerization of LA as well as the proposed polymerization mechanisms is discussed. Effects of the geometry of the metal complexes, solvent, and temperature on the stereocontrol of ROP of *rac*-LA are also discussed.

### 1.39.2 ROP of LA by Main-Group Metals

Generally, efficient catalysts/initiators for controlled ROP of LA require the following conditions: (1) metal center with high Lewis acidity to increase the bonding with LA; (2) M–OR should be labile to speed up alcohol exchange and insertion reactions with C–O bonds to introduce chain transfer and functionality into the polymer; (3) metal should be redox inactive and inert to  $\beta$ -hydrogen abstraction; and (4)  $L_nM$  template should remain inert with respect to ligand scrambling to prevent the formation of oligomeric metal species and loss of single-site catalysis. On this basis, numerous well-defined main-group metal complexes of the type  $L_nMX$  (M = metal, X = initiating unit commonly an alkoxide or rarely an amide, and  $L_n$  = ancillary ligand) have been developed in order to minimize the aggregation of metal complexes and therefore to enhance their catalytic activity and reduce the transesterification site reactions for ROP of LA over the past decades. An overview of well-defined metal catalysts is presented in this section and comparative studies of the ROP activity of the structurally similar catalysts are included wherever appropriate.

#### 1.39.2.1 ROP of LAs by Alkali Metals (Li, Na, and K)

An important task for developing new catalytic systems is to make the catalyst more compatible with the purpose of biomedical application. Among group 1 metals, also known as alkali metals, sodium and potassium are nontoxic and essential for human life. Lithium is also present in our body at about 30 ppb, though it has several biological effects. For instance, patients with bipolar disorder benefit from taking lithium carbonate. Therefore, these three metals are potential candidates as initiators for ROP of LA.

Anionic polymerization of LAs initiated by BuLi, RO Li, and ROK was investigated as early as the 1990s.<sup>21</sup> In most cases, the afforded PLAs showed broad-molecular-weight distribution (MDW) or worse molecular control due to the side transesterification reactions. ROP of LA by LiCl in the presence of ethylene glycol also showed poor control of polymerization. Recently, dinuclear lithium and macroaggregates with phenolate ligands have attracted substantial interest, mainly due to their distinctly diverse structural features and ability in catalyzing the polyester formation and various other polymeric materials via ROP.<sup>19b,c</sup> A series of lithium complexes coordinated with 2,2'-ethylidenebis(4,6-di-*tert*-butylphenol) (EDBP- $H_2$ ) 2–6 have shown excellent activity for the ROP of *L*-LA in  $CH_2Cl_2$  at moderate temperature (Scheme 4) in which PDIs of the obtained PLAs have been quite narrow (1.04–1.14).<sup>22</sup>

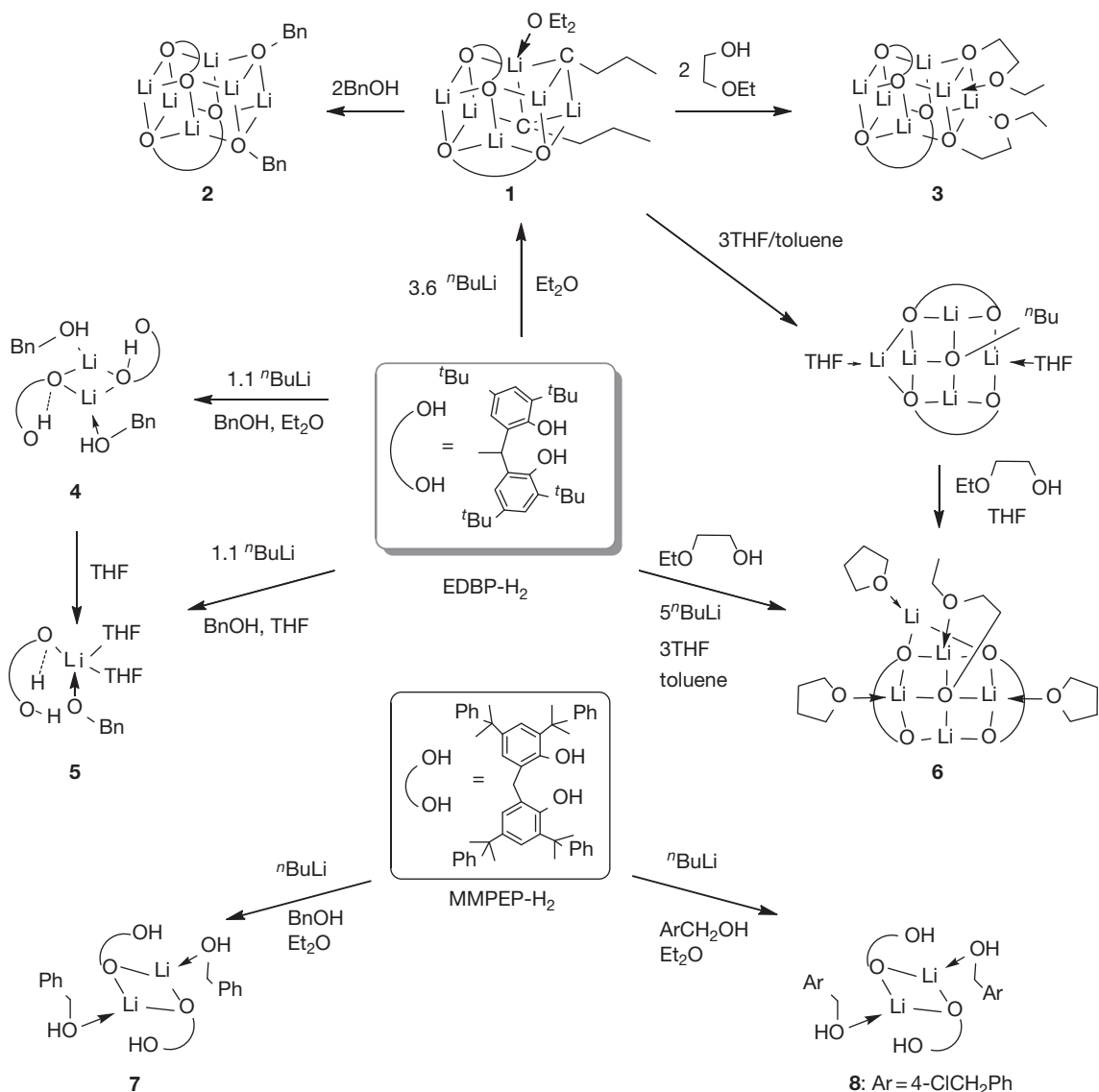
Among them, dinuclear complexes 4 and 6 are the most efficient in polymerizing *L*-LA at low temperature (0 °C) in the presence of benzyl alcohol as a chain-transfer agent, giving polymers with narrow PDIs (1.04–1.08) in  $CH_2Cl_2$ .<sup>22</sup> Similarly, 2,2'-methylenebis[4,6-di(1-methyl-1-phenylethyl)phenol] (MMPEP- $H_2$ ) supported lithium alkoxide complexes [(MMPEP- $H$ )Li•(BnOH)]<sub>2</sub> 7 and [(MMPEP- $H$ )Li•(HOCH<sub>2</sub>C<sub>6</sub>H<sub>4</sub>CH<sub>2</sub>Cl)]<sub>2</sub> 8, bearing a Li<sub>2</sub>O<sub>2</sub> core and phenoxy oxygen bridges, catalyzed ROP of *L*-LA giving PLLAs with PDIs ranging from 1.06 to 1.16.<sup>23</sup>

Chisholm and coworkers have developed two tetranuclear lithium aggregates [( $\mu$ , $\mu$ -biphenolate)Li<sub>2</sub>( $\mu$ -OCH(<sup>*t*</sup>Pr)<sub>2</sub>)<sub>2</sub>Li<sub>2</sub>(L)<sub>2</sub>] (9-THF, L = THF; 9-CyHO, L = CyHO) supported by 5,5,6,6-tetramethyl-3,3-di-*tert*-butyl-1,1-bi-2,2-phenolate of which 9-THF acts as an efficient initiator for ROP of *L*-LA displaying a temperature-dependent reaction rate (Figure 3).<sup>24</sup> A series of tetranuclear lithium complexes (Li<sub>2</sub>O<sub>2</sub>NNMe)<sub>2</sub> 10, (Li<sub>2</sub>O<sub>2</sub>NNPy)<sub>2</sub> 11, and (Li<sub>2</sub>O<sub>2</sub>NOMe)<sub>2</sub> 12 [H<sub>2</sub>O<sub>2</sub>NNMe = Me<sub>2</sub>NCH<sub>2</sub>CH<sub>2</sub>N-(CH<sub>2</sub>-2-HO-3,5-C<sub>6</sub>H<sub>2</sub>(<sup>*t*</sup>Bu)<sub>2</sub>)<sub>2</sub>; H<sub>2</sub>O<sub>2</sub>NNPy = (2-C<sub>3</sub>H<sub>4</sub>N)CH<sub>2</sub>N-(CH<sub>2</sub>-2-HO-3,5-C<sub>6</sub>H<sub>2</sub>(<sup>*t*</sup>Bu)<sub>2</sub>)<sub>2</sub>; H<sub>2</sub>O<sub>2</sub>NOMe = MeOCH<sub>2</sub>CH<sub>2</sub>N-(CH<sub>2</sub>-2-HO-3,5-C<sub>6</sub>H<sub>2</sub>(<sup>*t*</sup>Bu)<sub>2</sub>)<sub>2</sub>]<sup>25a</sup> have been prepared by Chen et al. Recently, tetranuclear Li<sub>2</sub>(O(ArO)<sub>2</sub>)<sub>2</sub> 13 [H<sub>2</sub>O<sub>2</sub>ArO = O(CH<sub>2</sub>-2-OH-3,5-(C(Ph)(Me)<sub>2</sub>)<sub>2</sub>)] and dinuclear complexes [Li(O(ArO)(ArOH))]<sub>2</sub> 14, [Li(O(PhO)(PhOH))]<sub>2</sub> 15, [Li(THF)(O(PhO)(PhOH))]<sub>2</sub> 16, and [Li(O(PhO)(PhOH))(BnOH)]<sub>2</sub> 17 [H<sub>2</sub>O<sub>2</sub>ArO = O(CH<sub>2</sub>-2-OH-3,5-(C<sub>6</sub>H<sub>2</sub>(C(Ph)Me<sub>2</sub>)<sub>2</sub>)<sub>2</sub>; H<sub>2</sub>O<sub>2</sub>PhO = O(CH<sub>2</sub>-2-OH-3,5-(C<sub>6</sub>H<sub>2</sub>(<sup>*t*</sup>Bu)<sub>2</sub>)<sub>2</sub>)] were prepared.<sup>25b</sup> Dinuclear complexes 18–21 derived from pendant aminophenolate ligands were also reported.<sup>25c</sup> All of these lithium derivatives have been found to be active in ROP of *L*-LA with a 'living' character of polymerization. In a similar study, the sterically hindered lithium acetamidinate [Li(tbptamd)(THF)] [tbptamd = *N*-ethyl-*N'*-*tert*-butylbis(3,5-di-*tert*-butylpyrazol-1-yl)acetamidinate] complex 22 has been shown to be an active catalyst for the polymerization of unactivated *L*-LA at 110 °C in toluene without a cocatalyst.<sup>25d</sup> Comparative ROP catalysis data of lithium complexes are presented in Table 1.

Apart from the promising LA polymerization activity of a considerable number of lithium initiators reported in the literature, only a limited number of sodium and potassium initiators are known.<sup>26</sup> Among them, the first reported sodium complex [EDBPH-Na(MeOH)<sub>2</sub>(THF)<sub>2</sub>] 23 (Figure 4) with a sterically bulky ligand, EDBP- $H_2$ , as an efficient initiator for the polymerization of *L*-LA resulted in PLAs with controlled molecular weights and narrow to moderate PDIs (1.08–1.38).<sup>25c</sup> Additionally, di- or tetranuclear complexes, Na<sub>2</sub>(O(ArO)<sub>2</sub>)<sub>2</sub> 24, [Li(O(ArO)(ArOH))]<sub>2</sub> 25 [H<sub>2</sub>O<sub>2</sub>ArO = O(CH<sub>2</sub>-2-OH-3,5-(C<sub>6</sub>H<sub>2</sub>(C(Ph)Me<sub>2</sub>)<sub>2</sub>)<sub>2</sub>],<sup>25b</sup> and [Na(EDBP)((CH<sub>2</sub>)<sub>2</sub>O(CH<sub>2</sub>)<sub>2</sub>OMe)]<sub>2</sub> 26 have also shown similar polymerization results.<sup>26</sup> Furthermore, potassium complexes [K(EDBP((CH<sub>2</sub>)<sub>2</sub>O(CH<sub>2</sub>)<sub>2</sub>OMe))]<sub>2</sub> 27 and [EDBPH-K(THF)<sub>2</sub>] 28 have been demonstrated as efficient catalysts for the ROP of *L*-LA in a controlled manner, yielding PLAs with expected molecular weights and moderate PDIs (1.24–1.58).<sup>26</sup>

#### 1.39.2.2 ROP of LA by Group 2 Metals (Mg, Ca, Sr, Ba) and Zn

Alkaline earth metals such as Mg, Ca, Sr, and Ba are biocompatible, nontoxic, and essential for life.<sup>27</sup> Among these metal



**Scheme 4** Synthesis of lithium complexes **2–8** derived from bisphenolate ligands EDBP-H<sub>2</sub> and MMPEP-H<sub>2</sub>.<sup>22</sup>

ions, Ca<sup>2+</sup> and Mg<sup>2+</sup> are hard and kinetically labile.<sup>28</sup> Therefore, they have attracted most attention as catalysts for developing biocompatible polymers.<sup>29</sup> For instance, Ca(acac)<sub>2</sub> was the first calcium compound reported as initiator for copolymerization of glycolide with LA.<sup>30</sup> Among the heavier group 2 metals, simple strontium complexes such as amino isopropoxyl strontium (Sr-PO) efficiently initiate polymerization of L-LA in a controlled manner under mild conditions.<sup>31</sup> By contrast, well-defined barium initiators for the polymerization of LA are not common probably due to high ionicity and large size which favors the formation of insoluble material and leads to unplanned association of metal centers.<sup>32</sup> Only a few examples of barium complexes as catalysts for LA polymerization have been reported. One of them is the trinuclear barium complex **29** reported by Davidson et al. Polymerization of LA by the unusual trinuclear amino-bis(phenolate) barium complex resulted in PLA in moderate yield (60%) with a reasonable degree of control ( $M_n = 25\,500$ , PDI = 1.57)

(Figure 5).<sup>33a</sup> Recently, Sarazin et al. demonstrated three well-defined cationic barium complexes, **30a–b** and **30c**, stabilized by strong Ba···F—C secondary interactions as shown in Figure 5. Both **30a** and **30b** show high activity toward ROP L-LA in the presence of benzyl alcohol at room temperature. It is worth noting that **30b** reveals an excellent ‘immortal’ character with high turn over frequency (1940 [h<sup>-1</sup>], [L-LA]<sub>0</sub>/[**30b**]/[BnOH]<sub>0</sub> = 1000:1:50, 97%) and a remarkably high L-LA/catalyst ratio in quantitative conversion (95%) at room temperature ([L-LA]<sub>0</sub>/[**30b**]/[BnOH]<sub>0</sub> = 5000:1:100, PDI = 1.08).<sup>33b</sup>

Furthermore, all group 2 metal ions are redox inactive and inert toward β-hydrogen abstraction from growing polymer chains; however, all of these metal ions are kinetically labile and are prone to ligand disproportionation via a Schlenk equilibrium between homoleptic and heteroleptic forms. For instance, the Schlenk equilibrium was found to be favored on the side of the heteroleptic complex in the case of the calcium system and it is controlled by steric as well as electronic effects

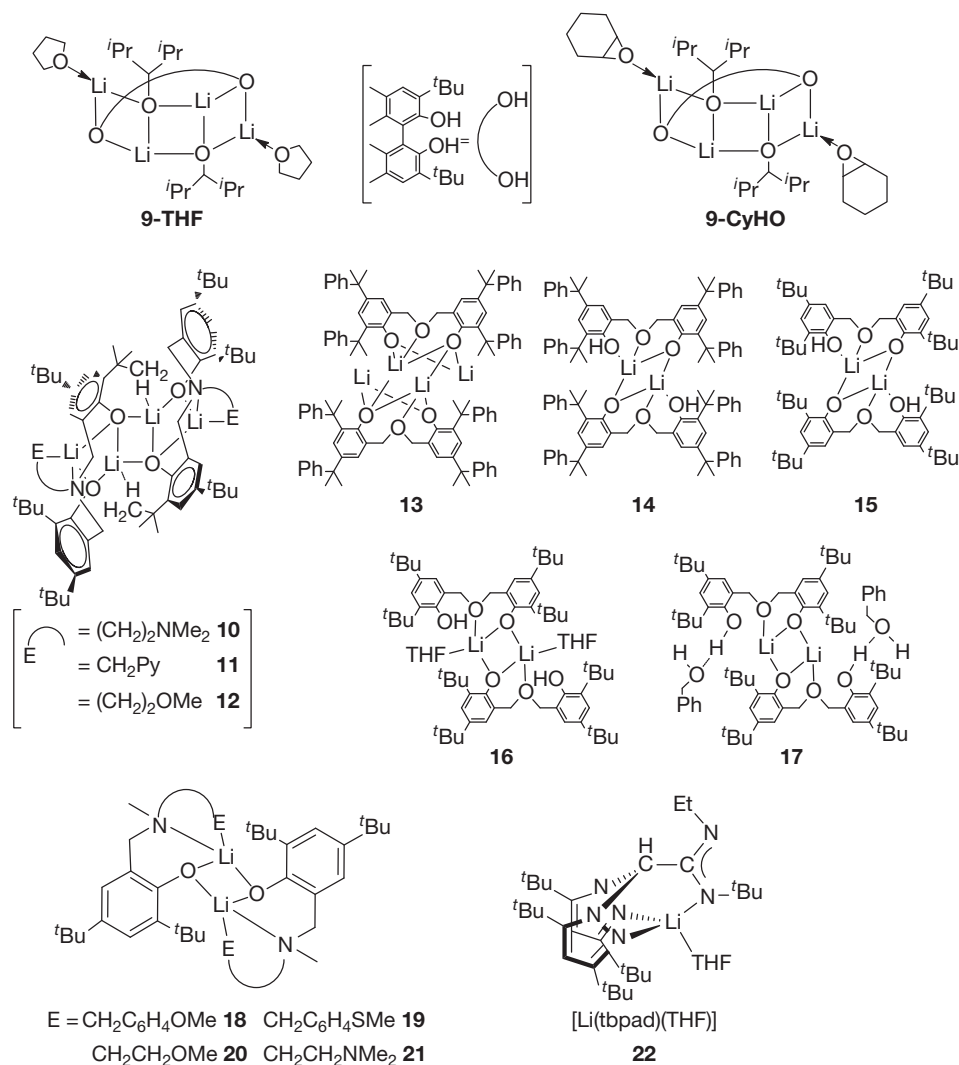


**Figure 3** Other lithium initiators for L-LA polymerization.<sup>24,25</sup>

of the ancillary ligand (Scheme 5(a)).<sup>34</sup> In certain calcium systems, ligand disproportionation was also dependent on the nature of the solvent.<sup>35</sup> Similarly, Schlenk equilibrium between homo- and heteroleptic complexes of barium was also reported as shown in Scheme 5(b).<sup>36</sup>

In order to prevent disadvantages of ligand exchange, suitable steric protection of the ancillary ligands is highly desirable for preventing catalysts from Schlenk equilibrium. A recently developed method of grafting of the calcium reagents on a silica surface to control the Schlenk equilibrium<sup>37</sup> may also provide a new route for designing group 2 metal catalysts for the efficient ROP. However, commonly used ligands for the Mg and Zn initiators were trispyrazolyl hydroborate,  $\beta$ -diketiminates (BDI), bis(phenolate) (diol), Schiff base, and various other ligands.  $\text{Zn}^{2+}$  has  $d^{10}$  pseudo-noble gas configuration and similar ionic radius as magnesium,<sup>38</sup> but the latter is a hard metal, while  $\text{Zn}^{2+}$  is soft in nature<sup>39</sup>; therefore, they exhibit similar but different chemical properties. Regarding a possible incorporation of trace amount of metal residues in end-product PLAs, polymerization catalysts consisting of biocompatible  $\text{Ca}^{2+}$ ,  $\text{Mg}^{2+}$ , and  $\text{Zn}^{2+}$  are therefore much preferred. Therefore, the

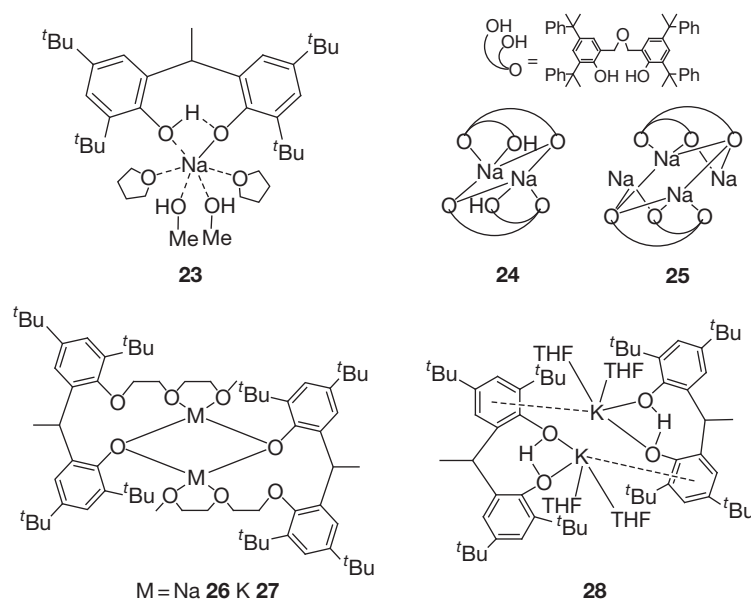
polymerization behaviors of Mg and Zn initiators are summarized and compared in this section.

### 1.39.2.2.1 Tripodal complexes

Monoanionic tridentate ancillary ligands, trispyrazolyl- and trisindazolyl-hydroborate, were introduced by Chisholm et al. to offer the required sterics around the central metal and prevent unwanted aggregation during polymerization of LA. As a result, a series of mononuclear magnesium (31a, 32) and zinc (31b, 33, 34) alkoxides supported by tripodal ligands were prepared (Figure 6) in which 32 produces PLAs with an OEt end group via an acyl cleavage of LA monomer as revealed.<sup>40</sup> Controlled polymerization of L-LA with a linear relationship between number-average molecular weight ( $M_n$ ) and the conversion of monomer with low PDIs (1.10–1.25) was observed using complexes 31a–b as catalysts. Experimental results indicated that magnesium complex 31a is more active than its Zn(II) analogs due to the expected high polarity of the Mg–OR bond as compared to that of the zinc complexes. Kinetic studies revealed that the polymerization followed a first-order

**Table 1** Comparative L-LA polymerization data of lithium complexes

Entry	Initiator	$[M]_0/[I]_0$	$CH_2Cl_2$ (ml)	Temperature ( $^{\circ}C$ )	Time (min)	$M_w/M_n$	$M_n(GPC)^a$	$M_n(NMR)$	Conversion (%)
1	<b>2</b>	150/1	10	25	60	1.43	22 100(12 800)	–	>99
2	<b>2</b>	150/1	20	25	60	1.24	15 200(8800)	–	95
3	<b>3</b>	100/1	10	0	360	1.06	12 400(7200)	6800	95
4	<b>4</b>	100/1	10	0	120	1.08	22 800(13 200)	11 100	92
5	<b>4</b>	200/1	10	0	120	1.05	41 100(23 800)	22 100	92
6	<b>5</b>	25/1	10	0	180	1.05	6300(3700)	3600	92
7	<b>6</b>	100/1	15	0	180	1.07	10 800(6300)	4900	94
8	<b>6</b>	150/1	15	0	180	1.06	15 600(9000)	9600	93
9	<b>8</b>	150/1	10	0	450	1.06	8600(5000)	6900	80
10	<b>9</b>	200/1	10	0	510	1.07	15 400(8900)	11 700	92
11	<b>10</b>	100/1	10	25	15	1.13	23 900(13 900)	–	92
12	<b>11</b>	100/1	10	25	20	1.09	21 400(12 400)	–	92
13	<b>12</b>	100/1	10	25	25	1.08	19 300(11 200)	–	90
14	<b>13</b>	100/1	10	20	50	1.06	25 900(15 000)	14 000	93
15	<b>14</b>	100/1	10	20	120	1.09	26 200(15 200)	14 600	91
16	<b>15</b>	100/1	10	20	60	1.10	18 000(10 300)	12 000	83
17	<b>16</b>	50/1	10 <sup>b</sup>	30	10	1.11	9600(5600)	6000	79
18	<b>17</b>	100/1	10 <sup>b</sup>	30	18	1.08	26 500(15 300)	13 800	85
19	<b>18</b>	100/2	10	25	15	1.23	13 500(7800)	–	97
20	<b>19</b>	100/2	10	25	20	1.22	13 900(8100)	–	96
21	<b>20</b>	100/2	10	25	15	1.14	12 900(7500)	–	95
22	<b>21</b>	50/1	10	15	15	1.14	11 000(6400)	–	92

<sup>a</sup>Obtained from GPC analysis and values in parentheses are from GPC times 0.58.<sup>b</sup>Toluene.**Figure 4** Bis(phenolate)-supported sodium and potassium initiators in L-LA polymerization.

dependence in both LA and metal complex. Achiral initiators **31a–b** also displayed a significant preference for the polymerization of *meso*-LA over L- and D-LA in  $CH_2Cl_2$  at 22  $^{\circ}C$ . However, chiral magnesium complex **32** demonstrated a marked preference for the polymerization of *meso*-LA over *rac*-LA. In sharp contrast to the behavior of complex **31a**, the copolymerization of a 1:1 mixture of *meso*- and *rac*-LA catalyzed by the chiral zinc complex **32** in  $CD_2Cl_2$  at 22  $^{\circ}C$  revealed that both monomers (D- and L-LA) were polymerized essentially at the same rate during the initial phase of the process (~30% conversion).

The chiral complex **32** with (*R,R*) stereocenters at the *t*Pr- and Me-substituted carbon atoms exhibits a modest preference for the polymerization of L-LA from *rac*-LA. Complex **33** was nearly inactive for polymerization of L-LA due to the attachment of electron-withdrawing  $CF_3$  groups.

### 1.39.2.2.2 BDI complexes

$\beta$ -Diketiminato ligands are one of the most versatile ligands in coordination chemistry for their strong metal–ligand bonds and these ligands are readily tunable to access derivatives

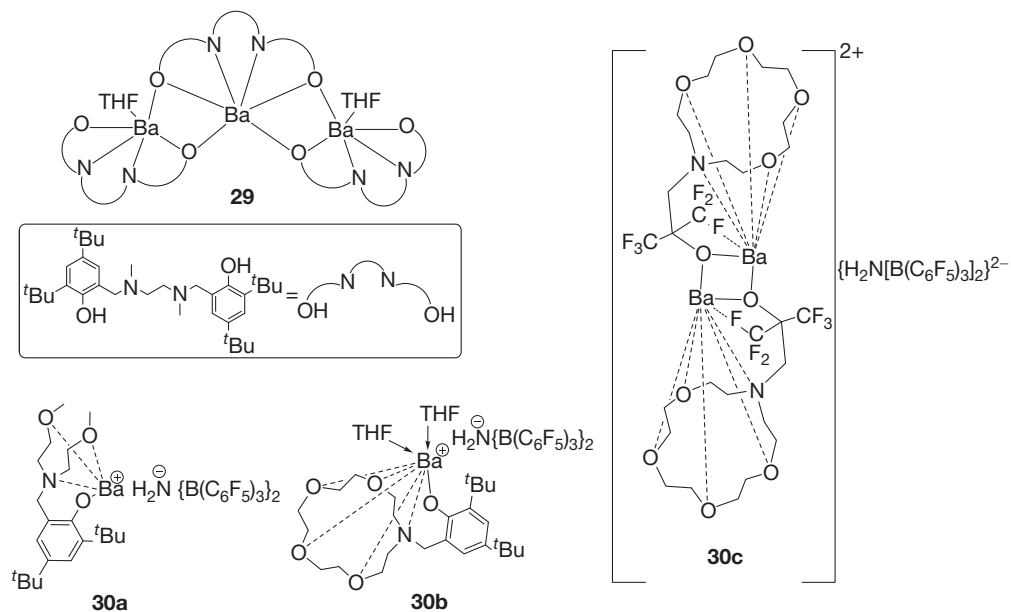
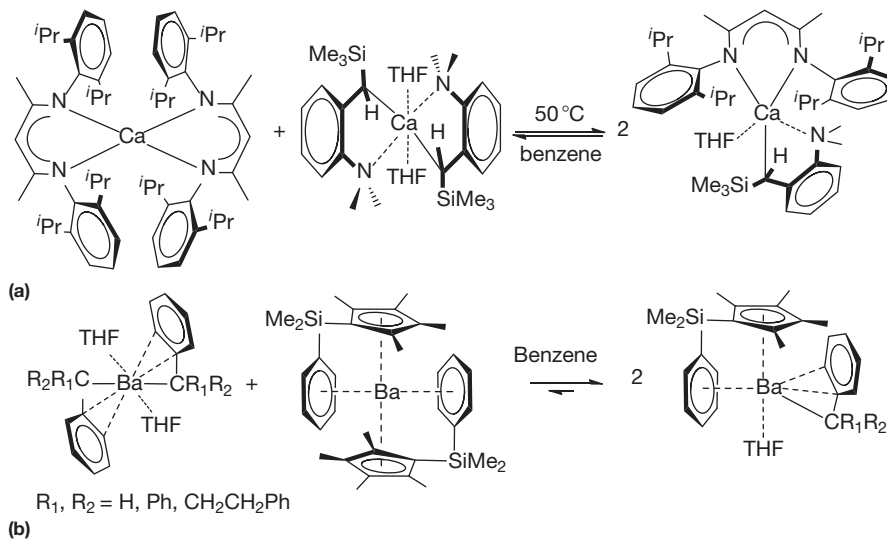


**Figure 5** Trinuclear barium complexes **29** and cationic barium complexes **30a–30c**.



**Scheme 5** Schlenk equilibrium of the homo- and heteroleptic forms complexes of calcium (a) and barium (b).<sup>34–36</sup>

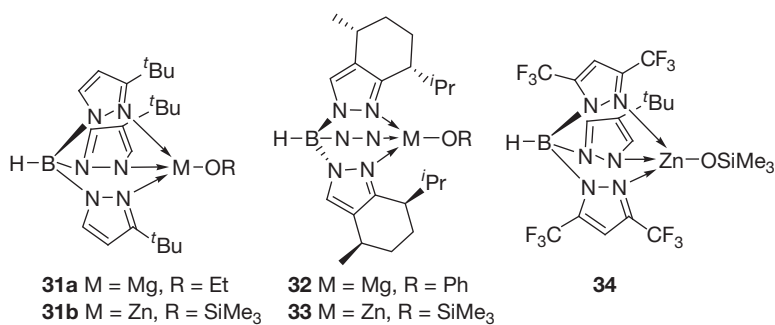


**Figure 6** Trispyrazolyl- and trisindazolyl-hydroborate-supported Mg and Zn complexes.

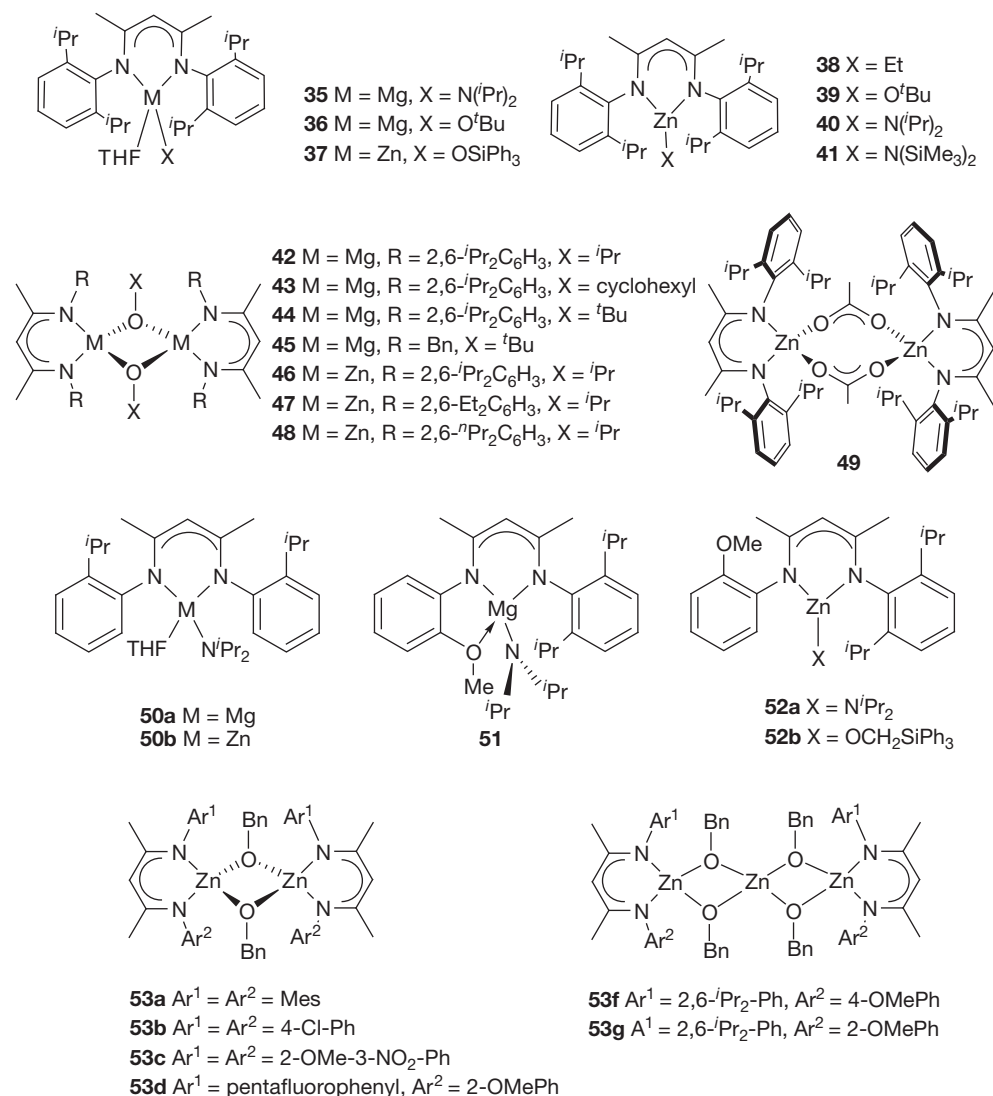


**Figure 7**  $\beta$ -Diketiminate supported Mg and Zn complexes.

containing a range of substituents around the ligand skeleton. A variety of magnesium and zinc alkoxide initiators supported on the sterically bulky BDIs 35–53 (Figure 7) have been developed for polymerization of LA.<sup>41,42</sup> Experimental results indicate that polymerization of LA depends on the initiating groups of the polymerization initiators with the order O<sup>t</sup>Bu > N(*i*Pr)<sub>2</sub> > NSi<sub>2</sub>Me<sub>6</sub> > OSiPh<sub>3</sub>. This order reflects the influence of both electronic and steric factors. For example, while N(*i*Pr)<sub>2</sub> is the most basic initiating unit, its lone pair is sterically less accessible than that of O<sup>t</sup>Bu.<sup>43a</sup> Complexes with alkoxy groups closely mimic the putative propagating groups, producing PLAs of predictable molecular weight and narrow MWD ( $M_w/M_n = 1.10$ ). By contrast, other functional groups are likely to react with impurities such as water resulting in a slow initiation rate of the polymerization.

When compared to diketiminate zinc alkoxide complexes, magnesium analogs are more active for the polymerization of LA. For example, complex 42 has demonstrated a rapid completion of polymerization of *rac*-LA in 2 min at 20 °C ( $[Mg]_0 = 2$  mM;  $[LA]_0 = 0.4$  M;  $[LA]_0/[Mg]_0 = 200$ ) while

complex 46 catalyzed complete conversion in 20 min.<sup>42c</sup> A similar result has been recorded in the case of the Mg complex 36 (2 min) and Zn complex 39 (10 min) with the  $[LA]_0/[Metal]_0$  ratio = 100 in CH<sub>2</sub>Cl<sub>2</sub> at 20 °C.<sup>42b</sup> The PDIs of the resulting polymers produced by magnesium complexes were relatively broader ( $M_w/M_n = 1.20$ – $1.35$ ) than those of the related zinc complexes ( $M_w/M_n = 1.02$ – $1.18$ ).

Tridentate diketiminate-supported magnesium and zinc complexes (51–53) (Figure 7) are highly active for the ROP of LA affording 80–90% conversion to PLA within 10 min.<sup>43a</sup> However, the magnesium initiator 51 displayed far less controlled polymerization than its zinc analogs 52a. Although initiation has been poor, the chain length increases linearly with monomer conversion (plot of  $M_n = 20\,000$ – $50\,000$  vs. % conversion 40–95%) in the presence of complex 52b as catalyst as revealed from the polymerization experiments with  $[LA]:[52b] = 100$  in CDCl<sub>3</sub> at 25 °C with a PDI 1.12–1.21. Recently, Chen et al. illustrated a series of zinc complexes, 53a–g, supported by asymmetric and symmetric BDI ligands with respect to the steric and electronic effect of substituents on the polymerization of *l*-LA.<sup>43b</sup>

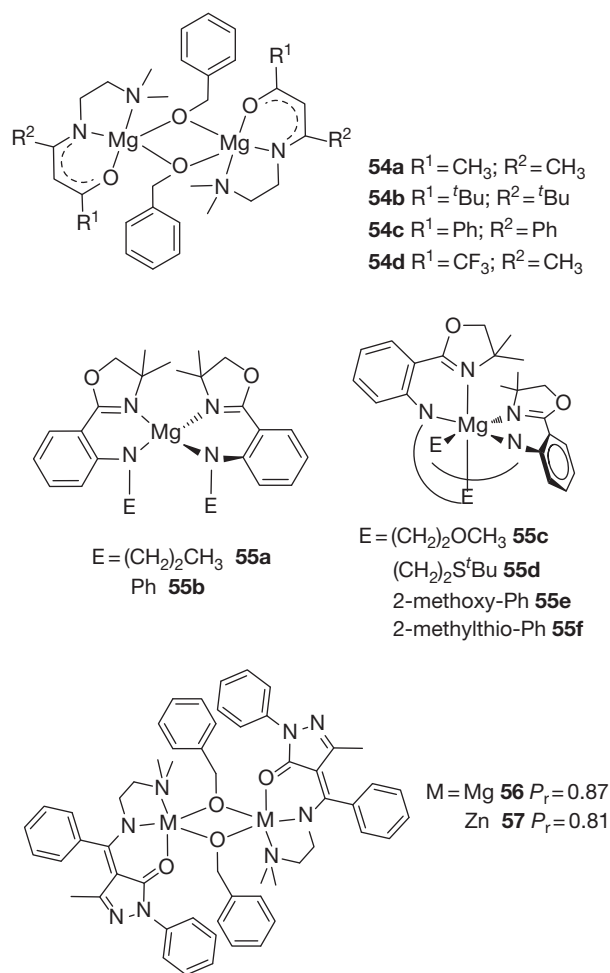


**Figure 8** Tridentate ketimine-supported Mg and Zn complexes.

Catalytic results show that the polymerization rates correlate with the *N*-aryl substituents to a certain extent in the order: alkyl/BnOH  $\sim$  alkoxy (2–5 min, room temp., 94–99%)  $>$  halide (120–290 min, room temp., 87–99%)  $>$  nitro group (360 min, 100 °C, 86%). According to the kinetic studies of **53d**, it shows both first order with respect to the concentration of complex and monomer as well as the overall rate equation concluded with  $-\text{d}[\text{LA}]/\text{d}t = k[\text{LA}]^2[\text{53d}]^1$

### 1.39.2.2.3 Tridentate ketimine complexes

Because of lack of steric effect on one side, the ketimine ligand is insufficient to protect metal complexes forming a disproportionation side reaction. This problem can be overcome by the addition of a pendant-functional coordination site. A series of dinuclear magnesium complexes  $[\text{LMg}(\mu\text{-OBn})_2]$  with NNO-tridentate ketimine ligands (L) **54a–d** (Figure 8) displayed a dramatic steric and electronic influence of the substituents of the ketimine ligand on their *l*-LA polymerization activity. Specifically, a sterically bulkier group increases the activity of a magnesium complex; however, an electron-withdrawing group decreases its activity. In this case, on the basis of the  $^1\text{H}$  NMR results, a mononuclear–dinuclear equilibrium in solution is believed to occur in which the mononuclear form is the most active species. Polymerization probably

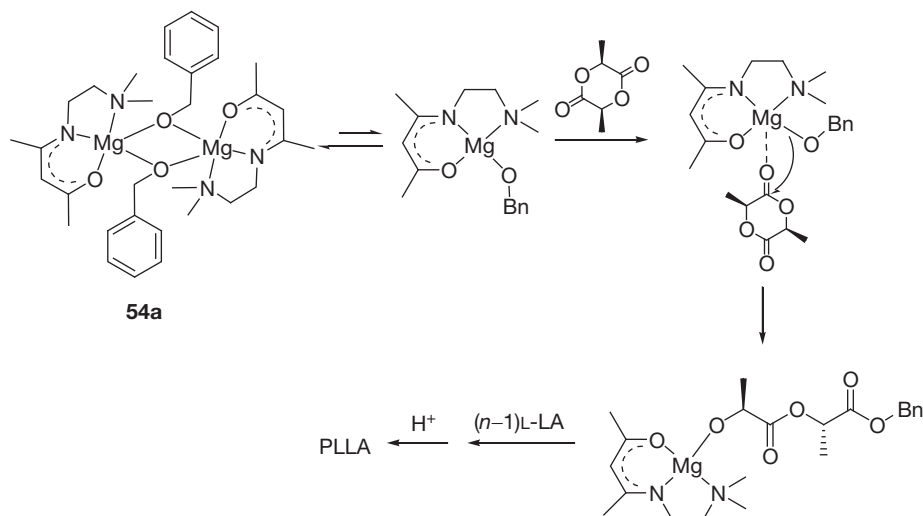
proceeds with the coordination of the LA to the mononuclear complex giving a five-coordinated Mg complex as an intermediate. *l*-LA polymerization results showed a high conversion by all initiators with a range of PDIs 1.13–1.46 of resulting PLAs in toluene at room temperature or 0 °C.<sup>44</sup> In order to quantify the presence of the mononuclear form as the active species during polymerization, a freezing point depression experiment was performed from which the dissociation percentage of the dinuclear species can be calculated which provides 64% dissociation in the case of **54a**. On the basis of the polymerization results, variable-temperature  $^1\text{H}$  NMR and melting-point depression studies, a mechanism for the ROP of *l*-LA initiated by **54a** is proposed as shown in Scheme 6.

Magnesium complexes bearing bis-amido-oxazolate complexes **55a–f**, structurally very similar to the NNO-tridentate ketimine systems, were promoted for deriving PLA from *l*-LA in the presence of benzyl alcohol.<sup>45a</sup> The low activity of **55e** and **55f** is probably due to the retardation in propagation which is attributed to (1) the interaction between phenyl backbone pendant functionalities and magnesium and (2) the rigidity of the phenyl group leading to a hindrance of the coordination of benzyl alcohol or monomer to the metal center. More recently, aromatic heterocyclic pyrazol-5-one-based tridentate NNO donor ketimine-supported magnesium and zinc benzylalkoxide systems  $[\text{L}_2\text{M}_2(\mu\text{-OBn})_2]$  ( $M = \text{Mg}$  **56** or  $\text{Zn}$  **57**,  $L = 4$ -((2-(dimethylamino)ethylamino)(phenyl)-methylene)-3-methyl-1-phenyl-pyrazol-5-one) have been developed and these dinuclear dimeric systems were demonstrated to polymerize *l*-LA rapidly (1.67 to 4 h) with good-molecular-weight control and narrow MWD (PDI 1.04–1.08) in the resulting PLAs.<sup>45b</sup> The kinetic studies for the polymerization of *l*-LA with compound **56** show first order in concentration of both **56** and LA with a polymerization rate constant,  $k$ , of  $6.94 \text{ M min}^{-1}$ . Interestingly, faster polymerizations were recorded for both *l*- and *rac*-LA when using zinc complex **57** as initiator.

### 1.39.2.2.4 Bisphenolate complexes

A series of bis(phenolate) ligands such as EDBP-H<sub>2</sub> and MCIMP-H<sub>2</sub> supported dinuclear magnesium and zinc complexes **58a–58e** as well as a tetranuclear magnesium complex **58g** were obtained by reactions of bisphenol ligands with  $\text{Mg}^t\text{Bu}_2$  or  $\text{Et}_2\text{Zn}$  in THF or diethyl ether (Figure 9).<sup>46,47</sup> All of these complexes exhibit dimeric structures or higher aggregates in the solid state despite the presence of bulky substituents in the *ortho* positions of phenyls. It is found that magnesium complex **58d** is more active than the other magnesium complexes, probably due to a more sterically bulky group in the bridging carbon of the MEMPEP<sup>2-</sup> ligand. ROP of LA by **58d** gives a complete conversion in 2 h at 25 °C at  $[\text{LA}]_0/[\text{Cat}]_0/[\text{BnOH}]_0$  200:1:2, while complex **58b** does so in 2 h at 83 °C. In addition to these systems, this divalent ancillary has been changed into a monovalent analog by conversion of the alkoxide group into methoxy group recently. Like BDI and tripodal systems, bisphenolato zinc complexes **58e** and **58f** are somewhat less active than their magnesium analogues **58c** and **58d**. Polymerization of LA requires 40 h to proceed to 96% conversion at room temperature with PDI = 1.41 using zinc complex **59** as initiator.<sup>24</sup>

EDBP-(Me)H-supported dinuclear magnesium initiator  $\{[\text{EDBP}(\text{Me})]\text{Mg}(\mu\text{-OBn})\}_2$  **60** is also active in *l*-LA



**Scheme 6** Proposed mechanism for the ROP of L-LA initiated by **54a**.<sup>44</sup>

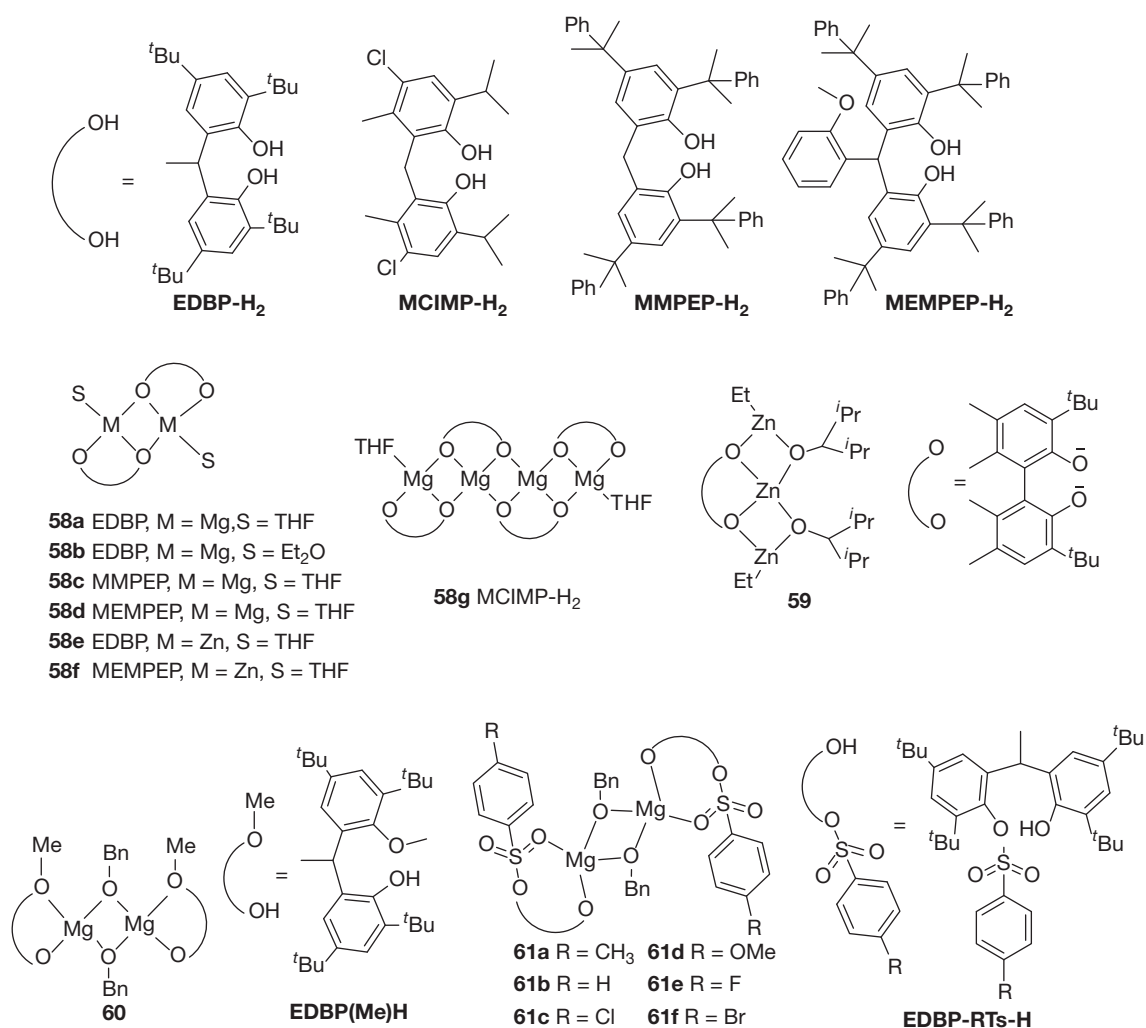


**Figure 9** Bisphenolate-supported Mg and Zn complexes.

polymerization resulting in the molecular weight of the PLLA twice that as expected, indicating that only one of the two benzyl alkoxy groups is active in the polymerization process.<sup>48a</sup> Similar results are obtained in the case of ROP of LA using [(EDBP-RTs)Mg(OBn)]<sub>2</sub> **61** as an initiator.<sup>48b</sup> The polymerization activity of **60** is higher (99% conversion in 10 min) than its EDBP analog probably due to the higher activity of RO<sup>-</sup> compared to ROH. In addition, the activity of **61** is much higher than that of **60** due to more electron deficiency on the metal center of **61**. The mechanism initiated by **60** and **61** is proposed as shown in Scheme 7.

### 1.39.2.2.5 Schiff base complexes

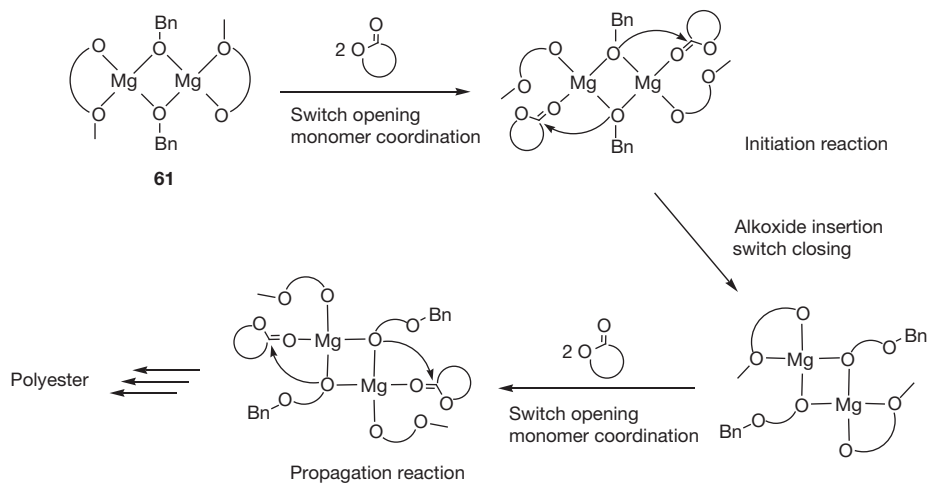
Because of their diverse forms and ease of preparation, many Schiff-base-supported metal complexes have been widely used in ROP of LA. The first Schiff-base-supported zinc complexes **62a** and **62b** (Figure 10) were reported by Chisholm et al.<sup>49</sup> which catalyzed polymerization of L-LA with conversion up to 90% at room temperature in 3 h for **62a** and 72 h for **62b**. The difference in the reaction rate is probably due to the sterically bulkier 2,6-*tert*-butylphenoxide initiating unit in **62b**. Recently, we have developed a series of NNO-tridentate Schiff base-supported zinc alkoxides **63a**–**63e**, excluding **63c** from 90% with 240 min at 80 °C, efficiently initiate the polymerization of L-LA at 25 °C with conversion of >90% within 30–80

min.<sup>50</sup> The polymerization was well controlled (PDI = 1.04–1.09) and the reactivity decreases with an electron-withdrawing group on the ligand. Increasing the steric bulk of substituents at the imine carbon, **63f**–**63i**, increases the catalytic activity dramatically with the conversion of L-LA reaching >87% within 4 min at 0 °C, and yielding a polymer with low PDI (1.07–1.16).<sup>51</sup>

Furthermore, experimental results show that sterically congested monoether salen-supported dinuclear magnesium complex **64a** initiates polymerization of LA at 25 °C in 50 min with a 96% conversion, while the zinc complex **64b** requires 4 h at 60 °C to reach 95% conversion on the ratio of [LA]<sub>0</sub>/[I]<sub>0</sub> = 100.<sup>52a</sup> Kinetic studies of L-LA polymerization revealed a second-order dependency on [LA] and a first-order dependency on concentration of complex **64a**, while complex **64b** favors a dinuclear initiation mechanism since the polymerization rate has a first-order dependency on both [LA] and catalyst concentration. Based on the <sup>1</sup>H NMR spectroscopic studies and kinetic results, a dinuclear intermediate has been proposed for the polymerization initiated by complex **64a** as shown in Scheme 8.

### 1.39.2.2.6 Miscellaneous ligands

Ko et al. have prepared a new type of NNO-tridentate bis(amine)benzotriazole phenol (<sup>C<sup>8</sup>N<sup>N</sup></sup>BTP-H) ligand according



**Scheme 7** Proposed switch opening/closing mechanism for the ROP of cyclic ester.

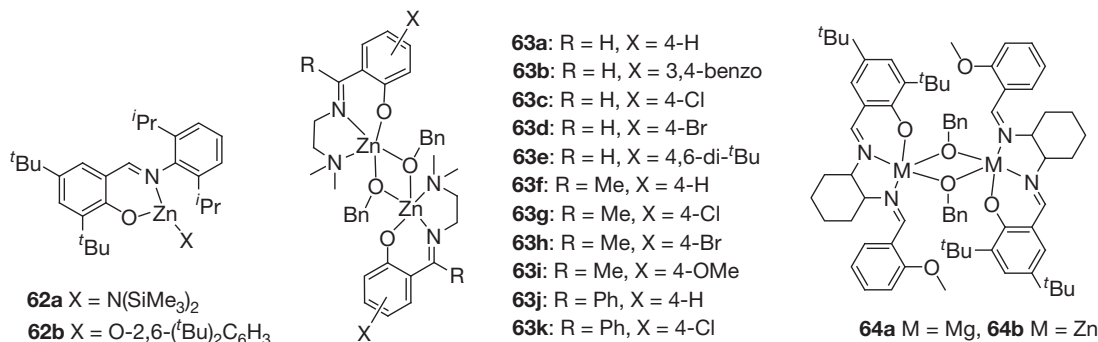
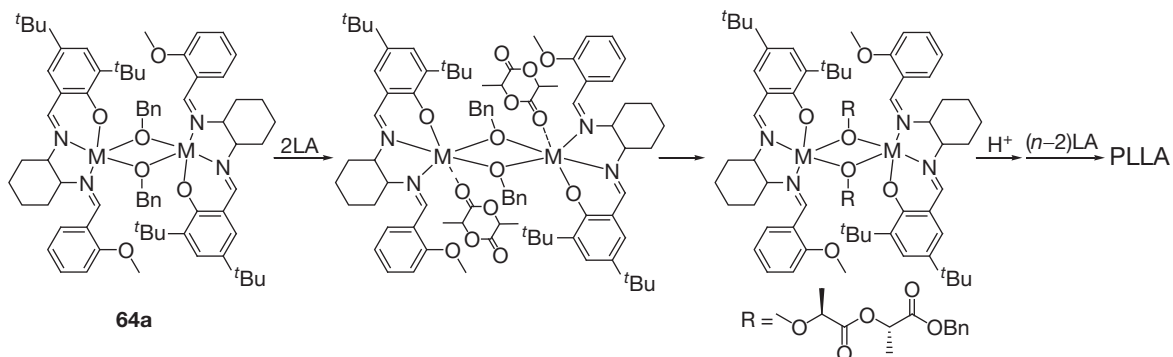


**Figure 10** Schiff-base-ligand-supported zinc and magnesium complexes.



**Scheme 8** Proposed mechanism for ROP of L-LA initiated by **64a**.<sup>52a</sup>

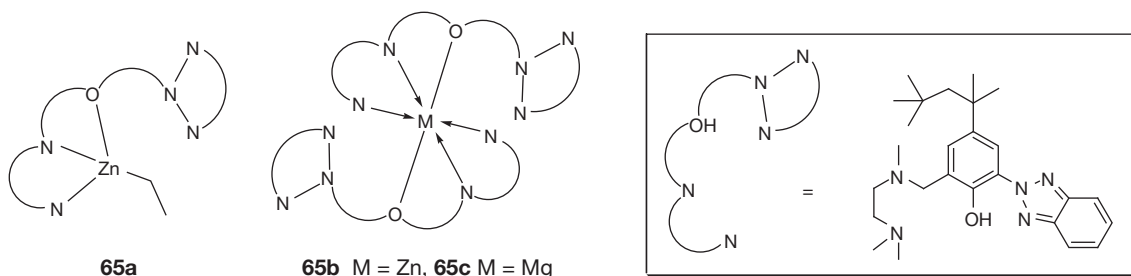


**Figure 11** BTP-H ligand-supported zinc and magnesium complexes.

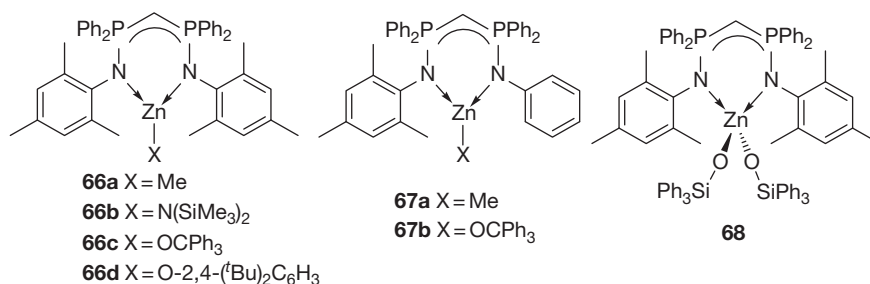


**Figure 12** Bis(phosphinimino)methyl ligand-supported zinc complexes.

to Mannich condensation (Figure 11).<sup>52b</sup> Monomeric metal complexes **65a**–**65c** were synthesized and further utilized for the ROP of LA in the presence of 9-anthracenemethanol (9-AnOH). Experimental results show that homoleptic zinc complex, **65a**, undergoes efficient catalytic activity with a quantitative conversion in a controlled fashion (3 h, 30 °C, PDI = 1.06–1.20). Magnesium complex, **65c**, has relatively lower activity (20 h, 61%) than its zinc analog **65b** (10 h, 97%) in the same condition.

Excellent ROP activity of Coates' sterically bulky BDI zinc complexes inspired the design and synthesis of several bis(phosphinimino)methyl ligand-supported zinc complexes **66**–**68** (Figure 12).<sup>53</sup> Complexes **66c**, **66d**, and **67b** are active for the ROP of *rac*-LA and effect >95% conversion of 100 equiv. of LA in toluene at 60 °C. Among them, **67b** is the most active because of the decreased steric demands of the ligand. The ROP activity of these phosphinimino-based zinc

initiators is lower than that reported for BDI zinc alkoxides **45**–**47** probably due to the strong carbanionic character of the noncoordinating bridge-headed carbon atom.

Hillmyer and Tolman et al. reported a dinuclear NNO-aminophenolate zinc ethoxide **69** which has displayed rapid polymerization of *rac*-LA in CH<sub>2</sub>Cl<sub>2</sub> at room temperature with a [LA]<sub>0</sub>/[I]<sub>0</sub> ratio of 300 (Figure 13).<sup>54</sup> <sup>1</sup>H NMR spectra showed that the polymerization of *D,L*-LA and *L*-LA yielded atactic and isotactic PLA, respectively, implying no epimerization of stereogenic centers. Similarly, zinc alkyl complexes **70a**, **70b**, and alkoxy-bridged dimeric complex **71** were introduced.<sup>55</sup> Complex **71** is highly active for the polymerization of *rac*-LA in CH<sub>2</sub>Cl<sub>2</sub> at ambient temperature, with an activity of 8.2 times higher than that of **69**. Meanwhile, they reported the first *N*-heterocyclic carbene-supported zinc initiator **72** for ROP of LA where each zinc center is in a distorted tetrahedral geometry bound to a carbene and two bridging and one terminal

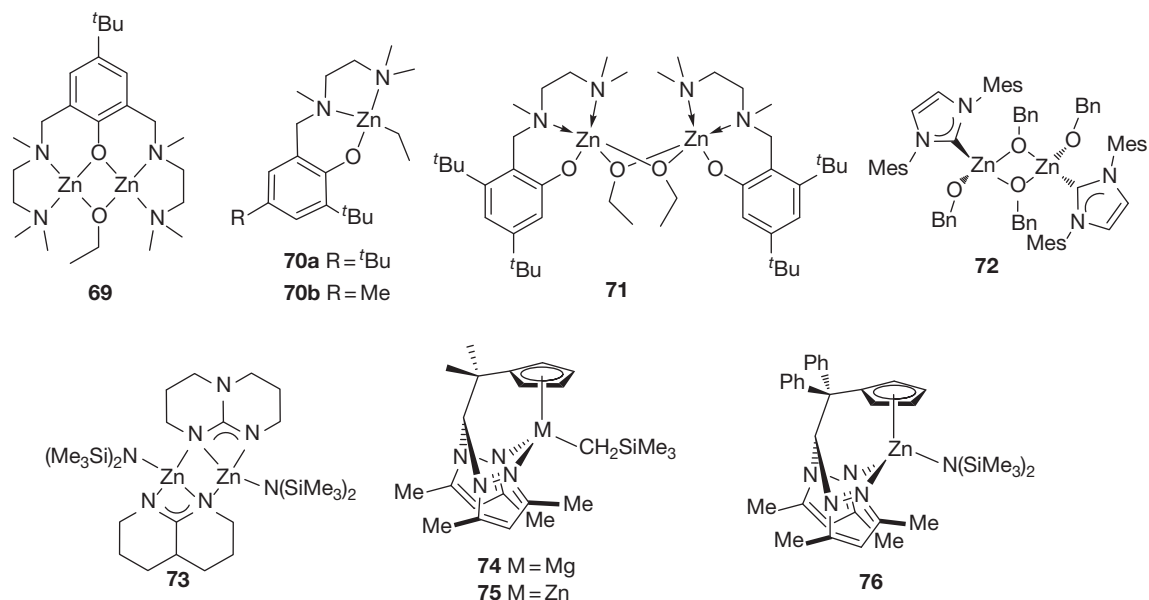


**Figure 13** Zinc complexes of NNO-aminophenolate, NHC, and scorpionate ligands.

benzyloxy units.<sup>56</sup> Kinetic studies revealed a first-order dependence on [LA] for the complex 72 in the polymerization of LA. A similar mixed (guanidinate)(amide) complex  $[\text{Zn}(\text{hpp})\{\text{N}(\text{SiMe}_3)_2\}]_2$  73, which exists as a dimer in the solid state, displays a 95% conversion of *rac*-LA to PLA in 2 h with a linear relationship between molecular weight of the polymers and percentage of conversion, proving the 'living' nature of polymerization.<sup>57</sup>

Structurally characterized hybrid scorpionate/cyclopentadienyl Mg and Zn catalysts afford PLAs with medium molecular weights and narrow polydispersities.<sup>58</sup> Among them, magnesium complex 74 is much more active than the others with the polymerization of *l*-LA of 200 equiv. in toluene at 90 °C for 2.5 h with 97% conversion for 74. However, it takes 30 h for zinc complexes 75 and 76 under the same conditions. Some representative structural types of the magnesium and zinc complexes are listed in **Table 2** as they display closely related ROP activity of LA.

### 1.39.2.2.7 Comparison of activity of Mg and Zn complexes

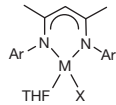
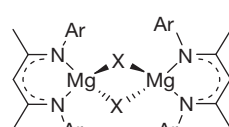
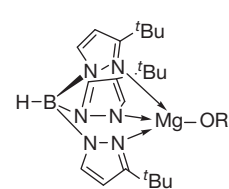
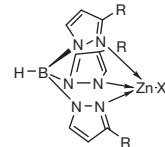
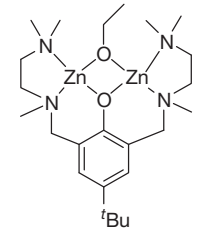
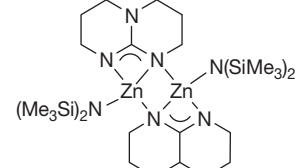
In comparison, it has been found that magnesium complexes supported with bidentate BDI, NNO-tridentate ketiminate, and diol ligands are more active than their structurally analogous zinc complexes in the ROP of LAs. The faster rate of polymerization of magnesium complexes was such that almost complete conversion (97%) occurred in 1 min at 20 °C for the BDI magnesium complex  $[(\text{BDI-1})\text{Mg}(\text{O}^i\text{Pr})]_2$  42 whereas the zinc analog required 33 min for a similar conversion at the same temperature (**Table 3**, entry 1).<sup>42a</sup> Similar distinctly higher activity of polymerization for LAs was noted for a magnesium complex 64 in comparison to its zinc analog of a salen-type Schiff-base ligand (entry 2).<sup>52</sup> A deviation of the normally observed trend of higher activity of magnesium initiators in comparison to the analogous zinc derivatives was noted in the case of the NNO-tridentate ketiminate ligand systems (**Table 3**, entry 3).<sup>45b</sup> In this case, faster polymerizations were recorded for

both *l*- and *rac*-LA when using zinc complex 57 as an initiator. The reason for such a reversal has not been ascertained. Determination of the rate law for the polymerization process did not explain the reversal of ROP activity. Qualitatively, it could be argued that  $\text{M}-\text{O}_{\text{alkoxy}}$  bond breaking occurs more easily for the zinc complex 57 in comparison to its magnesium analog due to the favorable electronics of the ketiminate ligand which facilitates the formation of the new metal-alkoxy species during the initiation process of polymerization. This phenomenon might be reversed in the case of the diketiminate and salen-type Schiff-base ligands which makes their magnesium complexes more active than the zinc analog. In support of this argument, the  $\text{Zn}-\text{O}_{\text{benzyloxy}}$  bond lengths (2.0287(15) and 2.0296(15) Å) of the tridentate ketiminate-supported zinc complex 57 were found to be significantly longer than  $\text{Mg}-\text{O}_{\text{benzyloxy}}$  lengths (1.9752(12) and 1.9901(12) Å) from the analysis of their respective solid-state x-ray structures.<sup>45b</sup>

### 1.39.2.2.8 Calcium complexes

Due to their biocompatible property, calcium-based initiators are expected to be excellent alternative catalysts for preparing PLA. Feijen et al. reported the first highly active calcium examples, generated *in situ* from the reaction of bis(tetrahydrofuran) calcium bis[bis(trimethylsilyl)amide] and isopropanol, for the living and controlled ROP of cyclic esters under mild conditions (18 °C).<sup>58</sup> Calcium initiators  $[(\text{THF})\text{Ca}(\text{tmhd})]_2$  [*p*-N(SiMe<sub>3</sub>)<sub>2</sub>](*p*-tmhd) 77 and  $[(\text{THF})\text{Ca}(\text{tmhd})]_2$  [*p*-OCH(Me)Ph](*p*-tmhd) 78 (**Figure 14**) were derived from the chelating tmhd (H-tmhd = 2,2,6,6-tetramethylheptane-3,3-dione) ligand by the same group.<sup>59</sup> Though 77 is an active initiator for ROP of LA, the PDI of PLA obtained is rather broad. However, the *in situ* initiator 77/2-propanol, in which 2-propanol probably replaces the bridging bis(trimethylsilyl)amido ligand, has much higher activity than 77 in polymerizing LA with first-order polymerization kinetics and the polymerization is well controlled. Complex 78 is highly reactive and promotes a

**Table 2** The activity of Mg and Zn complexes in LA polymerization

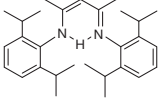
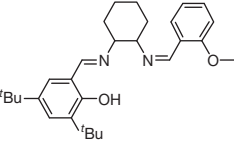
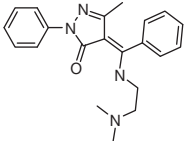
Initiators	Solvent (T/°C) [I] <sub>0</sub> :[LA] <sub>0</sub>	Activity
 <p>M = Mg, Zn, Ar = 2,6-<i>i</i>-Pr<sub>2</sub>C<sub>6</sub>H<sub>3</sub>, 2-<i>t</i>-BuC<sub>6</sub>H<sub>4</sub>, X = N(SiMe<sub>3</sub>)<sub>2</sub>, N(P<sup><i>i</i></sup>Pr)<sub>2</sub>, OSiPh<sub>3</sub>, O<sup><i>t</i></sup>Bu</p>	THF (25) 1:100	5 min, 95% (M = Mg, Ar = 2,6- <i>i</i> -Pr <sub>2</sub> C <sub>6</sub> H <sub>3</sub> , X = O <sup><i>t</i></sup> Bu) 80 min, 95% (M = Zn, Ar = 2,6- <i>i</i> -Pr <sub>2</sub> C <sub>6</sub> H <sub>3</sub> , X = O <sup><i>t</i></sup> Bu) OCH(Me)Ph
 <p>Ar = 2,6-<i>i</i>-Pr<sub>2</sub>C<sub>6</sub>H<sub>3</sub>, 2,6-Pr<sub>2</sub>C<sub>6</sub>H<sub>3</sub>, X = Et, N(SiMe<sub>3</sub>)<sub>2</sub>, OAc, O<sup><i>i</i></sup>Pr</p>	CH <sub>2</sub> Cl <sub>2</sub> (25) 1:490	$k_p = 9 \times 10^{-4} \text{ s}^{-1}$ ( <i>rac</i> -LA, [LA] <sub>0</sub> = 1 M, [I] <sub>0</sub> = 2 mM, R = 2,6- <i>i</i> -Pr <sub>2</sub> C <sub>6</sub> H <sub>3</sub> , X = O <sup><i>i</i></sup> Pr)
 <p>Ar = 2,6-<i>i</i>-Pr<sub>2</sub>C<sub>6</sub>H<sub>3</sub>, X = O<sup><i>i</i></sup>Pr</p>	CH <sub>2</sub> Cl <sub>2</sub> (25) 1:200	2 min, 99% ([LA] <sub>0</sub> = 0.4 M, [I] <sub>0</sub> = 2 mM)
 <p>R = Ph, Et</p>	CH <sub>2</sub> Cl <sub>2</sub> (25) 1:500	60 min, 90% $k_{app} = 6.5 \times 10^{-4} \text{ s}^{-1}$ ([LA] <sub>0</sub> = 5.5 M, [I] <sub>0</sub> = 11 mM, R = <i>t</i> Bu, X = OEt)
 <p>R = <i>t</i>Bu, indazolyl, CF<sub>3</sub>, X = OSiMe<sub>3</sub></p>	CH <sub>2</sub> Cl <sub>2</sub> (25) 1:500	60 days, 90% $k_{app} = 1.3 \times 10^{-5} \text{ s}^{-1}$ ([LA] <sub>0</sub> = 5.5 M, [I] <sub>0</sub> = 11 mM, R = <i>t</i> Bu, X = OEt)
	CH <sub>2</sub> Cl <sub>2</sub> (25)	$k_p = 0.37 \text{ M}^{-1} \text{ s}^{-1}$ (M = Zn)
	CD <sub>2</sub> Cl <sub>2</sub> (25) 1:100	2 h, 95%

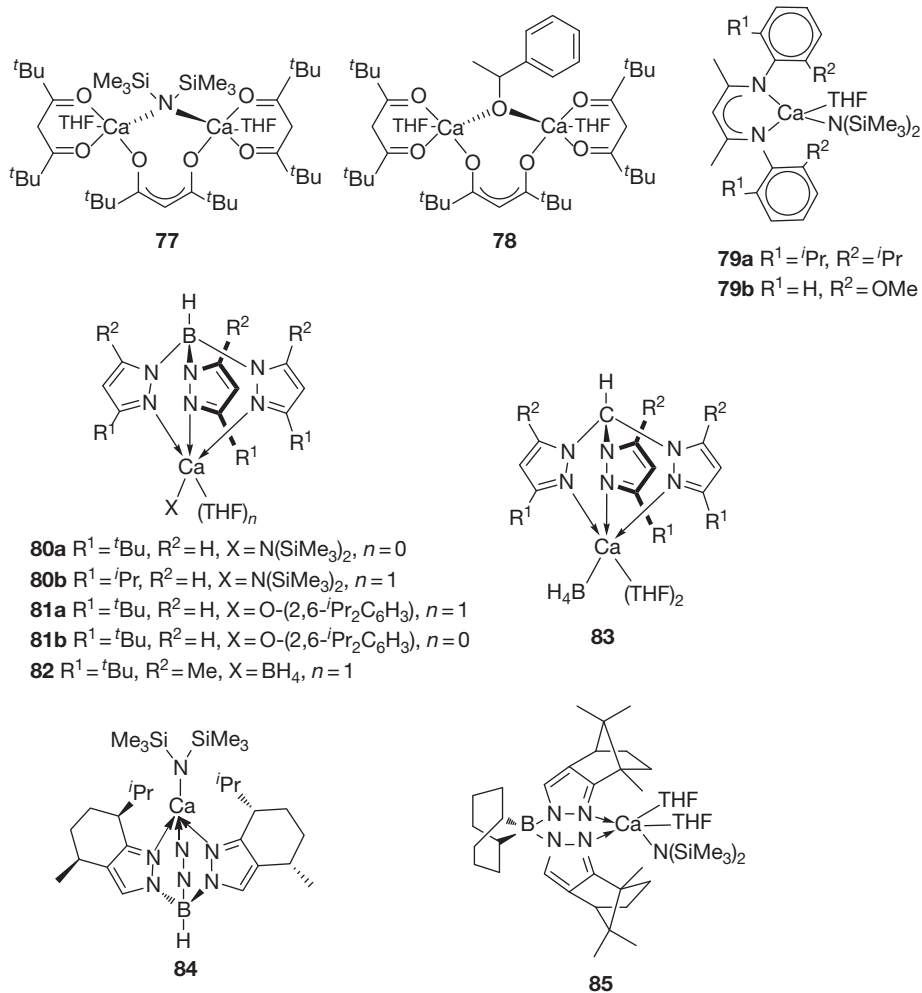
rapid ROP of L-LA under mild conditions producing PLAs with narrow PDIs (1.13–1.19) and controlled molecular weight.

Inspired by the successful application of tris(pyrazolyl)borate-supported magnesium and zinc catalysts, Chisholm et al. and Mountford et al. independently investigated a series of

calcium complexes 79–85 supported by sterically bulky BDI-H, tris(pyrazolyl)borate([HB(3-Rpz)<sub>3</sub>]), and tris(pyrazolyl)methylene([HC(3-Rpz)<sub>3</sub>]).<sup>60</sup> Complex (BDI)CaN(SiMe<sub>3</sub>)<sub>2</sub>THF **79a** reacted with *rac*-LA (200 equiv.) in THF at room temperature giving conversion up to >90% in 2 h. By contrast, the

**Table 3** Comparison of the polymerization activity of structurally analogous Mg and Zn complexes

Entry	Ligand	Metal	Monomer	Solvent	Temperature (°C)	Time (min)	Conversion (%)	$M_w/M_n$
1		Mg	<i>rac</i> -LA	CH <sub>2</sub> Cl <sub>2</sub>	20	1	97	1.20
		Zn	<i>rac</i> -LA	CH <sub>2</sub> Cl <sub>2</sub>	20	33	97	1.10
2		Mg	L-LA	Toluene	25	75	98	1.09
		Zn	<i>rac</i> -LA	Toluene	25	75	98	1.09
		Zn	L-LA	Toluene	60	4 h	95	1.03
		Zn	<i>rac</i> -LA	CH <sub>2</sub> Cl <sub>2</sub>	25	24 h	95	1.05
3		Mg	L-LA	CH <sub>2</sub> Cl <sub>2</sub>	30	1.67 h	95	1.07
		Zn	<i>rac</i> -LA	CH <sub>2</sub> Cl <sub>2</sub>	30	12 h	71	1.09
		Zn	L-LA	CH <sub>2</sub> Cl <sub>2</sub>	0	40	96	1.04
		Zn	<i>rac</i> -LA	CH <sub>2</sub> Cl <sub>2</sub>	0	75	98	1.05

**Figure 14** Calcium complexes supported by various ligands.

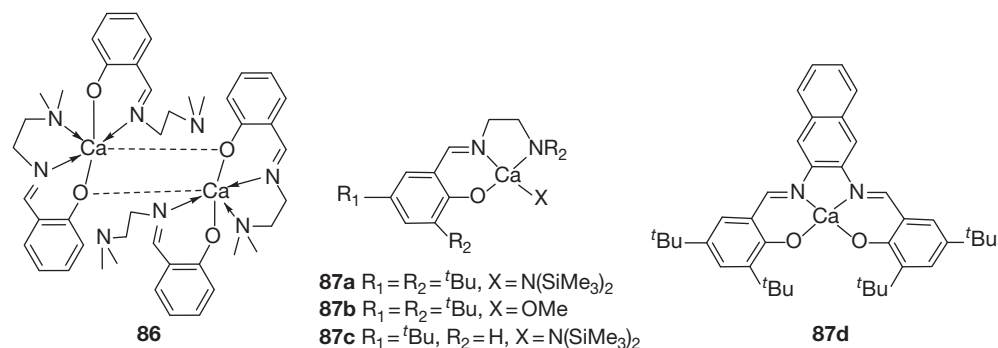


**Figure 15** Calcium complexes supported by Schiff-base and salen-type ligands.

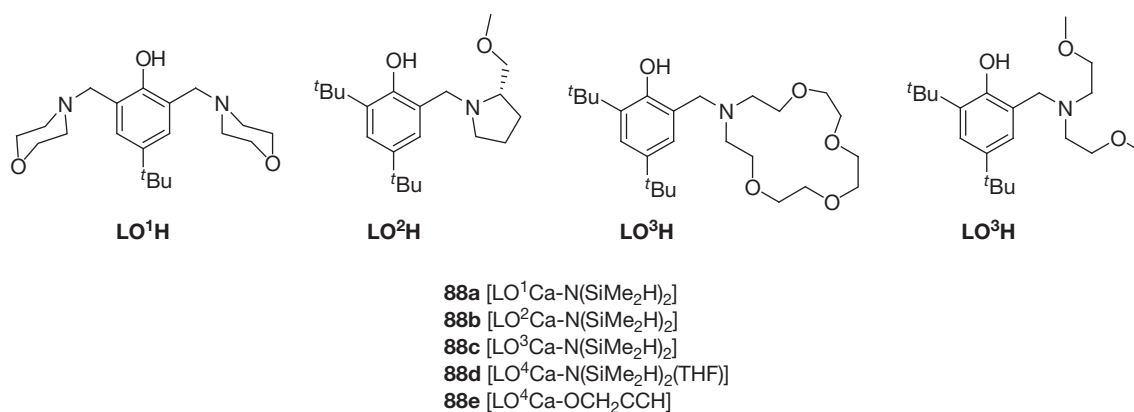


**Figure 16** Heteroleptic silylamido phenolate calcium complexes.

magnesium complex  $(\text{BDI})\text{MgN}(\text{SiMe}_3)_2$  displayed ca. 90% conversion to PLA within only 5 min. The opposite reactivity order of  $\text{Mg} > \text{Ca}$  is probably due to the larger size of  $\text{Ca}^{2+}$  in comparison to  $\text{Mg}^{2+}$  as well as insufficient steric protection of the BDI ligand to prevent aggregation or ligand scrambling. To further evaluate this suggestion, the reaction of  $(\text{BDI})\text{CaN}(\text{SiMe}_3)_2$  **79a** with 1 equiv. of  $\text{HO}^i\text{Pr}$  at  $-78^\circ\text{C}$  was performed and  $(\text{BDI})_2\text{Ca}$  was obtained as the major product. All of the complexes **80–85** displayed extremely fast conversion with a  $>90\%$  conversion of LA in less than 5 min and a broad PDI.

Recently, a novel NNO-Schiff-base-supported dinuclear calcium complex  $[(\text{DAIP})_2\text{Ca}]_2$  ( $\text{DAIP} = 2\text{-}[2\text{-}(\text{dimethylaminoethylimino})\text{methyl}]\text{phenol}$ ) **86** (Figure 15) has been shown to initiate ROP of L-LA in a controlled fashion in the presence of benzyl alcohol giving a 96% conversion within 30–60 min at room temperature, yielding polymers with expected molecular weight and low PDIs.<sup>61a</sup> Later, Darensbourg et al. reported a series of well-defined calcium complexes **87a–87d** for ROP of LAs.<sup>61b,c</sup> Complex **87a** initiated polymerization of LA producing PLAs with high molecular weight (65 000–110 600) and narrow polydispersities (1.02–1.04) at  $110^\circ\text{C}$  in 30 min using a monomer:initiator ratio of 350–700:1. The complex **87a** displayed moderate heteroselectivity ( $P_1 = 0.73$ ) in the polymerization of *rac*-LA in THF at  $-33^\circ\text{C}$ .

More recently, Carpentier et al. reported a series of silylamido and alkoxide calcium complexes **88a–88e** based on N, O-donor ligands as shown in Figure 16.<sup>62</sup> Among them, **88c** reveals the highest catalytic activity toward ROP of L-LAs, giving

**Table 4** Ca complexes in polymerization of LAs

Initiator	Solvent ( $T/^\circ\text{C}$ ) [I] <sub>0</sub> :[LA] <sub>0</sub>	Activity
<b>78</b>	THF (room temperature) 1:150	120 min, 96%
<b>79–80</b>	THF (room temperature) 1:200	1 min, $>90\%$
<b>81</b>	THF (room temperature) 1:200 ( <i>rac</i> -LA)	5 min, $>90\%$
<b>82</b>	THF (room temperature) 1:200 ( <i>rac</i> -LA)	2 h, $>90\%$
<b>83</b>	THF (room temperature) 1:200	2 h, $>90\%$
<b>85</b>	THF (room temperature) 1:200	5 min, 90%
<b>87a</b>	Melt (110) 1:350	30 min, 80%
<b>88d</b>	THF (0) 1:20 (L-LA)	60 min, 76%
<b>88e</b>	THF (0) 1:50 (L-LA)	15 min, 99%

87–91% conversion within 2 min at  $30^\circ\text{C}$  in the presence of propargyl alcohol, BnOH, or 9-anthracenylmethanol, yielding polymers with expected molecular weight and narrow PDIs (1.10–1.17). The activity order of this series complexes is **88c**  $>$  **88d**  $>$  **88a**  $\approx$  **88b**. The aforementioned calcium initiators and their LA polymerization data are listed in Table 4.

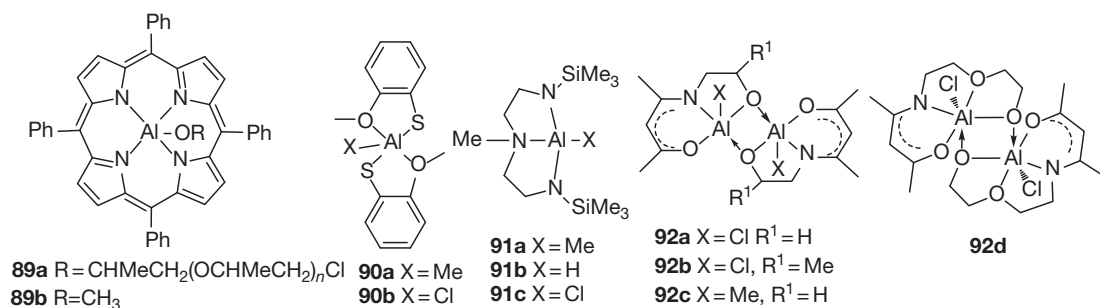


**Figure 17** Achiral Al alkyl and alkoxide initiators.

**Table 5** Polymerization of L-LA initiated by complex **93**

Entry	$[M]_0/[Al]_0/[ROH]_0$	Time (h)	$M_w/M_n$	$M_n(\text{GPC})^a$	$M_n(\text{calcd.})^b$	$M_n(\text{NMR})^c$	Conversion (%) <sup>c</sup>
1	10/1/0	25	1.07	3300	1100	1700	66
2	20/1/0	25	1.11	3800	2100	2400	68
3	25/1/0	25	1.08	5800	2600	3500	70
4	40/1/0	25	1.06	7200	3600	4200	61
5	50/1/0	25	1.07	10200	4900	6000	66
6	20/1/0	48	1.08	6600	2600	3800	87
7	50/1/0	48	1.09	13000	5900	7000	81
8	50/1/1 <sup>d</sup>	25	1.07	8900	3600	4500	97

<sup>a</sup>Obtained from GPC analysis.

<sup>b</sup>Calculated from the molecular weight of L-LA times  $[M]_0/[Al]_0$  times conversion yield divided by  $([ROH] + 1)$  plus the molecular weight of BnOH.

<sup>c</sup>Obtained from <sup>1</sup>H NMR analysis.

<sup>d</sup>Polymerization of LA in the presence of 1 molar equiv. of benzyl alcohol.

### 1.39.2.3 Group 13 Metals (Al, Ga, In)

Within group 13 metals, aluminum catalysts have been extensively exploited for the ROP of cyclic esters. A variety of well-defined aluminum-alkyl, halide, and alkoxide complexes supported by porphyrin, diamine, ketiminate, diketiminate, and biphenolates ligands have been designed in ROP of LA.<sup>63–66</sup> In addition, a large number of aluminum initiators surrounded with chiral or achiral ligands have exhibited highly controlled ROP of L- and rac-LA. However, the polymerization rate for most of the aluminum complexes is generally slow and requires high temperature (70–100 °C) over a relatively long period of time. Porphyrin-supported aluminum complexes **89a** and **89b** (Figure 17) were demonstrated by Inoue et al. to give PLAs with expected molecular weights and narrow PDIs (<1.25) at 100 °C.<sup>64,65</sup> Based on the <sup>1</sup>H NMR spectroscopic studies, polymerization takes place via the insertion of 1 equiv. LA to the aluminum center followed by ring cleavage at the acyl–oxygen bond. Kinetic studies on related systems revealed that the polymerization follows a second-order rate law with respect to the concentration of Al complex, suggesting that the propagation involves two molecules of Al, one as a nucleophilic species which is involved in chain growth and the other as a Lewis-acidic monomer activator. Monomeric Al complexes **90a** and **90b** were synthesized in our laboratory for producing polyesters with thiolate end groups.<sup>66</sup> These complexes initiate polymerization in boiling toluene or xylene forming PLAs with narrow-molecular-weight distributions (PDIs 1.15–1.25).

A series of neutral and cationic aluminum complexes **91a–91c** supported with triamine ligands were prepared.<sup>63</sup> Though both complexes **91a** and **91b** are capable of initiating the polymerization of rac-LA in benzene at 80 °C, hydride complex **91b** is about twice as active as the methylaluminum derivative **91a**. However, only a low-molecular-weight polymer with a narrow MWD has been obtained with a maximum 46% conversion after 5 days. Complexes **92a**, **92b**, and **92d** displayed a poor activity toward polymerization of rac-LA in toluene at 70 °C giving distinctly low conversions (5–11%) even after 7 days.<sup>67</sup> Interestingly, with the addition of a stoichiometric quantity of propylene oxide or cyclohexene oxide, the corresponding Al–OR derived from propylene oxide ring-opening insertion into the [Al]–Cl bond, catalyzed the completed polymerization of LA in 18 h at 70 °C in toluene giving PLAs with expected molecular weights and narrow PDIs (1.13–1.27).

Bisphenolates and substituted phenolate derivatives with bi- or multidentate group such as N, O, ONO, OSSO, and Schiff base are commonly used to prepare aluminum complexes, particularly with sterically hindered substituents in order to stabilize the chelated metal complexes with a single catalytic site. For example, complex **93** can be synthesized by treatment of MMPEP-H<sub>2</sub> with trimethylaluminum in Et<sub>2</sub>O followed by further reaction with benzyl alcohol in toluene.<sup>68</sup> The structure of the complex **93** shows a dimeric feature and distorted tetrahedral geometry around the Al metal center containing an Al<sub>2</sub>O<sub>2</sub> core bridging through the O atom of the benzyl alkoxide groups. It reveals a living character in the polymerization of L-LA with a narrow PDI (Table 5).

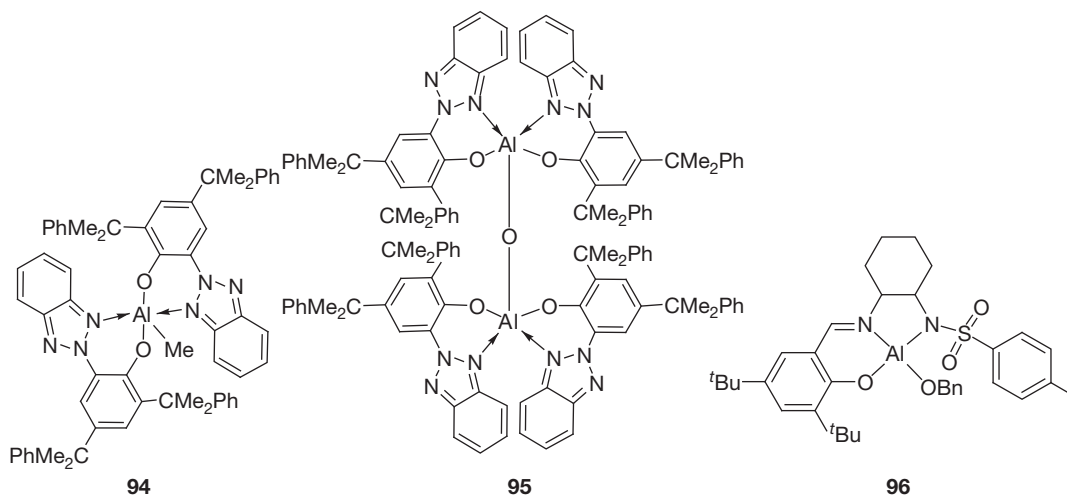


**Figure 18** Structures of aluminum complexes **94**, **95**, and **96**.

**Table 6** Ring-opening polymerization of L-LA (L-LA) catalyzed by complexes **94** or **95** in the presence of 9-AnOH and **96** in toluene

Entry	Catalyst	$[M]_0/[Cat]_0/[9-AnOH]_0$	Time (h)	Temperature (°C)	Conversion (%) <sup>a</sup>	$M_n^b$ (calcd.)	$M_n^c$ (obs.)	$M_n^d$ (nmr)	$PDI^e$
1	<b>94</b>	200/1/2	48	110	47	6700	8000(4600)	7000	1.12
2	<b>95</b>	200/1/0	48	90	35	10100 <sup>f</sup>	12200(7100)	— <sup>f</sup>	1.16
3	<b>95</b>	200/1/2	48	90	71	10200	16000(9300)	11900	1.06
4	<b>95</b>	200/1/2	48	110	85	12200	21000(12000)	12500	1.05
5	<b>95</b>	200/1/2	48	110	94	13500	22300(13000)	13000	1.04
6	<b>95</b>	50/1/2	48	110	92	3300	4900(2800)	3400	1.16
7	<b>95</b>	100/1/2	48	110	92	6600	9200(5300)	7500	1.13
8	<b>95</b>	150/1/2	48	110	94	10000	16000(9300)	11500	1.06
9	<b>96</b>	25/1/0	24	110	98	3600	6300(3700)	3700	1.03
10	<b>96</b>	50/1/0	24	110	98	7200	11300(6600)	6600	1.07
11	<b>96</b>	75/1/0	24	110	94	10300	21000(12100)	11000	1.05
12	<b>96</b>	100/1/0	30	110	96	13900	27300(15800)	15500	1.08
13	<b>96</b>	50(50)/1/0	24(24)	110	95	13800	25900(15000)	13100	1.10

<sup>a</sup>Obtained from <sup>1</sup>H NMR determination.

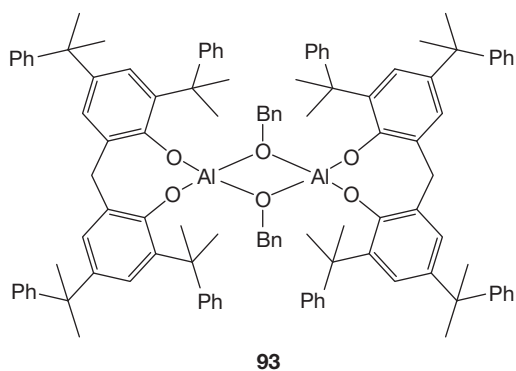
<sup>b</sup>Calculated from the molecular weight of L-LA times  $[LA]_0/[9-AnOH]_0$  times conversion yield plus the molecular weight of 9-AnOH.

<sup>c</sup>Obtained from GPC analysis and calibrated by polystyrene standard. Values in parentheses are the values obtained from GPC times 0.58.

<sup>d</sup>Obtained from <sup>1</sup>H NMR analysis.

<sup>e</sup>Calculated from the molecular weight of L-LA times 200 times conversion yield.

<sup>f</sup>Not available.



Aluminum complexes **94–96** bearing either a sterically hindered benzotriazole-phenoxide ligand 2-(2H-benzotriazol-2-yl)-4,6-bis(1-methyl-1-phenylethyl)phenol (<sup>CMe<sub>2</sub>Ph</sup>BTP-H)<sup>69</sup> or a sulfonamide/Schiff base ligand derived from the condensation of 4,6-di-*tert*-butyl-2-aldehydephenol and *N*-(2-aminocyclohexyl)-toluylsulfonamide<sup>70</sup> have been synthesized. Complexes **94** and **95** exhibited a penta-coordinated environment around the aluminum centers with trigonal-bipyramidal geometry of their respective monomeric and dimeric structures (Figure 18). Ko et al. reported that there are two kinds of  $\pi$ - $\pi$  stacking interactions enhancing the stability of the alumoxane **94**, which is stable to air in the solid state. Both **94** and **95** have been shown to be efficient catalysts in ROP of L-LA in the presence of 9-anthracenemethanol and the polymer is produced in a controlled fashion and exhibits narrow PDIs (Table 6). Wu and coworkers illustrated that the monomeric complex **96** is also an

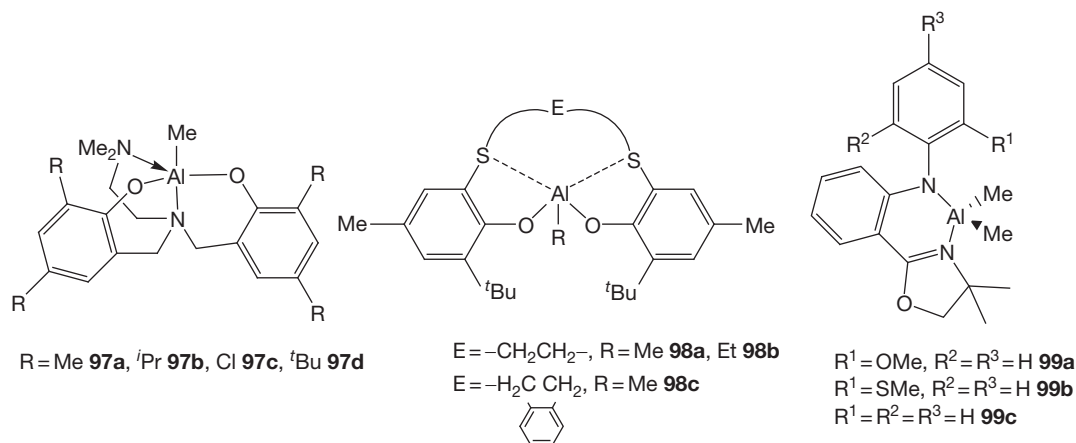


**Figure 19** Aluminum complexes supported with anilido-oxazolinato and other ligands.

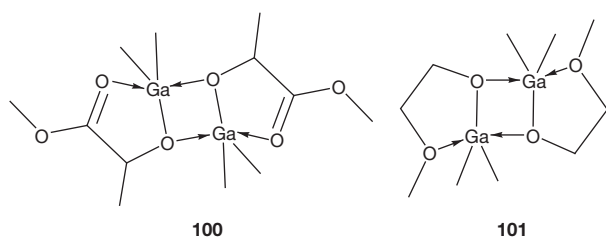


**Figure 20** Structures of gallium complexes **100** and **101**.

efficient initiator for the living ROP of L-LA without epimerization of the chiral centers.

In addition, several single-site alkylaluminum complexes supported with bi- or multidentate auxiliary ligands such as anilido-oxazolinato,<sup>71</sup> *N,N*-bis(3,5-diisopropyl-2-hydroxybenyl)-*N',N'*-dimethyl-1,2-diaminoethane,<sup>70</sup> and 1,4-dithiabutenediylbis(6-*tert*-butyl-4-methylphenol) (etbmpH<sub>2</sub>)<sup>72</sup> have been reported (**Figure 19**). All of these complexes are employed as catalysts to investigate the activity for ROP of *rac*-LA or L-LA in the presence of a suitable alcohol. They all demonstrate well-controlled polymerization within narrow MWD (<1.30) but only moderate tacticity (*P*<sub>m</sub>: 0.35–0.73) for ROP of *rac*-LA.

There was no report of gallium complexes as initiators for the ROP of cyclic esters until Horeglad et al. described the first example of gallium alkoxides (**Figure 20**) accessible for living and controlled polymerization of *rac*-LA in the presence of a Lewis base such as  $\gamma$ -picoline, leading to heterotactically enriched PLA (**Table 7**).<sup>73</sup>

Indium complexes have been increasingly important in organic synthesis because of their rich reactivity profile and remarkable water tolerance.<sup>74</sup> However, structurally well-defined indium complexes used as catalysts for the ROP of LA are still limited. Mehrkhodavandi et al. reported an unusual alkoxy-bridged dinuclear indium complex supported by an amino-phenolato ligand, [ $\{(NNO)InCl\}_2(\mu\text{-OEt})(\mu\text{-Cl})$ ] **102** (**Scheme 9**), and its application in the ROP of LA. It shows a rapid and living polymerization of *rac*-LA, but only modest selectivity, under moderate conditions (25 °C, 30 min, *P*<sub>m</sub> = 0.53–0.62).<sup>75</sup>

Okuda et al. have reported tetradentate (OSSO)-type ligand-supported well-defined indium complexes as initiators for the

ROP of L- and *rac*-LA (*vide infra*).<sup>76</sup> Both of the indium isopropoxy complexes [In(etbbp)(O<sup>*t*</sup>Pr)] **103** and [In(etccp)(O<sup>*t*</sup>Pr)] **104** (**Figure 21**), supported by (OSSO)-type 1,4-dithiabutenediylbis(4,6-di-*tert*-butylphenol) (etbbpH<sub>2</sub>) and 1,4-dithiabutenediylbis{4,6-di(2-phenyl-2-propyl)phenolato} (etccpH<sub>2</sub>) ligands, are efficient in polymerizing L-LA in toluene to form isotactic PLAs with narrow MWD (*M*<sub>w</sub>/*M*<sub>n</sub> = 1.03–1.18). Recently, a series of indium alkoxide compounds derived from the chiral ligand (*t*Bu)<sub>2</sub>P(O)CH<sub>2</sub>CH(*t*Bu)OH has been reported. Interestingly, all three indium complexes show efficient catalytic activity for ROP of *rac*-LA over a wide range of monomer-to-initiator ratios at 25 °C (**Scheme 10**).<sup>77</sup>

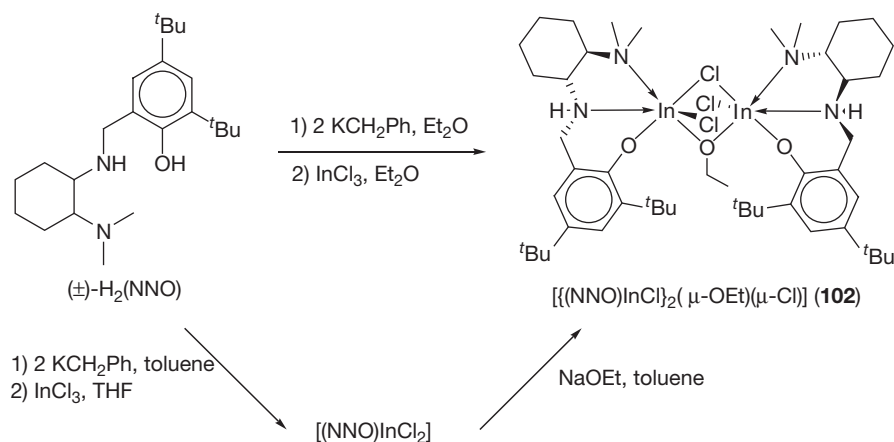
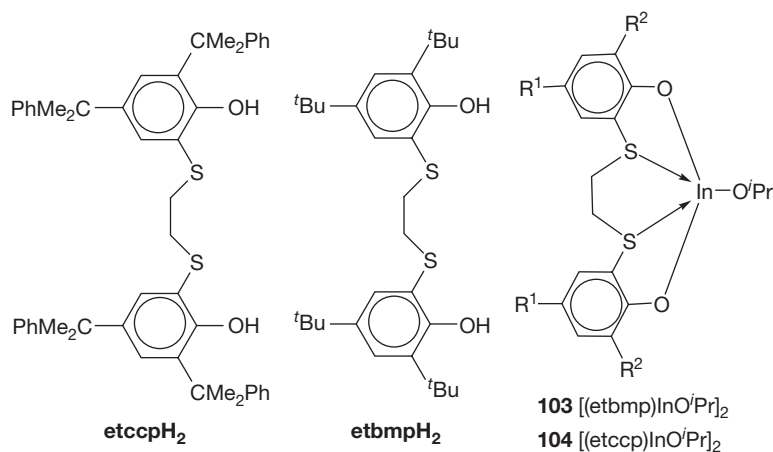
### 1.39.2.4 Group 14 Metals (Ge, Sn)

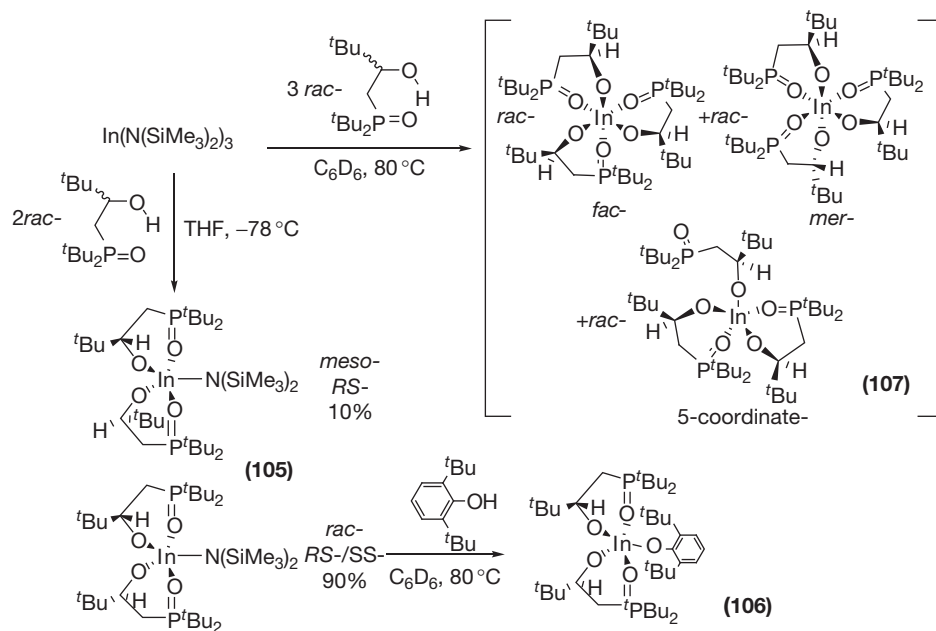
Germanium is a well-established semiconductor and has been used in various electronic devices. An alloy of germanium with uranium and rhodium is the first reported metallic superconductor in the presence of an extremely strong electromagnetic field.<sup>78</sup> Silicon–germanium alloys are rapidly becoming important semiconductor materials for use in high-speed integrated circuits.<sup>79</sup> Though organic germanium compounds have been found to be nontoxic, immuno-enhancing, and potent analgesics,<sup>80</sup> only a few germanium alkoxides have been investigated for applications in the polymerization of cyclic esters.<sup>80–82</sup> Kricheldorf and Langanke reported the first example in the polymerization of lactones catalyzed by germanium alkoxides, Et<sub>3</sub>GeOMe, Ge(OEt)<sub>4</sub> and Ge[μ<sub>2</sub>-O(CH<sub>2</sub>)<sub>3</sub>O]<sub>2</sub>.<sup>81</sup> Albertsson et al. elaborated the ROP of L-LA by three new spirocyclic germanium initiators **108**, **109**, and **110** yielding PEG-*b*-PLA copolymers with different lengths of ethylene oxide units which offer flexibility to the block copolymer and render a more hydrophilic character that can lead to a polymer with very interesting properties for applications in the biomedical field (**Figure 22** and **Table 8**).<sup>80</sup> Furthermore, Davidson et al. demonstrated a germanium alkoxide **111** supported by a C<sub>3</sub>-symmetric ligand which initiates ROP of *rac*-LA producing PLA with medium-to-high heterotacticity of PLA (0.78–0.82) in bulk (**Scheme 11**).<sup>82</sup>

Among main-group organometallic compounds, organotin compounds have the widest range of uses. The major

**Table 7** Selected polymerization data of **100** and **101**

Entry	Catalyst, solvent	Time (h)	Conversion (%)	$10^{-3}M_n^a$	$10^{-3}M_w^b$	$M_w/M_n$	$P_r/P_m^c$
1 <sup>d</sup>	<b>100</b> , CH <sub>2</sub> Cl <sub>2</sub>	144	93	15.4	10.1	1.1	0.5/0.5
2 <sup>e</sup>		240	99	28.1	20.6	1.1	0.5/0.5
3 <sup>d</sup>	<b>100</b> , THF	144	97	18.2	12.9	1.5	0.68/0.32
4 <sup>e</sup>		240	98	28.0	23.8	1.5	0.68/0.32
5 <sup>d</sup>	<b>100</b> / $\gamma$ -pic(1:6), CH <sub>2</sub> Cl <sub>2</sub>	144	98	17.4	12.9	1.1	0.78/0.22
6 <sup>e</sup>		240	99	26.4	16.2	1.1	0.78/0.22
7 <sup>f</sup>	<b>101</b> , THF	72	93	4.2	2.4	1.2	0.65/0.35
8 <sup>g</sup>	<b>101</b> , CH <sub>2</sub> Cl <sub>2</sub>	72	>99	3.9	4.4	1.1	0.78/0.22

<sup>a</sup>Determined by <sup>1</sup>H NMR.<sup>b</sup>Determined by gel permeation chromatography (GPC) in THF, relative to polystyrene standard.<sup>c</sup>Probability of isotactic enchainment ( $P_m$ ) and probability of heterotactic enchainment ( $P_r$ ) were calculated on the basis of homonuclear-decoupled <sup>1</sup>H NMR spectra according to Coates et al.<sup>d</sup>250 equiv. of *rac*-LA.<sup>e</sup>400 equiv. of *rac*-LA; 150 equiv. added after 144 h.<sup>f</sup>60 equiv. of *rac*-LA.<sup>g</sup>**1**/ $\gamma$ -pic, 6 equiv.**Scheme 9** Different routes for the synthesis of **102**.**Figure 21** Dimeric and monomeric indium initiators for the ROP of L-LA.<sup>74a</sup>



**Scheme 10** Syntheses of indium complexes **105**–**107**.

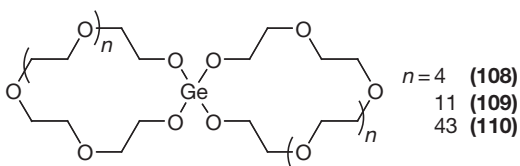


**Figure 22** Spirocyclic germanium initiators of structures **108**, **109**, and **110**.

application is in the stabilization of halogenated PVC plastics, which would otherwise rapidly degrade under light, heat, and atmospheric oxygen, to give discolored and brittle products. It is believed that the tin scavenges labile chlorine ions, which would otherwise initiate loss of HCl from the plastic material.<sup>83</sup> Tin(II) octanoate ( $\text{Sn}(\text{Oct})_2$ ) has been the most commonly applied metal catalyst for the industrial preparation of PLA, which provides polyesters with high molecular weights and high levels of end-group accuracy for biomedical applications including biodegradable fibers and tissue engineering scaffolds.<sup>84</sup> Moreover, it is well known that stannous octoate is extensively utilized as an efficient catalyst in ROP of cyclic esters and the stannous complex can be used either alone or in combination with a coinitiator. Prud'homme et al. report the polymerization of L-LA catalyzed by using stannous octoate with 2-(2-methoxyethoxy)ethanol (MEE) under mild conditions (70 °C in toluene) as shown in **Figure 23**.<sup>85</sup> Similarly, Seppälä et al. demonstrated that linear and star-shaped PLAs were prepared by utilizing  $\text{Sn}(\text{Oct})_2$  as a catalyst in the presence of coinitiators with different numbers of hydroxyl groups such as BnOH, 1,4-butanediol, pentaerythritol, and polyglycerine. It is interesting to note that the coinitiator with increasing hydroxyl end-group content induces a faster polymerization and higher molecular weight without enhancing backbiting during propagation in the maximum conversions (>90%).<sup>86</sup> Albertsson et al. used the cyclic tin alkoxides, **112/113** and

**114/115** (**Figure 24**), to initiate the ROP of L-LA giving a series of L-LA macromonomers with narrow PDI from low to high molecular weights as shown in **Table 9**.<sup>87</sup>

Although numerous explorations concerning living ROP of LA by stannous octoate have been described in the past decade, there have been no reports of tin initiators with well-defined ancillary ligands until Gibson et al. demonstrated the first sample of a single-site tin(II) complex, **116**, as a catalyst for the ROP of LA (**Scheme 12**).<sup>88</sup> Experimental results show that **116** has living characteristic of polymerization yielding polymers with narrow PDIs ( $M_w/M_n = 1.05$ ) (**Figure 25**).

Hillmyer and Tolman et al. reported two monomeric LSn(II)OR compounds,  $\text{L}^{\text{SiMe}_3}\text{Sn}(\text{OCPh}_3)$  and  $\text{L}^{\text{SiMe}_2\text{Ph}}\text{Sn}(\text{OCPh}_3)$  (**Figure 26**), incorporating sterically bulky benzamidinate and alkoxide ligands.<sup>89</sup> These two Sn(II) alkoxides are effective for the ROP of *rac*-LA in toluene at 80 °C with monomer/initiator ratio up to 500 and a PDI of 1.18. In the presence of equivalent BnOH as an added initiator,  $\text{L}^{\text{SiMe}_2\text{Ph}}\text{Sn}(\text{OCPh}_3)$  displays good control behavior of molecular weight and kinetic studies show the process to be first order in monomer and one-third order in initial concentration of  $\text{L}^{\text{SiMe}_2\text{Ph}}\text{Sn}(\text{OCPh}_3)$  (**Figure 27**).

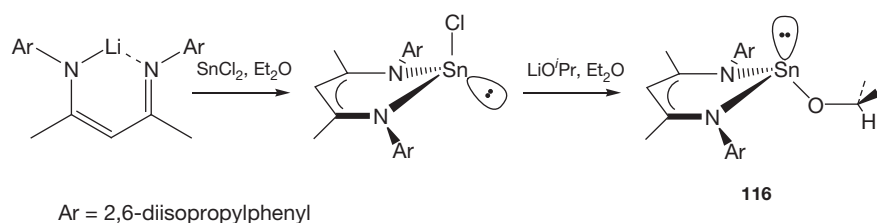
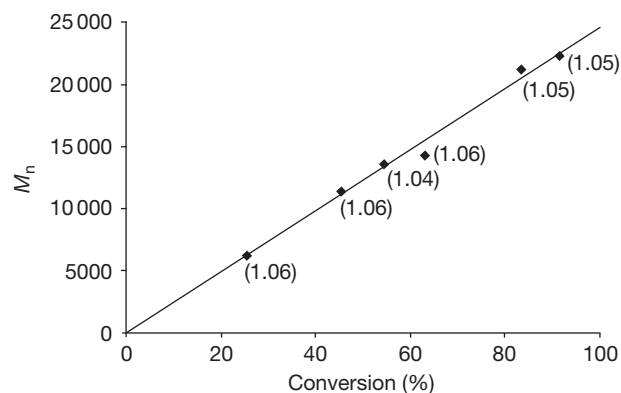
### 1.39.2.5 Group 15 Metals (Bi)

Bismuth is considered to be the heaviest naturally occurring stable element and bismuth compounds are widely used in cosmetics, medicines, and in medical procedures. For instance, about 1000 tons of bismuth were consumed in 2008 in United States, of which 55% were pharmaceuticals, cosmetics, and pigments and 34% were metallurgical additives for galvanizing and casting.<sup>90</sup> Despite the investigation of the other main metal complexes in ROP, there are only a limited number of reports of using a bismuth complex in related research. The first reference to the polymerization of cyclic esters catalyzed by

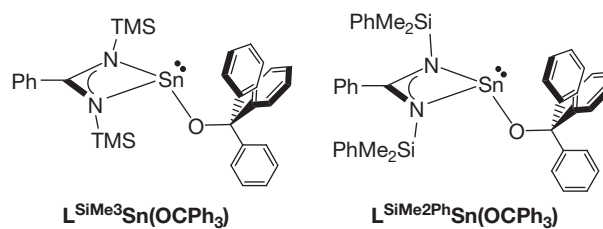


**Table 9** Ring-opening polymerization of L-LA with tin alkoxide **112/113** or **114/115** as initiator; reaction was conducted at 60 °C in chloroform with  $[M]_0 = 0.5$  M

Initiator	$[M]/[I]^a$	Time (h)	$M_n^b$	$M_n^c$	$M_n^d$	$PDI^d$	Conversion (%) <sup>c</sup>	Yield (%) <sup>e</sup>
<b>112/113</b>	20	6	3200	3000	5900	1.06	98	72
	50	16	7520	7500	14 400	1.07	98	86
	100	28	14 720	19 700	29 200	1.05	90	83
	250	71	36 320	39 000	41 800	1.10	78	68
	500	140	72 320	79 000	104 400	1.09	83	76
<b>114/115</b>	20	8	3250	3000	4800	1.07	95	40
	50	16	7570	7300	11 700	1.11	96	83
	100	32	14 770	14 400	21 300	1.11	95	78
	500	160	72 370	72 500	52 200	1.08	65	63

<sup>a</sup>Molar feed ratio calculated from the unimeric species.<sup>b</sup>Value calculated assuming living polymerization.<sup>c</sup>Calculated from <sup>1</sup>H NMR on crude reaction mixture.<sup>d</sup>Determined by SEC analysis calibrated with polystyrene standards.<sup>e</sup>Amount of polymer formed after precipitation in methanol.**Scheme 12** Single-site tin(II) initiator with  $\beta$ -diketiminato ligand.**Figure 25** Living ROP of L-LA catalyzed by complex **116** ( $\text{CH}_2\text{Cl}_2$ , 4 h, 85%,  $M_w/M_n = 1.05$ ).

bismuth compounds was published by Kricheldorf and Serra.<sup>91</sup> They showed that Bi(III) 2-ethylhexanoate caused less racemization than other metal salts when compared under rather harsh conditions (48 h at 180 °C). Bismuth salts such as  $\text{BiCl}_3$ ,  $\text{BiAc}_3$ ,  $\text{BiO}_3$ ,  $\text{Bi}(n\text{-hexanoate})_3$ , or bismuth subsalicylate (BSS) have several advantages as initiators including low price, stability on storage, and nontoxicity in the quantities needed. For example, as mentioned by Kricheldorf,<sup>92</sup> BSS has a tradition of almost 100 years as a commercial over-the-counter drug against travelers' diarrhea, nonulcer dyspepsia, and gastrointestinal complaints such as heartburn and nausea. It has been reported that BSS should be used as a catalyst with TEG (tetraethyleneglycol) as initiator for copolymerization of  $\epsilon$ -CL, glycolide and L-LA

**Figure 26** Structures of  $L^{\text{SiMe}_3}\text{Sn}(\text{OCPh}_3)$  and  $L^{\text{SiMe}_2\text{Ph}}\text{Sn}(\text{OCPh}_3)$ .

within a range of PDIs (1.54–2.00). In addition, bismuth hexanoate or bismuth acetate has also been shown to produce different types (linear, telechelic, star-shaped) and block copolymers (A–B–A or multiblock) of PLLA (**Figure 28** and **Scheme 13**).<sup>93</sup>

### 1.39.2.6 ROP of LAs by Mixed-Metal Initiators

Despite the aforementioned examples, there are only a few reports that describe the ROP of LAs catalyzed by mixed-metal systems involving main-group metals. Li et al. have published the first example of ROP of L-LA catalyzed by sodium bis(2-methoxyethoxy)aluminum hydride (Red-Al) **117** in which **117** shows the living characteristic of ROP in bulk generating a PLLA with moderate molecular weight (19 300–23 000), high yield (>96%), narrow PDI (<1.32), and high isotacticity (95.2%).<sup>94</sup> The mechanism is also proposed as shown in **Scheme 14**.

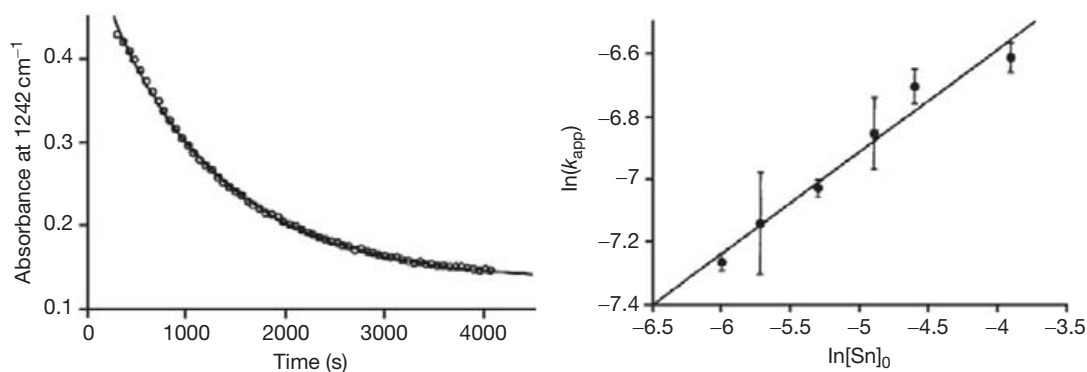


**Figure 27** The curve depicts a fit to the equation for first-order decay:  $\text{abs}_t (\text{abs}_0 - \text{abs}_\infty) \exp(-k_{\text{app}}t) + \text{abs}_\infty$ , affording  $k_{\text{app}}t = (8.68 \pm 0.08) \times 10^{-4} \text{ s}^{-1}$ ,  $\text{abs}_0 = 0.529 \pm 0.02$ , and  $\text{abs}_\infty = 0.1338 \pm 0.007$ . Plot of  $\ln(k_{\text{app}})$  vs.  $\ln[\text{Sn}]_0$ , where 'Sn' refers to  $\text{L}^{\text{SiMe}_2\text{Ph}}\text{Sn}(\text{OCPh}_3)$ . Polymerization conditions:  $[\text{Sn}]_0 = [\text{BnOH}]_0$ ,  $[\text{LA}]_0 = 1.0 \text{ M}$ , toluene,  $80^\circ \text{C}$ . All measurements of  $k_{\text{app}}$  were made in triplicate, and the error bars on  $\ln(k_{\text{app}})$  values correspond to one standard deviation. The slope of the indicated line is  $0.33 \pm 0.02$ .

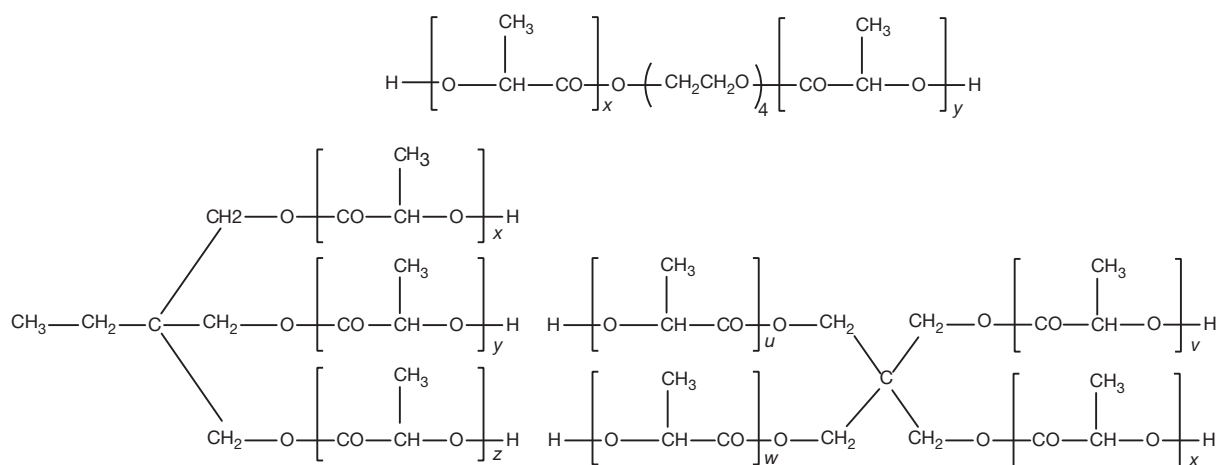


**Figure 28** Telechelic and star-shaped PLLA.

A series of bis(phenolato) ligands, such as EDBP- $\text{H}_2$ , TBBP- $\text{H}_2$ , and 1,4-bis(2-hydroxy-3,5-di-*tert*-butyl-benzyl)-piperazine, have been reported in the syntheses of heterobimetallic complexes in order to investigate the catalytic behavior in the ROP of *L*-LA. Various substituents on the bis(phenolato) ligand structurally similar to EDBP- $\text{H}_2$  have been synthesized and characterized (Scheme 15).<sup>95</sup> According to the experimental results, these heterobimetallic complexes reveal high activity for the ROP of *L*-LA in a controlled manner (Table 10) with a prominent decrease in catalytic activity found in the order  $123 > 121 > 122 > 120$  for Ti-Zn complexes and  $126 > 125 > 124$  for Ti-Mg complexes, indicating that electron-donating substituents at the *ortho* position are advantageous for the polymerization process. Kinetic studies using 121 showed that the polymerization reaction proceeds with first-order rate dependence on both the monomer and initiator concentrations (Figure 29).

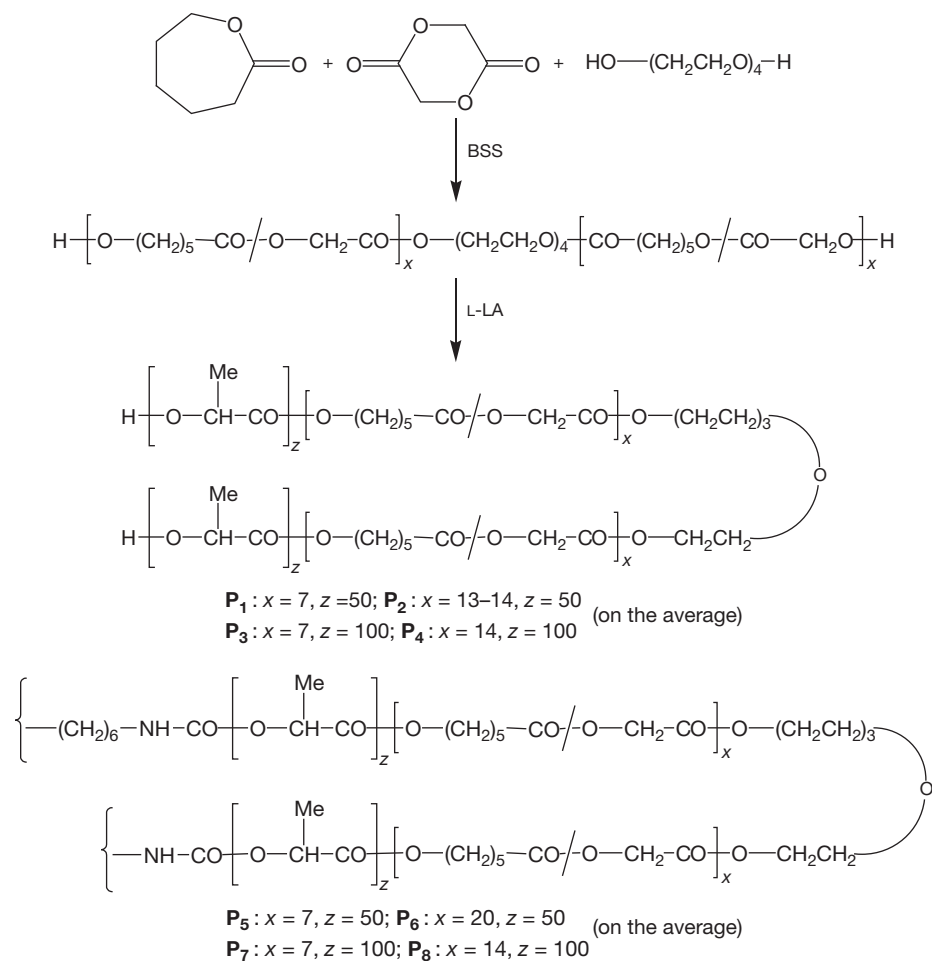
Wu et al. have also described zinc-sodium/lithium heterometallic aryloxides coordinated by a sterically bulky ligand, TBBP- $\text{H}_2$  (3,3',5,5'-tetra-*tert*-butyl-2,2'-biphenol) and their applications toward the polymerization of *L*-LA (Scheme 16).<sup>96</sup> The experimental results show that 128 and 129 efficiently initiate the polymerization (Table 11) without epimerization according to homonuclear-decoupled  $^1\text{H}$  NMR data in the

methine carbon region and a living nature of polymerization was noted. In addition, 128 catalyzes the polymerization in a controlled manner with high conversion by using commercial *L*-LA without further treatment even in the presence of water (Table 12).

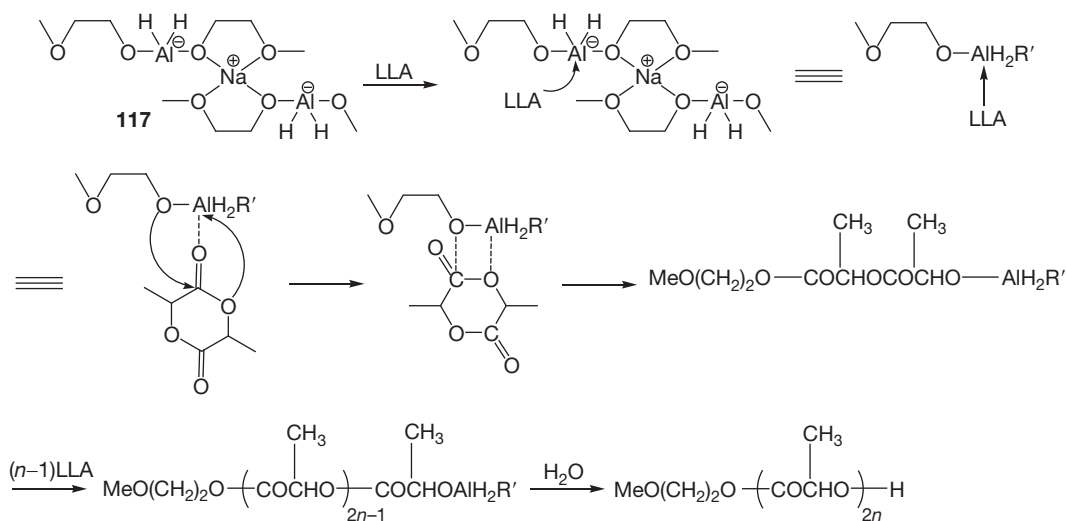
Furthermore, Yao et al. reported an 'ate' and neutral ytterbium/lithium bimetallic complex supported by an auxiliary ligand with a flexible piperazine-bridged bis(phenolato) group (Scheme 17).<sup>97</sup> Complex 130 was also found to be an efficient initiator for the ROP of *L*-LA with a high molar ratio of monomer to initiator of about 1000 and high conversion up to 97% within 30 min. From the preliminary results, the bimetallic complex 130 has higher activity than the mononuclear ytterbium amides toward the ROP of *L*-LA.

### 1.39.3 Stereocontrolled ROP of LAs

Because of the chiral nature of LA, PLA with several distinct forms such as atactic, isotactic, heterotactic, and syndiotactic can be derived as shown in Scheme 18.<sup>42e</sup> The tacticity of PLA is quantified by  $P_m$  and  $P_t$  values which can be determined by homonuclear-decoupled  $^1\text{H}$  NMR spectroscopic studies in the methine region ( $\delta = 5.15\text{--}5.25 \text{ ppm}$ ) (Figure 30).<sup>98</sup> It has



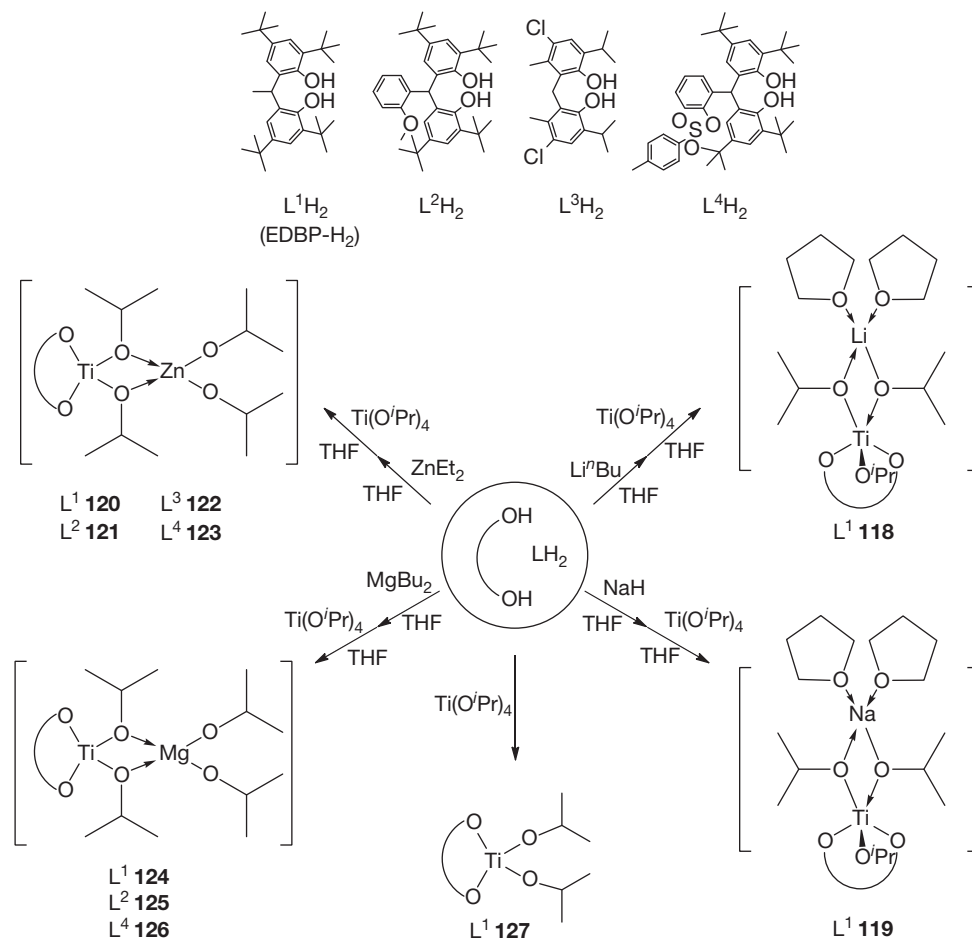
**Scheme 13** BSS-catalyzed copolymerization of  $\epsilon$ -CL and GL in the presence of TEG for the preparation of A-B-A triblock copolymers or multiblock copolymers having the typical character of thermoplastic elastomers.



**Scheme 14** Proposed mechanism for ROP of L-LA by Red-Al.

been known that the physical, biological, and mechanical properties of PLA rely on the stereochemistry of the chiral unit within PLA. For instance, polymer melting ( $T_m$ ) and glass transition ( $T_g$ ) temperatures changed with differences in tacticity. The isotactic PLLA possesses  $T_m \sim 175^\circ\text{C}$  and

$T_g \sim 50^\circ\text{C}$ .<sup>99</sup> However, the melting point can be increased to  $205^\circ\text{C}$  for PLA with  $P_r$  up to 97%.<sup>100</sup> Heterotactic PLA displays a  $T_m$  ( $130^\circ\text{C}$ ) and no observable  $T_g$ . However, a 50:50 mixture of PLLA and PDLA displays a comparable  $T_g$  to PLLA but a significantly increased  $T_m$  (ca.  $230^\circ\text{C}$ ). This



**Scheme 15** Synthesis of metal complexes supported by bis(phenolato) ligands.

**Table 10** Polymerization of L-LA in toluene (15 ml) using complexes **120–125** (0.05 mmol) as initiators

Entry	Initiator	[M]/[ini]	Temperature (°C)	Time (h)	Conversion (%) <sup>a</sup>	$M_n$ (calcd.) <sup>b</sup>	$M_n$ (obs.) <sup>c</sup>	$M_n$ (NMR) <sup>d</sup>	PDI
1	<b>120</b>	100	30	0.25	27				
2	<b>120</b>	100	30	0.5	91	6600	8800	6800	1.27
3	<b>124</b>	100	70	1.5	94	6800	7900	5900	1.18
4	<b>124</b>	100	30	3.5	89	6500	6300	6900	1.28
5	<b>124</b>	100	50	1	56				
6	<b>121</b>	50	30	0.5	89	3300	3600	3700	1.13
7	<b>121</b>	100	30	0.5	94	6800	7800	7200	1.15
8	<b>121</b>	150	30	0.5	94	10200	11400	10500	1.16
9	<b>121</b>	200	30	0.5	95	13700	14800	14000	1.15
10	<b>125</b>	100	30	1	13				
11	<b>125</b>	50	50	1	85	3100	3900	3300	1.23
12	<b>125</b>	100	50	1	92	6700	8700	6800	1.19
13	<b>125</b>	150	50	1	91	9900	12200	10600	1.15
14	<b>125</b>	200	50	1	91	13200	16200	13600	1.12
15	<b>122</b>	100	30	0.25	5				
16	<b>122</b>	100	30	0.5	94	3400	3800	3700	1.17
17	<b>123</b>	100	30	0.25	93	6800	7700	7900	1.29
18	<b>123</b>	100	30	1	32				
19	<b>123</b>	100	50	0.5	47				
20	<b>123</b>	100	50	1	95	6900	5000	5100	1.29

<sup>a</sup>Obtained from <sup>1</sup>H NMR analysis.

<sup>b</sup>Calculated from the molecular weight of LA  $\times$   $[M]_0/[O^iPr^-]_0 \times$  conversion yield +  $M_w(\text{PrOH})$ .

<sup>c</sup>Obtained from GPC analysis and calibrated by polystyrene standard.

<sup>d</sup>Obtained from <sup>1</sup>H NMR analysis.

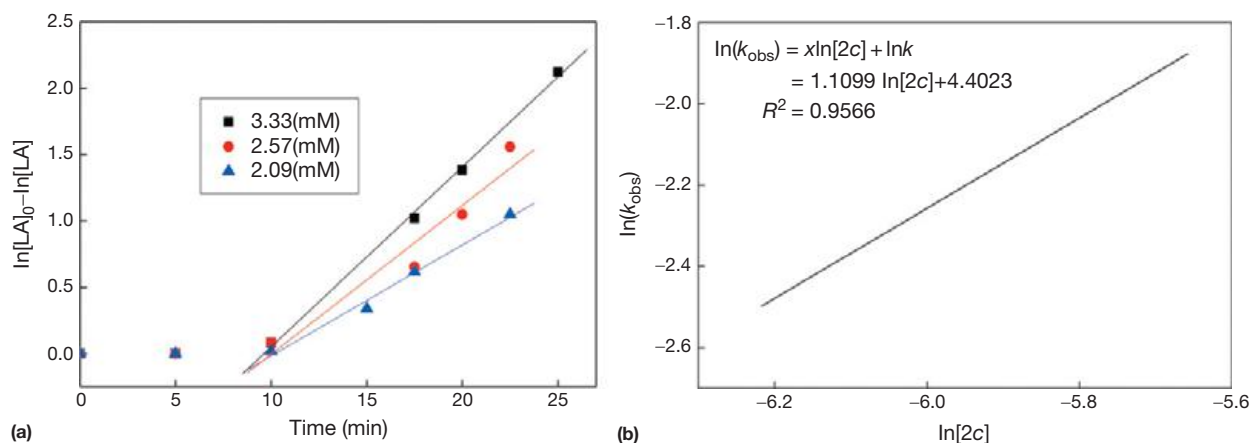
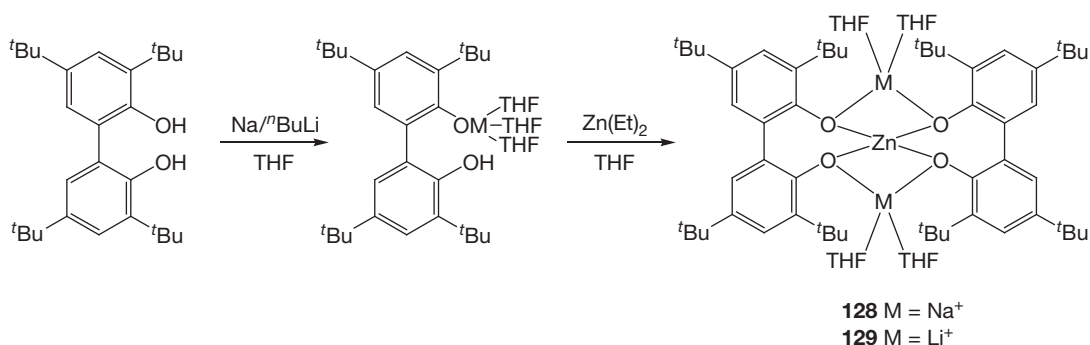


**Figure 29** (a) First-order kinetic plots for L-LA polymerizations with time in toluene with different concentration of **[121]** = **[2c]** as an initiator. (b) Linear plot of  $\ln(k_{\text{obs}})$  vs.  $\ln[121]$  with  $[LA]_0 = 0.167$  M in toluene.



**Scheme 16** Preparation of compounds **128** and **129**.

**Table 11** Ring-opening polymerization of L-LA with complexes **128** and **129**<sup>a</sup>

Entry	Catalyst	$[M]_0/[complex]_0$	Conversion [%]	$M_n$ (obs.) <sup>b</sup>	$M_n$ (calcd.) <sup>c</sup>	PDI
1	<b>128</b>	125	90.6	18 800	16 400	1.36
2	<b>128</b>	150	89.5	19 300	19 300	1.40
3	<b>128</b>	200	91.0	25 500	26 200	1.42
4	<b>128</b>	250	91.6	29 000	33 000	1.45
5	<b>129</b>	100	89.0	12 800	12 300	1.40
6	<b>129</b>	150	91.3	22 200	19 700	1.46
7	<b>129</b>	175	87.0	23 900	22 200	1.40
8	<b>129</b>	200	95.0	27 400	27 360	1.26

<sup>a</sup>Conditions: All manipulations were carried out under a dry nitrogen atmosphere, 0.02 mmol of complex, 10 ml of toluene, 90 °C, reaction time 48 h.

<sup>b</sup>Obtained from GPC analysis times 0.58 and calibrated by polystyrene standard.

<sup>c</sup> $M_n(\text{calcd.}) = ([M]_0/[complex]_0) \times 144.13 \times \text{conv.}$

increase in melting transition is attributed to a stereocomplex microstructure.<sup>99</sup> Consequently, there has been greater demand for the control of the stereochemistry of insertion of the LA monomer into the PLA chain. The stereochemistry of PLA can be controlled by either chain-end control (depending on stereochemistry of the monomer) or site control (depending on chirality of the catalyst).<sup>101</sup>

The first example of highly stereocontrolled polymerization of rac-LA through an enantiomorphic site-control mechanism was reported by Spassky et al. in 1996 in which (R,R)-LA was converted to isotactic PLA by an enantiomerically pure

Al complex (R)-**131** (Figure 31).<sup>102</sup> Furthermore, complex **131** is the only efficient catalyst reported for the stereoselective preparation of syndiotactic enriched PLA in an ROP of meso-LA resulting in a syndiotactic PLA ( $P_r$  96%) with alternating arrangement of stereocenters.<sup>98a</sup> Thereafter, many metal complexes containing chiral ligands have been developed. For instance, enantiopure aluminum complex (R,R)-**132** exhibited an excellent reverse stereocontrol by preferential polymerization of L-LA over D-LA monomer ( $K_{SS}/K_{RR} = 14$ ) resulting PLA with  $P_m = 0.93$ .<sup>103</sup> Natural amino acid (L-phenylalanine, L-leucine, and L-methionine)-derived

**Table 12** Ring-opening polymerization of L-LA with complexes **128** and **129** under moist conditions<sup>a</sup>

Entry	Catalyst	$[M]_0/[complex]_0$	Conversion [%]	$M_n$ (obs.) <sup>b</sup>	$M_n$ (calcd.) <sup>c</sup>	PDI
1	<b>128</b> <sup>d</sup>	100	87.0	17 300	12 500	1.47
2	<b>128</b> <sup>d</sup>	125	90.0	21 700	19 400	1.49
3	<b>128</b> <sup>d</sup>	150	92.0	24 700	23 200	1.50
4	<b>128</b> <sup>d</sup>	175	93.7	27 300	26 900	1.36
5	<b>128</b> <sup>e</sup>	100	85.0	13 000	12 200	1.33
6	<b>129</b> <sup>f</sup>	100	25.4	n.d.	n.d.	n.d.

<sup>a</sup>Conditions: 0.02 mmol of complex, 10 ml of toluene, 90 °C, reaction time 48 h.

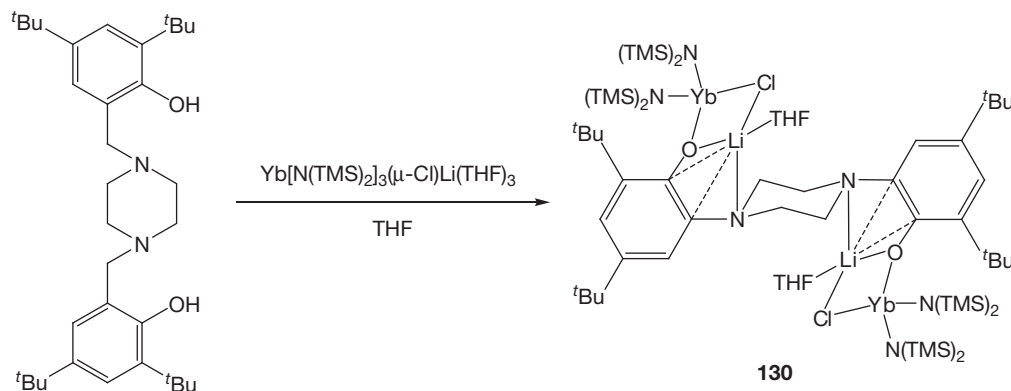
<sup>b</sup>Obtained from GPC analysis times 0.58 and calibrated by polystyrene standard.

<sup>c</sup> $M_n(\text{calcd.}) = ([M]_0/[complex]_0) \times 144.13 \times \text{conv.}$

<sup>d</sup>The LA was not recrystallized, the polymerization reactions were exposed to air.

<sup>e</sup>18  $\mu\text{l}$  of H<sub>2</sub>O added.

<sup>f</sup>3.6  $\mu\text{l}$  of H<sub>2</sub>O added.

**Scheme 17** Synthesis of mixed-metal complex **130**.

Schiff-base metal complexes **133a–133d** (Figure 31) demonstrate a temperature-dependent heteroselectivity with  $P_r$  0.68–0.83 at 22 °C and 0.85–0.89 at –30 °C.<sup>104</sup> Al complexes **134a–134c**/propan-2-ol offered mixed stereoselection with  $P_m = 0.66$  for **134a** and  $P_r = 0.64$  and 0.55 for **134b** and **134c**, respectively.<sup>105</sup> In addition, a *rac*-indium complex **107** (InL<sub>3</sub>) with chiral L ligand (L = (tBu)<sub>2</sub>P(O)CH<sub>2</sub>CH(tBu)-OH) exhibited moderate isotactic selectivity ( $P_m = 0.63$ ).<sup>77</sup>

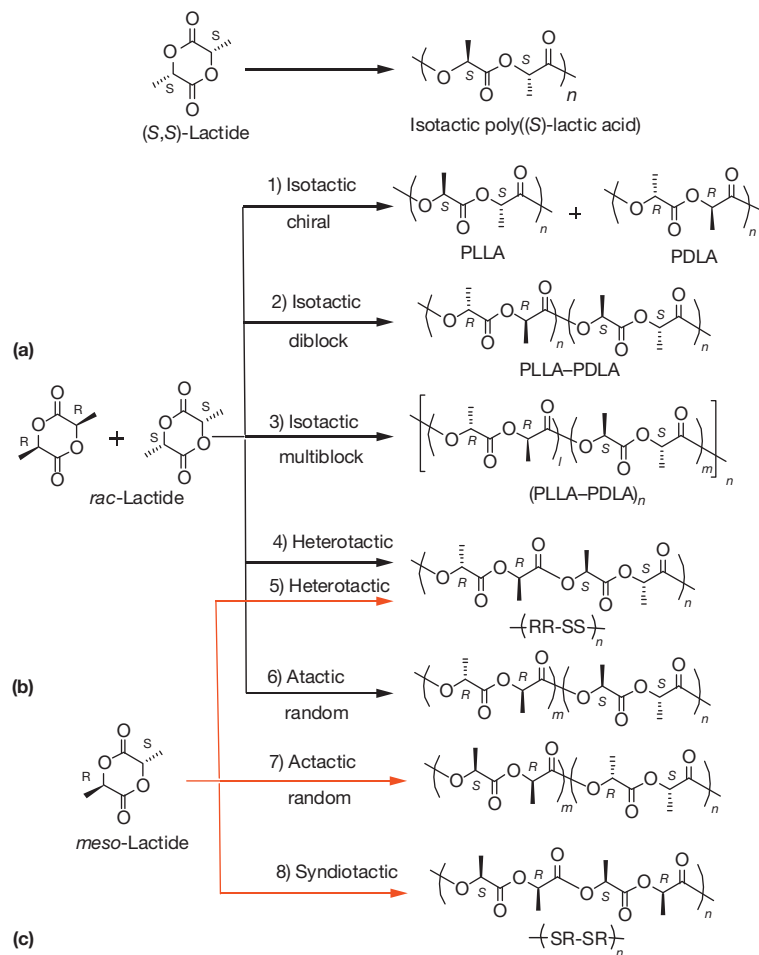
The most widely used stereocontrolled polymerization processes are using achiral initiators through chain-end control and the selectivity is rather random and unpredictable. Achiral  $\beta$ -diiminate zinc initiators **45–47** exhibit high stereocontrol of heterotactic PLA formation from *rac*-LA with  $P_r = 0.94$  at 0 °C for complex **45**.<sup>42,106</sup> Chisholm et al. reported calcium trispyrazolyl borate complexes (Tp<sup>t</sup>Bu)CaX (**79** and **81**) which also offered high heterotactic selectivity with  $P_r = 0.90$ .<sup>60</sup> However, achiral Al–salen complex **135** shows high isotactic selectivity with  $P_m = 0.91$  in the presence of BnOH.<sup>107</sup> Similarly, achiral Al–salen complex **136**/2-propanol offered isotactic selectivity ( $P_m = 0.90$ ).<sup>108</sup> Gibson and coworkers demonstrated heterotactic preference ( $P_r = 0.80–0.96$ ) with achiral tetradentate *N*, *N'*-disubstituted bis(aminophenoxide) (SALAN) aluminum complexes **137a–137d** (Figure 32).<sup>109</sup> It is interesting to note that polymerization of *rac*-LA by indium trichloride in the presence of BnOH/Et<sub>3</sub>N without a multidentate ligand yields highly heterotactic PLA with  $P_r = 0.97$  at 0 °C.<sup>110</sup> Aluminum alkoxides **138a–138c** are highly stereoselective in the ROP of

*rac*-LA producing PLA with 94–97% enantiomeric selectivity ( $P_m$ ) at high conversion. Their high enantioselectivity leads to PLA with high  $T_m$  (205 °C).<sup>100</sup>

The stereoselectivity of PLA is dramatically solvent and temperature dependent. For instance, NNO-tridentate magnesium and zinc complexes [(L<sup>1</sup>)<sub>2</sub>Mg<sub>2</sub>( $\mu$ -OBn)<sub>2</sub>] **56** exhibited heteroselective preference with  $P_r = 0.85$  at 30 °C and  $P_r = 0.87$  at 0 °C in THF.<sup>45b</sup> However, it showed the isotactic preference with  $P_m = 0.64$  at 30 °C in CH<sub>2</sub>Cl<sub>2</sub>. Similarly, a solvent-dependent heteroselectivity has been noted for [(salenMe)Zn(OBn)]<sub>2</sub> (**65**) with  $P_r = 0.75$  in CH<sub>2</sub>Cl<sub>2</sub> and  $P_r = 0.57$  in THF.<sup>52</sup> Stereocontrol of ROP of *rac*-LA is also affected by the steric hindrance. For instance, an increase in steric restraint of the ligand on Schiff-base-zinc alkoxide **63a–63e** results in an improvement in  $P_r$  from 59% to 74%.<sup>50</sup>

### 1.39.4 Conclusion

Over the past decades, the development of metal catalysts for ROP of LA for the control of the molecular weight, molecular-weight distribution, and tacticity of the resulting polymers has increased rapidly. A variety of metal complexes supported by various well-designed ligands have been synthesized. Main-group metal initiators such as lithium alkoxides and their aggregates have certainly proved to be amazingly efficient for the production of PLAs with high molecular-weight and



**Scheme 18** LA stereochemistry and PLA microstructures obtained from ROP of *rac*-LA and *meso*-LA.

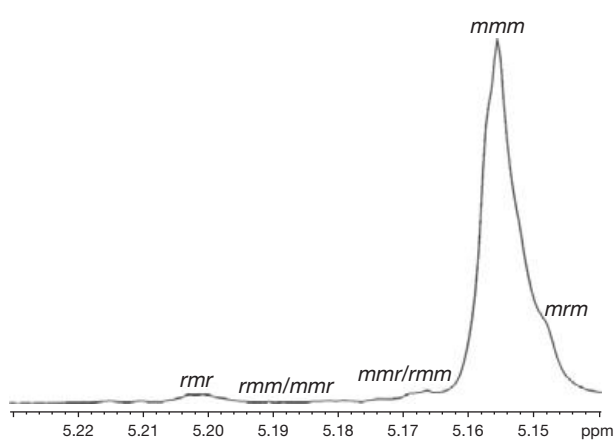


**Figure 30** Homonuclear-decoupled  $^1\text{H}$  NMR spectrum of the methine ( $-\text{CH}(\text{CH}_3)-$ ) region of heterotactic PLA ( $P_m = 96\%$ ) obtained from ROP of *rac*-LA in which  $P_m$  values were calculated from (area of *mmm* tetrad)/(total area in the methine proton region).  $[\text{mmm}] = P_m^2 + (1 - P_m)P_m/2$ ;  $[\text{mrm}] = [\text{rmm}] = (1 - P_m)P_m/2$ ;  $[\text{rrr}] = (1 - P_m)^2/2$ ; and  $[\text{rrm}] = [(1 - P_m)^2 + P_m(1 - P_m)]/2$ .<sup>101</sup>

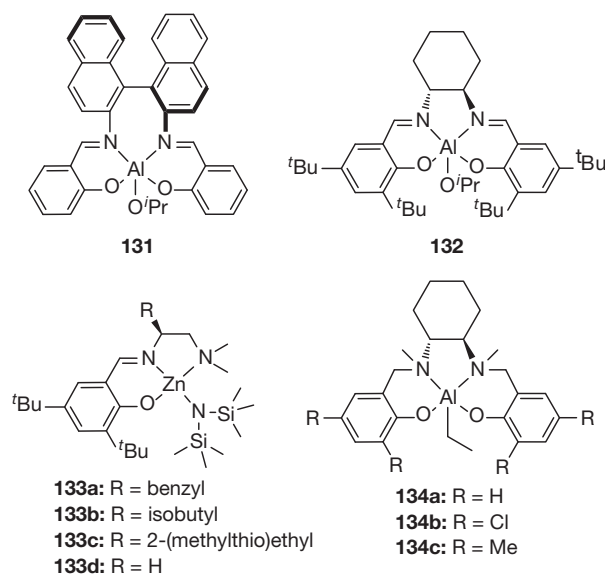


**Figure 31** Metal complexes containing chiral ligands.

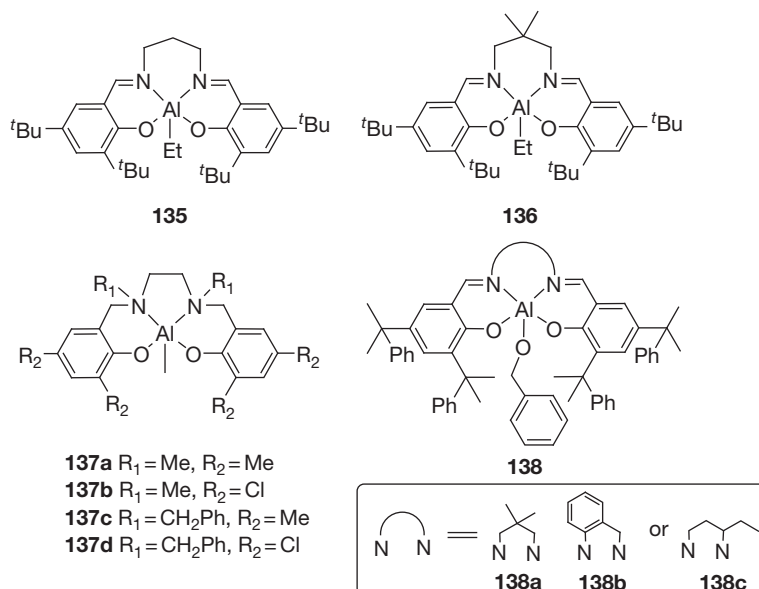


**Figure 32** Aluminum complexes with achiral ligands.

narrow-molecular-weight distribution. Crucially, zinc and magnesium initiators have been the most widely investigated systems because of their biologically benign nature.

It can be expected that many interesting architectures of the ligands and applications of their metal complexes in polymerization of LA and related monomers will be presented in the future. It will be highly desirable to accomplish the solid version of high-performance LA polymerization catalytic systems for improving the quality of the resulting PLA in their high commercial applications. For a related chapter in this Comprehensive, we refer to **Chapter 7.01**.

## Acknowledgment

Financial support from the National Science Council and the Ministry of Economic Affairs of Taiwan, Republic of China is gratefully appreciated.

## References

- (a) Swift, G. *Acc. Chem. Res.* **1993**, *26*, 105; (b) Fujisato, T.; Ikada, Y. *Macromol. Symp.* **1996**, *103*, 73.
- (a) Endo, M.; Aida, T.; Inoue, S. *Macromolecules* **1987**, *20*, 2982; (b) Duda, A.; Florjanczyk, Z.; Hofman, A.; Słomkowski, S.; Penczek, S. *Macromolecules* **1990**, *23*, 1640; (c) Kowalski, A.; Duda, A.; Penczek, S. *Macromol. Rapid Commun.* **1998**, *19*, 567; (d) Gan, Z.; Jim, T. F.; Jim, M.; Yuer, Z.; Wang, S.; Wu, C. *Macromolecules* **1999**, *32*, 590.
- Chamberlain, B. M.; Sun, Y.; Hagadorn, J. R.; Hemmesch, E. W.; Young, V. G., Jr.; Pink, M.; Hillmyer, M. A.; Tolman, W. B. *Macromolecules* **1999**, *32*, 2400.
- (a) Hovestadt, W.; Müller, J. A.; Höcker, H. *Macromol. Chem., Rapid Commun.* **1990**, *11*, 271; (b) Hovestadt, W.; Keul, H.; Höcker, H. *Polymer* **1992**, *33*, 1941.
- (a) Ni, Q.; Yu, L. *J. Am. Chem. Soc.* **1998**, *120*, 1645; (b) Jeong, B.; Bae, Y. H.; Lee, D. S.; Kim, S. W. *Nature* **1997**, *388*, 860; (c) Gref, R.; Minamitake, Y.; Peracchia, M. T.; Trubetskoy, V.; Torchilin, V.; Langer, R. *Science* **1994**, *263*, 1600.
- (a) Fujisato, T.; Ikada, Y. *Macromol. Symp.* **1996**, *103*, 73; (b) Hutchinson, F. G.; Furr, B. J. A. In *High Value Polymers*; Fawcett, A. H., Ed.; The Royal Society of Chemistry: Science Park, Cambridge, 1991.
- Wehrenberg, R. H., II. *Mater. Eng.* **1981**, *94*, 63.
- Spinu, M.; Jackson, C.; Keating, M. Y.; Gardner, K. H. *J. Macromol. Sci. Pure Appl. Chem.* **1996**, *A33*, 1497.
- (a) Athanasiou, K. A.; Niederauer, G. G.; Agrawal, C. M. *Biomaterials* **1996**, *17*, 93; (b) Yamamoto, T.; Matsusue, Y.; Uchida, A.; Shimda, K.; Shimozaki, E.; Kitaoka, K. *Int. Orthop.* **1994**, *18*, 332.
- (a) Langer, R. *Nature* **1998**, *392*, 5; (b) Zhu, K. J.; Xiangzhou, L.; Shilin, Y. *J. Appl. Polym. Sci.* **1990**, *39*, 1.
- (a) Pack and Proper Co., Ltd. <http://www.packproper.com.tw>; (b) BioTech One Inc. <http://www.biotech-one.com>; (c) Robb, M. J.; Connal, L. A.; Lee, B. F.; Lynd, N. A.; Hawker, C. J. *Polym. Chem* **2012**, *3*, 1618.
- Kricheldorf, H. R. *Chemosphere* **2001**, *43*, 49.
- Carothers, W. H.; Dorough, G. L.; Van Natta, F. J. *J. Am. Chem. Soc.* **1932**, *54*, 761.
- Duda, A.; Penczek, S. *Macromolecules* **1990**, *23*, 1636.
- van Hummel, G. J.; Harkema, S.; Kohn, F. E.; Feijen, J. *Acta Crystallogr. B* **1982**, *38*, 1679.
- Wang, Y.; Hillmyer, M. A. *Macromolecules* **2000**, *33*, 7395.
- (a) Penczek, S.; Cypriak, M.; Duda, A.; Kubisa, P.; Słomkowski, S. *Prog. Polym. Sci.* **2007**, *32*, 247; (b) Adamus, G.; Kowalczyk, M. *Biomacromolecules* **2008**, *9*, 696; (c) Kasperczyk, J. E. *Macromolecules* **1995**, *28*, 3937; (d) Dove, A. P. *Chem. Commun.* **2008**, 6446.
- Dittrich, W.; Schulz, R. C. *Angew. Makromol. Chem.* **1971**, *15*, 109.
- (a) Dechy-Cabaret, O.; Martin-Vaca, B.; Bourissou, D. *Chem. Rev.* **2004**, *104*, 6147; (b) Wu, J.; Yu, T. L.; Chen, C. T.; Lin, C. C. *Coord. Chem. Rev.* **2006**, *250*, 602; (c) Sutar, A. K.; Maharana, T.; Dutta, S.; Chen, C. T.; Lin, C. C. *Chem. Soc. Rev.* **2010**, *39*, 1724; (d) Patel, R. H.; Hodgson, L. M.; Williams, C. K. *Polym. Rev.* **2008**, *48*, 11; (e) Wheaton, W. G.; Hayes, P. G.; Ireland, B. J. *Dalton Trans.* **2009**, 4832.
- (a) Thomas, C. M. *Chem. Soc. Rev.* **2010**, *39*, 165; (b) Standford, M. J.; Dove, A. P. *Chem. Soc. Rev.* **2010**, *39*, 486.
- Sipos, L.; Zsuga, M. *J. Macromol. Sci. A: Pure Appl. Chem.* **1997**, *34*, 1269.
- (a) Hsueh, M. L.; Huang, B. H.; Wu, J.; Lin, C. C. *Macromolecules* **2005**, *38*, 9482; (b) Huang, B. H.; Ko, B. T.; Athar, T.; Lin, C. C. *Inorg. Chem.* **2006**, *45*, 7348; (c) Ko, B. T.; Lin, C. C. *J. Am. Chem. Soc.* **2001**, *123*, 7973.
- Yu, T. L.; Huang, B. H.; Hung, W. C.; Lin, C. C.; Wang, T. C.; Ho, R. M. *Polymer* **2007**, *48*, 4401.
- Chisholm, M. H.; Lin, C. C.; Gallucci, J. C.; Ko, B. T. *Dalton Trans.* **2003**, 406.
- (a) Huang, C. A.; Chen, C. T. *Dalton Trans.* **2007**, *47*, 5561; (b) Huang, Y.; Tsai, Y. H.; Hung, W. C.; Lin, C. S.; Wang, W.; Huang, J. H.; Dutta, S.; Lin, C. C. *Inorg. Chem.* **2010**, *49*, 9416; (c) Huang, C. A.; Ho, C. L.; Chen, C. T. *Dalton*

- Trans.* **2008**, *26*, 3502; (d) Alonso-Moreno, C.; Garcés, A.; Sánchez-Barba, L. F.; Fajardo, M.; Fernández-Baeza, J.; Otero, A.; Lara-Sánchez, A.; Antiñolo, A.; Broomfield, L.; López-Solera, M. I.; Rodríguez, A. M. *Organometallics* **2008**, *27*, 1310.
26. (a) Chen, H. Y.; Zhang, J. B.; Lin, C. C.; Reibenspies, J. H.; Miller, S. A. *Green Chem.* **2007**, *9*, 1038; (b) Chen, L.; Jia, L.; Cheng, F.; Wang, L.; Lin, C. C.; Wu, J.; Tang, N. *Inorg. Chem. Commun.* **2011**, *14*, 26; (c) Pan, X.; Liu, A.; Yang, X.; Wu, J.; Tang, N. *Inorg. Chem. Commun.* **2010**, *13*, 376.
  27. Campbell, N. A. *Biology*, 3rd ed.; Benjamin/Cummings: Upper Saddle River, NJ, 1993; 718.
  28. Greenwood, N. N.; Earnshaw, A. *Chemistry of the Elements*, 2nd ed.; Butterworth-Heinemann: Oxford, 1997.
  29. Goeke, G. L.; Park, K.; Karol, P. J.; Mead, B. U.S. Patent 4,193,892.
  30. (a) Dobrzyński, P.; Kasperczyk, J.; Bero, M. *Macromolecules* **1999**, *32*, 4735; (b) Li, S. M.; Rashkov, I.; Espartero, J. L.; Manolova, N.; Vert, M. *Macromolecules* **1996**, *29*, 57.
  31. Tang, Z.; Chen, X.; Liang, Q.; Bian, X.; Yang, L.; Piao, L.; Jing, X. *J. Polym. Sci. A: Polym. Chem.* **2003**, *41*, 1934.
  32. Tesh, K. F.; Hanusa, T. P. *J. Chem. Soc. Chem. Commun.* **1991**, 879.
  33. (a) Davidson, M. G.; O'Hara, C. T.; Jones, M. D.; Keir, C. G.; Mahon, M. F.; Kociok-Köhn, G. *Inorg. Chem.* **2007**, *46*, 7686; (b) Liu, B.; Roisnel, T.; Sarazin, Y. *Inorg. Chim. Acta* **2012**, *380*, 2.
  34. Harder, S. *Angew. Chem. Int. Ed.* **2003**, *42*, 3430.
  35. Sockwell, S. C.; Hanusa, T. P.; Huffman, J. C. *J. Am. Chem. Soc.* **1992**, *114*, 3393.
  36. Weeber, A.; Harder, S.; Brintzinger, H. H. *Organometallics* **2000**, *19*, 1325.
  37. Gauvin, R. M.; Buch, F.; Delevoye, L.; Harder, S. *Chem. Eur. J.* **2009**, *15*, 4382.
  38. Cotton, F. A.; Wilkinson, E.; Murillo, C. A. *Advanced Inorganic Chemistry*, 6th ed.; Wiley and Sons: New York, 1999; 1302.
  39. Huheey, J. E.; Keiter, E. A.; Keiter, R. L. *Inorganic Chemistry: Principles of Structure and Reactivity*, 4th ed.; Harper Collins College Publishers: New York, 1993; p 292.
  40. (a) Chisholm, M. H.; Eilerts, N. W. *Chem. Commun.* **1996**, 853; (b) Chisholm, M. H.; Eilerts, N. W.; Huffman, J. C.; Iyer, S. S.; Pacold, M.; Phomphrai, K. *J. Am. Chem. Soc.* **2000**, *122*, 11845; (c) Chisholm, M. H.; Gallucci, J.; Phomphrai, K. *Chem. Commun.* **2003**, 48.
  41. (a) Parks, J. E.; Holm, R. H. *Inorg. Chem.* **1968**, *7*, 1408; (b) Bourget-Merle, L.; Lappert, M. F.; Severn, J. R. *Chem. Rev.* **2002**, *102*, 3031; (c) Dove, A. P.; Gibson, V. C.; Marshall, E. L.; White, A. J. P.; Williams, D. J. *Dalton Trans.* **2004**, 570.
  42. (a) Chisholm, M. H.; Huffman, J. C.; Phomphrai, K. *J. Chem. Soc. Dalton Trans.* **2001**, 222; (b) Chisholm, M. H.; Gallucci, J.; Phomphrai, K. *Inorg. Chem.* **2002**, *41*, 2785; (c) Chisholm, M. H.; Phomphrai, K. *Inorg. Chim. Acta* **2003**, *350*, 121; (d) Cheng, M.; Attygalle, A. B.; Lobkovsky, E. B.; Coates, G. W. *J. Am. Chem. Soc.* **1999**, *121*, 11583; (e) Chamberlain, B. M.; Cheng, M.; Moore, D. R.; Oviitt, T. M.; Lobkovsky, E. B.; Coates, G. W. *J. Am. Chem. Soc.* **2001**, *123*, 3229; (f) Drouin, F.; Whitehorn, T. J. J.; Schaper, F. *Dalton Trans.* **2011**, *40*, 1396.
  43. (a) Dove, A. P.; Gibson, V. C.; Marshall, E. L.; White, A. J. P.; Williams, D. J. *Dalton Trans.* **2004**, 570; (b) Chen, H. Y.; Peng, Y. L.; Huang, T. H.; Sutar, A. K.; Miller, S. A.; Lin, C. C. *J. Mol. Catal. A: Chem.* **2011**, *339*, 61.
  44. Tang, H. Y.; Chen, H. Y.; Huang, J. H.; Lin, C. C. *Macromolecules* **2007**, *40*, 8855.
  45. (a) Chen, M. T.; Chang, P. J.; Huang, C. A.; Peng, K. F.; Chen, C. T. *Dalton Trans.* **2009**, 9068; (b) Huang, Y.; Hung, W. C.; Liao, M. Y.; Tsai, T. E.; Peng, Y. L.; Lin, C. C. *J. Polym. Sci. A: Polym. Chem.* **2009**, *47*, 2318.
  46. Shueh, M. L.; Wang, Y. S.; Huang, B. H.; Kuo, C. Y.; Lin, C. C. *Macromolecules* **2004**, *37*, 5155.
  47. Yu, T. L.; Wu, C. C.; Chen, C. C.; Huang, B. H.; Wu, J.; Lin, C. C. *Polymer* **2005**, *46*, 5909.
  48. (a) Shen, M. Y.; Peng, Y. L.; Hung, W. C.; Lin, C. C. *Dalton Trans.* **2009**, 9906; (b) Wu, J.; Chen, Y. Z.; Hung, W. C.; Lin, C. C. *Organometallics* **2008**, *27*, 4970.
  49. Chisholm, M. H.; Gallucci, J. C.; Zhen, H. S. *Inorg. Chem.* **2001**, *40*, 5051.
  50. Chen, H. Y.; Tang, H. Y.; Lin, C. C. *Macromolecules* **2006**, *39*, 3745.
  51. Hung, W. C.; Huang, Y.; Lin, C. C. *J. Polym. Sci. A: Polym. Chem.* **2008**, *46*, 6466.
  52. (a) Wu, J.; Huang, B. H.; Hsueh, M. L.; Lai, S. L.; Lin, C. C. *Polymer* **2005**, *46*, 9784; (b) Sung, C. Y.; Li, C. Y.; Su, J. K.; Chen, T. Y.; Lin, C. H.; Ko, B. T. *Dalton Trans.* **2012**, *41*, 953.
  53. Hill, M. S.; Hitchcock, P. B. *Dalton Trans.* **2002**, 4694.
  54. Williams, C. K.; Brooks, N. R.; Hillmyer, M. A.; Tolman, W. B. *Chem. Commun.* **2002**, 2132.
  55. Williams, C. K.; Breyfogle, L. E.; Choi, S. K.; Nam, W.; Young, V. G., Jr.; Hillmyer, M. A.; Tolman, W. B. *J. Am. Chem. Soc.* **2003**, *125*, 11350.
  56. Jensen, T. R.; Breyfogle, L. E.; Hillmyer, M. A.; Tolman, W. B. *Chem. Commun.* **2004**, 2504.
  57. Coles, M. P.; Hitchcock, P. B. *Eur. J. Inorg. Chem.* **2004**, 2662.
  58. Zhong, Z. Y.; Dijkstra, P. J.; Birg, C.; Westerhausen, M.; Feijen, J. *Macromolecules* **2001**, *34*, 3863.
  59. Zhong, Z. Y.; Schneiderbauer, S.; Dijkstra, P. J.; Westerhausen, M.; Feijen, J. *Polym. Bull.* **2003**, *51*, 175.
  60. (a) Chisholm, M. H.; Gallucci, J. C.; Phomphrai, K. *Inorg. Chem.* **2004**, *43*, 6717; (b) Cushion, M. G.; Mountford, P. *Chem. Commun.* **2011**, 47, 2276.
  61. (a) Chen, H. Y.; Tang, H. Y.; Lin, C. C. *Polymer* **2007**, *48*, 2257; (b) Darensbourg, D. J.; Choi, W.; Karroonirun, O.; Bhuvanesh, N. *Macromolecules* **2008**, *41*, 3493; (c) Darensbourg, D. J.; Choi, W.; Richers, C. P. *Macromolecules* **2007**, *40*, 3521.
  62. Liu, B.; Roisnel, T.; Guegan, J. P.; Carpentier, J. F.; Sarazin, Y. *Chem. Eur. J.* **2012**, *18*, 6289.
  63. Emig, N.; Nguyen, H.; Krautscheid, H.; Réau, R.; Cazaux, J. B.; Bertrand, G. *Organometallics* **1998**, *17*, 3599.
  64. (a) Shimasaki, K.; Aida, T.; Inoue, S. *Macromolecules* **1987**, *20*, 3076; (b) Trofimoff, L.; Aida, T.; Inoue, S. *Chem. Lett.* **1987**, 991.
  65. Aida, T.; Inoue, S. *Acc. Chem. Res.* **1996**, *29*, 39.
  66. Huang, C. H.; Wang, F. C.; Ko, B. T.; Yu, T. L.; Lin, C. C. *Macromolecules* **2001**, *34*, 356.
  67. Doherty, S.; Errington, R. J.; Housley, N.; Clegg, W. *Organometallics* **2004**, *23*, 2382.
  68. Liu, Y. C.; Ko, B. T.; Lin, C. C. *Macromolecules* **2001**, *34*, 6196.
  69. Li, C. Y.; Tsai, C. Y.; Lin, C. H.; Ko, B. T. *Dalton Trans.* **2011**, *40*, 1880.
  70. Wu, J.; Pan, X.; Tang, N.; Lin, C. C. *Eur. Polym. J.* **2007**, *43*, 5040.
  71. Chen, C. T.; Weng, H. J.; Chen, M. T.; Huang, C. A.; Peng, K. F. *Eur. J. Inorg. Chem.* **2009**, 2129.
  72. Ma, H.; Mellillo, G.; Spaniol, T. P.; Englert, U.; Okuda, J. *Dalton Trans.* **2005**, 721.
  73. Horeglad, P.; Kruk, P.; Pécaut, J. *Organometallics* **2010**, *29*, 3729.
  74. (a) Shanthi, G.; Perumal, P. T. *Synlett* **2008**, *18*, 2791; (b) Shen, Z. L.; Ji, S. J.; Loh, T. P. *Tetrahedron* **2008**, *64*, 8159; (c) Chapin, R. E.; Harris, M. W.; Hunter, E. S. I. I.; Davis, B. J.; Collins, B. J.; Lockhart, A. C. *Fundam. Appl. Toxicol.* **1995**, *27*, 140.
  75. Douglas, A. F.; Patrick, B. O.; Mehrhodavandi, P. *Angew. Chem. Int. Ed.* **2008**, *47*, 2290.
  76. Peckermann, I.; Kapelski, A.; Spaniol, T. P.; Okuda, J. *Inorg. Chem.* **2009**, *48*, 5526.
  77. Buffet, J. C.; Okuda, J.; Arnold, P. L. *Inorg. Chem.* **2010**, *49*, 419.
  78. Lévy, F.; Sheikin, I.; Grenier, B.; Huxley, A. D. *Science* **2005**, *309*, 1343.
  79. Washio, K. *IEEE Trans. Electron Dev.* **2003**, *50*, 656.
  80. Finne, A.; Reema, A.; Albertsson, A. C. *J. Polym. Sci. A: Polym. Chem.* **2003**, *41*, 3074.
  81. Kricheldorf, H. R.; Langanke, D. *Polymer* **2002**, *43*, 1973.
  82. Chmura, A. J.; Chuck, C. J.; Davidson, M. G.; Jones, M. D.; Lunn, M. D.; Bull, S. D.; Mahon, M. F. *Angew. Chem. Int. Ed.* **2007**, *46*, 2280.
  83. Atkins, P.; Shriver, A. J. *Inorganic Chemistry*, 4th ed.; Oxford University Press: New York, 2006.
  84. Baran, J.; Duda, A.; Kowalski, A.; Szymanski, R.; Penczek, S. *Macromol. Symp.* **1997**, *123*, 93.
  85. Jalabert, M.; Frascini, C.; Prud'homme, R. E. *J. Polym. Sci. A: Polym. Chem.* **2007**, *45*, 1944.
  86. Korhonen, H.; Helminen, A.; Seppälä, J. V. *Polymer* **2001**, *42*, 7541.
  87. Ryner, M.; Finne, A.; Albertsson, A. C.; Kricheldorf, H. R. *Macromolecules* **2001**, *34*, 7281.
  88. Dove, A. P.; Gibson, V. C.; Marshall, E. L.; White, A. J. P.; Williams, D. J. *Chem. Commun.* **2001**, 283.
  89. Aubrecht, K. B.; Hillmyer, M. A.; Tolman, W. B. *Macromolecules* **2002**, *35*, 644.
  90. Carlin, J. F., Jr. *Bismuth [Advance Release], 2008 Minerals Yearbook, U.S. Department of the Interior*, Oct. 2009, U.S. Geological Survey.
  91. Kricheldorf, H. R.; Serra, A. *Polym. Bull. (Berlin)* **1985**, *44*, 497.
  92. Kricheldorf, H. R. *Chem. Rev.* **2009**, *109*, 5579.
  93. Kricheldorf, H. R.; Rost, S. *Polymer* **2005**, *46*, 3248.
  94. Li, H.; Wang, C.; Bai, F.; Yue, J.; Woo, H. G. *Organometallics* **2004**, *23*, 1411.
  95. Chen, H. Y.; Liu, M. Y.; Sutar, A. K.; Lin, C. C. *Inorg. Chem.* **2010**, *49*, 665.
  96. Wang, L.; Pan, X.; Yao, L.; Tang, N.; Wu, J. *Eur. J. Inorg. Chem.* **2011**, 632.
  97. Zhang, Z. J.; Xu, X. P.; Sun, S.; Yao, Y. M.; Zhang, Y.; Shen, Q. *Chem. Commun.* **2009**, 7414.

98. (a) Ovitt, T. M.; Coates, G. W. *J. Am. Chem. Soc.* **1999**, *121*, 4072; (b) Zell, M. T.; Padden, B. E.; Paterick, A. J.; Thakur, K. A. M.; Kean, R. T.; Hillmyer, M. A.; Munson, E. J. *Macromolecules* **2002**, *35*, 7700.
99. Fukushima, K.; Kimura, Y. *Polym. Int.* **2006**, *55*, 626.
100. Chen, H.-L.; Dutta, S.; Huang, P.-Y.; Lin, C.-C. *Organometallics* **2012**, *31*, 2016.
101. Byers, J. A.; Bercaw, J. E. *Proc. Natl. Acad. Sci.* **2006**, *103*, 15303.
102. Spassky, N.; Wisniewski, M.; Pluta, C.; Le Borgne, A. *Macromol. Chem. Phys.* **1996**, *197*, 2627.
103. Zhong, Z.; Dijkstra, P. J.; Feijen, J. *J. Am. Chem. Soc.* **2003**, *125*, 11291.
104. Darensbourg, D. J.; Karroonnirun, O. *Inorg. Chem.* **2010**, *49*, 2360.
105. Du, H.; Velders, A. H.; Dijkstra, P. J.; Sun, J.; Zhong, Z.; Chen, X.; Feijen, J. *Chem. Eur. J.* **2009**, *15*, 9836.
106. Cheng, M.; Attygalle, A. B.; Lobkovsky, E. B.; Coates, G. W. *J. Am. Chem. Soc.* **1999**, *121*, 11583.
107. Nomura, N.; Ishii, R.; Akakura, M.; Aoi, K. *J. Am. Chem. Soc.* **2002**, *124*, 5938.
108. Tang, Z.; Chen, X.; Pang, X.; Yang, Y.; Zhang, X.; Jing, X. *Biomacromolecules* **2004**, *5*, 965.
109. Hormnirun, P.; Marshall, E. L.; Gibson, V. C.; White, A. J. P.; Williams, D. J. *J. Am. Chem. Soc.* **2004**, *126*, 2688.
110. Pietrangelo, A.; Hillmyer, M. A.; Tolman, W. B. *Chem. Commun.* **2009**, 2736.

This page intentionally left blank